

**Signals
and
Communication
Technology**

Y. S. Shmaliy



**Continuous-Time
Systems**

 Springer

CONTINUOUS-TIME SYSTEMS

Continuous-Time Systems

by

Yuriy Shmaliy
*Guanajuato University,
Mexico*

 Springer

A C.I.P. Catalogue record for this book is available from the Library of Congress.

ISBN 978-1-4020-6271-1 (HB)
ISBN 978-1-4020-6272-8 (e-book)

Published by Springer,
P.O. Box 17, 3300 AA Dordrecht, The Netherlands.

www.springer.com

Printed on acid-free paper

All Rights Reserved

© 2007 Springer

No part of this work may be reproduced, stored in a retrieval system, or transmitted in any form or by any means, electronic, mechanical, photocopying, microfilming, recording or otherwise, without written permission from the Publisher, with the exception of any material supplied specifically for the purpose of being entered and executed on a computer system, for exclusive use by the purchaser of the work.

To the memory of my father and mother

Preface

Any real system be it physical, biological, chemical, astronomical, electrical, electronic, etc. operates in continuous time and is governed by differential equations. To learn the world we are living in and so comprehend the laws inherent to its organisms, the mathematical methods of system analysis, synthesis, and design have been under development for centuries. With time, these methods have framed what we now call the “system theory” covering all aspects of mathematical modeling of structures comprising subsystems and even components.

A very specific area unites electronic systems, such as navigation, positioning, radar, sonar, control, broadcasting, television, communications, measurements, remote sensing, etc. with permanently increasing fields of applications, such as military, space exploration, aviation, bioengineering, cartography, astronomy, manufacturing, robotics, medicine, metrology, scientific, entertainment, and this list is not exhausted.

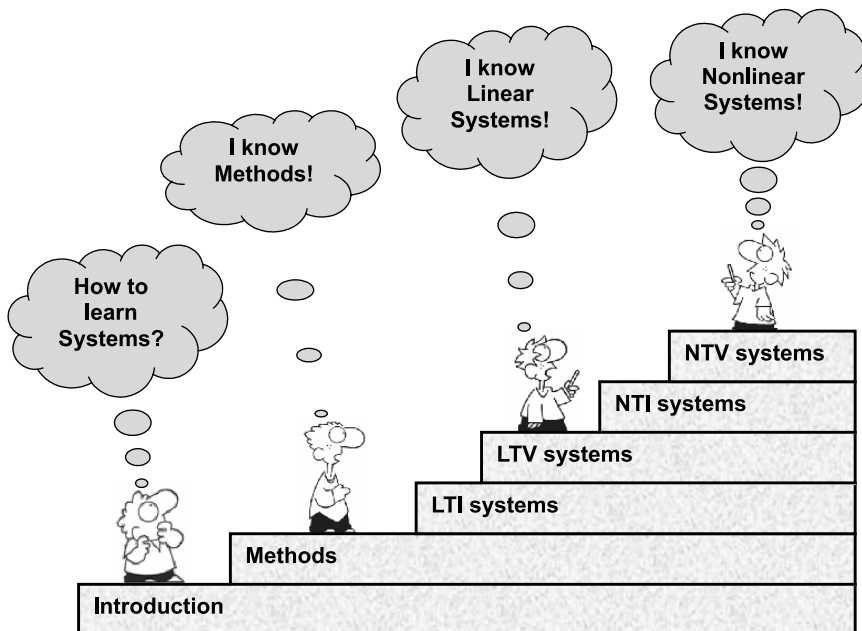
In spite of a relatively short history, electronic systems have passed a way of tremendous development starting from the early days of communication by telephone (Elisha Gray and Graham Bell, 1870s) and radio broadcasting (Aleksandr Popov and Guglielmo Marconi, 1890s) up to the automatic control (1940s), chaotic systems (1970s) (mechanical chaotic system have been studied for over 200 years), and fractals (1980s). An enormous number of papers have been published for decades as associated with different aspects of the system theory and applications and the number of publications intensively grows every year.

This book introduces the reader to the deterministic theory of the continuous-time linear and nonlinear systems assuming them to be either time-varying or time-invariant. We do not give cross-references to the critical and widely recognized works (the list of these works is applied). Instead, we mention short biographies of the most outstanding people contributing to the field, whenever the name first appears in the text.

To keep the development logical and more understandable, the systems are observed from the linear time-invariant (LTI), to linear time-varying (LTV),

nonlinear time-invariant (NTI), and nonlinear time-varying (NTV). The main material is supplied with the Introduction and two Chapters presenting the qualitative and quantitative methods.

The organization of the book is illustrated by the following humorous diagram with a personage taken from the Education Cartoons for Teachers, by Randy Glasbergen.



The following chapters elucidate the theory of the continuous-time systems:

1. In Introduction (Chapter 1), basic principles of operation of the most typical electronic systems are first observed. The systems are then classified in nowadays seemingly obvious and acceptable terms. Finally, basic operations with signals are briefly outlined for all general types of systems: linear and nonlinear, time-invariant and time-varying.
2. Chapter 2 addresses the quantitative methods of systems analysis. It starts with the definitions of the system responses to test signals. The rigorous methods are then observed for both linear and nonlinear systems. The rigor is not for its own sake and not always necessary. Therefore, in the sequel, the approximate methods are discussed for nonlinear systems. Among these methods, the two far reaching approaches called averaging and equivalent linearization are observed in detail. An analysis is finished with the system norms and theory of stability.

3. The qualitative methods are observed in Chapter 3. System presentation in phase plane is given along with a description of phase trajectories (limit cycles, homoclinic and heteroclinic, and attractors). Structural stability, bifurcations, chaotic orbits, and fractals are also discussed. Finally, conservative and dissipative structures are presented with the methods of their analysis.
4. Beginning with Chapter 4, the systems are analyzed systematically using the conceptual cannons, foundations, and methods given in Chapters 1–3. In Chapter 4, the LTI systems are examined in the time domain. Starting with the convolution, the LTI systems are then described by the ordinary differential equations (ODEs), simulated with block diagrams, and represented in state space.
5. In Chapter 5, the LTI systems are examined in the frequency (transform) domain. Major tools here are the Fourier transform and Laplace transform (bilateral and unilateral) applied to earlier observed the different forms in the time domain. Stability analysis in the frequency domain and transform domain is also given.
6. Chapter 6 is devoted to LTV systems. In the time domain, this system is represented with the time-varying impulse response (standard and modified) and general convolution. It is also represented with the ODEs and in state space. In the transform domain, the tool is mostly the time-varying frequency response. Linear periodic systems are observed and analyzed as suggested by Floquet's theory. Examples are taken from the frequency transformation, parametric modulation, parametric excitation, parametric amplification, and synchronous detection.
7. NTI systems are observed and analyzed in Chapter 7. Here, a memoryless nonlinearity is described, interpolated, and approximated. The Volterra and Wiener approaches are applied to memory systems both in the time and frequency domains. As applications, the Hammerstein and Wiener models are considered. Systems are also represented approximately with the describing function method. Description by the ODEs is supported with examples of nonlinear piezoelectric filter, harmonic oscillator, bi-harmonic oscillatory system, and synchronized harmonic oscillator. Finally, state space presentation is given and illustrated with the phase locked loop.
8. In the last Chapter 8, the most general system model, namely NTV, is examined. The memoryless nonlinearity is considered in time and the Volterra approach is extended to the time-variant coefficients of a memory system. The system is also analyzed with the ODE and illustrated with the voltage controlled oscillator. Periodic (modulated) NTV systems are described with the modulation functions method and supported by examples of FM oscillators. Finally, state space presentation is given for the time-varying Hammerstein and Wiener systems.

The remainder of the book is build with Appendices reviewing the properties of the Dirac delta function (Appendix A), matrices (Appendix B), the Fourier transform and transform properties (Appendix C), and the Laplace transform and transform properties (Appendix D). Useful mathematical formulas are postponed to Appendix E.

As well as the first part Signals¹, this book is essentially an extensive revision and development of my Lectures on Radio Signals, Circuits, and Systems given during a couple of decades in Kharkiv Military University of Ukraine and several courses on Signals and Systems, System Theory, and Signal Processing in the Guanajuato University of Mexico in recent years. The book is intended for the sophomore-junior and upper level electrical engineering student who wants to acquire knowledge in classical and modern system analysis and comprehend the links between linear and nonlinear, time-invariant and time-varying structures. It may also be useful for post graduate studies and specialists in electronic and other systems.

Salamanca, Mexico,

Yuriy S. Shmaliy

¹ Shmaliy, Y.S., Continuous-Time Signals, Springer, Dordrecht, 2006.

Contents

1	Introduction	1
1.1	Principles of Operation of Typical Systems	2
1.1.1	Communications	2
1.1.2	Distance Measurement by Phase Radars	4
1.1.3	Radial Velocity Measurement of an Aircraft	5
1.1.4	Control	6
1.1.5	Medical Ultrasonography	7
1.1.6	Robot Positioning	8
1.1.7	Remote Sensing	10
1.1.8	Reference Source of Frequency	10
1.2	Systems Performance and Classification	12
1.2.1	Regularity	12
1.2.2	Continuity	13
1.2.3	Dimensionality	13
1.2.4	Memory	14
1.2.5	Causality	15
1.2.6	Linearity	16
1.2.7	Time Invariance	17
1.2.8	Observability and Controllability	19
1.2.9	Detectability and Stabilizability	20
1.2.10	Accuracy and Precision	20
1.2.11	Uncertainty and Robustness	21
1.2.12	Stability	24
1.3	Basic Structures	25
1.3.1	Open (Input-to-output) System	25
1.3.2	Closed Loop System	25
1.3.3	Closed Loop Control System	26
1.3.4	Interconnection	27
1.4	Basic Operations with Signals in Systems	28
1.4.1	Linear Time-invariant Systems	28
1.4.2	Linear Time-varying Systems	32

1.4.3	Nonlinear Time-invariant Systems	33
1.4.4	Nonlinear Time-varying Systems	37
1.5	Summary	37
1.6	Problems	38
2	Quantitative Methods of Systems Description	43
2.1	System Responses to Test Signals	43
2.1.1	Impulse Response	44
2.1.2	Step Response	46
2.1.3	Frequency Response	46
2.2	Methods for Linear Systems	49
2.2.1	Convolution	49
2.2.2	Differential Equations	51
2.2.3	Transfer Function	52
2.2.4	State Space Representation	54
2.3	Common Methods for Nonlinear Systems	57
2.3.1	Volterra Series	57
2.3.2	Differential Equation Method	60
2.3.3	State Space Representation	60
2.4	Approximation and Linearization	61
2.4.1	Polynomial Approximation	61
2.4.2	Methods of Linearization	62
2.5	Averaging	66
2.5.1	Method of Expansion (Perturbation Method)	67
2.5.2	Van der Pol's Method	68
2.5.3	Asymptotic Methods of Krylov-Bogoliubov-Mitropolskiy	70
2.5.4	Systems with Slowly Changing Parameters	74
2.6	Equivalent Linearization	77
2.6.1	Classical Method of Harmonic Balance	78
2.6.2	Stationary Solutions by Harmonic Balance	79
2.6.3	Double Harmonic Balance Method	81
2.6.4	Describing Function Method	85
2.7	Norms	87
2.7.1	Norms for Signals	87
2.7.2	Norms for Systems	91
2.7.3	System Norms via Signal Norms	94
2.8	System Stability	95
2.8.1	External (Bounded Input/Bounded Output) Stability	95
2.8.2	Internal Stability	98
2.8.3	Stability of Linear Systems	103
2.8.4	The First Lyapunov Method	105
2.8.5	The Second Lyapunov Method	108
2.9	Summary	112
2.10	Problems	113

3	Qualitative Methods of Systems Description	119
3.1	Qualitative Analysis	119
3.1.1	Phase Plane	120
3.1.2	Stability of Linearized Nonlinear Systems	121
3.2	Phase Trajectories	124
3.2.1	Limit Cycles	126
3.2.2	Homoclinic and Heteroclinic Trajectories	128
3.2.3	Attractors	130
3.2.4	Structural Stability of Systems	131
3.3	Bifurcations	131
3.4	Chaotic Orbits and Fractals	134
3.4.1	Lyapunov Exponents	137
3.5	Conservative Systems	138
3.5.1	Hamiltonian Systems	141
3.6	Dissipative (Near Conservative) Systems	143
3.6.1	Near Conservative Time-varying Systems	145
3.6.2	Melnikov's Method	146
3.7	Summary	148
3.8	Problems	149
4	LTI Systems in the Time Domain	153
4.1	Introduction	153
4.2	Convolution	153
4.2.1	System Step Response	157
4.2.2	Properties of the Convolution	157
4.2.3	Properties of LTI Systems	161
4.2.4	Problems Solved with Convolution	164
4.2.5	Convolution Form for Multiple Systems	167
4.3	Representation by Differential Equations	168
4.3.1	CARMA model	169
4.3.2	Properties of the ODE Operator	170
4.4	Electric Circuit Presentation by ODEs	175
4.4.1	LTI Systems of the First Order	175
4.4.2	LTI Systems of the Second Order	179
4.5	System Simulation by Block Diagrams	188
4.5.1	Basic Blocks of LTI Systems	188
4.5.2	Generalized Structures of LTI Systems	189
4.6	State Space Representation	195
4.6.1	The First Direct Forms of SISO Systems in State Space	196
4.6.2	The Second Direct Forms of SISO Systems in State Space	200
4.6.3	MIMO Systems in State Space	203
4.6.4	LTI Systems with Feedback	206
4.6.5	Properties of State Space Model	211
4.6.6	Stability	218

4.7	Solution of State Space Equations	222
4.7.1	Matrix Exponential	223
4.7.2	System Impulse Response in State Space	228
4.7.3	System Step Response in State Space	228
4.8	Summary	229
4.9	Problems	230
5	LTI Systems in the Frequency Domain (Transform Analysis)	239
5.1	Introduction	239
5.2	Fourier Analysis	239
5.2.1	Frequency Response	240
5.2.2	Phase Distortions	246
5.2.3	Distortionless Transmission	249
5.2.4	Filtering	250
5.2.5	LTI Systems of the First Order	254
5.2.6	LTI Systems of the Second Order	260
5.2.7	LTI Systems of High Orders	266
5.2.8	Piezoelectric Structures	267
5.3	Laplace Transform	276
5.3.1	Bilateral Laplace Transform vs. Fourier Transform	276
5.3.2	Region of Convergence	279
5.3.3	Properties of the Bilateral Laplace Transform	282
5.3.4	System Characterization with Transfer Function	291
5.3.5	The Inverse Laplace Transform	293
5.4	Unilateral Laplace transform	297
5.4.1	Properties of the Unilateral Laplace Transform	297
5.4.2	Laplace Transforms of Some Common Functions	302
5.5	Applications of Laplace transform	304
5.5.1	Solution of ODEs of LTI Systems	304
5.5.2	Application to Electric Circuits	307
5.5.3	Block Diagram Presentation by the Laplace Transform	313
5.5.4	State Space Analysis via Laplace Transform	317
5.6	Stability Analysis of Feedback Systems	319
5.6.1	Transfer Function of Closed Systems	319
5.6.2	Routh-Hurwitz Criterion	322
5.6.3	Nyquist Criterion	323
5.6.4	Gain and Phase Stability Margins	325
5.6.5	Bandwidth Correction by Feedback	328
5.7	Selective Filter Approximations	333
5.7.1	Butterworth Filter	333
5.7.2	Chebyshev Filter	336
5.8	Summary	341
5.9	Problems	341

6	Linear Time-Varying Systems	349
6.1	Introduction	349
6.2	Time-varying Impulse Response and General Convolution ...	349
6.2.1	Modified Time-varying Impulse Response.....	352
6.2.2	Time-varying Frequency Response	356
6.2.3	Time-varying Transfer Function	362
6.2.4	Classification of LTV Systems.....	364
6.3	Properties of LTV Systems	366
6.3.1	Linearity	366
6.3.2	Non-commutativity	367
6.3.3	Associativity	367
6.3.4	Inconvertibility of Impulse and Step Responses	369
6.3.5	BIBO Stability	371
6.4	Representation by Differential Equations	371
6.4.1	LTV System of the First Order.....	372
6.4.2	Application to Electrical Circuits	375
6.4.3	Block Diagrams	378
6.5	State Space Representation	383
6.5.1	State Space Model via the Second Direct Form for $M = 0$	383
6.5.2	Block Diagram Representation	384
6.5.3	Solution of State Space Equations	386
6.5.4	System Impulse Response in State Space	391
6.5.5	BIBO Stability of MIMO LTV Systems	393
6.5.6	Controllability	394
6.5.7	Observability	396
6.6	Linear Periodically Time-varying Systems	396
6.6.1	Basic Foundations	397
6.6.2	Floquet's Theory	398
6.6.3	Frequency Transformation	402
6.6.4	Parametric Modulation	404
6.6.5	Synchronous Detection	405
6.6.6	Linear Parametric Excitation	407
6.6.7	Linear Parametric Oscillator. Mathieu's Equation	409
6.6.8	Parametric Amplification	414
6.7	Summary.....	417
6.8	Problems.....	418
7	Nonlinear Time Invariant Systems	425
7.1	Introduction	425
7.2	Memoryless Systems	426
7.2.1	Lagrange Interpolation	427
7.2.2	Newton Method.....	428
7.2.3	Splines	429
7.2.4	Exponential Approximation.....	433

7.2.5	Taylor Series Expansion	434
7.2.6	Linearization Techniques	435
7.3	Representation of Memory Systems by Volterra Series	436
7.3.1	A Noble Example	438
7.3.2	Hammerstein and Wiener Systems	439
7.3.3	Properties of the Volterra Operator	442
7.3.4	Wiener approach	447
7.4	Representation in the Transform Domain	450
7.4.1	Properties of the Multivariate Laplace Transform	450
7.4.2	Laplace Transform of the Volterra Series	453
7.4.3	System Representation in the Transform Domain	455
7.5	Approximation by Describing Functions	458
7.5.1	System Representation with Describing Functions	458
7.5.2	Properties of Describing Functions	465
7.6	Description by Differential Equations	470
7.6.1	System of the First Order (Bernoulli's Equation)	470
7.6.2	Linearization of Nonlinear ODEs	471
7.6.3	Nonlinear Piezoelectric Filter	473
7.6.4	Harmonic Oscillator	477
7.6.5	Biharmonic Oscillatory System	480
7.6.6	Synchronized Harmonic Oscillator	486
7.7	State Space Representation	493
7.7.1	Linearization of State Space Model	494
7.7.2	Hammerstein System	496
7.7.3	Wiener System	499
7.7.4	Cascade Hammerstein and Wiener Systems	501
7.7.5	Closed Loop Systems	502
7.7.6	Phase Locked Loop	506
7.8	Summary	512
7.9	Problems	513
8	Nonlinear Time Varying Systems	519
8.1	Introduction	519
8.2	Memoryless Time-varying Nonlinearities	520
8.2.1	Bias Voltage Control	520
8.2.2	Interpolation of Time-varying Memoryless Nonlinearities	523
8.2.3	Taylor Series Expansion for Time-varying Characteristics	523
8.3	Volterra Series Expansion	525
8.3.1	Properties of the Time-varying Volterra Operator	528
8.3.2	Representation in the Frequency Domain	531
8.3.3	Representation in the Transform Domain	535
8.4	Description by Differential Equations	535
8.4.1	Systems of the First Order	536
8.4.2	Voltage Controlled Oscillator	539
8.5	Nonlinear Periodically Time-varying Systems	542

8.5.1	Bogolubov-Mitropolskiy Model	543
8.5.2	Modulation Functions Method (Slow Modulation)	544
8.5.3	Oscillator with a Modulated Inductance	551
8.5.4	Frequency Modulated Crystal Oscillator	557
8.5.5	Modulation Functions Method (Fast Modulation)	562
8.5.6	Butler Type FM Crystal Oscillator	569
8.6	State Space Representation	574
8.6.1	Linearization	577
8.6.2	Time-varying Hammerstein System	578
8.6.3	Time-varying Wiener System	581
8.7	Summary	583
8.8	Problems	584
A	Dirac Delta Function	589
B	Matrices	593
C	Tables of Fourier Series, Transform, and Properties	609
D	Tables of Laplace Transform and Transform Properties	613
E	Mathematical Formulas	617
	References	625
	Index	629

Introduction

All physical systems are governed by differential equations and operate in continuous time. Therefore, they are labeled as *dynamical systems* and interpreted as functions that map input signals into output signals. This mapping may be linear or nonlinear, time-invariant or time-variant, deterministic or stochastic (random). The system input may fully be specified by its output and the system then becomes closed loop (no input) being either passive (negative feedback) or active or oscillating (positive feedback). If a closed loop system has an auxiliary control input, then it is a closed loop control system or merely a control system. Contrary, if a system is designed without output, then it is an isolated system (no output) also called a closed system. A common idea about a *system* may thus be formulated as follows:

System: A *system* is an assemblage of physical or mathematical components organized and interacting to convert an input signal (also called excitation signal or driving force) to an output signal (also called response signal). □

A system is presented as a mathematical model of a physical process that relates the input signal to the output signal. Therefore, basically, the system theory is forwarded toward solving four major problems:

- **System analysis**, to understand properties of a given system. □
- **System design**, to find a proper system that meets given specifications. □
- **System synthesis**, to find a system structure or a proper block diagram. □
- **System implementation**, to realize a system practically. □

In modern signals mapping, attention is focused not solely on how the function is defined, but also on what is the domain and range of signals. Domains and ranges are often converted that makes a modern system typically complex but also optimized. An example is when an analog signal is converted

to the discrete form, then processed digitally, and returned back to the analog form. In the other example, to transmit a digital signal through the telephone system, the digital signal has to be converted into a bandlimited audio signal in the analog domain of the telephone system.

Many systems are designed to have constant coefficients with negligible noise. Such systems labeled deterministic are considered throughout this book. For a long time, researchers were deeply convinced that deterministic systems always give a deterministic output. It then occurred that, under certain conditions, the deterministic system may produce the output that is not strongly deterministic, but chaotic.

The essential feature of system theory is that the analytical results for dynamical systems with discrete time are not always applicable in the continuous-time systems. This is why the dynamical systems in continuous time, also often called *flows*, and the discrete-time dynamic systems have different mathematics, even though the fundamental concepts are common for both types.

In this book, we consider fundamentals and basic canons of all types of the continuous-time deterministic systems, namely linear and nonlinear, time-invariant and time-varying, with their presentations in the time and frequency (transform) domains. Since the material relates to electrical engineering, prime attention is paid to linear electronic systems associated with 2π signal periodicity and methods of description of time-varying and nonlinear systems with applications to their principle representatives, such as frequency transformers, oscillators, nonlinear amplifiers, modulators, demodulators, control systems, phase locked loops, etc. The reader is encouraged to follow fundamentals, definitions, and basic canons of signals given in [Shmaliy, Yu.S., *Continuous-Time Signals*, Springer, 2006] that is referred to throughout the book as Signals.

1.1 Principles of Operation of Typical Systems

As many physical processes are of interest, many systems may be designed to meet practical needs. In the modern view, systems exploiting electrical and/or electromagnetic nature of signals can quite fully be represented with the following examples grounded on practical usefulness.

1.1.1 Communications

In communications, a system is called a device that realizes a transformation of the information in its input signal to the information in its output signal. Via the communication channel, the information is submitted by the *transmitter* at a distance and received by the *receiver*. Two structures are practically feasible: the communication channel may be either wireless (Fig. 1.1a) or wire (Fig. 1.1b).

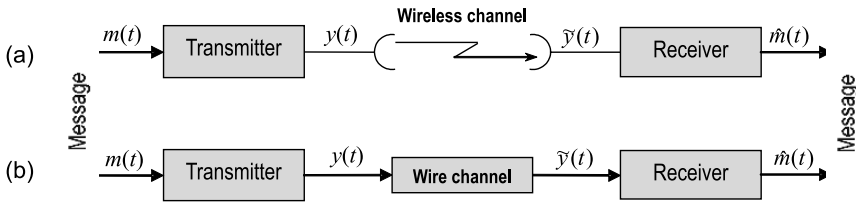


Fig. 1.1. Structures of communication systems: (a) wireless and (b) wire.

A typical situation is when the information is represented not in electrical media. It may be voice or image, for example. Therefore, an important block is a *modulator* that performs the transformation of the nonelectric information (voice) to the electric signal (voice-like). At the receiver, the electric signal (voice-like) is transformed back to the nonelectric information (voice) by what is called the *demodulator*. The other important operation of the transmitter is information coding necessary to detect different signals. The receiver also provides amplification, demodulation, filtering, and information decoding.

The information is transmitted via the amplitude or/and angle of a carrier signal, so that a general form of a transmitted signal may be performed as

$$y(t) = A(t) \cos \Psi(t), \tag{1.1}$$

where various kinds of amplitude modulation (AM) are realized by variations in the amplitude $A(t)$. Frequency modulation (FM) and phase modulation (PM) are provided by altering the signal angle $\Psi(t)$.

With AM, the signal (1.1) may be written as

$$y(t) = A_0 [1 + k_a m(t)] \cos(\omega_0 t + \psi_0), \tag{1.2}$$

where $m(t)$ is the baseband *message*, A_0 is the mean amplitude without AM, k_a is the *amplitude sensitivity*, ω_0 is a carrier frequency, and ψ_0 is a initial constant phase. By FM, the function (1.1) is transformed to

$$y(t) = A_0 \cos \left[\omega_0 t + k_\omega \int_0^t m(t) dt + \psi_0 \right], \tag{1.3}$$

where $k_\omega = 2\pi k_f$ and k_f is the *frequency sensitivity*. Finally, with PM, the signal is formed as

$$y(t) = A_0 \cos[\omega_0 t + k_p m(t) + \psi_0], \tag{1.4}$$

where k_p is the *phase sensitivity*.

At the receiver, the signal $\tilde{y}(t)$ appears as a corrupted version of $y(t)$ owing to the channel imperfection. It is then detected and the message estimate $\hat{m}(t)$ is formed. With ideal wireless transmission, it is assumed that $\hat{m}(t) = m(t)$.

1.1.2 Distance Measurement by Phase Radars

The principle of distance measurement between a stationary object (car) and phase radar (acronym for radio detection and ranging) is illustrated in Fig. 1.2. The radar system consists of the transmitter and receiver organized in the same equipment. A precision oscillator (Osc) generates the reference signal

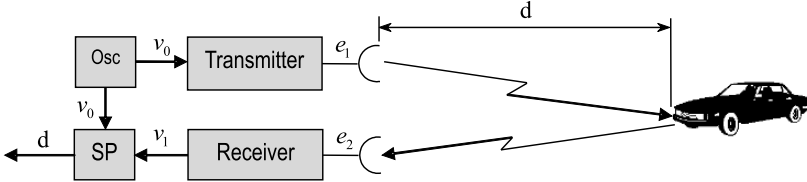


Fig. 1.2. Distance measuring radar system.

$$v_0(t) = V_0 \cos(\omega_0 t + \psi_0), \quad (1.5)$$

where V_0 , ω_0 , and ψ_0 are constant.

The transmitter gains oscillations, which are then radiated by the antenna as an electromagnetic field with an electric intensity

$$e_1(t) = E_1 \cos(\omega_0 t + \psi_0 + \varphi_t), \quad (1.6)$$

where φ_t a phase shift caused by signal amplification and propagation. While propagating, an electromagnetic field acquires a phase shift

$$2\pi \frac{(2d)}{\lambda} = \frac{4\pi d}{\lambda}, \quad (1.7)$$

where d is a distance between the measurement set (radar) and an object (car) and λ is the wave length determined by the frequency ω_0 and the phase speed ν of the wave propagation in the medium.

At the receiving antenna, an electric intensity of the electromagnetic field becomes

$$e_2(t) = E_2 \cos \left(\omega_0 t + \psi_0 + \varphi_t - \frac{4\pi d}{\lambda} \right), \quad (1.8)$$

and, after amplified and properly transformed at the receiver, the following signal goes to the signal processing (SP) block,

$$v_1(t) = V_1 \cos \left(\omega_0 t + \psi_0 + \varphi_t - \frac{4\pi d}{\lambda} + \varphi_r \right), \quad (1.9)$$

where φ_r the phase shift induced by the receiver. The SP block calculates the phase difference between two signals, $v_0(t)$ and $v_1(t)$; that is,

$$\phi = \frac{4\pi d}{\lambda} - \varphi_t - \varphi_r, \tag{1.10}$$

and the distance d is then defined by

$$d = \frac{\lambda}{4\pi} \phi + \frac{\lambda}{4\pi} (\varphi_t + \varphi_r), \tag{1.11}$$

where the phase shifts, φ_t and φ_r , are measured at the early stage while testing the system.

1.1.3 Radial Velocity Measurement of an Aircraft

Every pilot needs to know true airspeed to avoid critical situations. A geometrical interpretation of a possibility of determining a radial velocity of an aircraft is shown in Fig.1.3. The ground-placed equipment is located at a center point 0 of the stationary coordinates (x, y, z) . The point A , associated with the aircraft, lies at the plane y_1z_1 of the moving coordinates $[x_1(t_1), y_1, z_1]$ with a center at 0_1 . It is also assumed that the axes x and x_1 coincide, time t_1 corresponds to the moving coordinates, and that the aircraft moves along the direction r with a constant velocity \dot{r} .

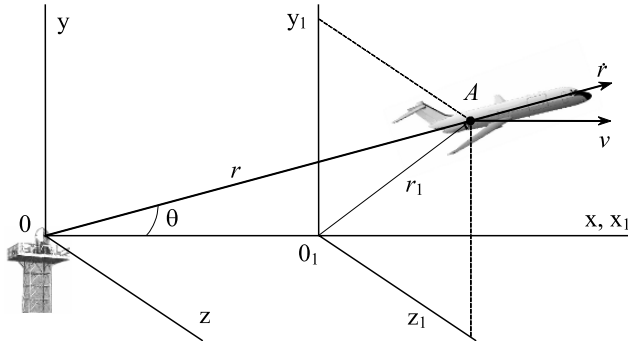


Fig. 1.3. Flying aircraft.

To measure \dot{r} , the system (Fig. 1.4) is organized such that the ground-placed transmitter radiates toward the aircraft a continuous harmonic wave with a reference frequency ω_0 . Owing to the Doppler¹ effect caused by the aircraft movement, the frequency ω_1 of the received signal differs from ω_0 and $\omega_0 - \omega_1$ is proportional to \dot{r} .

¹ Christian Andreas Doppler, Austrian mathematician, 29 November 1803–17 March 1853.

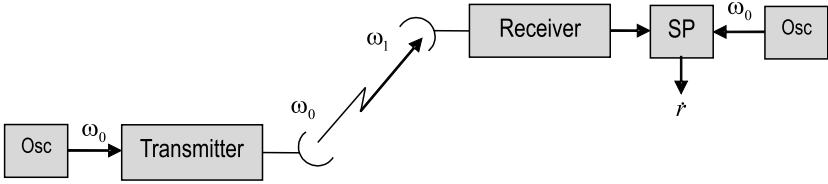


Fig. 1.4. Measurements of the radial velocity of an aircraft.

For the velocity ν in the direction x and velocity of a radio wave v , the time t_1 is defined by the direct Lorentz² transform that gives

$$t_1 = \frac{t - \frac{\nu}{v^2}x}{\sqrt{1 - \left(\frac{\nu}{v}\right)^2}}. \tag{1.12}$$

Since the signal phase is invariant to the coordinate system, it is supposed that $\varphi = \varphi_1$, where

$$\varphi = \omega_0 \left(t - \frac{r}{\nu} \right), \quad \text{and} \quad \varphi_1 = \omega_1 \left(t_1 - \frac{r_1}{\nu} \right). \tag{1.13}$$

If we now differentiate an equality $\varphi = \varphi_1$ with account of (1.12), we shall go, by $r_1 = \text{const}$ and $\dot{x} = \nu$, to

$$\omega_0 \left(1 - \frac{\dot{r}}{v} \right) = \omega_1 \sqrt{1 - \left(\frac{\nu}{v}\right)^2}. \tag{1.14}$$

By taking into consideration that $\nu = \dot{r} \cos \theta$, the Doppler frequency $\Omega = \omega_0 - \omega_1$ is approximately calculated as

$$\Omega = \omega_0 \left(\frac{\dot{r}}{v} - \frac{1}{2} \frac{\dot{r}^2}{v^2} \cos \theta \right). \tag{1.15}$$

The aircraft-placed electronic system measures Ω and its SP block calculates, by (1.15), the radial velocity \dot{r} for known θ and v .

1.1.4 Control

A critically important kind of problem is solved with control systems. An example of application of such systems to manage a manufacturing process is shown in Fig. 1.5.

It is supposed that the manufacturing plant produces some multiple output (production) $\mathbf{y}(t)$ that is evaluated by sensors to convert $\mathbf{y}(t)$ to $\mathbf{x}_1(t)$. The latter value is compared to the reference input (plan) $\mathbf{x}(t)$ and the evaluated

² Hendrik Antoon Lorentz, Dutch physicist and mathematician, 18 July 1853–4 February 1928.

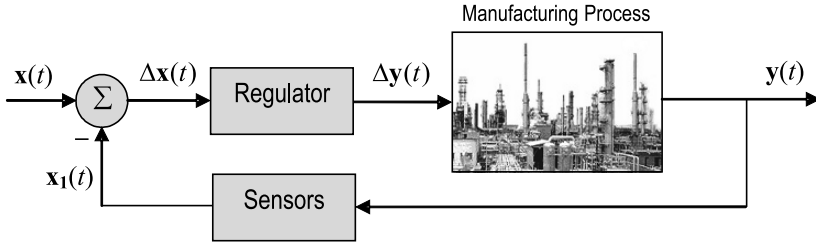


Fig. 1.5. Control of a manufacturing process.

difference $\Delta\mathbf{x}(t) = \mathbf{x}(t) - \mathbf{x}_1(t)$ goes to a regulator. To manage the process, a regulator produces the value $\Delta\mathbf{y}(t)$ such that the difference $\Delta\mathbf{x}(t)$ decreases toward zero.

In an ideal case of $\mathbf{x}_1(t) = \mathbf{x}(t)$, the value $\Delta\mathbf{y}(t)$ becomes zero and no adjustment is necessary for the process. If $\mathbf{x}_1(t) > \mathbf{x}(t)$ or $\mathbf{x}_1(t) < \mathbf{x}(t)$, the manufacturing process develops under the external control.

1.1.5 Medical Ultrasonography

An example of application of systems in medicine is ultrasonography illustrated in Fig. 1.6. Here, a short pulse signal is generated and sent through the attenuator to the ultrasonic acoustic transducer. For the Gaussian waveform, the generated signal may be written as

$$v_0(t) = V_0 e^{-a^2 t^2} \cos \omega_0 t, \tag{1.16}$$

where V_0 and ω_0 are the constant peak amplitude and carrier frequency, respectively, and the coefficient a is responsible for the pulse width. The

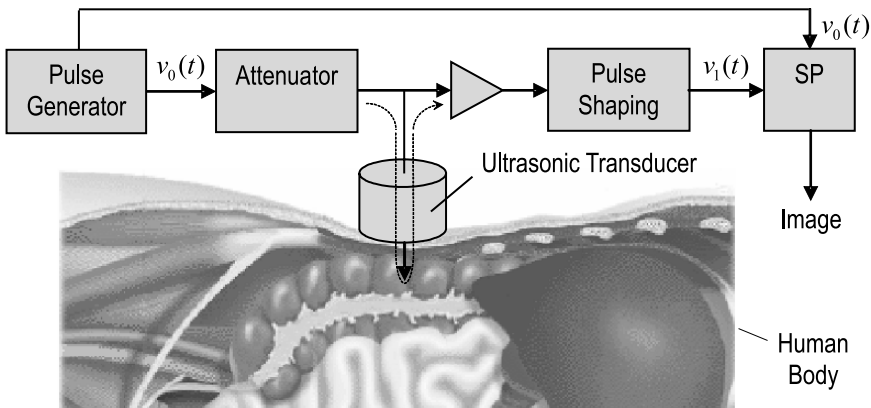


Fig. 1.6. Medical ultrasonography of a human body.

transducer converts $v_0(t)$ to the acoustic wave and forwards it into a human body.

Whenever a sound wave encounters a material with a different acoustical impedance, part of the sound wave is reflected, which the probe detects as an echo. The signal, reflected and converted back to electric form, becomes

$$v_1(t) = \alpha(t)V_0e^{-a^2(t-t_1)^2} \cos[\omega_0t - \varphi_1(t)], \quad (1.17)$$

where α , t_1 , and φ_1 indicate the depth of the tissue interface causing the echo at time $t = t_1$. The greater the difference between acoustic impedances, the larger the echo is. Along with the reference pulse $v_0(t)$, the reflected pulses $v_1(t)$ go through the pulse shaper to the SP block, where they are jointly processed to produce an electronic image.

Real ultrasonographs (Fig. 1.7a) exploit multiple transducers with high resolution in space. Owing to this, an electronic image (Fig. 1.7b) looks like a section of a human body allowing for qualified medical personnel to make a decision about a state of human organs.

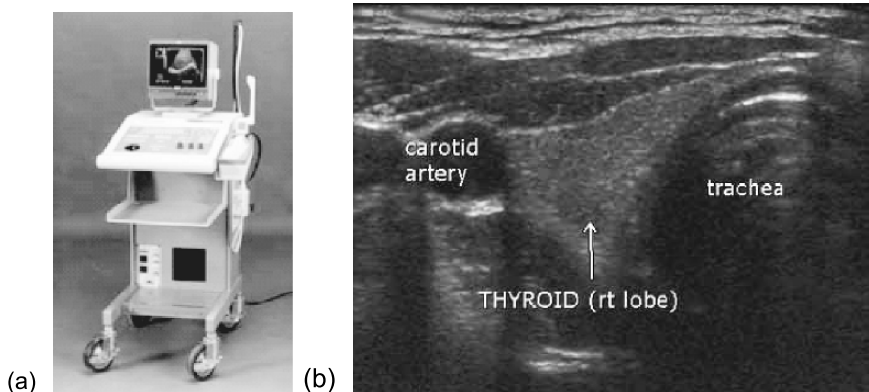


Fig. 1.7. Medical ultrasonography: (a) ultrasonographer and (b) example of an electronic image.

1.1.6 Robot Positioning

In many ways a position of a robot can be determined. Electronic, mechanical, optical, and even satellite systems such as the Global Positioning System (GPS) are used. An example is a wireless electronic system (Fig. 1.8a) consisting of the three transmitters placed at the points A , B , and C and radiating electromagnetic signals at given frequencies. The rotating antenna of a robot determines directions to every transmitter and indicates the relevant angles, φ_1 , φ_2 , and φ_3 .

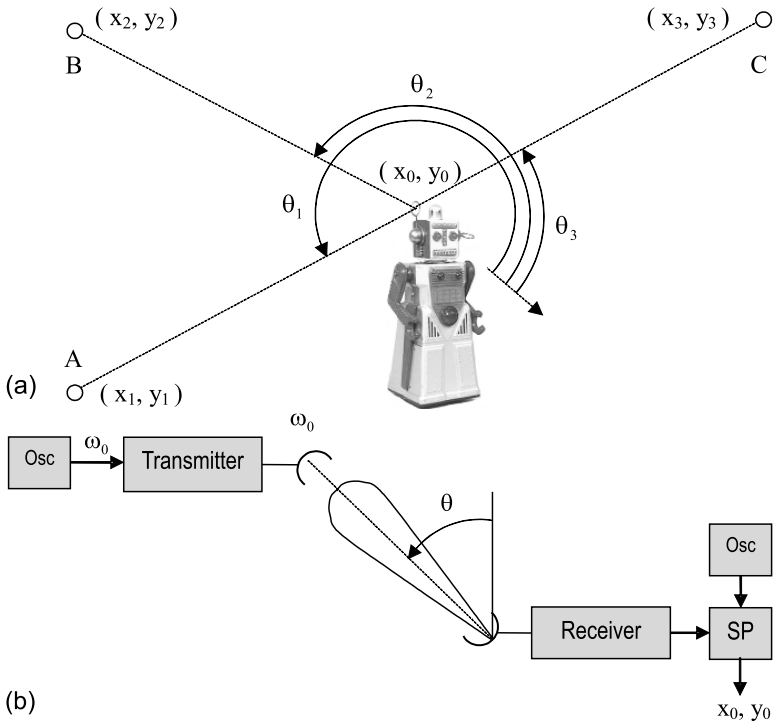


Fig. 1.8. Robot positioning for three spaced local stations with known coordinates: (a) geometrical interpretation and (b) measuring system.

An interaction of the robot’s receiver with every transmitter is shown in Fig. 1.8b. An antenna of the receiver is designed to have a narrow directional pattern such that an angle θ is measured for the maximum signal at the receiver with high accuracy. When all angles are measured, the SP block of a receiver calculates the robot coordinates x_0, y_0 as follows.

For known coordinates of all of the transmitters (Fig. 1.8b), the distances d_1 and d_2 between A and B , and B and C , respectively, are defined by

$$d_1 = \sqrt{(x_1 - x_2)^2 + (y_2 - y_1)^2}, \tag{1.18}$$

$$d_2 = \sqrt{(x_3 - x_2)^2 + (y_2 - y_3)^2}. \tag{1.19}$$

Distances between the robot and each of the transmitters are defined in a like manner, so that, for A , B , and C , respectively, we can write

$$a_1 = \sqrt{(y_0 - y_1)^2 + (x_0 - x_1)^2}, \tag{1.20}$$

$$a_2 = \sqrt{(y_2 - y_0)^2 + (x_0 - x_2)^2}, \tag{1.21}$$

$$a_3 = \sqrt{(y_3 - y_0)^2 + (x_3 - x_0)^2}. \quad (1.22)$$

The unknown coordinates x_0 and y_0 are then calculated by solving jointly the equations

$$d_1^2 = a_1^2 + a_2^2 - 2a_1a_2 \cos(\theta_1 - \theta_2), \quad (1.23)$$

$$d_2^2 = a_2^2 + a_3^2 - 2a_2a_3 \cos(\theta_2 - \theta_3), \quad (1.24)$$

comprising the functions defined by (1.18)–(1.22). This simple algorithm illustrates a system operation for a stationary robot. Most generally, for a moving robot, the equations complicate by accounting the parameters of movement (velocity and acceleration).

1.1.7 Remote Sensing

Nowadays, remote sensing is used widely for geophysical, meteorological, oceanographical and other purposes. In passive satellite sensing (Fig. 1.9a), energy E_I from an external source, e.g., the sun, leads to radiation with energy E_R that is received by the satellite-placed system. In an active method, energy generated by the satellite-placed sensor system is beamed outward and the fraction returned is measured. Radiation bears information about color and positioning (longitude, altitude, latitude), so that an image may be restored, in principle, as two-dimensional (2D) or three-dimensional (3D).

A critical component of the remote sensing system is the sensor (detector) that instantaneously measures radiation coming from the entire scene. The whole picture is then electronically recorded, processed, and restored to obtain a more or less true imagination about the scene. Fig. 1.9b shows a restored image of the western U.S. and adjoining Pacific Ocean provided by the GOES 10 geostationary satellite.

1.1.8 Reference Source of Frequency

Even a quick look at the above-considered structures selects a separate block called “Osc” (oscillator). It is presumed that the carrier frequency ω_0 of a signal generated by “Osc” is constant, so time invariant. To meet this requirement, special systems termed reference sources of frequency are designed.

The widely used “Osc” is the Oven Controlled Crystal Oscillator (OCXO), which basic structure is shown in Fig. 1.10. The principle component here is a precision quartz crystal resonator, whose resonant frequency is highly accurate, precise, and low sensitive to environment. The resonator is excited in an oscillator scheme with small nonlinearity. To reduce the amplitude-to-frequency conversion, a power supply voltage E_{PS} is stabilized. Also, to diminish a frequency vs. temperature dependence, an electronic block is placed to an oven, whose temperature is sustained at the point of a minimum temperature sensitivity of a resonator.

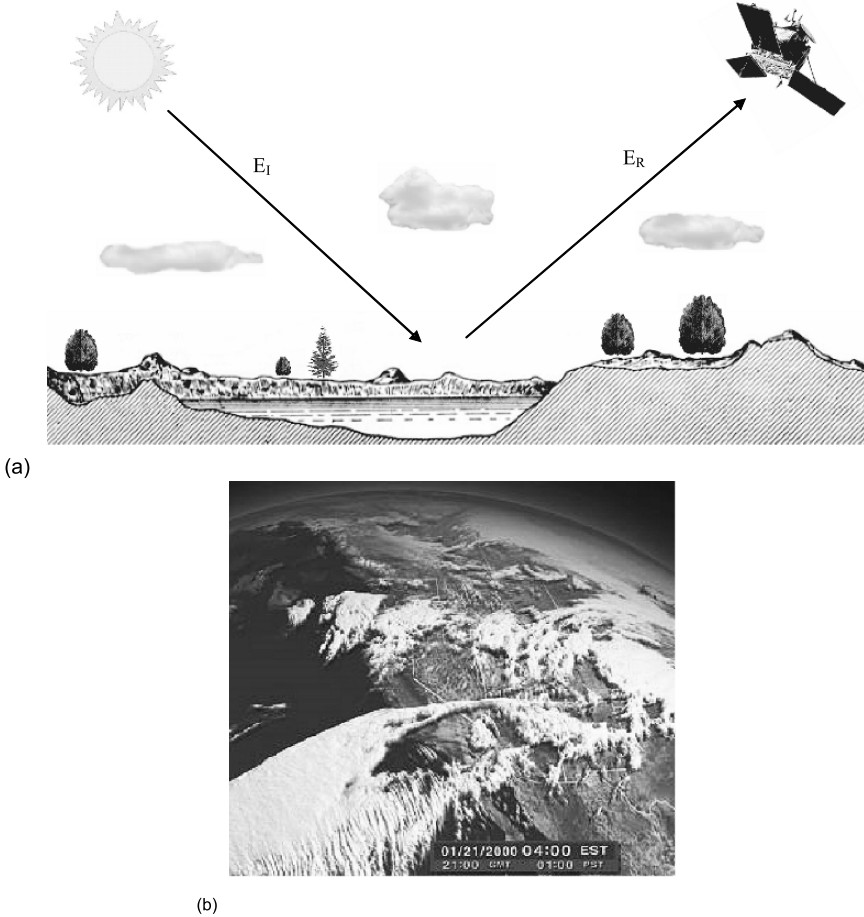


Fig. 1.9. Remote sensing: (a) principle of passive sensing and (b) electronic image.

The output signal of a reference source of frequency is obtained to be almost harmonic $y(t) = A_0 \cos[\omega_0 t + \Psi(t)]$, where the amplitude A_0 is near constant and the frequency instability is small being predetermined by the time derivative of a nonstationary phase $\Psi(t)$. The phase $\Psi(t)$ is affected by a number of internal and external factors such that the frequency instability $\Delta\omega(t)$ may be evaluated by

$$\Delta\omega(t) = \frac{d\Psi(t)}{dt} = \Delta\omega_0 + at + \frac{d}{dt}e_{PM}(t) + e_{FM}(t), \quad (1.25)$$

where $\Delta\omega_0$ is a small frequency offset for the desired (required) reference frequency, a is a linear frequency drift coefficient due to aging, and $e_{PM}(t)$ and $e_{FM}(t)$ are components of phase and frequency modulations, respectively,

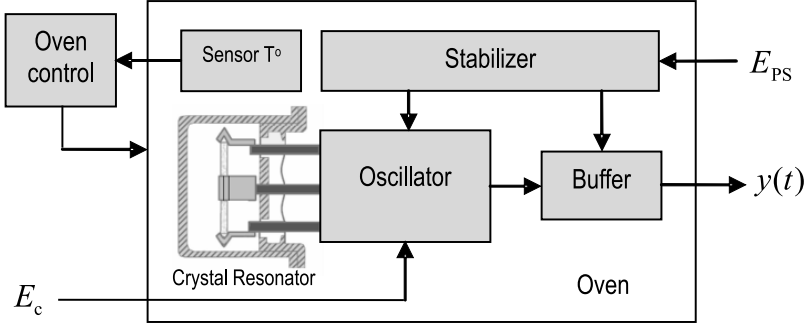


Fig. 1.10. Basic structure of an oven controlled crystal oscillator.

caused by noise and environment. Seemingly obvious is that the goal of any reference source of frequency is to set $\Delta\omega(t)$ to zero. If the internal resources are insufficient to fulfill this requirement, an external signal E_c is applied of the higher level reference frequency source to discipline an oscillator. Frequently, an OCXO is disciplined with the GPS timing signals. If such signals are not available or the GPS timing receiver induces too much noise, the ground-placed rubidium, cesium, and even hydrogen atomic standards of frequency are used.

1.2 Systems Performance and Classification

Most generally, a system may be described with some operator (function) \mathcal{O} that couples the vector input signal $\mathbf{x}(t)$ with the vector output signal $\mathbf{y}(t)$ by the relation

$$\mathbf{y}(t) = \mathcal{O}\mathbf{x}(t). \quad (1.26)$$

In the sequel, we conventionally will denote a system operator as in Table 1.1 and, when a system is not specified, use a simple \mathcal{O} , as in (1.26). The operator may be either scalar \mathcal{O} or vector \mathbf{O} .

Depending on the properties of operator \mathcal{O} , continuous-time systems may be performed to have different characteristics. Classification of systems is given below.

1.2.1 Regularity

It is commonly desirable to have a system, which operator is exactly described by mathematical functions (usually simple) at every time instant. Such a system is called *deterministic* meeting the requirements of *regularity*. If the operator can be described only in statistical terms or in frames of the probability

Table 1.1. System operator

System	Operator
Linear time-invariant	\mathcal{O}
Linear time-varying	$\mathcal{O}(t)$
Nonlinear time-invariant	$\mathcal{O}(x) \equiv \mathcal{O}[x(t)]$
Nonlinear time-varying	$\mathcal{O}(x, t) \equiv \mathcal{O}[x(t), t]$

theory, the system is said to be *random* or *stochastic*. For example, if multiple measurements of the input-to output characteristic of a square amplifier give the same table, the amplifier may be said to be deterministic. If every new measurement differs from others owing to fluctuations in the amplifier components, the characteristic (and so amplifier) will be noisy or random.

Throughout this book we consider only deterministic systems.

1.2.2 Continuity

In the modern world, time-continuity is the simplest and one of the most important properties of all signals and systems. It gives the idea of continuous-time and discrete-time.

Continuity: A system, where input and output are both continuous, is the *continuous-time system* (1.26) and the one having the input and output both discrete, is the *discrete-time system*.

□

If a system operates in discrete time t_n , where n is integer, the relation (1.26) is written as $\mathbf{y}[n] = \mathcal{O}\mathbf{x}[n]$.

The definition of continuity is certainly conditional in a sense. Indeed, many modern systems operating in continuous-time scale utilize computers in their signal processing blocks, thereby becoming *continuous/discrete-time*. On the other hand, in some systems having discrete-time scale, signals are converted to analog forms, then transmitted, received, and returned back to discrete forms. Such systems may be said to be *discrete/continuous-time*.

1.2.3 Dimensionality

Systems can be designed in different configurations to have not only one input and one output. Depending on a number of inputs and outputs, the following types of systems are recognized:

- **Multiple-input multiple-output (MIMO)** system is the one having more than one input and more than one output. The MIMO system has a structure (Fig. 1.11a) with a multiple $k \times 1$ input and multiple $p \times 1$ output, respectively,

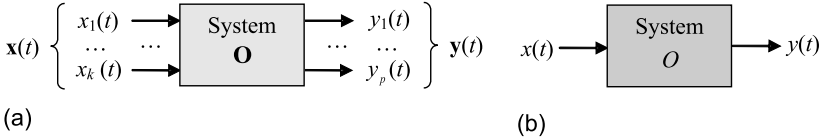


Fig. 1.11. Generalized system models: (a) MIMO and (b) SISO.

$$\mathbf{x}(t) = \begin{bmatrix} x_1(t) \\ x_2(t) \\ \vdots \\ x_k(t) \end{bmatrix} \quad \text{and} \quad \mathbf{y}(t) = \begin{bmatrix} y_1(t) \\ y_2(t) \\ \vdots \\ y_p(t) \end{bmatrix}, \quad (1.27)$$

which components are $x_i(t)$, $i = 1, 2, \dots, k$, and $y_j(t)$, $j = 1, 2, \dots, p$. \square

- **Single-input single-output (SISO)** system is the one having only one input $x(t)$ ($k = 1$) and only one output $y(t)$ ($p = 1$)(Fig. 1.11b). \square
- **Single-input multiple-output (SIMO)** system is designed, having only one input $x(t)$ ($k = 1$), but more than one output, $\mathbf{y}(t)$ ($p > 1$). \square
- **Multiple-input single-output (MISO)** system has several inputs, $\mathbf{x}(t)$ ($k > 1$), but only one output $y(t)$ ($p = 1$). \square

1.2.4 Memory

Memory of a system is predetermined by the form of its operator allowing for two structures.

Memoryless Systems: A system is memoryless (or static) if a system output at a time instant t depends on only a system input at the same time instant t . \square

For MIMO memoryless linear systems, the following relation holds true,

$$\mathbf{y}(t) = \mathcal{O}\mathbf{x}(t) = \mathbf{A}\mathbf{x}(t), \quad (1.28)$$

where an operator \mathcal{O} is just a matrix \mathbf{A} with constant components. An example of SISO memoryless nonlinear systems is a square amplifier described with

$$y(t) = \mathcal{O}(x)x(t) = ax^2(t),$$

where $\mathcal{O}(x)$ means the product $x(t)x(t)$ gained with a .

Memory Systems: A system is memory (or dynamic) if a system output at a time instant t depends on not only a system input at t , but also on some past history. \square

Examples of memory systems are integrators and differentiators. The memory operation of integration

$$\mathbf{y}(t) = \mathcal{O}\mathbf{x}(t) = \int_{-\infty}^t \mathbf{x}(\tau) d\tau \quad (1.29)$$

is provided by the system operator $\mathcal{O} \equiv \int_{-\infty}^t dt$ involving all past history and the memory operation of differentiation

$$\mathbf{y}(t) = \mathcal{O}\mathbf{x}(t) = \frac{d}{dt}\mathbf{x}(t) \quad (1.30)$$

is obtained with the system operator $\mathcal{O} \equiv \frac{d}{dt}$ exploiting the most nearest past.

1.2.5 Causality

This property is usually associated with physical realizability of systems.

Causal Systems: A system is said to be *causal* if its output $\mathbf{y}(t)$ at an arbitrary time instant t depends on only its input $\mathbf{x}(t - \theta)$ for $\theta \geq 0$.

□

In other words, the output of a causal system at the present time depends on only the present and/or past values of the input and does not depend on its future values, suggesting that

$$\mathbf{y}(t) = \mathcal{O}\mathbf{x}(t - \theta), \quad \theta \geq 0. \quad (1.31)$$

Practically, (1.31) means that, in causal systems, the output cannot appear before the input is applied to a system. In fact, in real communication channels a signal can only be delayed with time that meets (1.31) and never be advanced.

Noncausal Systems: A system is said to be *noncausal* if its output $\mathbf{y}(t)$ at an arbitrary time instant t depends on its input $\mathbf{x}(t + \theta)$ for $\theta \geq 0$.

□

The definition suggests that

$$\mathbf{y}(t) = \mathcal{O}\mathbf{x}(t + \theta), \quad \theta \geq 0, \quad (1.32)$$

and thus a noncausal system requires future (thus unknown) points of the input. An example is the Fourier transform claiming a signal to be known from $t = -\infty$ to $t = \infty$ that obviously cannot be met in practice.

It is worth remembering that all memoryless systems are causal, but not every causal system is memoryless.

1.2.6 Linearity

The most natural engineering approach is to model a system in simple forms and functions. First of all, a system is examined for linearity and, if so, the well developed methods and transforms are applied.

Linear Systems: A system is said to be linear if a system operator \mathcal{O} satisfies the conditions of both homogeneity (scaling) and additivity (superposition). Otherwise, a system is nonlinear. □

The condition of *homogeneity* (also called *scaling property*) implies that the operator \mathcal{O} is linear (and so a system is linear) if for a given input $a\mathbf{x}(t)$ the output $\mathbf{y}(t)$ is provided in two equal forms of

$$\mathbf{y}(t) = \mathcal{O}[a\mathbf{x}(t)] = a\mathcal{O}[\mathbf{x}(t)]. \quad (1.33)$$

The property (1.33) is illustrated in Fig. 1.12a for a constant coefficient a .

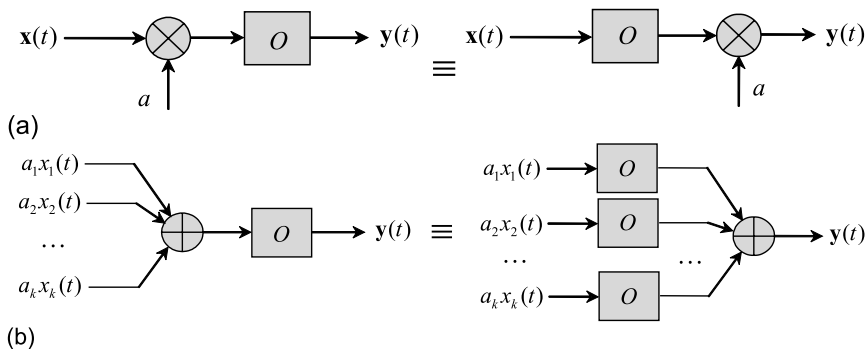


Fig. 1.12. Linearity conditions: (a) scaling and (b) additivity.

The other condition termed *additivity* and often called the *superposition principle* implies that the operator \mathcal{O} is linear if the following relation holds true for the given inputs $a_1x_1(t)$, $a_2x_2(t)$, \dots , $a_kx_k(t)$:

$$\mathbf{y}(t) = \mathcal{O} \sum_{i=1}^k a_i x_i(t) = \sum_{i=1}^k \mathcal{O}[a_i x_i(t)]. \quad (1.34)$$

This property also realizable in two equal forms is illustrated in Fig. 1.12b for constant coefficients a_i , $i = 1, 2, \dots, k$.

Typically, the conditions of homogeneity and additivity are met in the same linear operator. An example is the relation (1.34) that, by the homogeneity property (1.33), may ultimately be written as

$$y(t) = \mathcal{O} \sum_{i=1}^k a_i x_i(t) = \sum_{i=1}^k \mathcal{O}[a_i x_i(t)] = \sum_{i=1}^k a_i \mathcal{O}x_i(t).$$

The other example is a linear memoryless operation of the transformation of a vector input $\mathbf{x}(t)$ to the vector output $\mathbf{y}(t)$ by means of a matrix \mathbf{A} , namely $\mathbf{y}(t) = \mathbf{A}\mathbf{x}(t)$.

1.2.7 Time Invariance

One of the most critical properties of a system is a dependence of its operator on time.

Time-invariant system: A system is said to be *time-invariant* if any time shift θ in the input signal causes the same time shift in the output signal; that is,

$$y(t \pm \theta) = \mathcal{O}x(t \pm \theta). \tag{1.35}$$

A system is *time-varying* or *time-variant* otherwise. □

In the theory of random (or stochastic) systems, time invariance is related to mean values. Therefore, time-invariant systems are often called *stationary*. Fig. 1.13 illustrates the property (1.35) and we notice that, by Table 1.1, the operators of both linear and nonlinear systems can demonstrate time invariance.

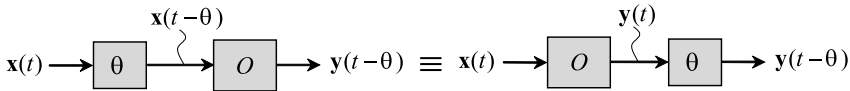


Fig. 1.13. Time invariance of systems.

The most general classification of input-to-output systems relates to whether the system is linear and/or time-invariant or not.

Linear Time-invariant (LTI) System

The linear time-invariant system is a linear system that is also time-invariant (all its coefficients are time constants). The simplest LTI system is described with an operator $\mathcal{O} = a$, where a is a constant; that is,

$$y(t) = \mathcal{O}x(t) = ax(t). \tag{1.36}$$

A generalized structure of an LTI system is shown in Fig. 1.14a.

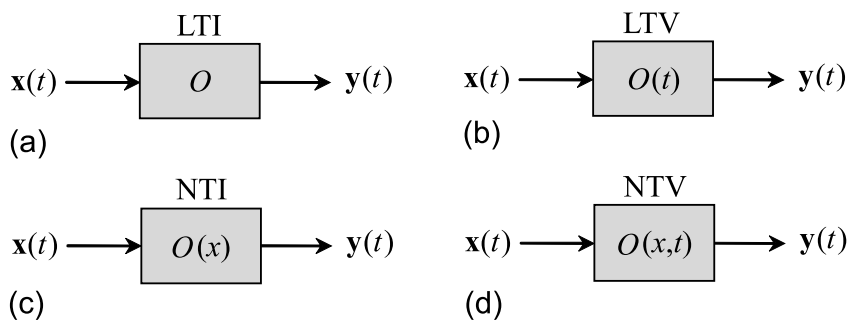


Fig. 1.14. Continuous-time systems: (a) LTI, (b) LTV, (c) NTI, and (d) NTV.

Linear Time-varying (LTV) System

The LTV system is a linear system, in which at least one of the coefficients is time-varying and thus its operator \mathcal{O} is time-variant as well (Fig. 1.14b). The simplest example of an LTV system is a memoryless mapping

$$y(t) = \mathcal{O}(t)x(t) = a(t)x(t), \quad (1.37)$$

where $a(t)$ is a time-varying coefficient, provided $\mathcal{O}(t) = a(t)$. Note that, in practice, communication and other wireless channels are always time-variant, since they are affected by environment and thus the coefficients are not time-constant. All adaptive and modulated linear systems are also time-varying, by the definition.

Nonlinear Time-invariant (NTI) System

The NTI system is a system, whose operator is time-invariant but depends on the input (Fig. 1.4c). An example is a square amplifier, provided

$$y(t) = \mathcal{O}[x(t)]x(t) = ax^2(t). \quad (1.38)$$

Other examples are rectifiers, oscillators, phase-locked loops (PLL), etc. Note that all real electronic systems become practically nonlinear owing to saturation.

Nonlinear Time-varying (NTV) System

The NTV system is a nonlinear system, in which at least one of the coefficients depends on time (Fig. 1.14d). For instance, if a coefficient a in (1.38) changes with time by some reasons, the system becomes NTV, provided

$$y(t) = \mathcal{O}[x(t), t]x(t) = a(t)x^2(t). \quad (1.39)$$

All synchronized oscillators and adaptive nonlinear structures are NTV. The NTV systems seem more “mystical” from the standpoint of stability, but typically have simpler structures and, in a modern view, often solve problems in the most accurate and even optimum way.

Let us notice that, owing to the environmental influence, aging in components, temperature effects caused by large values of signals, and saturation, all real physical continuous-time systems are virtually time-varying and nonlinear. Digital systems are much lesser affected by those factors and any software is absolutely insensitive to them.

1.2.8 Observability and Controllability

Every dynamic system may be described in terms of states. The terms *state observability* and *state controllability* were introduced by Kalman³ in 1960 as characterizing the system structure.

Observability: A system is *completely observable* on the finite time interval $[t_0, t_1]$ if for any t_0 an initial state $\mathbf{q}(t_0)$ can be determined from observation of the output $\mathbf{y}(t)$ over this interval with the input $\mathbf{x}(t)$ known over the same interval. □

State observability is thus a measure for how well internal states of a system can be inferred by knowledge of its external outputs. Formally, a system is said to be observable if, for any possible sequence of state and control vectors, the current state can be determined in finite time using only the outputs. In other words, this means that we can watch the system outputs and figure out what is going on inside the system with its states, even if it takes a very long time.

In turn, the term *state controllability* is associated with “state control.” Even intuitively, it predetermines that the system state is supposed to be adjusted in some way.

Controllability: A system is *completely controllable* on the finite time interval $[t_0, t_1]$ if for any initial state $\mathbf{q}(t_0)$ there may be found an input $\mathbf{x}(t)$ to transfer the system to the other given state $\mathbf{q}(t_1)$. □

A system is thus *controllable* if its state variables can be directly controlled by the input(s). Contrary, in the *uncontrollable* or *partly controllable* system, all or some state variables cannot be “adjusted” in finite time by the admissible input(s).

³ Rudolf Emil Kalman, Hungarian-born American scientist, 19 May 1930 – .

1.2.9 Detectability and Stabilizability

Closely related to controllability and observability are two other fundamental properties of systems called *detectability* and *stabilizability*.

Suppose the system is unobservable but the unobservable mode is stable. Detectability requires the unobservable part of the system to be asymptotically stable and hence is a weaker concept than observability, provided the definition:

Detectability: An LTI system is *detectable* if every unobservable state is stable. □

It then follows that an observable system is automatically detectable, since it has no unobservable states.

Stabilizability: An LTI system is *stabilizable* if every uncontrollable state is stable. □

This definition suggests that the effective control law may be found even though a system is uncontrollable. It can be shown that an LTI system is stabilizable by feedback if there exists a feedback matrix gain such that the system behavior is asymptotically stable. Note that for finite-dimensional linear systems if the system is open-loop stabilizable then it is stabilizable by feedback and conversely.

1.2.10 Accuracy and Precision

No one system is ideal, and each system operates with errors. When a system is one of measurement, such as radar, GPS, etc., the error limits its functional facilities, so must somehow be evaluated and, if possible, reduced. The error is typically random (deterministic or methodological errors are usually eliminated at the early stage) and the system “mistakes” are usually evaluated in terms of *accuracy* and *precision*.

Accuracy: Accuracy is the degree of conformity with an ideal (or reference) system also called standard. □

A simple treatment of accuracy may be done by associating the system input with a ball and its output with a target. A system is thus accurate (Fig. 1.15a) if it hits the center of a target with the scattering allowed.

It is accepted that accuracy relates to the quality of a system, and is distinguished from precision, which relates to the quality of the system operation by which the result is obtained.

Precision: Precision is the degree of perfection in the system or the degree of refinement in the performance of the system operation.

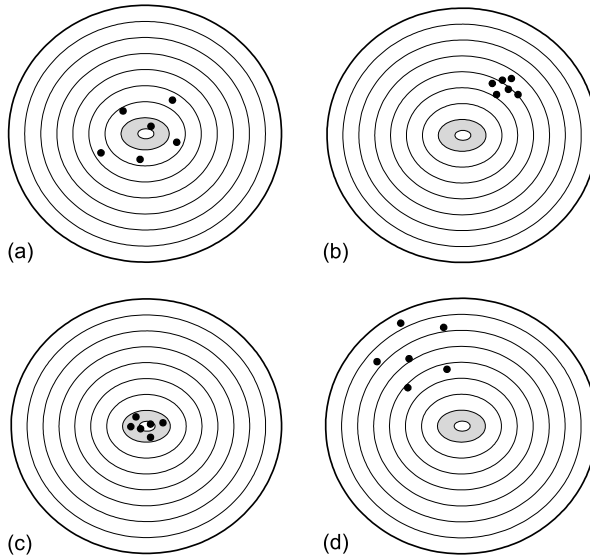


Fig. 1.15. Accuracy and precision: (a) accurate, (b) precise, (c) both accurate and precise, and (d) neither accurate nor precise.

□

Fig. 1.15b illustrates the system precision associated with the small scattering of hits on target. In other words, precision indicates reproducibility of a result obtained by a system. As such, precision relates to the quality of a system operation, by which a result is obtained, and is distinguished from accuracy, which relates to the quality of the result.

It follows from the comparison of Fig. 1.15a and Fig. 1.15b that an accurate system is not obligatory precise and a precise system is not always accurate. Fig. 1.15c gives an idea about the system that is both accurate and precise. In turn, the performance sketched in Fig. 1.15d addresses the system that is neither accurate nor precise. Let us notice that highly precise and accurate systems, such as GPS, are typically very costly.

1.2.11 Uncertainty and Robustness

Readers may wonder if the system can be designed to operate with infinite accuracy and precision and, if not, what are the limitations?

An important physical (and theoretical) limitation on the combined accuracy of certain pairs of simultaneous measurements was introduced in 1927 by Heisenberg⁴ that is now known as the *uncertainty principle*.

⁴ Werner Karl Heisenberg, German physicist, 5 December 1901-1 February 1976.

Heisenberg’s uncertainty principle: The conjugate quantities such as pairs of observables (position and momentum) of a single elementary particle cannot be measured with arbitrary precision. \square

Specifically for applications in systems, this principle suggests that the system states cannot be measured all at once with infinite accuracy and precision. In fact, whenever we describe a system as state space, we commonly think about the system states (phase, frequency, linear frequency drift rate, etc.) as related to the current time t . Such values are called *instantaneous*. However, the frequency, for example, is evaluated by the phase rate. So, we need two different (even very closely placed) points to evaluate frequency. Therefore the term *instantaneous* may only be used in the sense of a theoretical limit for the evaluated quantity.

Reasoning similarly for the other system states, one arrives at the conclusion that any dynamic system (with nonzero states) inherently has “internal faults” that gives certain problems to system design. For example, decision making under uncertainty is a central problem in robotics, plant control, and machine learning. Therefore, closely tied to the problem of uncertainty is that of approximation. For instance, in large scale system problems, learning decisions under uncertainty inevitably requires approximation.

The uncertainty may be evaluated as follows. Let an LTI system be characterized with the operator \mathcal{O} in the transform domain, so with the transfer function $\tilde{H}(s)$. The function may then be composed with the nominal frequency response $H(s)$ and the uncertainty addition $\Delta(s)$, namely $\tilde{H}(s) = H(s) + \Delta(s)$. If the magnitude response $|\Delta(j\omega)|$ does not exceed unity over all frequencies, the disturbance Δ is called *allowable*. Usually, allowable uncertainties Δ are assumed in applications.

It seems that the first solution for the uncertainty problem was found by Black⁵ in the 1930s for the telephone industry regarding the constructing feedback amplifiers insensitive to variations in their units and supply voltages. The achieved pioneering result by Black was lately recognized among 25 seminal papers in control published in 20th century.

The system uncertainty is closely related to the required system robustness. “Robust” is a term introduced by Box⁶ in the 1950s as relevant to devising tests on data “contaminated” and other relevant problems. Furthermore, the term was applied to system problems and Black’s amplifier was treated as an example of robust systems.

Robustness: System robustness is the measure of its ability to operate correctly in the presence of invalid inputs and despite the internal faults. \square

⁵ Harold Stephen Black, American engineer and inventor, 1898-1983.

⁶ George Edward Pelham Box, English statistician, 18 October 1919 -.

To diminish an influence of the uncertainty Δ upon the system performance, the weighting transfer function $W(s)$ is searched, satisfying the conditions for the system to be *robust*. Three basic models may be observed in designing robust systems:

- Additive (Fig. 1.16a): $\tilde{H} = H + W\Delta$,
- Multiplicative (Fig. 1.16b): $\tilde{H} = H(1 + W\Delta)$,
- Feedback (Fig. 1.16c): $\tilde{H} = \frac{H}{1 + HW\Delta}$.

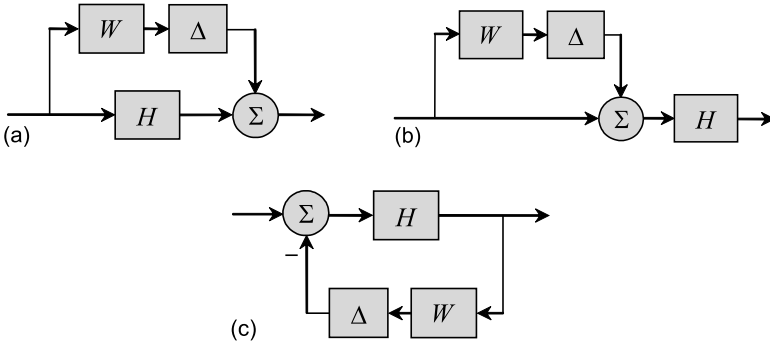


Fig. 1.16. Robust system models with uncertainty: (a) additive, (b) multiplicative, and (c) feedback.

Example 1.1. An ideal integrator is given with the nominal transfer function $H(s) = 1/s$. The first order real physical integrator is described with $\tilde{H} = 1/(s+a)$, where a is a small constant. Find the weight W for the multiplicative model (Fig. 1.16b).

Having $\tilde{H} = H(1 + W\Delta)$, we may write $\frac{\tilde{H}}{H} - 1 = W\Delta$. For the allowable $|\Delta| < 1$, the relation yields an inequality

$$\left| \frac{\tilde{H}}{H} - 1 \right| \leq |W|$$

that, for the transfer functions given, results in $\left| \frac{s}{a+s} - 1 \right| \leq |W|$. The weighting transfer function is thus

$$W(s) = \frac{a}{a + s}.$$

It follows that, by $a = 0$, the weight is zero, $W = 0$. Indeed, without uncertainty, $a = 0$, no correction is necessary and the relevant branch in Fig. 1.16b vanishes. Overall, the weight derived claims that the integrator would be robust for the uncertainty associated with a small coefficient a . \square

1.2.12 Stability

Any system is critically sensitive to stability. Independently on types and applications, it is usually highly desirable for the systems to be stable in order to operate properly and fulfil the requirements. If we think that the necessary condition of system operation is to fulfil some operator (function), then stability of this operator may be treated as a sufficient condition of system operation. Basically, two factors (external and internal) affect the system operation, and provided the definition:

Stability: The system is stable 1) if its output does not diverge as long as the input does not diverge and 2) a slight disturbance in a system does not produce a significant disrupting effect on that system. □

Systems with the input $\mathbf{x}(t)$ and output $\mathbf{y}(t)$ are always desirable to be stable. The closed-loop systems (no input) are usually oscillatory. Such systems (oscillators) are underdamped with low input signals, critically damped with normal amplitudes, and overdamped with large amplitudes. Therefore, oscillators are typically unstable at zero and stable at an equilibrium point.

There are several approaches of how to ascertain stability of systems in a different sense depending on stationarity and linearity. In the sequel, we shall observe most of them in the time and transform domains as well as in the phase plane. For now, it seems in order to give the reader an idea about the seemingly most obvious input-to-output stability.

The requirement for the system output not to diverge as long as the input does not diverge relates to whether the signal is bounded or not.

BIBO Stability: A system is said to be *bounded-input/bounded-output* (BIBO) *stable* if for any bounded input $x(t)$ the corresponding output $y(t)$ is also bounded; that is,

$$|x(t)| \leq \alpha \iff |y(t)| = |\mathcal{O}x(t)| \leq \beta, \quad (1.40)$$

where α and β are finite real constants. A system is BIBO unstable if (1.40) is not met, i.e. $y(t)$ grows without limit (diverges) from a bounded input. □

Note that the BIBO stability of an LTI system is neatly described in terms of whether or not its impulse response is absolutely integrable (satisfies the Dirichlet conditions).

Example 1.2. The SISO memory systems are described with the equations,

$$y(t) = ax(t) + \frac{1}{b} \int_{-\infty}^t x(\tau) d\tau + c \frac{d}{dt} x(t), \quad (1.41)$$

$$y(t) = at|x(t)| + \frac{1}{b} \int_{-\infty}^{t+\theta} x(\tau)d\tau + \frac{d}{dt}c(t)x(t), \quad \theta \geq 0. \quad (1.42)$$

The first system (1.41) is causal, linear, time-invariant, and BIBO-stable. The second system (1.42) is not causal (the integration involves future points at θ), nonlinear (due to the term $|x(t)|$), time-variant (due to the time-dependent coefficient $c(t)$), and BIBO-unstable (the first term evolves proportionally with time t and hence the upper bound of $|y(t)|$ lies at infinity). \square

1.3 Basic Structures

Three basic structures of systems are recognized, namely the *open system* or *input-to-output system*, *closed loop system*, and *closed loop control system*.

1.3.1 Open (Input-to-output) System

A simple system structure implies an input $\mathbf{x}(t)$ and output $\mathbf{y}(t)$ coupled with an operator \mathcal{O} by (1.26). Systems shown in Fig. 1.14 are examples of input-to-output systems.

1.3.2 Closed Loop System

If the system output is coupled with the system input by an operator \mathcal{O}_1 as $\mathbf{y}(t) = \mathcal{O}_1\mathbf{x}(t)$ and the input in turn is fully defined by the output via some other operator \mathcal{O}_2 as $\mathbf{x}(t) = \mathcal{O}_2\mathbf{y}(t)$, then the system becomes *closed loop* (having no input) (Fig. 1.17a).

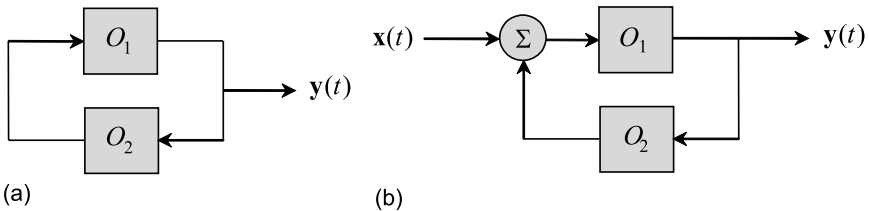


Fig. 1.17. Feedback systems: (a) closed loop and (b) closed loop control.

It can be shown that a closed loop system also called *feedback system* is described with the equation

$$(1 - \mathcal{O}_1\mathcal{O}_2)\mathbf{y}(t) = 0. \quad (1.43)$$

The term “feedback” suggests that the output “feeds back” the input through the block \mathcal{O}_2 . Two possible realizations of the closed loop systems are feasible. The feedback can be organized to be either positive or negative.

Negative Feedback

If an operator \mathcal{O}_2 inverts a signal $\mathbf{x}(t)$ on its way round the closed loop, the system is said to be the *negative feedback closed loop system*. Practically, such systems have limited applications, since they have no input and are unable to generate the output signal. For the cascade-connected system, the negative feedback closed loop system plays typically a role of a load.

Positive Feedback

If an operator \mathcal{O}_2 does not invert a signal in the feedback, the system is said to be the *positive feedback system*. When an open loop gain in such a system overcomes unity, the feedback causes the output to increase. Otherwise, the output attenuates. With unit feedback gain, a dissipated energy is fully recovered that is used in oscillators at steady state.

Example 1.3. An LTI system is described with the ODE

$$y'' + ay' + by = ax' \quad (1.44)$$

and, by $x = Ky$, becomes closed loop performed by

$$y'' + a(1 - K)y' + by = 0. \quad (1.45)$$

It can be shown, by the theory of the ODEs, that stability of a system described with (1.45) is guaranteed if $a(1 - K) > 0$. Thus, having negative feedback with $K < 0$, the system is always stable. With positive feedback and $0 < K < 1$, it is still stable and oscillations attenuate with time. If $K = 1$, the system becomes conservative to mean that oscillations have constant amplitude. Finally, if $K > 1$, the system is unstable and oscillations develop. \square

1.3.3 Closed Loop Control System

Without an input, a closed loop (Fig. 1.17a) has a practical meaning if it generates oscillations, thus is nonlinear and with positive feedback. To extend an application range for feedback systems, a control input is induced as shown in Fig. 1.17b. Such a system is called *closed loop control*.

The input $\mathbf{x}_1(t)$ of a block \mathcal{O}_1 is predefined to be $\mathbf{x}_1(t) = \mathcal{O}_2\mathbf{y}(t) + \mathbf{x}(t)$. Therefore, the system equation is given by

$$\mathcal{O}_1\mathbf{x}(t) = (1 - \mathcal{O}_1\mathcal{O}_2)\mathbf{y}(t). \quad (1.46)$$

In line with the closed loop, any closed loop control system can also be designed to have either negative or positive feedback. Negative feedback is often deliberately introduced to increase the stability and accuracy of a system. Positive feedback is usually an unwanted consequence of system behavior. It is induced when a nonlinear system is intended to generate oscillations.

Example 1.4. A system (1.44) is closed with a feedback $x_1(t) = Ky(t) + x(t)$ and described by an equation

$$y'' + a(1 - K)y' + by = ax' \quad (1.47)$$

with zero initial conditions. The Laplace transform of (1.47) is

$$s^2Y(s) + a(1 - K)sY(s) + bY(s) = asX(s),$$

producing the system transfer function

$$H(s) = \frac{Y(s)}{X(s)} = \frac{as}{s^2 + a(1 - K)s + b}. \quad (1.48)$$

The roots of the denominator of (1.48) are defined by

$$s_{1,2} = -\frac{a(1 - K)}{2} \pm \sqrt{\frac{a^2(1 - K)^2}{4} - b}.$$

It can be shown, by the theory of the ODEs, that the system is stable if the real parts of $s_{1,2}$ are negative that is only possible if $K < 1$. Stability is thus always guaranteed with the negative feedback, $K < 0$, and with the positive feedback, if $0 < K < 1$. \square

1.3.4 Interconnection

Different interconnections are used in system design: cascade, parallel, and feedback.

Cascade Interconnection

When the output of one system with the operator \mathcal{O}_1 is connected to the input of another one with the operator \mathcal{O}_2 , the interconnection is called *cascade* (Fig. 1.18a). Two systems included in cascade are described with the equation

$$\mathbf{y}(t) = \mathcal{O}_2\mathcal{O}_1\mathbf{x}(t). \quad (1.49)$$

Examples of cascade interconnections may be found in Fig. 1.16. Note that, in some cases, the ordering of the systems matters, in others it does not.

Parallel Interconnection

A signal $\mathbf{x}(t)$ may go simultaneously to several (two and more) systems, which outputs are added together to create a signal $\mathbf{y}(t)$. This is what is called *parallel interconnection* (Fig. 1.18b). Two subsystems included in parallel are described with the equation

$$\mathbf{y}(t) = (\mathcal{O}_1 + \mathcal{O}_2)\mathbf{x}(t). \quad (1.50)$$

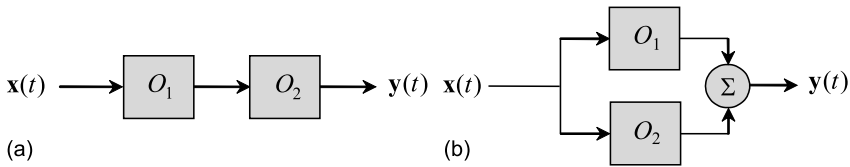


Fig. 1.18. Interconnection of systems: (a) cascade and (b) parallel.

Feedback Interconnection

This subtle type of interconnection was already discussed when considered closed loops (Fig. 1.17). What is worth keeping in mind is that each of the subsystems, \mathcal{O}_1 and \mathcal{O}_2 , in both structures (Fig. 1.17a and Fig. 1.17b) can also be feedback.

1.4 Basic Operations with Signals in Systems

Irrespective of the physical nature of systems, their basic operation principles remain virtually the same. Below, we will not subtilize (details are elucidated in the following Chapters) and list only the basic operations peculiar to continuous-time LTI, LTV, NTI, and NTV electronic systems.

1.4.1 Linear Time-invariant Systems

Every LTI electronic system be it very sophisticated obeys the following basic principles of operation:

Amplitude Scaling

Assume that a signal $x(t)$ passes through a system and appears at the output with a gain factor a (Fig. 1.19a). The output is thus provided with the memoryless operation of scaling

$$y(t) = \mathcal{O}x(t) = ax(t), \quad (1.51)$$

representing the product of a constant coefficient a and a signal $x(t)$ both having arbitrary signs and values. An electric equivalent of (1.51) is shown in Fig. 1.19b meaning that the output voltage $v_R(t)$ is induced on a resistor R by an electric current $i(t)$ without shifting in time and violating the waveform of $i(t)$. Vectors $i(t)$ and $v_R(t)$ hence coincide in direction (Fig. 1.19d) that is supported by the direct and inverse memoryless relations (Fig. 1.19c), respectively,

$$v_R(t) = Ri(t), \quad (1.52)$$

$$i(t) = \frac{1}{R}v_R(t), \quad (1.53)$$

associated with (1.51).

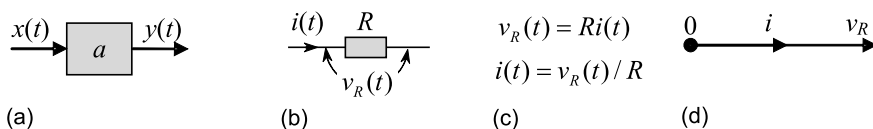


Fig. 1.19. Amplitude scaling: (a) basic structure, (b) memoryless electric circuit, (c) basic equations, and (d) vector diagram.

Ideal Integration

An ideal integration of $x(t)$ (Fig. 1.20a) is provided in a purely capacitive electric circuit (Fig. 1.20b). Such a system comprises the only memory element, a capacitor C . Accordingly, the waveform of an electric current $i(t)$ leads the waveform of an electric voltage $v_C(t)$ by 90° in phase (Fig. 1.20d) that is represented by the direct and inverse relations (Fig. 1.20c), respectively,

$$v_C(t) = \frac{1}{C} \int_{-\infty}^t i(\tau) d\tau, \quad (1.54)$$

$$i(t) = C \frac{d}{dt} v_C(t). \quad (1.55)$$

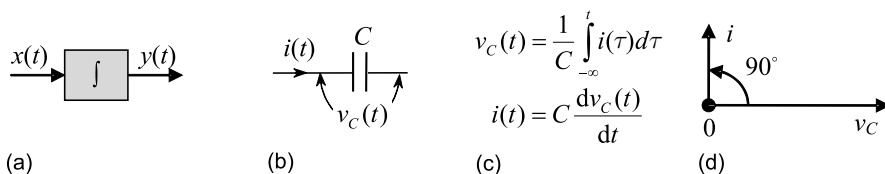


Fig. 1.20. Ideal integration: (a) basic structure, (b) memory capacitive electric circuit, (c) basic equations, and (d) vector diagram.

If to apply the Fourier transform to either (1.54) or (1.55) and assign $X_C(j\omega) = V(j\omega)/I(j\omega)$, the purely imaginary impedance of a capacitor will be defined in the frequency domain by

$$X_C(j\omega) = \frac{1}{j\omega C} = -j \frac{1}{\omega C}. \quad (1.56)$$

One thus concludes that the memory operation of integration is associated with a complex gain of a system.

Ideal Differentiation

The other ideal memory operation provides differentiation (Fig. 1.21a) in the purely inductive electric circuit (Fig. 1.21b). A system consists of only the component, the inductor L . It can be shown that the voltage $v_L(t)$ induced on L leads the electric current $i(t)$ by 90° in phase (Fig. 1.21d) that is supported by the relationships (Fig. 1.21c):

$$v_L(t) = L \frac{d}{dt} i(t), \quad (1.57)$$

$$i(t) = \frac{1}{L} \int_{-\infty}^t v_L(\tau) d\tau. \quad (1.58)$$

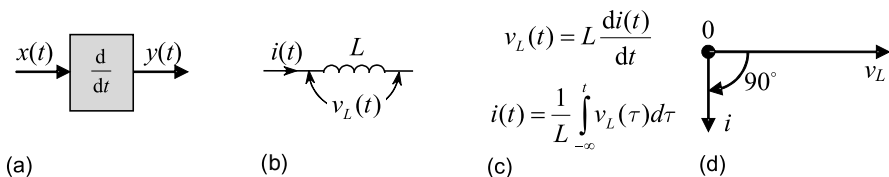


Fig. 1.21. Ideal differentiation: (a) basic structure, (b) memory inductive electric circuit, (c) basic equations, and (d) vector diagram.

Analogously to (1.56), the Fourier transform applied to either (1.57) or (1.58) allows finding the purely imaginary impedance of an inductor

$$X_L(j\omega) = j\omega L. \quad (1.59)$$

Again one can notice that an ideal differentiation (as the memory operation) is also associated with a complex gain of a system.

Addition

Given k signals $x_i(t)$, $i = 1, 2, \dots, k$, each of which is gained with a constant coefficient a_i , $i = 1, 2, \dots, k$. For LTI systems, the following additive operation is fundamental,

$$y(t) = a_1 x_1(t) + a_2 x_2(t) + \dots + a_i x_i(t). \quad (1.60)$$

An example of an addition of two harmonic signals $x_1(t)$ (Fig. 1.22a) and $x_2(t)$ (Fig. 1.22b) is given in Fig. 1.22c.

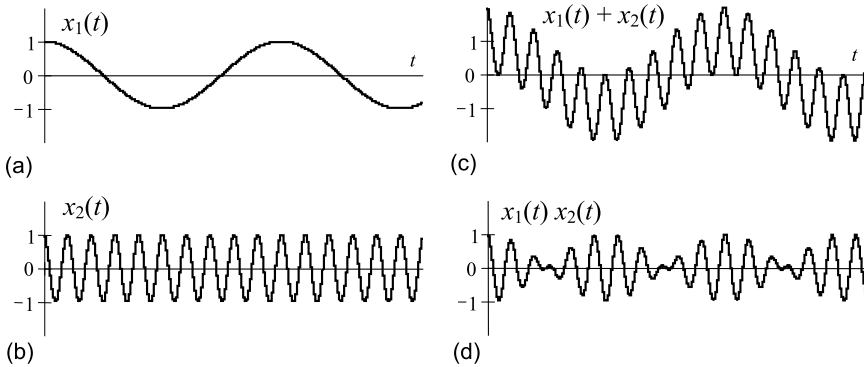


Fig. 1.22. Operations with signals in systems: (a) signal $x_1(t)$, (b) signal $x_2(t)$, (c) addition $x_1(t) + x_2(t)$, and (d) product $x_1(t)x_2(t)$.

Ideal Time Shifting

In system channels, a signal $x(t)$ (electric voltage or current) is typically delayed in time on some amount t_0 . The ideal operation of delay (time shifting) produces the output signal $y(t)$ (electric voltage or current)

$$y(t) = x(t - t_0). \tag{1.61}$$

Note that an advance shifting $x(t + t_0)$ cannot physically be realized as involving future points, thus unknown.

Basic ideal operations with signals in electrical LTV systems are postponed to Table 1.2.

Table 1.2. Basic ideal operations with signals in electrical linear systems

Operation	LTI system	LTV system
Amplitude scaling	$v(t) = Ri(t)$ $i(t) = \frac{1}{R}v(t)$	$v(t) = R(t)i(t)$ $i(t) = \frac{1}{R(t)}v(t)$
Integration	$v(t) = \frac{1}{C} \int_{-\infty}^t i(\tau) d\tau$ $i(t) = \frac{1}{L} \int_{-\infty}^t v(\tau) d\tau$	$v(t) = \int_{-\infty}^t \frac{1}{C(\tau)} i(\tau) d\tau$ $i(t) = \frac{1}{L(t)} \int_{-\infty}^t v(\tau) d\tau$
Differentiation	$v(t) = L \frac{d}{dt} i(t)$ $i(t) = C \frac{d}{dt} v(t)$	$v(t) = \frac{d}{dt} L(t) i(t)$ $i(t) = C(t) \frac{d}{dt} v(t)$
Time delay	$y(t) = x(t - t_0)$	$y(t) = x[t - t_0(t)]$

Example 1.5. A series connection of a resistor R , capacitor C , inductance L , and a source of an electric voltage $v(t)$ is described with an equation

$$v(t) = Ri(t) + \frac{1}{C} \int_{-\infty}^t i(\tau) d\tau + L \frac{d}{dt} i(t). \quad (1.62)$$

This system realizes the LTI operations of scaling (1.51), integration (1.54), differentiation (1.57), and addition (1.60). \square

1.4.2 Linear Time-varying Systems

In LTV systems, at least one of the coefficients is varied with time (intentionally or randomly). Assuming that a system has only one such coefficient $a(t)$, the basic operations peculiar to LTV systems can be performed for a signal $x(t)$ (referring to the comments given for LTI systems) as in the following:

- *Amplitude scaling* of a signal $x(t)$ is provided by

$$y(t) = \mathcal{O}x(t) = a(t)x(t). \quad (1.63)$$

This operation has two electrical equivalents supported by the equations given in Table 1.2. \square

- *Ideal integration* of a signal $x(t)$ is obtained with

$$y(t) = \int_{-\infty}^t a(\tau)x(\tau) d\tau \quad \text{or} \quad y(t) = a(t) \int_{-\infty}^t x(\tau) d\tau \quad (1.64)$$

by two electrical equivalents described with the equations postponed to Table 1.2. \square

- *Ideal differentiation* of a signal $x(t)$ can be realized in two forms of

$$y(t) = \frac{d}{dt} a(t)x(t) \quad \text{or} \quad y(t) = a(t) \frac{d}{dt} x(t) \quad (1.65)$$

associated with two electrical equivalents given in Table 1.2. \square

- *Addition.* Given k signals $x_i(t)$ (electric voltages or currents), $i = 1, 2, \dots, k$, each of which is gained with the time-variant coefficient $a_i(t)$, $i = 1, 2, \dots, k$. An additive sum of these signals is defined by

$$y(t) = a_1(t)x_1(t) + a_2(t)x_2(t) + \dots + a_i(t)x_i(t). \quad (1.66)$$

\square

Example 1.6. A low-pass RC system has the bandwidth controlled by a time-varying capacitor $C(t)$. The ODEs of this system written with respect to the input voltage $v(t)$ and output voltage $v_C(t)$ are, respectively,

$$v(t) = R[C(t)v_C(t)]' + v_C(t),$$

$$v_C' + \left(\frac{1}{RC} + \frac{C'}{C}\right)v_C = \frac{1}{RC}v.$$

As can be seen, the equations combine the operations of scaling (1.63), differentiation⁷ (1.65), and addition (1.66). \square

1.4.3 Nonlinear Time-invariant Systems

It is seemingly obvious that nonlinear systems can utilize an infinite variety of nonlinear operations. Nevertheless, the following operations might be most frequently met in electrical and electronic systems.

Nonlinear Memoryless Amplification

Amplifiers can be designed to provide the input-to-output memoryless (or functional) nonlinear transformations with arbitrary laws. Not all nonlinear functions meet practical needs. Most frequently, the following nonlinear amplifiers are used.

Square-law amplifier. The memoryless transformation may follow what is called a “square-law” curve, meaning that the output is proportional to the input power,

$$y(t) = \mathcal{O}(x)x(t) = a^2x^2(t), \quad (1.67)$$

where a is constant.

Example 1.7. Given a harmonic signal $x(t) = a \cos \omega_0 t$ with period $T = 2\pi/\omega_0$. Its average power is defined by

$$P_x = \frac{a^2}{T} \int_{-T/2}^{T/2} \cos^2 \omega_0 t \, dt = \frac{a^2}{2}.$$

A signal goes through a square amplifier, which output calculates

$$y(t) = a^2 \cos^2 \omega_0 t = \frac{a^2}{2} + \frac{1}{2} \cos 2\omega_0 t.$$

The signal average power $a^2/2$ is evaluated by attaching a low-pass filter at the output of an amplifier. \square

⁷ Remark: Throughout the book we also equivalently use the following notation of differentiation: $\frac{d}{dt}y = y'$.

Logarithmic amplifier. Sometimes the output voltage of an amplifier may want to represent the natural logarithm of its input voltage. This can be done using feedback. Fig. 1.23a shows the circuit diagram of a logarithmic amplifier, which feedback includes a diode. Here the output voltage $y(t) = V_{\text{out}}(t)$ depends on its input voltage $x(t) = V_{\text{in}}(t)$ as

$$y(t) = \mathcal{O}(x)x(t) = -a \ln \frac{x(t)}{b}, \quad (1.68)$$

where a and b are constants.

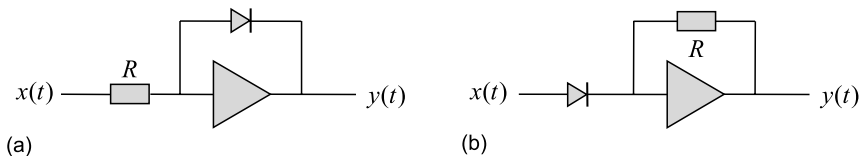


Fig. 1.23. Nonlinear amplifiers: (a) logarithmic and (b) exponential.

Exponential amplifier. An exponential curve is achieved by interchanging the diode and resistor as in Fig. 1.23b. Accordingly, the operator of an exponential amplifier is performed by

$$y(t) = \mathcal{O}(x)x(t) = -b \exp \frac{x(t)}{a}, \quad (1.69)$$

where a and b are still constants.

Power amplification. In power amplification, they typically design the amplifier structure with two nonlinear subamplifiers. A harmonic wave $x(t) = \cos \omega_0 t$ is gained here so that one of its parts passes through one subamplifier and another one through the other subamplifier. The operator of a subamplifier is defined by

$$y(t) = \mathcal{O}(x)x(t) = \begin{cases} a \cos \omega_0 t, & -\varphi + 2\pi n \leq \omega_0 t \leq \varphi + 2\pi n \\ 0, & \text{otherwise} \end{cases}, \quad (1.70)$$

where n is integer. Depending on an angle φ , the following classes of nonlinear amplifiers are distinguished:

- *Class B* is when $\varphi = \pi/2$ and thus only 50% of the input signal is used, meaning that a half of a harmonic wave is gained and the other half cut-off. A disadvantage of this class is that two gained waveforms cannot typically be fused without distortions caused by real circuits. \square

- *Class AB* relates to $\pi < \varphi < \pi/2$ and hence more than 50% but less than 100% is used. In the limiting case of *Class A* ($\varphi = \pi$), an amplifier gains a full signal and becomes linear. \square
- *Class C* refers to as employing $\pi/2 < \varphi < 0$. Here less than 50% of a signal is used. \square
- *Class D* unites amplifiers, which are also known as switching amplifiers or digital amplifiers. Operating in switch mode, such an amplifier is either completely turned on or completely turned off by an input signal. \square

One needs to remember that all linear amplifiers become nonlinear, when the input voltage exceeds the power supply voltage. This effect is termed *saturation*.

Product (Multiplication)

For the two-dimensional vector input $\mathbf{x}(t) = [x_1(t) \ x_2(t)]^T$, the operation of multiplication of its components is provided with the product

$$y(t) = \mathcal{O}(x)\mathbf{x}(t) = ax_1(t)x_2(t). \quad (1.71)$$

An example is given in Fig. 1.22d for two harmonic signals $x_1(t)$ (Fig. 1.22a) and $x_2(t)$ (Fig. 1.22b). Following Fig. 1.22c and Fig. 1.22d, one could realize the difference between the sum and product of two signals.

Example 1.8. Given two signal, $x_1(t) = a \sin(\omega_1 t + \varphi)$ and $x_2(t) = \cos \omega_2 t$. The product produced by a unit-gain multiplier can be written as

$$\begin{aligned} y(t) &= a \sin(\omega_1 t + \varphi) \cos \omega_2 t \\ &= \frac{a}{2} \sin[(\omega_1 - \omega_2)t + \varphi] + \frac{a}{2} \sin[(\omega_1 + \omega_2)t + \varphi]. \end{aligned}$$

By applying a LP filter with a gain factor of 2 and cut-off frequency $\omega_1 - \omega_2 \ll \omega_c \ll \omega_1 + \omega_2$, we save only the first component with the frequency $\omega_1 - \omega_2$, thereby supporting two useful applications:

- With $\omega_1 \neq \omega_2$, a signal $x_1(t)$ might be supposed to be removed by a reference signal $x_2(t)$ from ω_1 to $\omega_1 - \omega_2$ that is used in heterodyne receivers.
- With $\omega_1 = \omega_2$ and $|\varphi| \ll \pi$, the output varies as a function of φ , namely $y = \sin \varphi$, that is exploited in phase detectors and phase locked loops. \square

In applications, the products are used to realize different nonlinear operations exploited, for example, in conventional AM with double sideband large carrier, synchronous demodulation of AM, signals heterodyning, and phase detection. In each of these cases, a mixer multiplies the signals together and the product (or its part) is thereafter filtered to produce a desired quality.

Rectification

Rectifiers are used to restore the envelope $\tilde{x}(t)$ of a signal $y(t) = x(t)z(t)$, where $x(t)$ is a message signal and $z(t)$ is a carrier signal, or to convert an alternative current (AC) waveform into a direct current (DC) waveform. Typically, two rectification schemes are used: the *half-wave rectifier* (Fig. 1.24a) and the *full-wave rectifier* (Fig. 1.24b). Both schemes utilize semiconductor diodes.

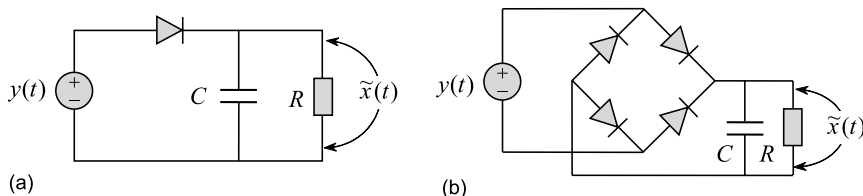


Fig. 1.24. Rectifiers: (a) half-wave and (b) full-wave (bridge method).

The nonlinear part of a half-wave rectifier may be described with the operator

$$\tilde{y}(t) = \mathcal{O}(y)y(t) = \begin{cases} ax(t)z(t), & z(t) \geq 0 \\ 0, & z(t) < 0 \end{cases} \quad (1.72)$$

and that of a full-wave rectifier by

$$\tilde{y}(t) = \mathcal{O}y(t) = |ax(t)z(t)|. \quad (1.73)$$

In a simplest case of each of the schemes, the envelope $\tilde{x}(t)$ associated with a message signal $x(t)$ carried by the input $y(t)$ is obtained by using an RC LP filter.

Comparison

To go from an analog signal to the impulse signal, a *comparator* is used as a nonlinear device intended to compare the input $x(t)$ to the reference voltage x_r and switch the output $y(t)$ to A if the input is above the threshold, $x(t) > x_r$. If drops below that value, $x(t) < x_r$, the output is switched to B . The operator of the transformation is therefore

$$y(t) = \mathcal{O}(x)x(t) = \begin{cases} A, & x(t) > x_r \\ B, & x(t) < x_r \end{cases}. \quad (1.74)$$

A schematic realization of (1.74) is shown in Fig. 1.25, where a resistor R obtains the necessary gain of a comparator at the threshold $x(t) = x_r$.

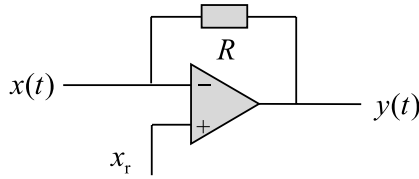


Fig. 1.25. Comparison of two voltages, $x(t)$ and x_r .

A comparator (Fig. 1.25) is also often used in filter structures as a high gain linear amplifier.

Limitation

A comparator (or a system of comparators) can be used to gain the input linearly in a gap between two thresholds (reference voltages), $x_{r1} < x < x_{r2}$, and limit (hold) the input at some level A when $x(t)$ drops below x_{r1} and at B if $x(t)$ exceeds x_{r2} . The relevant nonlinear operator of limitation can be described with the piecewise function

$$y(t) = \mathcal{O}(x)x(t) = \begin{cases} ax(t), & x_{r1} < x(t) < x_{r2} \\ A, & x(t) < x_{r1} \\ B, & x(t) > x_{r2} \end{cases}. \quad (1.75)$$

We notice that, typically, any linear amplifier with saturation fits (1.75).

1.4.4 Nonlinear Time-varying Systems

In applications, nonlinear systems may undergo intentional and/or “annoying” changes in their structures, thereby becoming time-varying. Because the nonlinear blocks are typically designed to be memoryless, time variations in their components result merely in time dependencies of the coefficients in the above-discussed nonlinear memoryless operators.

So, we passed over the most typical and thus basic linear and nonlinear, memory and memoryless operations in systems. Using them separately, or combining the memoryless nonlinear subsystems with linear memory blocks allows designing a variety of linear and nonlinear systems and structures, such as filters, resonant amplifiers, oscillators, control systems, modulators, demodulators, phase locked loops (PLLs), etc. Methods of analysis and examples of systems will be considered in the following chapters.

1.5 Summary

What we discussed above introduces the reader to the fundamental canons of systems and, in what follows, we shall start elucidating the methods of systems

description. To keep the development more understandable and transparent, the reader has to remember the fundamental definitions and classifications of systems based on the following foundations:

- A system is a mathematical model of a physical process that relates the input signal to the output signal.
- System analysis is provided to understand major properties of a system.
- System design is used to find a proper system that meets given specifications.
- System synthesis is carried out to find a proper system structure or block diagram.
- System simplification is necessary to realize a system practically.

1.6 Problems

1.1 (Systems). A message is transmitted in the communication channel simultaneously via the amplitude and angle of a modulated carrier signal. Based upon (1.1)–(1.4), write the modulated signals for simultaneous

1. AM and FM
2. AM and PM
3. FM and PM
4. AM, FM and PM

1.2. The radar (Fig. 1.2) has measured a frequency shift Ω between the transmitted and received signals. Write properly the received signal model (1.9) and explain why the frequency shift may occur? How it might be coupled with the vehicular velocity?

1.3. The Doppler frequency of a measurement is given by (1.15). Based upon and following Fig. 1.3, derive the radial velocity \dot{r} and define the velocity

1. in direction \mathbf{x}
2. in direction \mathbf{y}
3. in direction \mathbf{z}

1.4. Write an equation of the control system shown in Fig. 1.5. How the function would be changed if there is an external additive factor $\mathbf{v}(t)$ at the output of the “Manufacturing Process”?

1.5. Analyze the operation principle of ultrasonography (Fig. 1.6) and deduce what information about the human body may be extracted from the amplitude, phase, and frequency of the reflected signal (1.17)?

1.6. Following (1.18)–(1.24), solve the positioning problem for the robot in the three coordinates \mathbf{x}_0 , \mathbf{y}_0 , and \mathbf{z}_0 . Suppose that the 3D coordinates of the transmitters, \mathbf{x}_i , \mathbf{y}_i , and \mathbf{z}_i , at the points A, B, and C are known. Note that an antenna of the robot can be rotated only in a horizontal plane.

1.7. Analyze the principle equation (1.25) of an OXCO and explain a physical essence of every term in its right-hand side. Suggest practical ways to diminish the annoying components to zero.

1.8 (Systems classification). A system is performed with an input $x(t)$ and output $y(t)$, which in vector forms are, $\mathbf{x}(t)$ and $\mathbf{y}(t)$, respectively. System equations are given below. Realize whether the system is SISO, MISO, SIMO, or MIMO?

$$\begin{aligned} 1. \quad & \mathbf{q}'(t) = \mathbf{A}\mathbf{q}(t) + \mathbf{B}x(t) \\ & \mathbf{y}(t) = \mathbf{C}\mathbf{q}(t) + \mathbf{D}x(t) \end{aligned}$$

$$2. \quad y(t) = \mathbf{A}\mathbf{x}(t) + b\frac{d^2}{dt^2}y(t) + \frac{d}{dt}c(t)y(t)$$

$$\begin{aligned} 3. \quad & \mathbf{q}'(t) = \mathbf{A}\mathbf{q}(t) + \mathbf{B}x(t) \\ & y(t) = \mathbf{C}\mathbf{q}(t) \end{aligned}$$

$$4. \quad \mathbf{A}\mathbf{y}(t) = a\frac{d}{dt}y_1(t) + bx(t) + c\frac{d}{dt}x(t)$$

$$5. \quad ax(t) = \mathbf{B}\mathbf{y}(t)$$

$$\begin{aligned} 6. \quad & \mathbf{q}'(t) = \mathbf{A}\mathbf{q}(t) + \mathbf{B}\mathbf{x}(t) \\ & \mathbf{y}(t) = \mathbf{C}\mathbf{q}(t) \end{aligned}$$

$$\begin{aligned} 7. \quad & \mathbf{q}'(t) = \mathbf{A}\mathbf{q}(t) + \mathbf{B}\mathbf{x}(t) \\ & y(t) = \mathbf{C}\mathbf{q}(t) + \mathbf{D}\mathbf{x}(t) \end{aligned}$$

1.9. Given the following SISO system:

$$1. \quad y(t) = ax(t) + e^{at} \int_{-\infty}^{t+\theta} x(\tau) d\tau + c\frac{d}{dt}x(t), \quad \theta \geq 0$$

$$2. \quad y(t) = at|x(t)| + b\frac{d^2}{dt^2}x(t) + \frac{d}{dt}c(t)x(t)$$

$$3. \quad y(t) = a\frac{d}{dt}y(t) + bx(t) + c\frac{d^2}{dt^2}x(t) + \frac{d}{dt}d(t)x(t)$$

$$4. \quad y(t) = a\frac{d}{dt}y(t) + b\frac{d^2}{dt^2}y(t) + c\frac{d^3}{dt^3}y(t) + dx(t)$$

$$5. \quad y(t) = ax(t) + c\frac{d}{dt}[x(t) - g]^2$$

$$6. \quad y(t) = at|x(t)| + b\frac{d}{dt}x(t)$$

Which system is memory and which is not? Why?

Which system is causal and which is not causal? Why?

Which system is linear and which is nonlinear? Why?

Which system is time-invariant and which is time-variant? Why?

Which system may be said to be BIBO stable? Why?

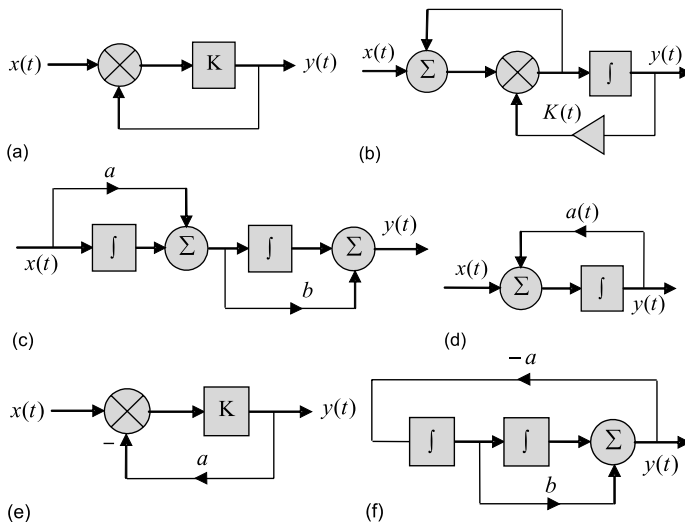


Fig. 1.26. System block diagrams.

1.10. A systems is represented with the block diagram (Fig. 1.26). Analyze the system structure and deduce whether a system is LTI, LTV, NTI, or NTV.

1.11. Write an equation of the system shown in Fig. 1.26 in the form used in Problem 1.9.

1.12. Analyze the system shown in Fig. 1.26 and realize whether a system is BIBO stable or not obligatorily BIBO stable. Formulate conditions (constraints) under which a system would always be BIBO stable.

1.13. Realize, which system structure shown in Fig. 1.26 is closed loop and which is not? Which closed loop has a positive feedback and which has a negative feedback? Which is closed loop control and which is not?

1.14. Consider any two systems shown in Fig. 1.26 and sketch a new structure with their

1. Series interconnection
2. Parallel interconnection
3. Feedback interconnection

If possible, simplify a resulting structure. Write an equation of a new system.

1.15. An electric circuit is shown in Fig. 1.27. Implying that all its electric units are time constants and using Table 1.2, write an ODE of the system.

1.16. All memory electric units (C and L) in the scheme shown in Fig. 1.27 are assumed to be time-controllable. Using Table 1.2, write an ODE of the system.

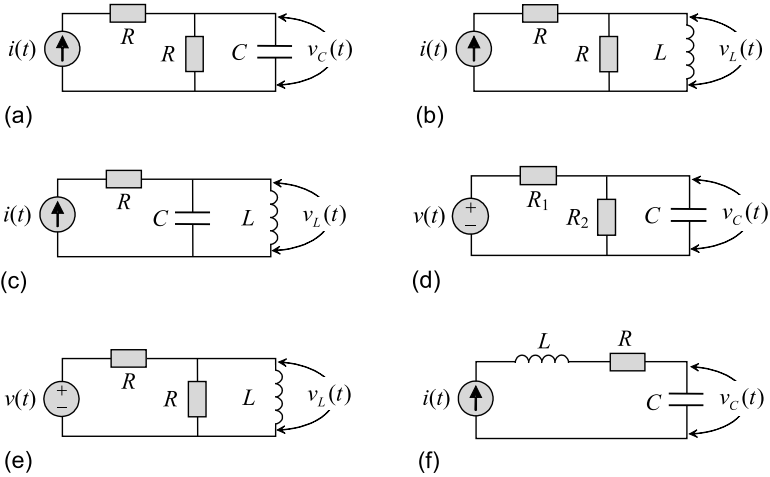


Fig. 1.27. Electrical systems.

1.17. A nonlinear memoryless system is represented with the below given mapping equation:

1. $y(t) = a + bx(t) + cx^2(t)$
2. $y(t) = a^2x^2(t) - a \ln \frac{x(t)}{b}$
3. $y(t) = ax(t) - b \exp \frac{x(t)}{a}$
4. $y(t) = a \ln \frac{b}{x(t)}$
5. $y(t) = ax^{-1}(t) + b \exp \frac{c}{x(t)}$

Supposing that $x(t) = \cos \omega_0 t$, determine the frequency content of the output $y(t)$ in the range of $0 \leq \omega \leq 2\omega_0$.

1.18. The system input $x(t)$ and output $y(t)$ are represented with the magnitude spectra, $|C_{xk}|$ and $|C_{yk}|$, respectively, as shown in Fig. 1.28. Realize, which system is linear and which is nonlinear.

1.19 (Accuracy and precision). Positioning systems provide measurements of the coordinates (x, y) of a linearly moving object (Fig. 1.29). Observe the measurements and make a conclusion about accuracy and precision of each of the systems.

1.20 (Uncertainty and robustness). The nominal performance of a system (Problem 1.19) is shown in Fig. 1.29 with a bold line. Analyze the actual performance and realize the system uncertainty 1) at every time instant, 2) at particular parts of measurements, and 3) over all measurements.

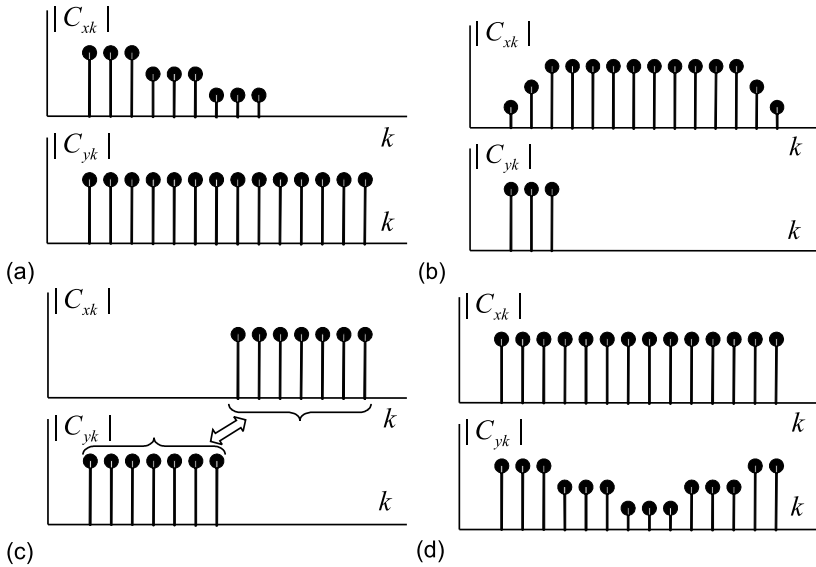


Fig. 1.28. Magnitude spectra, $|C_{xk}|$ and $|C_{yk}|$, of the input signal $x(t)$ and output signal $y(t)$, respectively.

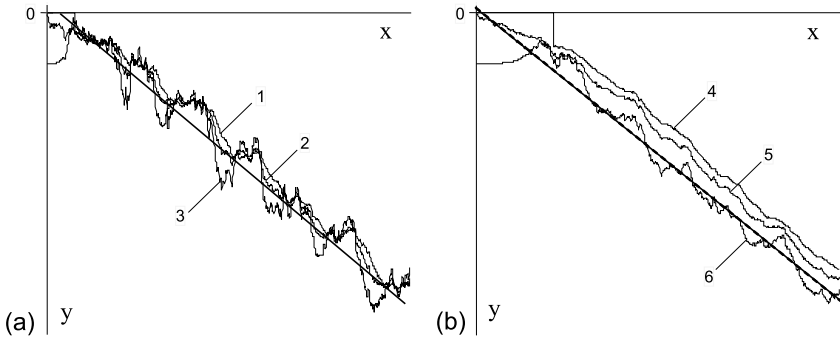


Fig. 1.29. Coordinates measured of a linearly moving object (bold) with different systems.

1.21. Following Example 1.1, specify the weighting transfer function for the additive and feedback robust system models with uncertainty. Verify that, by $\tilde{H} = \frac{1}{s+a}$ and $H = \frac{1}{s}$, the weights are $W = \frac{a}{s(s+a)}$ and $W = as$ for the additive and feedback cases, respectively.

Quantitative Methods of Systems Description

Any system represents some physical process with a mathematical model. Therefore, its operator \mathcal{O} is not always defined to be absolutely rigorous, but rather described appropriately with some methods. Depending on applications and practical needs, different methods may be used and different forms of system presentation can be found. The most well developed methods are created for LTI systems. All general responses of LTI systems are coupled with each other by the transforms and already quite complete the LTI system theory seems rigorous and strong. The other systems (LTV, NTI, and NTV) also demonstrate abilities for generalization that will be shown in the sequel. Even so, many nonlinear problems are still being solved involving approximation and linearization as well as decomposing a system to well-studied blocks. Below, we observe the most efficient methods of systems description in the time and frequency (transform) domains. Such methods are called quantitative.

2.1 System Responses to Test Signals

Any input-to-output system responds to the input signal with its own unique output signal. To generalize a system performance, the following standard test waveforms are used.

The *unit impulse* $\delta(t)$ also called the *Dirac*¹ *delta function* possesses the following fundamental properties:

$$\delta(t) = \begin{cases} \infty, & t = 0 \\ 0, & t \neq 0 \end{cases} \quad \text{and} \quad \int_{-\infty}^{\infty} \delta(t) dt = 1. \quad (2.1)$$

The other useful properties of $\delta(t)$ are postponed to Appendix A. The *unit step* function $u(t)$ is defined by

¹ Paul Adrien Maurice Dirac, English mathematician, 8 August 1902–20 October 1984.

$$u(t) = \begin{cases} 1, & t \geq 0 \\ 0, & t < 0 \end{cases} \quad (2.2)$$

and is coupled with $\delta(t)$ by a pair of the transformations:

$$\delta(t) = \frac{du(t)}{dt} \quad \text{and} \quad u(t) = \int_{-\infty}^t \delta(\tau) d\tau. \quad (2.3)$$

Finally, the *complex exponential signal* $e^{j\omega t}$ is defined, as a test signal, by two harmonic functions as

$$e^{j\omega t} = \cos \omega t + j \sin \omega t, \quad (2.4)$$

where ω is an angular frequency. Note that, in some special cases, albeit not commonly, other test signals may be useful.

The response of a system to the standard test waveform (function) is then described mathematically to be the system *general response*: impulse, step, or frequency.

2.1.1 Impulse Response

When we use $\delta(t)$ as a test signal, we think about the response of a system to the unit impulse, so about the *impulse response*, provided the definition:

Impulse response: The response of a system to the unit impulse is the system impulse response. □

More specifically, an LTI system is characterized by the impulse response $h(t)$ that is its response at time t to the unit impulse at time t ,

$$h(t) = \mathcal{O}\delta(t). \quad (2.5)$$

In turn, an LTV system is characterized by the time-varying impulse response $h(t, \theta)$ that is its response at time t to the unit impulse at time θ ,

$$h(t, \theta) = \mathcal{O}(t)\delta(t - \theta). \quad (2.6)$$

Example 2.1. An LTI system (Fig. 2.1a) is described with the ODE

$$\frac{d}{dt}v_C(t) + \frac{1}{\tau_c}v_C(t) = \frac{1}{\tau_c}v(t),$$

where $\tau_c = RC$ is a system time constant, having a general solution

$$v_C(t) = v_C(0)e^{-\frac{t}{\tau_c}} + e^{-\frac{t}{\tau_c}} \frac{1}{\tau_c} \int_{-0}^t e^{\frac{\theta}{\tau_c}} v(\theta) d\theta. \quad (2.7)$$

Suppose that the input is shaped with the unit impulse, $v(t) = \delta(t)$. Then, by the sifting property of the delta function (Appendix A) and $v_C(0) = 0$, the solution (2.7) produces the system impulse response function

$$h(t) = v_C(t) = \begin{cases} \frac{1}{\tau_c} e^{-t/\tau_c}, & t \geq 0 \\ 0, & t < 0 \end{cases}, \quad (2.8)$$

illustrated in Fig. 2.1b. □

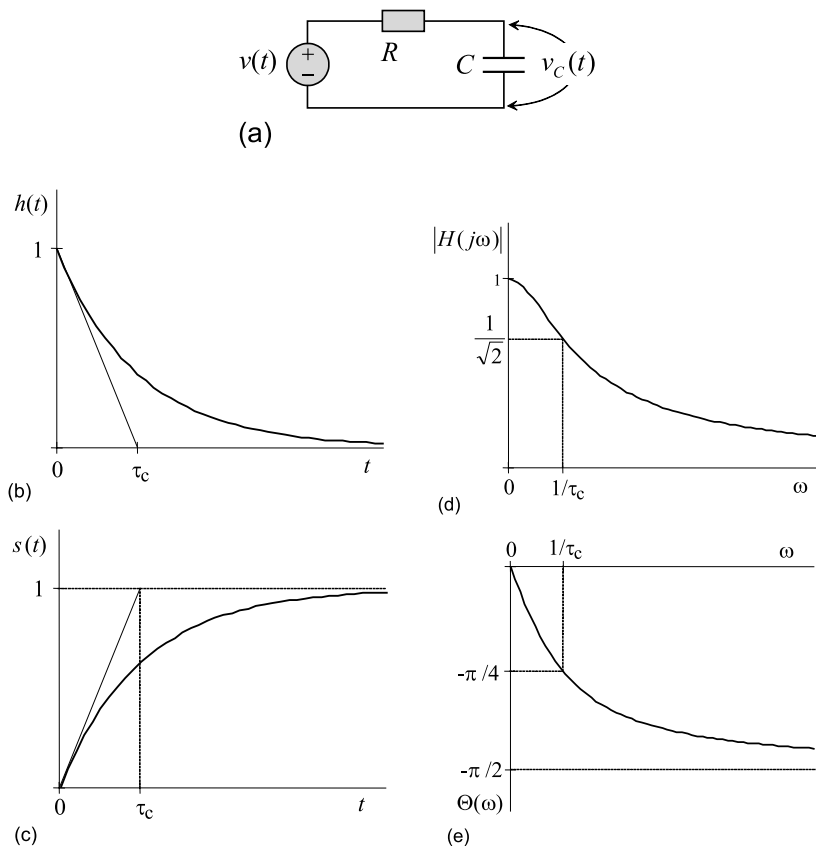


Fig. 2.1. General responses of a system: (a) low-pass LTI system, (b) impulse response $h(t)$, (c) step-response $s(t)$, (d) magnitude response $|H(j\omega)|$, and (e) phase response $\Theta(\omega)$.

Examples of the impulse responses of time-varying and nonlinear systems will be considered in the relevant Chapters.

2.1.2 Step Response

The other standard test signal, the unit step $u(t)$, is associated with the step response of a system, provided the definition:

Step response: The response of a system to the unit-step is the system step response. □

Similarly to the impulse response, the step response is specifically measured for time-invariant and time-varying systems. For LTI systems, the step response $g(t)$ is defined as the system response at time t to $u(t)$ at t ,

$$g(t) = \mathcal{O}u(t). \quad (2.9)$$

For LTV systems, it is characterized by the time-varying step response $g(t, \theta)$ that is its response at time t to the unit step at time θ ,

$$g(t, \theta) = \mathcal{O}(t)u(t - \theta). \quad (2.10)$$

It can be shown that, for LTI systems, the step response is equivalently defined by integrating the impulse response and the impulse response by differentiating the step response, respectively,

$$g(t) = \int_0^t h(\tau) d\tau \quad \text{and} \quad h(t) = \frac{d}{dt}g(t). \quad (2.11)$$

Note that for time-varying and nonlinear systems the relevant pair of the transformations (2.11) is not commonly valid.

Example 2.2. Given a system (Fig. 2.1a) described in Example 2.1. Let the input be a unit-step function, $v(t) = u(t)$. Then (2.7) produces, by $v_C(0) = 0$, the system step response

$$g(t) = v_C(t) = \begin{cases} 1 - e^{-t/\tau_c}, & t \geq 0 \\ 0, & t < 0 \end{cases}, \quad (2.12)$$

shown in Fig. 2.1c. It may easily be verified that, by (2.11), the function (2.12) becomes the impulse response (2.8) and integrating (2.8) produces the step response (2.12). □

2.1.3 Frequency Response

In the frequency domain, a system is characterized with the *frequency response* also called the *system function* that is the measure of its response to a harmonic signal, which amplitude is unit and which frequency can be arbitrary, provided the definition:

Frequency response: The ratio of the system response to the complex exponential signal $x(t) = e^{j\omega t}$ and $e^{j\omega t}$ is the system frequency response,

$$\text{Frequency response} = \frac{\text{Response to } e^{j\omega t}}{e^{j\omega t}}. \quad (2.13)$$

□

Because a system is typically with memory, its frequency response is commonly a complex function. The absolute value of this function is called the *magnitude response* and its phase the *phase response*.

Specifically for LTI systems, the frequency response is defined by

$$H(j\omega) = \frac{\text{Response to } e^{j\omega t}}{e^{j\omega t}} = |H(j\omega)|e^{j\varphi_H(\omega)}, \quad (2.14)$$

where $|H(j\omega)|$ is the *magnitude response* and $\varphi_H(\omega)$ *phase response*. The frequency response of an LTI system can be measured as follows. Sweep a unit amplitude harmonic input signal through the bandwidth of a system and measure the magnitude and phase of a relevant harmonic signal at the output.

It is of high importance that the impulse and frequency responses of an LTI system are coupled by the Fourier² transform (Appendix C)

$$H(j\omega) \stackrel{\mathcal{F}}{\Leftrightarrow} h(t). \quad (2.15)$$

For LTI systems we thus can say that the frequency response $H(j\omega)$ is the Fourier transform of its impulse response $h(t)$ and the impulse response is the inverse Fourier transform of its frequency response. Overall, all general responses of LTI systems are interchangeable by the transformations. Therefore, both SISO and MIMO LTI systems are consistently described in the time and frequency (transform) domains.

If a system is LTV, its frequency response as well as magnitude and phase responses become time-varying,

$$H(j\omega, t) = \frac{\text{Response to } e^{j\omega t}}{e^{j\omega t}} = |H(j\omega, t)|e^{j\varphi_H(\omega, t)}. \quad (2.16)$$

However, the time-varying impulse and frequency responses are not coupled by the Fourier transform, contrary to (2.15) valid for LTI systems.

Note that nonlinear systems respond to the input signal with new harmonics. Therefore the definition of the frequency response can only be used as related to the harmonic of the same frequency as in the input.

Example 2.3. Consider a system described in Example 2.1. To define the frequency response, the input signal must be set to be harmonic (cosine or sine) with unit amplitude. Then suppose that $v(t) = \sin \omega t$. The output is thus predetermined to be

² Jean Baptiste Joseph Fourier, French mathematician, 21 March 1768–16 May 1830.

$$v_C(t) = |H(j\omega)| \sin[\omega t + \varphi_H(\omega)].$$

Exploiting the general solution (2.7) with $v_C(0) = 0$, substituting the harmonic input and output, and using the Euler³ formula (Appendix E) allows us to write

$$\begin{aligned} |H(j\omega)| \sin[\omega t + \varphi_H(\omega)] &= e^{-\frac{t}{\tau_c}} \frac{1}{\tau_c} \int_{-0}^t e^{\frac{\theta}{\tau_c}} \sin \omega \theta \, d\theta \\ &= e^{-\frac{t}{\tau_c}} \frac{1}{\tau_c} \int_{-0}^t e^{\frac{\theta}{\tau_c}} \frac{e^{j\omega\theta} - e^{-j\omega\theta}}{2j} \, d\theta \\ &= \frac{e^{-\frac{t}{\tau_c}}}{2j\tau_c} \left[\int_0^t e^{(\frac{1}{\tau_c} + j\omega)\theta} \, d\theta - \int_0^t e^{(\frac{1}{\tau_c} - j\omega)\theta} \, d\theta \right] \\ &= \frac{1}{1 + \omega^2\tau_c^2} (\sin \omega t - \omega\tau_c \cos \omega t). \end{aligned}$$

The expression results in two equations,

$$|H(j\omega)| \sin \varphi_H(\omega) = -\frac{\omega\tau_c}{1 + \omega^2\tau_c^2},$$

$$|H(j\omega)| \cos \varphi_H(\omega) = \frac{1}{1 + \omega^2\tau_c^2},$$

yielding the magnitude and phase responses of a system, respectively,

$$|H(j\omega)| = \frac{1}{\sqrt{1 + \omega^2\tau_c^2}}, \quad (2.17)$$

$$\tan \varphi_H(\omega) = -\omega\tau_c \quad (2.18)$$

The functions (2.17) and (2.18) are sketched in Fig. 2.1d and Fig. 2.1e, respectively. \square

Example 2.4. In a much lesser sophisticated way, the responses (2.17) and (2.18) can be derived exploiting (2.15). Indeed, by the Fourier transform applied to (2.8), the frequency response is easily found to be

$$H(j\omega) = \int_0^{\infty} e^{-\frac{t}{\tau_c}} e^{-j\omega t} \, dt = \frac{1}{1 + j\omega\tau_c} \quad (2.19)$$

and it is evident that the magnitude and phase responses associated with (2.19) are given by (2.17) and (2.18), respectively. \square

³ Leonhard Euler, Swiss mathematician, 15 April 1707–18 September 1783.

Nonlinear systems can also be characterized by responses to test signals, following the general definitions. However, for such systems, the general responses are not interchangeable by the transformations, unlike the LTI systems case. For many nonlinear systems, the test responses cannot mathematically be performed at all and approximate methods of identification are applied. The other problem is here that the test responses can differ cardinally for different values in different regions of signals. Therefore, nonlinear systems are often locally linearized that makes the responses of linear systems to be fundamental in the system theory.

2.2 Methods for Linear Systems

As follows from what was observed above, all LTI systems are exhaustively characterized by responses to the standard test signals both in the time and frequency (transform) domains. Their time responses (impulse and step) predefine each other by integration and differentiation and the impulse and frequency responses are coupled by the Fourier transform. These splendid properties have created solid foundation for the methods of LTI systems analysis.

2.2.1 Convolution

In the time domain, the operator of an LTI system is called the *convolution*. By the convolution, the output $y(t)$ of a SISO LTI system is coupled with its input $x(t)$ via the impulse response $h(t)$ as follows:

$$\begin{aligned} y(t) &= \mathcal{O}x(t) = \int_{-\infty}^{\infty} x(\theta)h(t - \theta) d\theta = x(t) * h(t) \\ &= \int_{-\infty}^{\infty} h(\theta)x(t - \theta) d\theta = h(t) * x(t), \end{aligned} \quad (2.20)$$

where the symbol “ $*$ ” commonly denotes a convolution. Relations in (2.20) hold true for both noncausal signals and systems and suggest that $x(t)$ and $h(t)$ are commuting. When signals and systems are both causal, the lower integral bound becomes zero and the upper equal to the current time value t . By the convolution, a generalized structure of an LTI system in the time domain appears as in Fig. 2.2a.

Example 2.5. Given a noncausal signal $x(t) = e^{j\omega_0 t}$, driving a system represented with the impulse response

$$h(t) = \frac{1}{\tau_c} e^{-\frac{t}{\tau_c}} u(t).$$

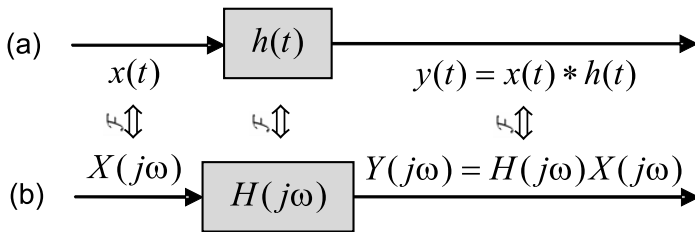


Fig. 2.2. A generalized structure of a SISO LTI system: (a) in the time domain and (b) in the frequency domain.

By (2.20), the output is calculated to be

$$y(t) = \frac{1}{\tau_c} \int_{-\infty}^t e^{j\omega_0\theta} e^{-\frac{t-\theta}{\tau_c}} d\theta = \frac{e^{-t/\tau_c}}{\tau_c} \int_{-\infty}^t e^{(j\omega_0 + \frac{1}{\tau_c})\theta} d\theta = \frac{e^{j\omega_0 t}}{1 + j\omega_0\tau_c}. \quad (2.21)$$

With $\tau_c \rightarrow \infty$, the system is absolutely inertial (infinite memory) that tends the output toward zero. In the other limiting case of $\tau_c \rightarrow 0$, the system is memoryless having unity gain and the output becomes equal to the input. \square

If the Fourier transforms are known of

$$X(j\omega) \stackrel{\mathcal{F}}{\Leftrightarrow} x(t), \quad Y(j\omega) \stackrel{\mathcal{F}}{\Leftrightarrow} y(t), \quad \text{and} \quad H(j\omega) \stackrel{\mathcal{F}}{\Leftrightarrow} h(t),$$

then the Fourier transform applied to the convolution integral (2.20) produces an equivalent form in the frequency domain,

$$Y(j\omega) = H(j\omega)X(j\omega). \quad (2.22)$$

Relation (2.22) suggests that the operator of an LTI system in the frequency domain is the frequency response $H(j\omega) = |H(j\omega)|e^{j\varphi_H(\omega)}$ specified by (2.14). We thus can say that the frequency response of an LTI system is the ratio of the Fourier transform of its output $Y(j\omega)$ and the Fourier transform $X(j\omega)$ of its input, namely

$$H(j\omega) = \frac{Y(j\omega)}{X(j\omega)}. \quad (2.23)$$

A generalized structure of an LTI system in the frequency domain is shown in Fig. 2.2b.

Example 2.6. Given a signal

$$x(t) = e^{j\omega_0 t} \stackrel{\mathcal{F}}{\Leftrightarrow} X(j\omega) = 2\pi\delta(\omega - \omega_0)$$

driving a SISO LTI system (Example 2.5) having the impulse response

$$h(t) = \frac{1}{\tau_c} e^{-\frac{t}{\tau_c}} u(t) \stackrel{\mathcal{F}}{\Leftrightarrow} H(j\omega) = \frac{1}{1 + j\omega\tau_c}.$$

It can easily be verified that the Fourier transform applied to the output (2.21) and the product $H(j\omega)X(j\omega)$ produce the same result, respectively,

$$Y(j\omega) = \frac{2\pi}{1 + j\omega_0\tau_c} \delta(\omega - \omega_0)$$

that is the spectral density (Fourier transform) of the output. \square

If a system is LTV, then its input $x(t)$ and output $y(t)$ are coupled via the *time-varying impulse response* $h(t, \theta)$ by the *general convolution*

$$y(t) = \mathcal{O}(t)x(t) = \int_{-\infty}^{\infty} x(\theta)h(t, \theta) d\theta \quad (2.24)$$

that, contrary to (2.20), commonly does not commute.

2.2.2 Differential Equations

In the time domain, an LTI system can be described with the N -order linear ordinary differential equation (ODE)

$$\sum_{n=0}^N a_n \frac{d^n}{dt^n} y(t) = \sum_{m=0}^M b_m \frac{d^m}{dt^m} x(t), \quad (2.25)$$

where a_n and b_m are real constant coefficients bearing all dynamic (memory) properties of a system and N refers to the highest order derivative of the output, meaning that the condition $N \geq M$ ensures *physical realizability*. The system output can then be expressed as follows

$$y(t) = \sum_{m=0}^M \frac{b_m}{a_0} \frac{d^m}{dt^m} x(t) - \sum_{n=1}^N \frac{a_n}{a_0} \frac{d^n}{dt^n} y(t), \quad (2.26)$$

where the first sum in the right-hand side represents the direct transformation of $x(t)$ to $y(t)$ and the second one accounts for the feedback branches.

Example 2.7. A system (Example 2.1) is generalized with

$$\sum_{n=0}^1 a_n \frac{d^n}{dt^n} y(t) = \sum_{m=0}^0 b_m \frac{d^m}{dt^m} x(t),$$

where $y(t) = v_C(t)$, $x(t) = v(t)$, $a_0 = 1/\tau_c$, $a_1 = 1$, and $b_0 = 1/\tau_c$. \square

A generalized N -order ODE of an LTV system is written as

$$\sum_{n=0}^N \frac{d^n}{dt^n} [a_n(t)y(t)] = \sum_{m=0}^M \frac{d^m}{dt^m} [b_m(t)x(t)], \quad (2.27)$$

where at least one of the real coefficients, a_n and b_m , is time-varying. By differentiating the products, (2.27) can be transformed to (2.25) with at least one coefficient time-varying.

CARMA Model

An alternative form of the linear system ODE (2.26) came from the series analysis and is known as the *continuous-time autoregressive moving average* (CARMA) model,

$$y(t) = \sum_{m=0}^M \beta_{M-m} \frac{d^m}{dt^m} x(t) - \sum_{n=1}^N \alpha_{N-n} \frac{d^n}{dt^n} y(t), \quad (2.28)$$

where the coefficients β_m and α_n are constants. Originally, the CARMA model was used to investigate correlation in discrete-time series. Therefore, the first sum in the right-hand side was called the *moving average* (MA) model and the second one *autoregressive* (AR) model. It is evident that two models, (2.26) and (2.28), have no substantial differences, because of, by $\alpha_{N-n} = a_n/a_0$ and $\beta_{M-m} = b_m/a_0$, they convert to each other.

2.2.3 Transfer Function

It is known from the theory of ODEs that a solution of either (2.26) or (2.28) cannot typically be found in the time domain in simple forms when N is large. An alternative way implies applying the Laplace⁴ transform (Appendix D) to both sides of the linear ODE, exploiting the transforms of the input $X(s) \stackrel{\mathcal{L}}{\Leftrightarrow} x(t)$ and output $Y(s) \stackrel{\mathcal{L}}{\Leftrightarrow} y(t)$, and representing (2.25) as follows

$$Y(s) \sum_{n=0}^N a_n s^n = X(s) \sum_{m=0}^M b_m s^m, \quad (2.29)$$

where $s = \sigma + j\omega$ is the Laplace variable. This equation gives another form of the system operator that can now be represented in the transform domain as the system *transfer function*, provided the definition:

Transfer function: The transfer function of a LTI system is the ratio of the Laplace transform $Y(s)$ of its output and the Laplace transform $X(s)$ of its input,

⁴ Pierre Simon Laplace, French physicist and mathematician, 23 March 1749–5 March 1827.

$$H(s) = \frac{Y(s)}{X(s)}. \tag{2.30}$$

□

By (2.29) and (2.30), the system transfer function can be expressed as

$$\begin{aligned} H(s) = \frac{Y(s)}{X(s)} &= \frac{\sum_{m=0}^M b_m s^m}{\sum_{n=0}^N a_n s^n} = \frac{b_0 + b_1 s + \dots + b_M s^M}{a_0 + a_1 s + \dots + a_N s^N} \\ &= \frac{b_M (s - z_1)(s - z_2) \dots (s - z_M)}{a_N (s - p_1)(s - p_2) \dots (s - p_N)}, \end{aligned} \tag{2.31}$$

where the roots z_m , $m = 1, 2, \dots, M$, of the polynomial in the numerator are called the *zeros* to mean that $H(s)$ by each of these roots will tend toward zero. In turn, the roots p_n , $n = 1, 2, \dots, N$, of the polynomial in the denominator are called the *poles*, because $H(s)$ goes to infinite by each of them.

It is of importance that the transfer function and impulse response of an LTI system are coupled by the pair of the Laplace transform, i. e.

$$H(s) \stackrel{\mathcal{L}}{\Leftrightarrow} h(t). \tag{2.32}$$

The generalized structure of a SISO LTI system in the s domain is shown in Fig. 2.3b along with its counterpart in the time domain (Fig. 2.3a).

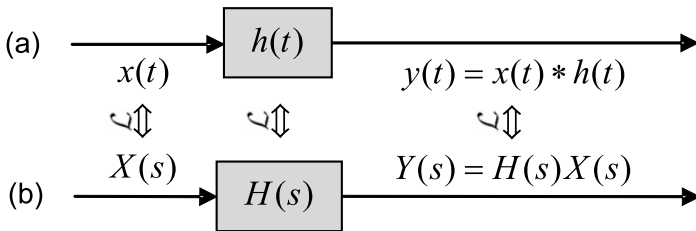


Fig. 2.3. A generalized structure of a SISO LTI system: (a) in the time domain and (b) in the s domain.

Example 2.8. A system is given with the ODE (Example 2.1). Applying the Laplace transform to the both sides of this equation, we have

$$sV_C(s) + \frac{1}{\tau_c} V_C(s) = \frac{1}{\tau_c} V(s),$$

where $V_C(s) \stackrel{\mathcal{L}}{\Leftrightarrow} v_C(t)$ and $V(s) \stackrel{\mathcal{L}}{\Leftrightarrow} v(t)$, that allows us to write the system transfer function as

$$H(s) = \frac{V_C(s)}{V(s)} = \frac{1}{1 + s\tau_c}. \quad (2.33)$$

Note that, by $s = j\omega$, (2.33) becomes the system frequency response $H(j\omega)$ given in Example 2.6. \square

Overall, the transfer function, as a mathematical statement, is a relationship between the input and the output of an LTI system in terms of the transfer characteristics. Because the Fourier transform is a special case of the bilateral Laplace transform then, by $\sigma = 0$, the system frequency response $H(j\omega)$ is a special case of the system transfer function $H(s)$.

2.2.4 State Space Representation

The ODE (2.25) is coupled straightforwardly with the system model in *state space*. The term “*space*” may be treated as a “*memory element*” of the system and therefore the number of *states* is associated with the number of derivatives. The set of all state variables is called the *system’s state*. Because the set describes a system completely, it also contains sufficient information to compute all future system’s states and outputs.

Most commonly, a MIMO LTV system is described with the so-called *state equation* that is the first-order matrix ODE and *state observation equation* that is a matrix algebraic equation, respectively,

$$\mathbf{q}'(t) = \mathbf{A}(t)\mathbf{q}(t) + \mathbf{B}(t)\mathbf{x}(t), \quad (2.34)$$

$$\mathbf{y}(t) = \mathbf{C}(t)\mathbf{q}(t) + \mathbf{D}(t)\mathbf{x}(t), \quad (2.35)$$

where $\mathbf{q}(t)$ is the $N \times 1$ vector of the system states and $\mathbf{q}'(t) = \frac{d}{dt}\mathbf{q}(t)$ is its time derivative of the same dimensions. The $k \times 1$ vector of a multiple input $\mathbf{x}(t)$ and the $p \times 1$ vector of a multiple output $\mathbf{y}(t)$ are, respectively,

$$\mathbf{x}(t) = \begin{bmatrix} x_1(t) \\ x_2(t) \\ \vdots \\ x_k(t) \end{bmatrix} \quad \text{and} \quad \mathbf{y}(t) = \begin{bmatrix} y_1(t) \\ y_2(t) \\ \vdots \\ y_p(t) \end{bmatrix}. \quad (2.36)$$

The $N \times N$ matrix $\mathbf{A}(t)$ is called the *system matrix*, $\mathbf{B}(t)$ of dimensions $N \times k$ the *input matrix*, $\mathbf{C}(t)$ of $p \times N$ the *observation matrix* or *measurement matrix*, and $\mathbf{D}(t)$ of $p \times k$ the *output matrix*.

At least one of the matrices in (2.34) and (2.35) must be time-variant for the system to be LTV. Otherwise, the system is LTI and the equations become

$$\mathbf{q}'(t) = \mathbf{A}\mathbf{q}(t) + \mathbf{B}\mathbf{x}(t), \quad (2.37)$$

$$\mathbf{y}(t) = \mathbf{C}\mathbf{q}(t) + \mathbf{D}\mathbf{x}(t). \quad (2.38)$$

If it is also a SISO LTI system, then its input $x(t)$ and output $y(t)$ are both scalars, and the state-space model simplifies to

$$\mathbf{q}'(t) = \mathbf{A}\mathbf{q}(t) + \mathbf{B}x(t), \quad (2.39)$$

$$y(t) = \mathbf{C}\mathbf{q}(t) + \mathbf{D}x(t), \quad (2.40)$$

where \mathbf{A} has the same dimensions and the matrices \mathbf{B} , \mathbf{C} , and \mathbf{D} possess the dimensions $N \times 1$, $1 \times N$, and 1×1 , respectively. Moreover, if $M < N$ in (2.25), then the last term in the right-hand side of (2.40) vanishes, because $\mathbf{D} = [0]$.

Example 2.9. A SISO system is described with the ODE (2.25). By assigning the state variables

$$\begin{aligned} q_1(t) &= y(t), \\ q_2(t) &= y'(t) = q_1'(t), \\ q_3(t) &= y''(t) = q_2'(t), \\ &\vdots \\ q_N(t) &= y^{(N-1)}(t) = q_{N-1}'(t), \end{aligned}$$

we arrive at the state space model (2.39) and (2.40), for the $N \times 1$ system's state vector

$$\mathbf{q}(t) = [q_1(t) \ q_2(t) \ \dots \ q_N(t)]^T \quad (2.41)$$

and matrices

$$\mathbf{A} = \begin{bmatrix} 0 & 1 & 0 & \dots & 0 \\ 0 & 0 & 1 & & 0 \\ \vdots & \vdots & & \ddots & \vdots \\ 0 & 0 & 0 & & 1 \\ -a_0/a_N & -a_1/a_N & \dots & -a_{N-2}/a_N & -a_{N-1}/a_N \end{bmatrix}, \quad (2.42)$$

$$\mathbf{B} = [0 \ 0 \ \dots \ 1/a_N]^T, \quad (2.43)$$

$$\mathbf{C} = \begin{bmatrix} b_0 - a_0 b_N/a_N \\ b_1 - a_1 b_N/a_N \\ \vdots \\ b_{N-1} - a_{N-1} b_N/a_N \end{bmatrix}^T, \quad (2.44)$$

$$\mathbf{D} = [b_N/a_N]. \quad (2.45)$$

□

Just from the definition of the system state, it follows that the state space equation describes the internal dynamic structure of a system and the observation equation shows how the states result in the system output.

Example 2.10. A system described by the ODE (Example 2.1) is SISO LTI. Therefore, its equations in state space are (2.39) and (2.40) with $x(t) = v(t)$ and $y(t) = v_C(t)$. Having $N = 1$, the state variable may be assigned to be $q_1(t) = y(t) = v_C(t)$ and then the state vector becomes of 1×1 dimensions,

$$\mathbf{q}(t) = [q_1(t)].$$

By the known coefficients of the system generalized ODE (2.25): $a_0 = 1/\tau_c$, $a_1 = 1$, and $b_0 = 1/\tau_c$, the matrices of the state space model become, respectively,

$$\mathbf{A} = \left[-\frac{1}{\tau_c} \right], \quad \mathbf{B} = [1], \quad \mathbf{C} = \left[\frac{1}{\tau_c} \right], \quad \text{and} \quad \mathbf{D} = [0].$$

□

The state space model of a MIMO LTI system readily converts to the system transfer function. In fact, by applying the Laplace transform to (2.39), we can write

$$\begin{aligned} s\mathbf{Q}(s) &= \mathbf{A}\mathbf{Q}(s) + \mathbf{B}\mathbf{X}(s), \\ \mathbf{Q}(s) &= (s\mathbf{I} - \mathbf{A})^{-1}\mathbf{B}\mathbf{X}(s), \end{aligned}$$

where \mathbf{I} is an identity matrix and $\mathbf{Q}(s) \stackrel{\mathcal{L}}{\Leftrightarrow} \mathbf{q}(t)$ and $\mathbf{X}(s) \stackrel{\mathcal{L}}{\Leftrightarrow} \mathbf{x}(t)$. The transform of the output equation (2.38) then becomes

$$\mathbf{Y}(s) = [\mathbf{C}(s\mathbf{I} - \mathbf{A})^{-1}\mathbf{B} + \mathbf{D}]\mathbf{X}(s),$$

where $\mathbf{Y}(s) \stackrel{\mathcal{L}}{\Leftrightarrow} \mathbf{y}(t)$, producing

$$\mathbf{H}(s) = \mathbf{C}(s\mathbf{I} - \mathbf{A})^{-1}\mathbf{B} + \mathbf{D}, \tag{2.46}$$

where

$$\mathbf{H}(s) = [H_1(s) H_2(s) \dots H_N(s)]^T$$

is the $N \times 1$ transfer function matrix.

Example 2.11. By the matrices given in Example 2.10, the 1×1 transfer function matrix (2.46) associated with the system ODE (Example 2.1) acquires the component equal to (2.33), namely

$$H(s) = \left[\frac{1}{\tau_c} \right] \left(s[1] - \left[-\frac{1}{\tau_c} \right] \right)^{-1} [1] + [0] = \frac{1}{1 + s\tau_c}.$$

□

On the whole, it follows that all basic methods intended for LTI systems are interchangeable that creates an appreciable convenience and makes the theory of these systems rigorous and strong. The same can be said, in part, about the LTV systems. The case of nonlinear systems is apparently more sophisticated requiring other methods of analysis.

2.3 Common Methods for Nonlinear Systems

So far, we observed the methods intended for linear systems. When a system is nonlinear, the functional dependence between its input and output is described with a nonlinear operator,

$$y(t) = \mathcal{O}(x)x(t), \quad (2.47)$$

that can also be time-varying, $\mathcal{O}(x, t)$. In line with linear systems, both NTI and NTV systems can be described by the ODEs and represented in state space. However, a general solution of the ODE with an arbitrary nonlinearity apparently does not exist, except for some particular cases. Therefore, several other methods were developed to describe nonlinear systems. In the remainder of this Chapter, we shall consider the most common rigorous methods and widely used approximate methods associated with nonlinear systems.

2.3.1 Volterra Series

In linear systems, the output $y(t)$ is coupled with the input $x(t)$ via the impulse response by the convolution (2.20) (LTI systems) or via the time-varying impulse response by the general convolution (2.24) (LTV systems). If a system is memoryless NTI, we commonly expand its output $y(x)$ to the Taylor⁵ series around some point x_0 ,

$$\begin{aligned} y(x) = y(x_0) + \left. \frac{\partial y(x)}{\partial x} \right|_{x=x_0} (x - x_0) + \frac{1}{2} \left. \frac{\partial^2 y(x)}{\partial x^2} \right|_{x=x_0} (x - x_0)^2 \\ + \dots + \frac{1}{k!} \left. \frac{\partial^k y(x)}{\partial x^k} \right|_{x=x_0} (x - x_0)^k + \dots \end{aligned} \quad (2.48)$$

The Volterra⁶ series method considers a system to be nonlinear and memory either. Therefore, the Volterra series is often called the Taylor series with memory. The output accordingly is calculated by the *Volterra series* operator

$$\begin{aligned} y(t) = \mathcal{V}x(t) = H_0x(t) + H_1x(t) + \dots + H_nx(t) + \dots \\ = h_0 + \sum_{n=1}^{\infty} \int_{-\infty}^{\infty} \dots \int_{-\infty}^{\infty} h_n(\theta_1, \dots, \theta_n)x(t - \theta_1) \dots x(t - \theta_n)d\theta_1 \dots d\theta_n, \end{aligned} \quad (2.49)$$

where $h_n(\theta_1, \dots, \theta_n)$ is called the *Volterra kernel*. By these kernels, the components of the series (2.49) are found to possess the important functional properties, namely

⁵ Brook Taylor, English mathematician, 18 August 1685–29 December 1731.

⁶ Vito Volterra, Italian mathematician, 3 May 1860–11 October 1940.

$$H_0x(t) = h_0 \quad (2.50)$$

is a constant (the output with zero input),

$$H_1x(t) = \int_{-\infty}^{\infty} h_1(\theta_1)x(t - \theta_1)d\theta_1 \quad (2.51)$$

is the output (convolution) corresponding to the linear system term, and the rest of the components is calculated similarly:

$$H_2x(t) = \int_{-\infty}^{\infty} \int_{-\infty}^{\infty} h_2(\theta_1, \theta_2)x(t - \theta_1)x(t - \theta_2)d\theta_1d\theta_2, \quad (2.52)$$

$$H_3x(t) = \int_{-\infty}^{\infty} \int_{-\infty}^{\infty} \int_{-\infty}^{\infty} h_3(\theta_1, \theta_2, \theta_3)x(t - \theta_1)x(t - \theta_2)x(t - \theta_3)d\theta_1d\theta_2d\theta_3, \quad (2.53)$$

⋮

An expansion (2.49) suggests that, similarly to any LTI system that is exhaustively characterized by the impulse response, any nonlinear system described by the Volterra series is exhaustively characterized by the Volterra kernels. In fact, the first term (2.50) is a constant value associated with the system output for zero input. The second term (2.51) means nothing more than the response of a linearized system. The third term (2.52) is the system response produced by the square component. The fourth one (2.53) by the cubic component, and so on. Therefore, if a nonlinear system is expandable to the Volterra series, they often call its response to $\delta(t)$ the *generalized impulse response* and say that its output is coupled with the input by the *generalized convolution*.

Example 2.12. Consider an NTI system, in which a signal $x(t)$ goes through a series connection of an LTI filter with the impulse response $h(t)$ and square-law amplifier. The system block diagram can be performed as in Fig. 2.4.

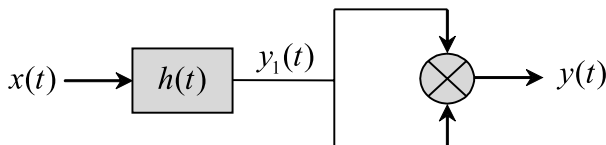


Fig. 2.4. An NTI system with quadratic nonlinearity.

First, the output of a filter can be defined by the convolution

$$y_1(t) = \int_{-\infty}^{\infty} h(\theta)x(t - \theta)d\theta$$

and then the square value of $y_1(t)$ produces the system output

$$\begin{aligned} y(t) = y_1^2(t) &= \int_{-\infty}^{\infty} h(\theta_1)x(t - \theta_1)d\theta_1 \int_{-\infty}^{\infty} h(\theta_2)x(t - \theta_2)d\theta_2 \\ &= \int_{-\infty}^{\infty} \int_{-\infty}^{\infty} h_2(\theta_1, \theta_2)x(t - \theta_1)x(t - \theta_2)d\theta_1d\theta_2, \end{aligned} \tag{2.54}$$

where $h_2(\theta_1, \theta_2) = h(\theta_1)h(\theta_2)$ is the Volterra kernel. The system is thus performed with the only term $H_2x(t)$ (2.52) of the Volterra series (2.49). □

Example 2.13. A linear part of the system (Fig. 2.4) is described with the impulse response $h(t) = \frac{1}{\tau_c}e^{-\frac{t}{\tau_c}}u(t)$ and the input is the unit step $x(t) = u(t)$. The system output is thus the step response defined, by (2.54), to be

$$\begin{aligned} g(t) &= \frac{1}{\tau_c^2} \int_0^t \int_0^t e^{-\frac{\theta_1}{\tau_c}} e^{-\frac{\theta_2}{\tau_c}} d\theta_1 d\theta_2 \\ &= \frac{1}{\tau_c^2} \left(\int_0^t e^{-\frac{\theta}{\tau_c}} d\theta \right)^2 = \left(1 - e^{-\frac{t}{\tau_c}} \right)^2. \end{aligned}$$

□

In spite of a seemingly obvious generality and convertibility of (2.49) to the transform domain, there are two typical problems in applications of the Volterra series: How to measure the Volterra kernels? How to transfer from the system differential equation to the Volterra series? One more problem is that the terms in the Volterra series are not orthogonal, therefore must be identified all at once.

To orthogonalize the Volterra series, Wiener⁷ proposed a solution that is known now as the Wiener method (Chapter 7). The method is based on a simulation of the NTI memory system in a special manner via the functional Volterra series, assuming a Brownian⁸ motion in the input. In line with the Volterra and Wiener approaches, some other methods have been developed, among them the Fliess generating power series. All these methods can equivalently be used in the transform domain. However, effectiveness of series expansions is typically acceptable if systems have weak nonlinearities.

⁷ Norbert Wiener, American scientist, 26 November 1894–18 March 1964.

⁸ Robert Brown, British botanist, 21 December 1773–10 June 1858.

2.3.2 Differential Equation Method

Both NTI and NTV systems can be performed by the N-order nonlinear ODEs with respect to the highest order time derivative of the output as follows, respectively,

$$\frac{d^N y}{dt^N} = f \left(y, \frac{dy}{dt}, \dots, \frac{d^{N-1}y}{dt^{N-1}}, x, \frac{dx}{dt}, \dots, \frac{d^M x}{dt^M} \right), \quad (2.55)$$

$$\frac{d^N y}{dt^N} = f \left(y, \frac{dy}{dt}, \dots, \frac{d^{N-1}y}{dt^{N-1}}, x, \frac{dx}{dt}, \dots, \frac{d^M x}{dt^M}, t \right), \quad (2.56)$$

where $M \leq N$. It is evident that general solutions of these equations cannot be found. Instead, the analytical solutions exist only for several particular cases.

Example 2.14. An NTI system is represented with the block diagram shown in Fig. 2.5. Assign $y_1(t)$ to be the output of the first integrator. Then the system equations for the inputs of each integrator may be written as

$$\begin{aligned} y' &= -0.5y^2 + y_1, \\ y_1' &= bx - ay. \end{aligned}$$

Differentiating the first equation and substituting for the second one leads to the system nonlinear ODE

$$y'' + yy' + ay = bx \quad (2.57)$$

that is modeled by Fig. 2.5 and can be represented in the Volterra form. □

2.3.3 State Space Representation

It is known that any ODE of high order can be represented by the equations system of the first order. If a system is NTI, then its state space model can be performed with the equations

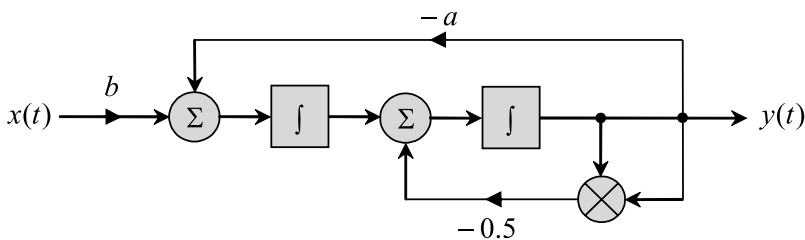


Fig. 2.5. An NTI system with a quadratic nonlinearity.

$$\mathbf{q}'(t) = \Psi[\mathbf{q}(t), \mathbf{x}(t)], \quad (2.58)$$

$$\mathbf{y}(t) = \Upsilon[\mathbf{q}(t), \mathbf{x}(t)], \quad (2.59)$$

where Ψ and Υ are some nonlinear operators. Supposing that both operators are linear, we go from (2.58) and (2.59) to (2.37) and (2.38), respectively.

Example 2.15. Consider an NTI system (Fig. 2.5). Assign its output to be the first state, $q_1(t) = y(t)$, and the output of the second integrator $y_1(t)$ to be the second state, $q_2(t) = y_1(t)$. The system nonlinear state space equations then appear by simple manipulations:

$$\mathbf{q}'(t) = \mathbf{A}[\mathbf{q}(t)]\mathbf{q}(t) + \mathbf{B}x(t),$$

$$y(t) = \mathbf{C}\mathbf{q}(t),$$

where

$$\mathbf{q}(t) = \begin{bmatrix} q_1(t) \\ q_2(t) \end{bmatrix}, \quad \mathbf{A} = \begin{bmatrix} -0.5q_1(t) & 1 \\ -a & 0 \end{bmatrix}, \quad \mathbf{B} = \begin{bmatrix} 0 \\ b \end{bmatrix}, \quad \mathbf{C} = [1 \ 0].$$

Note that these equations cannot be solved in a manner similar to the linear ODEs, in which \mathbf{A} does not depend on the state vector. \square

If a system is NTV, its generalized state space model becomes time-varying,

$$\mathbf{q}'(t) = \Psi[\mathbf{q}(t), \mathbf{x}(t), t], \quad (2.60)$$

$$\mathbf{y}(t) = \Upsilon[\mathbf{q}(t), \mathbf{x}(t), t], \quad (2.61)$$

that evidently complicates a solution. The most well investigated solutions for particular structures of NTI and NTV systems in state space will be considered in the relevant Chapters.

2.4 Approximation and Linearization

Any real electronic system is nonlinear by saturation and not every input-to-output nonlinearity can be described analytically by physical laws. In many cases, the function is first measured and then approximated and linearized. Linearization is often included to the approximation procedure.

2.4.1 Polynomial Approximation

A great deal of nonlinear problems is efficiently solved by polynomial approximation using the Taylor series. For memoryless SISO systems, (2.48) is usually written as an approximating k -degree polynomial

$$y(x) = y(x_0) + a_1(x - x_0) + a_2(x - x_0)^2 + \dots + a_k(x - x_0)^k, \quad (2.62)$$

for which the coefficients a_k are calculated analytically by $a_k = \frac{1}{k!} \frac{\partial^k y(x)}{\partial x^k} \Big|_{x=x_0}$ or determined experimentally. If the point x_0 is fixed, then (2.62) is very often written for increments of the variable and function, namely as

$$\Delta y = a_1 \Delta x + a_2 \Delta x^2 + \dots + a_k \Delta x^k, \quad (2.63)$$

where $\Delta y = y(x) - y(x_0)$ and $\Delta x = x - x_0$.

Example 2.16. The input-to-output dependence $y(x)$ of a system was measured at three points: $y(0) = 0$, $y(1) = 1$, and $y(2) = 3$. By (2.63), the coefficients of the approximating polynomial of the second degree, $y(x) = a_1 x + a_2 x^2$, are defined by solving the equations $1 = a_1 + a_2$ and $3 = 2a_1 + 4a_2$ to be $a_1 = a_2 = 0.5$. That yields $y(x) = 0.5x(1 + x)$. Fig. 2.6a shows the measured points along with the approximating curve. \square

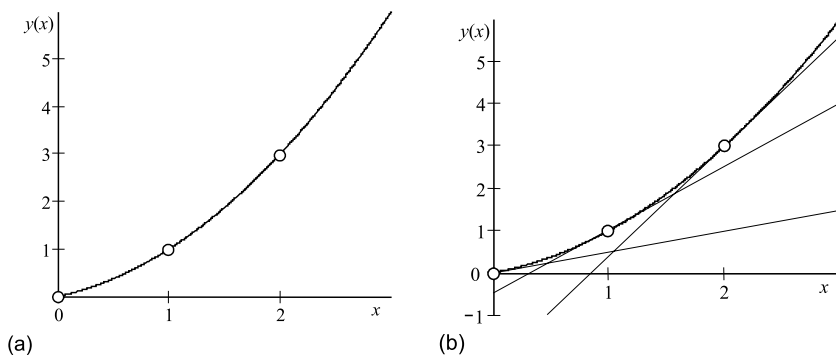


Fig. 2.6. Measured nonlinear function: (a) approximation and (b) linearization.

2.4.2 Methods of Linearization

The most common method of analytical linearization implies describing a nonlinear system by linear functions around some points. Linearization may be provided by the piecewise-linear (PWL) approach or linear spline interpolation. Exponential, quadratic, cubic, and other piecewise-functions and splines are also often used.

Analytic Linearization

Analytic linearization of the input-to-output dependence around some operation point is provided by saving only two first terms (constant and linear)

in the Taylor series (2.48). If a nonlinear SISO system is memoryless, then a linearizing expansion in the vicinity of x_0 becomes, by (2.48),

$$y(x) \cong y(x_0) + a_1(x - x_0), \quad (2.64)$$

where the coefficient

$$a_1 = \left. \frac{\partial y(x)}{\partial x} \right|_{x=x_0} \quad (2.65)$$

is defined either analytically or experimentally.

Example 2.17. Given a memoryless SISO system represented with $y(x) = 0.5x(1 + x)$ (Example 2.16). By (2.65), we have $a_1 = 0.5 + x_0$ and then, by (2.64), the linearizing function becomes

$$y(x) = y(x_0) + \left(\frac{1}{2} + x_0 \right) (x - x_0).$$

Fig. 2.6b shows this line at three discrete points $y(0) = 0$, $y(1) = 1$, and $y(2) = 3$. \square

Linearization of Nonlinear ODE

Likewise, linearization can be obtained for the N -order nonlinear ODE (2.55). The Taylor expansion is applied at some desirable operation point x_0, y_0 with seemingly known derivatives $y'_0, y''_0, \dots, y_0^{(N)}$, $x'_0, x''_0, \dots, x_0^{(M)}$. Only constant and linear terms are saved and a linearized equation is complete:

$$\begin{aligned} \tilde{y}^{(N)}(t) &= \left. \frac{\partial f}{\partial y} \right|_0 \tilde{y}(t) + \left. \frac{\partial f}{\partial y'} \right|_0 \tilde{y}'(t) + \dots + \left. \frac{\partial f}{\partial y^{(N-1)}} \right|_0 \tilde{y}^{(N-1)}(t) + \dots \\ &+ \left. \frac{\partial f}{\partial x} \right|_0 \tilde{x}(t) + \left. \frac{\partial f}{\partial x'} \right|_0 \tilde{x}'(t) + \dots + \left. \frac{\partial f}{\partial x^{(M)}} \right|_0 \tilde{x}^{(M)}(t), \end{aligned} \quad (2.66)$$

where

$$\left. \frac{\partial f}{\partial \text{var}} \right|_0 \triangleq \left. \frac{\partial f}{\partial \text{var}} \right|_{x=x_0, y=y_0, x^m=x_0^m, y^m=y_0^m},$$

$n = 1, 2, \dots, N - 1$, $m = 1, 2, \dots, M$, and, for the sake of accuracy, all increments

$$\begin{aligned} \tilde{y} &= y - y_0, \quad \tilde{y}' = y' - y'_0, \quad \dots, \quad \tilde{y}^{(N-1)} = y^{(N-1)} - y_0^{(N-1)}, \\ \tilde{x} &= x - x_0, \quad \tilde{x}' = x' - x'_0, \quad \dots, \quad \tilde{x}^{(M)} = x^{(M)} - x_0^{(M)} \end{aligned}$$

are commonly preserved to be reasonably small. By assigning

$$\tilde{a}_0 = \left. \frac{\partial f}{\partial y} \right|_0, \quad \tilde{b}_0 = \left. \frac{\partial f}{\partial x} \right|_0, \quad \tilde{a}_n = \left. \frac{\partial f}{\partial y^{(n)}} \right|_0, \quad \text{and} \quad \tilde{b}_n = \left. \frac{\partial f}{\partial x^{(m)}} \right|_0, \quad (2.67)$$

(2.66) becomes a linear ODE

$$\begin{aligned} \tilde{y}^N(t) &= \tilde{a}_0 \tilde{y}(t) + \tilde{a}_1 \tilde{y}'(t) + \dots + \tilde{a}_{N-1} \tilde{y}^{(N-1)}(t) + \dots \\ &\quad + \tilde{b}_0 \tilde{x}(t) + \tilde{b}_1 \tilde{x}'(t) + \dots + \tilde{b}_M \tilde{x}^{(M)}(t) \end{aligned} \quad (2.68)$$

that can be written in the standard form (2.25) and then solved, by $a_N = 1$. In time-varying problems, the operation point changes with time, $y_0(t)$ and $x_0(t)$. Therefore, the ODE linearized by (2.68) possesses at least one time-varying coefficient.

Example 2.18. An NTI system is given with the ODE (2.57),

$$y'' = -yy' - ay + bx.$$

By (2.67), the coefficients are defined to be $\tilde{a}_0 = -y'_0 - a$, $\tilde{a}_1 = -y_0$, and $\tilde{b}_0 = b$ and then the linearized ODE becomes

$$\tilde{y}'' = -(y'_0 + a)\tilde{y} - y_0\tilde{y}' + b\tilde{x},$$

having a general solution. □

Linearization of State Space Model

In a manner similar to the ODEs, an NTI system state space model, (2.58) and (2.59), can also be linearized. Assume that the system is examined in the vicinity of the point \mathbf{y}_0 , \mathbf{x}_0 corresponding to the state \mathbf{q}_0 and its time derivative \mathbf{q}'_0 . The actual system state, input, and output may then be defined by, respectively,

$$\mathbf{q}(t) = \mathbf{q}_0(t) + \tilde{\mathbf{q}}(t), \quad (2.69)$$

$$\mathbf{x}(t) = \mathbf{x}_0(t) + \tilde{\mathbf{x}}(t), \quad (2.70)$$

$$\mathbf{y}(t) = \mathbf{y}_0(t) + \tilde{\mathbf{y}}(t), \quad (2.71)$$

where $\tilde{\mathbf{q}}(t)$, $\tilde{\mathbf{x}}(t)$, and $\tilde{\mathbf{y}}(t)$ are small time varying increments. By (2.69)–(2.71), the state space model, (2.58) and (2.59), transforms to

$$\mathbf{q}'_0(t) + \tilde{\mathbf{q}}'(t) = \mathbf{\Psi}[\mathbf{q}_0(t) + \tilde{\mathbf{q}}(t), \mathbf{x}_0(t) + \tilde{\mathbf{x}}(t)], \quad (2.72)$$

$$\mathbf{y}_0(t) + \tilde{\mathbf{y}}(t) = \mathbf{\Upsilon}[\mathbf{q}_0(t) + \tilde{\mathbf{q}}(t), \mathbf{x}_0(t) + \tilde{\mathbf{x}}(t)]. \quad (2.73)$$

Expanding both sides of these equations to the Taylor series and truncating for the constant and linear terms makes them linearized in the forms of (2.37) and (2.38), respectively,

$$\tilde{\mathbf{q}}'(t) = \mathbf{A}\tilde{\mathbf{q}}(t) + \mathbf{B}\tilde{\mathbf{x}}(t), \quad (2.74)$$

$$\tilde{\mathbf{y}}(t) = \mathbf{C}\tilde{\mathbf{q}}(t) + \mathbf{D}\tilde{\mathbf{x}}(t), \quad (2.75)$$

in which all matrices are Jacobian being predetermined by

$$\mathbf{A} = \left. \frac{\partial \Psi}{\partial \mathbf{q}} \right|_0, \quad \mathbf{B} = \left. \frac{\partial \Psi}{\partial \mathbf{x}} \right|_0, \quad \mathbf{C} = \left. \frac{\partial \Upsilon}{\partial \mathbf{q}} \right|_0, \quad \mathbf{D} = \left. \frac{\partial \Upsilon}{\partial \mathbf{x}} \right|_0, \quad (2.76)$$

where Φ and Υ are taken from (2.58) and (2.59), respectively.

Because the approach is the same, the linearized state space model is akin to the linearized nonlinear ODE having the same range of applications.

Example 2.19. Following Example 2.14, an NTI system (Fig. 2.5) is described in state space with

$$\mathbf{q}'(t) = \Psi[\mathbf{q}(t), \mathbf{x}(t)], \quad (2.77)$$

$$\mathbf{y}(t) = \mathbf{C}\mathbf{q}(t), \quad (2.78)$$

where

$$\mathbf{q}(t) = \begin{bmatrix} q_1(t) \\ q_2(t) \end{bmatrix} \quad \text{and} \quad \Psi = \begin{bmatrix} -0.5q_1^2(t) + q_2(t) \\ -aq_1(t) + bx(t) \end{bmatrix}. \quad (2.79)$$

By (2.76), the matrices of the linearized equations (2.74) and (2.75) are defined to be

$$\mathbf{A} = \begin{bmatrix} -q_{10}(t) & 1 \\ -a & 0 \end{bmatrix}, \quad \mathbf{B} = \begin{bmatrix} 0 \\ b \end{bmatrix}, \quad \mathbf{C} = [1 \ 0], \quad \mathbf{D} = [0]. \quad (2.80)$$

Because $y(t) = q_1(t)$, the matrix equations may be performed as

$$\begin{bmatrix} y'(t) \\ q_2'(t) \end{bmatrix} = \begin{bmatrix} -y_0(t) & 1 \\ -a & 0 \end{bmatrix} \begin{bmatrix} y(t) \\ q_2(t) \end{bmatrix} + \begin{bmatrix} 0 \\ b \end{bmatrix} x \quad (2.81)$$

that, equivalently, leads to

$$y'(t) = -y_0(t)y(t) + q_2(t), \quad (2.82)$$

$$q_2'(t) = -ay(t) + bx(t). \quad (2.83)$$

By differentiating (2.82) and substituting for the second equation (2.83), one arrives at the same linearized equation as in Example 2.18. \square

Linearization Techniques

Technical linearization implies using some auxiliary nonlinear blocks to make the system linear. Several linearization techniques are used, among them the feedforward linearization, feedback linearization, and nonlinear predistortion of signals can most frequently be met in designs. The linearization techniques are expounded in Chapter 7.

2.5 Averaging

Special approximate methods of *averaging* have been developed for centuries to investigate the fundamental properties of nonlinear systems. The approach relates to the closed loop systems typically modeled with the nonlinear ODE of the second order

$$y'' + \omega_0^2 y = \epsilon f(y, y'), \quad (2.84)$$

where $f(y, y')$ is a nonlinear function, $\epsilon \sim 2\delta$ is a small parameter proportional to the open system bandwidth $2\delta \ll \omega_0$, and ω_0 is the system resonance angular frequency. If a system is of higher order, then, by small ϵ , its high order time derivatives are commonly reduced to y or y' . A solution of (2.84) is usually found by linearization and many linearization methods are based on averaging.

The history of application of averaging to different physical system problems returns us back to the works of Lagrange⁹, Poisson¹⁰, Poincaré¹¹, Laplace, Lyapunov¹², Brillouin¹³, Wentzel¹⁴ Kramers¹⁵ (BWK method), and many others. However, a historical breakthrough was done only in the 1920s by van der Pol¹⁶ with his heuristical method of “slowly changing amplitude”. Considering solely an electronic oscillator, van der Pol, virtually, discovered a new approach to solve a great deal of problems in vibrating and oscillating nonlinear systems. Soon after, in the 1930s, Krylov¹⁷ with his student Bogoliubov¹⁸ justified the van der Pol method mathematically, extended it to higher-order approximations, and presented the *asymptotic theory* of oscillations. The first-order approximation of the *asymptotic method* was then widely cited as the Krylov-Bogoliubov (KB) method. Thereafter, the theory has been extended by Krylov, Bogoliubov, and Mitropolskiy¹⁹ to the other method known as the *equivalent linearization* associated with *harmonic balance*. Furthermore, the theory was greatly developed by Bogoliubov and his student Mitropolskiy and the asymptotic method of the higher-order approximations was called the Krylov-Bogoliubov-Mitropolskiy (KBM) method (also

⁹ Joseph-Louis Lagrange, French/Italian mathematician, 25 January 1736–10 April 1813.

¹⁰ Simon Denis Poisson, French mathematician, 21 June 1781–25 April 1840.

¹¹ Jules Henri Poincaré, French mathematician, 29 April 1854–17 July 1912.

¹² Aleksandr Mikhailovich Lyapunov, Russian/Ukrainian mathematician, 6 June 1857–3 November 1918.

¹³ Léon Nicolas Brillouin, French physicist, 7 August 1889–4 October 1969.

¹⁴ Georg Wentzel, German/Swiss physicist, 17 February 1898–12 August 1978.

¹⁵ Hendrik Antony Kramers, Dutch physicist, 17 December 1894–24 April 1952.

¹⁶ van der Pol, Balthasar, Dutch engineer, 1889–1959.

¹⁷ Nikolay Mitrofanovich Krylov, Russian born Ukrainian mathematician, 29 November 1879–11 May 1955.

¹⁸ Nikolai Nikolaevich Bogoliubov, Russian born Ukrainian mathematician, 21 August 1909–13 February 1992.

¹⁹ Yuriy Alekseevich Mitropolskiy, Ukrainian mathematician, 1917– .

cited as the *generalized method of averaging*). In line with these works, albeit not commonly, several other approaches are also used, among them the shortened (truncated) equations method, averaging by transforming variables (canonical variables method), and others.

It is worth remembering that almost all approximate methods elaborated for nonlinear systems are applicable for linear systems with sometimes a shorter way, although approximate, to reach the result.

2.5.1 Method of Expansion (Perturbation Method)

Even though the *perturbation method* (or *method of expansion*) does not exploit an idea of averaging straightforwardly, it is an asymptotic approach. We therefore shall consider it in conjunction with the methods of averaging.

Historically, an application of the perturbation method to nonlinear problems was first formulated by Poisson, then studied by many scientists, and finally generalized by Poincaré.

An idea of the method is to perform a solution for (2.84) by the series

$$y = y_0 + \epsilon y_1 + \epsilon^2 y_2 + \dots + \epsilon^n y_n + \dots = \sum_{i=0}^{\infty} \epsilon^i y_i. \quad (2.85)$$

Substituting (2.85) to (2.84) formally produces

$$\sum_{i=0}^{\infty} \epsilon^i y_i'' + \omega_0^2 \sum_{i=0}^{\infty} \epsilon^i y_i = -\epsilon f \left(\sum_{i=0}^{\infty} \epsilon^i y_i, \sum_{i=0}^{\infty} \epsilon^i y_i' \right). \quad (2.86)$$

Supposing that the nonlinear function is multiply differentiable (so analytic), the right-hand side of (2.86) is expanded, by the method, to the Taylor series for the powers of a small parameter ϵ . Herewith, the terms with ϵ^i are discarded if i is higher than n . Equating the coefficients of ϵ^i , $i \leq n$, yields the equations

$$\begin{aligned} y_0'' + \omega_0^2 y_0 &= 0, \\ y_1'' + \omega_0^2 y_1 &= f(y_0, y_0'), \\ y_2'' + \omega_0^2 y_2 &= f_y'(y_0, y_0') y_1 + f_{y'}'(y_0, y_0') y_1', \\ &\vdots \end{aligned} \quad (2.87)$$

further solved for the unknown values of y_0, y_1, \dots, y_n .

It can be shown that the series expansion often predetermines a critical disadvantage neatly demonstrated by a harmonic wave

$$\sin(\omega_0 + \epsilon)t = \sin \omega_0 t + \epsilon t \cos \omega_0 t - \frac{\epsilon^2 t^2}{2!} \sin \omega_0 t - \frac{\epsilon^3 t^3}{3!} \cos \omega_0 t + \dots$$

As it is seen, in line with the first harmonic term $\sin \omega_0 t$, there exist the so-called *secular terms*, which amplitudes increase with time infinitely. It is evident that, by large n and relatively short observation time, the secular terms will compensate each other. In practice, however, only small n is of importance. Therefore, the perturbation method has not gained wide currency in the nonlinear system problems.

2.5.2 Van der Pol's Method

Let us come back to the closed loop system equation $y'' + a(1 - K)y' + by = 0$ (1.45), set $a = -\epsilon$, $b = \omega_0^2$, and $K = y^2$, and represent it in the form of (2.84). We thus arrive at what is known as the *van der Pol oscillator equation*,

$$y'' + \omega_0^2 y = \epsilon(1 - y^2)y', \quad (2.88)$$

in which the nonlinear function is represented with $f(y, y') = (1 - y^2)y'$. Note that the classical van der Pol oscillator is normalized for the dimensionless time $\tau = \omega_0 t$ to be

$$y'' + y = \epsilon(1 - y^2)y', \quad (2.89)$$

where $\epsilon \sim 2\delta/\omega_0 = 1/Q \ll 1$, and Q is the *quality factor* of an open system.

An heuristical (although correct!) suggestion by van der Pol was to find a solution of (2.88) in the forms of

$$y = r \cos \psi, \quad (2.90)$$

$$y' = -\omega_0 r \sin \psi, \quad (2.91)$$

where $\psi(t) = \omega_0 t + \vartheta(t)$ and $\vartheta(t)$ is a time-varying phase. In further, validity of (2.90) and (2.91) was justified by many authors and these forms have become a common feature of most of the methods considering the amplitude $r(t)$ and phase $\vartheta(t)$ of harmonic oscillations as slowly varying with time.

Now, let us write the first time-derivative of (2.90) completely:

$$y' = r' \cos \psi - \omega_0 r \sin \psi - \vartheta' r \sin \psi. \quad (2.92)$$

Since we also want to allow (2.91), the following constraint appears, by comparing (2.92) and (2.91),

$$r' \cos \psi - \vartheta' r \sin \psi = 0. \quad (2.93)$$

Substituting (2.90) and (2.91) to (2.84) produces

$$r' \sin \psi + \vartheta' r \cos \psi = -\frac{\epsilon}{\omega_0} f(r \cos \psi, -\omega_0 r \sin \psi) \quad (2.94)$$

and, by solving (2.94) with (2.93), we arrive at the solutions

$$r' = -\frac{\epsilon}{\omega_0} f(r \cos \psi, -\omega_0 r \sin \psi) \sin \psi, \quad (2.95)$$

$$\vartheta' = -\frac{\epsilon}{\omega_0 r} f(r \cos \psi, -\omega_0 r \sin \psi) \cos \psi. \quad (2.96)$$

Because both functions, r and ϑ , are presumed to change slowly, they may also be assumed to be constants during period $T = 2\pi/\omega$. Based upon this and averaging (2.95) and (2.96) over T , we arrive at

$$r' = -\frac{\epsilon}{2\pi\omega_0} \int_0^{2\pi} f(r \cos \psi, -\omega_0 r \sin \psi) \sin \psi \, d\psi, \quad (2.97)$$

$$\vartheta' = -\frac{\epsilon}{2\pi\omega_0 r} \int_0^{2\pi} f(r \cos \psi, -\omega_0 r \sin \psi) \cos \psi \, d\psi. \quad (2.98)$$

For the van der Pol equation (2.88), substituting $f(y, y')$ to (2.97) and (2.98) first gives

$$r' = \frac{\epsilon}{2\pi} \int_0^{2\pi} r(1 - r^2 \cos^2 \psi) \sin^2 \psi \, d\psi, \quad (2.99)$$

$$\vartheta' = \frac{\epsilon}{4\pi r} \int_0^{2\pi} r(1 - r^2 \cos^2 \psi) \sin 2\psi \, d\psi \quad (2.100)$$

and then leads to the final ODEs regarding the amplitude and phase, respectively,

$$r' = \frac{\epsilon}{2} r \left(1 - \frac{r^2}{4} \right), \quad (2.101)$$

$$\vartheta' = 0. \quad (2.102)$$

To solve (2.101), it is in order, first, to change a variable, $z = r^2$, then separate variables, and integrate the both sides to get

$$\int \frac{dz}{z(z-4)} = -\frac{\epsilon}{4} t + C,$$

where C is an integration constant. An integral identity $\int \frac{dx}{x(x+a)} = \frac{1}{a} \ln \left| \frac{x}{x+a} \right|$ then leads to

$$\begin{aligned} -\frac{1}{4} \ln \left| \frac{z}{z-4} \right| &= \frac{1}{4} \ln \left| \frac{z-4}{z} \right| = -\frac{\epsilon}{4} t + C, \\ \ln \left| 1 - \frac{4}{z} \right| &= -\epsilon t + 4C, \quad 1 - \frac{4}{z} = e^{-\epsilon t} e^{4C}, \\ z &= \frac{4}{1 - e^{-\epsilon t} e^{4C}}, \quad \text{and} \quad r = \frac{2}{\sqrt{1 - e^{-\epsilon t} e^{4C}}}. \end{aligned}$$

For the initial value of $r_0 = 0$, the last relation produces $e^{4C} = 1 - \frac{4}{r_0^2}$ and the solution finally becomes

$$r(t) = \frac{2}{\sqrt{1 + \left(\frac{4}{r_0^2} - 1\right) e^{-\epsilon t}}}. \quad (2.103)$$

Hence, van der Pol's oscillator generates oscillations

$$y(t) = r(t) \cos(\omega_0 t + \vartheta_0)$$

with a constant phase ϑ_0 and the transient in the amplitude determined by (2.103). Fig. 2.7 illustrates (2.103) for the particular values of $r_0 = 0.01$, $\epsilon = 0.1$, $\omega_0 = 1$, and $\vartheta_0 = 0$. It is seen that the oscillations sustain at $r(t) = r_0 = 2$.

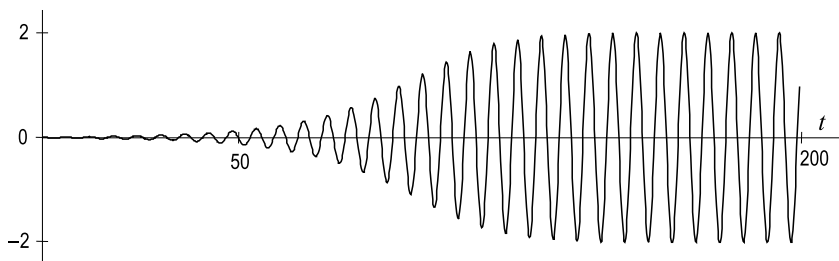


Fig. 2.7. Oscillations in van der Pol's oscillator with $r_0 = 0.01$, $\epsilon = 0.1$, $\omega_0 = 1$, and $\vartheta_0 = 0$.

An importance of van der Pol's equation (2.88) resides in the fact that it models with a sufficient accuracy a great deal of particular oscillator schemes. On the other hand, the method ignores high harmonics [a solution of (2.102) produces a constant ϑ_0] and, consequently, does not allow us to evaluate the effect caused by the amplitude-to-phase conversion associated with nonlinearities. This disadvantage is overcome in the asymptotic methods.

2.5.3 Asymptotic Methods of Krylov-Bogoliubov-Mitropolskiy

Created by Krylov and Bogoliubov and thereafter developed by Bogoliubov and Mitropolskiy, the asymptotic methods are mathematically rigorous.

The main idea of the approach is to find a solution for (2.84) in a series form of

$$y = r \cos \psi + \epsilon u_1(r, \psi) + \epsilon^2 u_2(r, \psi) + \epsilon^3 u_3(r, \psi) + \dots, \quad (2.104)$$

where $u_1(r, \psi)$, $u_2(r, \psi)$, \dots are 2π -periodic functions of ψ , and slowly changing with time the values of r and ψ are defined by the differential equations, respectively,

$$r' = \epsilon A_1(r) + \epsilon^2 A_2(r) + \dots, \quad (2.105)$$

$$\psi' = \omega_0 + \epsilon B_1(r) + \epsilon^2 B_2(r) + \dots, \quad (2.106)$$

in which the functions $A_1(r)$, $A_2(r)$, \dots , $B_1(r)$, $B_2(r)$, \dots are determined by averaging the nonlinear functions of the relevant harmonics of oscillations.

Typically, dealing with high order terms of the asymptotic series entail difficulties. On the other hand, only the amplitude and its influence upon the phase are commonly of practical importance. Therefore, application of the method is usually restricted with the first and second orders of approximation.

The First Order Approximation

In the first order approximation, equations (2.105) and (2.106) are shortened to, respectively,

$$r' = \epsilon A_1(r), \quad (2.107)$$

$$\psi' = \omega_0 + \epsilon B_1(r), \quad (2.108)$$

and the functions $A_1(r)$ and $B_1(r)$ are given by, respectively,

$$A_1(r) = -\frac{1}{2\pi\omega_0} \int_0^{2\pi} f(r \cos \psi, -r\omega_0 \sin \psi) \sin \psi \, d\psi, \quad (2.109)$$

$$B_1(r) = -\frac{1}{2\pi r\omega_0} \int_0^{2\pi} f(r \cos \psi, -r\omega_0 \sin \psi) \cos \psi \, d\psi. \quad (2.110)$$

As follows from a comparison of (2.97), (2.98) and (2.107), (2.110), the first order approximation of the Krylov and Boboliubov asymptotic method coincides with the van der Pol method.

The Second Order Approximation

In the second order approximation, a solution is found as

$$y = r \cos \psi + \epsilon u_1(r, \psi), \quad (2.111)$$

where the function $u_1(r, \psi)$ is defined by the series

$$u_1(r, \psi) = \frac{g_0(r)}{\omega_0^2} - \frac{1}{\omega_0^2} \sum_{n=2}^{\infty} \frac{g_n(r) \cos n\psi + h_n(r) \sin n\psi}{n^2 - 1}, \quad (2.112)$$

in which

$$g_n(r) = \frac{1}{\pi} \int_0^{2\pi} f(r \cos \psi, -r\omega_0 \sin \psi) \cos n\psi \, d\psi, \quad (2.113)$$

$$h_n(r) = \frac{1}{\pi} \int_0^{2\pi} f(r \cos \psi, -r\omega_0 \sin \psi) \sin n\psi \, d\psi. \quad (2.114)$$

The slowly changing averaged amplitude and phase are described by, respectively,

$$r' = \epsilon A_1(r) + \epsilon^2 A_2(r), \quad (2.115)$$

$$\psi' = \omega_0 + \epsilon B_1(r) + \epsilon^2 B_2(r), \quad (2.116)$$

where, the functions $A_1(r)$ and $B_1(r)$ are still given by (2.109) and (2.110), respectively. The remaining functions are defined with

$$A_2(r) = -\frac{1}{2\omega_0} \left(2A_1 B_1 + A_1 \frac{\partial B_1}{\partial r} r \right) - \frac{1}{2\pi\omega_0} \int_0^{2\pi} \left[u_1(r, \psi) f'_y + \left(A_1 \cos \psi - r B_1 \sin \psi + \omega_0 \frac{\partial u_1}{\partial \psi} \right) f'_{y'} \right] \sin \psi \, d\psi, \quad (2.117)$$

$$B_2(r) = -\frac{1}{2\omega_0} \left(B_1^2 - \frac{A_1}{r} \frac{\partial A_1}{\partial r} \right) - \frac{1}{2\pi\omega_0 r} \int_0^{2\pi} \left[u_1(r, \psi) f'_y + \left(A_1 \cos \psi - r B_1 \sin \psi + \omega_0 \frac{\partial u_1}{\partial \psi} \right) f'_{y'} \right] \cos \psi \, d\psi, \quad (2.118)$$

where

$$f'_y = \frac{\partial f(y, y')}{\partial y} \Big|_{\substack{y=r \cos \psi \\ y'=-r\omega_0 \sin \psi}}, \quad f'_{y'} = \frac{\partial f(y, y')}{\partial y'} \Big|_{\substack{y=r \cos \psi \\ y'=-r\omega_0 \sin \psi}}.$$

The reader should not be confused by complexity of the functions $u_1(r, \psi)$, $A_2(r)$ and $B_2(r)$, since they are given in the most common forms. For particular NTI systems, substantial simplifications could take place that we demonstrate below traditionally analyzing the van der Pol's oscillator.

Example 2.20 (Solutions of van der Pol's equation in the second order approximation). Consider van der Pol's equation (2.89) and find its solutions in the second-order approximation by the asymptotic method.

We first transform (2.113) and (2.114) and realize that

$$g_n(r) = 0|_{n \geq 0}, \quad h_n(r) = \begin{cases} r^3/4, & n = 3 \\ 0, & n \neq 3 \end{cases}.$$

The function (2.112) is then defined to be

$$u_1(r, \psi) = -\frac{r^3}{32\omega_0} \sin 3\psi$$

and the solution (2.111) in the second order approximation becomes

$$y = r \cos \psi - \frac{\epsilon r^3}{32\omega_0} \sin 3\psi. \quad (2.119)$$

To obtain the functions of the slowly changing r and ψ , we first determine

$$f'_y = r^2 \omega_0 \sin 2\psi, \quad f'_{y'} = 1 - r^2 \cos^2 \psi$$

and thereafter, by (2.117) and (2.118), define

$$A_2(r) = 0, \quad B_2(r) = -\frac{1}{8} + \frac{r^2}{8} - \frac{7r^4}{256}.$$

By (2.115) and (2.116), the differential equations for the time-varying amplitude and phase become, respectively,

$$r' = \frac{\epsilon}{2} r \left(1 - \frac{r^2}{4} \right), \quad (2.120)$$

$$\psi' = \omega_0 - \frac{\epsilon^2}{8\omega_0} \left(1 - r^2 + \frac{7r^4}{32} \right). \quad (2.121)$$

A solution of (2.120) is given by (2.103) that allows integrating (2.121) straightforwardly to obtain a solution

$$\psi = \omega_0 t - \frac{\epsilon^2}{8\omega_0} \left(1 - r^2 + \frac{7r^4}{32} \right) t + \vartheta_0, \quad (2.122)$$

where ϑ_0 is an initial phase.

We then deduce that, in the second order approximation, the amplitude of van der Pol's oscillator is still obtained by the first order approximation and that the main effect is in the amplitude-to-phase conversion produced by the second term in the right-hand side of (2.122). \square

Overall, asymptotic approximation in the first order (error $\sim \epsilon^2$) gives solutions for the variable amplitude and constant phase, second order (error $\sim \epsilon^3$) contributes for with the amplitude-to-phase conversion, third order (error $\sim \epsilon^4$) accounts for the phase-to-amplitude conversion, and so on. Let us notice again that, since of prime importance is the amplitude behavior and its influence upon the phase, an analysis is usually restricted with the first and second order approximations.

2.5.4 Systems with Slowly Changing Parameters

Bogoliubov and Mitropolskiy showed that the asymptotic approach still can be useful if a closed loop system is NTV and its coefficients change with time slowly as compared to period T . It was also shown that a generalized form of the ODE for such systems is written as

$$[m(\tau)y']' + k(\tau)y = \epsilon f(\tau, y, y'), \quad (2.123)$$

where $\tau = \epsilon t$ is a “slow” time. The model implies that the coefficients, $m(\tau)$ and $k(\tau)$, are both nonzero and multiply differentiable (analytical) on the observable time interval.

A solution of (2.123) is searched in frames of the asymptotic methods as

$$y = r \cos \psi + \epsilon u_1(\tau, r, \psi) + \epsilon^2 u_2(\tau, r, \psi) + \dots, \quad (2.124)$$

where the functions $u_1(\tau, r, \psi)$, $u_2(\tau, r, \psi)$, \dots are 2π -periodic regarding an angle ψ . The amplitude and phase associated with (2.124) are then defined by the ODEs, respectively,

$$r' = \epsilon A_1(\tau, r) + \epsilon^2 A_2(\tau, r) + \dots, \quad (2.125)$$

$$\psi' = \omega_0(\tau) + \epsilon B_1(\tau, r) + \epsilon^2 B_2(\tau, r) + \dots, \quad (2.126)$$

where

$$\omega_0^2(\tau) = \frac{k(\tau)}{m(\tau)} \quad (2.127)$$

defines the square natural frequency. As well as for (2.84), here the functions $A_1(\tau, r)$, $A_2(\tau, r)$, \dots , $B_1(\tau, r)$, $B_2(\tau, r)$, \dots are determined by averaging the nonlinear function in the right-hand side of (2.123) from 0 to 2π over ψ for the relevant harmonic of oscillations. The first and second orders of approximation obtained by this approach are observed below.

The First Order Approximation

It seems obvious that in the first order approximation a solution of (2.123) is still found as

$$y = r \cos \psi, \quad (2.128)$$

where the amplitude and phase are defined by the restricted series (2.125) and (2.126), respectively,

$$r' = \epsilon A_1(\tau, r), \quad (2.129)$$

$$\psi' = \omega_0(\tau) + \epsilon B_1(\tau, r). \quad (2.130)$$

For the time-varying coefficients, the functions $A_1(\tau, r)$ and $B_1(\tau, r)$ are given by, respectively,

$$A_1(\tau, r) = -\frac{r}{2m(\tau)\omega_0(\tau)} \frac{d[m(\tau)\omega_0(\tau)]}{d\tau} - \frac{1}{2\pi m(\tau)\omega_0(\tau)} \int_0^{2\pi} f_0(\tau, r, \psi) \sin \psi \, d\psi, \quad (2.131)$$

$$B_1(\tau, r) = -\frac{1}{2\pi r m(\tau)\omega_0(\tau)} \int_0^{2\pi} f_0(\tau, r, \psi) \cos \psi \, d\psi, \quad (2.132)$$

where

$$f_0(\tau, r, \psi) = f[\tau, r \cos \psi, -r\omega_0(\tau) \sin \psi]. \quad (2.133)$$

An important conclusion follows instantly. Because the time-varying parameters, $m(\tau)$ and $k(\tau)$, affect both A_1 and B_1 , one should expect variations in both the amplitude and phase.

Example 2.21 (Van der Pol's oscillator with modulated frequency).

We will now think that the frequency of van der Pol's oscillator is harmonically modulated with a small amplitude $a \ll 1$ and frequency $0 < \Omega \sim \epsilon \ll \omega_0$; that is,

$$\omega_0(t) = \omega_0(1 + a \cos \Omega t). \quad (2.134)$$

The equation (2.84) may therefore be written as

$$y'' + \omega_0^2(1 + a \cos \gamma \tau)^2 y = \epsilon(1 - y^2)y', \quad (2.135)$$

where $\tau = \epsilon t$ and $\gamma = \Omega/\epsilon$. In terms of (2.123), this gives the coefficients $m(\tau) = 1$ and $k(\tau) = \omega_0^2(1 + a \cos \gamma \tau)^2$.

By (2.131) and (2.132), the functions $A_1(\tau, r)$ and $B_1(\tau, r)$ become, respectively,

$$A_1(\tau, r) \cong \frac{r}{2} \left(1 - \frac{r^2}{4}\right) + \frac{r}{2} a \gamma \sin \gamma \tau, \quad (2.136)$$

$$B_1(\tau, r) = 0 \quad (2.137)$$

that transforms (2.129) and (2.130) to, respectively,

$$r' = \frac{\epsilon}{2} r \left(1 - \frac{r^2}{4}\right) + \frac{\epsilon}{2} r a \gamma \sin \gamma \tau, \quad (2.138)$$

$$\psi' = \omega_0(1 + a \cos \gamma \tau). \quad (2.139)$$

It is seen that the first time derivative of the phase (2.139) equals exactly to the function (2.134) of a modulated frequency. Herewith, the amplitude (2.138) also undergoes modulation. Inherently, by $\gamma = 0$, both equations become solutions of the classical van der Pol oscillator. \square

The Second Order Approximation

In the second order approximation, a solution (2.124) saves two terms,

$$y = r \cos \psi + \epsilon u_1(\tau, r, \psi), \quad (2.140)$$

where r and ψ are defined by equations of the second order approximation

$$r' = \epsilon A_1(\tau, r) + \epsilon^2 A_2(\tau, r), \quad (2.141)$$

$$\psi' = \omega_0(\tau) + \epsilon B_1(\tau, r) + \epsilon^2 B_2(\tau, r). \quad (2.142)$$

The functions $A_1(\tau, r)$ and $B_1(\tau, r)$ are still defined by (2.131) and (2.132), respectively. Expressions for $A_2(\tau, r)$ and $B_2(\tau, r)$ are given below, respectively,

$$\begin{aligned} A_2(\tau, r) = & -\frac{1}{2\omega_0(\tau)} \left[r \frac{\partial B_1}{\partial r} A_1 + r \frac{dB_1}{d\tau} + 2A_1 B_1 + \frac{r}{m(\tau)} \frac{dm(\tau)}{d\tau} B_1 \right] \\ & - \frac{1}{2\pi m(\tau) \omega_0(\tau)} \int_0^{2\pi} f_1(\tau, r, \psi) \sin \psi \, d\psi, \end{aligned} \quad (2.143)$$

$$\begin{aligned} B_2(\tau, r) = & \frac{1}{2r\omega_0(\tau)} \left[\frac{\partial A_1}{\partial r} A_1 + \frac{dA_1}{d\tau} - r B_1^2 + \frac{1}{m(\tau)} \frac{dm(\tau)}{d\tau} A_1 \right] \\ & - \frac{1}{2\pi r m(\tau) \omega_0(\tau)} \int_0^{2\pi} f_1(\tau, r, \psi) \cos \psi \, d\psi. \end{aligned} \quad (2.144)$$

An auxiliary nonlinear function $f_1(\tau, r, \psi)$ in (2.143) and (2.144) is performed as

$$\begin{aligned} f_1(\tau, r, \psi) = & f'_y u_1 + f'_{y'} \left[A_1 \cos \psi - r B_1 \sin \psi + \frac{\partial u_1}{\partial \psi} \omega(\tau) \right] \\ & - m(\tau) \left[2 \frac{\partial^2 u_1}{\partial \tau \partial \psi} \omega(\tau) + 2 \frac{\partial^2 u_1}{\partial r \partial \psi} A_1 \omega(\tau) + 2 \frac{\partial^2 u_1}{\partial \psi^2} \omega(\tau) B_1 \right. \\ & \left. + \frac{\partial u_1}{\partial \psi} \frac{d\omega(\tau)}{d\tau} + \frac{\partial u_1}{\partial \psi} \frac{\omega(\tau)}{m(\tau)} \frac{dm(\tau)}{d\tau} \right], \end{aligned} \quad (2.145)$$

where

$$f'_y = \left. \frac{\partial f(\tau, y, y')}{\partial y} \right|_{y=r \cos \psi, y'=-r\omega_0(\tau) \sin \psi}, \quad (2.146)$$

$$f'_{y'} = \left. \frac{\partial f(\tau, y, y')}{\partial y'} \right|_{y=r \cos \psi, y'=-r\omega_0(\tau) \sin \psi}, \quad (2.147)$$

and the function $u_1(\tau, r, \psi)$ is defined by

$$u_1(\tau, r, \psi) = \frac{1}{2\pi k(\tau)} \sum_{n \neq \pm 1} \frac{e^{jn\psi}}{1-n^2} \int_0^{2\pi} f_0(\tau, r, \psi) e^{-jn\psi} d\psi, \quad (2.148)$$

in which $f_0(\tau, r, \psi)$ is given by (2.133).

We notice that in all above-given relevant functions, integration is provided assuming r and ψ to be constants over period 2π , even though the functions depend on “slow” time τ . In spite of such important simplifications, for many cases, solutions cannot be performed analytically in simple functions and numerical analysis often becomes the only choice to investigate a system.

2.6 Equivalent Linearization

When the signal phase is not of importance, the first order approximation serves with a sufficient accuracy. Furthermore, if the phase of an oscillator signal is constant (or zero) with time, then the amplitude-to-phase conversion is absent that is only possible in absence of overtones, so the oscillator is linear. Referring to this fact, Bogoliubov and Mitropolskiy proposed to transform an original nonlinear ODE with constant coefficients to the linear ODE with time-varying coefficients. In other words, they suggested to go from the NTI oscillator model to the LTV oscillator model. The method was called *equivalent linearization*.

In accordance with the approach, equation (2.84),

$$y'' + \omega_0^2 y = \epsilon f(y, y'),$$

is substituted by the linear ODE

$$y'' + \lambda(r)y' + k(r)y = 0, \quad (2.149)$$

where both the time-variant (amplitude-dependent) equivalent bandwidth $\lambda(r)$ and square resonance frequency $k(r)$ are defined by, respectively,

$$\lambda(r) = \frac{\epsilon}{\pi r \omega_0} \int_0^{2\pi} f(r \cos \psi, -r \omega_0 \sin \psi) \sin \psi d\psi, \quad (2.150)$$

$$k(r) = \omega_0^2 - \frac{\epsilon}{\pi r} \int_0^{2\pi} f(r \cos \psi, -r \omega_0 \sin \psi) \cos \psi d\psi. \quad (2.151)$$

The equations of the first order approximation associated with (2.149)–(2.151) are represented with

$$r' = -\frac{r}{2}\lambda(r), \quad (2.152)$$

$$\psi' = k^{1/2}(r). \quad (2.153)$$

A transition from (2.84) to (2.149) produces an error of the first order approximation ($\sim \epsilon^2$). In many cases, such an error is allowed. Therefore, the method of equivalent linearization has gained currency in different modifications.

Example 2.22 (Equivalent linearization of van der Pol's equation). Represent (2.88) in the form of (2.149). By (2.150) and (2.151), the relevant coefficients are defined to be, respectively,

$$\lambda(r) = -\epsilon \left(1 - \frac{r^2}{4} \right),$$

$$k(r) = \omega_0^2.$$

Instantly, (2.152) and (2.153) become (2.101) and (2.102), respectively, meaning that equivalent linearization produces the same result as the van der Pol' method and first order approximation, by Krylov and Bogoliubov. \square

Largely, one can conclude that the method of equivalent linearization is closely related to the method of averaging.

2.6.1 Classical Method of Harmonic Balance

The term *harmonic balance* was introduced in the text by Krylov, Bogoliubov, and Mitropolskiy, who also developed the *harmonic balance method*. The method is akin to equivalent linearization leading, in the first order approximation, to the same results as by the van der Pol's and asymptotic methods.

An idea of classical harmonic balance is to perform a system by the ODE similarly to (2.84), substitute the solutions

$$y = r \cos \psi,$$

$$y' = -r\omega_0 \sin \psi,$$

$$y'' = -r'\omega_0 \sin \psi - r\omega_0^2 \cos \psi - r\omega_0\psi' \cos \psi, \quad (2.154)$$

expand the function $f(y, y')$ to the Fourier series, equate the amplitudes of the first overtone, and go to the equations for the amplitude and phase.

Indeed, by substituting (2.154) to (2.84) and expanding $f(y, y')$ to the Fourier series with only one harmonic, we can write

$$-r'\omega_0 \sin \psi - r\omega_0\psi' \cos \psi$$

$$\begin{aligned}
&= \left[\frac{\epsilon}{2\pi} \int_0^{2\pi} f(r \cos \psi, -r\omega_0 \sin \psi) \cos \psi \, d\psi \right] \cos \psi \\
&+ \left[\frac{\epsilon}{2\pi} \int_0^{2\pi} f(r \cos \psi, -r\omega_0 \sin \psi) \sin \psi \, d\psi \right] \sin \psi. \quad (2.155)
\end{aligned}$$

By equating the amplitudes of $\cos \psi$ and $\sin \psi$ to zero and assigning

$$\lambda(r) = -\frac{2\epsilon}{r} A_1(r), \quad (2.156)$$

$$k(r) = \omega_0^2 + 2\epsilon\omega_0 B_1(r), \quad (2.157)$$

where A_1 and B_1 are given by (2.109) and (2.110), respectively, we arrive at the equations of the first order approximation,

$$r' = \epsilon A_1(r) = -\frac{r}{2} \lambda(r), \quad (2.158)$$

$$\vartheta' = \epsilon B_1(r) = -\frac{1}{2} \left[\omega_0 - \frac{k(r)}{\omega_0} \right]. \quad (2.159)$$

Despite the original duty to deal with weakly nonlinear ODEs of the second order, the method is often applied to higher order ODEs. In the latter case, the high order time derivatives are first reduced to basic functions $y = r \cos \psi$ and $y' = -r\omega_0 \sin \psi$ as in the following scheme

$$\begin{aligned}
y''' &= r\omega_0^3 \sin \psi = -\omega_0^2 y', \\
y^{(4)} &= -r\omega_0^4 \cos \psi = -\omega_0^4 y, \\
&\vdots
\end{aligned} \quad (2.160)$$

Solutions of the reduced equation are then obtained by (2.158) and (2.159).

2.6.2 Stationary Solutions by Harmonic Balance

An important significance of the harmonic balance approach is that it can universally be used to define stationary solutions in different orders of approximation. Most generally, an idea is to express the periodic solution by the finite Fourier series

$$y(t) = \sum_{i=0}^N y_i(t), \quad (2.161)$$

where N can be arbitrary and $y_i(t)$ is defined by

$$y_i(t) = U_i \cos i\omega t + V_i \sin i\omega t \quad (2.162)$$

with still unknown constant amplitudes U_i and V_i .

A solution (2.161) is then substituted into the nonlinear ODE neglecting time derivatives of U_i and V_i . For the second order nonlinear ODE (2.84), this gives

$$\sum_{i=0}^N y_i'' + \omega_0^2 \sum_{i=0}^N y_i = -\epsilon f \left(\sum_{i=0}^N y_i, \sum_{i=0}^N y_i' \right). \quad (2.163)$$

To find U_i and V_i , the right-hand side of (2.163) is expanded to the Fourier series. Thereafter, neglecting harmonics with the order higher than N and equating the constant terms and amplitudes of $\cos(i\omega t)$ and $\sin(i\omega t)$ to zero, one goes to a system of $2N + 1$ algebraic equations for unknown U_i and V_i . In the first order approximation, by $N = 1$, the solution produces U_0 , U_1 , and V_1 . In the second order, we additionally have U_2 and V_2 , and so on.

Example 2.23 (Solution of van der Pol's equation by harmonic balance in the second order approximation). To find a stationary solution of the van der Pol equation (2.88) in the second order approximation, we suppose that, by (2.119), the series (2.161) is

$$y = U_1 \cos \omega t + V_3 \sin 3\omega t. \quad (2.164)$$

Setting all the time derivatives of the amplitude and phase to zero, we then write

$$\begin{aligned} y' &= -U_1 \omega \sin \omega t + 3V_3 \omega \cos 3\omega t, \\ y'' &= -U_1 \omega^2 \cos \omega t - 9V_3 \omega^2 \sin 3\omega t \end{aligned}$$

that, neglecting the higher order overtones and equating to zero the amplitudes of $\cos \omega t$, $\sin \omega t$, and $\sin 3\omega t$ allows transferring from (2.89) to

$$\begin{aligned} \omega^2 - \omega_0^2 &= \frac{1}{4} \epsilon U_1 V_3 \omega, \\ 1 - \frac{U_1^2}{4} - \frac{V_3^2}{2} &= 0, \\ V_3(9\omega^2 - \omega_0^2) &= -\frac{1}{4} \epsilon U_1^3 \omega. \end{aligned}$$

Since $\omega \cong \omega_0$, we let $\omega = \omega_0$ in the last equation and derive the amplitude of the third harmonic

$$V_3 = -\frac{\epsilon U_1^3}{32\omega_0} \quad (2.165)$$

that is equal to that (2.119) obtained by the asymptotic method. For small ϵ , we also allow $U_1^2 \gg V_3^2$ and then the second equation, by setting $V_3^2 = 0$, produces $U_1 = r_0 = 2$ that coincides with the asymptotical solution (2.120) in the steady state when $r' = 0$.

Finally, involving (2.165), the first equation, by $\omega + \omega_0 \cong 2\omega$ and $\Delta\omega = \omega - \omega_0$, produces

$$\Delta\omega = -\frac{\epsilon^2 r_0^4}{256\omega_0} \quad (2.166)$$

that, by $r_0 = 2$, gives the same steady state value $\Delta\omega = -\epsilon^2/16\omega_0$ that was earlier provided by (2.121) in frames of the asymptotic method. \square

An advantage of harmonic balance is that, by the Fourier series, it simultaneously solves the analysis and synthesis problems for the output $y(t)$. However, to apply the method efficiently, the solution form, like (2.164), must somehow be predicted. Otherwise, the burden of the transformations, although algebraic, can be very large owing to extra terms involved.

2.6.3 Double Harmonic Balance Method

For modulated oscillators (closed loop NPTV systems), the method of harmonic balance modifies to what is called *double harmonic balance*. An idea is, first, to exploit harmonic balance for the nonlinear ODE and go to ODEs for the amplitudes of overtones. At the second stage, the time-varying parameters are expanded to the finite Fourier series for the “slow” (modulation) frequency and the method of harmonic balance is applied once again.

Let us consider a general form of the second order nonlinear ODE (2.123) assuming that its coefficients are periodically varied (modulated),

$$[m(t)y']' + k(t)y = \epsilon f(t, y, y'). \quad (2.167)$$

Supposing a solution (2.161), (2.167) can be rewritten as follows

$$\left[m(t) \sum_{i=0}^N y_i' \right]' + k(t) \sum_{i=0}^N y_i = -\epsilon f \left(t, \sum_{i=0}^N y_i, \sum_{i=0}^N y_i' \right) \quad (2.168)$$

and, by substituting (2.162) and rearranging the terms, represented with

$$\begin{aligned} & \sum_{i=0}^N [i\omega V_i m'(t) - i^2 \omega^2 U_i m(t) + U_i k(t)] \cos i\omega t \\ & + \sum_{i=0}^N [-i\omega U_i m'(t) - i^2 \omega^2 V_i m(t) + V_i k(t)] \sin i\omega t \\ = & -\epsilon f \left[t, \sum_{i=0}^N (U_i \cos i\omega t + V_i \sin i\omega t), \sum_{i=0}^N (-i\omega U_i \sin i\omega t + i\omega V_i \cos i\omega t) \right]. \end{aligned} \quad (2.169)$$

Further extending the right-hand side of (2.169) to the Fourier series and thereafter equating the amplitudes of the harmonic functions to zero gives $2N + 1$ differential equations for U_i and V_i .

The time-varying known functions $m(t)$ and $k(t)$ and unknown functions U_i and V_i can now also be extended to the finite Fourier series as in the following,

$$m(t) = \sum_{k=0}^M (m_{ck} \cos k\Omega t + m_{sk} \sin k\Omega t) , \quad (2.170)$$

$$k(t) = \sum_{k=0}^M (k_{ck} \cos k\Omega t + k_{sk} \sin k\Omega t) , \quad (2.171)$$

$$U_i = \sum_{k=0}^M (a_{ik1} \cos k\Omega t + a_{ik2} \sin k\Omega t) , \quad (2.172)$$

$$V_i = \sum_{k=0}^M (b_{ik1} \cos k\Omega t + b_{ik2} \sin k\Omega t) , \quad (2.173)$$

where, it is implied, all amplitudes of the harmonic functions in right-hand sides are small constant values. In the first order approximation, the series length is restricted with $M = 1$, in the second with $M = 2$, and so on. By substituting (2.170)–(2.173) to (2.169), equating to zero the constant terms and amplitudes of the harmonic functions, and neglecting products of small values, a system of the algebraic equations is formed to solve for the unknown amplitudes a_{ik1} , a_{ik2} , b_{ik1} , and b_{ik2} .

A solution of (2.167) is hence generally performed by

$$\begin{aligned} y = & \sum_{i=0}^N \sum_{k=0}^M (a_{ik1} \cos k\Omega t + a_{ik2} \sin k\Omega t) \cos i\omega t \\ & + \sum_{i=0}^N \sum_{k=0}^M (b_{ik1} \cos k\Omega t + b_{ik2} \sin k\Omega t) \sin i\omega t . \end{aligned} \quad (2.174)$$

Note that not all the amplitudes a_{ik1} , a_{ik2} , b_{ik1} , and b_{ik2} play the same role in the model (2.174). For example, in the first order of approximation, the phase is not of importance and hence the terms with b_{ik1} and b_{ik2} can be neglected.

Example 2.24 (Solution of the modified van der Pol' equation by double harmonic balance in the first order approximation). Consider an FM van der Pol oscillator represented with (2.135),

$$y'' + \omega_0^2(1 + \alpha \cos \Omega t)^2 y = \epsilon(1 - y^2)y' , \quad (2.175)$$

and the harmonically modulated frequency

$$\omega_0(t) = \omega_0(1 + \alpha \cos \Omega t), \quad \omega'_0(t) = -\alpha\omega_0\Omega \sin \Omega t. \quad (2.176)$$

By harmonic balance, solutions of the first order approximation, by $\psi = \omega_0 t + \vartheta$ and neglecting products of small values such as $r'\vartheta'$, can be found as

$$\begin{aligned} y &= r \cos \psi, \\ y' &= -r(\omega_0 + \vartheta') \sin \psi, \\ y'' &= -r\omega_0(\omega_0 + 2\vartheta') \cos \psi - r'\omega_0 \sin \psi, \end{aligned} \quad (2.177)$$

where

$$\vartheta(t) = \frac{\omega_0}{\Omega} \alpha \sin \Omega t, \quad \vartheta'(t) = \alpha\omega_0 \cos \Omega t.$$

Substituting (2.177) to (2.175), neglecting higher overtones, and equating to zero the terms with a sine function leads to

$$\frac{\omega'_0(t)}{\omega_0(t)} = \epsilon \left(1 - \frac{r^2}{4} \right) - 2\frac{r'}{r},$$

where $\omega_0(t)$ is given by (2.176). By simple transformations, the equation becomes that, (2.138), derived in frames of the asymptotical methods,

$$r' = \frac{\epsilon}{2} r \left(1 - \frac{r^2}{4} \right) + \frac{\alpha}{2} r \Omega \sin \Omega t. \quad (2.178)$$

Now, by (2.172), the modulated amplitude can be performed as

$$\begin{aligned} r &= r_0 + a_{11} \cos \Omega t + a_{12} \sin \Omega t, \\ r' &= -a_{11} \Omega \sin \Omega t + a_{12} \Omega \cos \Omega t, \end{aligned} \quad (2.179)$$

where r_0 is the mean amplitude (unmodulated) and a_{11} and a_{12} are small additions caused by modulation. Substituting (2.179) to (2.178), neglecting products of small values, and equating to zero the constant term and the amplitudes of cosine and sine functions produce

$$\begin{aligned} 1 &= \frac{r_0^2}{4}, \\ a_{11} \frac{\epsilon}{2} \left(1 - \frac{3}{4} r_0^2 \right) - a_{12} \Omega &= 0, \\ a_{11} \Omega + a_{12} \frac{\epsilon}{2} \left(1 - \frac{3}{4} r_0^2 \right) &= -\frac{\alpha}{2} r_0 \Omega. \end{aligned}$$

The first equation gives $r_0 = 2$ and two remaining yield

$$a_{11} = -2\alpha \frac{\nu^2}{\nu^2 + (G-1)^2}, \quad (2.180)$$

$$a_{12} = 2\alpha \frac{(G-1)\nu}{\nu^2 + (G-1)^2}, \quad (2.181)$$

where $\nu = \Omega/\delta$ is a modulation frequency normalized for a system half bandwidth $\delta = 1/2$ and $G = 3r_0^2/4$ is the open loop gain.

The steady state solution of a modulated van der Pol oscillator is thus approximated by the finite Fourier series

$$\begin{aligned} y(t) &= 2 \left[1 - \frac{\alpha\nu^2}{\nu^2 + (G-1)^2} \cos \frac{\nu t}{2} + \frac{\alpha(G-1)\nu}{\nu^2 + (G-1)^2} \sin \frac{\nu t}{2} \right] \cos \omega t \\ &= \left[\frac{c_0}{2} + c_1 \cos(\Omega t - \Psi_1) \right] \cos \omega t, \end{aligned} \quad (2.182)$$

where $c_0 = 4$,

$$c_1 = \frac{2\alpha\nu}{\sqrt{\nu^2 + (G-1)^2}}, \quad (2.183)$$

$$\Psi_1 = -\arctan \frac{G-1}{\nu}. \quad (2.184)$$

□

Example 2.24 neatly demonstrates an important feature of the double harmonic balance method. It follows that, by the method, we can reflect the modulating signal in the amplitude, frequency, and phase of oscillations. Furthermore, given spectral contents of the modulating and modulated signals, the linearized modulator can be represented with the relevant frequency responses. This approach was first used by Sokolinskiy and then developed by Shmaliiy to be known as the *modulation functions method* or *dynamic modulation characteristics method*. The method and its application to the closed loop NPTV systems is expounded in Chapter 8. Below, we illustrate its main idea traditionally considering the van der Pol's oscillator.

Example 2.25. The van der Pol oscillator (2.175) is modulated with a signal

$$s(t) = a \cos \nu \tau, \quad (2.185)$$

where $\nu = \Omega/\delta$, $\tau = \delta t$ and a is a constant, causing the frequency to vary by (2.176). FM is accompanied with spurious AM associated with the amplitudes (2.180) and (2.181).

By small values of a , an oscillator can be linearized and the response of its frequency to (2.185) can be specified with the *frequency modulation function* (FMF)

$$H_\omega(j\nu) = |H_\omega(j\nu)| e^{j\vartheta_\omega(\nu)} = 1 \quad (2.186)$$

that apparently is unit, because of the direct modulation and zero values of b_{ik1} and b_{ik2} , in the first order approximation.

The response of the oscillator amplitude to (2.185) can be specified with the *amplitude modulation function* (AMF)

$$H_r(j\nu) = |H_r(j\nu)|e^{j\vartheta_r(\nu)}, \quad (2.187)$$

where, by (2.182)–(2.184), the magnitude AMF and phase AMF are derived to be, respectively,

$$|H_r(j\nu)| = \frac{c_1}{a} = \frac{2\nu}{\sqrt{\nu^2 + (G-1)^2}}, \quad (2.188)$$

$$\vartheta_r(\nu) = \Psi_r(\nu) = -\arctan \frac{\mu-1}{\nu}. \quad (2.189)$$

As may be seen, spurious AM becomes negligible with $\nu \ll 1$ and attains a maximum with $\nu \gg 1$. Therefore, with a broadband modulation, an amplitude limiter would be in order. \square

2.6.4 Describing Function Method

With time, classical equivalent linearization has been developed to the engineering approach called the *describing function method* (DF method). Well elaborated, the method is reminiscent of the familiar harmonic balance, but proposes its own philosophy. Actually, it deals not with the whole system, but only with its input-to-output nonlinear part, be it even with memory.

The basic idea of the DF method is to present an input of the nonlinear system as a periodic harmonic wave (sine or cosine) having the amplitude r and frequency ω , save only the first harmonic in the output, and describe the gain of such a linearized system by a ratio of the complex amplitudes of the output and input vectors. The gain $N(r, j\omega)$ called the *describing function* is thus kind of frequency response of a linearized system. Accordingly, the input-to-output relation is written as

$$y(t) = N(r, j\omega)x(t). \quad (2.190)$$

The cosine-input FD is defined by

$$N(r, j\omega) = \frac{1}{\pi r} \int_{-\pi}^{\pi} y(r \cos \omega t, -r\omega \sin \omega t) e^{-j\omega t} d\omega t \quad (2.191)$$

that, if a system is memoryless, becomes

$$N(r) = \frac{1}{\pi r} \int_{-\pi}^{\pi} y(r \cos \omega t) e^{-j\omega t} d\omega t. \quad (2.192)$$

Example 2.26. A memoryless NTI system is performed with $y(t) = x^3(t)$. Supposing $y(t) = r \cos \omega t$, the DF is defined, by (2.192), to be

$$N(r) = \frac{r^2}{\pi} \int_{-\pi}^{\pi} e^{-j\omega t} \cos^3 \omega t \, d\omega t = \frac{3}{4} r^2. \quad (2.193)$$

It can be shown that (2.193) also appears by direct equivalent linearization. \square

Example 2.27 (Linearization of van der Pol's equation with DF). Consider van der Pol's oscillator (2.88). The cosine input DF for the nonlinear function $f(y, y')$ is defined, by (2.192), to be

$$\begin{aligned} N(r, j\omega) &= -\frac{\omega}{\pi} \int_{-\pi}^{\pi} (1 - r^2 \cos^2 \psi) e^{-j\psi} \sin \psi \, d\psi \\ &= -\frac{\omega}{2\pi} \int_{-\pi}^{\pi} (1 - r^2 \cos^2 \psi) \sin 2\psi \, d\psi + \frac{j\omega}{\pi} \int_{-\pi}^{\pi} (1 - r^2 \cos^2 \psi) \sin^2 \psi \, d\psi \\ &= \left(1 - \frac{r^2}{4}\right) j\omega. \end{aligned} \quad (2.194)$$

By the operators identity, $j\omega \equiv \frac{d}{dt}$, we thus have

$$f(y, y') = N(r, j\omega)y = \left(1 - \frac{r^2}{4}\right) y'$$

and the linearized equation becomes

$$y'' - \epsilon \left(1 - \frac{r^2}{4}\right) y' + \omega_0^2 y = 0$$

that was derived earlier, by equivalent linearization. \square

If the input is sinusoidal, the DF is defined by

$$N(r, j\omega) = \frac{j}{\pi r} \int_{-\pi}^{\pi} y(r \sin \omega t, r\omega \cos \omega t) e^{-j\omega t} \, d\omega t, \quad (2.195)$$

$$N(r) = \frac{j}{\pi r} \int_{-\pi}^{\pi} y(r \sin \omega t) e^{-j\omega t} \, d\omega t \quad (2.196)$$

for memory and memoryless systems, respectively,

Example 2.28. A memoryless system with a nonlinearity $y(t) = x^3(t)$ has an input $y(t) = r \sin \omega t$. The DF is defined, by (2.196), to be

$$N(r) = \frac{jr^2}{\pi} \int_{-\pi}^{\pi} \sin^3 \omega t e^{-j\omega t} d\omega t = \frac{3}{4}r^2. \quad (2.197)$$

As can be seen, the function is exactly that (2.193) obtained for the cosine input. \square

Like in other attempts of linearization, simplifications allowed by the DF method do not seem to be useful for subtle nonlinear structures. Moreover, in some cases, the DF does not fit principle features of systems. The approach, however, allows predicting and investigating with sufficient trustworthiness limit cycles in closed loops and solves several other engineering problems. On the whole, as a product of equivalent linearization, the DF method substitutes an NTI system by an LTV one with all advantages and disadvantages.

2.7 Norms

An important quantitative measure of system performance is provided by *norms*. Basically, evaluation with norms answers on the question how large will be the output signal for the given input or allowed information about the input.

Norm: The norm means a measure of the “size” of a signal and, thereby, a system. \square

System norms are used in evaluating robustness, minimizing the peak of the largest singular value or all singular values in the frequency domain, specifying the performance in terms of sensitivity, etc. The system norms are evaluated via the impulse response function and its transform. For some problems, the system norms are expressed via the signal norms.

2.7.1 Norms for Signals

In mathematics, the vector length is called the *norm*. Accordingly, a linear space \mathbb{L} is said to be *normed*, if every vector $x(t) \in \mathbb{L}$ is specified by its norm $\|x\|$. For the normed space, the following axioms are valid :

- *Positivity:* The norm is non negative, $\|x\| \geq 0$. \square
- *Positive definiteness:* The norm is $\|x\| = 0$ if and only if $x = \emptyset$. \square
- *Homogeneity:* For any a , the following equality holds $\|ax\| = |a| \cdot \|x\|$. \square

- *Triangle inequality:* If $x(t) \in \mathbb{L}$ and $y(t) \in \mathbb{L}$, then the following triangle inequality is valid: $\|x + y\| \leq \|x\| + \|y\|$. \square

Different types of norms of scalar-valued signals are used in applications depending on their physical meanings and geometrical interpretations.

L_1 -norm

The L_1 -norm of a signal $x(t)$ is the integral of the absolute value $|x(t)|$ representing its *length* or *total resources*,

$$\|x\|_1 = \int_{-\infty}^{\infty} |x(t)| dt. \quad (2.198)$$

The finite value of this norm $\|x\|_1 < \infty$ means that the function is *absolutely integrable* and, by the *Dirichlet*²⁰ conditions, its transform exists.

L_2 -norm

The L_2 -norm of a real $x(t)$ is defined as the square root of the integral of $x^2(t)$,

$$\|x\|_2 = \sqrt{\int_{-\infty}^{\infty} x^2(t) dt}, \quad (2.199)$$

and if a signal is complex, then $\|x\|_2$ is specified by

$$\|x\|_2 = \sqrt{\int_{-\infty}^{\infty} x(t)x^*(t) dt} = \sqrt{\int_{-\infty}^{\infty} |x(t)|^2 dt}, \quad (2.200)$$

where a symbol (*) means complex conjugate. By the Rayleigh²¹ theorem (Parseval²² relation or Plancherel²³ identity), the L_2 -norm can also be defined by

$$\|x\|_2 = \|X\|_2 = \sqrt{\frac{1}{2\pi} \int_{-\infty}^{\infty} |X(j\omega)|^2 d\omega}. \quad (2.201)$$

The L_2 -norm is appropriate for electrical signals at least by two reasons:

²⁰ Johann Peter Gustav Lejeune Dirichlet, Belgium-born German/French mathematician, 13 February 1805–5 May 1859.

²¹ John William Strutt (Lord Rayleigh), English mathematician, 12 November 1842–30 June 1919.

²² Marc-Antoine de Parseval des Chsnes, French mathematician, 27 April 1755–16 August 1836.

²³ Michel Plancherel, Swiss mathematician, 16 January 1885–4 March 1967.

- Frequently, a signal is evaluated in terms of the energy effect, for example, by the amount of warmth induced on a resistance. The squared norm may thus be treated as a *signal energy*; that is

$$E_x = \|x\|_2^2 = \int_{-\infty}^{\infty} x(t)x^*(t)dt. \quad (2.202)$$

For instance, suppose that $i(t)$ is a current through a 1Ω resistor. Then the instantaneous power equals $i^2(t)$ and the total energy equals the integral of this, namely, $\|i\|_2^2$.

- The energy norm is “insensitive” to changes in the signal waveform. These changes may be substantial but existing in a short time. Therefore, their integral effect may be insignificant.

L_p -norm

The L_p -norm of $x(t)$ is a generalization for both the L_1 -norm and L_2 -norm. It is defined as

$$\|x\|_p = \sqrt[p]{\int_{-\infty}^{\infty} |x(t)|^p dt}. \quad (2.203)$$

The necessity to use the L_p -norm refers to the fact that the integrand in (2.203) should be Lebesgue²⁴-integrable for the integral to exist. Therefore, this norm is a generalization of the standard Riemann²⁵ integral to a more general class of signals.

L_∞ -norm

The L_∞ -norm is often called the ∞ -norm. It is characterized as the maximum of the absolute value (*peak value*) of $x(t)$,

$$\|x\|_\infty = \max_t |x(t)|, \quad (2.204)$$

assuming that the maximum exists. Otherwise, if there is no guarantee that it exists, the correct way to define the L_∞ -norm is to calculate it as the least upper bound (*supremum*) of the absolute value,

$$\|x\|_\infty = \sup_t |x(t)|. \quad (2.205)$$

²⁴ Henri Léon Lebesgue, French mathematician, 28 June 1875–26 July 1941.

²⁵ Georg Friedrich Bernhard Riemann, German mathematician, 17 September 1826–20 July 1866.

Root-Mean-Square Norm

The root-mean-square (RMS) norm or just RMS is calculated by

$$\|x\|_{\text{rms}} = \sqrt{\lim_{T \rightarrow \infty} \frac{1}{T} \int_{-T/2}^{T/2} |x(t)|^2 dt}. \quad (2.206)$$

Example 2.29. Given a signal $x(t) = e^{-at}u(t)$, $a > 0$. It can be shown that its norms are defined by $\|x\|_1 = \frac{1}{a}$, $\|x\|_2 = \|X\|_2 = \frac{1}{\sqrt{2a}}$, and $\|x\|_\infty = 1$.

Given the other signal $y(t) = \frac{1}{b-a}(e^{-at} - e^{-bt})u(t)$, $a > 0$ and $b > 0$. The norms of this signal are given by $\|y\|_1 = \frac{1}{ab}$, $\|y\|_2 = \frac{1}{\sqrt{2ab(a+b)}}$, and $\|y\|_\infty = \frac{1}{b} \left(\frac{b}{a}\right)^{\frac{a}{a-b}}$. \square

In a similar manner are defined the norms of vector signals. If $\mathbf{x}(t) = [x_1(t), x_2(t), \dots, x_n(t)]^T$ is a $n \times 1$ vector of some linear n -dimensional space \mathbb{L}^n , $\mathbf{x}(t) \in \mathbb{L}^n$, then the relevant norms for this vector are ascertained by

$$\|\mathbf{x}\|_1 = \int_{-\infty}^{\infty} \sum_i |x_i(t)| dt, \quad (2.207)$$

$$\|\mathbf{x}\|_2 = \sqrt{\int_{-\infty}^{\infty} \sum_i |x_i(t)|^2 dt} = \sqrt{\int_{-\infty}^{\infty} \mathbf{x}^H(t)\mathbf{x}(t) dt}, \quad (2.208)$$

$$\|\mathbf{x}\|_p = \left(\int_{-\infty}^{\infty} \sum_i |x_i(t)|^p dt \right)^{\frac{1}{p}}, \quad (2.209)$$

$$\|\mathbf{x}\|_\infty = \sup_t \max_i |x_i(t)|, \quad (2.210)$$

$$\|\mathbf{x}\|_{\text{rms}} = \sqrt{\lim_{T \rightarrow \infty} \frac{1}{T} \int_{-T/2}^{T/2} \sum_i |x_i(t)|^2 dt}, \quad (2.211)$$

where a symbol (H) means conjugate transpose.

Of applied importance is also the following *multiplication condition*. Let two signals $\mathbf{x} \in \mathbb{L}^n$ and $\mathbf{y} \in \mathbb{L}^n$ be coupled by the relevant matrix \mathbf{A} of the transformation, $\mathbf{x} = \mathbf{A}\mathbf{y}$. Then the following inequality holds true

$$\|\mathbf{A}\mathbf{x}\| \leq \|\mathbf{A}\| \|\mathbf{x}\| \quad \text{for } \mathbf{x} \in \mathbb{L}^n.$$

We notice that the presentation of signals by norms may be useful in defining the norms for systems. Yet, if the waveform of an input is known and the norm of an output is given, then the norm of a system may be predicted.

2.7.2 Norms for Systems

Consider an LTI system characterized with the impulse response $h(t)$, frequency response $H(j\omega)$, or transfer function $H(s)$. The norms of such systems are commonly defined for the following recognized types of the transfer function, namely for

- Stable, if $\operatorname{Re} s \geq 0$ □
- Proper, if $H(j\infty) < \infty$ □
- Strictly proper, if $H(j\infty) = 0$ □
- Biproper, if $H(s)$ and $H^{-1}(s)$ are both proper □

Typically, causal systems are evaluated with two norms, termed the H_2 -norm and H_∞ -norm.

The H_2 -norm

For stable SISO systems, the H_2 -norm characterizes an average gain and is defined similarly to (2.199) by

$$\begin{aligned} \|H\|_2 &= \sqrt{\frac{1}{2\pi j} \int_{-j\infty}^{j\infty} H(s)H(-s) ds} \\ &= \sqrt{\frac{1}{2\pi} \int_{-\infty}^{\infty} |H(j\omega)|^2 d\omega}. \end{aligned} \quad (2.212)$$

By the Rayleigh theorem, this norm can also be calculated via the impulse response function as

$$\|H\|_2 = \sqrt{\int_0^{\infty} h^2(t) dt}. \quad (2.213)$$

Example 2.30. An LP filter is described with the ODE $y' + ay = bx$, $a > 0$, $b > 0$, that corresponds to the frequency response $H(j\omega) = \frac{b}{a+j\omega}$ and impulse response $h(t) = be^{-at}u(t)$. The square magnitude response of the filter becomes $|H(j\omega)|^2 = \frac{b^2}{a^2+\omega^2}$ that, by (2.212), symmetry of $|H(j\omega)|$, and an identity $\int_0^{\infty} \frac{dz}{a^2+z^2} = \frac{\pi}{2a}$, yields

$$\|H\|_2 = \sqrt{\frac{1}{\pi} \int_0^{\infty} \frac{b^2}{a^2 + \omega^2} d\omega} = \frac{b}{\sqrt{2a}}.$$

The same value appears if one applies (2.213) to the impulse response. □

If a SISO system is performed in state space by equations (2.39) and (2.40) with $\mathbf{D} = 0$, its transfer function is predetermined by (2.46) with $\mathbf{D} = 0$ and the H_2 -norm is specified by

$$\|H\|_2 = \sqrt{\mathbf{C}\mathbf{L}\mathbf{C}^T}, \quad (2.214)$$

where the so-called observability Gramian²⁶ matrix is given by

$$\mathbf{L} = \int_0^{\infty} e^{\mathbf{A}t} \mathbf{B}\mathbf{B}^T e^{\mathbf{A}^T t} dt. \quad (2.215)$$

The H_2 -norm for MIMO systems represented by the transfer function matrix $\mathbf{H}(s)$ with the components $H_{km}(s)$ and by the impulse response matrix $\mathbf{h}(t)$ with the components $h_{km}(t)$, is usually evaluated via the *Frobenius*²⁷ norm, sometimes also called the *Euclidean*²⁸ norm,

$$\|\mathbf{A}\|_F = \sqrt{\sum_k \sum_m |a_{km}|^2} = \sqrt{\text{trace}(\mathbf{A}\mathbf{A}^H)}. \quad (2.216)$$

Employing this norm and taking into account the Rayleigh theorem, the H_2 -norm of a MIMO system is found to be

$$\begin{aligned} \|\mathbf{H}\|_2 &= \sqrt{\frac{1}{2\pi} \int_{-\infty}^{\infty} \|\mathbf{H}(j\omega)\|_F^2 d\omega} \\ &= \sqrt{\int_0^{\infty} \|\mathbf{h}(t)\|_F^2 dt}. \end{aligned} \quad (2.217)$$

If a MIMO system is represented in state space with equations (2.37) and (2.38), then, by $\mathbf{D} = 0$, its H_2 -norm is defined by

$$\|H\|_2 = \sqrt{\text{trace}[\mathbf{C}\mathbf{L}\mathbf{C}^T]}, \quad (2.218)$$

where \mathbf{L} is still given by (2.215).

²⁶ Jørgen Pedersen Gram, Danish mathematician, 27 June 1850–29 April 1916.

²⁷ Ferdinand Georg Frobenius, German mathematician, 26 October 1849–3 August 1917.

²⁸ Euclid of Alexandria, Mathematician of antiquity, about 325 BC–about 265 BC.

The H_∞ -norm

The other widely used fundamental H_∞ -norm is associated with a peak-value of the system performance. For instance, if a nominal frequency response of a system is supposed to be uniform, then the H_∞ -norm characterizes a measure of the maximum excursion in the actual frequency response. Therefore, this norm is useful in ascertaining the system instability.

For SISO systems, similarly to the L_∞ -norm, the H_∞ -norm is characterized as the maximum of the absolute value (peak value) of $H(j\omega)$,

$$\|H\|_\infty = \max_{\omega} |H(j\omega)|, \quad (2.219)$$

implied that the maximum exists. If there is no guarantee that it exists, the correct way to define the H_∞ -norm is to calculate it as the least upper bound of the absolute value,

$$\|H\|_\infty = \sup_{\omega} |H(j\omega)|. \quad (2.220)$$

Example 2.31. A channel is described with the ODE $y' + ay = bx' + cx$ having $a > 0$, $b = 1$, and $c > 0$. By this equation, the frequency response of a channel is defined to be $H(j\omega) = \frac{c+j\omega}{a+j\omega}$. The square magnitude response is thus $|H(j\omega)|^2 = \frac{c^2+\omega^2}{a^2+\omega^2}$. A simple observation shows that, by $c < a$, a maximum of $|H(j\omega)|$ is unity at $\omega \rightarrow \infty$. When $c = a$, we have unity for all ω . If $c > a$, a local maximum c/a exists at $\omega = 0$. One can thus conclude that

$$\|H\|_\infty = \begin{cases} \frac{c}{a}, & \text{if } c > a \\ 1, & \text{if } c \leq a \end{cases}.$$

□

Example 2.32. A SISO LTI system is represented with the impulse response $h(t) = e^{-bt}u(t)$, $b > 0$. The norms of this system can be found to be $\|H\|_2 = \frac{1}{\sqrt{2b}}$ and $\|H\|_\infty = \frac{1}{b}$.

A simple analysis shows that the above-defined system norms are specified by the signals norms given in Example 2.29 as follows: $\|H\|_2 = \sqrt{\|y\|_1}$ and $\|H\|_\infty = \frac{\|y\|_1}{\|x\|_1}$. □

For a SISO system characterized with the strictly proper transfer function and represented in state space with $\mathbf{D} = 0$, an important theorem claims that $\|H\|_\infty < \gamma$, where γ is positive and real, if and only if the following Hamiltonian²⁹ matrix has no eigenvalues on the imaginary axis,

$$\mathbf{M} = \begin{bmatrix} \mathbf{A} & \gamma^{-2}\mathbf{B}\mathbf{B}^T \\ -\mathbf{C}^T\mathbf{C} & -\mathbf{A}^T \end{bmatrix}. \quad (2.221)$$

²⁹ William Rowan Hamilton, Irish mathematician, physicist, and astronomer, 4 August 1805–2 September 1865.

If a system is MIMO, then the H_∞ -norm is often determined by the least upper bound of the *maximum singular value*, denoted $\bar{\sigma}\mathbf{H}(j\omega)$, of the matrix $\mathbf{H}(j\omega)$; that is,

$$\|\mathbf{H}\|_\infty = \sup_\omega \bar{\sigma}\mathbf{H}(j\omega). \quad (2.222)$$

If such a system is represented in state space with $\mathbf{D} \neq 0$, then the above-mentioned theorem relates to the Hamiltonian matrix

$$\mathbf{M} = \begin{bmatrix} \mathbf{A} + \mathbf{B}\mathbf{R}^{-1}\mathbf{D}^T\mathbf{C} & \mathbf{B}\mathbf{R}^{-1}\mathbf{B}^T \\ -\mathbf{C}^T(\mathbf{I} + \mathbf{D}\mathbf{R}^{-1}\mathbf{D}^T)\mathbf{C} & -(\mathbf{A} + \mathbf{B}\mathbf{R}^{-1}\mathbf{D}^T\mathbf{C})^T \end{bmatrix}, \quad (2.223)$$

where $\mathbf{R} = \gamma^2\mathbf{I} - \mathbf{D}^T\mathbf{D}$. We notice that, by $\mathbf{D} = 0$, the relation (2.223) degenerates to (2.221).

2.7.3 System Norms via Signal Norms

We have already mentioned above and illustrated by Example 2.32 that system norms can be expressed via signal norms.

More specifically, if we consider a SISO LTI system with the input $x(t) \stackrel{\mathcal{F}}{\leftrightarrow} X(j\omega)$, output $y(t) \stackrel{\mathcal{F}}{\leftrightarrow} Y(j\omega)$, and impulse response $h(t) \stackrel{\mathcal{F}}{\leftrightarrow} H(j\omega)$, we can specify, by (2.201), its L_2 -norm as follows

$$\begin{aligned} \|y\|_2^2 &= \|Y\|_2^2 = \frac{1}{2\pi} \int_{-\infty}^{\infty} |H(j\omega)X(j\omega)|^2 d\omega \\ &\leq \frac{1}{2\pi} \int_{-\infty}^{\infty} |H(j\omega)|^2 |X(j\omega)|^2 d\omega \leq \|H\|_\infty^2 \frac{1}{2\pi} \int_{-\infty}^{\infty} |X(j\omega)|^2 d\omega \\ &= \|H\|_\infty^2 \|X\|_2^2 = \|H\|_\infty^2 \|x\|_2^2. \end{aligned}$$

The norms mapping is thus $\|y\|_2 \leq \|H\|_\infty \|x\|_2$.

Reasoning similarly, the other relations between the signal and system norms have been found and generalized by the authors. For example, let a stable SISO LTI system be represented with the input $x(t)$, output $y(t)$, impulse response $h(t)$, and frequency response $H(j\omega) \stackrel{\mathcal{F}}{\leftrightarrow} h(t)$. Doyle, Francis, and Tannenbaum showed that Table 2.1 gives the input/output norms for such a system.

We notice that the mapping given in Table 2.1 is not exact, but rather representing useful inequalities, as in the above considered case of $\|y\|_2 \leq \|H\|_\infty \|x\|_2$.

Table 2.1. Norms mapping in SISO LTI systems

	$\ x\ _2$	$\ x\ _\infty$
$\ y\ _2$	$\ H\ _\infty$	∞
$\ y\ _\infty$	$\ H\ _2$	$\ h\ _1$

2.8 System Stability

Stability is one of the fundamental properties of any system. Even intuitively, we think about the system operation as desirably insensitive (so stable) to slight internal and external disturbances. We also want the output signal to track the transformed input signal and not to be infinite even at one or several points. To fit these needs, the system stability must somehow be evaluated and the relevant conditions described mathematically.

Depending on the system linearity, stationarity, and even application, the terms “stable” and “stability” are used in rather special and often different senses. Therefore, when we speak about stability, we usually need to supply this term with the addition “in the sense of ...”

Most generally, the definitions of stability may be related to the common state space model of a system, (2.65) and (2.66),

$$\mathbf{q}'(t) = \Psi[\mathbf{q}(t), \mathbf{x}(t), t], \quad (2.224)$$

$$\mathbf{y}(t) = \Upsilon[\mathbf{q}(t), \mathbf{x}(t), t], \quad (2.225)$$

and to its particular forms associated with linear and/or time-invariant realizations. In what follows, we observe the most widely used definitions of stability.

2.8.1 External (Bounded Input/Bounded Output) Stability

Let us consider a SISO system with the input $x(t)$ and output $y(t)$. We have already mentioned before, when classified systems, that a system is *bounded-input/bounded-output* (BIBO) *stable* if for any bounded input $x(t)$ the corresponding output $y(t)$ is also bounded. The definition involves solely the external resources. Therefore, the *BIBO stability* is often called the *external stability* as related to the relaxed systems (with zero initial states). Mathematically, the condition for a system to be BIBO stable reads as follows:

BIBO stability: The system is BIBO stable if for any input $x(t)$ with $\|x(t)\|_\infty \leq M_x < \infty$ there is the output $y(t)$ with $\|y(t)\|_\infty \leq M_y < \infty$, where M_x and M_y are finite positive real constants.

□

If this condition is not met, i.e. $y(t)$ grows without limit (diverges) from a bounded input, then the system is BIBO unstable.

BIBO Stability via the Impulse Response

Because the convergence of the output can only be possible if the impulse response $h(t)$ of the LTI system has finite total resources, the necessary and sufficient condition for the LTI system to be BIBO stable is the finite value of the L_1 -norm of the impulse response,

$$\|h\|_1 = \int_{-\infty}^{\infty} |h(t)| dt \leq M < \infty, \quad (2.226)$$

where M is a constant. Let us verify (2.226) recalling that, in LTI systems, the output and input are coupled by the convolution

$$y(t) = \int_{-\infty}^{\infty} x(\vartheta)h(t - \vartheta) d\vartheta. \quad (2.227)$$

We can now take the absolute values of both sides of (2.227) and go to

$$\begin{aligned} |y(t)| &= \left| \int_{-\infty}^{\infty} x(\theta)h(t - \theta) d\theta \right| = \int_{-\infty}^{\infty} |x(\theta)h(t - \theta)| d\theta \\ &\leq \int_{-\infty}^{\infty} |x(\theta)||h(t - \theta)| d\theta. \end{aligned}$$

Substituting the absolute value $|x(t)|$ with the norm $\|x\|_{\infty}$,

$$\begin{aligned} \int_{-\infty}^{\infty} |x(\theta)||h(t - \theta)| d\theta &\leq \int_{-\infty}^{\infty} \|x\|_{\infty}|h(t - \theta)| d\theta \\ &= \|x\|_{\infty} \int_{-\infty}^{\infty} |h(t - \theta)| d\theta = \|x\|_{\infty}\|h\|_1, \end{aligned}$$

yields $|y(t)| \leq \|x\|_{\infty}\|h\|_1$. If $y(t)$ and $x(t)$ are both bounded, then $\|h\|_1$ must be finite, $\|h\|_1 < \infty$, and the verification of (2.226) is complete.

Example 2.33. A filter is characterized with the impulse response $h(t) = te^{-bt}u(t)$. By (2.226) and an identity $\int xe^{\alpha x} dx = e^{\alpha x} \left(\frac{x}{\alpha} - \frac{1}{\alpha^2} \right)$, the L_1 -norm is defined to be

$$\|h\|_1 = \frac{1}{b} \left(\frac{1}{b} - e^{-b\infty} \infty \right).$$

Exploiting the limits $\lim_{z \rightarrow \infty} ze^{-az} = 0$ and $\lim_{z \rightarrow \infty} ze^{az} = \infty$, $a > 0$, we conclude that the filter is BIBO stable only if $b > 0$. \square

If an LTI system is MIMO with the impulse response matrix $\mathbf{h}(t)$ having the components $h_{kl}(t)$, then it is BIBO stable if and only if all the components of $\mathbf{h}(t)$ are absolutely integrable, so satisfying (2.226).

If a SISO system is LTV, it is characterized with the time-varying impulse response $h(t, \theta)$. The BIBO stability condition for such systems is that there must exist a finite value of the integral

$$\int_{t_0}^t |h(t, \theta)| d\theta \leq M < \infty, \quad (2.228)$$

where $t > t_0$ takes any value exceeding an initial time t_0 .

Example 2.34. An LTV channel is characterized with the impulse response

$$h(t, \theta) = \delta(t - \tau_0 - \theta) e^{j\Omega_0 t} u(t - \theta).$$

In view of $|e^{j\Omega_0 t}| = 1$, the absolute value of $h(t, \theta)$ becomes $|h(t, \theta)| = \delta(t - \tau_0 - \theta) u(t - \theta)$. The integral (2.228) thus produces unity and the channel is hence BIBO stable. \square

The relevant condition for a MIMO LTV system is that there must exist a positive constant M such that

$$\int_{-\infty}^t \|\mathbf{h}(t, \theta)\|_F d\theta \leq M < \infty \quad (2.229)$$

for all values of t , where $\|\mathbf{h}(t, \theta)\|_F$ is the Frobenius (or Euclidean) norm (2.216) of the impulse response matrix.

BIBO Stability via the Transfer Function

If a SISO LTI system is given with the transfer function $H(s)$, the relevant condition for a system to be BIBO stable can be derived as in the following.

Consider (2.226). Because $|e^{-j\omega t}| = 1$, we can write the L_1 -norm (2.198) for $h(t)$ as

$$\begin{aligned} \|h\|_1 &= \int_{-\infty}^{\infty} |h(t)| dt = \int_{-\infty}^{\infty} |h(t)| |e^{-j\omega t}| dt \\ &\geq \int_{-\infty}^{\infty} |h(t) e^{-j\omega t}| dt = \left| \int_{-\infty}^{\infty} h(t) e^{-st} dt \right|_{\sigma=0} = |H(s)|_{\sigma=0}. \end{aligned}$$

It follows from these manipulations that the only condition for the system to be BIBO stable is that the region of convergence (ROC) of the Laplace

transform includes the imaginary axis. The condition is satisfied with $\sigma = 0$ and may be interpreted in the following way.

A SISO LTI system with the proper rational transfer function $H(s)$ is BIBO stable if and only if every pole of $H(s)$ has a negative real part (lies in the left-hand part of s -plane).

Example 2.35. An LTI system is represented with the transfer function

$$H(s) = \frac{s(s-2)}{(s+3)(s-1)(s+2)}.$$

The poles have real parts $\sigma_1 = -3$, $\sigma_2 = 1$, and $\sigma_3 = -2$. Because the real part of one of the poles is positive (lies in the right half of a plane), the system is BIBO unstable. \square

Likewise, a MIMO LTI system with the proper rational transfer function matrix $\mathbf{H}(s)$ having the components $H_{kl}(s)$ is BIBO stable if and only if every pole of each component in $\mathbf{H}(s)$ has a negative real part.

We notice that the modern theory of dynamic systems and control offers many other definitions and forms of BIBO stability for systems that may be found in the relevant books.

2.8.2 Internal Stability

So far, we defined the system stability in terms of its input and output avoiding discussing the system itself. This is what was called the external (or BIBO) stability. The only condition for ascertaining the external stability is the zero initial states of a system.

Contrary to the external stability, the internal one is evaluated solely in terms of the system performance. Therefore, the input is required to be zero and we are thus deal only with the state equation (2.224) that, by $\mathbf{x}(t) \equiv \mathbf{0}$ becomes

$$\mathbf{q}'(t) = \Psi[\mathbf{q}(t), t]. \quad (2.230)$$

Let us think that the system (2.230) has N points of equilibrium $\mathbf{q}_1, \mathbf{q}_2, \dots, \mathbf{q}_N$ such that

$$\Psi(\mathbf{q}_1, t) = 0, \quad \Psi(\mathbf{q}_2, t) = 0, \quad \dots, \quad \Psi(\mathbf{q}_N, t) = 0.$$

For an arbitrary value of $\mathbf{q}(t)$, we can introduce time-varying increments

$$\tilde{\mathbf{q}}_1(t) = \mathbf{q}(t) - \mathbf{q}_1, \quad \tilde{\mathbf{q}}_2(t) = \mathbf{q}(t) - \mathbf{q}_2, \quad \dots, \quad \tilde{\mathbf{q}}_N(t) = \mathbf{q}(t) - \mathbf{q}_N,$$

which differentiation produces, respectively,

$$\tilde{\mathbf{q}}_1'(t) = \Psi[\tilde{\mathbf{q}}_1(t) + \mathbf{q}_1, t] \equiv \mathbf{f}_1[\tilde{\mathbf{q}}_1(t), t],$$

$$\begin{aligned}
\tilde{\mathbf{q}}_2'(t) &= \Psi[\tilde{\mathbf{q}}_2(t) + \mathbf{q}_2, t] \equiv \mathbf{f}_2[\tilde{\mathbf{q}}_2(t), t], \\
&\vdots \\
\tilde{\mathbf{q}}_N'(t) &= \Psi[\tilde{\mathbf{q}}_N(t) + \mathbf{q}_N, t] \equiv \mathbf{f}_N[\tilde{\mathbf{q}}_N(t), t].
\end{aligned} \tag{2.231}$$

By (2.231), every equilibrium point of the system is reduced to the center of the coordinates to mean that, for example, $\mathbf{q}_1'(t) = \mathbf{f}_1(0, t) = 0$. By the way, if a system (2.231) is further linearized, it attains the form of the linearized state space model described earlier.

Instead of (2.231), we shall now consider an equation

$$\tilde{\mathbf{q}}'(t) = \mathbf{f}[\tilde{\mathbf{q}}(t), t] \tag{2.232}$$

to represent a system at an arbitrary equilibrium point such that $\tilde{\mathbf{q}}'(t) = \mathbf{f}(0, t) = 0$. Exploiting (2.232), the definitions of the system stability may be given in a different sense.

In what follows, we shall illustrate definitions of stability with an example of the phase locked loop (PLL). The phase $\phi(t)$ of a local oscillator is measured for the reference phase ϕ_0 . A signal proportional to the phase difference $\varphi(t) = \phi(t) - \phi_0$ adjusts the local oscillator to tend $\varphi(t)$ toward zero. Owing to time variations in $\phi(t)$, the difference $\varphi(t)$ is not always zero, but rather contains some amount of error $\tilde{\varphi}(t)$. We therefore wonder whether the system is internally stable or not to small excursions in $\varphi(t)$.

To find an answer, it needs returning back to works of Lyapunov, who followed Chebyshev³⁰ and created the theory of stability. The theory was presented by Lyapunov in 1892 in his Doctoral thesis “The general problem of the stability of motion,” in which several fundamental definitions of stability were given. We shall give all definitions of stability as adapted to the notations given above.

Stability (in the sense of Lyapunov): An equilibrium point “0” of (2.232) is said to be stable in the sense of Lyapunov if for any real $\varepsilon > 0$ there exists a real $\delta(\varepsilon, t_0) > 0$ such that

$$\|\tilde{\mathbf{q}}(t_0)\| < \delta \quad \text{and} \quad \|\tilde{\mathbf{q}}(t)\| < \varepsilon \quad \text{for} \quad t \geq t_0. \tag{2.233}$$

□

Typically, it is assumed that $\varepsilon \geq \delta$. Therefore the above-given definition is often called *local*. If the initial value $\delta(\varepsilon, t_0)$ is supposed to be arbitrary and hence $\varepsilon \leq \delta < r < \infty$, the stability is said to be *global*.

It is seen that the bounds δ and ε are not absorbed by the conditions (2.233), although in other interpretations of Lyapunov’s stability they are absorbed. If they are absorbed and a system is linear, then the Lyapunov stability is often called *marginal*.

³⁰ Pafnuty Lvovich Chebyshev, Russian mathematician, 16 May 1821–8 December 1894.

With respect to the above-mentioned phase system, Lyapunov’s definition of stability means that the phase $\varphi(t)$ with $t \geq t_0$ must trace within the bounds $|\varepsilon|$ without actually touching them. Examples of locally and globally Lyapunov stable phase systems are shown in Fig. 2.8a and Fig. 2.8b, respectively.

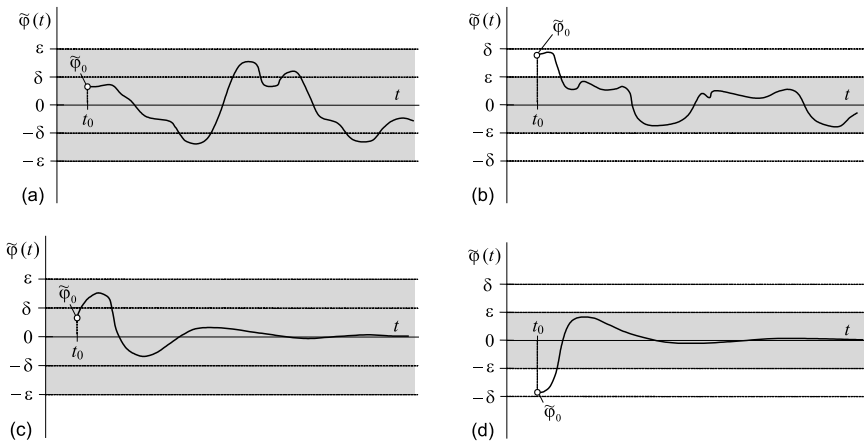


Fig. 2.8. System stability: (a) local in the sense of Lyapunov, (b) global in the sense of Lyapunov, (c) local asymptotic, and (d) global asymptotic.

In other words, Lyapuniv’s stability does not guarantee that the system is absolutely insensitive to any internal disturbances. Instead, it claims that the sensitivity is just such that the system behaves with time within the certain bounds $|\varepsilon|$. For a great deal of applications the condition (2.233) is appropriate. Therefore, this measure has gained wide currency.

Uniform stability (in the sense of Lyapunov): An equilibrium point “0” of (2.232) is said to be uniformly stable in the sense of Lyapunov if it is stable in the sense of Lyapunov with $\delta(\varepsilon) > 0$, meaning that δ does not depend on t_0 .

□

This definition is illustrated by Fig. 2.8a if we think that δ takes values independently on the start moment t_0 .

Asymptotic stability: An equilibrium point “0” of (2.232) is said to be asymptotically stable if

1. It is stable,
2. Every movement beginning closely to zero tends toward zero with $t_0 \leq t \rightarrow \infty$ such that

$$\|\tilde{\mathbf{q}}(t_0)\| < \delta \quad \text{and} \quad \lim_{t \rightarrow \infty} \tilde{\mathbf{q}}(t) = 0. \quad (2.234)$$

□

As well as the Lyapunov stability, the asymptotic stability is classified to be local and global. Examples of both kinds are shown in Fig. 2.8c and Fig. 2.8d, respectively. The difference between the Lyapunov and asymptotic stabilities is that, in the first case, the system behaves within the bounds $|\varepsilon|$, whereas the second case claims the system to behave toward zero with time.

Example 2.36. Consider an electrical circuit shown in Fig. 2.9 and described

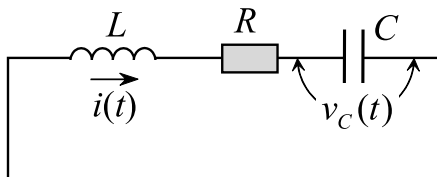


Fig. 2.9. Electric circuit of the second order.

for the voltage v_C induced on the capacitor C with the ODE

$$v_C'' + \frac{R}{L}v_C' + \frac{1}{LC}v_C = 0.$$

Let us assign v_C to be the first state, $q_1(t) = v_C(t)$, and an electric current to be the second state, $i(t) = q_2(t) = Cv_C' = Cq_1'(t)$. We thus go to the equations

$$q_1' = \frac{1}{C}q_2, \quad q_2' = -\frac{1}{L}q_1 - \frac{R}{L}q_2.$$

To ascertain stability, we find the internal energy of the circuit,

$$E = \frac{Cv_C^2}{2} + \frac{Li^2}{2} = \frac{Cq_1^2}{2} + \frac{Lq_2^2}{2},$$

and then define its time derivative (rate)

$$E'(t) = -Rq_2^2(t) = -Rv_L^2(t).$$

Immediately one concludes that, by $R > 0$, the energy dissipates with time to zero (by negative rate) and the circuit is thus stable. One then can suppose some $\varepsilon > 0$ and $\delta > 0$ and realize that this system is stable in the sense of Lyapunov. Because δ can be set arbitrary, the stability is global. Moreover, since energy dissipates with time to zero, the circuit is asymptotically stable and, by arbitrary δ , it is globally asymptotically stable. \square

When we think about asymptotic convergence of any function, we also wonder if this convergence is exponential or not. From the standpoint of engineering needs, if any behavior is expressed in terms of simple functions, then such a behavior is perceived as generalized. Therefore, the asymptotic stability is often considered to be the exponential stability, provided the definition:

Exponential stability: An equilibrium point “0” of (2.232) is said to be *exponentially stable* if there exists positive-valued constants $\beta > 0$, $\alpha > 0$, and $\varepsilon > 0$ such that

$$\|\tilde{\mathbf{q}}(t)\| \leq \beta e^{-\alpha(t-t_0)} \|\tilde{\mathbf{q}}(t_0)\| \quad \text{for} \quad \|\tilde{\mathbf{q}}(t_0)\| \leq \varepsilon \quad \text{and} \quad t \geq t_0, \quad (2.235)$$

where the largest allowed α is called the *rate of convergence*. □

Because the bound ε is not limited and hence the initial state $\mathbf{q}(t_0)$ may take any value, this kind of stability is also called the *global exponential stability* often abbreviated as G.E.S. In analogous to the asymptotic stability, if $\varepsilon < \beta$, the exponential stability may be said to be *local*. In applications, exponential stability has appeared to be a strong form of stability, since both uniform and asymptotic stability definitions are absorbed. In particular, exponential convergence was shown to be robust to perturbations that makes it to be essential for control algorithms.

The most loose definition of stability arises from the works of Lagrange on the stability of equilibrium states of discrete conservative system. Lagrange showed that if the potential energy reaches its minimum at a position of equilibrium, then this position is stable, whereas if the potential energy reaches its maximum, the position is unstable. Developed in further by Dirichlet and some other authors, the definition of Lagrange’s stability may be formulated as follows:

Stability (in the sense of Lagrange): The state $\tilde{\mathbf{q}}(t_0)$ of (2.232) is said to be restricted or stable in the sense of Lagrange if for any t_0 there exists a real $B[\tilde{\mathbf{q}}(t_0), t_0] < \infty$ such that

$$\|\tilde{\mathbf{q}}(t)\| < B \quad \text{for} \quad t \geq t_0. \quad (2.236) \quad \square$$

As follows from this definition, the Lagrange stable system is not obligatorily staying at equilibrium.

Links with External Stability

It follows from the above-given definitions that the internal stability is completely determined via the system states. Contrary, the external stability involves the system input and output. In recent decades, many efforts have been made to find a link between two concepts of stability and ascertain stability in

some common sense. Consequently, new “cross” definitions were introduced and elaborated as connected with the important system properties such as *stabilizability* and *detectability*. The problem is still under investigation, because the externally stable system is not always internally stable. Below we refer only to several important results:

- *Input/output to state stability* (IOSS): This property is also called *detectability* and *strong unboundedness observability*. The notion suggests that if the input and output are both small, the state must be eventually small. It was also mentioned by Sontag and Wang that it is not a notion of stability, because, for example, the unstable system $\mathbf{q}'(t) = \mathbf{q}(t)$, $\mathbf{y}(t) = \mathbf{q}(t)$ is IOSS. Rather, it represents a property of zero-state detectability. \square
- *Input to output stability* (IOS): If a system is IOS, then it is also *robustly output stable* (ROS). However, there is ROS system that is not IOS. \square
- *Input to state stability* (ISS): A system is ISS if and only if it is IOSS and IOS. \square
- *Output to state stability* (OSS): This property is associated with the property of detectability. \square

Overall, there is an opinion that internal system stability is equivalent to detectability plus external stability. The proof, however, follows by routine arguments.

Based on the above-given definitions of system stability, we may now continue with observing general conditions for linear and nonlinear systems to be stable in different senses.

2.8.3 Stability of Linear Systems

If a system is linear and, possibly, time-varying, its stability at zero is ascertained by the state space equation

$$\mathbf{q}'(t) = \mathbf{A}(t)\mathbf{q}(t) \quad (2.237)$$

Moreover, by the theory of ODEs, the equilibrium point is unique if the determinant of $\mathbf{A}(t)$ is not zero, $|\mathbf{A}(t)| \neq 0$ for $t \geq t_0$.

It will be shown in Chapter 4 that a general solution of (2.237) is given by

$$\mathbf{q}(t) = \mathbf{\Phi}(t, t_0)\mathbf{q}(t_0), \quad (2.238)$$

where $\mathbf{\Phi}(t, t_0)$ is the so-called *state transition matrix* of a system, characterized by two major properties: $\mathbf{\Phi}'(t, t_0) = \mathbf{A}(t)\mathbf{\Phi}(t, t_0)$ and $\mathbf{\Phi}(t_0, t_0) = \mathbf{I}$. Employing $\mathbf{\Phi}(t, t_0)$, the condition for a system to be stable can be found as in the following.

Stability in the Sense of Lyapunov

An equilibrium point of a system described by (2.237) is stable in the sense of Lyapunov if for any real $\varepsilon > 0$ there exists a real $\delta > 0$ such that

$$\|\Phi(t, t_0)\mathbf{q}(t_0)\| < \varepsilon \quad \text{for} \quad \|\mathbf{q}(t_0)\| < \delta. \quad (2.239)$$

On the other hand, by the multiplication condition, we have

$$\|\Phi(t, t_0)\mathbf{q}(t_0)\| \leq \|\Phi(t, t_0)\| \|\mathbf{q}(t_0)\|,$$

where $\|\mathbf{q}(t_0)\|$ is restricted with δ and thus it is in order to write

$$\|\Phi(t, t_0)\mathbf{q}(t_0)\| < \|\Phi(t, t_0)\| \delta. \quad (2.240)$$

Comparing (2.239) and (2.240), one concludes that the condition (2.239) is satisfied for any real value M such that

$$\|\Phi(t, t_0)\| < M < \infty \quad \text{with} \quad \delta = \frac{\varepsilon}{M}. \quad (2.241)$$

In other words, a linear system is stable in the sense of Lyapunov if the norm of its state transition matrix does not reach $M = \varepsilon/\delta$ with $\|\mathbf{q}(t_0)\| < \delta$. If so, the system behavior is bounded by $\|\mathbf{q}(t)\| < \varepsilon$ for $t \geq t_0$.

Stability in the Sense of Lagrange

If a linear system (2.237) is supposed to work with any initial state $\mathbf{q}(t_0)$ having the finite norm $\|\mathbf{q}(t_0)\| < \infty$, the system is stable in the sense of Lagrange if and only if its transition matrix satisfies

$$\|\Phi(t, t_0)\| < M < \infty \quad \text{with} \quad t \geq t_0, \quad (2.242)$$

where M is some allowed finite real bound. It then follows that an equilibrium point $\mathbf{q}(t_0)$ of a linear system is Lyapunov stable if and only if it is Lagrange stable.

Asymptotic Stability

In a similar manner, the asymptotic stability can be ascertained. An equilibrium point of a linear system (2.237) is asymptotically stable if, and only if, the norm of the state transition matrix is finite with time and tends toward infinity with $t \rightarrow \infty$. This means that

$$\|\Phi(t, t_0)\| < M < \infty \quad \text{with} \quad t \geq t_0 \quad \text{and} \quad \lim_{t \rightarrow \infty} \|\Phi(t, t_0)\| = 0, \quad (2.243)$$

where M is still some allowed finite real value. So long as the condition (2.243) deals solely with the norm of the state transition matrix, it is also the condition for the global asymptotic stability.

Exponential Stability

The concept of asymptotic stability may now be extended to the exponentially decaying envelope. By the definition, an equilibrium point is exponentially stable if there exists positive-valued constants $\beta > 0$, $\alpha > 0$, and $\varepsilon > 0$ such that

$$\|\Phi(t, t_0)\mathbf{q}(t_0)\| \leq \beta e^{-\alpha(t-t_0)} \|\mathbf{q}(t_0)\|$$

for $\|\mathbf{q}(t_0)\| \leq \varepsilon$ and $t \geq t_0$. Applying the multiplication condition, we go to the relation

$$\begin{aligned} \|\Phi(t, t_0)\mathbf{q}(t_0)\| &\leq \|\Phi(t, t_0)\| \|\mathbf{q}(t_0)\| \leq \beta e^{-\alpha(t-t_0)} \|\mathbf{q}(t_0)\|, \\ \|\Phi(t, t_0)\| &\leq \beta e^{-\alpha(t-t_0)}, \end{aligned} \quad (2.244)$$

meaning that a system is exponentially stable if the norm of its state transition matrix traces with time toward zero starting at $\mathbf{q}(t_0)$ within the exponential bound.

The above conditions given for linear systems cannot commonly be applied to nonlinear systems and some other approaches are used. An exception is when the initial condition is placed closely to equilibrium. In this case, a nonlinear system is linearized and the above-given definitions guarantee the system stability. Below we observe the most common methods for nonlinear systems.

2.8.4 The First Lyapunov Method

Let us come back to the general state equation for nonlinear systems (2.224) and discuss how the conditions of stability can be derived from. Commonly, the procedure entails difficulty that, for NTI and NTV systems, is circumvented by the first and second Lyapunov methods, respectively. However, some other approaches are also efficiently used.

By his first method also called *indirect*, Lyapunov solved the problem with stability by linearizing an NTI system at the point of equilibrium. To follow, assume that an autonomous NTI system is described with the state equation $\mathbf{q}'(t) = \Psi[\mathbf{q}(t)]$ that is the time-invariant version of (2.230). Let this system has n points of equilibrium \mathbf{q}_i , $i \in [1, n]$, at which $\Psi[\mathbf{q}_i] = 0$. The following theorem states how stability of such a system can be ascertained.

Theorem (the first Lyapunov method): A point of equilibrium \mathbf{q}_i of a system described by the nonlinear ODE

$$\mathbf{q}'(t) = \Psi[\mathbf{q}(t)], \quad \Psi[\mathbf{q}_i] = 0, \quad (2.245)$$

is asymptotically stable if the point of equilibrium $\tilde{\mathbf{q}}_i$ of the corresponding linearized system described by the linear ODE

$$\tilde{\mathbf{q}}'(t) = \mathbf{A}\tilde{\mathbf{q}}(t), \quad (2.246)$$

where $\mathbf{A} = \left. \frac{\partial \Psi[\mathbf{q}(t)]}{\partial \mathbf{q}(t)} \right|_{\tilde{\mathbf{q}}_i}$, is asymptotically stable. □

To verify, one must expand the function $\Psi[\mathbf{q}(t)]$ to the Taylor series at the point of equilibrium. Saving the terms in the second order of approximation, we thus have

$$\tilde{\mathbf{q}}'(t) = \mathbf{A}\tilde{\mathbf{q}}(t) + \mathbf{e}(t),$$

where every component of the vector $\mathbf{e}(t) \equiv \mathbf{e}(\|\tilde{\mathbf{q}}(t)\|^2)$ is a small value predefined by the relevant component of $\|\tilde{\mathbf{q}}(t)\|^2$. Considering $\mathbf{e}(t)$ to be the “input”, one can write a general solution of this ODE as follows (in Chapter 4, we shall discuss the solution in detail)

$$\tilde{\mathbf{q}}(t) = \Phi(t, t_0)\tilde{\mathbf{q}}(t_0) + \int_{t_0}^t \Phi(t, \theta)\mathbf{e}(\theta) d\theta,$$

where $\Phi(t, t_0) = e^{\mathbf{A}(t-t_0)}$ is the state transition matrix. Exploiting the multiplication condition and triangle inequality, the norm of the solution can be expressed by

$$\|\tilde{\mathbf{q}}(t)\| \leq \|\Phi(t, t_0)\|\|\tilde{\mathbf{q}}(t_0)\| + \int_{t_0}^t \|\Phi(t, \theta)\|\|\mathbf{e}(\theta)\| d\theta.$$

Now recall that, by (2.244), the exponential stability of a system like (2.246) is guaranteed if there exist real positive numbers $\beta > 0$ and $\alpha > 0$ such that $\|\Phi(t, t_0)\| = \|e^{\mathbf{A}(t-t_0)}\| \leq \beta e^{-\alpha(t-t_0)}$ for $t \geq t_0$. By this condition, we immediately have

$$\|\tilde{\mathbf{q}}(t)\| \leq \beta e^{-\alpha(t-t_0)}\|\tilde{\mathbf{q}}(t_0)\| + \int_{t_0}^t \beta e^{-\alpha(t-\theta)}\|\mathbf{e}(\theta)\| d\theta.$$

On the other hand, the exponentially decaying function must satisfy the condition for asymptotical stability. This means that for the given real positive $\varepsilon > 0$ and $\delta > 0$ the norm $\|\mathbf{e}(t)\|$ must be such that

$$\|\mathbf{e}(t)\| \leq \frac{\varepsilon}{\beta}\|\tilde{\mathbf{q}}(t)\| \quad \text{for} \quad \|\tilde{\mathbf{q}}(t)\| \leq \delta.$$

Accordingly, we go to

$$e^{\alpha(t-t_0)}\|\tilde{\mathbf{q}}(t)\| \leq \beta\|\tilde{\mathbf{q}}(t_0)\| + \varepsilon \int_{t_0}^t e^{\alpha(\theta-t_0)}\|\tilde{\mathbf{q}}(\theta)\| d\theta$$

and, by the Grönwall³¹-Bellman³² inequality (Appendix E), arrive at

$$e^{\alpha(t-t_0)} \|\tilde{\mathbf{q}}(t)\| \leq \beta \|\tilde{\mathbf{q}}(t_0)\| e^{\varepsilon(t-t_0)}$$

that readily produces

$$\|\tilde{\mathbf{q}}(t)\| \leq \beta \|\tilde{\mathbf{q}}(t_0)\| e^{-(\alpha-\varepsilon)(t-t_0)}.$$

For a system to be exponentially stable, the value of ε in the latter relation must be set such that $\varepsilon < \alpha$. If so and still $\|\tilde{\mathbf{q}}(t)\| \leq \delta$, we can write $\|\tilde{\mathbf{q}}(t)\| \leq \beta \|\tilde{\mathbf{q}}(t_0)\|$. This means, in turn, that $\|\tilde{\mathbf{q}}(t_0)\| < \frac{\delta}{\beta}$ and we finally get

$$\|\tilde{\mathbf{q}}(t)\| \leq \delta e^{-(\alpha-\varepsilon)(t-t_0)} \quad \text{for } t \geq t_0. \quad (2.247)$$

An importance of the inequality (2.247) resides in the following fact. It proves that the exponential stability of an NTI system at the point of equilibrium is guaranteed by the exponential stability of its linearized version at the same point.

Example 2.37. The amplitude $V(t)$ of a signal of a crystal oscillator is modeled at low drive levels with the ODE

$$V' = \left(\alpha - \frac{\gamma}{V^2} \right) V, \quad \gamma > 0.$$

By setting $V' = 0$, the equilibrium point is defined as $V_0 = \sqrt{\gamma/\alpha}$. Following the linearization procedure, the equation is linearized at V_0 to be

$$\tilde{V}' = 2\alpha\tilde{V}.$$

The conclusion follows instantly. If $\alpha > 0$, the amplitude develops without bounds with V_0 real. By $\alpha < 0$, the amplitude attenuates to zero exponentially, but a real V_0 does not exist (V_0 is imaginary). So, the point V_0 is unstable. \square

Example 2.38. Consider the Rayleigh oscillator

$$y' = -\omega z, \quad z' = \omega y + \epsilon(1 - \mu z^2)z$$

with $\omega = \epsilon = 1$ and μ arbitrary. Because the factor ϵ is not small, averaging cannot be allowed. Instead, assigning $q_1 = y$ and $q_2 = z$, we go to the state space model

$$\mathbf{q}'(t) = \Psi[\mathbf{q}(t)],$$

where

$$\mathbf{q} = \begin{bmatrix} q_1 \\ q_2 \end{bmatrix}, \quad \Psi = \begin{bmatrix} -q_2 \\ q_1 + (1 - \mu q_2^2)q_2 \end{bmatrix}.$$

³¹ Thomas Hakon Grönwall, Swedish-born US mathematician, 16 January 1877–9 May 1932.

³² Richard Ernest Bellman, US mathematician, 26 August 1920–19 March 1984.

Following (2.246), the linearized system matrix appears to be

$$\mathbf{A} = \begin{bmatrix} 0 & -1 \\ 1 & 1 - 3\mu q_{20}^2 \end{bmatrix},$$

where q_{20} is the second state at equilibrium. The characteristic equation associated with this matrix is $\lambda^2 + \sigma\lambda + \Delta = 0$, where $\sigma = 3\mu q_{20}^2 - 1$ and $\Delta = 1 > 0$. It is known from the theory of ODEs that if $\sigma > 0$ and $\Delta > 0$, then the linearized system is asymptotically stable. Accordingly, a solution is asymptotically stable if $\mu > 1/3q_{20}^2$. \square

Example 2.39. A system is described with the equations

$$q_1' = 2q_1(1 + q_2) + 3q_2^2, \quad q_2' = q_1 + q_2(1 + q_1),$$

having the point of equilibrium at zero. For this point, $q_1 = q_2 = 0$, the linearized system is performed, following (2.246), by

$$\begin{bmatrix} q_1' \\ q_2' \end{bmatrix} = \left. \begin{bmatrix} 2(1 + q_2) & 2q_1 + 6q_2 \\ 1 + q_2 & 1 + q_1 \end{bmatrix} \right|_0 \begin{bmatrix} q_1 \\ q_2 \end{bmatrix},$$

$$\begin{bmatrix} q_1' \\ q_2' \end{bmatrix} = \begin{bmatrix} 2 & 0 \\ 1 & 1 \end{bmatrix} \begin{bmatrix} q_1 \\ q_2 \end{bmatrix}.$$

The characteristic equation of the linearized system matrix \mathbf{A} is given by $\lambda^2 - 3\lambda + 2 = 0$. Because one of the coefficients is negative, the equilibrium point is unstable. \square

As one can see, the first method by Lyapunov implies that the linearized solution of a nonlinear ODE can be found. If it cannot be found or a nonlinear system is time-varying, the *second method of Lyapunov* also known as the *method of Lyapunov functions* is used.

2.8.5 The Second Lyapunov Method

In the second method by Lyapunov often called *direct*, the stability problem of an NTV system

$$\mathbf{q}'(t) = \Psi[\mathbf{q}(t), t] \tag{2.248}$$

at a point of equilibrium is solved by finding some scalar continuous function $V(\mathbf{q})$ (the *Lyapunov function*) possessing the certain properties. There is no universal receipt how to find this function, except for some classes of nonlinear ODEs. Despite this fact, the method has appeared to be highly efficient in solving many theoretical and applied problems associated with system stability.

An idea of the approach can easily be caught by imitating a system with a football player kicking a ball in some media to hit a target placed in Fig. 2.10 at “0” of the coordinates q_1, q_2, z .

A system is supposed to be stable if with any even absolutely incredible trajectory (although featured to this system) a ball hits a target. Otherwise, a system is unstable. If all trajectories hitting a target are closed within some function $V(q_1, q_2, t)$, the latter is said to be the *Lyapunov function*. One therefore can truly interpret the Lyapunov function as a “snare for a ball”.

Most generally, the Lyapunov function is a function of n variables and we can write it as $V[\mathbf{q}(t), t]$. If we now analyze this function for a situation sketched in Fig. 2.10, we can come to the conclusion that the Lyapunov function possesses some necessary properties. First of all, it could be thought of as *generalized energy function* for a system. In fact, in passive media the energy always dissipates (except at 0) and the function thus reduces with time to zero. Moreover, in such media, energy dissipates monotonously, to mean that the time derivative of V should always be negative. This deduction extends to NTV systems, in which V is time-varying. Indeed, if we want the system to work stably, we must think that no time variations are able to affect the monotonously dissipated energy to be not dissipated.

From what is observed, it follows that the Lyapunov function V must be *positive definite*, provided the definition:

Positive definite function: A function $V[\mathbf{q}(t), t]$ is positive definite in some space \mathbb{R} if

- V is continuous and differentiable □
- $V \geq 0$ for all $\mathbf{q}(t)$ and t □
- $V(0, t) = 0$ if and only if $\mathbf{q}(t) = 0$ □
- $V \rightarrow \infty$ as $\mathbf{q}(t) \rightarrow \infty$ □

□

The following Lyapunov theorem states when a system is stable in terms of the positive definite function V .

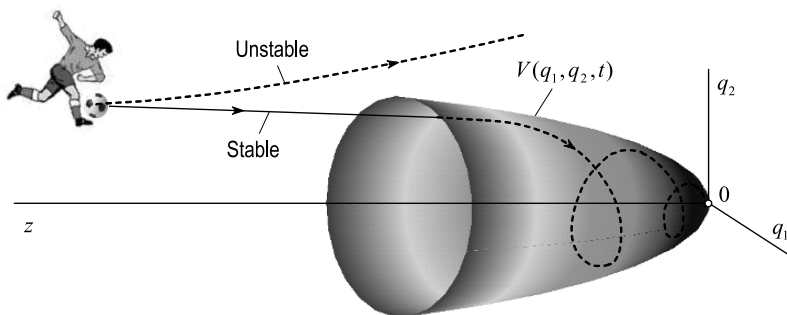


Fig. 2.10. Interpretation of the second Lyapunov method.

Lyapunov theorem: A point of equilibrium “0” of a system (2.248) is stable if there exists a positive definite function $V[\mathbf{q}(t), t]$ such that its time derivative V' is *non-positive* for all trajectories $\mathbf{q}(t)$ of a system. \square

Because the time derivative of V is allowed to be zero, stability stated by this theorem is often understood in the sense of Lyapunov. This means that a stable solution for a system will exist in some bound $\delta > 0$ such that $\|\mathbf{q}(t)\| < \delta$. If the system behavior is required to be asymptotically stable, the other theorem is applied.

Lyapunov theorem (asymptotic stability): A point of equilibrium “0” of a system (2.248) is asymptotically stable (every trajectory converges to zero at $t \rightarrow \infty$) if there exists a positive definite function $V[\mathbf{q}(t), t]$ such that its time derivative V' is *negative* for all trajectories $\mathbf{q}(t)$ of a system. \square

In this case, the time derivative of V is always negative. Therefore the system solution tends toward zero with time. Because the Lyapunov function can take any positive finite value, such stability is also called the *global asymptotic stability* (G.A.S).

Let us prove this theorem. Suppose a solution of (2.248) converges to some value $\xi \geq 0$ and we wonder if this value should obligatory be zero. Having a nonzero value at $t \rightarrow \infty$, the Lyapunov function may be searched such that

$$\xi \leq V[\mathbf{q}(t)] \leq V[\mathbf{q}(0)].$$

We can also think that a solution converges with a maximum rate $V'_{\max} = -v < 0$ and hence $V' \leq -v$ for $t \geq 0$.

Accounting for the above-given considerations, the Lyapunov function related to some time instant T must satisfy

$$\xi \leq V[\mathbf{q}(T)] = V[\mathbf{q}(0)] + \int_0^T V'(z) dz \leq V[\mathbf{q}(0)] - vT$$

that yields

$$\xi \leq V[\mathbf{q}(T)] \leq V[\mathbf{q}(0)] - vT.$$

If we now increase T , the right-hand side will become negative with $T > V[\mathbf{q}(0)]/v$ that leads to a contradiction. Because the function V cannot be negative, the only reasonable value for ξ is zero and the proof is complete.

Example 2.40. Let us come back to the circuit (Fig. 2.9) and ascertain its stability with the direct Lyapunov method. In state space, by $q_1(t) = v_C(t)$ and $q_2(t) = i(t) = Cv'_C = Cq'_1(t)$, the circuit is described with the equations

$$q'_1 = \frac{1}{C}q_2, \quad q'_2 = -\frac{1}{L}q_1 - \frac{R}{L}q_2.$$

The best candidate to the Lyapunov function is therefore an equation of internal energy

$$V[\mathbf{q}(t)] = \frac{Cq_1^2}{2} + \frac{Lq_2^2}{2},$$

which time-derivative gives

$$V'[\mathbf{q}(t)] = -Rq_2^2(t),$$

where R is real and positive. It may easily be verified that the function V is continuous, differentiable, and positive for all $\mathbf{q}(t)$ and t . Yet, $V(0, t) = 0$ and $V \rightarrow \infty$ with $\mathbf{q}(t) \rightarrow \infty$. So, this is the Lyapunov function. Because for real positive R the rate V' is always negative, the circuit is asymptotically stable. Recall that in Example 2.38 we arrived at the same conclusion via the dissipated energy. \square

Example 2.41. Consider an oscillator loop combined with two RC circuits and two limiters, direct and inverting, respectively,

$$f_1(q_1) = \begin{cases} 1, & q_1 > 0 \\ -1, & q_1 < 0 \end{cases} \quad \text{and} \quad f_2(q_2) = \begin{cases} -1, & q_2 > 0 \\ 1, & q_2 < 0 \end{cases}$$

as shown in Fig. 2.11.

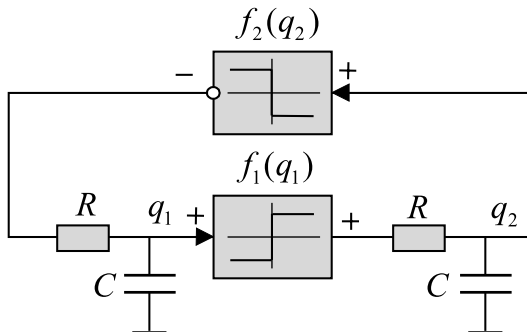


Fig. 2.11. Closed oscillator loop.

The voltages at the outputs of the limiters are defined by $f_1(q_1) = q_2 + RCq_2'$ and $f_2(q_2) = q_1 + RCq_1'$. The system is thus described in state space with $\mathbf{q}'(t) = \Psi[\mathbf{q}(t)]$, where, by $C = 1$ and $R = 1$,

$$\mathbf{q} = \begin{bmatrix} q_1 \\ q_2 \end{bmatrix}, \quad \Psi = \begin{bmatrix} -q_1 + f_2(q_2) \\ -q_2 + f_1(q_1) \end{bmatrix}.$$

To ascertain stability, let us choose the Lyapunov function such that

$$V(\mathbf{q}) = \frac{Cq_1^2}{2} + \frac{Cq_2^2}{2} = \frac{q_1^2}{2} + \frac{q_2^2}{2}.$$

The time-derivative of V is given by

$$V'(\mathbf{q}) = -(q_1^2 + q_2^2) + q_1 f_2(q_2) + q_2 f_1(q_1).$$

An analysis of two last terms shows that they take values $\pm 1(q_1 - q_2)$, where the multiplier “1” represents the maximum unit voltage in the loop. Over period of oscillations, the terms produce zero and we have

$$V'(\mathbf{q}) = -(q_1^2 + q_2^2) = -2V,$$

meaning that the time-derivative of V is negative and the system is hence stable. \square

Following the definition, the asymptotic stability can readily be extended to the exponential stability, provided the definition:

Lyapunov theorem (exponential stability): A point of equilibrium “0” of a system (2.148) is exponentially stable, meaning that every trajectory of $\mathbf{q}'(t) = \Psi[\mathbf{q}(t), t]$ satisfies

$$\|\mathbf{q}(t)\| \leq \beta e^{-\frac{\alpha t}{2}} \|\mathbf{q}(0)\|,$$

where $\beta > 0$, if there exists a positive definite function $V[\mathbf{q}(t), t]$ and a constant $\alpha > 0$ such that $V' \leq -\alpha V$. \square

A motivation to satisfy an inequality $V' \leq -\alpha V$ arises from the observation that the latter guarantees minimum dissipation rate, proportional to energy. Because β is allowed to be any positive finite value, this stability is global exponential (G.E.S).

In this Chapter, we considered the most efficient and thus basic *quantitative* methods of linear and nonlinear systems analysis in the time and frequency (transform) domains. It turns out that in many cases time and frequency are not the proper scales to learn systems and another methods called *qualitative* are often used to complete an analysis with information taken from the so-called *phase plane*.

2.9 Summary

Quantitative methods unite the most powerful tools of system analysis in the time and frequency (transform) domains. Before continuing with applying these methods to different kinds of systems, the reader is encouraged to go over the material once again emphasizing the following fundamentals:

- The response of a system to the unit impulse is the system impulse response.
- The response of a system to the unit step is the system step response.
- The response of a system to $e^{j\omega t}$ is the system frequency response, represented with the magnitude and phase responses.
- For LTI systems, the impulse and frequency responses are coupled with the Fourier transform. This is not valid for another types of systems.
- In LTI systems, the output is coupled with the input via the impulse response by the convolution.
- In LTV systems, the output is coupled with the input via the time-varying impulse response by the general convolution.
- In nonlinear systems, the output is coupled with the input via the generalized impulse response (Volterra kernels) by the generalized convolution (Volterra series).
- Any dynamic system can be described with the ODE of a proper order and represented in state space.
- System states are associated with time derivatives.
- The transfer function of an LTI system is a ratio of the Laplace transform of its output and the Laplace transform of its input. This is not valid for another type of systems.
- The ODE of a nonlinear system with a small parameter may be substituted with two nonlinear ODEs of the first order for the amplitude and phase.
- By equivalent linearization, an NLI system is converted to the LTV system.
- The “norm” means a measure of the “size” of a signal and, thereby, a system.
- Stability means a negligible sensitivity of a system to slight external and internal disturbances.
- Stability can be internal and external. Both can be ascertained in a different sense.
- The most general theory of stability was created by Lyapunov.

2.10 Problems

2.1. Find simple words and examples to explain the difference between linear and nonlinear, time-invariant and time-varying systems.

2.2. They say that the methods for linear systems are not applicable for nonlinear systems. Is it true? If yes, then why is the theory of LTI systems fundamental for other systems? Explain with examples.

2.3 (Response of a system). An LTI system is represented with the following impulse response. Define the step response, frequency response, magnitude response, and phase response of a system.

1. $h(t) = \delta(t)$

2. $h(t) = u(t) - u(t - 1)$
3. $h(t) = ae^{-bt}u(t) + c\delta(t)$
4. $h(t) = au(t) - au(t - 1) + b\delta(t)$
5. $h(t) = u(t)$

2.4. An LTI system is represented with the following frequency response. Define the magnitude, phase, impulse, and step responses of a system.

1. $H(j\omega) = a$
2. $H(j\omega) = a[u(\omega + \omega_0) - u(\omega - \omega_0)]$
3. $H(j\omega) = ae^{|a\omega|}$
4. $H(j\omega) = \delta(\omega)$
5. $H(j\omega) = \delta(j\omega - j\omega_0)$
6. $H(j\omega) = ae^{jb\omega}$

2.5 (Convolution). A causal input signal is described by $x(t) = Ae^{-bt}u(t)$. Using the convolution integral, define the output signal $y(t)$ for the impulse response of a system specified in Problem 2.3.

2.6. An input signal has a rectangular waveform $x(t) = A[u(t + \tau/2) - u(t - \tau/2)]$. Write the spectral density of the input and determine the spectral density of the output for the frequency response specified in Problem 2.4. By the inverse Fourier transform, define the time function of the output.

2.7 (Volterra series). A nonlinear system is shown in Fig. 2.4 and described with the Volterra series (2.54). Define the system output for $x(t) = A$ and the impulse response given in Problem 2.3.

2.8. Using the Volterra approach, write the integral equations of the nonlinear systems shown in Fig. 2.12.

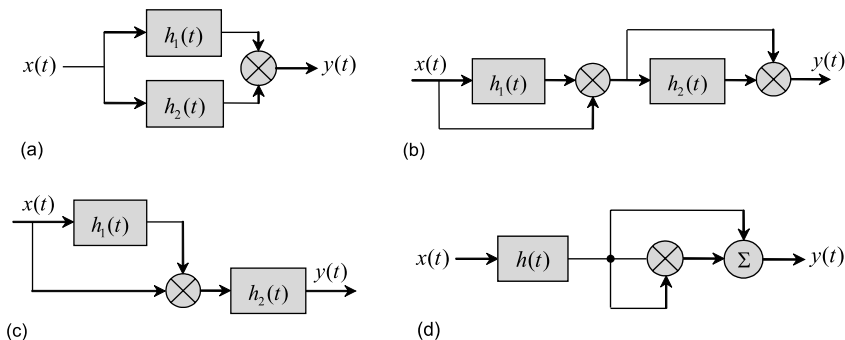


Fig. 2.12. Nonlinear systems.

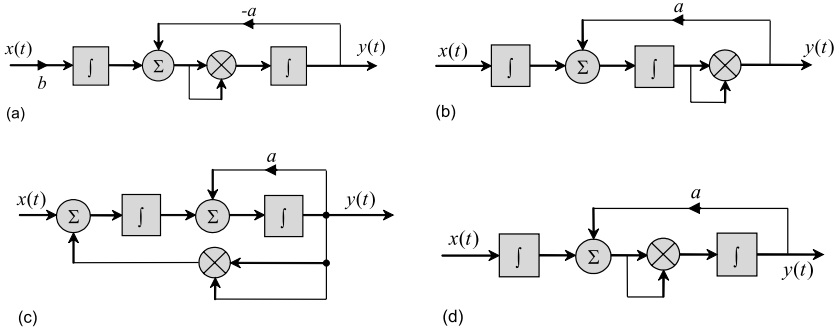


Fig. 2.13. Systems performed with block diagrams.

2.9 (Differential equation). A nonlinear system is performed with the block diagram shown in Fig. 2.13. Write the differential equation of a system.

2.10. Consider a system shown in Fig. 2.13. Suppose that the multiplier is absent in the structure and the system is thus linear. Write the differential equation of a system. Find the impulse and frequency responses of a system.

2.11. A system is represented with the following differential equation. Show the block diagram of a system.

1. $y'' - 3y' + 4y = -2x' + x$
2. $3y'' + yy' = x$
3. $2x' + y' = y$
4. $2x + y'' = 2yy'$
5. $x' + x = y' + y$
6. $y'' + 2y' - y = x'' - 2x' + x$

2.12 (Transfer function). A linear system is represented with the following differential equation. Define the system transfer function.

1. $2y'' + 4y = -2x' + x$
2. $a_2y'' + a_1y' = b_1x$
3. $v' + 2v = 5v_C$
4. $y(t) = \sum_{m=0}^2 \beta_{2-m} \frac{d^m}{dt^m} x(t) - \sum_{n=1}^2 \alpha_{2-n} \frac{d^n}{dt^n} y(t)$
 $\beta_0 = 2, \beta_1 = 1, \beta_2 = 2, \alpha_1 = 3, \alpha_2 = 1$
5. $\sum_{n=0}^3 a_n \frac{d^n}{dt^n} y(t) = \sum_{m=0}^2 b_m \frac{d^m}{dt^m} x(t)$
 $a_0 = 1, a_1 = 2, a_2 = 3, a_3 = 2, b_0 = 1, b_1 = 3, b_2 = 2$
6. $y(t) = \sum_{m=0}^2 \frac{b_m}{a_0} \frac{d^m}{dt^m} x(t) - \sum_{n=1}^1 \frac{a_n}{a_0} \frac{d^n}{dt^n} y(t)$

2.13. A system is described with the following transfer function. Convert the transfer function to the differential equation.

1. $H(s) = s$
2. $H(s) = \frac{1}{s}$
3. $H(s) = \frac{1}{s^2 + 2s + 1}$
4. $H(s) = s^2 + 2s + 1$
5. $H(s) = \frac{(s+1)(s+2)}{(s-1)(s-2)}$
6. $H(s) = 1 + \frac{1}{s}$

2.14 (State space presentation). A system is given with the following state space model. Write the differential equation of a system.

1.

$$\begin{bmatrix} dq_1(t) \\ dq_2(t) \\ dq_3(t) \end{bmatrix} = \begin{bmatrix} 0 & 1 & 0 \\ 0 & 0 & 1 \\ 0 & 0 & 0 \end{bmatrix} \begin{bmatrix} q_1(t) \\ q_2(t) \\ q_3(t) \end{bmatrix} dt, \quad y(t) = [1 \ 0 \ 0] \begin{bmatrix} q_1(t) \\ q_2(t) \\ q_3(t) \end{bmatrix}$$

2.

$$\begin{bmatrix} dq_1(t) \\ dq_2(t) \end{bmatrix} = \begin{bmatrix} 0 & A \\ 0 & 0 \end{bmatrix} \begin{bmatrix} q_1(t) \\ q_2(t) \end{bmatrix} dt, \quad y(t) = [B \ 0] \begin{bmatrix} q_1(t) \\ q_2(t) \end{bmatrix}$$

3.

$$\begin{bmatrix} dq'_1(t) \\ dq'_2(t) \end{bmatrix} = \begin{bmatrix} 1 & 0.5 \\ 0 & 1 \end{bmatrix} \begin{bmatrix} q_1(t) \\ q_2(t) \end{bmatrix} dt, \quad y(t) = [1 \ 0] \begin{bmatrix} q_1(t) \\ q_2(t) \end{bmatrix}$$

2.15. A system is represented in state space with the equations (Problem 2.14). Write the differential equation of the system.

2.16. The differential equation of a system is defined by the transfer function derived in Problem 2.12. Represent the system in state space.

2.17. A system is performed with the differential equation derived in Problem 2.10. Represent the system in state space.

2.18 (Linearization). The following nonlinear differential equation describes a system. Using the method of linearization, rewrite the equation in the linearized form around the given initial point $y_0, y'_0, \dots, x_0, x'_0, \dots$

1. $y'' - 3yy' = 4y - 2x' + x$
2. $3y'' + (y')^2 = x$
3. $2x' = y' + y^2$
4. $2x^2 + y'' = 2yy'$
5. $xx' + x = y' + y$
6. $y'' + y^2 = -2x' + x$

2.19. A system is described with the differential equation associated with the block diagram (Fig. 2.12). Represent this system with the linearized equation around the point $y_0, y'_0, \dots, x_0, x'_0, \dots$

2.20 (Averaging). The oscillatory system is represented with the following differential equation, in which ϵ is a small parameter. Using the method by Krylov and Bogoliubov, write the system equations for the amplitude and phase in the first order approximation.

1. $y'' + 3y = \epsilon(1 - y^3)y'$
2. $3y'' + \epsilon y' + y - \epsilon(y^3)' = 0$
3. $y'' + \epsilon(1 - ay^2)y' + y = 0$

2.21 (Equivalent linearization). Using the method of equivalent linearization, write the linearized ODEs for the system described in Problem 2.20.

2.22. An oscillatory system is described with the ODE (Problem 2.20). Using the classical harmonic balance method, define the stationary solution for the system in the first order approximation.

2.23. Using the method of describing functions, linearize the nonlinear equations given in Problem 2.20.

2.24 (Norms). Give simple interpretations for norms of signals and systems. Why not to characterize signals just with the maximum and minimum values and systems with the peak-values of the responses?

2.25. A system is represented with the impulse response (Problem 2.3). Define the H_2 -norm of a system.

2.26. A system is represented with the transfer function (Problem 2.13). Define the H_1 -norm, H_2 -norm, and H_∞ -norm of a system.

2.27 (Stability). A system is given with the impulse response (Problem 2.3) and transfer function (Problem 2.13). Ascertain the BIBO stability of a system.

2.28. Analyze the block diagrams (Fig. 2.13) and realize how the coefficient a can affect stability of a system? Which system is stable and which is potentially not?

2.29. A system is represented with the transfer function found in Problem 2.12. Investigate the poles of the transfer function and make a conclusion about the BIBO stability of a system.

2.30. A system is described in state space with the following equations. The equilibrium point lies at zero. Investigate stability of a system at this point by the first Lyapunov method.

1. $q_1' = q_1^2(2 + q_2) + 3q_2$, $q_2' = q_1(2 + q_2^2)(q_1^2 + q_2^2 - 1) + 3q_2$
2. $q_1' = q_1^2(2 + q_2)(q_1^2 + q_2^2 - 1) + q_2$, $q_2' = q_1$
3. $q_1' = q_2 + q_1q_2^2 + q_1^2q_2$, $q_2' = 3q_2 - 2q_1^2q_2^2 - q_1^2 + q_2^2$
4. $q_1' = q_2q_1(1 - 3q_2q_1)$, $q_2' = (q_2 - 3q_1^2)(2q_2^2 - q_1^2) + q_2^2$

2.31. A system is described in state space with the following equations. Assuming that the Lyapunov function $V(\mathbf{q}) = (q_1^2 + q_2^2)/2$ is truly selected for this system, make a conclusion about its stability by the second Lyapunov method.

1. $q_1' = -q_1 - 2q_2^3$, $q_2' = -q_2 - q_1^3$

2. $q_1' = -q_1 + q_2$, $q_2' = -q_2 - 3q_1$

3. $q_1' = -2q_1 - q_2^2$, $q_2' = -2q_2 + q_1^2$

4. $q_1' = -q_1 + 2q_2$, $q_2' = -q_2 + 4q_1$

If a system does not seem to be stable for the Lyapunov function given, try to find some other function. Alternatively, prove that the Lyapunov function does not exist and the system is thus unstable.

Qualitative Methods of Systems Description

In Chapter 2, we were concerned about the rigorous and approximate quantitative methods of linear and nonlinear systems analysis in the time and frequency (transform) domains. It follows from what was observed that if a system is nonlinear then not every corresponding ODE can be solved analytically in simple functions. However, we can glean a lot of information about the behavior of solutions by looking carefully at what the equation says, without actually solving it. Well elaborated the methods organized into the relevant theory and based, first of all, on the works of Poincaré, are called *qualitative*.

In this Chapter we consider fundamentals of the qualitative theory having no intention to examine all aspects of this very powerful tool (for more profound learning, the reader should open the *dynamic systems theory*). Instead, we elucidate only the most recognized and widely used methods in the language suitable for electrical engineering. Several modern qualitative effects such as chaos, for example, are discussed in brief as the theory still does not offer simple and distinct engineering methods for their prediction.

3.1 Qualitative Analysis

In the *qualitative theory*, time is commonly excluded from the direct variables and the system ODE is investigated in the so-called *phase space* that is the collection of possible states of a dynamical system. To investigate, the N -order ODE is represented with N ODEs of the first order related to each of the system states. If $N = 2$, an analysis is provided on the *phase plane*, since only two states exist. So long as the states may be assigned in different ways, different ODEs of the first order may represent the same system.

Example 3.1. Consider a familiar equation by van der Pol,

$$y'' + \omega_0^2 y = \epsilon(1 - y^2)y'.$$

If we assign $z = y'$, we have

$$y' = z, \quad z' = \epsilon(1 - y^2)z - \omega_0^2 y, \quad (3.1)$$

where the states are y and z . We may also let $z = y' - \epsilon(y - \frac{1}{3}y^3)$ and then equivalently write

$$y' = z + \epsilon \left(y - \frac{1}{3}y^3 \right), \quad z' = -\omega_0^2 y. \quad (3.2)$$

Because the states in (3.1) and (3.2) have different meanings, one should expect different results of an analysis, even though the whole picture of a system will be the same. \square

3.1.1 Phase Plane

Let us assume that a system of the second order, like van der Pol's oscillator, is represented with two ODEs of the first order. The most common form of such a system in state space is performed with

$$\frac{dy}{dt} = P(y, z, t), \quad \frac{dz}{dt} = Q(y, z, t), \quad (3.3)$$

where $P(y, z, t)$ and $Q(y, z, t)$ are some linear or nonlinear, time varying or time invariant functions. In the qualitative analysis, we typically let $z = y'$ and go from (3.3) to the function

$$\frac{dz}{dy} = \frac{dy'}{dy} = \frac{Q(y, z, t)}{P(y, z, t)} \quad (3.4)$$

that is useful, first of all, when both functions, Q and P , are time invariant and such that

$$\frac{dz}{dy} = \frac{dy'}{dy} = \frac{Q(y, z)}{P(y, z)}. \quad (3.5)$$

Function (3.5) can now be investigated on a plane of two variables, $z = y'$ and y , called the *phase plane*. The term suggests that, for any initial condition (y_0, z_0) , a solution may be found as $z(y)$ or $y(z)$ and represented with the so-called *phase trajectories*. Seemingly obvious is that every point of each of these trajectories corresponds to a certain time instant and depends on the initial conditions.

Because the initial conditions can be set arbitrary, a number of the phase trajectories is infinite. Therefore, researchers, first of all, are interested of considering some special points, functions, and ranges, by means of which the system demonstrates its major properties.

As a first step toward sketching the phase trajectories, one needs to find and mark on a phase plane the functions associated with $z' = Q = 0$ and $y' = P = 0$. It follows from (3.5) that the function derived by $Q = 0$ will give

us the points, where the phase trajectory has a zero slope (traces horizontally). A set of these points form a function called the z -*nullcline* being the *isocline* with a zero tangent to the axis y . Analogously, the function derived by $P = 0$ gives us the points, where the phase trajectory has an infinite slope (traces vertically). A function formed by a set of these points is called the y -*nullcline* or the *isocline* with a zero tangent to the axis z . One can also let $dz/dy = m$ and find the isoclines with a slope m .

The special points of a system in phase plane are specified by $Q = P = 0$. Since the latter relation means $z' = y' = 0$ and thus there is no behavior, the relevant points are called *fixed* as associated with a system in equilibrium. Every fixed may be stable or unstable.

3.1.2 Stability of Linearized Nonlinear Systems

To study stability of a system at a fixed point means, first, to write

$$P(y, z) = Q(y, z) = 0, \quad (3.6)$$

then find some solution z_0, y_0 , linearize a system at this point, and finally investigate it. Defined a solution y_0, z_0 , a linearized system is represented in the matrix form

$$\begin{bmatrix} y' \\ z' \end{bmatrix} = \begin{bmatrix} a & b \\ c & d \end{bmatrix} \begin{bmatrix} y \\ z \end{bmatrix}, \quad (3.7)$$

using the Jacobian¹ matrix (Appendix B)

$$\mathbf{J}(z, y) = \mathbf{A} = \begin{bmatrix} a & b \\ c & d \end{bmatrix}, \quad (3.8)$$

in which

$$\begin{aligned} a &= P'_y(y_0, z_0) = \left. \frac{\partial P(y, z)}{\partial y} \right|_{y=y_0, z=z_0}, & b &= P'_z(y_0, z_0) = \left. \frac{\partial P(y, z)}{\partial z} \right|_{y=y_0, z=z_0}, \\ c &= Q'_y(y_0, z_0) = \left. \frac{\partial Q(y, z)}{\partial y} \right|_{y=y_0, z=z_0}, & d &= Q'_z(y_0, z_0) = \left. \frac{\partial Q(y, z)}{\partial z} \right|_{y=y_0, z=z_0}. \end{aligned} \quad (3.9)$$

The characteristic equation, associated with the matrix \mathbf{A} (3.8), is written as

$$\begin{vmatrix} a - \lambda & b \\ c & d - \lambda \end{vmatrix} = \lambda^2 + \sigma\lambda + \Delta = 0, \quad (3.10)$$

¹ Carl Gustav Jacob Jacobi, German mathematician, 10 December 1804-18 February 1851.

where the coefficients are predetermined to be $\sigma = -(a + d)$ and $\Delta = ad - bc$. The roots of (3.10) are defined by

$$\lambda_{1,2} = -\frac{\sigma}{2} \pm \sqrt{\frac{\sigma^2}{4} - \Delta}, \quad (3.11)$$

being simultaneously the *eigenvalues* of the Jacobian matrix. If the eigenvalues are found, a linearized system can fully be described via the *eigenvectors*.

Analyzing (3.11), we recognize several special cases. First, it is important to remember that the necessary and sufficient condition for the linear system to be stable is satisfied by $\sigma > 0$ and $\Delta > 0$. All points placed in the first quadrant of the coordinates (Fig. 3.1) are thus stable.

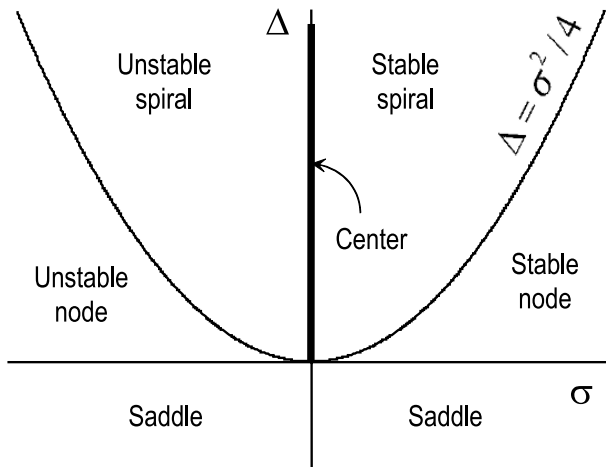


Fig. 3.1. Fixed points on phase plane.

With $\sigma^2 - 4\Delta < 0$, the roots are complex and an equilibrium is *spiral* also called *focus*. The relevant points lie within the parabola depicted in Fig. 3.1. Here, if $\sigma > 0$, spiral is stable (Fig. 3.2a) and, by $\sigma < 0$, it is unstable (Fig. 3.2b). In a special case of $\sigma = 0$, spiral degenerates to *center* also called *neutral center* (Fig. 3.2f). In Fig. 3.2 and in the following, a stable point is depicted by a bold point “•” and unstable by a cycle “○”.

If $\sigma^2 - 4\Delta > 0$ and $\Delta > 0$, an equilibrium point in the topographical nature is *node*. The node is stable (Fig. 3.2d) if $\sigma > 0$ and it is unstable (Fig. 3.2c) if $\sigma < 0$.

It is seen that, by $\Delta < 0$, the roots are always real with, however, different signs. The relevant fixed points lie in the third and fourth quadrants and an equilibrium here, in the topographical nature, is *saddle* (Fig. 3.2e).

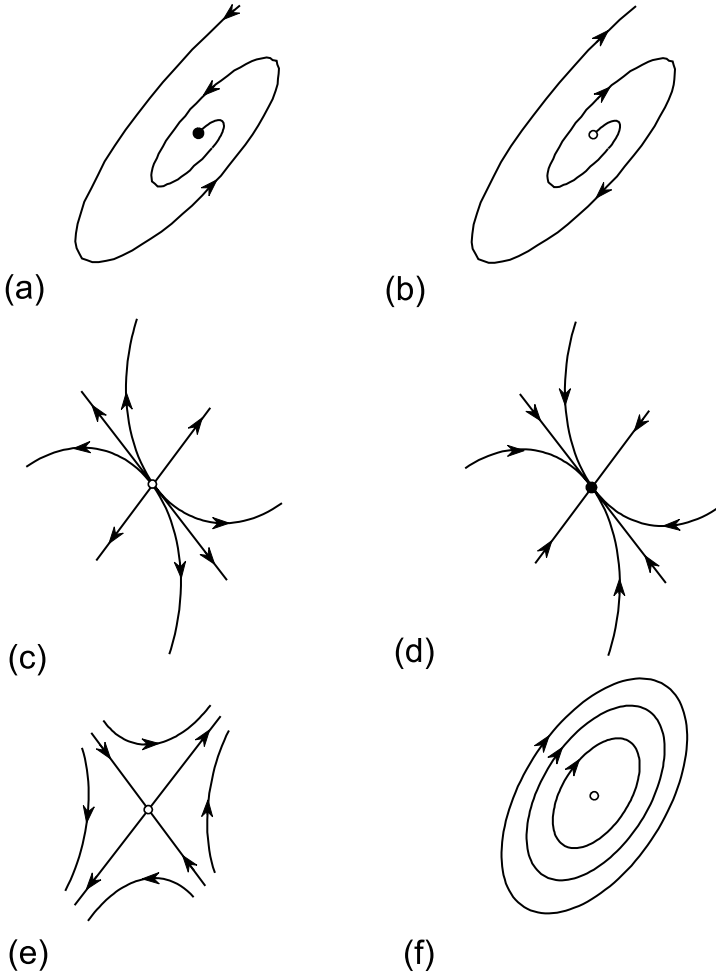


Fig. 3.2. Topological nature of fixed points on phase plane: (a) stable spiral (or focus), (b) unstable spiral (or focus), (c) unstable node, (d) stable node, (e) saddle, and (f) center.

In applications, it sometimes seems convenient to deal directly with the components a , b , c , and d of the Jacobian matrix rather than with their functions σ and Δ . Allowing this, the topological nature of the fixed points is specified by the roots

$$\begin{aligned}
 2\lambda_{1,2} &= a + d \pm \sqrt{(a + d)^2 - 4(ad - bc)} \\
 &= a + d \pm \sqrt{(a - d)^2 + 4bc}
 \end{aligned}
 \tag{3.12}$$

that is summarized in Table 3.1.

Table 3.1. Topographical nature of fixed points

Condition	Fixed point
$(a - b)^2 + 4bc > 0$	
$ad - bc < 0$	Saddle
$ad - bc > 0$	
$a + d < 0$	Stable node
$a + d > 0$	Unstable node
$(a - b)^2 + 4bc < 0$	
$a + d = 0$	Center
$a + d \neq 0$	
$a + d < 0$	Stable spiral
$a + d > 0$	Unstable spiral

Example 3.2. A system is described with the linear differential equation

$$y'' = y. \quad (3.13)$$

Its state plane form is $y' = z$ and $z' = y$. Therefore, the z -nullcline $(z, 0)$ coincides with the axis z and the y -nullcline $(0, y)$ is the axis y (Fig. 3.3a). The only fixed point here is $y_0 = 0$ and $z_0 = 0$ and, therefore, the characteristic equation $\lambda^2 + 0 \cdot \lambda - 1 = 0$ gives $\lambda_1 = 1$ and $\lambda_2 = -1$ and produces $\sigma = 0$ and $\Delta = -1$. It then follows from Fig. 3.1 that an equilibrium is saddle. \square

3.2 Phase Trajectories

To define the phase trajectories in the phase plane, one needs solving the differential equation of the first order (3.5),

$$\frac{dz}{dy} = \frac{Q(y, z)}{P(y, z)}, \quad (3.14)$$

that can be brought about in different ways depending on the functions $P(y, z)$ and $Q(y, z)$. An assemblage of the phase trajectories caused by different initial conditions will represent what we call the *phase portrait*. Every phase trajectory traces in phase plane in some direction. The rule to determine the direction at an arbitrary point (y, z) is established by Table 3.2.

Among all the phase trajectories there are special curves separating the regions of different behaviors. The curve is called the *separatrix* that is not crossed by any other trajectory. The separatrix goes from the unstable saddle to the stable node or spiral. It may close two branches of the saddle or go from one saddle to the other.

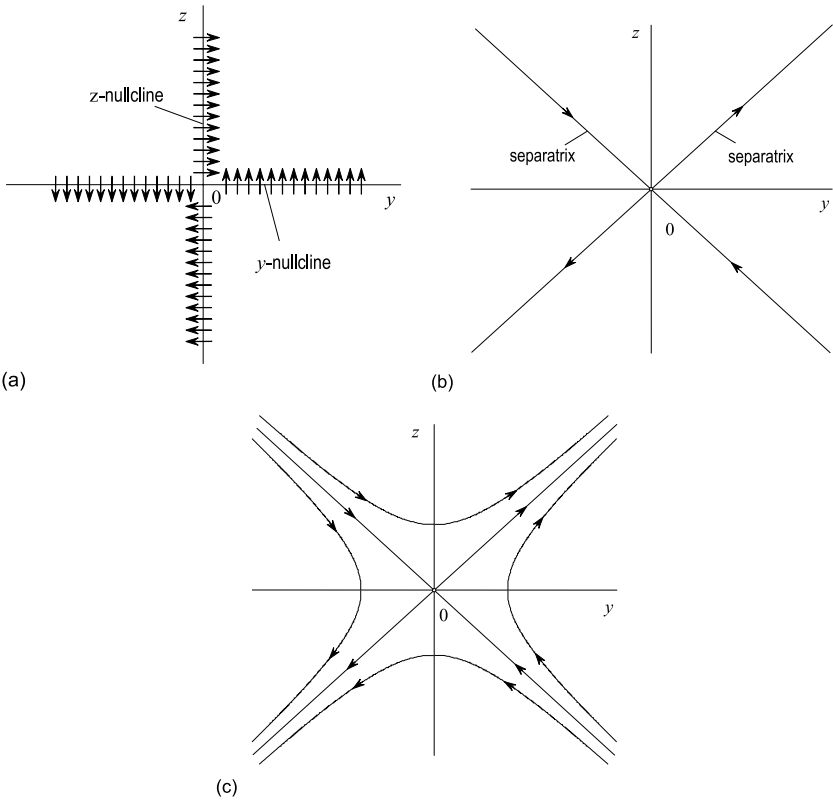


Fig. 3.3. Solutions of equations $y' = z$ and $z' = y$ on phase plane: (a) nullclines, (b) separatrices, and (c) phase portrait of phase trajectories.

Table 3.2. Directions of a phase trajectory at y, z

Function	Direction
$P(y, z) > 0$	y directs \rightarrow
$P(y, z) < 0$	y directs \leftarrow
$Q(y, z) > 0$	z directs \uparrow
$Q(y, z) < 0$	z directs \downarrow

If a system is linearized or linear, (3.7), the separatrices at each of the fixed points are specified by two 2×1 eigenvectors \mathbf{V} corresponding to each of the eigenvalues. The basic relation is

$$\mathbf{A}\mathbf{V} = \lambda\mathbf{V}, \tag{3.15}$$

where λ is either λ_1 or λ_2 . To solve (3.15), one usually fixes one of the coordinate values and then calculates the other one. The eigenvectors corresponding

to λ_1 and λ_2 represent the separatrix curves. The phase trajectories are defined by solving (3.14), where $P(y, z)$ and $Q(y, z)$ are linear functions of y and z .

Example 3.3. Consider a system $y'' = y$ (Example 3.2), which Jacobian matrix is

$$\mathbf{A} = \begin{bmatrix} 0 & 1 \\ 1 & 0 \end{bmatrix}$$

and the eigenvalues are $\lambda_1 = 1$ and $\lambda_2 = -1$. For the first eigenvalue $\lambda_1 = 1$, the eigenvector is defined, by (3.15), with an equation

$$\begin{bmatrix} 0 & 1 \\ 1 & 0 \end{bmatrix} \begin{bmatrix} y_1 \\ z_1 \end{bmatrix} = \lambda_1 \begin{bmatrix} y_1 \\ z_1 \end{bmatrix},$$

producing two equal equations $z_1 = y_1$ and $y_1 = z_1$. For $y_1 = 1$ we hence have $z_1 = 1$. Reasoning similarly, one can find $y_2 = 1$ and $z_2 = -1$ for the second eigenvalue $\lambda_2 = -1$. The eigenvectors directed along the separatrices (Fig. 3.3b) are thus

$$\mathbf{V}_1 = \begin{bmatrix} 1 \\ 1 \end{bmatrix}, \quad \mathbf{V}_2 = \begin{bmatrix} 1 \\ -1 \end{bmatrix}.$$

Table 3.2 suggests that the phase trajectories are directed as follows. In the 1st quadrant as $\uparrow\rightarrow$, in the 2st as $\downarrow\rightarrow$, in the 3st as $\leftarrow\downarrow$, and in the 4st as $\leftarrow\uparrow$. Fig. 3.3a illustrates this directions for the relevant nullclines. \square

3.2.1 Limit Cycles

A special phase trajectory exhibited by nonlinear systems originates a so-called *limit-cycle* or a *closed trajectory* in phase space. A limit cycle is initiated in a nonlinear dynamical system when the latter evolves with time and its trajectory might tend to spiral approaching a closed loop in the phase plane.

The following Bendixson's² criterion helps figuring out if a system has closed trajectories:

Theorem 3.1 (Bendixson's criterion). *Consider a system $y' = P(y, z)$ and $z' = Q(y, z)$ within the given closed region D . If*

$$\frac{\partial P(y, z)}{\partial y} + \frac{\partial Q(y, z)}{\partial z} \neq 0, \quad (3.16)$$

then there cannot be a periodic orbit inside D .

\square

In line with the node and spiral, a limit cycle can also be either stable or not. If the neighboring trajectories evolve towards the limit cycle, then it is a *stable limit cycle* (Fig. 3.4a). Otherwise it is an *unstable limit cycle* (Fig. 3.4b).

² Ivar Otto Bendixson, Swedish mathematician, 1 August 1861-1935.

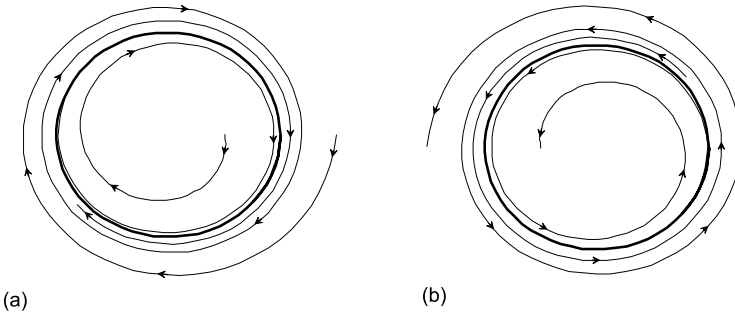


Fig. 3.4. Limit cycles: (a) stable and (b) unstable.

Stable limit-cycles are associated with self sustained oscillations in systems such as van der Pol's oscillator. An important peculiarity of a stable limit cycle is that any small perturbation from its closed loop would cause the system to return back. The following Poincaré-Bendixson theorem is often used to determine if there is a closed trajectory in a system.

Theorem 3.2 (Poincaré-Bendixson theorem). *Consider a system*

$$y' = P(y, z), \quad z' = Q(y, z)$$

in the closed bounded region D , where $P(y, z)$ and $Q(y, z)$ are smoothed differentiable functions. If a system trajectory of the dynamic system is such that it remains in D for $t \geq 0$, then this trajectory is either a limit cycle or it converges to a limit cycle.

□

Example 3.4. Consider a system that is known to be oscillatory,

$$y' = -y + az + y^2z = P(y, z), \quad z' = b - az - y^2z = Q(y, z),$$

where $a = 0.08$ and $b = 0.6$. A system has a fixed point $y_0 = b$, $z_0 = b/(a + b^2)$ that is an unstable spiral. The divergence of the trajectory is ascertained from

$$\frac{\partial P(y, z)}{\partial y} + \frac{\partial Q(y, z)}{\partial z} = 2yz - 1 - a - y^2,$$

it may be zero at some points, and thus, by the Bendixson criterion, a system has a limit cycle. It can be shown that all the trajectories exist in some closed range. Hence, by the Poincaré-Bendixson theorem, a system has a limit cycle. Fig. 3.5 demonstrates, for two different initial conditions, that the trajectories approach a stable limit cycle.

□

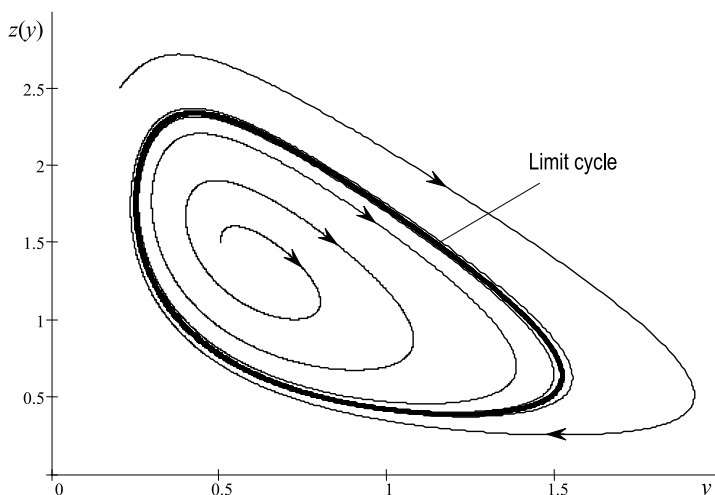


Fig. 3.5. Limit cycle in a system.

3.2.2 Homoclinic and Heteroclinic Trajectories

Let us assume that a system has a saddle or two saddles. Then two particular cases can be considered. A separatrix may go from a saddle O and come back to the same point with $t \rightarrow +\infty$ or $t \rightarrow -\infty$. Such a closed trajectory is called the *homoclinic orbit* or *horseshoe* (Fig. 3.6a). In the other case, a separatrix may go, for example, from a saddle O_2 to a saddle O_1 and reach this point at $t \rightarrow +\infty$ or $t \rightarrow -\infty$ (Fig. 3.6b). This trajectory is called the *heteroclinic path* (*cycle* or *trajectory*).

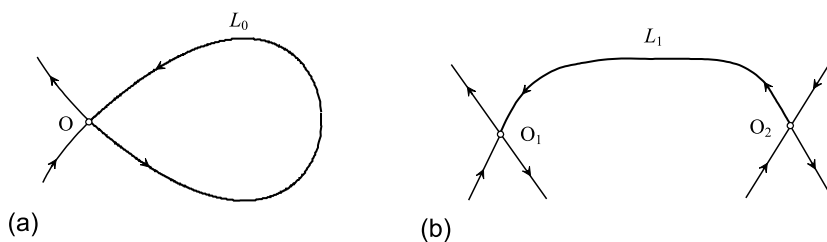


Fig. 3.6. Saddle trajectories: (a) homoclinic and (b) heteroclinic.

If such trajectories exist, the questions arise if they are stable or not and what are the conditions for them to be stable? In 1923, Dulac has proved the following theorem that was further justified by Andronov³:

³ Aleksandr Aleksandrovich Andronov, Russian physicist, 11 April 1901-31 October 1952.

Theorem 3.3 (Dulac theorem). Consider a system $y' = P(y, z)$ and $z' = Q(y, z)$, in which the right-hand sides are analytic and a system has a homoclinic trajectory L_0 (Fig. 3.6a). Then L_0 is stable if

$$\sigma_0 = \left(\frac{\partial P}{\partial y} + \frac{\partial Q}{\partial z} \right) \Big|_{y_0=0, z_0=0} < 0 \quad (3.17)$$

and it is unstable if

$$\sigma_0 = \left(\frac{\partial P}{\partial y} + \frac{\partial Q}{\partial z} \right) \Big|_{y_0=0, z_0=0} > 0. \quad (3.18)$$

□

A special case here is when $\sigma_0 = 0$. Studied by many authors, this case results in the following theorem:

Theorem 3.4. Consider a system $y' = P(y, z)$ and $z' = Q(y, z)$ such that $\sigma_0 = \left(\frac{\partial P}{\partial y} + \frac{\partial Q}{\partial z} \right) \Big|_{y_0=0, z_0=0} = 0$.

If the integral measure is negative,

$$\sigma_1 = \int_{-\infty}^{\infty} \left(\frac{\partial P}{\partial y} + \frac{\partial Q}{\partial z} \right) \Big|_{y, z \in L_0} dt < 0, \quad (3.19)$$

then the homoclinic trajectory L_0 is stable and if

$$\sigma_1 = \int_{-\infty}^{\infty} \left(\frac{\partial P}{\partial y} + \frac{\partial Q}{\partial z} \right) \Big|_{y, z \in L_0} dt > 0, \quad (3.20)$$

then L_0 is unstable.

□

The other special case of $\sigma_0 = \sigma_1 = 0$ is more complicated to justify theoretically, even though it has simple examples with analytically derived trajectories. It follows that, in this case, a system has closed cycles within the homoclinic cycle.

Example 3.5. Given a system

$$y' = 2z = P(y, z), \quad z' = 12y - 2y^2 = Q(y, z).$$

It can be shown that, for this system, $\sigma_0 = \sigma_1 = 0$ and one should expect for the closed cycles if the homoclinic trajectory exists. The system has two fixed points: $y = 0, z = 0$ and $y = 4, z = 0$. It can easily be verified that the first point is saddle and the second one is center. The general integral of a system is given by

$$y^3 - 6y^2 + z^2 = C$$

and we determine

$$z = \pm \sqrt{6y^2 - y^3 + C}$$

that, by $C = 0$, is represented by a saddle with a homocline (Fig. 3.7). \square

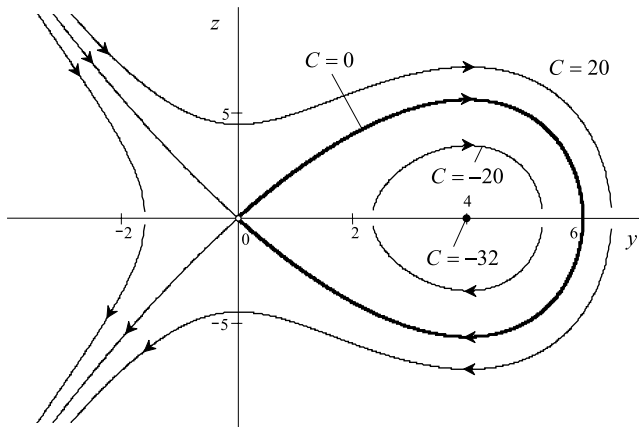


Fig. 3.7. System with a homoclinic trajectory (bold).

So far, we discussed the homoclinic cycle. If the trajectory occurs to be heteroclinic, it goes from one saddle O_1 to the other one O_2 (Fig. 3.6b), then the most important question is if this trajectory is sensitive to small perturbations or it is not. The theorem proved by Andronov et al. claims that the heteroclinic trajectory is not structurally stable, meaning that even an insignificant perturbation is able to “destroy” this connection.

3.2.3 Attractors

Typically, the phase portrait of trajectories exhibits one or several curves, points, or manifolds which the trajectories asymptotically approach. If such special states are invariant under the dynamics, then they are said to be *attractors*.

A stable limit cycle (Fig. 3.4a) acts as an attractor also called *regular attractor*. A stable fixed point (node and spiral) surrounded by a dissipative region is an attractor known as a *map sink*. It needs to remember that systems without dissipation of energy do not have attractors, since the motion is periodic. An attractor may also be a complicated set with fractal structures known as a *strange attractor*. The strange attractor may be watched both in the deterministic and chaotic systems. For the latter case, the special theory known as *chaos theory* is developed.

3.2.4 Structural Stability of Systems

An important feature of any system is how it responds to small perturbations being at equilibrium. The problem was first considered by Andronov applying the Poincaré theory. Then the definition of a “rough” system or *structurally stable system* that is akin to physical *robustness* was stated by the Andronov-Pontryagin⁴ theorem. By Andronov, the rough system is the one, which topography in the considered region is not changed by small perturbations. Accordingly, the system is called “subtle” or (*structurally unstable*) if it changes the topography in the considered region, by small variations in its parameters. This results in the following theorem:

Theorem 3.5 (Andronov-Pontryagin theorem). *Consider a system $y' = P(y, z)$ and $z' = Q(y, z)$. If the condition*

$$\Delta = \begin{vmatrix} P'_y(y_0, z_0) & P'_z(y_0, z_0) \\ Q'_y(y_0, z_0) & Q'_z(y_0, z_0) \end{vmatrix} \neq 0 \quad (3.21)$$

is met at the fixed point (y_0, z_0) , then the system is “rough” at this point.

□

Since a fixed point may have different nature (Table 3.1), it is of practical importance to estimate *roughness* of each of the fixed points. Table 3.3 summarizes such estimates for several equilibria.

Table 3.3. Structural stability

Condition	Fixed point	Roughness
$\Delta > 0, \sigma \neq 0$	Node or spiral	Rough
$\Delta < 0$	Saddle	Rough
$\Delta > 0, \sigma = 0$		Subtle
Separatrix	Saddle to saddle	Subtle
	Simple limit cycle	Rough

3.3 Bifurcations

The word “bifurcate” means to “divide into two parts or branches” and the term *bifurcation* in the system theory means splitting of attractors. Accordingly, the *bifurcation theory* learns changes in the topology (or attractor’s structure) of dynamic systems caused by changes in systems.

⁴ Lev Semenovich Pontryagin, Russian mathematician, 3 September 1908-3 May 1988.

Bifurcation parameter: The value μ_0 of a parameter μ is said to be the bifurcation parameter, if a topological structure of a dynamic system associated with μ_0 differs from that associated with μ .

□

Any coefficient of a nonlinear system can play a role of the bifurcation parameter if some its value changes cardinally a topological structure of the phase portrait.

Example 3.6. Consider a system described with the equations

$$y' = 2z, \quad z' = 2y - 3\mu y^2,$$

where μ can take different values. The general integral of a system is

$$z^2 - y^2 + \mu y^3 = C,$$

where C is a constant, and the trajectories are described by

$$z = \pm \sqrt{y^2(1 - \mu y) + C}.$$

Fig. 3.8 shows phase portraits of this system for three different values of $\mu = 0.3$, $\mu = 0$, and $\mu = -0.3$. It is seen that the topology is changed with $\mu = 0$ (only one saddle point) and hence this value is bifurcation, $\mu_0 = 0$. With another value of μ , the topology has two fixed points: saddle and center.

□

Bifurcation diagram: A bifurcation diagram shows the possible long-term values a variable of a system can obtain in function of a parameter of the system.

□

It follows from the definition of the *bifurcation diagram* that it is a graph showing the location of a system equilibrium point at different values of the parameter. Typically, a location of a stable equilibrium is depicted by a solid curve and that of unstable equilibrium by dashed curve.

A classical illustration for the bifurcation diagram is provided by the logistic map

$$y_{t+1} = \mu y_t(1 - y_t),$$

where time takes discrete values with a step 1. Fig. 3.9 shows what happens with the equilibria if changing a parameter μ . It is seen that for $0 \leq \mu \leq 1$, all the points are plotted at zero and thus zero is the one-point attractor here. For $1 < \mu < 3$, there is still one-point attractor, which is stable and which value $y = (\mu - 1)/\mu$ increases as μ increases. At $\mu = 3$, there is the flip bifurcation. With further increase of μ , the fixed point becomes unstable. Then, again, bifurcations occur, approximately, at $r = 3.45, 3.54, 3.564, 3.569, \dots$, until

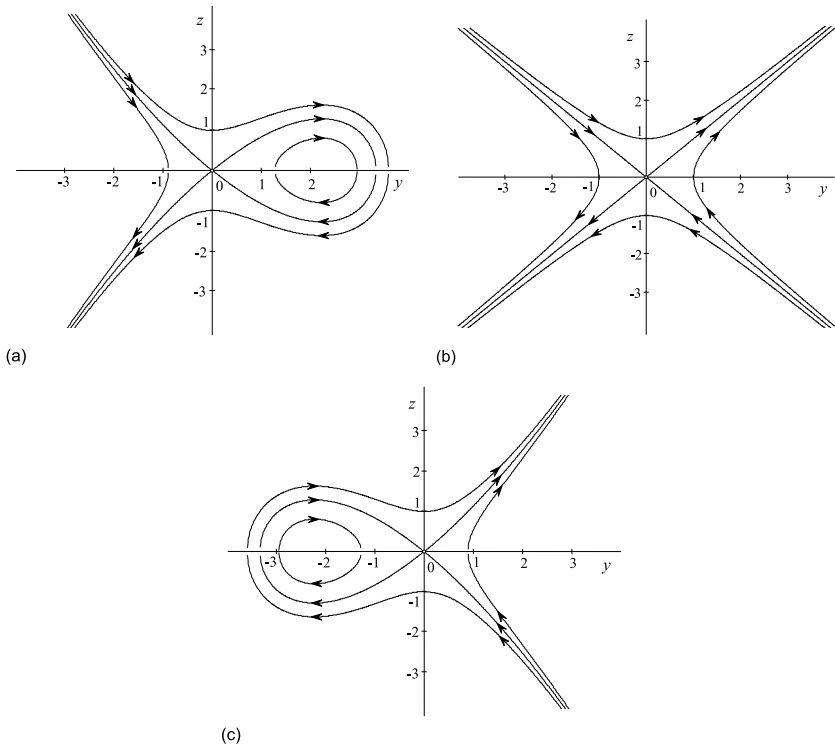


Fig. 3.8. Bifurcation: (a) $\mu = 0.3$, (b) $\mu = 0$, and (c) $\mu = -0.3$.

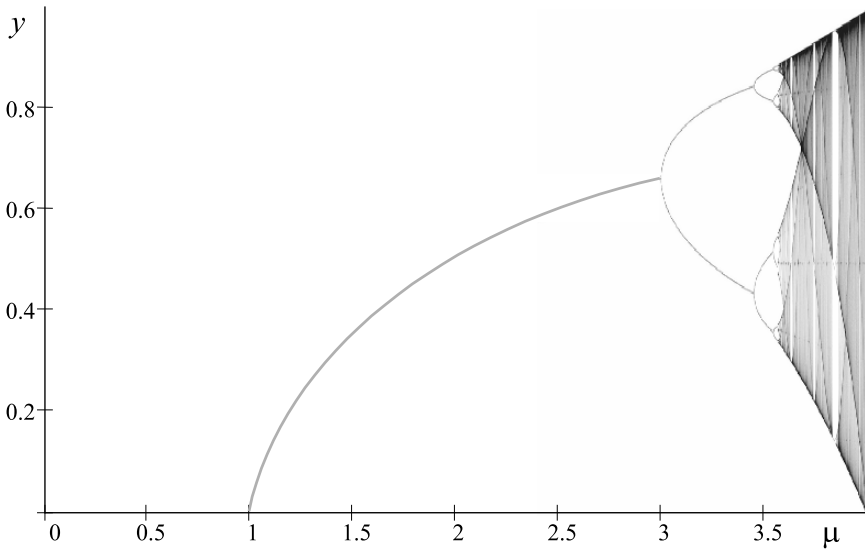


Fig. 3.9. Bifurcation diagram of a logical map.

the value 3.57, at which the system is chaotic. However, the system is not chaotic for all values of $\mu > 3.57$.

Investigated by Poincaré, Andronov, Pontriagin, Hopf⁵, and many other scientists, nowadays, the bifurcation theory proposes to readers a broad classification of bifurcation phenomena. Table 3.4 gives examples of the several most typical bifurcations in continuous-time dynamic systems.

Table 3.4. Typical bifurcations in dynamic systems

Bifurcation	Fixed points	Example
Fold	Stable and unstable \Leftrightarrow no	$y' = \mu - y^2$
Pitchfork	Stable \Leftrightarrow unstable and two stable	$y' = \mu y - y^3$
Pitchfork	Stable and two unstable \Leftrightarrow unstable	$y' = \mu y + y^3$
Transcritical	Stable and unstable \Leftrightarrow unstable and stable	$y' = \mu y - y^2$
Saddle node	Saddle \Leftrightarrow stable and unstable	$y' = \mu - y^2$
Cusp	Stable \Leftrightarrow two stable and one unstable	$y' = -b + ay - y^3$
Andronov-Hopf	Stable spiral \Leftrightarrow center \Leftrightarrow unstable spiral	$y' = [\alpha - (y^2 + z^2)]y - \beta z$ $z' = [\beta y + [\alpha - (y^2 + z^2)]]y$

3.4 Chaotic Orbits and Fractals

The theory of *chaotic orbits* or just *chaos* is very recent, even though its roots are in the works of Henri Poincaré (about 1900), who wrote:

“It so happens that small differences in the initial state of the system can lead to very large differences in its final state. A small error in the former could then produce an enormous one in the latter. Prediction becomes impossible, and the system appears to behave randomly.”

□

Poincaré also found that there can be orbits in the motion of three objects in mutual gravitational attraction which are nonperiodic. This deduction of Poincaré however, was not properly appreciated and, much later, it had been thought that chaos is available in complex systems and is a consequence of a large number of degrees of freedom. Therefore, formally, the theory of

⁵ Heinz Hopf, German mathematician, 19 November 1894-3 June 1971.

chaos is often defined as the study of complex (with recursion) nonlinear dynamic (time-varying and nonperiodic) systems. Most recently, it was found that chaotic orbits may nucleate even in deterministic systems with a number of states no less than three.

With time, the essence of chaos has become more and more clear and its practical applications were found, despite mathematicians still having not decided on the definition of chaos. It turned out that chaotic behaviors in nonlinear systems may be used in modulation to transmit messages in what was further called chaos-based communications and telecommunications. Other areas of applications are information compression, image recognition, medical diagnostics, electronic archives, etc.

Based upon the classical notions, the evolution of an initial condition y_0 under a system operator does not behave chaotically, because of its predictability, if the function $y(t)$

- Goes to an equilibrium when $t \rightarrow \infty$, □
- Goes to a periodic orbit when $t \rightarrow \infty$, □
- Escapes to ∞ as $t \rightarrow \infty$. □

Contrary to periodic behaviors, a chaotic orbit is not periodic or eventually periodic. Such an orbit occurs if, as accepted conventionally, the Lyapunov exponent (which we introduce below) is positive. An example of chaotic behaviors is the Lorenz system.

Example 3.7 (Lorenz oscillator). To illustrate the chaotic orbits, we show below a numerical solution for a system described with the Lorenz equations,

$$x' = \sigma(y - x), \quad y' = x(\rho - z) - y, \quad z' = xy - \beta z,$$

where $\rho = 28$, $\sigma = 10$, and $\beta = 8/3$. The initial conditions are set to be $x(0) = y(0) = z(0) = 1$. It is seen (Fig. 3.10) that the behaviors of all three states have some carrier and that they are not periodic on a long time scale.

Fig. 3.11 shows the trajectories in three phase space sections. As it is seen, the trajectories chaotically behave between two attractors, say “left” and “right”. Let us consider, for example, the plane $z-x$ (Fig. 3.11b). A trajectory starts at $t = 0$ at the point $x = y = z = 1$, makes only one semi loop, and goes to the left part, where it moves around the unstable attractor (loop) during a lot of periods. At $t = 14$, it leaves the left attractor and appears closely to the start point. Again, it makes a semi loop and comes back to the left attractor. It then twice returns at about $t = 21$ and $t = 23.3$. But thereafter, before coming back to the left attractor, the trajectory makes a full loop in the right part. In a like manner, the trajectories behave in the planes $y-x$ (Fig. 3.11a) and $z-y$ (Fig. 3.11c). If we look at the picture in a long-time base, we find two brightly pronounced attractors, called the butterfly attractors, as it is shown in Fig. 3.11d in the $y-x$ plane.

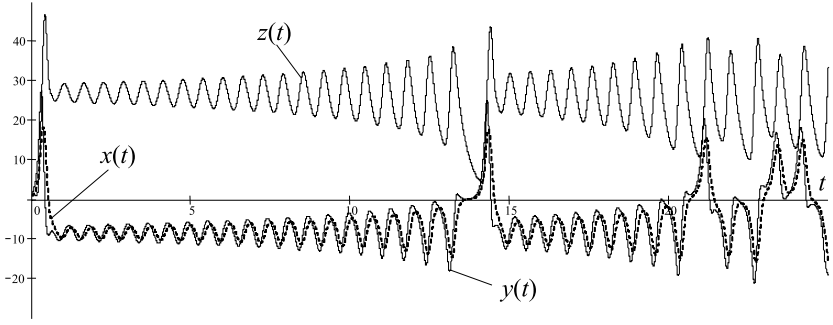


Fig. 3.10. Numerical solutions of Lorenz's equations for $\rho = 28$, $\sigma = 10$, $\beta = 8/3$, and $x(0) = y(0) = z(0) = 1$.

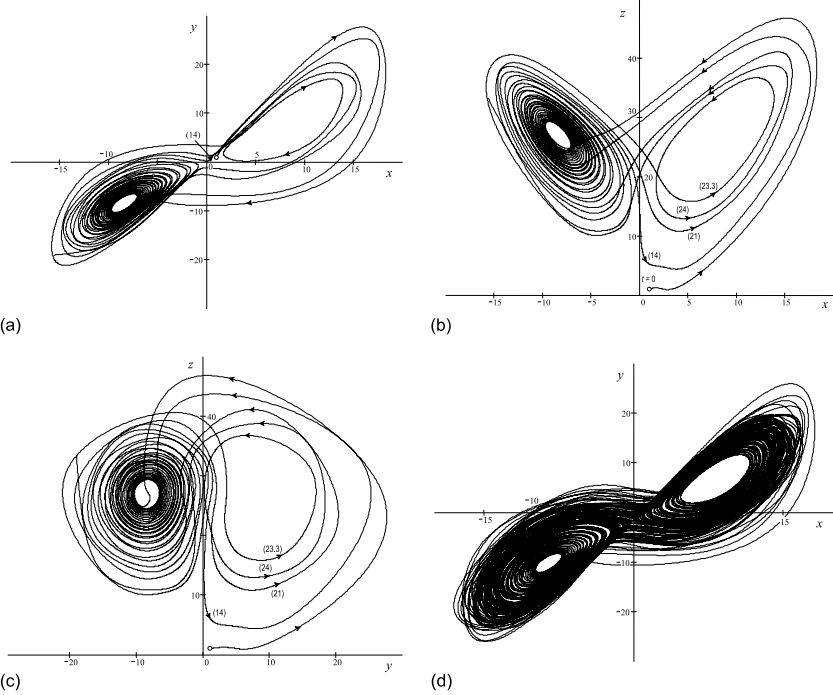


Fig. 3.11. Lorenz chaotic orbits and attractors: (a) y - x plane, (b) z - x plane, (c) z - y plane, and (d) y - x plane in long-term time.

An applied significance of a picture shown in Fig. 3.11d is that it is nothing less than a chaotic bit sequence. Such an unexpectedly splendid property of Lorenz's oscillator has found applications in digital communications. \square

Fractals

The word “*fractal*” was introduced by Benoit Mandelbrot⁶ in 1975 from the Latin *fractus* (meaning “broken” or “fractured”) to describe an object which has partial dimension. It is a geometric object that satisfies a specific technical condition, namely having a Hausdorff⁷-Besicovitch⁸ dimension greater than its topological dimension. The fractal denotes a shape that is recursively constructed or self-similar: a shape that appears similar at all scales of magnification.

Fractals are usually created by recursive equations in discrete time. Therefore, they are typically so irregular that they cannot be described by smooth, differentiable structures; thus, they are not directly associated with continuous-time systems.

3.4.1 Lyapunov Exponents

A convenient mathematical tool to determine what kind of attractors may exist in a system is the *Lyapunov characteristic exponent* or just the *Lyapunov exponent*. These exponents describe the mean exponential rate of divergence of two (or more) trajectories initially close to each other in phase space.

For the sake of simplicity, we shall first demonstrate the meaning of the Lyapunov exponent considering a one-state system. So, let us assume that a system is described with

$$y' = P(y), \quad (3.22)$$

where $P(y)$ is a nonlinear function, and select two nearby initial points y and y_0 of a trajectory. The distance between y and y_0 is supposed to be small and we expand a nonlinear function in the right-hand side to the Taylor series around y_0

$$y' = P(y_0) + \left. \frac{\partial P(y)}{\partial y} \right|_{y=y_0} (y - y_0) + \dots,$$

We now let $y'_0 = P(y_0)$, neglect the nonlinear terms, and write

$$\Delta y' = \left. \frac{\partial P(y)}{\partial y} \right|_{y=y_0} \Delta y, \quad (3.23)$$

⁶ Benoit Mandelbrot, Polish-born French mathematician, 20 November 1924-.

⁷ Felix Hausdorff, German mathematician, 8 November 1868-26 January 1942.

⁸ Abram Samoilovitch Besicovitch, Ukrainian-born Russian/English mathematician, 24 January 1891-2 November 1970.

where $\Delta y = y - y_0$ and $\Delta y' = y' - P(y_0) = y' - y'_0$. A general solution of the linear ODE (3.23) is exponential,

$$\Delta y(t) = e^{\lambda t} \Delta y(0), \quad (3.24)$$

that, being rewritten for λ , gives

$$\lambda = \frac{1}{t} \ln \frac{|\Delta y(t)|}{|\Delta y(0)|}.$$

In applications, a value derived is of interest on a long time scale. Therefore, an equation is rewritten as

$$\lambda = \lim_{t \rightarrow \infty} \frac{1}{t} \ln \frac{|\Delta y(t)|}{|\Delta y(0)|} \quad (3.25)$$

and is called the Lyapunov exponent.

If we now differentiate (3.24), $\Delta y' = \lambda e^{\lambda t} \Delta y(0)$, and then substitute Δy and $\Delta y'$ to (3.23), we arrive at an analytical measure of the Lyapunov exponent; that is,

$$\lambda = \left. \frac{\partial P(y)}{\partial y} \right|_{y=y_0}. \quad (3.26)$$

An obvious conclusion follows instantly: if $\lambda > 0$, the trajectories diverge; when $\lambda = 0$, they conserve a mutual distance; and, if $\lambda < 0$, they converge.

Most generally, a closed loop system is described by a multi-state model with the Lyapunov exponent derived in a like manner,

$$\lambda = \lim_{t \rightarrow \infty} \frac{1}{t} \ln \frac{|\mathbf{y}(t) - \mathbf{y}_0(t)|}{|\mathbf{y}(0) - \mathbf{y}_0(0)|}, \quad (3.27)$$

where the value $|\mathbf{y}(t) - \mathbf{y}_0(t)|$ means a distance between the trajectories in state space at time t . It is commonly accepted that, like the one-state case, if the largest Lyapunov exponent is negative, then the trajectories will converge and the system will evolve to equilibria and limit cycles. With the positive largest Lyapunov exponent, the trajectories will diverge and a system will go to chaotic attractors. Finally, a zero largest Lyapunov exponent says that the trajectories have in average the same space distance with time and the system has regular attractors.

3.5 Conservative Systems

An important class of systems is formed by the *conservative systems* which satisfy an energy-balance equation, provided the definition given by Maxwell⁹:

⁹ James Clerk Maxwell, Scottish mathematical physicist, 13 June 1831-5 November 1879.

Conservative system: “A material system of such a nature that after the system has undergone any series of changes, and been brought back in any manner to its original state, the whole work done by external agents on the system is equal to the whole work done by the system overcoming external forces.”

James Clerk Maxwell □

In a conservative system, the sum of the energy stored in the system at some time t plus the outgoing energy equals the sum of the initial energy stored in the system and of the incoming energy. Therefore, the conservative systems are often called the system without a dissipation of energy, pointing out that the systems in which the energy is dissipated, the *dissipative systems*, are *not conservative*. For conservative systems, the sum of all Lyapunov exponents is zero and, for dissipative, it is negative.

If a system is described with the exact first-order differential equation of the form

$$P(y, z)dz - Q(y, z)dy = 0, \quad (3.28)$$

where

$$\frac{\partial P(y, z)}{\partial y} = -\frac{\partial Q(y, z)}{\partial z}, \quad (3.29)$$

then it is a conservative system. The solution to (3.28) is given by

$$\int_{z_0}^z P(y_0, z)dz - \int_{y_0}^y Q(y, z)dy = C, \quad (3.30)$$

where the integration constant C is associated with the initial conditions. An example of the conservative system is van der Pol's oscillator with a zero small parameter $\epsilon = 0$ that makes its equation to be $y'' + \omega_0^2 y = 0$. A great deal of systems governed by partial differential equations are also conservative.

Example 3.8. A system is described with the equations

$$y' = z + z(y^2 + z^2) = P(y, z), \quad z' = y - y(y^2 + z^2) = Q(y, z). \quad (3.31)$$

Since $P'_y = -Q'_z = 2yz$, then, by (3.29), the system is conservative. The system has three fixed points: $(-1, 0)$, $(0, 0)$, and $(1, 0)$. A general integral, by (3.29), is defined to be

$$(y^2 + z^2)^2 - 2(y^2 - z^2) = 4C. \quad (3.32)$$

If we now let $4C = c^4 - 1$, then an equation will attain the form

$$(y^2 + z^2)^2 - 2(y^2 - z^2) = c^4 - 1, \quad (3.33)$$

describing the Cassinian¹⁰ ovals (Fig. 3.12), in which the directions of the phase trajectories are readily defined by Table 3.2.

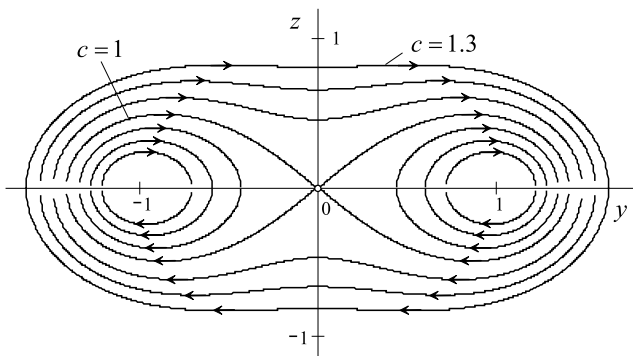


Fig. 3.12. Cassinian ovals following with a step $\Delta c = 0.1$.

It can be shown that, by $c = 0$, the oval degenerates into two points with the coordinates $(-1, 0)$ and $(1, 0)$. With $c = 1$, it is a so-called *lemniscate*. By $c \geq \sqrt{2}$, the curves are ovals, if $1 < c < \sqrt{2}$, they are “dog bones,” and, by $0 < c < 1$, the curve consists of two loops. \square

If (3.29) is not satisfied,

$$\frac{\partial P(y, z)}{\partial y} \neq -\frac{\partial Q(y, z)}{\partial z}, \quad (3.34)$$

the differential equation (3.28) is inexact. Inexact equations can be solved by defining an integration factor $\varrho(y, z)$ such that the resulting equation becomes exact, namely

$$\varrho(y, z)P(y, z)dz - \varrho(y, z)Q(y, z)dy = 0, \quad (3.35)$$

where the factor $\varrho(y, z)$ satisfies the partial differential equation (PDE)

$$\varrho \left(\frac{\partial Q}{\partial z} + \frac{\partial P}{\partial y} \right) = -P \frac{\partial \varrho}{\partial y} - Q \frac{\partial \varrho}{\partial z} \quad (3.36)$$

and (3.29) is satisfied with

¹⁰ Giovanni Domenico Cassini, French/Italian astronomer and mathematician, 8 June 1625–14 September 1712.

$$\frac{\partial \varrho(y, z)P(y, z)}{\partial y} = -\frac{\partial \varrho(y, z)Q(y, z)}{\partial z}. \quad (3.37)$$

It is seen that, by $\varrho(y, z) = 1$, a relation (3.36) becomes (3.29) and, so, a condition (3.36) is most general. But we still do not know if a system satisfying (3.36) is conservative. The definition given by Andronov claims that such a system is conservative if the factor $\mu(y, z)$ also called *conservative density* or *integral invariant density* is positive valued,

$$\varrho(y, z) \geq 0. \quad (3.38)$$

Defined $\varrho(y, z)$, a solution of (3.35) is obtained in a like manner,

$$\int_{z_0}^z \varrho(y, z)P(y_0, z)dz - \int_{y_0}^y \varrho(y, z)Q(y, z)dy = C. \quad (3.39)$$

Example 3.9. Given a system, performed by the equations

$$y' = 2z + y^2 + z^2 - 1 = P(y, z), \quad z' = -2y = Q(y, z). \quad (3.40)$$

Here we have $P'_y = 2y \neq Q'_z = 0$ and hence the associated differential equation (3.28) is inexact. To find a general integral, we exploit (3.36) and arrive at

$$2y\varrho = -(2z + y^2 + z^2 - 1)\frac{\partial \varrho}{\partial y} + 2y\frac{\partial \varrho}{\partial z}.$$

It is known that an equation like this has an exponential solution. It also follows that if ϱ does not depend on y , then an equality holds if $\varrho = e^z$. Since $e^z > 0$, then, by (3.38), a systems is conservative. By this value, a general integral applied to (3.35) is defined to be

$$(y^2 + z^2 - 1)e^z = C, \quad (3.41)$$

where the constant C corresponds to the certain trajectory of a system. \square

3.5.1 Hamiltonian Systems

An important class of conservative systems is united in what is known in physics as *Hamiltonian systems*. The dynamical system is said to be a Hamiltonian system if for a smooth function $H(\mathbf{y}, \mathbf{z})$, where \mathbf{y} and \mathbf{z} are $n \times 1$ vector functions associated with y and z , respectively, the following equations hold true:

$$y'_i = -\frac{\partial H}{\partial z_i}, \quad (3.42)$$

$$z'_i = \frac{\partial H}{\partial y_i}, \quad (3.43)$$

where $i \in [1, n]$. If the function H exists, then it is the *Hamiltonian function* or the *Hamiltonian*. Accordingly, (3.42) and (3.38) are called *Hamilton's equations*. A number of *degrees of freedom* of a Hamiltonian system is the number of (y_i, z_i) pairs in (3.42) and (3.43). This number is equal to n and the phase space is thus $2n$ -dimensional.

For example, in mechanics, the vector \mathbf{y} represents the coordinates of the system components, while \mathbf{z} is a set of momenta. Therefore, typically, the hamiltonian is often assumed to describe the total energy of a system, although this is not always the case. If the system energy is constant, the Hamilton function is constant as well that allows using this fact in integrating the equation (3.28).

If the Hamiltonian system is of the second order, equations (3.3) may be rewritten as

$$\frac{dy}{dt} = P(y, z) = -\frac{\partial H}{\partial z}, \quad (3.44)$$

$$\frac{dz}{dt} = Q(y, z) = \frac{\partial H}{\partial y}, \quad (3.45)$$

where the Hamiltonian H represents the system energy. It now follows straightforwardly that the Hamiltonian system is a particular case of a conservative system.

Example 3.10. Let us come back to the system (Example 3.2) and write its equations as follows,

$$y' = z = -\frac{\partial H}{\partial z}, \quad z' = y = \frac{\partial H}{\partial y}. \quad (3.46)$$

For the fixed point $(x_0 = 0, y_0 = 0)$, we have $P = z$, and $Q = y$, and the system energy is defined by

$$H = \int_0^z P(z)dz - \int_0^y Q(y)dy \quad (3.47)$$

$$= \frac{1}{2}z^2 - \frac{1}{2}y^2 = C. \quad (3.48)$$

As can be seen, the Hamiltonian derived (3.48) satisfies the equations (3.46). The phase trajectories are thus described by

$$z = \pm\sqrt{y^2 + 2C} \quad (3.49)$$

that gives, by $C = 0$, two separatrices, $z = y$ and $z = -y$ (Fig. 3.3b), represented in Example 3.3 by the eigenvectors. The phase portrait of a saddle associated with (3.49) is shown in Fig. 3.3c. \square

Example 3.11. Consider two general integrals, (3.32) and (3.41). It can easily be shown that, by assigning, respectively,

$$H = C = \frac{1}{4}(y^2 + z^2)^2 - \frac{1}{2}(y^2 - z^2),$$

$$H = \frac{C}{\mu} = \frac{C}{e^z} = (y^2 + z^2 - 1),$$

and then differentiating (3.44) and (3.45), we arrive at the relevant functions $P(y, z)$ and $Q(y, z)$ given in Examples 3.8 and 3.9, respectively. \square

3.6 Dissipative (Near Conservative) Systems

As we have already mentioned before, a great deal of nonlinear systems of practical importance is described by the ODE (2.84), in which ϵ is a small value. However, namely this small ϵ changes a picture cardinally: if $\epsilon = 0$, a system is conservative (idealized) and when $\epsilon > 0$ a system becomes dissipative (real physical). Referring to this fact, a qualitative analysis of a system may be provided in the mathematical form like that used in (2.84). Indeed, if we will think that there is a conservative system, (3.44) and (3.45), with known properties, then the dissipative (although near conservative) system can be described by

$$\frac{dy}{dt} = P(y, z) + \mu p(y, z, \mu) = P(y, z, \mu), \quad (3.50)$$

$$\frac{dz}{dt} = Q(y, z) + \mu q(y, z, \mu) = Q(y, z, \mu), \quad (3.51)$$

where μ is a small value and $p(y, z, \mu)$ and $q(y, z, \mu)$ are analytic functions in the observed range.

Referring to (3.44) and (3.45), the equations can be rewritten as

$$\frac{dy}{dt} = -\frac{\partial H}{\partial z} + \mu p_1(y, z) + \mu^2 p_2(y, z) + \dots, \quad (3.52)$$

$$\frac{dz}{dt} = \frac{\partial H}{\partial y} + \mu q_1(y, z) + \mu^2 q_2(y, z) + \dots, \quad (3.53)$$

where the products of small values μ^k , $k > 1$, may be neglected. The following Pontryagin theorem then helps to recognize whether a limit cycle in a system (3.52) and (3.53) exists or not.

Theorem 3.6 (Pontryagin theorem). *Let (3.52) and (3.53) be a near Hamiltonian system with a small value μ and L_0 a closed loop of a Hamiltonian system $\frac{dy}{dt} = -\frac{\partial H}{\partial z}$ and $\frac{dz}{dt} = \frac{\partial H}{\partial y}$. Let also $y = \varphi(t)$ and $z = \psi(t)$ be behaviors of a system with period T and G_0 a range within L_0 . Then, if*

$$\int \int_{G_0} [p'_{1y}(y, z) + q'_{1z}(y, z)] dy dz = 0, \quad (3.54)$$

$$l = \int_0^T \{p'_{1y}[\varphi(x), \psi(x)] + q'_{1z}[\varphi(x), \psi(x)]\} dx \neq 0, \quad (3.55)$$

then there exist values $a > 0$ and $b > 0$ such that

a) For any $|\mu| < b$, a system has only one closed loop L_μ that approaches L_0 if $\mu \rightarrow 0$,

b) A trajectory L_μ is a “rough” limit cycle that is stable when $\mu l < 0$ and unstable if $\mu l > 0$.

□

Example 3.12. Consider van der Pol’s oscillator

$$y'' + y = \varepsilon(1 - y^2)y',$$

where ε is a small value, and rewrite its equation in state space as

$$y' = -z, \quad z' = y + \varepsilon(1 - y^2)z.$$

With small ε , the oscillator may be considered to be a near Hamiltonian system,

$$y' = -z = -\frac{\partial H}{\partial z}, \quad z' = y = \frac{\partial H}{\partial y},$$

where the Hamiltonian is

$$H(y, z) = \frac{1}{2}(y^2 + z^2),$$

and the trajectories of a system are cycles with a center at $(y_0 = 0, z_0 = 0)$.

To study the original oscillator equations, we represent them in the forms of (3.52) and (3.53). Accordingly, we have

$$p_1(y, z) = 0, \quad q_1(y, z) = (1 - y^2)z.$$

In accordance with the Pontryagin theorem, it now needs evaluating the integral (3.54) attaining the form of

$$\int \int_{G_0} q'_{1z}(y, z) dy dz = \int \int_{G_0} (1 - y^2) dy dz.$$

To evaluate, we change the variables to $y = r \cos t$ and $z = r \sin t$, define the determinant of the Jacobian of the transformation $J = r$, and rewrite the integral as

$$\int_0^{2\pi} \int_0^r r(1 - r^2 \cos^2 \theta) dr d\theta = \frac{\pi}{4} r^2 (4 - r^2).$$

A simple observation shows that the integral is zero only if $r = 2$, since any radius cannot be negative.

Now let us evaluate the value l (3.55) that, for our conditions, becomes

$$l = \int_0^{2\pi} (1 - r^2 \cos^2 \theta) d\theta = 2\pi \left(1 - \frac{r^2}{2}\right) = -2\pi < 0.$$

It then follows, by Pontryagin’s theorem, that the closed trajectory, $y = -2 \cos t$ and $z = 2 \sin t$, of the Hamiltonian system originates the structurally stable limit cycle that is stable if $\varepsilon > 0$ and unstable with $\varepsilon < 0$. \square

Example 3.13. Given a system considered by Andronov et al.,

$$y' = z, \quad z' = y(z - 1) + y^2 + z^2 + \mu z,$$

where μ is a small parameter. The system has two fixed points: A ($y = 0, z = 0$) and B ($y = 1, z = 0$). The fixed point B is a saddle for an arbitrary μ . The eigenvalues of the point A are calculated by

$$\lambda_{1,2} = \frac{\mu}{2} \pm \sqrt{\frac{\mu^2}{4} - 1}$$

and we have the following characteristics of this point for different small values of μ :

- If $\mu \leq -2$, then the fixed point is stable node \square
- If $-2 < \mu < 0$, then the fixed point is stable spiral \square
- If $0 < \mu < 2$, then the fixed point is unstable spiral \square
- If $2 \leq \mu$, then the fixed point is unstable node \square
- If $\mu = +0$, then the fixed point is unstable spiral \square
- If $\mu = -0$, then the fixed point is stable spiral with an unstable cycle \square

3.6.1 Near Conservative Time-varying Systems

All real physical systems are affected by environment and many of them are controlled or synchronized by some external signal. In each of these cases, a system becomes time-varying, LTV or NTV.

In analogous to (3.50) and (3.51), equations for the near conservative time-varying systems may be written as

$$\frac{dy}{dt} = P(y, z) + \mu p(y, z, \mu, t), \tag{3.56}$$

$$\frac{dz}{dt} = Q(y, z) + \mu q(y, z, \mu, t), \tag{3.57}$$

where the functions $p(y, z, \mu, t)$ and $q(y, z, \mu, t)$ are time-dependent and we still think that μ is a small parameter making a system near conservative, although dissipative.

Certainly, we must know how the time-varying parts of (3.56) and (3.57) result in behaviors of systems. If we know everything about the unperturbed system described with $y' = P(y, z)$ and $z' = Q(y, z)$ and a system is at equilibrium, then the main question is if a system is still stable or it became chaotic owing to the perturbing terms. To come up with an answer to this question, one can apply the common methods and analyze a system at different time instances that usually entails difficulties. In some particular cases, the answer, even approximate, can be found faster. One of the cases is when a system is perturbed periodically. Here, a transition to chaos may approximately be predicted for a class of systems using the Melnikov method.

3.6.2 Melnikov's Method

One of the common cases of practical importance is when a system described by (3.56) and (3.57) has a homoclinic trajectory formed by a saddle loop such as that shown in Fig. 3.7 with $C = 0$. Most generally, the unperturbed system can have any periodic orbit. It is known that, under the certain circumstances, a system may become chaotic. To determine the relevant condition, let us perform a system with a matrix equation

$$\mathbf{z}' = \mathbf{f}(\mathbf{z}) + \mu \mathbf{g}(\mathbf{z}, t), \quad (3.58)$$

where

$$\mathbf{z}(t) = \begin{bmatrix} y(t) \\ z(t) \end{bmatrix}, \quad \mathbf{f}(\mathbf{z}) = \begin{bmatrix} P(y, z) \\ Q(y, z) \end{bmatrix}, \quad \mathbf{g}(\mathbf{z}, t) = \begin{bmatrix} p(y, z, t) \\ q(y, z, t) \end{bmatrix}.$$

Now consider Fig. 3.13 that shows a homoclinic trajectory (unperturbed closed loop of a saddle) associated with the equation $\mathbf{z}' = \mathbf{f}(\mathbf{z})$ and two separatrices (manifolds) of a saddle (perturbed open loop) occurred owing to the term $\mu \mathbf{g}(\mathbf{z}, t)$.

Let us suppose that at some time instant t_0 two separatrices of a perturbed saddle, r_1 and r_2 , trace at a distance $D(t_0)$. If this distance occurs to be zero, $D(t_0) = 0$, then the necessary condition is satisfied for a system to be chaotic. Melnikov has shown that $D(t_0)$ can be calculated by

$$D(t_0) = \frac{\mu}{|\mathbf{n}[\mathbf{z}_0(0)]|} M(t_0), \quad (3.59)$$

where the components of a vector $\mathbf{n}[\mathbf{z}_0(t - t_0)]$ are identified by the equations

$$\mathbf{f}[\mathbf{z}_0(t - t_0)]^T \mathbf{n}[\mathbf{z}_0(t - t_0)] = 0, \quad (3.60)$$

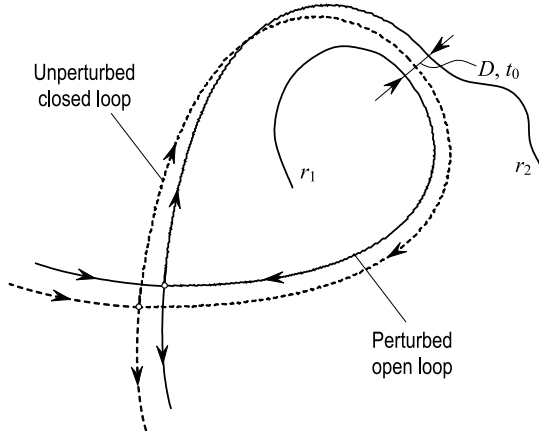


Fig. 3.13. Homoclinic trajectory.

$$|\mathbf{f}[\mathbf{z}_0(t - t_0)]| = |\mathbf{n}[\mathbf{z}_0(t - t_0)]|, \tag{3.61}$$

and $\mathbf{z}_0 = \mathbf{z}(t - t_0)$ is a solution of the equation $\mathbf{z}' = \mathbf{f}(\mathbf{z})$ associated with the separatrices.

The value $M(t_0)$ is provided by

$$M(t_0) = \int_{-\infty}^{\infty} \mathbf{g}[\mathbf{z}_0(\theta), \theta + t_0]^T \mathbf{n}[\mathbf{z}_0(\theta)] e^{-\int_0^\theta \nabla \cdot \mathbf{f}(\theta') d\theta'} d\theta \tag{3.62}$$

and has an alternative form of

$$M(t_0) = \int_{-\infty}^{\infty} \mathbf{f}[\mathbf{z}_0(\theta)] \wedge \mathbf{g}[\mathbf{z}_0(\theta), \theta + t_0] e^{-\int_0^\theta \nabla \cdot \mathbf{f}(\theta') d\theta'} d\theta, \tag{3.63}$$

where the divergence of the inner integral is ascertained by

$$\nabla \cdot \mathbf{f} = \frac{\partial P(y, z)}{\partial y} + \frac{\partial Q(y, z)}{\partial z} \tag{3.64}$$

and the wedge product of two vectors is defined by

$$\mathbf{f} \wedge \mathbf{g} = Pq - Qp. \tag{3.65}$$

The value $M(t_0)$ is proved by the Melnikov theorem and, therefore, is called the *Melnikov integral*.

There is an important particular case when $P(z)$ does not depend on y and $Q(y)$ on z . Thus, $\nabla \cdot \mathbf{f} = 0$ and the Melnikov integral becomes

$$M(t_0) = \int_{-\infty}^{\infty} \mathbf{f}[\mathbf{z}(\theta)] \wedge \mathbf{g}[\mathbf{z}_0(\theta), \theta + t_0] d\theta. \quad (3.66)$$

Solving Melnikov's integral equations helps understanding whether a system is addicted to chaos or its behavior is absolutely predictable for an arbitrary control signal.

3.7 Summary

So, we have observed in brief the qualitative theory of systems. Even though its roots are in the works of Poincaré and many studies have resulted in a number of books and papers, the qualitative theory is still in progress. Especially, it is related to chaotic systems. The theory helps investigating a great deal of problems, when an analytic solution of the system dynamic equation is problematic both in the time and frequency domains. Moreover, analytic solutions are often redundant. Summarizing, we list below the most fundamental canons of the qualitative theory:

- Qualitatively, a system is learned in phase space (multiple states) or phase plane (two states) with time excluded from the variables and existing indirectly.
- A line with a constant tangent in phase plane is called the isocline.
- The fixed points in phase plane are determined by zero time derivatives of all of the system states.
- The topological nature of a fixed point is defined by the coefficients of the characteristic equation of a linearized system.
- The phase trajectory is a curve of a system behavior in phase plane. An assemblage of phase trajectories is the phase portrait.
- A special trajectory that is not crossed by any other trajectory is called a separatrix.
- A special closed phase trajectory exhibited by nonlinear systems is a limit cycle.
- An attractor is a curve, or point, or manifold which the trajectories asymptotically approach. An attractor may be regular or chaotic.
- A fixed point, or trajectory, or manifold is structurally stable if it is robust to small perturbations.
- A parameter of a system is said to be bifurcation if a topological structure of a dynamic system associated with this parameter differs from that associated with other parameter.

- The conservative systems are often called the systems without a dissipation of energy.
- The Hamiltonian system is a particular case of conservative systems.
- If a system dissipates energy with time, then it is a dissipative system.

3.8 Problems

3.1 (Stability of linearized nonlinear systems). A system is given with the following differential equation. Define the fixed points of a system. Realize, whether the point is stable or not.

1. $y' = 2z$, $z' = 6y - 2y^2$
2. $y' = z^2 - 2z$, $z' = y$
3. $y' = 3z - 2z^2 + 2y^2$, $z' = 3y$
4. $y' = z^2 - y^2$, $z' = y^2 + z^2$
5. $y' = 12z - 6z^3$, $z' = 2y^2$
6. $y' = 2z$, $z' = 6y - 12y^3$
7. $y' = z + \frac{1}{2}(y^3 - yz^2)$, $z' = y - y^2 + y^2z - z^3$
8. $y' = -z + yz$, $z' = y + z^2$
9. $y' = y(2 - z - y)$, $z' = z(4y - y^2 - 3)$

3.2 (Phase trajectories). Given a system

1. $y'' = y + 2y'$
2. $y'' + ay' + by = 0$
3. $y' = 2y'' - y$

Represent the system in state space. Following Example 3.3, determine the eigenvalues and eigenvectors. Plot the separatrices and define their directions.

3.3. For the linearized system (Problem 3.1), following Example 3.3, define the eigenvectors at the fixed points. Determine the directions of the separatrices.

3.4. A system is represented in phase plane with the separatrices (Fig. 3.14). Assuming arbitrarily initial conditions, show the possible phase trajectories of a system.

3.5. In the phase portrait shown in Fig. 3.15, find errors in the separatrices and fixed points. Recall that a stable fixed point is depicted by a bold point, whereas unstable by a cycle.

3.6. Using the Bendixson criterion, realize whether the systems given in Problem 3.1 has a limit cycle or not.

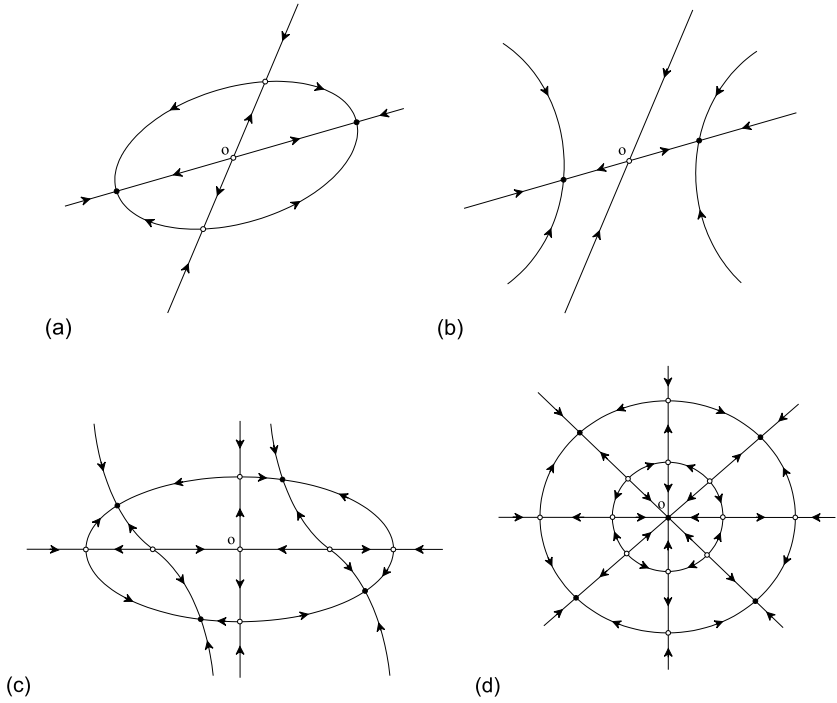


Fig. 3.14. Fixed points and separatrices in phase plane.

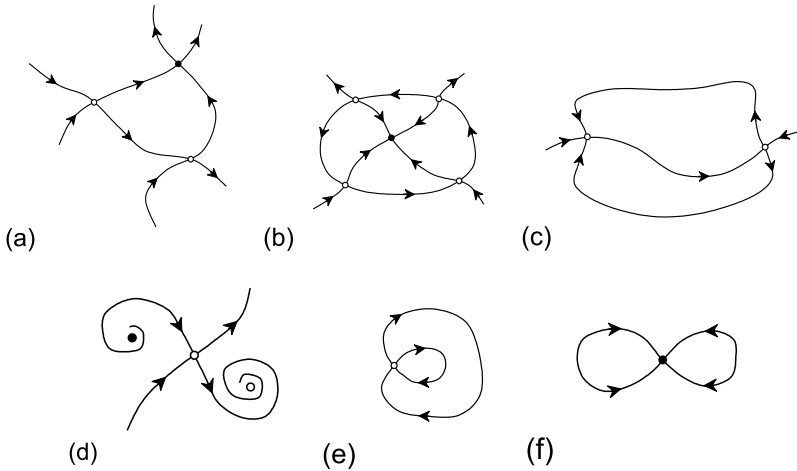


Fig. 3.15. Fixed points and separatrices in phase plane. What is wrong here? Find errors.

3.7. A system is given with

1. $y' = y^3 + z^2 + zy^2 - 2yz^2$, $z' = -2zy^2 - z^2y + z^3 + \sin y$
2. $y' = y - z - 2y(y^2 + z^2)$, $z' = y + z - z(y^2 + z^2)$

Using the Bendixson criterion, realize whether a systems has a limit cycle or not.

3.8 (Structural stability). A system is given with the differential equations (Problem 3.1). Using the Andronov-Pontriagin theorem, realize whether the system is structural stable at the fixed point or not.

3.9. Using the Andronov-Pontriagin theorem, ascertain the structural stability of a system described in Problem 3.7.

3.10 (Bifurcations). A system is given with the following differential equations having a free parameter μ :

1. $y' = 2z$, $z' = y(1 - \mu y)$
2. $y' = z(z - 2\mu)$, $z' = y$
3. $y' = z(3 - 2z) + 2\mu y^2$, $z' = 3y$
4. $y' = z^2 - (\mu - 1)y^2$, $z' = y^2 + \mu z^2$
5. $y' = z(2 - \mu z^2)$, $z' = 2y^2$
6. $y' = 2z$, $z' = 6y(1 - 2\mu y^2)$
7. $y' = z + y(\mu - 1)(y^2 - z^2)$, $z' = y(1 - y) + z(\mu - 1)(y^2 - z^2)$
8. $y' = -z(1 - \mu y)$, $z' = y + (\mu - 2)z^2$
9. $y' = y(2 - \mu z - y)$, $z' = z(4y - \mu y^2 - 3)$

Investigate the phase portrait of a system and define the bifurcation value of μ .

3.11. Analyze bifurcations in the systems presented in Problem 3.10. What kind of bifurcation it has? Use Table 3.4 as a reference.

3.12. Table 3.4 gives several equations associated with the distinguished kinds of bifurcations. Investigate these equations in the phase plane y', y and illustrate each bifurcation graphically.

3.13. Investigate and plot the bifurcation diagram for the systems given in Problem 3.10.

3.14. Investigate and plot the bifurcation diagram for the systems given in Table 3.4.

3.15 (Conservative systems). Consider a system given in Problem 3.1. Which system is conservative and which is not?

3.16. Consider a system given in Problem 3.10. Find a value of the parameter μ , making the conservative system to be non conservative and vise versa. Which system cannot transfer from the conservative to non conservative state?

3.17. Consider a system given in Problem 3.1. Whether this system is conservative or not? If not, find the function $\rho(y, z)$ to transform the non conservative system to conservative?

3.18. Given a system

$$y' = 2z + y^2 + z^2 - 1, \quad z' = -2y.$$

Verify that its general integral is $(y^2 + z^2 - 1)e^z = C$.

3.19. Given a system

$$y' = z + z(y^2 + z^2), \quad z' = y - y(y^2 + z^2).$$

Verify that its general integral is $(y^2 + z^2)^2 - 2(y^2 - z^2) = C$.

3.20 (Hamiltonian systems). A system is given with $y' = z$ and $z' = -ay - by^3$. Verify that the Hamiltonian of the system is

$$H = \frac{1}{2}z^2 + \frac{a}{4}y^2 + \frac{b}{4}y^4.$$

3.21. A system is given with $y' = z$ and $z' = -\sin y$. Verify that the Hamiltonian of the system is

$$H = \frac{1}{2}z^2 + 2 \sin^2 \frac{y}{2}.$$

3.22. Revise the systems given in Problem 3.1. If a system is conservative, write its Hamiltonian.

3.23 (Dissipative (near conservative) systems). Consider a dissipative system

$$y' = -z, \quad z' = y + \mu(a + by - cy^2)z,$$

describing an electronic oscillator.

1. How many fixed points has this system?
2. Characterize the fixed point of a system at zero.
3. What is the condition for the system to be Hamiltonian? Satisfied this condition, what will be the Hamiltonian?
4. What is the condition for the system to have a limit cycle?

LTI Systems in the Time Domain

4.1 Introduction

The most useful mathematical abstraction of real systems is a *linear time-invariant* (LTI) system. As a model, an LTI system is represented with some kind of a linear operator \mathcal{O} that maps the input $\mathbf{x}(t)$ to the output $\mathbf{y}(t)$. Typically, features and properties of a linear operator are much simpler than those peculiar to the nonlinear operator. Moreover, it is tacitly implied that the operator transforms signals linearly in the infinite range of values. Even though the latter cannot be met in practice, at least by saturation, the LTI model allows learning principle properties of many real structures and channels. Therefore, the LTI system analysis and synthesis are fundamental for the general systems theory.

There are three basic approaches to describe an LTI system in the time domain. One can use the *convolution* to couple an arbitrary input signal with the LTI system output via its *impulse response*. An LTI system can also be represented with the linear ordinary differential equation of some order. Alternatively, an LTI system could be performed by a set of its states in *state space* or, albeit less commonly, in some other coordinates. All these methods are interchangeable, thus universal for LTI modeling.

4.2 Convolution

Let us start with the mathematical description of LTI systems in the time domain. For the sake of simplicity, it is in order to first consider a single-input single-output (SISO) LTI system, whose output $y(t)$ is coupled with its input $x(t)$ by some linear and time-invariant operator \mathcal{O} ,

$$y(t) = \mathcal{O}x(t). \tag{4.1}$$

What could be this operator? To find an answer, one needs to apply the *test* unit impulse, $x(t) = \delta(t)$, and follow the fundamental definition:

Impulse response of an LTI system: The response $h(t)$ of an LTI system at time t to the unit impulse $\delta(t)$ at time t is the LTI system impulse response

$$h(t) = \mathcal{O}\delta(t). \quad (4.2)$$

□

If we now use the sifting property of the delta function (Appendix A), we can formally substitute a continuous-time input signal $x(t)$ by

$$x(t) = \int_{-\infty}^{\infty} x(\theta)\delta(t - \theta)d\theta. \quad (4.3)$$

Substituting (4.3) to (4.1), using the definition (4.2), and invoking the time shifting property of any linear operator that in our case gives $h(t - \theta) = \mathcal{O}\delta(t - \theta)$, we arrive at the rule

$$y(t) = \mathcal{O} \int_{-\infty}^{\infty} x(\theta)\delta(t - \theta)d\theta = \int_{-\infty}^{\infty} x(\theta)\mathcal{O}\delta(t - \theta)d\theta = \int_{-\infty}^{\infty} x(\theta)h(t - \theta)d\theta$$

that claims that the LTI system output $y(t)$ is coupled with its input $x(t)$ by the LTI system impulse response $h(t)$.

The integral relation derived is termed the *convolution*,

$$y(t) = x(t) * h(t) = \int_{-\infty}^{\infty} x(\theta)h(t - \theta)d\theta, \quad (4.4)$$

describing the process in a continuous-time LTI system that maps a continuous-time input $x(t)$ into a continuous-time output $y(t)$. The convolution (4.4) playing a fundamental role in the theory of LTI systems is also known as the *Duhamel's¹ integral* or the *Duhamel's convolution principle*.

The answer is thus the following. In the time domain, the operator \mathcal{O} of an LTI system is the convolution (4.4) representing the LTI system response $y(t)$ at time t to an arbitrary input $x(t)$ at time t .

Fig. 4.1 illustrates the convolution principle in the time domain. The system impulse response $h(t)$ is determined by applying a unit impulse to the input, $x(t) = \delta(t)$. Then the LTI system output represents the system impulse response $y(t) = h(t)$ as shown in Fig. 4.1a. Provided $h(t)$, the LTI system response $y(t)$ to an arbitrary signal $x(t)$ is obtained by the convolution (4.4) as shown in Fig. 4.1b for the rectangular pulse.

Example 4.1. An LTI system is represented with the impulse response

¹ Jean Marie Constant Duhamel, French mathematician, 5 February 1797–29 April 1872.

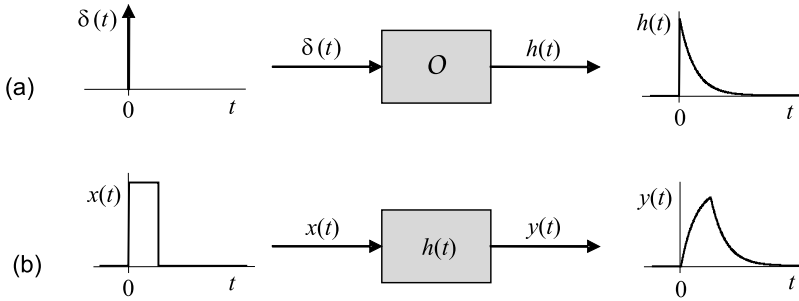


Fig. 4.1. The convolution principle for LTI systems: (a) determining the impulse response $h(t)$ and (b) response $y(t)$ to an arbitrary signal $x(t)$ via $h(t)$ and (4.4).

$$h(t) = \begin{cases} ae^{-bt} & \text{if } t \geq 0 \\ 0 & \text{otherwise} \end{cases} = ae^{-bt}u(t), \quad b > 0. \quad (4.5)$$

A signal acting at the system input is a rectangular pulse (Fig. 4.1b),

$$x(t) = \begin{cases} A_0 & \text{if } 0 \leq t \leq \tau \\ 0 & \text{otherwise} \end{cases}. \quad (4.6)$$

To define the system output by the convolution (4.4), perform the rectangular pulse (4.6) with two shifted unit-step functions as $x(t) = x_1(t) - x_2(t)$, where $x_1(t) = A_0u(t)$ and $x_2(t) = A_0u(t - \tau)$.

It is seen that both $h(t)$ and $x_1(t) = A_0u(t)$ are zero-valued with negative time. Therefore, by $t < 0$, $x_1(\theta)$ and $h(t - \theta)$ in (4.4) do not overlap. If $t > 0$, then $h(t)$ and $x_1(t) = A_0u(t)$ overlap from $\theta = 0$ to $\theta = t$. Accordingly, the bounds in (4.4) are changed and the system response $y_1(t)$ to $x_1(t)$ is provided with

$$\begin{aligned} y_1(t) &= \int_{-\infty}^{\infty} x_1(\theta)h(t - \theta)d\theta = aA_0 \int_0^t e^{-b(t-\theta)}d\theta \\ &= \frac{a}{b}A_0(1 - e^{-bt})u(t). \end{aligned} \quad (4.7)$$

Because the system response $y_2(t)$ to $x_2(t)$ is merely a shifted version of $y_1(t)$,

$$y_2(t) = y_1(t - \tau)u(t - \tau) = \frac{a}{b}A_0[1 - e^{-b(t-\tau)}]u(t - \tau),$$

we instantly arrive at the system response to (4.6); that is,

$$y(t) = y_1(t) - y_2(t) = \frac{a}{b}A_0(1 - e^{-bt})u(t) - \frac{a}{b}A_0[1 - e^{-b(t-\tau)}]u(t - \tau). \quad (4.8)$$

Fig. 4.2 demonstrates several stages of the convolution calculus, by (4.5) and (4.6). Geometrically, the convolution can be interpreted as a joint area

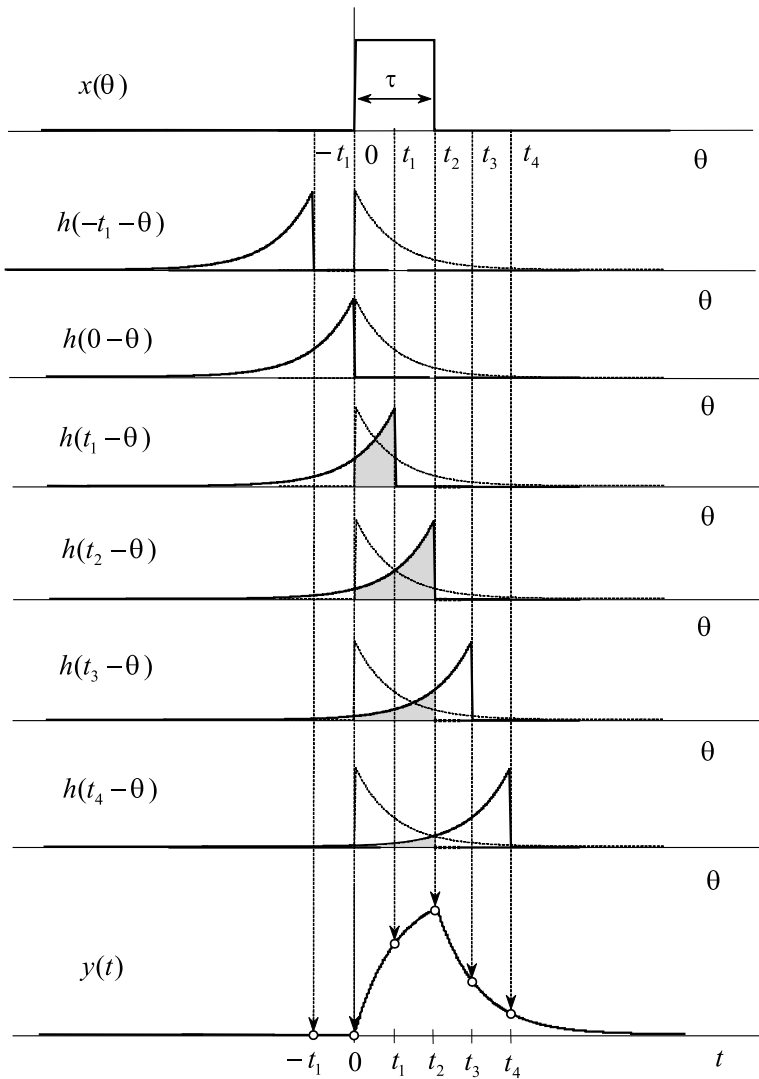


Fig. 4.2. Several stages of the convolution computation.

(shadowed) of two shifted and inversely related functions $x(t)$ and $h(t)$, for which the output equals zero if θ is negative. It is seen that the response increases in the amplitude when the area increases ($0 < t < t_2$). It then reduces with $t > t_2$ asymptotically approaching zero, when the area reduces.

□

A common conclusion following the convolution computation analysis (Fig. 4.2) is that the length of the system response $y(t)$ is the sum of the signal length τ and the impulse response $h(t)$ length.

4.2.1 System Step Response

If the input is formed with the test unit step function, $x(t) = u(t)$, the LTI system output is the step response, provided the other fundamental definition:

Step response of an LTI system: The response $g(t)$ of an LTI system at time t to the unit step $u(t)$ at time t is the LTI system step response

$$g(t) = \mathcal{O}u(t). \quad (4.9)$$

□

We now know that the operator \mathcal{O} of an LTI system in the time domain is the convolution. Therefore, the system step response can be defined by

$$g(t) = u(t) * h(t) = \int_{-\infty}^{\infty} u(\theta)h(t - \theta)d\theta = \int_0^t h(t - \theta)d\theta. \quad (4.10)$$

The integral form (4.10) establishes two fundamental relations between the LTI system impulse and step responses:

$$g(t) = \int_{-\infty}^t h(\tau)d\tau \quad \Leftrightarrow \quad h(t) = \frac{d}{dt}g(t), \quad (4.11)$$

meaning that $g(t)$ is performed by the instantaneous area of $h(t)$ and, in turn, $h(t)$ is represented by the time rate of $g(t)$.

Example 4.2. Consider the system response (4.7) to $x_1(t) = A_0u(t)$ that, by $A_0 = 1$, becomes the system step response and we can write

$$g(t) = \frac{a}{b} (1 - e^{-bt}) u(t).$$

Differentiating this relation, by (4.11), leads to the system impulse response

$$h(t) = ae^{-bt}u(t)$$

that was earlier specified by (4.5).

□

4.2.2 Properties of the Convolution

As we recently deduced analyzing Fig. 4.2, the convolution length is the sum of the signal length and the impulse response length. There are many other widely recognized and important properties of the convolution.

Commutativity

Consider the convolution integral (4.4). If to introduce a new variable $\eta = t - \theta$ and substitute $\theta = t - \eta$ and $d\theta = -d\eta$, then (4.4) transforms to

$$\begin{aligned} y(t) &= \int_{-\infty}^{\infty} x(\theta)h(t - \theta)d\theta = - \int_{\infty+t}^{-\infty+t} x(t - \eta)h(\eta)d\eta \\ &= \int_{-\infty}^{\infty} h(\eta)x(t - \eta)d\eta, \end{aligned}$$

establishing the following *commutativity* property:

$$y(t) = x(t) * h(t) = h(t) * x(t), \quad (4.12)$$

meaning that the input and impulse response are commuting in LTI systems.

Example 4.3. A system is characterized with the impulse response $h(t) = e^{-at}u(t)$, $a > 0$, and the input signal is $x(t) = e^{-bt}u(t)$, $b > 0$.

By the convolution (4.4), the system output is defined to be

$$\begin{aligned} y(t) &= \int_0^t e^{-b\theta} e^{-a(t-\theta)} d\theta = e^{-at} \int_0^t e^{-(b-a)\theta} d\theta \\ &= \frac{1}{b-a} (e^{-at} - e^{-bt}). \end{aligned}$$

One arrives at the same result, by using the commutativity property (4.12):

$$\begin{aligned} y(t) &= \int_0^t e^{-a\theta} e^{-b(t-\theta)} d\theta = e^{-bt} \int_0^t e^{-(a-b)\theta} d\theta \\ &= \frac{1}{a-b} (e^{-bt} - e^{-at}) = \frac{1}{b-a} (e^{-at} - e^{-bt}). \end{aligned}$$

Now observe that the functions $x(t)$ and $h(t)$ differ only by the coefficients a and b . A verification of the commutativity property follows immediately by interchanging a and b that does not affect the system response. \square

Distributivity

The property of *distributivity* is supported by the *superposition principle* and is critical for the distributed LTI systems. Distributivity suggests that if the impulse response is composed with an additive sum of N particular impulse responses, then the convolution can be calculated as

$$x(t) * \sum_{i=1}^N h_i(t) = \sum_{i=1}^N x(t) * h_i(t). \quad (4.13)$$

Inversely, if an input is a superposition of several particular subsignals, one can employ the rule

$$h(t) * \sum_{i=1}^N x_i(t) = \sum_{i=1}^N h(t) * x_i(t). \quad (4.14)$$

An application of (4.14) can be found in Example 4.1, where the input $x(t)$ is substituted with a sum of two subsignals $x_1(t)$ and $x_2(t)$.

Homogeneity

When one of the functions, $x(t)$ or $h(t)$, is multiplied (gained) with a constant a , then the following *homogeneity* property can be used,

$$x(t) * [ah(t)] = [ax(t)] * h(t) = a[x(t) * h(t)]. \quad (4.15)$$

One can find applications of this property in Example 4.1 and Example 4.2 as featured to LTI systems.

Linearity

Both distributivity and homogeneity imply *linearity* and it is seemingly obvious that the property of linearity is fundamental for all kinds of LTI systems. Examples are the convolution, integration, and differentiation representing the linear system operator \mathcal{O} .

Associativity

In applications, a signal $x(t)$ very often passes through two or more LTI subsystems, which impulse responses are presumed to be known. The response of a whole cascade system to $x(t)$ can be calculated using the property of *associativity*.

Let an LTI subsystem having the impulse response $h_1(t)$ responds to the input $x(t)$ as $y_1(t) = x(t) * h_1(t)$. If $y_1(t)$ acts in the input of some other LTI subsystem with the impulse response $h_2(t)$, then the output is calculated by

$$y(t) = y_1(t) * h_2(t) = [x(t) * h_1(t)] * h_2(t).$$

The property of associativity claims that

$$[x(t) * h_1(t)] * h_2(t) = x(t) * [h_1(t) * h_2(t)]. \quad (4.16)$$

To verify, one can rewrite the left-hand and right-hand sides of (4.16) separately as in the following:

$$\begin{aligned} [x(t) * h_1(t)] * h_2(t) &= \int_{-\infty}^{\infty} [x(\theta_1) * h_1(\theta_1)] h_2(t - \theta_1) d\theta_1 \\ &= \int_{-\infty}^{\infty} \int_{-\infty}^{\infty} x(\theta_2) h_1(\theta_1 - \theta_2) h_2(t - \theta_1) d\theta_1 d\theta_2, \end{aligned} \quad (4.17)$$

$$\begin{aligned} x(t) * [h_1(t) * h_2(t)] &= \int_{-\infty}^{\infty} x(\theta_3) [h_1(t - \theta_3) * h_2(t - \theta_3)] d\theta_3 \\ &= \int_{-\infty}^{\infty} \int_{-\infty}^{\infty} x(\theta_3) h_1(\theta_4) h_2(t - \theta_3 - \theta_4) d\theta_3 d\theta_4. \end{aligned} \quad (4.18)$$

Now change the variables in (4.18) to $\theta_3 = \theta_2$ and $\theta_4 = \theta_1 - \theta_2$. Having new variables, (4.18) needs to be multiplied with the determinant of the Jacobian of the transformation that in our case is unity, $J = \left| \frac{\partial(\theta_3, \theta_4)}{\partial(\theta_1, \theta_2)} \right| = 1$. Instantly (4.18) becomes (4.17) and the proof of the associative property is complete.

Example 4.4. Define the step response of a system composed by a cascade of two subsystems (Fig. 4.3a) having equal impulse responses,

$$h_1(t) = h_2(t) = ae^{-bt}u(t).$$

By the associativity property (4.16), we first ascertain the impulse response of the whole system

$$h(t) = \int_0^t h_1(\theta) h_2(t - \theta) d\theta = a^2 \int_0^t e^{-b\theta} e^{-b(t-\theta)} d\theta = a^2 e^{-bt} \int_0^t d\theta = a^2 t e^{-bt}.$$

Then, by the convolution integral and identity $\int x e^{\alpha x} dx = e^{\alpha x} \left(\frac{x}{\alpha} - \frac{1}{\alpha^2} \right)$, the system step response becomes

$$g(t) = a^2 \int_0^t (t - \theta) e^{-b(t-\theta)} d\theta = \frac{a^2}{b^2} (1 - e^{-bt}) - \frac{a^2}{b} t e^{-bt}$$

having a shape shown in Fig. 4.3b. In a bit more sophisticated way, the same result can be obtained by calculating first the output of the first subsystem and then the output of the second subsystem (the reader is encouraged to verify this). Fig. 4.3c illustrates the transformation stages for the latter case. \square

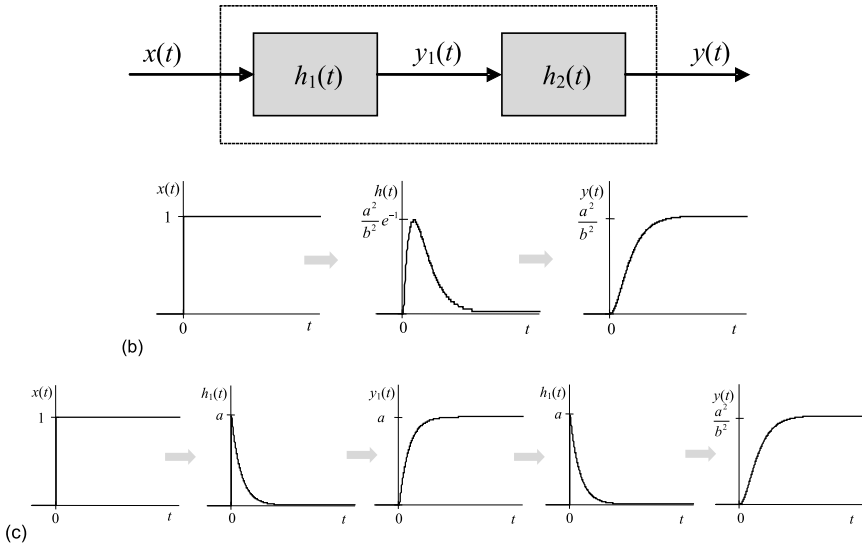


Fig. 4.3. A cascade LTI system: (a) system, (b) output via $h(t)$, and (c) output via $h_1(t)$ and $h_2(t)$.

Consistency with Cross-correlation

Convolution is closely related to cross-correlation. Consider the real input $x(t)$ and the impulse response $h(t)$. By the definition, the cross-correlation between two functions is evaluated with (see Signals)

$$\phi_{xh}(\theta) = \int_{-\infty}^{\infty} x(t)h(t - \theta)dt = x(t) \star h(t).$$

It is seen that, by the sign changed of a variable in $h(t)$, the cross-correlation function becomes the convolution (4.4) and we thus can write

$$x(t) \star h(t) = x(t) * h(-t), \tag{4.19}$$

$$x(t) * h(t) = x(t) \star h(-t). \tag{4.20}$$

The consistency relations (4.19) and (4.20) are often used to evaluate the correlation properties of a system via the convolution and vice versa.

4.2.3 Properties of LTI Systems

Using the properties of convolution, it becomes possible to outline many of the useful properties of applied importance featured to LTI systems. The most common of those are listed below.

Linearity

By definition, any LTI system is linear and time-invariant. The output and input of such a system are coupled by the convolution via the system impulse response. The convolution cannot be applied in its standard form (4.4) to time-variant and nonlinear systems.

Stationarity

The property of stationarity means time-invariance of the system operator that is the second fundamental property of any kind of LTI systems. Because the operator \mathcal{O} of an LTI system is time-constant, the system performance is not affected by time and it can be shown that, most generally, time shifting in the input results solely in time shifting in the output:

$$y(t - \tau) = \mathcal{O}x(t - \tau) = \int_{-\infty}^{\infty} h(\theta)x(t - \tau - \theta)d\theta.$$

Any linear system that does not meet this requirement belongs to the class of *time-variant* systems.

Memory (Inertia)

An LTI system can be with or without *memory*. The term “memory” in electronic systems is consistent with the term “inertia” in mechanical systems. In memoryless (inertialess) systems, the present output $y(t)$ depends on only the present input $x(t)$. The relationship between $y(t)$ and $x(t)$ thus can be of the form

$$y(t) = Gx(t), \quad (4.21)$$

where G is a constant gain factor representing the system operator by an identity $\mathcal{O} \equiv G$.

The impulse response of the memoryless system is delta-shaped,

$$h(t) = G\delta(t), \quad (4.22)$$

and hence does not equal to zero only at $t = 0$. Otherwise, if $h(t) \neq 0$ when $t \neq 0$, a system has some memory and thus is inertial or dynamical. An example of a memoryless system is amplitude scaling, whereas integration and differentiation are elements of memory systems. Based upon this definition, it can easily be observed that all systems considered in Examples 4.1–4.4 are memory.

Example 4.5. An LTI system is represented with the impulse response $h(t) = a\delta(t)$. The input is a harmonic signal $x(t) = A_0 \cos \omega_0 t$ with constant both the amplitude A_0 and carrier angular frequency ω_0 . By the convolution integral

(4.4) and sifting property of the delta function (Appendix A), the output is defined to be

$$y(t) = aA_0 \int_{-\infty}^{\infty} \delta(t - \theta) \cos \omega_0 \theta d\theta = aA_0 \cos \omega_0 t$$

and we see that the system provides amplitude scaling, thus is memoryless. \square

Causality

Most generally, the convolution (4.4) implies integration over the infinite bounds, thereby fitting the cases of both *causal* and *noncausal* signals and systems. If a signal or/and system is *causal*, then the convolution modifies, basically resulting in two special cases.

Convolution for either causal systems or signals. To modify the convolution for causal systems, one needs to recall that a system is causal if its output $y(t)$ at an arbitrary time instant t_1 depends on only its input $x(t)$ for $t_1 \geq t$. This means that a causal system does not respond to any input event until that event actually occurs. Indeed, the impulse response is generated by a unit impulse that exists at only zero point, $t = 0$. Thus, for causal LTI systems, we have

$$h(t) = \begin{cases} h(t) & \text{if } t \geq 0 \\ 0 & \text{if } t < 0 \end{cases} . \quad (4.23)$$

Applying (4.23) to (4.12), we arrive at two equal forms of convolution for causal systems:

$$y(t) = \int_{-\infty}^t x(\theta)h(t - \theta)d\theta = \int_0^{\infty} h(\theta)x(t - \theta)d\theta . \quad (4.24)$$

Reasoning along similar lines, one can verify that if a signal is causal; that is,

$$x(t) = \begin{cases} x(t) & \text{if } t \geq 0 \\ 0 & \text{if } t < 0 \end{cases} , \quad (4.25)$$

and a system is noncausal, then the convolution is calculated with

$$y(t) = \int_0^{\infty} x(\theta)h(t - \theta)d\theta = \int_{-\infty}^t h(\theta)x(t - \theta)d\theta .$$

Convolution for causal both systems and signals. Assume that a system is causal and thus its impulse response is defined by (4.23). Let

the input $x(t)$ be also causal as specified by (4.25). By (4.25), the convolution forms (4.24) modify to those associated with causal both systems and signals,

$$y(t) = \int_0^t x(\theta)h(t - \theta)d\theta = \int_0^t h(\theta)x(t - \theta)d\theta. \quad (4.26)$$

We notice that the forms (4.26) were used in the examples considered above in this Chapter.

Stability

For LTI systems, the critical property of *stability* is commonly associated with the *bounded-input/bounded-output* (BIBO) stability. To ascertain the BIBO stability, the absolute value of the impulse response is integrated over the infinite bounds. A finite value of the integral

$$\int_{-\infty}^{\infty} |h(\theta)|d\theta \leq M < \infty, \quad (4.27)$$

where $M < \infty$, means that a system is BIBO stable.

Example 4.6. A causal system has the impulse response $h(t) = ae^{-bt}u(t)$. Its BIBO stability is ascertained by (4.27) via the relation

$$B = a \int_0^{\infty} e^{-bt} dt = -\frac{a}{b} e^{-bt} \Big|_0^{\infty}.$$

Depending on the value of b , three particular cases can be distinguished:

- If $b > 0$, then $B = a/b < \infty$, the area of the impulse response is finite (Fig. 4.4a), and the system is thus BIBO stable.
- If $b < 0$, then $B \rightarrow \infty$, the area of the impulse response is infinite (Fig. 4.4c), and the system is thus BIBO unstable.
- If $b = 0$, we have an intermediate case (Fig. 4.4b).

□

4.2.4 Problems Solved with Convolution

As a rigorous and exact tool for LTI systems, the convolution allows solving three principle system problems.

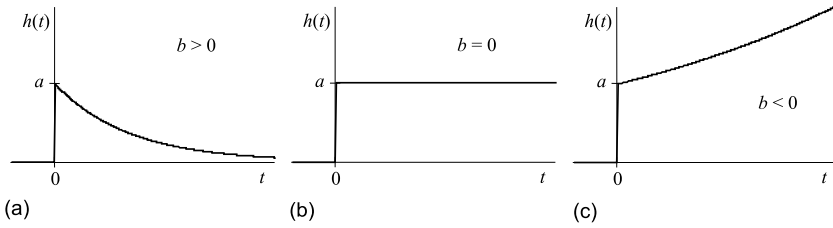


Fig. 4.4. Impulse response $h(t) = ae^{-bt}u(t)$: (a) $b > 0$, (b) $b = 0$, and (c) $b < 0$.

Direct Problem

Given the input signal $x(t)$, an LTI system is represented with the impulse response $h(t)$. Then the convolution straightforwardly solves the so-called *direct problem* defining, by (4.4), the system output $y(t)$. Examples 4.1, 4.3–4.5 illustrate solutions of the direct problem.

Inverse Problem

If an LTI system is represented with a known impulse response $h(t)$ and its output $y(t)$ is measured, then the input $x(t)$ can be restored using the convolution in what is called the *inverse problem*.

To define $x(t)$, one can try solving the integral equation (4.4) that commonly entails difficulties. Alternatively, we can recall that the Fourier transform of the convolution of two functions is the product of their spectral densities (Appendix C). Applying the transform to the both sides of (4.4), we thus have

$$Y(j\omega) = X(j\omega)H(j\omega),$$

where $H(j\omega) \stackrel{\mathcal{F}}{\Leftrightarrow} h(t)$ is the system transfer function defined as the Fourier transform of the impulse response $h(t)$ and $X(j\omega) \stackrel{\mathcal{F}}{\Leftrightarrow} x(t)$ and $Y(j\omega) \stackrel{\mathcal{F}}{\Leftrightarrow} y(t)$ are the spectral densities of $x(t)$ and $y(t)$, respectively.

Expressing $X(j\omega) = Y(j\omega)/H(j\omega)$ and thereafter applying the inverse transform to, we arrive at the time presentation of the input signal

$$x(t) = \frac{1}{2\pi} \int_{-\infty}^{\infty} \frac{Y(j\omega)}{H(j\omega)} e^{j\omega t} d\omega \quad (4.28)$$

and the inverse problem is solved.

Example 4.7. A causal LTI system is given with the impulse response $h(t) = ae^{-bt}u(t)$ and the output is measured to be $y(t) = B_0(1 - e^{-bt})u(t)$. The Fourier transforms of $h(t)$ and $y(t)$ are defined (Appendix C) by

$$h(t) = ae^{-bt}u(t) \quad \stackrel{\mathcal{F}}{\Leftrightarrow} \quad H(j\omega) = \frac{a}{b + j\omega},$$

$$y(t) = B_0(1 - e^{-bt})u(t) \quad \stackrel{\mathcal{F}}{\Leftrightarrow} \quad Y(j\omega) = \frac{B_0b}{j\omega(b + j\omega)}.$$

The inverse Fourier transform applied to the ratio $Y(j\omega)/H(j\omega)$ produces, by (4.28), the input signal

$$\frac{Y(j\omega)}{H(j\omega)} = B_0 \frac{b}{a} \frac{1}{j\omega} \quad \stackrel{\mathcal{F}}{\Leftrightarrow} \quad x(t) = B_0 \frac{b}{a} u(t)$$

that is gained with B_0b/a the step function $u(t)$. It then follows that the measured output $y(t)$ represents the step response of this system. \square

System Identification

In applications, especially in complex systems, they often consider a situation when the input $x(t)$ and output $y(t)$ are both measurable in the unknown system often called “black box”. The problem is thus to *identify* a system via its input and output.

To define the system impulse response, we can apply the inverse Fourier transform to the system transfer function $H(j\omega) = Y(j\omega)/X(j\omega)$ and go to its counterpart in the time domain,

$$h(t) = \frac{1}{2\pi} \int_{-\infty}^{\infty} \frac{Y(j\omega)}{X(j\omega)} e^{j\omega t} d\omega. \quad (4.29)$$

This, in turn, gives an alternative definition for the LTI system impulse response having an important practical significance. In fact, as can be seen, (4.29) does not claim the input $x(t)$ to be obligatorily the unit impulse. Instead, any input waveform can be applied if the system input is observable.

Example 4.8. The input and output of a “black box” were measured in the same time scale to be, respectively, $x(t) = A_0u(t)$ and $y(t) = B_0(1 - e^{-bt})u(t)$. The Fourier transforms of these signals (Appendix C) are, respectively,

$$x(t) = A_0u(t) \quad \stackrel{\mathcal{F}}{\Leftrightarrow} \quad X(j\omega) = \frac{A_0}{j\omega},$$

$$y(t) = B_0(1 - e^{-bt})u(t) \quad \stackrel{\mathcal{F}}{\Leftrightarrow} \quad Y(j\omega) = \frac{B_0b}{j\omega(1 + j\omega)}.$$

By (4.29), the system is identified to have the frequency and impulse responses, respectively,

$$H(j\omega) = \frac{Y(j\omega)}{X(j\omega)} = \frac{B_0}{A_0} \frac{b}{1 + j\omega} \quad \stackrel{\mathcal{F}}{\Leftrightarrow} \quad h(t) = \frac{B_0}{A_0} b e^{-bt} u(t).$$

We hence defined the system impulse response without actually applying the unit impulse. \square

4.2.5 Convolution Form for Multiple Systems

So far, we discussed applications of convolution for SISO LTI systems. If a system has more than one input and/or output, the approach virtually remains the same, albeit three basic structures shown in Fig. 4.5 are recognized. If an LTI system has one input and more than one output, then it is the *single-input multiple-output* (SIMO) LTI system (Fig. 4.5a). When several (more than one) inputs are organized such that the only output exists, we call the LTI system *multiple-input single-output* (MISO) (Fig. 4.5b). The most general LTI structure having more than one input and several outputs is termed *multiple-input multiple-output* (MIMO) (Fig. 4.5c).

Because the MIMO model obviously absorbs all others as its particular cases, we shall now discuss an LTI system having k inputs and p outputs performed by the $k \times 1$ and $p \times 1$ vectors, respectively,

$$\mathbf{x}(t) = [x_1(t) \ x_2(t) \ \dots \ x_k(t)]^T, \quad (4.30)$$

$$\mathbf{y}(t) = [y_1(t) \ y_2(t) \ \dots \ y_p(t)]^T. \quad (4.31)$$

Generally, in MIMO LTI systems, all of the inputs can interact with all of the outputs (Fig. 4.5c). Therefore, a system can be represented with the $k \times p$ impulse response matrix

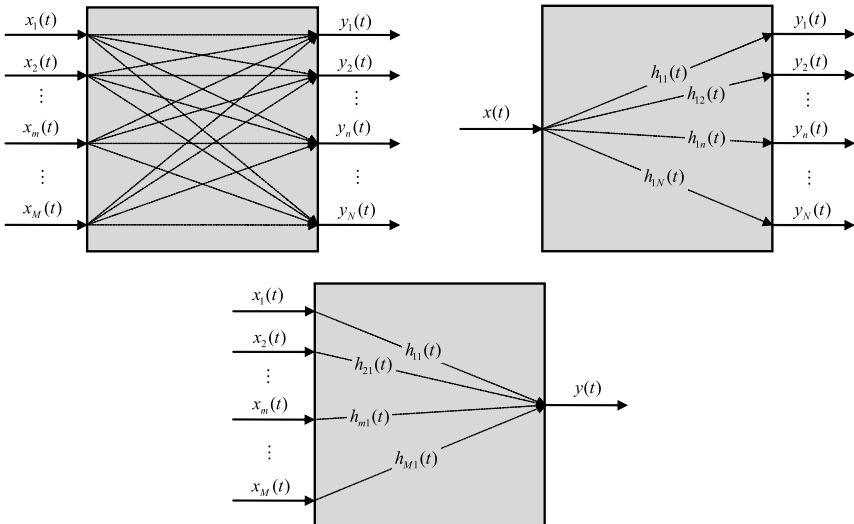


Fig. 4.5. Multiple LTI systems: (a) SIMO, (b) MISO, and (c) MIMO.

$$\mathbf{h}(t) = \begin{bmatrix} h_{11}(t) & h_{12}(t) & \dots & h_{1p}(t) \\ h_{21}(t) & h_{22}(t) & \dots & h_{2p}(t) \\ \vdots & \vdots & \ddots & \vdots \\ h_{k1}(t) & h_{k2}(t) & \dots & h_{kp}(t) \end{bmatrix}, \quad (4.32)$$

in which the component $h_{ij}(t)$, $i \in [1, k]$, $j \in [1, p]$, represents the impulse response at the j th output to i th input. Convolution for the MIMO LTI system is therefore commonly written as

$$\mathbf{y}(t) = \int_{-\infty}^{\infty} \mathbf{h}^T(t - \theta) \mathbf{x}(\theta) d\theta. \quad (4.33)$$

Example 4.9. A causal MIMO LTI system having two inputs and two outputs is represented with the impulse response matrix

$$\mathbf{h}(t) = \begin{bmatrix} ae^{-bt}u(t) & ae^{-2bt}u(t) \\ -ae^{-2bt}u(t) & ae^{-bt}u(t) \end{bmatrix}.$$

A vector of the causal input is described by

$$\mathbf{x}(t) = [A_0u(t) \ B_0u(t)]^T.$$

By (4.33), the system response to the input can be rewritten as

$$\begin{bmatrix} y_1(t) \\ y_2(t) \end{bmatrix} = a \int_0^t \begin{bmatrix} e^{-b(t-\theta)} & -e^{-2b(t-\theta)} \\ e^{-2b(t-\theta)} & e^{-b(t-\theta)} \end{bmatrix} \begin{bmatrix} A_0 \\ B_0 \end{bmatrix} d\theta$$

that produces two output signals

$$y_1(t) = A_0 \frac{a}{b} (1 - e^{-bt}) - B_0 \frac{a}{2b} (1 - e^{-2bt}),$$

$$y_2(t) = A_0 \frac{a}{2b} (1 - e^{-2bt}) + B_0 \frac{a}{b} (1 - e^{-bt}).$$

As it is seen, each of the outputs comprises two responses associated with two inputs. \square

4.3 Representation by Differential Equations

Convolution is not the only tool to couple the input and output of an LTI system in the time domain. Alternatively, because the output $y(t)$ is generated by the input $x(t)$, both $y(t)$ and $x(t)$ can be coupled by an ordinary differential equation (ODE) of some N th order. The coefficients of such an equation are predetermined by an LTI system to be constant and the order N is associated

with the system memory. The LTI system operator \mathcal{O} is thus also the ODE equation operator.

Most generally, an SISO system is described with the ODE as

$$\begin{aligned} a_0 y(t) + a_1 \frac{d}{dt} y(t) + a_2 \frac{d^2}{dt^2} y(t) + \dots + a_{N-1} \frac{d^{N-1}}{dt^{N-1}} y(t) + a_N \frac{d^N}{dt^N} y(t) \\ = b_0 x(t) + b_1 \frac{d}{dt} x(t) + b_2 \frac{d^2}{dt^2} x(t) + \dots + b_{M-1} \frac{d^{M-1}}{dt^{M-1}} x(t) + b_M \frac{d^M}{dt^M} x(t), \end{aligned} \quad (4.34)$$

where constant coefficients b_m , $m \in [0, M]$, and a_n , $n \in [0, N]$, are real. An important point to notice is that the system can physically be realized only if N is a highest order derivative in (4.34), i.e. $N \geq M$.

In a compact batch form, (4.34) becomes

$$\sum_{n=0}^N a_n \frac{d^n}{dt^n} y(t) = \sum_{m=0}^M b_m \frac{d^m}{dt^m} x(t) \quad (4.35)$$

and the output can be expressed straightforwardly as

$$y(t) = \sum_{m=0}^M \frac{b_m}{a_0} \frac{d^m}{dt^m} x(t) - \sum_{n=1}^N \frac{a_n}{a_0} \frac{d^n}{dt^n} y(t). \quad (4.36)$$

If the input $x(t)$ is known and the system coefficients, a_m and b_n , are completely determined, then the ODE, (4.35) or (4.36), can be solved for $y(t)$, provided the necessary initial conditions. This means, by extension, that if $x(t)$ is a unit impulse $\delta(t)$, then a solution of (4.35) is the system impulse response $h(t)$ and if $x(t)$ is a unit step $u(t)$, then the ODE produces the system step response $g(t)$. In this sense, the method of differential equations is consistent with convolution.

4.3.1 CARMA model

An alternative form of (4.36) came from the series analysis and is known as the *continuous-time autoregressive moving average* (CARMA) model. The model is performed as

$$y(t) = \sum_{m=0}^M \beta_{M-m} \frac{d^m}{dt^m} x(t) - \sum_{n=1}^N \alpha_{N-n} \frac{d^n}{dt^n} y(t), \quad (4.37)$$

where the coefficients β_m and α_n are constant. Originally, ARMA model was used to learn correlation in discrete-time series. Therefore, its part with the coefficients β_m is called the *moving average* (MA) model and the rest with the coefficients α_n the *autoregressive* (AR) model. By $\beta_{M-m} = b_m/a_0$ and $\alpha_{N-n} = a_n/a_0$, (4.37) becomes (4.36) and thus there is no principle difference between two models.

Example 4.10. A voltage $v(t) = x(t)$ forces an electric current $i(t) = y(t)$ to pass through a series connection of a resistance R , inductance L , and capacitance C . The system motion equation is therefore

$$x(t) = Ry(t) + L \frac{dy(t)}{dt} + \frac{1}{C} \int_{-\infty}^t y(\theta) d\theta.$$

By the first time derivative, the equation becomes

$$\frac{d^2y(t)}{dt^2} + \frac{R}{L} \frac{dy(t)}{dt} + \frac{1}{LC} y(t) = \frac{1}{L} \frac{dx(t)}{dt}$$

that, in the batch forms (4.35), is

$$\sum_{n=0}^2 a_n \frac{d^n}{dt^n} y(t) = \sum_{m=0}^1 b_m \frac{d^m}{dt^m} x(t),$$

where, the coefficients are defined by $a_0 = 1/LC$, $a_1 = R/L$, $a_2 = 1$, $b_0 = 0$, and $b_1 = 1/L$. By $\alpha_0 = LC$, $\alpha_1 = RC$, $\alpha_2 = 1$, $\beta_0 = C$, and $\beta_1 = 0$, the model is easily transformed to (4.37). \square

4.3.2 Properties of the ODE Operator

Application of the ODE operator to LTI systems, (4.35), presumes using some specific properties discussed below.

Solutions

A general solution of (4.35) comprises two functions,

$$y(t) = \bar{y}(t) + \tilde{y}(t), \tag{4.38}$$

where $\bar{y}(t)$ is known as a *homogenous solution* sometimes called *complimentary solution* and $\tilde{y}(t)$ is a *forced solution* also called *particular solution*, provided the definitions:

Homogenous solution: The system response to the initial conditions with zero input represents the homogenous solution $\bar{y}(t)$ of the system ODE. \square

In other words, to define $\bar{y}(t)$ starting at $t = t_0$, (4.35) must be solved under the condition that the input and all of its time derivatives are zero.

Forced solution: The system response to the input $x(t)$ with zero initial conditions represents the forced solution $\tilde{y}(t)$ of the system ODE.

□

It follows that, contrary to the homogenous solution, to define the system ODE solution $\tilde{y}(t)$ forced by the input $x(t)$ we must set all of the initial conditions to zero.

Homogenous solution. Following the definition, a homogenous solution $\bar{y}(t)$ is defined by setting to zero the right-hand side of (4.35) that gives

$$\sum_{n=0}^N a_n \frac{d^n}{dt^n} \bar{y}(t) = 0. \quad (4.39)$$

The exact solution of (4.39) is determined by N auxiliary initial conditions. In general, a set of these conditions is given at some start time point t_0 by the values of

$$\bar{y}(t_0), \quad \left. \frac{d\bar{y}(t)}{dt} \right|_{t=t_0}, \quad \dots, \quad \left. \frac{d\bar{y}^{N-1}(t)}{dt^{N-1}} \right|_{t=t_0}, \quad (4.40)$$

where t_0 is very often let to be zero, $t_0 = 0$.

The problem with solving (4.39) is coupled with finding the *eigenvalues* (roots) of the system's *characteristic equation*

$$\sum_{n=0}^N a_n \lambda^n = 0 \quad (4.41)$$

that is algebraic with exactly N roots λ_i , $i \in [1, N]$, which may be either real or complex conjugate.

It is known from the theory of ODEs that the first order linear ODE describing the first order LTI system has an exponential solution. The N -order linear ODE can be presented with N ODEs of the first order. Therefore, most commonly, when all of the roots of (4.41) are distinct and different, a solution of (4.39) can be found as a superposition of N weighted exponential functions called *eigenfunctions* as

$$\bar{y}(t) = \sum_{i=1}^N C_i e^{\lambda_i t}, \quad (4.42)$$

where each of the constant coefficients C_i is specified by the initial conditions (4.40) as follows. Take time derivatives of the right-hand side of (4.42) and set them to be equal at $t = t_0$ to the proper values of the initial conditions. We thus have N algebraic equations

$$\bar{y}(t_0) = \sum_{i=1}^N C_i e^{\lambda_i t_0},$$

$$\begin{aligned}
\left. \frac{d\bar{y}(t)}{dt} \right|_{t=t_0} &= \sum_{i=1}^N \lambda_i C_i e^{\lambda_i t_0}, \\
&\vdots \\
\left. \frac{d\bar{y}^{N-1}(t)}{dt^{N-1}} \right|_{t=t_0} &= \sum_{i=1}^N \lambda_i^{N-1} C_i e^{\lambda_i t_0},
\end{aligned} \tag{4.43}$$

where all λ_i are specified by (4.41), to solve for N unknown values of C_i .

It is seen that zero initial conditions degenerate (4.43) at $t_0 = 0$ to the linear algebraic equations system

$$\begin{aligned}
0 &= C_1 + C_2 + \dots + C_N, \\
0 &= \lambda_1 C_1 + \lambda_2 C_2 + \dots + \lambda_N C_N, \\
&\vdots \\
0 &= \lambda_1^{N-1} C_1 + \lambda_2^{N-1} C_2 + \dots + \lambda_N^{N-1} C_N
\end{aligned} \tag{4.44}$$

that can be solved for C_i in different ways.

In applications, the homogenous solution (4.42) is used to study stability, internal properties, and dynamics of systems in absence of any of the external signals and disturbances.

Forced solution. Because the input $x(t)$ can be of any waveform, the forced solution $\tilde{y}(t)$, contrary to $\bar{y}(t)$, cannot be generalized in closed form. Typically, to find a forced solution for the given $x(t)$, the function $\tilde{y}(t)$ must somehow be predicted to satisfy the ODE order. Then the unknown coefficients of this function are defined.

Linearity

The N -order equation (4.35) describing an LTI system belongs to the class of linear ODEs with constant coefficients. Linearity is thus an inherent property of this equation. Namely for this reason, its solution is defined as the sum (4.38) of the homogenous and forced solutions.

Causality

As we remember, causality is associated with physical realizability. An LTI system can physically be realized by the following principle constraints:

- **Order N .** The order N in (4.35) refers to the highest derivative of the output. This means that a signal in the LTI system feedback cannot be changed faster than in the direct way and hence $N \geq M$. Otherwise, a system does not meet physical imaginations and thus cannot be realized practically. \square

- **SISO system.** If the input $x(t)$ of a SISO system is such that $x(t) = 0$ for $t < t_0$, then its output must also be such that $y(t) = 0$ for $t < t_0$. This means that the response of a causal SISO system for $t \geq t_0$ is calculated by (4.35) with zero initial conditions (4.40). \square
- **MISO system.** If a causal MISO system has, for example, two inputs, $x_1(t)$ and $x_2(t)$, then its initial conditions for $x_1(t)$ may be defined by $x_2(t)$. Therefore, the system response $y(t)$ to $x_1(t)$ for $t \geq t_0$ cannot obligatory be associated with zero initial conditions. \square

Time-invariance

Time-invariance is an inherent property of LTI systems. With respect to the system ODE (4.35), the term “time-invariance” means that all of the coefficients in (4.35) are time-constant.

Test Responses

The impulse response $h(t)$ and step response $g(t)$ of an LTI system are derived, by (4.35), in the following forms, respectively,

$$\sum_{n=0}^N a_n \frac{d^n}{dt^n} h(t) = \sum_{m=0}^M b_m \frac{d^m}{dt^m} \delta(t), \quad (4.45)$$

$$\sum_{n=0}^N a_n \frac{d^n}{dt^n} g(t) = \sum_{m=0}^M b_m \frac{d^m}{dt^m} u(t). \quad (4.46)$$

Following the definition, all of the initial conditions in (4.45) and (4.46) must be set to zero.

Example 4.11. An LTI system is described with the ODE

$$\frac{d}{dt} y(t) + ay(t) = x(t), \quad (4.47)$$

in which a is constant and the input is performed by

$$x(t) = A_0 e^{-bt} u(t), \quad (4.48)$$

where A_0 and b are also constant. The initial condition is $y(0) = y_0$.

The characteristic equation (4.41) associated with (4.47) is $\lambda + a = 0$ having the only root $\lambda = -a$. Therefore, the homogenous solution is given by

$$\bar{y}(t) = C e^{\lambda t} = C e^{-at}.$$

By the initial condition applied to $\bar{y}(t)$ we have $\bar{y}(0) = y_0 = C$ and thus the homogenous solution is

$$\bar{y}(t) = y_0 e^{-at}. \quad (4.49)$$

Because $x(t)$ is performed with the exponential function (4.48) and $\bar{y}(t)$ also has an exponential solution (4.49), it is logical to suppose that the forced solution comprises two exponential functions. We therefore suppose that

$$\tilde{y}(t) = B e^{-at} + D e^{-bt}, \quad (4.50)$$

where B and D are still unknown. Now substitute (4.50) to (4.47), provide the transformation, define

$$D = \frac{A_0}{a-b},$$

and rewrite (4.50) as

$$\tilde{y}(t) = B e^{-at} + \frac{A_0}{a-b} e^{-bt}. \quad (4.51)$$

By the definition, the forced solution is defined for zero initial conditions. Letting $\tilde{y}(0) = 0$ at $t = 0$ in (4.51) produces

$$B = -\frac{A_0}{a-b}.$$

A common solution of (4.47) can now be written as

$$y(t) = \bar{y}(t) + \tilde{y}(t) = y_0 e^{-at} + \frac{A_0}{a-b} (e^{-bt} - e^{-at}), \quad t \geq 0. \quad (4.52)$$

Fig. 4.6 illustrates (4.52) for some given initial condition y_0 along with the input signal (4.48). As can be seen, a common solution $y(t)$ is strongly affected

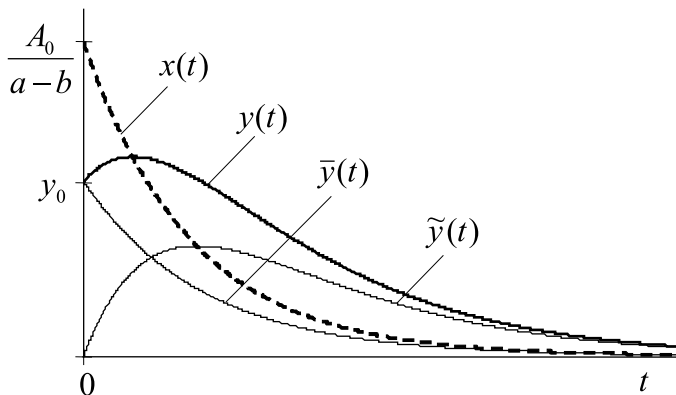


Fig. 4.6. Solutions of (4.47) for (4.48) and $y(0) = y_0$.

by both the homogenous and forced constituents. It is not unexpected, because the system (4.47) is almost equally sensitive to variations in the input and initial conditions. \square

As an exact and convenient tool, the ODE operator allows representing an LTI electronic system in two widely recognized forms:

- **Electric circuit presentation.** Any LTI system can be composed by the components of electric circuits, such as resistors R , inductances L , and capacitors C . At any point of such a system, signals can be gained with linear amplifiers. \square
- **Block diagram presentation.** Any LTI system can also be performed (simulated) by a proper connection of three linear blocks, such as integrators, adders, and amplifiers. \square

4.4 Electric Circuit Presentation by ODEs

An electronic LTI system is a real physical device having very often a great number of units, owing to which an exact solution of the system ODE becomes unwieldy and awkward. However, not all of the components of a system contribute equally to its dynamics. Therefore, many auxiliary units are usually omitted and the ODE is reduced to the more or less standard form of much lower order.

If the ODE order cannot be reduced without losing important features, the other way is to split a system into several subsystems, each of which can be presented with well studied elementary blocks of low order. Typically, the elementary blocks are associated with LTI systems of the first and second orders. A complex LTI system can then be composed by the elementary blocks and linear amplifiers.

4.4.1 LTI Systems of the First Order

An LTI system of the first order is often associated with the first order *low-pass* (LP) and *high-pass* (HP) filters. Two basic elementary configurations of the first order LTI systems are used, namely the RC circuit and the LR circuit, among which, the former has gained the most wide currency in applications.

A generalized ODE of an LTI system of the first order has the form of

$$\frac{d}{dt}y(t) + ay(t) = bx(t) \quad (4.53)$$

and its solution is found in the form of (4.38). A standard way to find a solution of (4.53) is to multiply both its sides with the so-called *integration factor* $e^{\int a dt}$ that transforms (4.53) to the equation

$$\frac{d}{dt} \left[e^{\int a dt} y(t) \right] = b e^{\int a dt} x(t),$$

which integration yields

$$y(t) = e^{-\int a dt} \left[\int bx(t)e^{\int a dt} dt + C \right], \quad (4.54)$$

where C is predetermined by the initial condition $y(t_0) = y_0$ and the integration must be provided from the start point t_0 up to the current time t . A solution (4.54) is general for both LTI and LTV systems. For LTI systems, in which all of the coefficients are constant, (4.54) attains the form of

$$y(t) = y_0 e^{-a(t-t_0)} + b e^{-a(t-t_0)} \int_{t_0}^t x(\tau) e^{a(\tau-t_0)} d\tau, \quad (4.55)$$

where the first term in the right-hand side represents the homogenous solution

$$\bar{y}(t) = y_0 e^{-a(t-t_0)} \quad (4.56)$$

that was derived earlier by (4.49) for $t = 0$, and the second term represents the forced solution

$$\tilde{y}(t) = b e^{-a(t-t_0)} \int_{t_0}^t x(\tau) e^{a(\tau-t_0)} d\tau \quad (4.57)$$

that must further be transformed for the particular input $x(t)$.

Example 4.12. Consider an LTI system described by (4.47) with the input given by (4.48). By (4.57), its forced solution is defined to be

$$\tilde{y}(t) = A_0 e^{-at} \int_0^t e^{-b\tau} e^{a\tau} d\tau = \frac{A_0}{a-b} (e^{-bt} - e^{-at})$$

that is equal to that obtained by (4.52). We thus conclude that a logical supposition about the form of a forced solution made in (4.50) was correct. \square

Response to Unit Impulse

If we let the input $x(t)$ to be a unit impulse acting at $t = 0$, then, by (4.45), the ODE (4.53) and so a solution (4.55) must produce the function associated with the system impulse response. Indeed, by setting $x(t) = \delta(t)$, we go to

$$h(t) = \left(y_0 e^{-at} + b e^{-at} \int_0^t \delta(\tau) e^{a\tau} d\tau \right) u(t)$$

that, by the sifting property of the delta function (Appendix A), reduces to

$$h(t) = (y_0 + b)e^{-at}u(t). \quad (4.58)$$

If we now set a zero initial condition $y_0 = 0$, (4.58) becomes

$$h(t) = be^{-at}u(t) \quad (4.59)$$

and we verify that a forced solution of the ODE of the first order causal LTI system for the input unit impulse represents its impulse response.

Note that a reciprocal $T = 1/a$ plays a role of the *system time constant*. Fig. 4.7a illustrates (4.59) and we notice that a tangent to $h(t)$ at $t = 0$ crosses the axis exactly at $t = T = 1/a$. Thus the time constant T of a system can easily be ascertained from the plot of the impulse response.

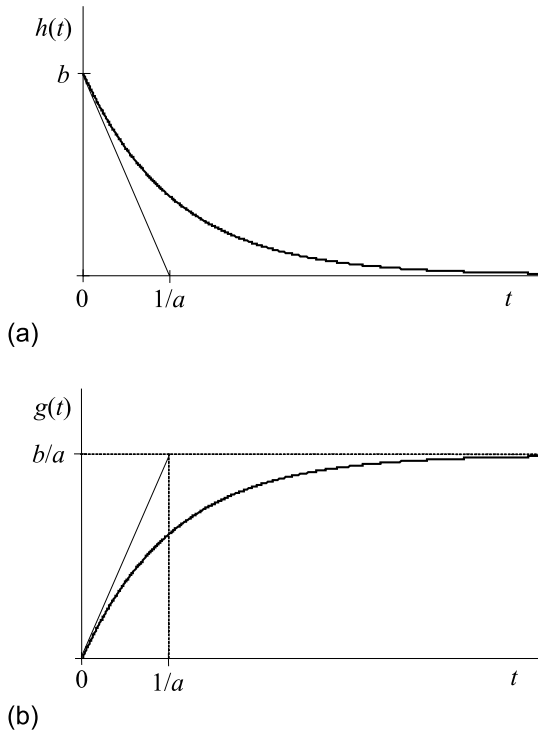


Fig. 4.7. Test responses of an LTI system of the first order: (a) impulse response and (b) step response.

Response to Unit Step

Let us now allow the input $x(t)$ to be the unit step $u(t)$ acting at $t = 0$. By the definition, a solution (4.55) must be associated with the system step response. In fact, setting $x(t) = u(t)$ gives

$$\begin{aligned} g(t) &= \left(y_0 e^{-at} + b e^{-at} \int_0^t e^{a\tau} d\tau \right) u(t) \\ &= y_0 e^{-at} u(t) + \frac{b}{a} (1 - e^{-at}) u(t) \end{aligned} \quad (4.60)$$

that, by $y_0 = 0$, yields the system step response

$$g(t) = \frac{b}{a} (1 - e^{-at}) u(t). \quad (4.61)$$

Note that (4.61) was earlier derived in the form of (4.7) via the convolution. And it is just a matter of simple manipulations to show that, by differentiating, (4.61) becomes (4.59) and, by integrating, (4.59) becomes (4.61) exactly as it is stated by (4.11). Fig. 4.7b illustrates the step response provided by (4.61).

Example 4.13. Fig. 4.8a represents the RC circuit as an LTI system of the first order. Here a resistor R causes the energy to dissipate and a capacitor C represents a memory component. A mechanical equivalent of a system is shown in Fig. 4.8b, where the force $x(t)$ acts on a spring in the presence of a friction that dissipates energy.

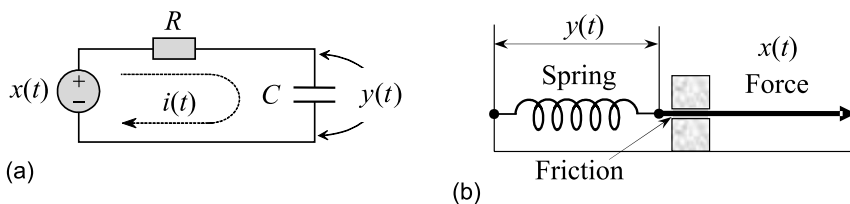


Fig. 4.8. LTI system of the first order: (a) electrical and (b) mechanical.

The system (Fig. 4.8a) is performed for the output voltage $y(t) = v_C(t)$ induced on a capacitor C and input voltage $x(t) = v(t)$ by the ODE of the first order

$$\frac{d}{dt} v_C(t) + \frac{1}{RC} v_C(t) = \frac{1}{RC} v(t).$$

In a causal system, we set $v(t) = 0$ for $t < 0$ and thus $v_C(0) = 0$. Accordingly, a solution of the equation is provided by (4.55) in the form of

$$v_C(t) = \frac{1}{RC} e^{-\frac{t}{RC}} \int_0^t v(\tau) e^{\frac{\tau}{RC}} d\tau.$$

The system impulse and step responses can now readily be obtained by letting $v(t) = \delta(t)$ and $v(t) = u(t)$, respectively,

$$h(t) = \frac{1}{RC} e^{-\frac{t}{RC}} u(t), \quad (4.62)$$

$$g(t) = (1 - e^{-\frac{t}{RC}}) u(t). \quad (4.63)$$

It can easily be verified that (4.62) and (4.63) are coupled by the rule established by (4.11). \square

4.4.2 LTI Systems of the Second Order

The other widely used elementary block is associated with LTI systems of the second order. Typically, this block is represented with the 2-order ODE

$$\frac{d^2}{dt^2} y(t) + a \frac{d}{dt} y(t) + by(t) = cx(t), \quad (4.64)$$

in which the coefficients a , b , and c are predetermined to be constant.

In applications, (4.64) commonly models oscillations and vibrations in selective LTI structures. The coefficient a has a meaning of the system bandwidth $BW = 2\delta$ and both b and c are typically associated with the system square *natural frequency* ω_0^2 . Therefore, (4.64) is usually rewritten in the other general form of

$$\frac{d^2}{dt^2} y(t) + 2\delta \frac{d}{dt} y(t) + \omega_0^2 y(t) = cx(t) \quad (4.65)$$

with arbitrary initial conditions at $t = 0$:

$$y(t_0) = y_0, \quad \left. \frac{dy(t)}{dt} \right|_{t=t_0} = y'_0. \quad (4.66)$$

An important characteristic of any bandpass or oscillatory system is the *quality factor* specified by

$$Q = \frac{\omega_0}{BW} = \frac{\omega_0}{2\delta}. \quad (4.67)$$

A system can also be characterized with the *damping factor*

$$\alpha = \frac{BW}{2\omega_0} = \frac{\delta}{\omega_0} = \frac{1}{2Q}. \quad (4.68)$$

It can be shown that the characteristic equation associated with (4.65) is

$$\lambda^2 + 2\delta\lambda + \omega_0^2 = 0, \quad (4.69)$$

having two complex-conjugate roots

$$\begin{aligned}\lambda_{1,2} &= -\delta \pm j\sqrt{\omega_0^2 - \delta^2} = -\delta \pm j\omega_s \\ &= \omega_0 \left(-\alpha \pm \sqrt{\alpha^2 - 1} \right),\end{aligned}\quad (4.70)$$

where $\omega_s = \sqrt{\omega_0^2 - \delta^2}$ is called the *system eigenfrequency*. In bandpass systems with high quality factor, $Q \gg 1$, losses of energy are usually small. Therefore, $\omega_0 \gg \delta$ and they typically allow $\omega_s \cong \omega_0$.

Homogenous Solution

The homogenous solution (4.42) associated with (4.65) is found in a like manner to comprise two exponential functions,

$$\bar{y}(t) = C_1 e^{\lambda_1 t} + C_2 e^{\lambda_2 t}, \quad (4.71)$$

where λ_1 and λ_2 are provided by (4.70) and C_1 and C_2 are predetermined by the initial conditions (4.66). By these conditions applied to (4.71) at $t = 0$, we arrive at two algebraic equations

$$y_0 = C_1 + C_2,$$

$$y'_0 = \lambda_1 C_1 + \lambda_2 C_2,$$

readily soluble for C_1 and C_2 ,

$$C_1 = \frac{-y'_0 + \lambda_2 y_0}{\lambda_2 - \lambda_1}, \quad C_2 = \frac{y'_0 - \lambda_1 y_0}{\lambda_2 - \lambda_1}. \quad (4.72)$$

By (4.70) and (4.72), the homogenous solution (4.71) becomes

$$\begin{aligned}\bar{y}(t) &= \frac{-y'_0 + \lambda_2 y_0}{\lambda_2 - \lambda_1} e^{\lambda_1 t} + \frac{y'_0 - \lambda_1 y_0}{\lambda_2 - \lambda_1} e^{\lambda_2 t} \\ &= \frac{y'_0 + (\delta + j\omega_s)y_0}{2j\omega_s} e^{-(\delta - j\omega_s)t} - \frac{y'_0 + (\delta - j\omega_s)y_0}{2j\omega_s} e^{-(\delta + j\omega_s)t}\end{aligned}\quad (4.73)$$

and it can easily be shown that, by $y_0 = 0$, (4.73) degenerates to

$$\begin{aligned}\bar{y}(t) &= \frac{y'_0}{\omega_s} e^{-\delta t} \sin \omega_s t \\ &= \frac{y'_0}{\omega_0 \sqrt{1 - \alpha^2}} e^{-\alpha \omega_0 t} \sin \omega_0 \sqrt{1 - \alpha^2} t.\end{aligned}\quad (4.74)$$

In applications, three particular cases are commonly analyzed for the homogenous solution (4.74) to provide the proper system quality associated with its dynamics (Fig. 4.9):

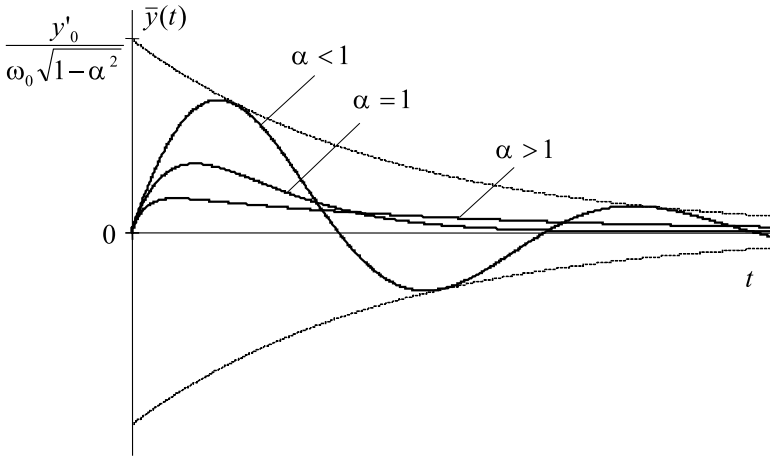


Fig. 4.9. Homogenous solutions for the 2-order LTI system with different damping factors.

- **Underdamping.** If $\alpha < 1$, then the system is said to be *underdamped*. The relevant solution oscillates about zero with an angular eigenfrequency ω_s that is lesser than the natural frequency, $\omega_s < \omega_0$. The oscillations envelope decays with time exponentially starting at $\bar{y}(0) = y'_0 / \omega_0 \sqrt{1 - \alpha^2}$ and having a time constant $T = 1 / \alpha \omega_0$. □
- **Overdamping.** With $\alpha > 1$, the solution has only positive values. It starts with zero, then goes up, attains a maximum, and thereafter attenuates to zero with time asymptotically. □
- **Critical damping.** The case of $\alpha = 1$ is intermediate. Therefore the systems is said to be *critically damped*. A solution for the critically damped system is $\bar{y}(t) = y'_0 t e^{-\omega_0 t}$. □

An applied convenience of the above used damping factor α resides in the fact that it, in a like manner, also separates the forced solutions.

Forced Solution

It can be shown that the closed forms forced solutions of (4.65) differ depending on the values of the damping factor α . Referring to the above-considered three cases, the solutions can be presented in the following forms:

- **Underdamping.** If a system is underdamped, $\alpha < 1$, the forced solution is given by

$$\tilde{y}(t) = \frac{ce^{-\alpha\omega_0 t}}{\omega_0 \sqrt{1 - \alpha^2}} \int_0^t x(\theta) e^{\alpha\omega_0 \theta} \sin[\omega_0 \sqrt{1 - \alpha^2}(t - \theta)] d\theta$$

$$= \frac{ce^{-\delta t}}{\omega_s} \int_0^t x(\theta)e^{\delta\theta} \sin \omega_s(t - \theta)d\theta. \quad (4.75)$$

□

- **Overdamping.** In the overdamped case, $\alpha > 1$, we have

$$\begin{aligned} \tilde{y}(t) &= \frac{ce^{-\alpha\omega_0 t}}{\omega_0\sqrt{\alpha^2 - 1}} \int_0^t x(\theta)e^{\alpha\omega_0\theta} \sinh[\omega_0\sqrt{\alpha^2 - 1}(t - \theta)]d\theta \\ &= \frac{ce^{-\delta t}}{\omega_s} \int_0^t x(\theta)e^{\delta\theta} \sinh \omega_s(t - \theta)d\theta. \end{aligned} \quad (4.76)$$

□

- **Critical damping.** A critical value of $\alpha = 1$ produces

$$\tilde{y}(t) = ce^{-\omega_0 t} \int_0^t x(\theta)(t - \theta)e^{\omega_0\theta}d\theta. \quad (4.77)$$

□

So, we now know both the homogenous solutions, (4.73) and (4.74), and forced solutions, (4.75)–(4.77), of a generalized LTI system of the second order. By applying the standard test functions, the solutions can easily be transformed to the the system test responses.

Impulse Response

The impulse response of an LTI system of the second order is defined by setting $x(t) = \delta(t)$ to (4.75)–(4.77). After the integration, we arrive at three different analytic results corresponding to the underdamped, overdamped, and critically damped systems, respectively,

$$\begin{aligned} h(t) &= \frac{ce^{\alpha\omega_0 t}}{\omega_0\sqrt{1 - \alpha^2}} \sin(\omega_0\sqrt{1 - \alpha^2}t) \\ &= \frac{c}{\omega_s} e^{-\delta t} \sin \omega_s t, \quad \alpha < 1, \end{aligned} \quad (4.78)$$

$$\begin{aligned} h(t) &= \frac{ce^{\alpha\omega_0 t}}{\omega_0\sqrt{\alpha^2 - 1}} \sinh(\omega_0\sqrt{\alpha^2 - 1}t) \\ &= \frac{c}{j\omega_s} e^{-\delta t} \sinh j\omega_s t, \quad \alpha > 1, \end{aligned} \quad (4.79)$$

$$h(t) = cte^{-\omega_0 t}, \quad \alpha = 1. \quad (4.80)$$

Fig. 4.10 exhibits what happens with the system impulse response, by changing the damping factor. It is seen that the functions differ cardinally in the underdamped and overdamped ranges. This is clearly illustrated in Fig. 4.10b, where the ranges for the underdamped and overdamped solutions are separated by the critical value of $\alpha = 1$. Two limiting cases can also be observed:

- **Zero damping factor**, $\alpha = 0$. With $\alpha \rightarrow 0$, a system works without dissipation of energy that, of course, cannot be met in practice and is just a useful mathematical idealization. Accordingly, the system bandwidth tends toward zero, $\delta \rightarrow 0$, and the ODE (4.65) degenerates to the form

$$\frac{d^2}{dt^2}y(t) + \omega_0^2 y(t) = cx(t), \quad (4.81)$$

associated with a linear *conservative system* of the second order, which impulse response is a sine wave with a natural frequency ω_0 and constant amplitude c/ω_0 ,

$$h(t) = \frac{c}{\omega_0} \sin \omega_0 t. \quad (4.82)$$

We notice that, even though this case cannot be reached fully, the goal of any precision nonlinear oscillatory system (reference oscillator) is to tend α toward zero as close as it is allowed by stability of the closed loop. \square

- **Infinite damping factor**, $\alpha \rightarrow \infty$. In the other limiting case of infinite α , the system bandwidth becomes infinite, $\delta \rightarrow \infty$, and the system hence totally loses its selectivity. It follows from (4.79) that, by $\delta \rightarrow \infty$, the system impulse response becomes zero. \square

Step Response

The step response function of an LTI system of the second order is defined by setting $x(t) = u(t)$ to (4.75)–(4.77). In line with the impulse response, three particular solutions characterize the step response as associated with the underdamped, overdamped, and critically damped systems, respectively

$$\begin{aligned} g(t) &= \frac{c}{\omega_0^2} \left[1 - e^{-\alpha\omega_0 t} \left(\cos \omega_0 \sqrt{1 - \alpha^2} t + \frac{\alpha}{\sqrt{1 - \alpha^2}} \sin \omega_0 \sqrt{1 - \alpha^2} t \right) \right] \\ &= \frac{c}{\omega_0^2} \left[1 - e^{-\delta t} \left(\cos \omega_s t + \frac{\delta}{\omega_s} \sin \omega_s t \right) \right], \quad \alpha < 1, \end{aligned} \quad (4.83)$$

$$g(t) = \frac{c}{\omega_0^2} \left[1 - e^{-\alpha\omega_0 t} \left(\cosh \omega_0 \sqrt{\alpha^2 - 1} t + \frac{\alpha}{\sqrt{\alpha^2 - 1}} \sinh \omega_0 \sqrt{\alpha^2 - 1} t \right) \right]$$

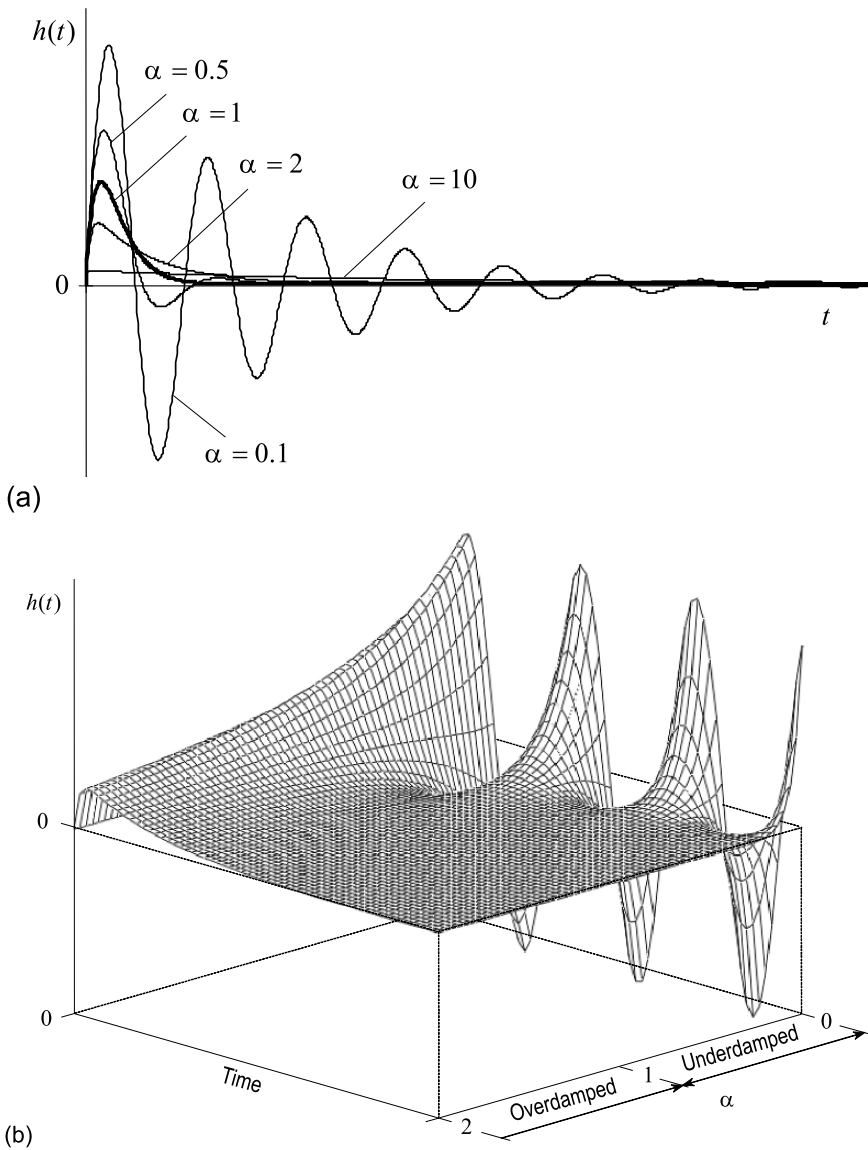


Fig. 4.10. Impulse response of a generalized LTI system of the second order with different damping factors: (a) several values of α and (b) transition from $\alpha = 0$ to $\alpha = 2$ through the critical value of $\alpha = 1$.

$$= \frac{c}{\omega_0^2} \left[1 - e^{-\delta t} \left(\cos \omega_s t + \frac{\delta}{\omega_s} \sin \omega_s t \right) \right], \quad \alpha > 1, \quad (4.84)$$

$$g(t) = \frac{c}{\omega_0^2} (1 - e^{-\omega_0 t} - \omega_0 t e^{-\omega_0 t}), \quad \alpha = 1. \quad (4.85)$$

Because a system is still linear and time-invariant, differentiating (4.83)–(4.85) yields the relevant impulse responses, (4.78)–(4.80), respectively. And, again, two limiting cases can be recognized:

- **Zero damping factor**, $\alpha = 0$. By (4.83) and $\alpha \rightarrow 0$, the step response of a conservative system becomes

$$g(t) = \frac{c}{\omega_0^2} (1 - \cos \omega_0 t) \quad (4.86)$$

that, by differentiating, inherently transforms to (4.82). \square

- **Infinite damping factor**, $\alpha \rightarrow \infty$. This case makes the system bandwidth 2δ to be extremely larger than the natural frequency ω_0 and the quality factor to be zero, $Q \rightarrow 0$. The system degenerates virtually to the RC circuit with extremely large R . Therefore, the step response, by (4.84), changes from zero exponentially and very slowly, approaching c/ω_0^2 at infinity. \square

In Fig. 4.11, we see how the step response of an LTI system of the second order evolves if to change α around unity. If to evaluate the transient time for the process envelope, then it can be shown that its minimum value corresponds to $\alpha = 1$. With $\alpha > 1$, the step response is almost exponential with the time constant proportional to α . The value $\alpha < 1$ makes the step response oscillating about c/ω_0^2 , whereas its envelope changes almost exponentially with the time constant reciprocal to α .

In applications, the transient time is fixed for some allowed level that often is 90 – 95% of the envelope at $t = \infty$. A shortest transient time is obtained by some value of $\alpha < 1$ when the first oscillation almost crosses this level.

Example 4.14. An RLC LTI system of the second order is performed by a cascade connection of L , R , and C as shown in Fig. 4.12a. Its mechanical equivalent is given in Fig. 4.12b. The system input is a voltage $v(t)$ and output is a voltage $v_C(t)$ induced on a capacitor C . In the mechanical equivalent, the force $x(t)$ acts to the mass connected via a spring to the fixed point. Mechanical shifts in this system are accomplished in the presence of friction leading to dissipation of energy.

An electric current in the scheme (Fig. 4.12a) can be performed via the voltage $v_C(t)$ as $i(t) = C dv_C(t)/dt$. Then the sum of all the voltages induced by $i(t)$ produces the system ODE of the second order

$$\frac{d^2}{dt^2} v_C(t) + \frac{R}{L} \frac{d}{dt} v_C(t) + \frac{1}{LC} v_C(t) = \frac{1}{LC} v(t)$$

that, in terms of (4.65), transforms to

$$\frac{d^2}{dt^2} v_C(t) + 2\delta \frac{d}{dt} v_C(t) + \omega_0^2 v_C(t) = \omega_0^2 v(t), \quad (4.87)$$

where $2\delta = R/L$ and $\omega_0^2 = 1/LC$. Properties of this system are completely specified by an equation (4.65) and its solutions if to substitute c with ω_0^2 . \square

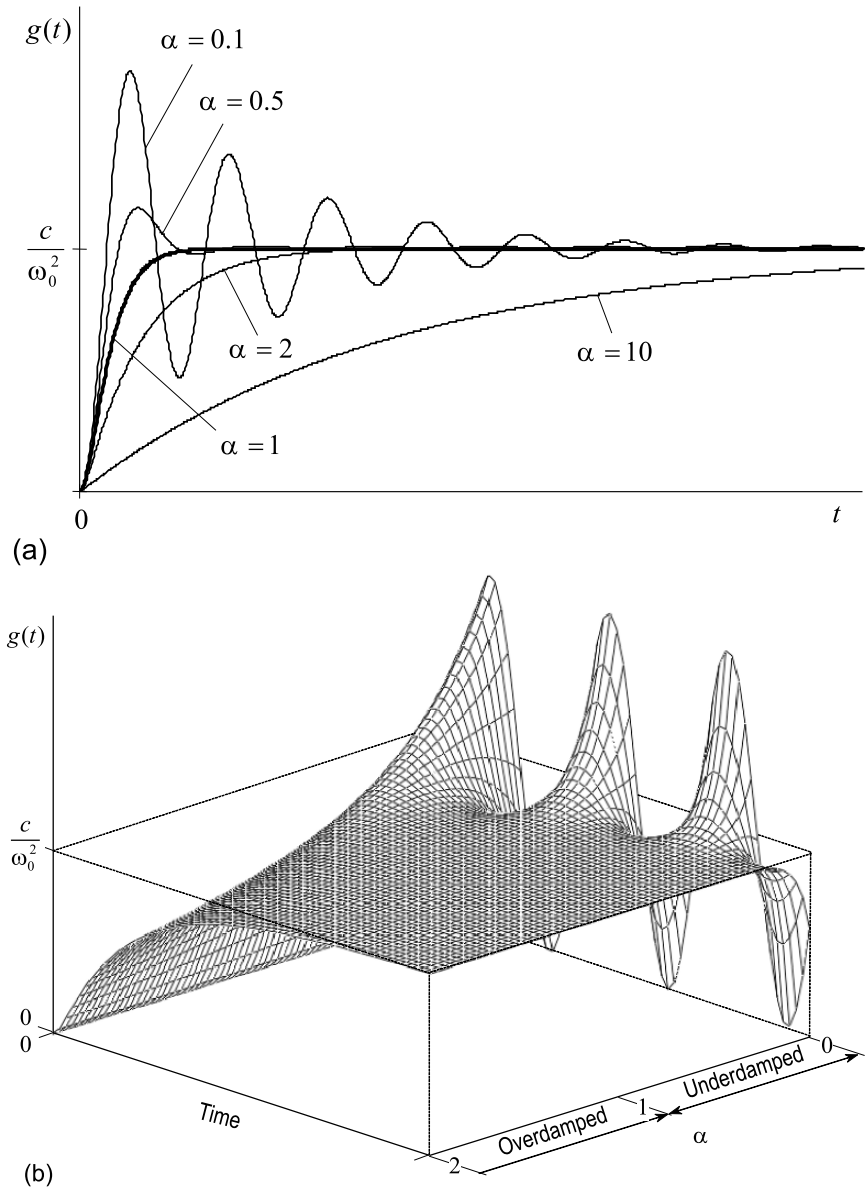


Fig. 4.11. Step response of a generalized LTI system of the second order for different damping factors: (a) several values of α and (b) transition from $\alpha = 0$ to $\alpha = 2$ through the critical value of $\alpha = 1$.

Example 4.15. Consider a system (Fig. 4.12a), in which the input voltage is constant, $v(t) = V_0$. With time, all transients in the system will finish and a capacitor C will be charged for the voltage $v_C = V_0$. Assuming such a

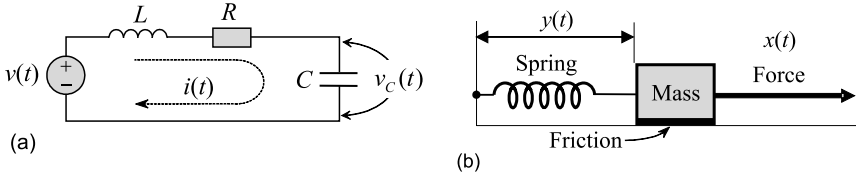


Fig. 4.12. LTI system of the second order: (a) electrical and (b) mechanical.

situation at $t = 0$, we set a switcher in a position shown in Fig. 4.13. This action forces an electric energy of a capacitor to be periodically exchanged with a magnetic energy of an inductance. Because of a real resistor, $R > 0$, dissipates energy, the amplitude of oscillations attenuates with time.

Transient in the electric current $i(t)$ (Fig. 4.13) is described by the homogenous ODE

$$\frac{d^2}{dt^2}i(t) + 2\delta \frac{d}{dt}i(t) + \omega_0^2 i(t) = 0. \tag{4.88}$$

At the first moment $t = 0$ after switched on, an inductance has a huge resistance (an electric current in any inductance cannot change instantly). Therefore, the first initial condition is zero, $i(0) = 0$. At the same time, the voltage on a capacitor is equal to the voltage on an inductance that produces the second initial condition,

$$\left. \frac{di(t)}{dt} \right|_{t=0} = -\frac{V_0}{L}.$$

The time function of $i(t)$ is then given by the homogenous solution (4.74) in the form of

$$i(t) = -\frac{V_0}{\omega_0 L \sqrt{1 - \alpha^2}} e^{-\alpha \omega_0 t} \sin \omega_0 \sqrt{1 - \alpha^2} t. \tag{4.89}$$

We notice that a negative sign in (4.89) indicates that the electric current generated by a voltage on a discharging capacity flows in an opposite direction. In Fig. 4.13 we have accounted for this fact. Therefore, referring to Fig.

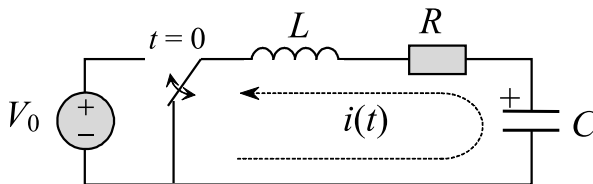


Fig. 4.13. Free discharge of a capacitor C in the RLC series tuned circuit.

4.13, a negative sign in (4.89) might be omitted. We also notice that Fig. 4.9 illustrates $i(t)$ in Fig. 4.13, by $y'_0 = V_0/L$.

□

4.5 System Simulation by Block Diagrams

Another form of description of LTI systems implies using the so-called *block diagrams*. The diagram is consistent with the system ODE and, actually, simulates a system mathematically rather than represents its physical nature. Therefore, it is also called the *simulation diagram*. The diagrams are useful in computed-aided systems design and analysis. They also help optimizing the system performance and resources.

4.5.1 Basic Blocks of LTI Systems

Any LTI system can be simulated by involving three basic blocks discussed below. No other kind of blocks is necessary.

- **Scalar multiplier.** This block is also called a *multiplier* (Fig. 4.14a), providing the multiplication (gaining) of any time signal $x(t)$ with any constant a by

$$y(t) = ax(t).$$

- **Adder.** The function of an *adder* is to obtain an addition of K signals $x_1(t), x_2(t), \dots, x_K(t)$ as shown in Fig. 4.14b by

$$y(t) = \sum_{k=1}^K x_k(t).$$

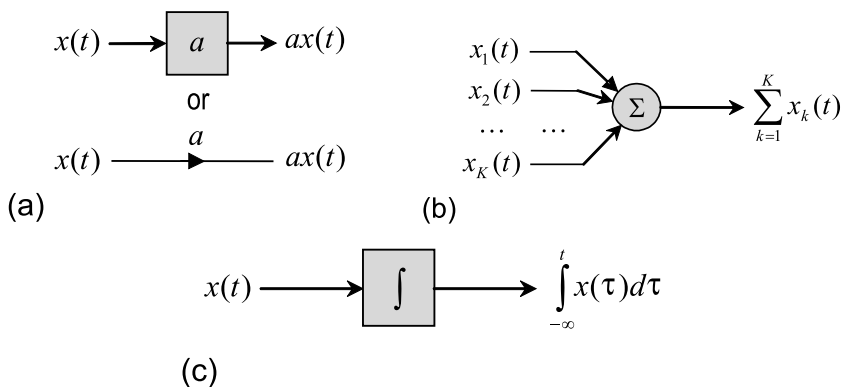


Fig. 4.14. Basic blocks of LTI systems: (a) scalar multiplier, (b) adder, and (c) ideal integrator.

- **Ideal integrator.** This block is also tacitly called an *integrator* (Fig. 4.14c) and its function is to integrate a signal $x(t)$ from some far point in the past up to the current time by

$$y(t) = \int_{-\infty}^t x(\tau) d\tau.$$

Combining the aforementioned blocks allows simulating any LTI system performed with the ODE of any order.

Example 4.16. An LTI system of the first order is described with the ODE

$$\frac{d}{dt}y(t) + 5y(t) = 2x(t).$$

The relevant block diagram is as shown in Fig. 4.15. Indeed, for the output

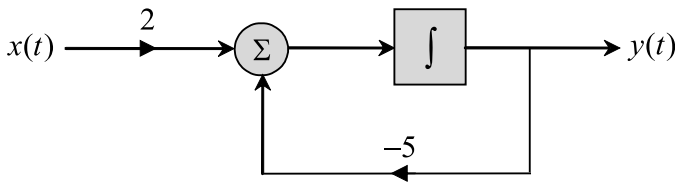


Fig. 4.15. Block diagram of the LTI systems of the first order.

$y(t)$, the input of an ideal integrator is $dy(t)/dt$. On the other hand, this input is formed by the sum of two signals, $2x(t)$ and $-5y(t)$, and we arrive at the system ODE. \square

4.5.2 Generalized Structures of LTI Systems

Let us come back to the ODE of a generalized LTI system (4.35),

$$\sum_{n=0}^N a_n \frac{d^n}{dt^n} y(t) = \sum_{m=0}^M b_m \frac{d^m}{dt^m} x(t). \tag{4.90}$$

Our purpose would be to represent a solution of this equation by the block diagram. To simplify the presentation form, it is in order to introduce the operator of multiple differentiation that we would like to denote by $\mathcal{D}^n \triangleq d^n/dt^n$, $n \geq 1$. Equation (4.90) can then be rewritten as

$$\sum_{n=0}^N a_n \mathcal{D}^n y(t) = \sum_{m=0}^M b_m \mathcal{D}^m x(t). \tag{4.91}$$

Further transformation of (4.91) is associated with two so-called the *canonic* forms of block diagrams, namely with the *first direct* and *second direct* forms. We notice that, albeit less commonly, some other forms are used.

The First Direct Form

The inverse operator \mathcal{D}^{-1} means integration, $\mathcal{D}^{-1} \triangleq \int_{-\infty}^t$. Aimed at providing the multiple N -times integration, we can formally multiply the both sides of (4.91) with \mathcal{D}^{-N} . Without loss in generality, we can even think that $N = M$ and normalize (4.91) with $a_N = 1$. The transformations lead to the form

$$\begin{aligned}
 y(t) &= - \sum_{n=0}^{N-1} a_n \mathcal{D}^{n-N} y(t) + \sum_{m=0}^N b_m \mathcal{D}^{m-N} x(t) \\
 &= \sum_{n=0}^{N-1} \mathcal{D}^{n-N} [-a_n y(t) + b_n x(t)] + b_N x(t)
 \end{aligned}
 \tag{4.92}$$

that can also be rewritten as

$$\begin{aligned}
 y(t) &= \mathcal{D}^{-N} [b_0 x(t) - a_0 y(t)] + \mathcal{D}^{-N+1} [b_1 x(t) - a_1 y(t)] + \dots \\
 &\quad + \mathcal{D}^{-1} [b_{N-1} x(t) - a_{N-1} y(t)] + b_N x(t).
 \end{aligned}
 \tag{4.93}$$

Both (4.92) and (4.93) are associated with the first direct (or canonic) form of the block diagram simulation of the LTI system ODE (4.90). By the property of distributivity, the operator of integration \mathcal{D}^{-1} can be applied either to each of the terms in (4.93) or to the sum of these terms. We thus have two equal structures of block diagrams shown in Fig. 4.16.

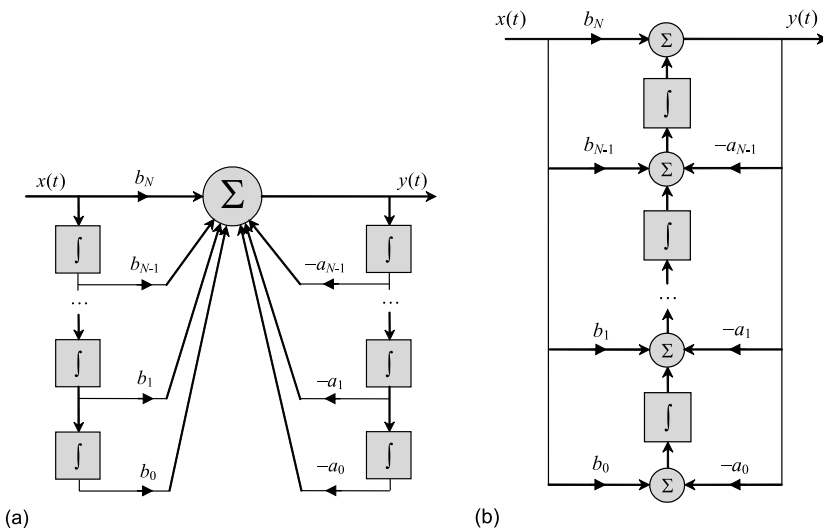


Fig. 4.16. The first direct form of LTI systems simulation: (a) addition efficient and (b) integration efficient.

In the first case (Fig. 4.16a), the structure exploits only one multi-input adder (addition efficient), however, suffers of a redundant number of integrators. The second diagram (Fig. 4.16b) utilizes a minimum number of integrators (integration efficient), but has a redundant number of adders. The latter structure is thus more preferable, because any integrator, as a memory device, is more complicated than any memoryless adder.

We notice that the power M might not obligatorily be equal to N , as we supposed in (4.93). If $M < N$, then the relevant branches with high-order coefficients b_m are omitted in Fig. 4.16.

Example 4.17. An LTI system of the second order is given with the block diagram of the first direct form shown in Fig. 4.17.

To go from the diagram to the system ODE, first express the output $y'(t) = dy(t)/dt$ of the first adder as

$$y'(t) = y_1(t) + 2x(t) - 2y(t).$$

Differentiating this relation gives

$$y''(t) = y_1'(t) + 2x'(t) - 2y'(t),$$

where the output $y_1'(t)$ of the second adder is performed by $y_1'(t) = 4x(t) + 4y(t)$. The system ODE then becomes

$$y''(t) = 2x'(t) + 4x(t) - 2y'(t) + 4y(t).$$

The reader is encouraged to verify that the above obtained ODE fits the block diagram shown in Fig. 4.17. \square

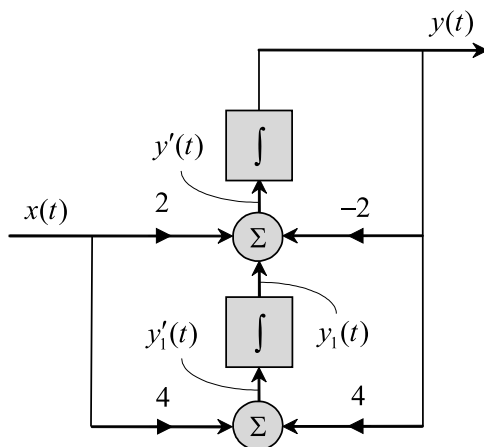


Fig. 4.17. Block diagram of an LTI system of the second order.

The Second Direct Form

The other direct (or canonic) form of diagrams appears if to represent (4.91) as follows. We first write

$$\left(\sum_{n=0}^N a_n \mathcal{D}^n \right) y(t) = \left(\sum_{m=0}^M b_m \mathcal{D}^m \right) x(t)$$

that identically can be represented as

$$\left(\sum_{n=0}^N a_n \mathcal{D}^n \right) \frac{y(t)}{\left(\sum_{m=0}^M b_m \mathcal{D}^m \right)} = x(t).$$

If now to substitute the ratio of the functions in the left-hand side with an auxiliary function $q(t)$, then the above equation can be split into two equations

$$\begin{aligned} \left(\sum_{n=0}^N a_n \mathcal{D}^n \right) q(t) &= x(t), \\ y(t) &= \left(\sum_{m=0}^M b_m \mathcal{D}^m \right) q(t), \end{aligned}$$

which, by multiplying the first of them with \mathcal{D}^{-N} , become, by $a_N = 1$,

$$\begin{aligned} q(t) &= - \sum_{n=0}^{N-1} a_n \mathcal{D}^{n-N} q(t) + \mathcal{D}^{-N} x(t), \\ y(t) &= \sum_{m=0}^M b_m \mathcal{D}^m q(t). \end{aligned} \tag{4.94}$$

Based upon (4.94), the block diagram is created in two steps. First, an auxiliary function $q(t)$ is expressed via the input $x(t)$ and then the output $y(t)$ is performed in terms of $q(t)$. The relevant diagram is shown in Fig. 4.18 for $N = M$.

One can deduce that, contrary to the first direct form (Fig. 4.16b), the second direct form requires a twice larger number of adders. In this sense, this form is not addition efficient that actually is not a great disadvantage.

Example 4.18. An LTI system is given with the ODE

$$y''(t) + 2y(t) = 4x'(t) + 2x(t).$$

To perform a system in the second direct form, substitute its ODE, by (4.94), with two equations

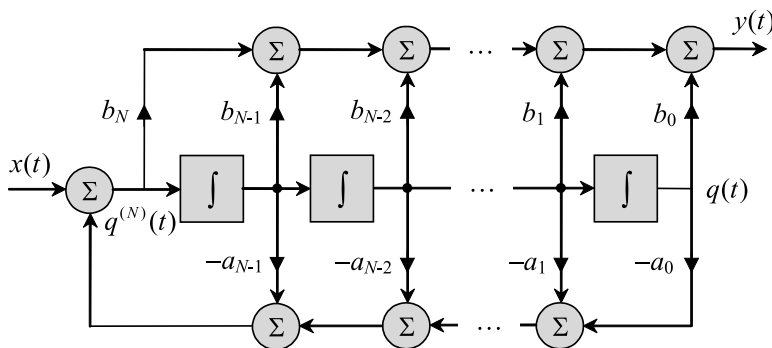


Fig. 4.18. The second direct form of the LTI system presentation.

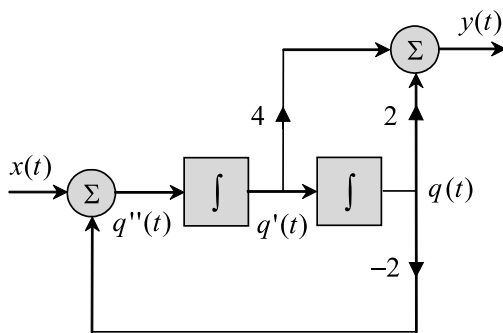


Fig. 4.19. Block diagram of an LTI system of the second order.

$$q''(t) + 2q(t) = x(t),$$

$$y(t) = 4q'(t) + 2q(t).$$

Simulation with the block diagram is then obtained as in Fig. 4.19. □

A particular case of $M = 0$. In applications, SISO LTI systems are often described by the ODE (4.90) with $M = 0$,

$$\sum_{n=0}^N a_n \frac{d^n}{dt^n} y(t) = b_0 x(t). \tag{4.95}$$

This degenerate version of (4.90) is simulated with two significantly simplified direct forms of block diagrams.

The first form (4.93), by $b_n = 0, n > 0$, leads to the equation

$$y(t) = \mathcal{D}^{-N} [b_0 x(t) - a_0 y(t)] - a_1 \mathcal{D}^{-N+1} y(t) - \dots - a_{N-1} \mathcal{D}^{-1} y(t) \tag{4.96}$$

that is simulated as in Fig. 4.20.

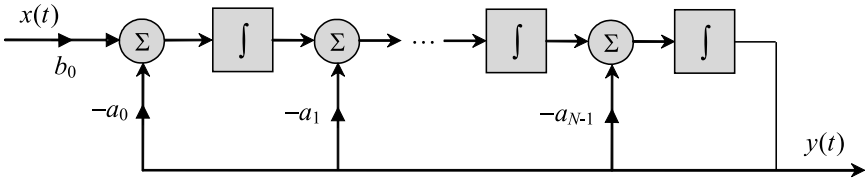


Fig. 4.20. The first direct form of a SISO LTI system diagram, by $M = 0$.

The second form (4.94), by $M = 0$, produces

$$\begin{aligned}
 q(t) &= - \sum_{n=0}^{N-1} a_n \mathcal{D}^{n-N} q(t) + x(t), \\
 y(t) &= b_0 q(t)
 \end{aligned}
 \tag{4.97}$$

and we arrive at the diagram shown in Fig. 4.21. Even a quick look at Fig. 4.20 and Fig. 4.21 leads to the immediate conclusion that they are equivalent having no substantial advantages to each other.

A special case of $M = 0$ and $b = 0$. There is an isolated case of LTI systems, when the ODE is performed with $M = 0$ and $b_0 = 0$. It follows from Fig. 4.20 that, by $b_0 = 0$, the system has no input. If it is still an LTI system then such a structure is of no essential practical importance. However, if some coefficients a_n are nonlinear, a system can become oscillating falling to the class of NTI systems. Contrary, in Fig. 4.21, the value $b_0 = 0$ makes the system isolated (no output) that is senseless. To avoid this confusion with simulation, the coefficient b_0 might be removed to the system input. Such a manipulation does not violate the model with $b_0 \neq 0$, but makes it equivalent to that shown in Fig. 4.20 when $b_0 = 0$.

An observation of the aforementioned forms of block diagrams assures that the tool is highly efficient in systems simulation. Indeed, while describing a real physical system (electrical and mechanical) by differential equations, we think in terms of energy bearers (electric current, voltage, charge, etc). Hereby, the ODE represents the LTI system via its physical resources. Contrary, the block

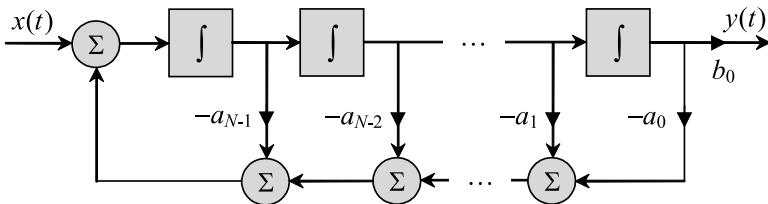


Fig. 4.21. The second direct form of a SISO LTI systems, by $M = 0$.

diagram simulates a system formally via its ODE using the assigned generalized signals, $x(t)$ and $y(t)$, without discussing their physical nature. Therefore, in systems design and optimization, it is worth passing over two important stages: 1) system presentation by the ODEs and 2) system simulation and optimization by the diagrams.

The other available and important tool of mathematical presentation of LTI systems is known as the *state space model*. The model implies presenting the system ODE of some N -order with a system of ODEs of the first order. Such a presentation employs a concept of the *system state variables*, which can or cannot be absolutely observable (measured) in real systems. The system state-space model is now well developed and used widely becoming principle for many applications.

4.6 State Space Representation

Any system operates with some signals. Any signal or its performance (amplitude and phase) can be expanded at some fixed time point t_1 to the Taylor series and thereby performed by an infinite set of weighted time derivatives. In phase systems, for example, the function of the information bearing phase can be characterized at t_1 by the phase value, linear phase drift rate (or frequency), linear frequency drift rate, and so on. Since a set of these characteristics represents an LTI system via the Taylor series explicitly, then we have one more form of the LTI system presentation.

This new form is called the *system state space model* or the *state space representation* of a system. The system's *state* is characterized by a set of *state variables* that at any given time completely describes the system. The variables may be assigned in different ways, however, the principle idea must be preserved: one needs to translate the N -order system ODE to a system of the 1-order ODEs. This can be done if the state variables are assigned to be the outputs of integrators in the block diagram. Returning to the phase system, we observe that the phase can be assigned to be the first state variable $q_1(t)$, the linear phase drift rate the second state variable $q_2(t)$, the linear frequency drift rate the third state variable $q_3(t)$, and the assignment can be extended infinitely.

If we will be able to perform a system with the state variables, we then will be required to couple these variables with the system input $x(t)$ and output $y(t)$. In state space modeling, this coupling is achieved with two equations. The first equation couples the system present state with its nearest past state and input. Therefore, it is called the *system state equation*, or *system equation*, or *state equation*. The second equation specifies the output via the system's state and input. Since the system state is observed (measured) in this equation indirectly, the equation is said to be the *observation equation* or *measurement equation*. Both the *system state equation* and the *observation equation* are called the *system state space equations* or just *state space equations*.

To understand the essence of state space modeling in more detail, let us come back to the second direct form (Fig. 4.18). Here, we use an auxiliary function $q(t)$ and its time derivatives to represent a system by two differential equations (4.94), rather than using only one equation (4.91). If to assign $q_1(t) = q(t)$, $q_2(t) = q'(t)$, \dots , $q_N(t) = q^{(N)}(t)$, we will get the second form in terms of the system state variables $q_1(t)$, $q_2(t)$, \dots , $q_N(t)$. The final step toward the state space model will be to translate the system ODE of the N -order to a system of the 1-order ODEs.

Before continuing with the mathematical presentation of the state space model, it is worth emphasizing that any LTI system can be described in state space if the following generic conditions are satisfied:

- **Initial conditions.** The system past history specifying the initial conditions must be known. □
- **System model.** A set of the system state variables or the system input-to-output equation specifying the system model must be known. □
- **Input signal.** The input must be known. □

After satisfying the conditions, the state space model inherently answers the following key questions: What is the system state at present? How did the system come at this state from the nearest past? What should we expect in the nearest future?

4.6.1 The First Direct Forms of SISO Systems in State Space

The state space model of an LTI system is readily created following the block diagram shown in Fig. 4.16b. We first assign the output of each of the integrators to be the proper state variable $q_n(t)$. Then, observing the diagram from up to down and differentiating consequently each of the states, we arrive at

$$\begin{aligned}
 y(t) &= q_1(t) + b_N x(t), \\
 q_1'(t) &= q_2(t) + b_{N-1} x(t) - a_{N-1} y(t), \\
 q_2'(t) &= q_3(t) + b_{N-2} x(t) - a_{N-2} y(t), \\
 &\vdots \\
 q_{N-1}'(t) &= q_N(t) + b_1 x(t) - a_1 y(t), \\
 q_N'(t) &= b_0 x(t) - a_0 y(t).
 \end{aligned} \tag{4.98}$$

The first equation in (4.98) can serve to eliminate $y(t)$ in the remaining equations. If to do so, we will go to the equations of the system's state,

$$q_1'(t) = q_2(t) - a_{N-1} q_1(t) + (b_{N-1} - a_{N-1} b_N) x(t),$$

$$\begin{aligned}
q'_2(t) &= q_3(t) - a_{N-2}q_1(t) + (b_{N-2} - a_{N-2}b_N)x(t), \\
&\vdots \\
q'_{N-1}(t) &= q_N(t) - a_1q_1(t) + (b_1 - a_1b_N)x(t), \\
q'_N(t) &= -a_0q_1(t) + (b_0 - a_0b_N)x(t)
\end{aligned}$$

that can be rewritten in matrix form as

$$\begin{bmatrix} q'_1(t) \\ q'_2(t) \\ \vdots \\ q'_{N-1}(t) \\ q'_N(t) \end{bmatrix} = \begin{bmatrix} -a_{N-1} & 1 & 0 & \dots & 0 \\ -a_{N-2} & 0 & 1 & & 0 \\ \vdots & \vdots & \vdots & \ddots & \vdots \\ -a_1 & 0 & 0 & & 1 \\ -a_0 & 0 & 0 & \dots & 0 \end{bmatrix} \begin{bmatrix} q_1(t) \\ q_2(t) \\ \vdots \\ q_{N-1}(t) \\ q_N(t) \end{bmatrix} + \begin{bmatrix} b_{N-1} - a_{N-1}b_N \\ b_{N-2} - a_{N-2}b_N \\ \vdots \\ b_1 - a_1b_N \\ b_0 - a_0b_N \end{bmatrix} x(t). \quad (4.99)$$

On the other hand, the first equation in (4.98) represents an observation of the system first state variable $q_1(t)$ via the input $x(t)$ and output $y(t)$ that can be reflected in matrix form as

$$y(t) = [1 \ 0 \ \dots \ 0] \begin{bmatrix} q_1(t) \\ q_2(t) \\ \vdots \\ q_N(t) \end{bmatrix} + b_N x(t). \quad (4.100)$$

Both the *state equation* (4.99) and the *observation equation* (4.100) have compact matrix forms of, respectively,

$$\mathbf{q}'(t) = \mathbf{A}\mathbf{q}(t) + \mathbf{B}x(t), \quad (4.101)$$

$$y(t) = \mathbf{C}\mathbf{q}(t) + \mathbf{D}x(t), \quad (4.102)$$

where the $N \times 1$ vector $\mathbf{q}(t)$ of the system's state is

$$\mathbf{q}(t) = [q_1(t) \ q_2(t) \ \dots \ q_N(t)]^T. \quad (4.103)$$

Here and in the following, the sign $(^T)$ means transpose (Appendix B). The time derivative of $\mathbf{q}(t)$ is defined by the $N \times 1$ vector

$$\mathbf{q}'(t) = \frac{d}{dt}\mathbf{q}(t) = [q'_1(t) \ q'_2(t) \ \dots \ q'_N(t)]^T. \quad (4.104)$$

The $N \times N$ matrix \mathbf{A} is called the *system matrix*,

$$\mathbf{A} = \begin{bmatrix} -a_{N-1} & 1 & 0 & \dots & 0 \\ -a_{N-2} & 0 & 1 & & 0 \\ \vdots & \vdots & \vdots & \ddots & \vdots \\ -a_1 & 0 & 0 & & 1 \\ -a_0 & 0 & 0 & \dots & 0 \end{bmatrix}. \quad (4.105)$$

The $1 \times N$ matrix \mathbf{C} is commonly called the *observation matrix* or *measurement matrix*,

$$\mathbf{C} = [1 \ 0 \ \dots \ 0] . \quad (4.106)$$

Finally, two auxiliary $N \times 1$ and 1×1 matrices are known as the *input matrix* and *output matrix*, respectively,

$$\mathbf{B} = \begin{bmatrix} b_{N-1} - a_{N-1}b_N \\ b_{N-2} - a_{N-2}b_N \\ \vdots \\ b_1 - a_1b_N \\ b_0 - a_0b_N \end{bmatrix} , \quad (4.107)$$

$$\mathbf{D} = [b_N] . \quad (4.108)$$

The block diagram presentation of SISO LTI systems in state space with $M = N$ is provided by (4.101) and (4.102) as shown in Fig. 4.22. Here we recognize two principle parts. The system state vector $\mathbf{q}(t)$ is evaluated for the given input $x(t)$ in the *state model* (dotted) described by (4.101). The output $y(t)$ is then calculated by (4.102) via $\mathbf{q}(t)$ and $x(t)$ in the *observation model* (dotted).

Example 4.19. A system (Example 4.10) is given with the ODE

$$\sum_{n=0}^2 a_n \frac{d^n}{dt^n} y(t) = \sum_{m=0}^1 b_m \frac{d^m}{dt^m} x(t) ,$$

where, the coefficients are $a_0 = 1/LC = \omega_0^2$, $a_1 = R/L = 2\delta$, $a_2 = 1$, $b_0 = 0$, and $b_1 = 1/L$. The first direct form of this equation is given in state space by (4.101) and (4.102), where the matrices are defined, by (4.105)–(4.108), as

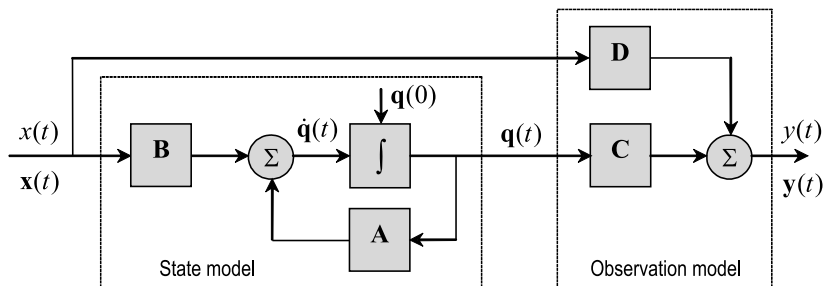


Fig. 4.22. Block diagram presentation of SISO LTI systems in state space for $M = N$.

$$\mathbf{A} = \begin{bmatrix} -2\delta & 1 \\ -\omega_0^2 & 0 \end{bmatrix}, \quad \mathbf{B} = \begin{bmatrix} 1/L \\ 0 \end{bmatrix}, \quad \mathbf{C} = [1 \ 0], \quad \mathbf{D} = [0].$$

It can easily be verified, by the inverse transformation, that the obtained state space model fits the original ODE. \square

Example 4.20. The ODE of an LTI system of the third order is given by

$$2y'''(t) + 4y''(t) - 2y'(t) + 6y(t) = 3x'''(t) + x''(t) + 6x(t).$$

The state space presentation of this equation in the first form is given by (4.101) and (4.102) if to specify the matrices as

$$\mathbf{A} = \begin{bmatrix} -2 & 1 & 0 \\ 1 & 0 & 1 \\ -3 & 0 & 0 \end{bmatrix}, \quad \mathbf{B} = \begin{bmatrix} -5/2 \\ 3/2 \\ -3/2 \end{bmatrix}, \quad \mathbf{C} = [1 \ 0 \ 0], \quad \mathbf{D} = [3/2].$$

The reader is encouraged to verify this, provide the inverse transformation, and come from the state space model to the original ODE. \square

A particular case of $M = 0$. Having $b_n = 0$ for $n > 0$, the system ODE becomes (4.95). In view of that, the state equation of the first direct form (4.99) degenerates to

$$\begin{bmatrix} q_1'(t) \\ q_2'(t) \\ \vdots \\ q_{N-1}'(t) \\ q_N'(t) \end{bmatrix} = \begin{bmatrix} -a_{N-1} & 1 & 0 & \dots & 0 \\ -a_{N-2} & 0 & 1 & & 0 \\ \vdots & \vdots & \vdots & \ddots & \vdots \\ -a_1 & 0 & 0 & & 1 \\ -a_0 & 0 & 0 & \dots & 0 \end{bmatrix} \begin{bmatrix} q_1(t) \\ q_2(t) \\ \vdots \\ q_{N-1}(t) \\ q_N(t) \end{bmatrix} + \begin{bmatrix} 0 \\ 0 \\ \vdots \\ 0 \\ b_0 \end{bmatrix} x(t). \quad (4.109)$$

By $b_N = 0$, we have $\mathbf{D} = 0$ and then (4.101) and (4.102) become

$$\mathbf{q}'(t) = \mathbf{A}\mathbf{q}(t) + \mathbf{B}x(t), \quad (4.110)$$

$$y(t) = \mathbf{C}\mathbf{q}(t), \quad (4.111)$$

where the system state vector $\mathbf{q}(t)$ and its time derivative $\mathbf{q}'(t)$ are defined by (4.103) and (4.104), respectively. The matrices \mathbf{A} and \mathbf{C} are described by (4.105) and (4.106), respectively. Finally, the $N \times 1$ matrix \mathbf{B} is given by

$$\mathbf{B} = [0 \ 0 \ \dots \ b_0]^T \quad (4.112)$$

and the output matrix is zero, $\mathbf{D} = 0$. Accordingly, the block diagram (Fig. 4.22) simplifies to that shown in Fig. 4.23.

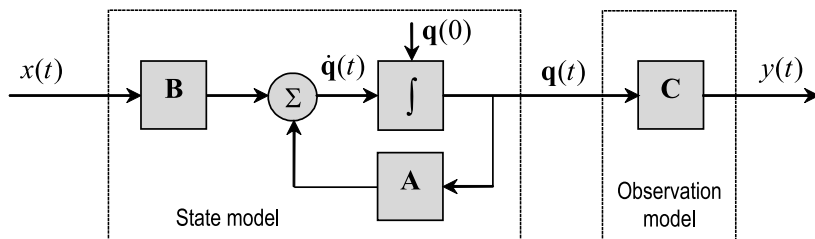


Fig. 4.23. Block diagram presentation of SISO LTI systems in state space for $M < N$.

4.6.2 The Second Direct Forms of SISO Systems in State Space

In a like manner, the state space presentation of a SISO LTI system can be provided for the second direct form (Fig. 4.18). In doing so, we first assign the output of each of the integrators to be the system state variable that leads to the equations

$$\begin{aligned}
 q_1'(t) &= q_2(t), \\
 q_2'(t) &= q_3(t), \\
 &\vdots \\
 q_{N-1}'(t) &= q_N(t), \\
 q_N'(t) &= -a_{N-1}q_N(t) - a_{N-2}q_{N-1}(t) - \dots - a_0q_1(t) + x(t), \\
 y(t) &= b_0q_1(t) + b_1q_2(t) + \dots + b_{N-1}q_N(t) \\
 &+ b_N[-a_0q_1(t) - a_1q_2(t) - \dots - a_{N-1}q_N(t) + x(t)]. \quad (4.113)
 \end{aligned}$$

Without any other transformations, these equations produce the system state and observation equations in matrix forms, respectively,

$$\begin{bmatrix} q_1'(t) \\ q_2'(t) \\ \vdots \\ q_{N-1}'(t) \\ q_N'(t) \end{bmatrix} = \begin{bmatrix} 0 & 1 & 0 & \dots & 0 \\ 0 & 0 & 1 & \dots & 0 \\ \vdots & \vdots & & \ddots & \vdots \\ 0 & 0 & 0 & \dots & 1 \\ -a_0 & -a_1 & -a_2 & \dots & -a_{N-1} \end{bmatrix} \begin{bmatrix} q_1(t) \\ q_2(t) \\ \vdots \\ q_{N-1}(t) \\ q_N(t) \end{bmatrix} + \begin{bmatrix} 0 \\ 0 \\ \vdots \\ 0 \\ 1 \end{bmatrix} x(t), \quad (4.114)$$

$$y(t) = \begin{bmatrix} b_0 - a_0b_N \\ b_1 - a_1b_N \\ \vdots \\ b_{N-1} - a_{N-1}b_N \end{bmatrix}^T \begin{bmatrix} q_1(t) \\ q_2(t) \\ \vdots \\ q_N(t) \end{bmatrix} + b_N x(t). \quad (4.115)$$

Now observe that (4.114) and (4.115) are still presented in the compact forms (4.101) and (4.102), respectively, if to specify the matrices of dimensions $N \times N$, $N \times 1$, $1 \times N$, and 1×1 by, respectively,

$$\mathbf{A} = \begin{bmatrix} 0 & 1 & 0 & \dots & 0 \\ 0 & 0 & 1 & & 0 \\ \vdots & \vdots & & \ddots & \vdots \\ 0 & 0 & 0 & & 1 \\ -a_0 & -a_1 & -a_2 & \dots & -a_{N-1} \end{bmatrix}, \quad (4.116)$$

$$\mathbf{B} = [0 \ 0 \ \dots \ 0 \ 1]^T, \quad (4.117)$$

$$\mathbf{C} = \begin{bmatrix} b_0 - a_0 b_N \\ b_1 - a_1 b_N \\ \vdots \\ b_{N-1} - a_{N-1} b_N \end{bmatrix}^T, \quad (4.118)$$

$$\mathbf{D} = [b_N]. \quad (4.119)$$

We thus deduce that, by $M = N$, both the first and the second direct forms are simulated with the same structure shown in Fig. 4.22 having an important common feature. With $M < N$ or $b_N = 0$, the matrix \mathbf{D} becomes identically zero, the matrix \mathbf{C} in both forms is calculated in a simpler way, and the block diagram becomes as in Fig. 4.23.

Example 4.21. An LTI system is given with the ODE considered in Example 4.20 being specified with the coefficients $a_0 = 6$, $a_1 = -2$, $a_2 = 4$, $a_3 = 2$, $b_0 = 6$, $b_1 = 0$, $b_2 = 1$, and $b_3 = 3$.

To go to the state space model, first, divide all of the coefficients by the factor of 2 to make $a_3 = 1$. The state space presentation of this equation in the second form will then be given by (4.101) and (4.102) if to define the matrices (4.116)–(4.119) by, respectively,

$$\mathbf{A} = \begin{bmatrix} 0 & 1 & 0 \\ 0 & 0 & 1 \\ -3 & 1 & -2 \end{bmatrix}, \quad \mathbf{B} = \begin{bmatrix} 0 \\ 0 \\ 1 \end{bmatrix}, \quad \mathbf{C} = \left[-\frac{3}{2} \ \frac{3}{2} \ -\frac{5}{2}\right], \quad \mathbf{D} = \left[\frac{3}{2}\right].$$

As can be observed, a difference between the first form given in Example 4.20 and the second one considered in this example is in the matrices \mathbf{A} , \mathbf{B} , and \mathbf{C} . This means that (4.101) and (4.102) can equivalently be filled with different matrix components for the same system. \square

A particular case of $M = 0$. Let us consider a SISO LTI system described with the ODE (4.95), in which $a_N = 1$. Since $M = 0$ implies $b_N = 0$, a system is performed in state space with (4.110) and (4.111), where the matrices \mathbf{A} and \mathbf{B} are given by (4.116) and (4.117), respectively. The $1 \times N$ matrix \mathbf{C} is

$$\mathbf{C} = [b_0 \ 0 \ \dots \ 0] \quad (4.120)$$

and the 1×1 matrix \mathbf{D} has a zero component, $\mathbf{D} = \mathbf{0}$. Having $b_N = 0$, this system is simulated with the block diagram shown in Fig. 4.23.

Example 4.22. A SISO *RLC*-system of the second order is given with the ODE (4.87),

$$v_C''(t) + 2\delta v_C'(t) + \omega_0^2 v_C(t) = \omega_0^2 v(t),$$

where $v(t)$ is the input and $v_C(t)$ is output. In terms of (4.95), the coefficients of the ODE are $a_0 = \omega_0^2$, $a_1 = 2\delta$, and $b_0 = \omega_0^2$. Its state space presentation is given by (4.101) and (4.102), where the matrices are defined by

$$\mathbf{A} = \begin{bmatrix} 0 & 1 \\ -\omega_0^2 & -2\delta \end{bmatrix}, \quad \mathbf{B} = \begin{bmatrix} 0 \\ 1 \end{bmatrix}, \quad \mathbf{C} = [\omega_0^2 \ 0].$$

The system is simulated with the block diagram shown in Fig. 4.23. \square

The other opportunity to perform a system in state space is to proceed directly with its ODE avoiding considering the diagram. The approach is akin to the second form and seems to be most “transparent” in explanation if to let $M = 0$ and $a_N = 1$, namely if a system is represented with the ODE

$$y^{(N)}(t) = - \sum_{n=0}^{N-1} a_n \frac{d^n}{dt^n} y(t) + b_0 x(t).$$

The state variables are assigned here as follows:

$$q_1(t) = y(t), \quad (4.121)$$

$$q_2(t) = y'(t) = q_1'(t),$$

$$q_3(t) = y''(t) = q_2'(t),$$

$$\vdots$$

$$q_{N-1}(t) = y^{(N-2)}(t) = q_{N-2}'(t),$$

$$q_N(t) = y^{(N-1)}(t) = q_{N-1}'(t),$$

$$-a_0 q_1(t) - a_1 q_2(t) - \dots - a_{N-1} q_N(t) + b_0 x(t) = y^{(N)}(t) = q_N'(t). \quad (4.122)$$

Then both (4.122) and (4.121) can be rewritten in matrix forms (4.110) and (4.111), respectively, representing the system state and observation equations, respectively,

$$\begin{bmatrix} q_1'(t) \\ q_2'(t) \\ \vdots \\ q_{N-1}'(t) \\ q_N'(t) \end{bmatrix} = \begin{bmatrix} 0 & 1 & 0 & \dots & 0 \\ 0 & 0 & 1 & & 0 \\ \vdots & \vdots & & \ddots & \vdots \\ 0 & 0 & 0 & & 1 \\ -a_0 & -a_1 & -a_2 & \dots & -a_{N-1} \end{bmatrix} \begin{bmatrix} q_1(t) \\ q_2(t) \\ \vdots \\ q_{N-1}(t) \\ q_N(t) \end{bmatrix} + \begin{bmatrix} 0 \\ 0 \\ \vdots \\ 0 \\ b_0 \end{bmatrix} x(t), \quad (4.123)$$

$$y(t) = [1 \ 0 \ \dots \ 0] \begin{bmatrix} q_1(t) \\ q_2(t) \\ \vdots \\ q_N(t) \end{bmatrix}. \quad (4.124)$$

Comparing (4.123) and (4.124) with (4.114) and (4.115) for $M = 0$, we find a difference only in the constant coefficient b_0 that is removed in the first case from matrix \mathbf{C} to matrix \mathbf{B} . This actually gives equivalent results. However, by $b_0 = 0$, the model, (4.123) and (4.124), has no input, whereas the model, (4.114) and (4.115), loses its output.

Example 4.23. A system is described with the ODE given in Example 4.22. By (4.123) and (4.124), the matrices for the state space model (4.110) and (4.111) are defined by

$$\mathbf{A} = \begin{bmatrix} 0 & 1 \\ -\omega_0^2 & -2\delta \end{bmatrix}, \quad \mathbf{B} = \begin{bmatrix} 0 \\ \omega_0^2 \end{bmatrix}, \quad \mathbf{C} = [1 \ 0].$$

In contrast to Example 4.22, here the coefficient ω_0^2 appears in \mathbf{B} and vanishes in \mathbf{C} . \square

4.6.3 MIMO Systems in State Space

The state space analysis is easily extended to the general case of MIMO systems. Assume that a system has k inputs and p outputs (Fig. 4.5c) and is described with N state variables. The state space model will then be represented by the equations

$$\mathbf{q}'(t) = \mathbf{A}\mathbf{q}(t) + \mathbf{B}\mathbf{x}(t), \quad (4.125)$$

$$\mathbf{y}(t) = \mathbf{C}\mathbf{q}(t) + \mathbf{D}\mathbf{x}(t), \quad (4.126)$$

where the $N \times 1$ vector of the system state $\mathbf{q}(t)$ and its time derivative $\mathbf{q}'(t)$ are given by (4.103) and (4.104), respectively. The $k \times 1$ vector of a multiple input $\mathbf{x}(t)$ and the $p \times 1$ vector of a multiple output $\mathbf{y}(t)$ are presented by, respectively,

$$\mathbf{x}(t) = [x_1(t) \ x_2(t) \ \dots \ x_k(t)]^T, \quad (4.127)$$

$$\mathbf{y}(t) = [y_1(t) \ y_2(t) \ \dots \ y_p(t)]^T. \quad (4.128)$$

The $N \times N$ system matrix and the $p \times N$ observation matrix are given as, respectively,

$$\mathbf{A} = \begin{bmatrix} a_{11} & a_{12} & \dots & a_{1N} \\ a_{21} & a_{22} & \dots & a_{2N} \\ \vdots & \vdots & \ddots & \vdots \\ a_{N1} & a_{N2} & \dots & a_{NN} \end{bmatrix}, \quad \mathbf{C} = \begin{bmatrix} c_{11} & c_{12} & \dots & c_{1N} \\ c_{21} & c_{22} & \dots & c_{2N} \\ \vdots & \vdots & \ddots & \vdots \\ c_{p1} & c_{p2} & \dots & c_{pN} \end{bmatrix}. \quad (4.129)$$

Finally, the $N \times k$ input matrix \mathbf{B} and $p \times k$ output matrix \mathbf{D} are performed by, respectively,

$$\mathbf{B} = \begin{bmatrix} b_{11} & b_{12} & \dots & b_{1k} \\ b_{21} & b_{22} & \dots & b_{2k} \\ \vdots & \vdots & \ddots & \vdots \\ b_{N1} & b_{N2} & \dots & b_{Nk} \end{bmatrix}, \quad \mathbf{D} = \begin{bmatrix} d_{11} & d_{12} & \dots & d_{1k} \\ d_{21} & d_{22} & \dots & d_{2k} \\ \vdots & \vdots & \ddots & \vdots \\ d_{p1} & d_{p2} & \dots & d_{pk} \end{bmatrix}. \quad (4.130)$$

We notice that all of the components in the matrices are defined by the coefficients of the system ODEs corresponding to the multiple input and output. It is also worth to notice that simulation of a MIMO system is provided by a familiar structure (Fig. 4.22). One merely needs substituting the scalar functions $x(t)$ and $y(t)$ with the vector functions $\mathbf{x}(t)$ and $\mathbf{y}(t)$, respectively.

Example 4.24. A MIMO system consists of two systems of the second order coupled via the mutual inductance M . The system has two inputs, $v_1(t)$ and $v_2(t)$, and two outputs, $v_{C1}(t)$ and $v_{C2}(t)$, as shown in Fig. 4.24. A straightforward description of a system gives two ODEs:

$$\begin{aligned} v_{C1}''(t) + 2\delta_1 v_{C1}'(t) + \omega_{01}^2 + \frac{\omega_{01}^2}{\omega_2^2} v_{C2}''(t) &= \omega_{01}^2 v_1(t), \\ v_{C2}''(t) + 2\delta_2 v_{C2}'(t) + \omega_{02}^2 + \frac{\omega_{02}^2}{\omega_1^2} v_{C1}''(t) &= \omega_{02}^2 v_2(t), \end{aligned}$$

where $\delta_1 = R_1/2L_1$, $\delta_2 = R_2/2L_2$, $\omega_{01}^2 = 1/L_1C_1$, $\omega_{02}^2 = 1/L_2C_2$, $\omega_1^2 = 1/MC_1$, and $\omega_2^2 = 1/MC_2$.

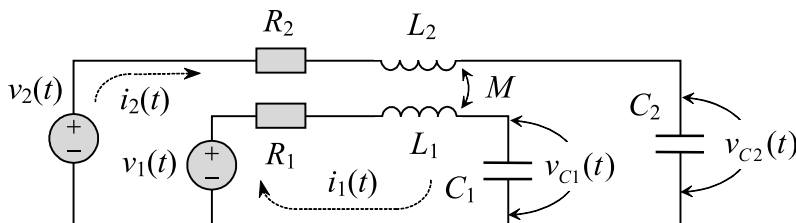


Fig. 4.24. A MIMO LTI electronic system.

To arrive at the standard forms, the equations can be rewritten for the high order time derivatives of the outputs as in the following:

$$v''_{C1} = -2\delta_1\gamma v'_{C1} - \omega_{01}^2\gamma v_{C1} + 2\delta_2\gamma \frac{\omega_{01}^2}{\omega_2^2} v'_{C2} + \omega_{02}^2\gamma \frac{\omega_{01}^2}{\omega_2^2} v_{C2} + \omega_{01}^2\gamma v_1 - \omega_{02}\gamma \frac{\omega_{01}^2}{\omega_2^2} v_2,$$

$$v''_{C2} = -2\delta_2\gamma v'_{C2} - \omega_{02}^2\gamma v_{C2} + 2\delta_1\gamma \frac{\omega_{02}^2}{\omega_1^2} v'_{C1} + \omega_{01}^2\gamma \frac{\omega_{02}^2}{\omega_1^2} v_{C1} + \omega_{02}^2\gamma v_2 - \omega_{01}\gamma \frac{\omega_{02}^2}{\omega_1^2} v_1,$$

where $\gamma = \omega_2^2\omega_1^2/(\omega_2^2\omega_1^2 - \omega_{01}^2\omega_{02}^2)$.

The state variables can now be assigned as follows:

$$q_1 = v_{C1},$$

$$q_2 = v'_{C1} = q'_1,$$

$$q'_2 = v''_{C1} = -2\delta_1\gamma q_2 - \omega_{01}^2\gamma q_1 + 2\delta_2\gamma \frac{\omega_{01}^2}{\omega_2^2} q_4 + \omega_{02}^2\gamma \frac{\omega_{01}^2}{\omega_2^2} q_3 + \omega_{01}^2\gamma v_1 - \omega_{02}^2\gamma \frac{\omega_{01}^2}{\omega_2^2} v_2,$$

$$q_3 = v_{C2},$$

$$q_4 = v'_{C2} = q'_3,$$

$$q'_4 = v''_{C2} = -2\delta_2\gamma q_4 - \omega_{02}^2\gamma q_3 + 2\delta_1\gamma \frac{\omega_{02}^2}{\omega_1^2} q_2 + \omega_{01}^2\gamma \frac{\omega_{02}^2}{\omega_1^2} q_1 + \omega_{02}^2\gamma v_2 - \omega_{01}\gamma \frac{\omega_{02}^2}{\omega_1^2} v_1.$$

Based upon, the system state and observation equations attain the forms of, respectively,

$$\begin{aligned} \begin{bmatrix} q'_1 \\ q'_2 \\ q'_3 \\ q'_4 \end{bmatrix} &= \begin{bmatrix} 0 & 1 & 0 & 0 \\ -\omega_{01}^2\gamma & -2\delta_1\gamma & \omega_{02}^2\gamma \frac{\omega_{01}^2}{\omega_2^2} & 2\delta_2\gamma \frac{\omega_{01}^2}{\omega_2^2} \\ 0 & 0 & 0 & 1 \\ \omega_{01}^2\gamma \frac{\omega_{02}^2}{\omega_1^2} & 2\delta_1\gamma \frac{\omega_{02}^2}{\omega_1^2} & -\omega_{02}^2\gamma & -2\delta_2\gamma \end{bmatrix} \begin{bmatrix} q_1 \\ q_2 \\ q_3 \\ q_4 \end{bmatrix} \\ &+ \begin{bmatrix} 0 & 0 \\ \omega_{01}^2\gamma & -\omega_{02}^2\gamma \frac{\omega_{01}^2}{\omega_2^2} \\ 0 & 0 \\ -\omega_{01}^2\gamma \frac{\omega_{02}^2}{\omega_1^2} & \omega_{02}^2\gamma \end{bmatrix} \begin{bmatrix} v_1 \\ v_2 \end{bmatrix}, \\ \begin{bmatrix} v_{C1} \\ v_{C2} \end{bmatrix} &= \begin{bmatrix} 1 & 0 & 0 & 0 \\ 0 & 0 & 1 & 0 \end{bmatrix} \begin{bmatrix} q_1 \\ q_2 \\ q_3 \\ q_4 \end{bmatrix}. \end{aligned}$$

We notice that, by the state variables assigned, the matrix \mathbf{D} in the observation equation (4.126) acquires zero components. Therefore the last equation lost its dependence on the input. \square

4.6.4 LTI Systems with Feedback

There is a class of LTI systems utilizing feedback. Systems of this kind are used in *control systems* and are often subject to the *control theory*.

Most commonly, two general models of LTI systems with feedback are recognized. The feedback can organize either a *closed loop* system with an output (no input) or a *closed loop control* system with an external control signal as an input.

Closed Loop LTI System

In closed loop LTI systems, the input vector $\mathbf{x}(t)$ is specified by the output vector $\mathbf{y}(t)$ and the $k \times p$ *feedback matrix*

$$\mathbf{K} = \begin{bmatrix} k_{11} & k_{12} & \dots & k_{1p} \\ k_{21} & k_{22} & \dots & k_{2p} \\ \vdots & \vdots & \ddots & \vdots \\ k_{k1} & k_{k2} & \dots & k_{kp} \end{bmatrix} \quad (4.131)$$

such that $\mathbf{x}(t) = \mathbf{K}\mathbf{y}(t)$. The components to \mathbf{K} are typically set such that some special requirements for the closed loop are satisfied.

Substituting $\mathbf{x}(t) = \mathbf{K}\mathbf{y}(t)$ to (4.101) and (4.102) yields

$$\mathbf{q}'(t) = \mathbf{A}\mathbf{q}(t) + \mathbf{B}\mathbf{K}\mathbf{y}(t), \quad (4.132)$$

$$\mathbf{y}(t) = \mathbf{C}\mathbf{q}(t) + \mathbf{D}\mathbf{K}\mathbf{y}(t). \quad (4.133)$$

The observation equation (4.133) can now be solved for $\mathbf{y}(t)$ and we arrive, by substituting $\mathbf{y}(t)$ in (4.132) and (4.133), at the state space model of a closed loop:

$$\mathbf{q}'(t) = [\mathbf{A} + \mathbf{B}\mathbf{K}(\mathbf{I} - \mathbf{D}\mathbf{K})^{-1}\mathbf{C}]\mathbf{q}(t), \quad (4.134)$$

$$\mathbf{y}(t) = (\mathbf{I} - \mathbf{D}\mathbf{K})^{-1}\mathbf{C}\mathbf{q}(t). \quad (4.135)$$

The block diagram simulating (4.134) and (4.135) is shown in Fig. 4.25. As it is seen, the system lost the input fitting the term “closed loop”.

Two particular cases of the model, (4.134) and (4.135), should also be mentioned. If the state variables are assigned such that the matrix \mathbf{D} has zero components, the equations simplify to

$$\mathbf{q}'(t) = (\mathbf{A} + \mathbf{B}\mathbf{K}\mathbf{C})\mathbf{q}(t), \quad (4.136)$$

$$\mathbf{y}(t) = \mathbf{C}\mathbf{q}(t). \quad (4.137)$$

And when the matrix \mathbf{C} is identity (we meet this case in many applications), then equations become

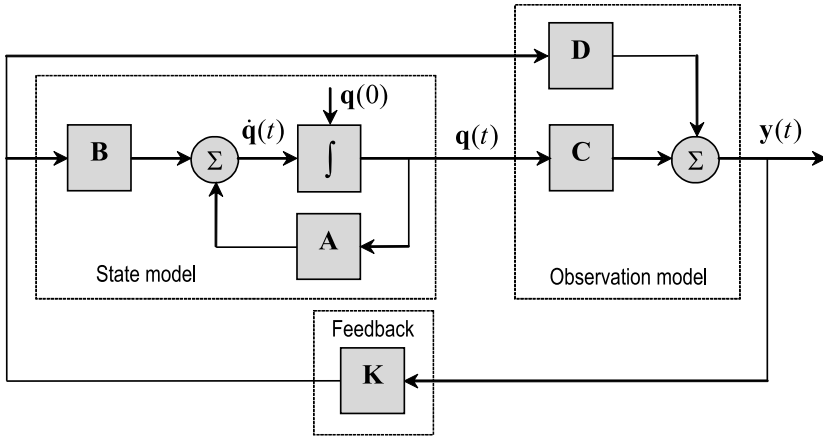


Fig. 4.25. Block diagram of a closed loop LTI system in state space.

$$\mathbf{q}'(t) = (\mathbf{A} + \mathbf{BK})\mathbf{q}(t), \tag{4.138}$$

$$\mathbf{y}(t) = \mathbf{C}\mathbf{q}(t). \tag{4.139}$$

As it is seen, the state equations (4.134), (4.136), and (4.138) are homogenous and therefore a composed matrix in their right-hand sides is totally responsible for system stability. Indeed, the unstable eigenvalues of \mathbf{A} can be made stable through appropriate choice of a matrix \mathbf{K} that is certainly an advantage of systems with feedback.

Of importance is that a stable closed loop is typically organized to have negative feedback. This means that the components in \mathbf{K} must be negative. Therefore, the coefficient \mathbf{K} very often appears in block diagrams (such as in Fig. 4.25) with a negative sign, namely as $-\mathbf{K}$, to emphasize that feedback is negative and the closed loop is stable.

Example 4.25. An LTI system of the second order represents a series tuned circuit shown in Fig. 4.26a. The scheme is described by the ODE

$$v_R''(t) + 2\delta v_R'(t) + \omega_0^2 v_R = 2\delta v'(t). \tag{4.140}$$

with known initial conditions, $v_R(0)$ and $v_R'(0)$.

The feedback induced (Fig. 4.26b) generates a voltage $v_{FB}(t) = v(t) = K v_R(t)$ and the system equation becomes homogenous

$$v_R''(t) + 2\delta(1 - K)v_R'(t) + \omega_0^2 v_R = 0. \tag{4.141}$$

It follows that, with $K < 1$, losses in the system are always positive and oscillations attenuate owing to energy dissipation. With $K > 1$, the losses are negative meaning that the feedback overcompensates dissipation of energy

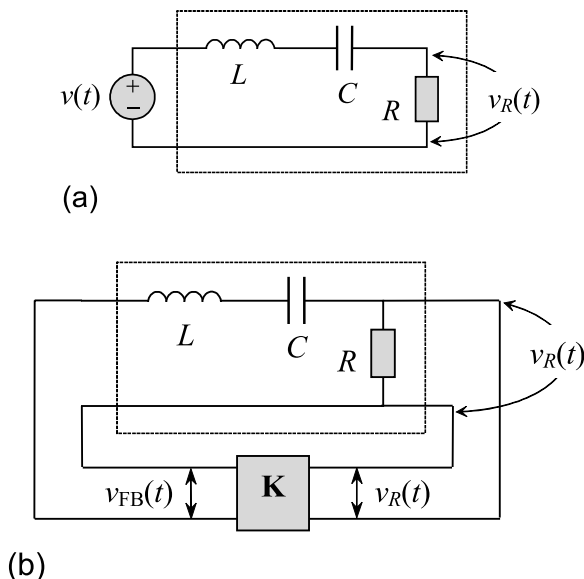


Fig. 4.26. LTI system of the second order: (a) input-to-output and (b) closed loop.

and oscillations develop. Finally, with $K = 1$, the losses are zero that can be met only if the dissipated energy is fully recovered by feedback.

The second direct form of (4.140) is given in state space by (4.136) and (4.137), if to define the matrices by

$$\mathbf{A} = \begin{bmatrix} 0 & 1 \\ -\omega_0^2 & -2\delta \end{bmatrix}, \quad \mathbf{B} = \begin{bmatrix} 0 \\ 1 \end{bmatrix}, \quad \mathbf{C} = [0 \ 2\delta], \quad \mathbf{D} = [0].$$

Having only one input and one output, the feedback matrix has 1×1 dimensions, $\mathbf{K} = [K]$. The state equation (4.136) and the observation equation (4.137) attain therefore the forms of, respectively,

$$\begin{bmatrix} q_1'(t) \\ q_2'(t) \end{bmatrix} = \left(\begin{bmatrix} 0 & 1 \\ -\omega_0^2 & -2\delta \end{bmatrix} + \begin{bmatrix} 0 \\ 1 \end{bmatrix} [K] [0 \ 2\delta] \right) \begin{bmatrix} q_1(t) \\ q_2(t) \end{bmatrix},$$

$$v_R = [1 \ 2\delta] \begin{bmatrix} q_1(t) \\ q_2(t) \end{bmatrix}.$$

After simple transformations, the state equation becomes

$$\begin{bmatrix} q_1'(t) \\ q_2'(t) \end{bmatrix} = \begin{bmatrix} 0 & 1 \\ -\omega_0^2 & -2\delta(1 - K) \end{bmatrix} \begin{bmatrix} q_1(t) \\ q_2(t) \end{bmatrix}.$$

It now becomes obvious that the coefficient K affects the system so that, by $K > 1$, the component A_{22} of \mathbf{A} is always positive. Furthermore, we will show

that such a value of K makes the system unstable to mean that the amplitude of oscillations develops with time. With $K < 1$, the system is always stable, once the amplitude of oscillations decreases with time. The case of $K = 1$ is intermediate. \square

Closed Loop Control LTI System

In the second important and widely used case, the input signal $\mathbf{x}(t)$ is formed as an additive sum of the output-generated signal $\mathbf{K}\mathbf{y}(t)$ and the external control signal $\mathbf{u}_c(t)$, namely we have $\mathbf{x}(t) = \mathbf{K}\mathbf{y}(t) + \mathbf{u}_c(t)$. By such an input, the state and observation equations become, respectively,

$$\mathbf{q}'(t) = \mathbf{A}\mathbf{q}(t) + \mathbf{B}\mathbf{K}\mathbf{y}(t) + \mathbf{B}\mathbf{u}_c(t), \tag{4.142}$$

$$\mathbf{y}(t) = \mathbf{C}\mathbf{q}(t) + \mathbf{D}\mathbf{K}\mathbf{y}(t) + \mathbf{D}\mathbf{u}_c(t). \tag{4.143}$$

The block diagram directly simulating (4.142) and (4.143) is presented in Fig. 4.27. As one can observe, the closed loop control system is the input-

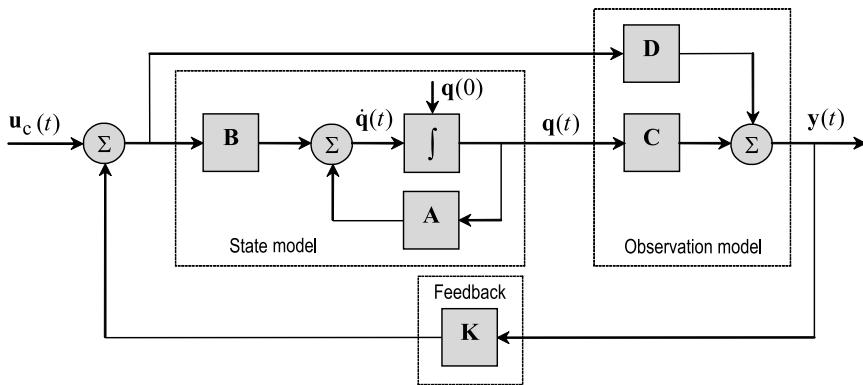


Fig. 4.27. Block diagram of a closed loop control LTI system in state space.

to-output system. However, unlike any open loop, the closed loop control possesses many useful properties of practical importance and its complexity is often compensated by its flexibility.

In a manner similar to the closed loop, one can solve (4.143) for $\mathbf{y}(t)$, substitute the result to (4.142) and go to the ultimate state space equations for the closed loop control:

$$\mathbf{q}'(t) = [\mathbf{A} + \mathbf{B}\mathbf{K}(\mathbf{I} - \mathbf{D}\mathbf{K})^{-1}\mathbf{C}]\mathbf{q}(t) + \mathbf{B}[\mathbf{I} + \mathbf{K}(\mathbf{I} - \mathbf{D}\mathbf{K})^{-1}\mathbf{D}]\mathbf{u}_c(t), \tag{4.144}$$

$$\mathbf{y}(t) = (\mathbf{I} - \mathbf{D}\mathbf{K})^{-1}\mathbf{C}\mathbf{q}(t) + (\mathbf{I} - \mathbf{D}\mathbf{K})^{-1}\mathbf{D}\mathbf{u}_c(t), \tag{4.145}$$

where \mathbf{I} is an identity matrix. By zero components in \mathbf{D} , the equations become

$$\mathbf{q}'(t) = (\mathbf{A} + \mathbf{BK})\mathbf{q}(t) + \mathbf{B}u_c(t), \quad (4.146)$$

$$\mathbf{y}(t) = \mathbf{C}\mathbf{q}(t) \quad (4.147)$$

and, if $\mathbf{C} = \mathbf{I}$, they degenerate to

$$\mathbf{q}'(t) = (\mathbf{A} + \mathbf{BK})\mathbf{q}(t) + \mathbf{B}u_c(t), \quad (4.148)$$

$$\mathbf{y}(t) = \mathbf{q}(t). \quad (4.149)$$

An advantage of this model is in its ability to be both stable and controllable by $u_c(t)$, if the feedback matrix \mathbf{K} is chosen appropriately.

Example 4.26. A system (Fig. 4.26b) is complicated for the control signal $u_c(t) = [u_c(t)]$ to be as in Fig. 4.28. The system is represented with the following ODE

$$v_R''(t) + 2\delta(1 - K)v_R'(t) + \omega_0^2 v_R = 2\delta u_c'(t), \quad (4.150)$$

having a forced solution affected by the control signal $u_c(t)$. The coefficients of the model (4.90) are $a_0 = \omega_0^2$, $a_1 = 2\delta(1 - K)$, $a_2 = 1$, $b_0 = b_2 = 0$, and $b_1 = 2\delta$.

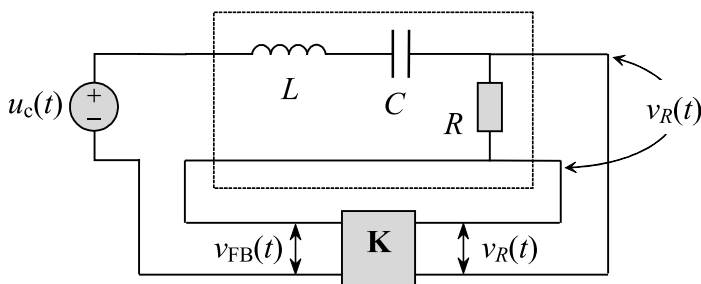


Fig. 4.28. Closed loop control LTI system of the second order.

Following Example 4.25, the second direct form of the system equations (4.146) and (4.147) becomes, after the transformations,

$$\begin{bmatrix} q_1'(t) \\ q_2'(t) \end{bmatrix} = \begin{bmatrix} 0 & 1 \\ -\omega_0^2 & -2\delta(1 - K) \end{bmatrix} \begin{bmatrix} q_1(t) \\ q_2(t) \end{bmatrix} + \begin{bmatrix} 0 \\ 1 \end{bmatrix} u_c(t),$$

$$v_R = [0 \ 2\delta] \begin{bmatrix} q_1(t) \\ q_2(t) \end{bmatrix}.$$

Except for the control input $u_c(t)$, the system has the same structure as in Fig. 4.26b. Therefore, K affects its stability in the same manner. It follows

from the state equation that with $K < 1$ the system is always stable, by $K > 1$, it is unstable, and $K = 1$ corresponds to the intermediate case. \square

4.6.5 Properties of State Space Model

As an incredibly effective and powerful tool of system description and presentation, the state space model possesses many of useful properties of importance.

Convertibility of State Variables

Returning back to the introduction on state space modeling, we recall that any LTI system can be performed either in the first or second direct forms of block diagrams. Moreover, although less commonly, other forms of diagrams are used. Because all of these forms can represent the same system with, however, different state variables, there must exist some rule to transfer from one set of state variables to the other one. The relevant rule is known as *similarity transformation*.

Assume that we have a system described for the state vector $\mathbf{q}(t)$ by (4.125) and (4.126), respectively,

$$\mathbf{q}'(t) = \mathbf{A}\mathbf{q}(t) + \mathbf{B}\mathbf{x}(t),$$

$$\mathbf{y}(t) = \mathbf{C}\mathbf{q}(t) + \mathbf{D}\mathbf{x}(t).$$

Let us also suppose that some other state vector $\mathbf{v}(t)$ of the same dimensions $N \times 1$ is of interest. Since the system is LTI, then $\mathbf{v}(t)$ and $\mathbf{q}(t)$ are coupled linearly and we can formally write

$$v_1(t) = p_{11}q_1(t) + p_{12}q_2(t) + \cdots + p_{1N}q_N(t),$$

$$v_2(t) = p_{21}q_1(t) + p_{22}q_2(t) + \cdots + p_{2N}q_N(t),$$

$$\vdots$$

$$v_N(t) = p_{N1}q_1(t) + p_{N2}q_2(t) + \cdots + p_{NN}q_N(t)$$

that in compact matrix form is

$$\mathbf{v}(t) = \mathbf{P}\mathbf{q}(t). \quad (4.151)$$

The $N \times N$ matrix \mathbf{P} is said to be the *similarity transformation matrix* (or merely *transformation matrix*) with constant components p_{ij} , $i, j \in [1, N]$. From (4.151) we have $\mathbf{q}(t) = \mathbf{P}^{-1}\mathbf{v}(t)$ and then substituting to (4.125) and (4.126) gives

$$\mathbf{P}^{-1}\mathbf{v}'(t) = \mathbf{A}\mathbf{P}^{-1}\mathbf{v}(t) + \mathbf{B}\mathbf{x}(t),$$

$$\mathbf{y}(t) = \mathbf{C}\mathbf{P}^{-1}\mathbf{v}(t) + \mathbf{D}\mathbf{x}(t).$$

By multiplying the first of the above equations with \mathbf{P} we finally arrive at the state space model performed in terms of a new state vector $\mathbf{v}(t)$,

$$\mathbf{v}'(t) = \mathbf{A}_v \mathbf{v}(t) + \mathbf{B}_v \mathbf{x}(t), \quad (4.152)$$

$$\mathbf{y}(t) = \mathbf{C}_v \mathbf{v}(t) + \mathbf{D}_v \mathbf{x}(t), \quad (4.153)$$

where

$$\mathbf{A}_v = \mathbf{PAP}^{-1}, \quad \mathbf{B}_v = \mathbf{PB}, \quad \mathbf{C}_v = \mathbf{CP}^{-1}, \quad \mathbf{D}_v = \mathbf{D}. \quad (4.154)$$

A new system state $\mathbf{v}(t)$ can now be expressed via the original state $\mathbf{q}(t)$.

Example 4.27. Consider a SISO LTI system (Example 4.22) described in state space with the matrices

$$\mathbf{A} = \begin{bmatrix} 0 & 1 \\ -\omega_0^2 & -2\delta \end{bmatrix}, \quad \mathbf{B} = \begin{bmatrix} 0 \\ 1 \end{bmatrix}, \quad \mathbf{C} = [\omega_0^2 \ 0], \quad \mathbf{D} = [0].$$

We want to describe the system's state in terms of a new state vector $\mathbf{v}(t)$ coupled with $\mathbf{q}(t)$ by the matrix

$$\mathbf{P} = \begin{bmatrix} \omega_0^2 & 0 \\ 0 & \omega_0^2 \end{bmatrix}.$$

By (4.154), we define

$$\mathbf{A}_v = \begin{bmatrix} \omega_0^2 & 0 \\ 0 & \omega_0^2 \end{bmatrix} \begin{bmatrix} 0 & 1 \\ -\omega_0^2 & -2\delta \end{bmatrix} \begin{bmatrix} \omega_0^{-2} & 0 \\ 0 & \omega_0^{-2} \end{bmatrix} = \begin{bmatrix} 0 & 1 \\ -\omega_0^2 & -2\delta \end{bmatrix},$$

$$\mathbf{B}_v = \begin{bmatrix} \omega_0^2 & 0 \\ 0 & \omega_0^2 \end{bmatrix} \begin{bmatrix} 0 \\ 1 \end{bmatrix} = \begin{bmatrix} 0 \\ \omega_0^2 \end{bmatrix},$$

$$\mathbf{C}_v = [\omega_0^2 \ 0] \begin{bmatrix} \omega_0^{-2} & 0 \\ 0 & \omega_0^{-2} \end{bmatrix} = [1 \ 0].$$

Now observe that, by this transformation, we arrived at the system model given in Example 4.23. \square

Example 4.28. An LTI system is represented in the second form (Example 4.21) by

$$\mathbf{A}_1 = \begin{bmatrix} 0 & 1 & 0 \\ 0 & 0 & 1 \\ -3 & 1 & -2 \end{bmatrix}, \quad \mathbf{B}_1 = \begin{bmatrix} 0 \\ 0 \\ 1 \end{bmatrix}, \quad \mathbf{C}_1 = \left[-\frac{3}{2} \ \frac{3}{2} \ -\frac{5}{2}\right], \quad \mathbf{D}_1 = \left[\frac{3}{2}\right]$$

and in the first form (Example 4.20) by

$$\mathbf{A}_2 = \begin{bmatrix} -2 & 1 & 0 \\ 1 & 0 & 1 \\ -3 & 0 & 0 \end{bmatrix}, \quad \mathbf{B}_2 = \begin{bmatrix} -5/2 \\ 3/2 \\ -3/2 \end{bmatrix}, \quad \mathbf{C}_2 = [1 \ 0 \ 0], \quad \mathbf{D}_2 = \left[\frac{3}{2} \right].$$

We want to identify the similarity transformation matrix \mathbf{P} to translate the first form to the second one.

The second relation in (4.154) gives $\mathbf{B}_2 = \mathbf{P}\mathbf{B}_1$,

$$\begin{bmatrix} -5/2 \\ 3/2 \\ -3/2 \end{bmatrix} = \begin{bmatrix} p_{11} & p_{12} & p_{13} \\ p_{21} & p_{22} & p_{23} \\ p_{31} & p_{32} & p_{33} \end{bmatrix} \begin{bmatrix} 0 \\ 0 \\ 1 \end{bmatrix}$$

that determines $p_{13} = -5/2$, $p_{23} = 3/2$, and $p_{33} = -3/2$. The third relation in (4.154), being rewritten as $\mathbf{C}_2\mathbf{P} = \mathbf{C}_1$,

$$[1 \ 0 \ 0] \begin{bmatrix} p_{11} & p_{12} & p_{13} \\ p_{21} & p_{22} & p_{23} \\ p_{31} & p_{32} & p_{33} \end{bmatrix} = \left[-\frac{3}{2} \ \frac{3}{2} \ -\frac{5}{2} \right],$$

produces $p_{11} = -3/2$, $p_{12} = 3/2$, and $p_{13} = -5/2$. Finally, the first equality in (4.154) performed as $\mathbf{A}_2\mathbf{P} = \mathbf{P}\mathbf{A}_1$,

$$\begin{bmatrix} -2 & 1 & 0 \\ 1 & 0 & 1 \\ -3 & 0 & 0 \end{bmatrix} \begin{bmatrix} p_{11} & p_{12} & p_{13} \\ p_{21} & p_{22} & p_{23} \\ p_{31} & p_{32} & p_{33} \end{bmatrix} = \begin{bmatrix} p_{11} & p_{12} & p_{13} \\ p_{21} & p_{22} & p_{23} \\ p_{31} & p_{32} & p_{33} \end{bmatrix} \begin{bmatrix} 0 & 1 & 0 \\ 0 & 0 & 1 \\ -3 & 1 & -2 \end{bmatrix},$$

allows getting the rest of the components of \mathbf{P} , namely: $p_{21} = 9/2$, $p_{31} = -3$, $p_{22} = -1$, and $p_{32} = 9/2$.

The similarity transformation matrix is thus identified by

$$\mathbf{P} = \begin{bmatrix} -3/2 & 3/2 & -5/2 \\ 9/2 & -1 & 3/2 \\ -3 & 9/2 & -3/2 \end{bmatrix}$$

that allows us to transfer from the first direct form to the second one and vice versa. \square

State Controllability

The term *state controllability* is akin to “state control.” Even intuitively, it predefines the system’s state to be adjustable in some way. The term was introduced to the text by Kalman in 1960, along with the other term *state observability* that we shall consider in the sequel.

Most commonly, we call a system *controllable* if its state variables can directly be controlled by the input(s). Contrary, in the *uncontrollable* or *partly controllable* system, all or some state variables cannot be steered in finite time by the admissible input(s). Specifically for LTI systems represented in state space, the definition of controllability means the following:

Controllability: An LTI system described by (4.125) and (4.126) is *completely controllable* on the finite time interval $[t_0, t_1]$ if for any initial state $\mathbf{q}(t_0)$ there may be found an input $\mathbf{x}(t)$ to transfer the system to the other given state $\mathbf{q}(t_1)$. □

The test for controllability is as follows. The system (4.125) and (4.125) is state controllable if the matrix

$$\mathbf{S}_c = [\mathbf{B} \quad \mathbf{A}\mathbf{B} \quad \mathbf{A}^2\mathbf{B} \quad \dots \quad \mathbf{A}^{N-1}\mathbf{B}] \quad (4.155)$$

has full rank (Appendix B); that is,

$$\text{rank } \mathbf{S}_c = N.$$

Recall that rank is the number of linearly independent rows in a matrix. Herewith, the matrix \mathbf{S}_c has to be non singular if it is square, but is not necessarily square. Note that the N -order square matrix \mathbf{S}_c is not singular if and only if its rank is N , i.e. $\det \mathbf{S}_c \neq 0$.

Example 4.29. The system state equation (4.125) is given as

$$\mathbf{q}'(t) = \begin{bmatrix} -1 & 0 \\ 0 & -2 \end{bmatrix} \mathbf{q}(t) + \begin{bmatrix} 0 \\ 1 \end{bmatrix} \mathbf{x}(t)$$

and the matrix \mathbf{S}_c is thus determined to be

$$\mathbf{S}_c = \left(\begin{bmatrix} 0 \\ 1 \end{bmatrix} \quad \begin{bmatrix} -1 & 0 \\ 0 & -2 \end{bmatrix} \begin{bmatrix} 0 \\ 1 \end{bmatrix} \right) = \begin{bmatrix} 0 & 0 \\ 1 & -2 \end{bmatrix}.$$

It can be shown that the rank of \mathbf{S}_c is unity, $\text{rank } \mathbf{S}_c = 1 < N = 2$. Therefore, the matrix is singular and the system's state is not controllable.

Alternatively, we can rewrite the system state equation as follows:

$$q_1'(t) = -q_1(t),$$

$$q_2'(t) = -2q_2(t) + x(t).$$

A conclusion about uncontrollability follows directly from the fact that the first state $q_1'(t)$ is not affected by the input and hence is not controllable. □

Example 4.30. Given the system state equation

$$\mathbf{q}'(t) = \begin{bmatrix} -1 & 0 \\ 0 & -2 \end{bmatrix} \mathbf{q}(t) + \begin{bmatrix} 1 \\ 1 \end{bmatrix} \mathbf{x}(t),$$

for which the matrix \mathbf{S}_c is calculated by

$$\mathbf{S}_c = \left(\begin{bmatrix} 1 \\ 1 \end{bmatrix} \quad \begin{bmatrix} -1 & 0 \\ 0 & -2 \end{bmatrix} \begin{bmatrix} 1 \\ 1 \end{bmatrix} \right) = \begin{bmatrix} 1 & -1 \\ 1 & -2 \end{bmatrix}.$$

This system is controllable, because the determinant of \mathbf{S}_c is not zero, $\det \mathbf{S}_c = -1 \neq 0$, and the rank is full, $\text{rank } \mathbf{S}_c = 2$. Alternatively, we can write

$$\begin{aligned} q_1'(t) &= -q_1(t) + x(t), \\ q_2'(t) &= -2q_2(t) + x(t) \end{aligned}$$

and conclude that system is controllable, because both the first and second states are affected by the input. \square

The definition of state controllability allows figuring out what the system is that is absolutely controllable? It can be shown that such a system is represented with the following *controllable canonic form*

$$\mathbf{q}'(t) = \begin{bmatrix} -a_1 & -a_2 & \dots & -a_{N-1} & -a_N \\ 1 & 0 & \dots & 0 & 0 \\ 0 & 1 & & 0 & 0 \\ \vdots & \vdots & \ddots & & \vdots \\ 0 & 0 & & 1 & 0 \end{bmatrix} \mathbf{q}(t) + \begin{bmatrix} 1 \\ 0 \\ 0 \\ \vdots \\ 0 \end{bmatrix} u_c(t), \quad (4.156)$$

$$y(t) = [b_1 \ b_2 \ \dots \ b_{N-1} \ b_N] \mathbf{q}(t) + D u_c(t). \quad (4.157)$$

As it follows from an analysis of (4.156), the first component $q_1'(t)$ of a vector $\mathbf{q}'(t)$ comprises all of the state variables and is controlled by $u_c(t)$. The system's state is thus absolutely controllable.

State Observability

Observability is a measure for how well internal states of a system can be inferred by knowledge of its external outputs. Formally, a system is said to be observable if, for any possible sequence of state and control vectors, the current state can be determined in finite time using only the outputs. Specifically for LTI systems, this means the following:

Observability: An LTI system described by (4.125) and (4.126) is *completely observable* on the finite time interval $[t_0, t_1]$ if for any t_0 an initial state $\mathbf{q}(t_0)$ can be determined from observation of the output $\mathbf{y}(t)$ over this interval with the input $\mathbf{x}(t)$ known over the same interval.

\square

In other words, we can watch the outputs of an observable system and figure out what is going on inside the system with its states, even if it takes a very long time. For LTI systems, a commonly used test for observability is as follows: the system is observable if the observability matrix

$$\mathbf{S}_o = \begin{bmatrix} \mathbf{C} \\ \mathbf{CA} \\ \vdots \\ \mathbf{CA}^{N-1} \end{bmatrix} \quad (4.158)$$

has full rank; that is,

$$\text{rank } \mathbf{S}_o = N.$$

Example 4.31. An LTI system (Example 4.26) is represented with the system and observation matrices, respectively,

$$\mathbf{A} = \begin{bmatrix} 0 & 1 \\ -\omega_0^2 & -2\delta(1-K) \end{bmatrix}, \quad \mathbf{C} = [0 \ 2\delta].$$

The observability matrix (4.156) of a system is defined to be

$$\mathbf{S}_o = 2\delta \begin{bmatrix} 0 & 1 \\ -\omega_0^2 & -2\delta(1-K) \end{bmatrix}.$$

Because the determinant of \mathbf{S}_o is not zero, its rank is full, $\text{rank } \mathbf{S}_o = 2 = N$, and the system is thus completely observable. \square

In line with the controllable canonic form, an LTI system can also be represented with the *observable canonic form*

$$\mathbf{q}'(t) = \begin{bmatrix} -a_1 & 1 & 0 & \dots & 0 \\ -a_2 & 0 & 1 & & 0 \\ \vdots & \vdots & \ddots & & \\ -a_{N-1} & 0 & 0 & & 1 \\ -a_N & 0 & 0 & \dots & 0 \end{bmatrix} \mathbf{q}(t) + \begin{bmatrix} b_1 \\ b_2 \\ \vdots \\ b_{N-1} \\ b_N \end{bmatrix} u_c(t), \quad (4.159)$$

$$y(t) = [1 \ 0 \ 0 \ \dots \ 0] \mathbf{q}(t) + Du_c(t). \quad (4.160)$$

Examining (4.159), one deduces that the first system state is specified via the second state. In turn, the second state is performed via the third state, and so on. In other words, the first system state $q_1(t)$ and thereby the system output (4.160) are performed by all of the other system states and the system is thus observable.

Duality of State Observability and Controllability

Both the *state observability* and *state controllability* are mathematically dual that is supported by the fact that controllability of the system described with

$$\mathbf{q}'(t) = \mathbf{A}\mathbf{q}(t) + \mathbf{B}u_c(t)$$

is the same as observability for the system represented by

$$\mathbf{q}'(t) = \mathbf{A}^T \mathbf{q}(t),$$

$$\mathbf{y} = \mathbf{B}^T \mathbf{q}.$$

In view of that, the test for controllability can be substituted by the test for observability through the following transformations:

$$\mathbf{A} \rightarrow \mathbf{A}^T, \quad \mathbf{B} \rightarrow \mathbf{C}^T, \quad \mathbf{S}_c \rightarrow \mathbf{S}_o. \quad (4.161)$$

Example 4.32. An LTI system (Example 4.26) is given in the state space form, (4.147) and (4.148), with the matrices

$$\mathbf{A} = \begin{bmatrix} 0 & 1 \\ -\omega_0^2 & -2\delta(1-K) \end{bmatrix}, \quad \mathbf{B} = \begin{bmatrix} 0 \\ 1 \end{bmatrix}, \quad \mathbf{C} = [0 \ 2\delta].$$

By (4.155), its controllability matrix is defined to be

$$\mathbf{S}_c = \begin{bmatrix} 0 & 1 \\ 1 & -2\delta(1-K) \end{bmatrix}.$$

Following (4.161), one arrives at the same result, by substituting \mathbf{A} with

$$\mathbf{A}^T = \begin{bmatrix} 0 & -\omega_0^2 \\ 1 & -2\delta(1-K) \end{bmatrix},$$

\mathbf{C} with $\mathbf{B}^T = [0 \ 1]$, and then \mathbf{S}_o with \mathbf{S}_c . □

Kalman Decomposition

Any LTI system can be performed in state space with what is called the *Kalman decomposition*. Kalman proposed splitting a system into the four qualitatively different substructures regarding the system states: controllable and observable q_{co} , controllable and not observable $q_{c\bar{o}}$, non-controllable and observable $q_{\bar{c}o}$, and non-controllable and not observable $q_{\bar{c}\bar{o}}$. Presenting the state vector as $\mathbf{q} = [q_{co} \ q_{c\bar{o}} \ q_{\bar{c}o} \ q_{\bar{c}\bar{o}}]^T$ allows formally writing the system state and observation equations as follows

$$\mathbf{q}'(t) = \begin{bmatrix} \mathbf{A}_{11} & 0 & \mathbf{A}_{13} & 0 \\ \mathbf{A}_{21} & \mathbf{A}_{22} & \mathbf{A}_{23} & \mathbf{A}_{24} \\ 0 & 0 & \mathbf{A}_{33} & 0 \\ 0 & 0 & \mathbf{A}_{43} & \mathbf{A}_{44} \end{bmatrix} \mathbf{q}(t) + \begin{bmatrix} \mathbf{B}_1 \\ \mathbf{B}_2 \\ 0 \\ 0 \end{bmatrix} u_c(t), \quad (4.162)$$

$$\mathbf{y}(t) = [\mathbf{C}_1 \ 0 \ \mathbf{C}_2 \ 0] \mathbf{q}(t), \quad (4.163)$$

where all of the auxiliary matrices are specified by the matrices \mathbf{A} , \mathbf{B} , and \mathbf{C} taken from the state and observation equations.

The block diagram simulating (4.162) and (4.163) is shown in Fig. 4.29 clearly illustrating all kinds of subsystems.

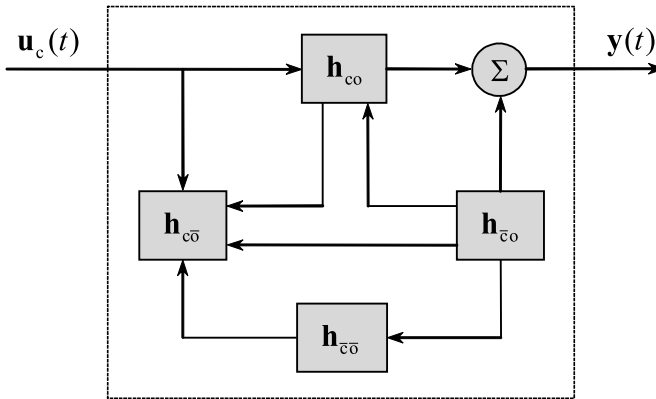


Fig. 4.29. Kalman decomposition of LTI systems.

As can be seen, a subsystem with the impulse response matrix \mathbf{h}_{co} has the input controlled by $\mathbf{u}_c(t)$ and the output connected to $\mathbf{y}(t)$. This block is thus both controllable and observable. Contrary, a subsystem $\mathbf{h}_{c\bar{o}}$ is disconnected from $\mathbf{u}_c(t)$ and $\mathbf{y}(t)$, therefore, is non-controllable and not observable. Connected to $\mathbf{u}_c(t)$ and disconnected from $\mathbf{y}(t)$, a subsystem $\mathbf{h}_{c\bar{o}}$ is controllable, but not observable. Finally, a subsystem $\mathbf{h}_{\bar{c}o}$ is observable, but non-controllable, because it is disconnected from $\mathbf{u}_c(t)$ and connected to $\mathbf{y}(t)$.

It would not be a big surprise that real systems do not always comprise all of the subsystems shown in Fig. 4.29. The seemingly obvious point is that the fully controllable and observable system would be represented by only the block \mathbf{h}_{co} .

4.6.6 Stability

As the Lyapunov theory suggests, stability of an LTI system can completely be ascertained by investigating the homogenous matrix state equation

$$\mathbf{q}' = \mathbf{A}\mathbf{q}, \tag{4.164}$$

where the $N \times N$ system matrix \mathbf{A} with constant components,

$$\mathbf{A} = \begin{bmatrix} a_{11} & a_{12} & \dots & a_{1N} \\ a_{21} & a_{22} & & a_{2N} \\ \vdots & \vdots & \ddots & \vdots \\ a_{N1} & a_{N2} & & a_{NN} \end{bmatrix}, \tag{4.165}$$

bears all the necessary information about behavior of a system. Ascertaining stability can be provided in different ways, by the following widely recognized criteria.

Lyapunov Criterion

The most widely used criterion of stability was proposed by Lyapunov. By the *Lyapunov criterion*, the sufficient condition for the trivial solution of (4.164) to be stable in the Lyapunov sense is that all of the roots of the characteristic equation

$$\det(a_{ij} - \lambda\delta_{ij}) = 0,$$

where $\delta_{ij} = \begin{cases} 1, & \text{if } i = j \\ 0, & \text{if } i \neq j \end{cases}$, $i, j \in [1, N]$, have negative real parts. If a square matrix \mathbf{A} possesses such a property, then it is called the *Hurwitz² matrix*.

The determinant can be rewritten in the form of

$$\begin{vmatrix} a_{11} - \lambda & a_{12} & \dots & a_{1N} \\ a_{21} & a_{22} - \lambda & & a_{2N} \\ \vdots & \vdots & \ddots & \vdots \\ a_{N1} & a_{N2} & & a_{NN} - \lambda \end{vmatrix} = 0, \quad (4.166)$$

allowing us to represent the characteristic equation by a polynomial

$$f(\lambda) = a_N\lambda^N + a_{N-1}\lambda^{N-1} + \dots + a_1\lambda + a_0 = 0, \quad a_0 > 0. \quad (4.167)$$

To apply the Lyapunov criterion, all of the roots of (4.167) must be found and investigated for negative real parts.

Example 4.33. An LTI system is represented in state space with the homogeneous matrix equation

$$\begin{bmatrix} q_1'(t) \\ q_2'(t) \end{bmatrix} = \begin{bmatrix} 0 & 1 \\ -\omega_0^2 & -2\delta(1-K) \end{bmatrix} \begin{bmatrix} q_1(t) \\ q_2(t) \end{bmatrix}.$$

The corresponding characteristic equation is written as

$$\begin{vmatrix} -\lambda & 1 \\ -\omega_0^2 & -2\delta(1-K) - \lambda \end{vmatrix} = 0,$$

$$\lambda^2 + 2\delta(1-K)\lambda + \omega_0^2 = 0,$$

having two roots,

$$\lambda_{1,2} = -\delta(1-K) \pm \sqrt{\delta^2(1-K)^2 - \omega_0^2}.$$

Because, typically, K is not large and $\omega_0 \gg 2\delta$, both roots are complex. For the real parts of the roots to be negative, we need to obtain $K < 1$. By the Lyapunov criterion, the system is thus stable only if $K < 1$. \square

² Adolf Hurwitz, German mathematician, 26 March 1859–18 November 1919.

Routh-Hurwitz Criterion

One can also realize if the characteristic equation (4.167) has roots with negative real parts, using the Routh³-Hurwitz criterion. In accordance with this criterion, all of the roots of (4.167) have negative real part if and only if all of the following determinants are positive-valued:

$$D_1 = a_1, \quad D_2 = \begin{vmatrix} a_1 & a_0 \\ a_3 & a_2 \end{vmatrix}, \quad D_3 = \begin{vmatrix} a_1 & a_0 & 0 \\ a_3 & a_2 & a_1 \\ a_5 & a_4 & a_3 \end{vmatrix}, \quad \dots, \\ D_N = \begin{vmatrix} a_1 & a_0 & 0 & 0 & \dots & 0 \\ a_3 & a_2 & a_1 & 0 & & 0 \\ \vdots & \vdots & \vdots & & \ddots & \vdots \\ a_{2N-1} & a_{2N-2} & a_{2N-3} & a_{2N-4} & & a_N \end{vmatrix}. \quad (4.168)$$

Example 4.34. Consider Example 4.33, in which the characteristic equation (4.167) is given with the coefficients $a_0 = \omega_0^2$, $a_1 = 2\delta(1 - K)$, and $a_2 = 1$. By the Routh-Hurwitz criterion (4.168), the relevant system would be stable if the determinants D_1 and D_2 are positive-valued.

Providing the necessary transformations, we arrive at

$$D_1 = a_1 = 2\delta(1 - K), \\ D_2 = \begin{vmatrix} 2\delta(1 - K) & \omega_0^2 \\ 0 & 1 \end{vmatrix} = 2\delta(1 - K)$$

and point out that D_1 and D_2 yield the same condition $2\delta(1 - K) > 0$ for the system to be stable. The latter is satisfied with $K < 1$ and thus the Lyapunov and Routh-Hurwitz criteria are consistent (Compare with Example 4.33). \square

Lyapunov Function Criterion

Because the Lyapunov functions method (Chapter 2) is applicable to any system, it could be used to ascertain stability of LTI systems. Before applying, it needs to introduce a concept of the *positive definite matrix* for LTI systems.

A matrix \mathbf{A} is said to be positive definite if the quadratic form $\mathbf{q}^T \mathbf{A} \mathbf{q}$ is positive definite. If so, then this quadratic form is the Lyapunov function

$$V(\mathbf{q}) = \mathbf{q}^T \mathbf{A} \mathbf{q} > 0 \quad (4.169)$$

that is positive for all $\mathbf{q} \neq 0$ and has a negative time-derivative, $V'(\mathbf{q}) < 0$. Using this definition, the following theorem is proved:

³ Edward John Routh, English mathematician, 20 January 1831-7 June 1907.

Theorem 4.1. *An LTI system (4.164) is asymptotically stable at zero if and only if for any given positive definite symmetric matrix \mathbf{Q} there exists a positive definite symmetric matrix \mathbf{P} such that the following equality is satisfied,*

$$\mathbf{A}^T \mathbf{P} + \mathbf{P} \mathbf{A} = -\mathbf{Q}. \quad (4.170)$$

□

To prove, let us think that \mathbf{P} and \mathbf{Q} are positive definite matrices. Then $V(\mathbf{q}) = \mathbf{q}^T \mathbf{P} \mathbf{q}$ is the Lyapunov function, because, first of all, it is positive-valued,

$$V(\mathbf{q}) = \mathbf{q}^T \mathbf{P} \mathbf{q} > 0, \quad (4.171)$$

and, second of all, by differentiating $V(\mathbf{q})$ and using (4.164) and (4.170), we have a negative-valued function

$$\begin{aligned} V'(\mathbf{q}) &= (\mathbf{q}^T)' \mathbf{P} \mathbf{q} + \mathbf{q}^T \mathbf{P} \mathbf{q}' = \mathbf{q}^T \mathbf{A}^T \mathbf{P} \mathbf{q} + \mathbf{q}^T \mathbf{P} \mathbf{A} \mathbf{q} \\ &= -\mathbf{q}^T \mathbf{Q} \mathbf{q} < 0. \end{aligned} \quad (4.172)$$

The proof is hence complete.

The reader has to remember that the goal is to define the matrix \mathbf{P} for the given matrix \mathbf{Q} and not vice versa. If one first define \mathbf{P} and then find \mathbf{Q} , then the conditions for the above-mentioned theorem are violated and an evaluation of the system stability may lead to wrong results.

Example 4.35. Consider two systems given with the system matrices and characteristic equations, respectively,

1. $\mathbf{A} = \begin{bmatrix} 0 & 1 \\ -2 & -1 \end{bmatrix}$, $\lambda^2 + \lambda + 2 = 0$
2. $\mathbf{A} = \begin{bmatrix} 1 & 0 \\ 2 & 1 \end{bmatrix}$, $\lambda^2 - 2\lambda - 1 = 0$

Because the coefficients of the first equation are both positive, the system is stable. The second characteristic equation has negative coefficients and the system is thus unstable.

To verify this fact by the second Lyapunov method, one can assign the positive definite symmetric matrix \mathbf{Q} and matrix \mathbf{P} as follows, respectively,

$$\mathbf{Q} = \begin{bmatrix} a & 0 \\ 0 & b \end{bmatrix}, \quad \text{and} \quad \mathbf{P} = \begin{bmatrix} p_{11} & p_{12} \\ p_{21} & p_{22} \end{bmatrix},$$

where $a > 0$, $b > 0$, and the components of \mathbf{P} are still unknown. Substituting \mathbf{Q} to (4.172), we realize that $-\mathbf{q}^T \mathbf{Q} \mathbf{q} = -(aq_1^2 + bq_2^2) < 0$ fits the Lyapunov function condition (4.172) for all q_1 and q_2 . The matrix \mathbf{Q} is thus positive definite.

We shall now determine \mathbf{P} separately for each of the systems to realize which matrix is symmetric and positive definite satisfying (4.171).

1. The first system. Substituting \mathbf{A} , \mathbf{Q} , and \mathbf{P} to (4.170) produces an equality

$$\begin{bmatrix} -2p_{21} - 2p_{12} & -2p_{22} + p_{11} - p_{12} \\ p_{11} - p_{21} - 2p_{22} & p_{12} - 2p_{22} + p_{21} \end{bmatrix} = - \begin{bmatrix} a & 0 \\ 0 & b \end{bmatrix},$$

which solution gives

$$\mathbf{P} = \begin{bmatrix} \frac{3a}{4} + b & \frac{a}{4} \\ \frac{a}{4} & \frac{1}{2}(\frac{a}{2} + b) \end{bmatrix}.$$

By this matrix, (4.171) yields the value

$$-\mathbf{q}^T \mathbf{P} \mathbf{q} = -\frac{a}{4}(q_1 + q_2)^2 - \left(\frac{a}{2} + b\right) q_1^2 - \frac{b}{2} q_2^2 < 0$$

that is negative for all q_1 and q_2 . The Lyapunov conditions are satisfied and the first system is thus stable.

2. Reasoning similarly regarding the second system, we have

$$\begin{bmatrix} p_{11} + p_{21} + p_{12} & p_{12} + p_{22} \\ p_{21} + p_{22} & p_{22} \end{bmatrix} = -\frac{1}{2} \begin{bmatrix} a & 0 \\ 0 & b \end{bmatrix}$$

that identifies the matrix \mathbf{P} to be

$$\mathbf{P} = \frac{1}{2} \begin{bmatrix} -a - 2b & b \\ b & -b \end{bmatrix}.$$

Now, by (4.171), we have

$$-\mathbf{q}^T \mathbf{P} \mathbf{q} = (a + b)q_1^2 + b(q_1 - q_2)^2 > 0$$

that is positive-valued for all q_1 and q_2 . The system is thus unstable. \square

4.7 Solution of State Space Equations

As any linear ODE of the first order, the state equation (4.125) associated with either SISO or MIMO LTI system can be solved for $\mathbf{q}(t)$. To arrive at the relevant solution, let us recall that a single ODE of the first order (4.53) is solved using the exponential integration factor. Similarly, the matrix ODE (4.125) can be solved using the integration factor $e^{-\mathbf{A}t}$.

To find a general solution of (4.125), we multiply both its sides with $e^{-\mathbf{A}t}$,

$$e^{-\mathbf{A}t} \mathbf{q}'(t) - e^{-\mathbf{A}t} \mathbf{A} \mathbf{q}(t) = e^{-\mathbf{A}t} \mathbf{B} \mathbf{x}(t).$$

The left-hand side is now the time derivative of the product and we go to the equation

$$[e^{-\mathbf{A}t} \mathbf{q}(t)]' = e^{-\mathbf{A}t} \mathbf{B} \mathbf{x}(t),$$

which integration from t_0 to t yields

$$e^{-\mathbf{A}t}\mathbf{q}(t) = e^{-\mathbf{A}t_0}\mathbf{q}(t_0) + \int_{t_0}^t e^{-\mathbf{A}\theta}\mathbf{B}\mathbf{x}(\theta)d\theta.$$

Multiplying the both sides of this equation with a reciprocal of the integration factor, $e^{\mathbf{A}t}$, results in the solution

$$\mathbf{q}(t) = e^{\mathbf{A}(t-t_0)}\mathbf{q}(t_0) + \int_{t_0}^t e^{\mathbf{A}(t-\theta)}\mathbf{B}\mathbf{x}(\theta)d\theta \quad (4.173)$$

that, by zero input $\mathbf{x}(t) = \mathbf{0}$, becomes homogenous,

$$\mathbf{q}(t) = e^{\mathbf{A}(t-t_0)}\mathbf{q}(t_0) = \mathbf{\Phi}(t, t_0)\mathbf{q}(t_0). \quad (4.174)$$

The matrix $\mathbf{\Phi}(t, t_0) = e^{\mathbf{A}(t-t_0)}$ in (4.174) predetermines a transition of the state vector \mathbf{q} from t_0 to t . Therefore, this matrix is termed the *state transition matrix*.

If we now substitute (4.173) to the observation equation (4.126), we arrive at a general solution of the state space equations

$$\begin{aligned} \mathbf{y}(t) &= \mathbf{C}e^{\mathbf{A}(t-t_0)}\mathbf{q}(t_0) + \mathbf{C} \int_{t_0}^t e^{\mathbf{A}(t-\theta)}\mathbf{B}\mathbf{x}(\theta)d\theta + \mathbf{D}\mathbf{x}(t), \\ &= \mathbf{C}\mathbf{\Phi}(t, t_0)\mathbf{q}(t_0) + \mathbf{C} \int_{t_0}^t \mathbf{\Phi}(t, \theta)\mathbf{B}\mathbf{x}(\theta)d\theta + \mathbf{D}\mathbf{x}(t). \end{aligned} \quad (4.175)$$

To compute (4.175), the state transition matrix $\mathbf{\Phi}(t, t_0)$ must somehow be evaluated in proper dimensions. As it follows, $\mathbf{\Phi}(t, t_0)$ is formed by a reciprocal of the integration factor, $\mathbf{\Phi}(t) = e^{\mathbf{A}t}$. The latter, owing to \mathbf{A} in its power, is called the *matrix exponential*, possessing several useful properties.

4.7.1 Matrix Exponential

Analogously to a reciprocal e^{at} of the integration factor e^{-at} for linear ODEs of the first order, the matrix exponential can be expanded to the Taylor series

$$\begin{aligned} \mathbf{\Phi}(t) &= e^{\mathbf{A}t} = \sum_{k=0}^{\infty} \frac{t^k}{k!} \mathbf{A}^k \\ &= \mathbf{I} + \mathbf{A}t + \frac{\mathbf{A}^2}{2!}t^2 + \dots + \frac{\mathbf{A}^k}{k!}t^k + \dots, \end{aligned} \quad (4.176)$$

where $\mathbf{I} = \mathbf{A}^0$ is the $N \times N$ identity matrix.

Example 4.36. The system matrix is specified with the components

$$\mathbf{A} = \begin{bmatrix} 0 & 1 & 2 \\ 0 & 0 & 3 \\ 0 & 0 & 0 \end{bmatrix}.$$

To expand the relevant matrix exponential $e^{\mathbf{A}t}$ to the Taylor series (4.176), first, define the product $\mathbf{A}^2 = \mathbf{A}\mathbf{A}$,

$$\mathbf{A}^2 = \begin{bmatrix} 0 & 1 & 2 \\ 0 & 0 & 3 \\ 0 & 0 & 0 \end{bmatrix} \begin{bmatrix} 0 & 1 & 2 \\ 0 & 0 & 3 \\ 0 & 0 & 0 \end{bmatrix} = \begin{bmatrix} 0 & 0 & 3 \\ 0 & 0 & 0 \\ 0 & 0 & 0 \end{bmatrix}.$$

Then the matrix $\mathbf{A}^3 = \mathbf{A}^2\mathbf{A}$ becomes nilpotent,

$$\mathbf{A}^3 = \begin{bmatrix} 0 & 0 & 3 \\ 0 & 0 & 0 \\ 0 & 0 & 0 \end{bmatrix} \begin{bmatrix} 0 & 1 & 2 \\ 0 & 0 & 3 \\ 0 & 0 & 0 \end{bmatrix} = \begin{bmatrix} 0 & 0 & 0 \\ 0 & 0 & 0 \\ 0 & 0 & 0 \end{bmatrix}$$

and all other higher order matrices \mathbf{A}^k , $k > 3$, are nilpotent as well. The matrix exponential $e^{\mathbf{A}t}$ is thus produced by the Taylor series to be

$$\begin{aligned} e^{\mathbf{A}t} &= \mathbf{I} + t\mathbf{A} + \frac{t^2}{2}\mathbf{A}^2 \\ &= \begin{bmatrix} 1 & 0 & 0 \\ 0 & 1 & 0 \\ 0 & 0 & 1 \end{bmatrix} + t \begin{bmatrix} 0 & 1 & 2 \\ 0 & 0 & 3 \\ 0 & 0 & 0 \end{bmatrix} + \frac{t^2}{2} \begin{bmatrix} 0 & 0 & 3 \\ 0 & 0 & 0 \\ 0 & 0 & 0 \end{bmatrix} \\ &= \begin{bmatrix} 1 & t & 2t + \frac{3t^2}{2} \\ 0 & 1 & 3t \\ 0 & 0 & 1 \end{bmatrix}, \end{aligned} \tag{4.177}$$

An important finding follows instantly. Disregarding the general infinite length of the Taylor series, the matrix exponential was produced by the finite Taylor series. The latter is obviously of high importance for state space modeling. \square

Based upon (4.176), several important properties of the matrix exponential $\Phi(t)$ can be distinguished:

- **Value at zero.** At $t = 0$, the matrix $\Phi(t)$ is identity,

$$\Phi(\mathbf{0}) = e^{\mathbf{0}} = \mathbf{I}. \tag{4.178}$$

\square

Example 4.37. As can be seen, by $t = 0$, the matrix exponential (4.177) becomes identity. \square

- **Time shifting.** An identity $e^{\mathbf{A}(t-\theta)} = e^{\mathbf{A}t}e^{-\mathbf{A}\theta}$ allows representing the state transition matrix $\Phi(t, \theta)$ by the matrix exponential as

$$\Phi(t - \theta) = \Phi(t, \theta) = \Phi(t)\Phi(-\theta). \tag{4.179}$$

□

- **Inverse matrix exponential.** Since $e^{\mathbf{A}t}e^{-\mathbf{A}t} = \mathbf{I}$ and hence $e^{-\mathbf{A}t} = (e^{\mathbf{A}t})^{-1}$, then

$$\Phi^{-1}(t) = \Phi(-t). \tag{4.180}$$

□

- **Differentiation.** Differentiating $\Phi(t)$ gives

$$\frac{d}{dt}e^{\mathbf{A}t} = \mathbf{A}e^{\mathbf{A}t} = e^{\mathbf{A}t}\mathbf{A} \tag{4.181}$$

that is supported by the manipulations:

$$\begin{aligned} \frac{d}{dt}e^{\mathbf{A}t} &= \mathbf{0} + \mathbf{A} + 2t\frac{\mathbf{A}^2}{2!} + \dots + kt^{k-1}\frac{\mathbf{A}^k}{k!} + \dots \\ &= \mathbf{A} \left(\mathbf{I} + \mathbf{A}t + \frac{\mathbf{A}^2}{2!} + \dots \right) = \left(\mathbf{I} + \mathbf{A}t + \frac{\mathbf{A}^2}{2!} + \dots \right) \mathbf{A}. \end{aligned}$$

□

Cayley-Hamilton Theorem

One more important property of the matrix exponential is established by the Cayley⁴-Hamilton theorem.

Generally, the Taylor series (4.176) evaluates $\Phi(t)$ via the infinite series length. The Cayley-Hamilton theorem states, in its applications to the LTI systems theory, that $\Phi(t)$ can be evaluated in the finite series of length N ,

$$\Phi(t) = e^{\mathbf{A}t} = \alpha_0\mathbf{I} + \alpha_1\mathbf{A} + \dots + \alpha_{N-1}\mathbf{A}^{N-1}, \tag{4.182}$$

if to specify properly the constant coefficients $\alpha_0, \alpha_1, \dots, \alpha_{N-1}$.

For the known eigenvalues $\lambda_k, k \in [1, N]$, of \mathbf{A} , the coefficients of (4.182) are defined by the linear equations system

$$\begin{aligned} \alpha_0 + \alpha_1\lambda_0 + \dots + \alpha_{N-1}\lambda_0^{N-1} &= e^{\lambda_0t}, \\ \alpha_0 + \alpha_1\lambda_1 + \dots + \alpha_{N-1}\lambda_1^{N-1} &= e^{\lambda_1t}, \\ &\vdots \\ \alpha_0 + \alpha_1\lambda_{N-1} + \dots + \alpha_{N-1}\lambda_{N-1}^{N-1} &= e^{\lambda_{N-1}t} \end{aligned} \tag{4.183}$$

⁴ Arthur Cayley, English mathematician, 16 August 1821-26 January 1895.

and it follows that the coefficients are commonly time-varying.

Because both (4.176) and (4.181) expand $\Phi(t)$ to the series regarding the same matrix \mathbf{A} , the coefficients $\alpha_0, \alpha_1, \dots, \alpha_{N-1}$ can be determined via the Taylor series (4.176), if to set all of the matrices \mathbf{A}^k for $k > N - 1$ to be nilpotent (having zero components).

Example 4.38. Consider the system matrix \mathbf{A} given in Example 4.36. The relevant characteristic equation is

$$\begin{vmatrix} -\lambda & 1 & 2 \\ 0 & -\lambda & 3 \\ 0 & 0 & -\lambda \end{vmatrix} = -\lambda^3 = 0,$$

having the only one zero root $\lambda = 0$. The coefficients of a polynomial (4.182) can be determined if to consider the first equation in (4.183) and supply two its time derivatives:

$$\begin{aligned} \alpha_0 + \alpha_1 \lambda + \alpha_2 \lambda^2 &= e^{\lambda t}, \\ \alpha_1 + 2\alpha_2 \lambda &= t e^{\lambda t}, \\ 2\alpha_2 &= t^2 e^{\lambda t}. \end{aligned}$$

From these equations, we have $\alpha_0 = 1$, $\alpha_1 = t$, and $\alpha_2 = t^2/2$. The matrix exponential is thus evaluated by

$$e^{\mathbf{A}t} = \mathbf{I} + t\mathbf{A} + \frac{t^2}{2}\mathbf{A}^2$$

that coincides with the Taylor expansion (4.177). \square

So, we now know how to evaluate the matrix exponential. One thus is able to find a closed form solution of a particular system state space model in the form of (4.175).

Example 4.39. An LTI system considered in Example 4.22 is assumed to have an infinite quality factor. Therefore, the bandwidth is zero, $2\delta = 0$, and the matrices of the state space model,

$$\begin{aligned} \mathbf{q}'(t) &= \mathbf{A}\mathbf{q}(t) + \mathbf{B}x(t), \\ y(t) &= \mathbf{C}\mathbf{q}(t), \end{aligned}$$

are specified by

$$\mathbf{A} = \begin{bmatrix} 0 & 1 \\ -\omega_0^2 & 0 \end{bmatrix}, \quad \mathbf{B} = \begin{bmatrix} 0 \\ 1 \end{bmatrix}, \quad \mathbf{C} = [\omega_0^2 \ 0].$$

By $t_0 = 0$, a solution (4.175) of the state space equations becomes

$$y(t) = \mathbf{C}e^{\mathbf{A}t}\mathbf{q}(0) + \mathbf{C} \int_0^t e^{\mathbf{A}(t-\theta)}\mathbf{B}x(\theta)d\theta \quad (4.184)$$

and the characteristic equation, for the given \mathbf{A} , is written as

$$\begin{vmatrix} -\lambda & 1 \\ -\omega_0^2 & -\lambda \end{vmatrix} = \lambda^2 + \omega_0^2 = 0$$

producing two roots,

$$\lambda_1 = j\omega_0, \quad \lambda_2 = -j\omega_0.$$

By the Carley-Hamilton theorem, the matrix exponential (4.182) is performed with

$$e^{\mathbf{A}t} = \alpha_0\mathbf{I} + \alpha_1\mathbf{A}$$

that, by (4.183), results in

$$\alpha_0 + \alpha_1j\omega_0 = e^{j\omega_0t},$$

$$\alpha_0 - \alpha_1j\omega_0 = e^{-j\omega_0t}.$$

The coefficients are thus determined to be

$$\alpha_0 = \cos \omega_0t,$$

$$\alpha_1 = \frac{1}{\omega_0} \sin \omega_0t$$

and we specify the matrix exponential with

$$\begin{aligned} e^{\mathbf{A}t} &= \mathbf{I} \cos \omega_0t + \mathbf{A} \frac{1}{\omega_0} \sin \omega_0t \\ &= \begin{bmatrix} \cos \omega_0t & \frac{1}{\omega_0} \sin \omega_0t \\ -\omega_0 \sin \omega_0t & \cos \omega_0t \end{bmatrix}. \end{aligned}$$

The solution (4.184) can now be written as

$$\begin{aligned} y(t) &= [\omega_0^2 \ 0] \begin{bmatrix} \cos \omega_0t & \frac{1}{\omega_0} \sin \omega_0t \\ -\omega_0 \sin \omega_0t & \cos \omega_0t \end{bmatrix} \begin{bmatrix} q_1(0) \\ q_2(0) \end{bmatrix} \\ &+ [\omega_0^2 \ 0] \int_0^t \begin{bmatrix} \cos \omega_0(t-\theta) & \frac{1}{\omega_0} \sin \omega_0(t-\theta) \\ -\omega_0 \sin \omega_0(t-\theta) & \cos \omega_0(t-\theta) \end{bmatrix} \begin{bmatrix} 0 \\ 1 \end{bmatrix} x(\theta)d\theta \\ &= q_1(0)\omega_0^2 \cos \omega_0t + q_2(0)\omega_0 \sin \omega_0t + \omega_0 \int_0^t x(\theta) \sin \omega_0(t-\theta)d\theta \quad (4.185) \end{aligned}$$

comprising a homogenous solution (two first terms) and a forced solution (the rest integral term). □

4.7.2 System Impulse Response in State Space

An inherent property of the general solution (4.175) is that it predefines the system impulse response by the unit impulse in the input.

For SISO LTI systems, (4.175) can be rewritten as

$$y(t) = \mathbf{C}e^{\mathbf{A}(t-t_0)}\mathbf{q}(t_0) + \mathbf{C} \int_{t_0}^t e^{\mathbf{A}(t-\theta)}\mathbf{B}x(\theta)d\theta. \quad (4.186)$$

Aimed at determining the system impulse response, we allow $t_0 = 0$, assume zero initial condition, $\mathbf{q}(0) = 0$, and set $x(t) = \delta(t)$. Instantly, by the sifting property of the delta function, the impulse response function appears to be

$$\begin{aligned} h(t) &= \mathbf{C} \int_0^t e^{\mathbf{A}(t-\theta)}\mathbf{B}\delta(\theta)d\theta \\ &= \mathbf{C}e^{\mathbf{A}t}\mathbf{B}. \end{aligned} \quad (4.187)$$

Example 4.40. An LTI system is given with the equation (4.185). By $q_1(0) = q_2(0) = 0$ and $x(t) = \delta(t)$, we go to the system impulse response

$$h(t) = \omega_0 \int_0^t \delta(\theta) \sin \omega_0 \theta d\theta = \omega_0 \sin \omega_0 t.$$

The same result appears, for known matrices (Example 4.39), if we employ the general solution (4.187):

$$\begin{aligned} h(t) &= [\omega_0^2 \ 0] \begin{bmatrix} \cos \omega_0 \theta & \frac{1}{\omega_0} \sin \omega_0 \theta \\ -\omega_0 \sin \omega_0 \theta & \cos \omega_0 \theta \end{bmatrix} \begin{bmatrix} 0 \\ 1 \end{bmatrix} \\ &= \omega_0 \sin \omega_0 t. \end{aligned}$$

Let us notice that the above derived impulse response function corresponds to conservative systems without dissipation of energy. Therefore, the function oscillates with time without attenuation that is illustrated in Fig. 4.10b for $\alpha = 0$. \square

4.7.3 System Step Response in State Space

In line with the impulse response, the system step response is readily produced by (4.186) if to set to zero the initial condition, $\mathbf{q}(0) = 0$, suppose $t_0 = 0$, and apply the unit step in the input. For SISO LTI systems, this leads to

$$g(t) = \mathbf{C} \int_0^t e^{\mathbf{A}(t-\theta)}\mathbf{B}u(\theta)d\theta = \mathbf{C} \int_0^t e^{\mathbf{A}(t-\theta)}\mathbf{B}d\theta. \quad (4.188)$$

Example 4.41. The step response function of an LTI system (Example 4.39) is calculated via its impulse response (Example 4.40) to be

$$g(t) = \int_0^t h(\tau) d\tau = \omega_0 \int_0^t \sin \omega_0 \tau d\tau = 1 - \cos \omega_0 t.$$

Equivalently, following (4.188), we arrive at the same result by

$$\begin{aligned} g(t) &= [\omega_0^2 \ 0] \int_0^t \begin{bmatrix} \cos \omega_0 \theta & \frac{1}{\omega_0} \sin \omega_0 \theta \\ -\omega_0 \sin \omega_0 \theta & \cos \omega_0 \theta \end{bmatrix} \begin{bmatrix} 0 \\ 1 \end{bmatrix} d\theta \\ &= [\omega_0^2 \ 0] \int_0^t \begin{bmatrix} \frac{1}{\omega_0} \sin \omega_0 \theta \\ \cos \omega_0 \theta \end{bmatrix} d\theta = \omega_0 \int_0^t \sin \omega_0 \theta d\theta \\ &= 1 - \cos \omega_0 t. \end{aligned}$$

Now note that the step response derived is illustrated in Fig. 4.11b, by $\alpha = 0$. \square

We finished with presentation and description of LTI systems in the time domain. As it follows from what was observed, such systems obey many useful properties and turn out to be particularly simpler than any other kind of systems. Their inherent properties are linearity (homogeneity and distributivity) and that they do not depend on when they occur (time-invariance). Especially important and often critical for applications is that the methods of LTI systems description (convolution, ODEs, and state space) are consistent, interchangeable, and produce equal results in rather different ways and forms, although translatable into each other. This splendid feature saves in the frequency (transform) domain.

4.8 Summary

As the most useful idealizations of real systems, LTI models are used widely to investigate a great deal of practical and applied problems. The following basic canons characterize LTI systems in the time domain:

- Any system that provides linear transformations with a time-invariant operator is the LTI system.
- Any linear system is time-invariant, if all of its coefficients are time-constant.
- The response of a system at time t to the unit impulse at time t is the LTI system impulse response.

- The response of a system at time t to the unit step at time t is the LTI system step response.
- Convolution couples the input and output of an LTI system via the impulse response by the integral equation; convolution in its standard form is not valid for time-variant and nonlinear systems.
- Convolution becomes cross-correlation by a sign changed in a variable of the impulse response.
- Any LTI system can be described by the N -order ODE; a solution of the ODE is consistent with that provided by convolution.
- The homogenous solution of the LTI system ODE is the LTI system response to the nonzero initial conditions with zero input.
- The forced solution of the LTI system ODE is the LTI system response to the input with zero initial conditions.
- Any LTI system can be simulated with the first and second direct (canonic) forms of block diagrams.
- The state variable is associated with time derivative and is commonly interpreted as the system “memory element”.
- Any LTI system can be represented in state space via the ODE or block diagram if the state variables are properly assigned.
- The state space representation of any LTI system is provided in matrix form by the state and observation equations (state space equations).
- The matrix form of state space equations is universal for both SISO and MIMO LTI systems.
- In state space, all of the properties of LTI systems are fully accounted by the time-invariant matrices (system, observation, input, and output).
- A general solution of the state space equations is universal for all kinds of LTI systems.

4.9 Problems

4.1. Observing different electronic systems (Chapter 1), find applications for LTI modeling in their structures.

4.2. An electronic system comprises the following blocks: Gaining amplifier, Reference oscillator, Phase modulator, Amplitude detector. Examine operation principles of these subsystems and realize which one can be analyzed by LTI modeling and which cannot.

4.3 (Convolution). A noncausal input signal has a waveform $x(t) = e^{-bt}$, $b > 0$. Using the convolution, define the output for the impulse response given:

1. $h(t) = e^{-at}u(t)$, $a > 0$
2. $h(t) = Au(t) - Au(t - \tau)$
3. $h(t) = Au(t) - 2Au(t - \tau) + Au(t - 2\tau)$
4. $h(t) = a\left(1 - \frac{t}{\tau}\right)[u(t) - u(t - \tau)]$
5. $h(t) = a\frac{t}{\tau}[u(t) - u(t - \tau)]$

4.4. Using the convolution, define the system output for the impulse response $h(t)$ and input $x(t)$ given, respectively,

- | | |
|--|--|
| 1. $h(t) = u(t)$ | $x(t) = te^{-2t}u(t)$ |
| 2. $h(t) = u(t)$ | $x(t) = t^2e^{-t}u(t)$ |
| 3. $h(t) = e^{-t}u(t)$ | $x(t) = u(t)$ |
| 4. $h(t) = u(t) - e^{-2t}u(t - \tau)$ | $x(t) = e^{-2t}u(t)$ |
| 5. $h(t) = a\frac{t}{\tau}[u(t) - u(t - \tau)]$ | $x(t) = a[u(t) - u(t - \tau)]$ |
| 6. $h(t) = a\left(1 - \frac{t}{\tau}\right)[u(t) - u(t - \tau)]$ | $x(t) = a\frac{t}{\tau}[u(t) - u(t - \tau)]$ |

4.5. An LTI system is characterized with the impulse response $h(t) = A[u(t) - u(t - \tau)]$. Using the convolution, define the system response to the causal and noncausal cosine inputs, $x(t) = u(t)\cos t$ and $x(t) = \cos t$, respectively. Give graphical interpretations.

4.6. Solve Problem 4.5 for the impulse response $h(t) = e^{-at}u(t)$, $a > 0$, and sinusoid inputs, $x(t) = u(t)\sin t$ and $x(t) = \sin t$.

4.7. Using the convolution, define the system step response for the impulse responses given in Problems 4.3 and 4.4. Verify the results by (4.11).

4.8 (Properties of LTI systems). The system impulse response and input are given by, respectively,

- | | |
|--|--|
| 1. $h(t) = e^{- t }$ | $x(t) = te^{-2t}u(t)$ |
| 2. $h(t) = 2e^{-4 t-\tau }$ | $x(t) = t^2e^{- t }$ |
| 3. $h(t) = 2e^{-4 t-\tau }\delta(t)$ | $x(t) = e^{- t }\cos\omega_0t$ |
| 4. $h(t) = te^{-t}u(t)$ | $x(t) = \cos\omega_0t$ |
| 5. $h(t) = u(t) - e^{-2t}$ | $x(t) = e^{-2t}u(t)$ |
| 6. $h(t) = a\frac{ t-\tau }{\tau}\delta(t)$ | $x(t) = a[u(t) - u(t - \tau)]$ |
| 7. $h(t) = a\left(1 - \frac{t}{\tau}\right)[u(t) - u(t - \tau)]$ | $x(t) = a\frac{ \sin\omega_0t }{\tau}$ |

Ascertain causality of each of these systems and signals and write properly the convolution integral.

4.9. Realize which system given in Problem 4.8 is stationarity and/or memory and which is not. Verify your deduction.

4.10. An LTI system characterized with the impulse response $h(t) = ae^{-bt}u(t)$ produces the output $y(t) = a^2(1/b + t)e^{-bt}u(t)$. Using the convolution, solve the inverse problem to define the input $x(t)$.

4.11. The input and output of an LTI system are represented with the spectral densities, respectively,

$$X(j\omega) = \begin{cases} A & \text{if } -\omega_c/2 \leq \omega \leq \omega_c/2 \\ 0 & \text{otherwise} \end{cases},$$

$$Y(j\omega) = \begin{cases} B & \text{if } -\omega_c/2 \leq \omega \leq \omega_c/2 \\ 0 & \text{otherwise} \end{cases},$$

where A and B are constant. Identify a system by the impulse response.

4.12 (LTI systems of the first order). Verify that an LTI system of the first order (Fig. 4.30) is described by the ODE

$$v_L'(t) + \frac{R_1}{L}v_L(t) = \frac{R_2}{R_1 + R_2}v'(t).$$

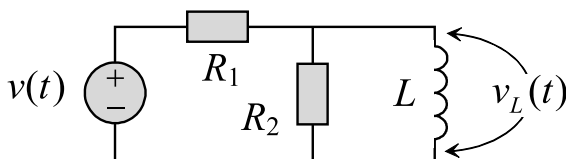


Fig. 4.30. An LTI system of the first order.

Write the general solution for an arbitrary initial condition. Investigate the homogenous solution. Define the system impulse and step responses.

4.13. Write the ODE and solve Problem 4.12 for an LTI system shown in Fig. 4.31.

4.14 (LTI systems of the second order). Verify that an LTI system given in Fig. 4.32 is described with the ODE

$$v_L''(t) + \frac{R_1}{L}v_L'(t) + \frac{1}{LC}v_L(t) = \frac{R_2}{R_1 + R_2}v''(t).$$

Write the general solution for arbitrary initial conditions. Investigate the homogenous solution. Define the system impulse and step responses. Investigate the responses numerically for $R_1 = R_2 = 100 \text{ Ohm}$, $L = 5 \times 10^{-3} \text{ H}$, and $C = 2 \times 10^{-6} \text{ F}$.

4.15. Write the ODE of an LTI system shown in Fig. 4.33 and solve Problem 4.14 for this system.

4.16 (Block diagrams). Verify that an LTI system described with the ODE (Problem 4.14) can be simulated by block diagrams in the first and second direct forms as shown in Fig. 4.34a and Fig. 4.34b.

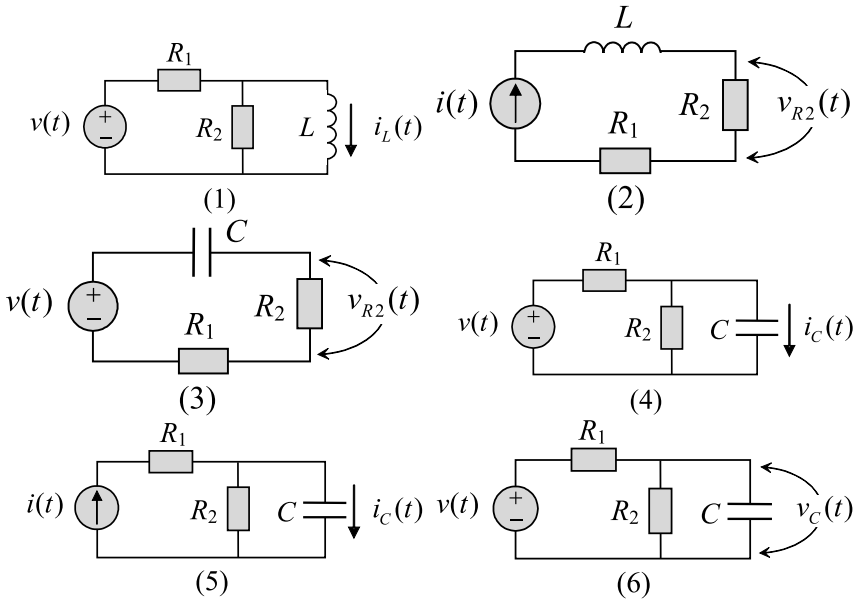


Fig. 4.31. LTI systems of the first order.

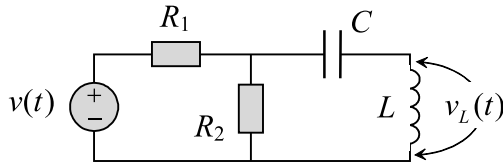


Fig. 4.32. An LTI system of the second order.

4.17. Write the ODE of an LTI systems represented in Fig. 4.35 with the block diagrams of the first direct form.

4.18. An LTI system is described with the following ODE

1. $ay'' + by' + cy = dx'' - ex'$
2. $3 \int y dt + 2y'' - 4y' + y = 3x'' - x$
3. $2y''' - 3y = 2x'' - x$
4. $y'' + \int y dt - 2y' = \sum_{m=0}^1 b_m \frac{d^m x}{dt^m}$, $b_0 = 2$, $b_1 = 1$
5. $x = \int y'' dt$
6. $2 \frac{d^2 x}{dt^2} + 4x + y = 2 \frac{d^3 y}{dt^3} + 4 \frac{dx}{dt}$
7. $4(y'' - x) = 3(y' - x'')$
8. $x' + \int x dt - 2y' = \int y dt - 2y''$
9. $a_2 y'' - b_0 x - a_1 y' - b_1 x' = 0$

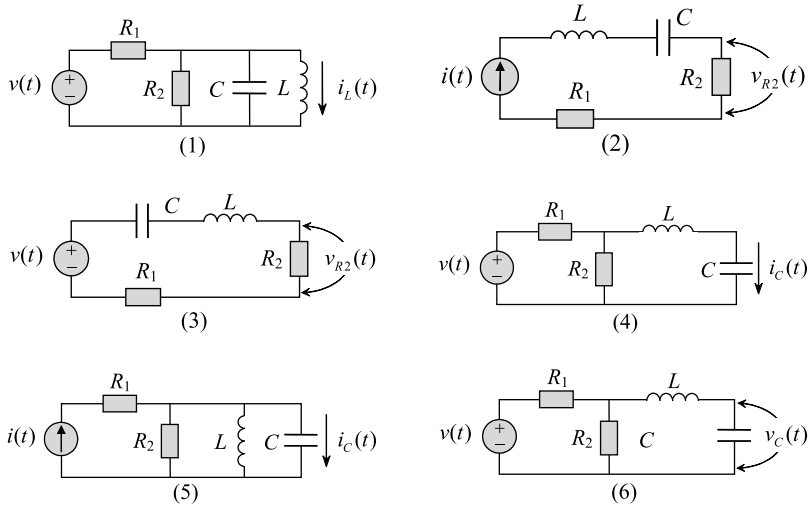


Fig. 4.33. LTI systems of the second order.

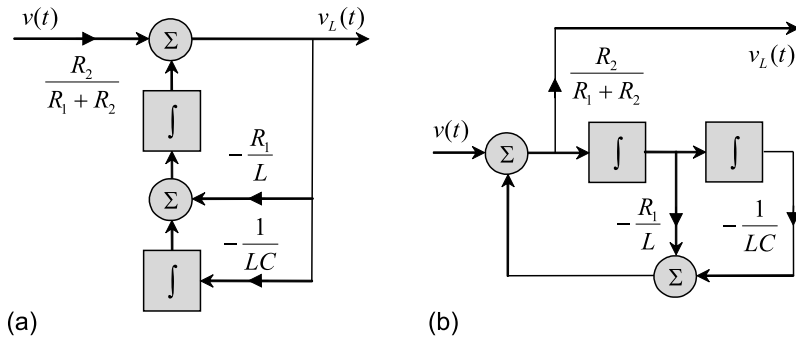


Fig. 4.34. Block diagrams of an LTI system: (a) the first direct form and (b) the second direct form.

10. $2y + \int x dt - 2y' = \int \int y dt dt - 2y$
11. $3y'' + 2 \int y dt = 2x$
12. $\sum_{n=0}^1 a_n \frac{d^n y}{dt^n} = x + \int x dt - 2y', a_0 = 2, a_1 = 1$
13. $\sum_{n=0}^1 a_n \frac{d^n y}{dt^n} + 2 \int x dt = \sum_{m=0}^1 b_m \frac{d^m x}{dt^m} + 2y + \int y dt,$
 $a_0 = 2, a_1 = 1, b_0 = 2, b_1 = 1$
14. $3y''' + \sum_{m=1}^2 b_m \frac{d^m x}{dt^m} - 4y' + y = 2x, b_2 = 2, b_1 = 1$

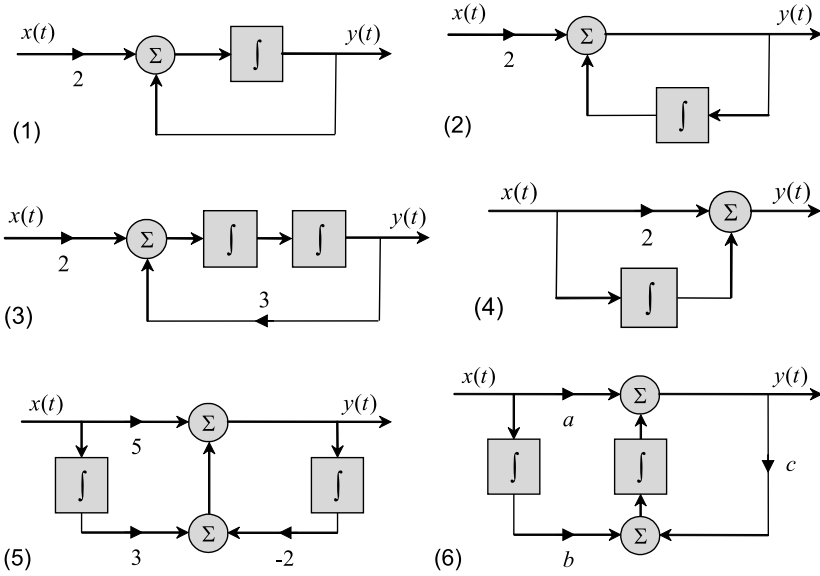


Fig. 4.35. LTI systems represented with the block diagrams of the first direct form.

15. $x + \int x dt - 2y' = \sum_{m=0}^1 b_m \frac{d^m x}{dt^m}$, $b_0 = 2$, $b_1 = 1$
 16. $2 \frac{d^2 y}{dt^2} + x + 2y = 2 \frac{d^3 y}{dt^3} + 4 \frac{dx}{dt}$

Represent a system with the diagrams of the first and second canonic forms.

4.19. An LTI system is simulated with the block diagram of the second direct form (Fig. 4.36). Using the diagram, write the ODE of the system.

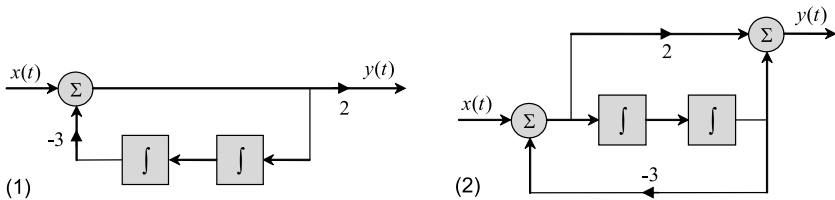


Fig. 4.36. LTI systems represented with the block diagrams of the second direct form.

4.20 (SISO systems in state space). A SISO LTI system of the first order is shown in Fig. 4.33. Represent this system in state space via the ODE defined in Problem 4.15.

4.21. A SISO LTI system is given with the block diagram shown in 4.35. Represent a system in state space via the ODE defined in Problem 4.17.

4.22 (MIMO systems in state space). A MIMO LTI system is given as in Fig. 4.37. Represent the system in state space.

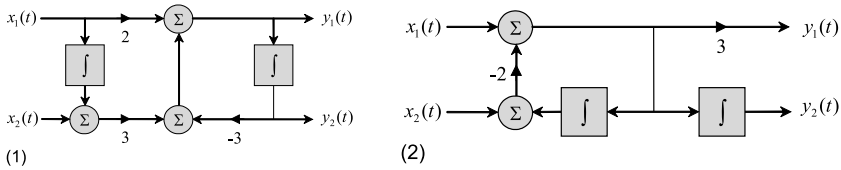


Fig. 4.37. MIMO LTI systems performed with block diagrams.

4.23 (LTI closed loop in state space). An LTI system is given with the block diagram as shown in Fig. 4.35. Assuming that the input is connected to the output with the function $x(t) = -2y(t)$, represent the system in state space.

4.24. The inputs and outputs of a MIMO feedback system (Fig. 4.37) are coupled with the functions $x_1(t) = -3y_2(t)$ and $x_2(t) = 0.2y_1(t)$. Represent a system in state space.

4.25 (LTI closed loop control in state space). Solve Problem 4.23 for $x(t) = -2y(t) + u_c(t)$, where $u_c(t)$ is a control signal.

4.26. Solve Problem 4.24 for $x_1(t) = -3y_2(t) + u_{c1}(t)$ and $x_2(t) = 0.2y_1(t) - u_{c2}(t)$.

4.27 (Convertibility of state variables). An LTI system is represented in Problem 4.19 in state space in the first direct form. Find a similarity matrix and transfer to the second direct form.

4.28 (Stability). An LTI system is given with one of the following system matrices

$$\mathbf{A}_1 = \begin{bmatrix} -1 & 2 & 1 \\ 1 & -1 & 1 \\ 0 & 0 & 1 \end{bmatrix}, \quad \mathbf{A}_2 = \begin{bmatrix} 1 & 2 & 1 \\ 0 & -1 & 1 \\ 1 & 2 & -1 \end{bmatrix}, \quad \mathbf{A}_3 = \begin{bmatrix} 1 & 2 & 3 \\ 0 & 1 & 2 \\ 0 & 0 & 1 \end{bmatrix}, \quad \mathbf{A}_4 = \begin{bmatrix} 1 & 1 & 1 \\ 0 & 1 & 1 \\ 0 & 0 & 1 \end{bmatrix}.$$

Using the Lyapunov criterion, realize which system is stable and which is not.

4.29 (Observability and controllability). An LTI system is given in state space with the following matrices

$$\mathbf{A} = \begin{bmatrix} -1 & 2 & 1 \\ 0 & -1 & 1 \\ 0 & 0 & 1 \end{bmatrix}, \quad \mathbf{B} = \begin{bmatrix} 1 \\ 0 \\ 1 \end{bmatrix}, \quad \mathbf{C} = [1 \ 1 \ 0].$$

Investigate a system for observability and controllability.

4.30 (Matrix exponential). Using the Cayley-Hamilton theorem, evaluate the matrix exponential of an LTI system given with the matrices (Problem 4.28).

4.31. An LTI system is represented in state space with the equations defined in Problem 4.20. Evaluate the matrix exponential for this system.

4.32 (Solution of state space equations). The system state space equations are defined in Problem 4.20. The relevant matrix exponential is evaluated in Problem 4.31. Using (4.171), write a general solution of the system state space equations.

4.33. Define and investigate numerically the impulse and step responses of an LTI system represented in Problem 4.32 with the general solution.

LTI Systems in the Frequency Domain (Transform Analysis)

5.1 Introduction

An alternative form of LTI systems presentation, although adequate and commonly used, is available in the *frequency domain*. Two approaches are basically employed. In *Fourier analysis* (the reader is encouraged to read Signals and follow Appendix C), an LTI system is described by the system *frequency response* that can be obtained as the Fourier transform of the system impulse response. In the more general *Laplace analysis*, an LTI system is represented by the system *transfer function* that turns out to be the Laplace transform of the system impulse response. All forms of an LTI system presentation in the time domain (convolution, ODE, and state space model) can be converted to the Fourier and Laplace transform domains equivalently, thus representing such a system explicitly and exhaustively.

5.2 Fourier Analysis

An efficient tool to study any LTI system in the frequency domain is based on the Fourier transform application. In the frequency domain often called Fourier transform domain, an LTI system is characterized with the *frequency response* that is the system complex function of frequency. The frequency response is characterized by the system *magnitude response*, often measured in dB, and *phase response*, typically measured in radians, both versus frequency.

To introduce the reader immediately to the essence of Fourier analysis, let us consider an SISO LTI system with known transforms of its input and output, respectively,

$$x(t) \xrightarrow{\mathcal{F}} X(j\omega), \quad y(t) \xrightarrow{\mathcal{F}} Y(j\omega).$$

Certainly, both spectral densities, $X(j\omega)$ and $Y(j\omega)$, must be coupled in the frequency domain by some system operator \mathcal{O} as

$$Y(j\omega) = \mathcal{O}X(j\omega). \quad (5.1)$$

Then what should be this operator?

To find an answer, we recall that, in the time domain, the output $y(t)$ is coupled with the input $x(t)$ via the system impulse response $h(t)$ by the convolution $h(t)*x(t)$. Then, the convolution property of the Fourier transform allows us to write

$$\mathcal{O}X(j\omega) = Y(j\omega) = \mathcal{F}y(t) = \mathcal{F}[h(t) * x(t)] = H(j\omega)X(j\omega). \quad (5.2)$$

Comparing the first and last expressions in (5.2), we deduce that the operator \mathcal{O} is a complex function $H(j\omega)$ that is identical to the Fourier transform of the system impulse response,

$$H(j\omega) \stackrel{\mathcal{F}}{\Leftrightarrow} h(t). \quad (5.3)$$

This means that the system impulse response is translated from the time domain to the frequency domain. Therefore, it would be absolutely logical to call $H(j\omega)$ the system frequency response. In the LTI system theory, Fourier analysis operates mostly with transforms of the system input, output, and impulse response.

Example 5.1. An LTI system is represented with the impulse response

$$h(t) = ae^{-at}u(t).$$

The Fourier transform produces the system frequency response (Appendix C)

$$\mathcal{F}h(t) = H(j\omega) = \frac{a}{a + j\omega}$$

and one can easily verify that the inverse Fourier transform applied to $H(j\omega)$ produces the impulse response $h(t)$. \square

5.2.1 Frequency Response

As one of the principle characteristics of LTI systems in the frequency domain, the frequency response is measured for the harmonic test signal, provided the definition:

Frequency response: The ratio of the LTI system response to the complex exponential signal $x(t) = e^{j\omega t}$ and $e^{j\omega t}$ is the system frequency response,

$$H(j\omega) = \frac{\text{Response to } e^{j\omega t}}{e^{j\omega t}}. \quad (5.4)$$

\square

Example 5.2. The ODE

$$y' + ay = bx$$

represents an LTI system of the first order, where a and b are time-constant. By (5.4), assuming $x(t) = e^{j\omega t}$ and $y(t) = H(j\omega)e^{j\omega t}$, we go to $j\omega H + aH = b$ that instantly yields the system frequency response

$$H(j\omega) = \frac{b}{a + j\omega}.$$

□

On the other hand, by (5.2) and (5.3), we have two other equivalent definitions valid for LTI systems, respectively:

Frequency response: The ratio of the Fourier transform (spectral density) $Y(j\omega)$ of the system output and the Fourier transform (spectral density) $X(j\omega)$ of the system input is the LTI system frequency response

$$H(j\omega) = \frac{Y(j\omega)}{X(j\omega)}. \quad (5.5)$$

□

Frequency response: The Fourier transform of the system impulse response $h(t)$ is the LTI system frequency response

$$H(j\omega) \stackrel{\mathcal{F}}{\Leftrightarrow} h(t).$$

□

Example 5.3. Consider an LTI system given with the ODE (Example 5.2). By applying the Fourier transform to both sides of this equation and using the transform properties (Appendix C), we go to

$$j\omega Y(j\omega) + aY(j\omega) = bX(j\omega)$$

that, by (5.5), leads to the same expression for the system frequency response as that found in Example 5.2. □

The above-considered Examples 5.2 and 5.3 neatly verify equivalency of both definitions of the system frequency response. Accordingly, by (5.5), the generalized structure of an LTI system in the frequency domain appears as shown in Fig. 5.1. It follows that if $X(j\omega)$ is unity with zero phase over all frequencies (input is the unit impulse), then the frequency response $H(j\omega)$ repeats the shape of the spectral density $Y(j\omega)$ of the output.

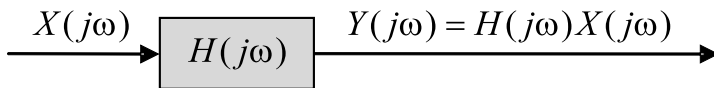


Fig. 5.1. Generalized structure of an LTI system in the frequency domain.

Magnitude and Phase Responses

By the above-given definitions, the frequency response is commonly a complex function. As such, it can be represented with

$$\begin{aligned} H(j\omega) &= \operatorname{Re}H(j\omega) + j\operatorname{Im}H(j\omega) \\ &= |H(j\omega)|e^{j\varphi_H(\omega)}, \end{aligned} \quad (5.6)$$

where $|H(j\omega)|$ is called the *magnitude response*, or *magnitude* of the frequency response, or *magnitude frequency response*, or sometimes *system gain*,

$$|H(j\omega)| = \sqrt{[\operatorname{Re}H(j\omega)]^2 + [\operatorname{Im}H(j\omega)]^2}. \quad (5.7)$$

In turn, the *phase response* $\varphi_H(\omega)$ is defined by

$$\varphi_H(\omega) = \arg H(j\omega) \quad \text{or} \quad \tan \varphi_H(\omega) = \frac{\operatorname{Im}H(j\omega)}{\operatorname{Re}H(j\omega)}. \quad (5.8)$$

In electronic systems and, in particular, in Fourier analysis of these systems we deal with signals possessing the property of 2π -periodicity (harmonic signals). Therefore, the phase response is assumed to range from $-\pi$ to π . The phase with such a property is called the *principle phase*, or *wrapped phase*, or very often *modulo 2π phase*, or just *phase mod 2π* . The phase response mod 2π can be calculated by

$$\varphi_H(\omega) = \begin{cases} \arctan(Q/I), & I \geq 0 \\ \arctan(Q/I) \pm \pi, & I < 0, \end{cases} \begin{cases} Q \geq 0 \\ Q < 0 \end{cases}, \quad (5.9)$$

where $I \equiv \operatorname{Re}H(j\omega)$ and $Q \equiv \operatorname{Im}H(j\omega)$.

We notice that the general definition of the phase response (5.8) allows restoring its *unwrapped* values existing in the infinite angular range if to account for a π -periodicity of the arctan-function.

If to substitute the spectral densities of the input and output as follows

$$X(j\omega) = |X(j\omega)|e^{-j\varphi_x(\omega)} \quad \text{and} \quad Y(j\omega) = |Y(j\omega)|e^{-j\varphi_y(\omega)},$$

where $|X(j\omega)|$ and $|Y(j\omega)|$ are the magnitude spectral densities of the input and output, respectively, and $\varphi_x(\omega)$ and $\varphi_y(\omega)$ are the phase spectral densities of the input and output, respectively, then the magnitude and phase frequency responses will attain the forms of, respectively,

$$|H(j\omega)| = \frac{|Y(j\omega)|}{|X(j\omega)|}, \quad (5.10)$$

$$\varphi_H(\omega) = \varphi_y(\omega) - \varphi_x(\omega). \quad (5.11)$$

By these relations, the magnitude response $|H(j\omega)|$ is determined as a ratio of the magnitude spectral densities of the output, $|Y(j\omega)|$, and input, $|X(j\omega)|$. In turn, the phase response is defined by the difference between the phase spectral densities of the output, $\varphi_y(\omega)$, and input, $\varphi_x(\omega)$.

Example 5.4. The spectral densities of the system input and output are performed with, respectively,

$$X(j\omega) = \frac{1}{3 + j\omega}, \quad Y(j\omega) = \frac{1}{2 + j\omega}.$$

By (5.5), the system frequency response attains the form of

$$H(j\omega) = \frac{3 + j\omega}{2 + j\omega} = 1 + \frac{1}{2 + j\omega}$$

causing the magnitude and phase responses to be, respectively,

$$|H(j\omega)| = \frac{\sqrt{(6 + \omega^2)^2 + \omega^2}}{4 + \omega^2},$$

$$\tan \varphi_H(\omega) = -\frac{\omega}{6 + \omega^2}.$$

By the inverse Fourier transform applied to $H(j\omega)$, the system impulse response is defined as

$$\mathcal{F}^{-1}H(j\omega) = h(t) = \delta(t) + e^{-2t}u(t).$$

It can easily be verified that the direct Fourier transform applied to $h(t)$ produces the above specified system frequency response. \square

As a product of the Fourier transform applied to the impulse response, the frequency response function possesses all of the Fourier transform properties featured to the spectral density of a signal. These properties are considered in detail in Signals and their review is postponed to Appendix C. The most critical characterizations of $H(j\omega)$ are the following:

- **Evenness (symmetry property):** $|H(j\omega)|$ is an even function; it is a symmetric function about zero. \square
- **Oddness (antisymmetry property):** $\varphi_H(\omega)$ is an odd function; it is an antisymmetric function about zero. \square

Cascade LTI Systems

Complex LTI systems are often performed by cascades of elementary (basic) systems. It can easily be shown that the frequency response of a cascade system is defined by the multiplication of the frequency responses of elementary blocks,

$$H(j\omega) = \prod_{i=1}^N H_i(j\omega) = \prod_{i=1}^N |H_i(j\omega)| e^{j\varphi_{H_i}(\omega)}, \quad (5.12)$$

therefore, the relevant magnitude and phase responses are specified by, respectively,

$$|H(j\omega)| = \prod_{i=1}^N |H_i(j\omega)|, \quad (5.13)$$

$$\varphi_H(\omega) = \sum_{i=1}^N \varphi_{H_i}(\omega). \quad (5.14)$$

Logarithmic Measures and Bode Plot

An important measure of the system performance in the frequency domain is the *logarithmic magnitude response* (in decibel units),

$$|H(j\omega)|_{\text{dB}} = 20 \log_{10} |H(j\omega)|. \quad (5.15)$$

If the frequency response occupies a wide frequency range of several decades, then the logarithmic measure of frequency, $\log(f)$, is also preferable. The display of $|H(j\omega)|_{\text{dB}}$ versus $\log(\omega)$ or $\log(f)$ is known as the *Bode¹ plot*. A benefit of Bode's plot is that 1) it allows evaluating the particular parts of the magnitude response in terms of the function rate in dB/decade and 2) the magnitude response may be bounded with lines that, in many cases, leads to useful generalizations.

Representation via Differential Equations

Many LTI systems are described by ODEs of the form

$$\sum_{n=0}^N a_n \frac{d^n}{dt^n} y(t) = \sum_{m=0}^M b_m \frac{d^m}{dt^m} x(t), \quad M \leq N. \quad (5.16)$$

Applying the Fourier transform to (5.16) and using the properties of linearity and differentiation, one can find out that

¹ Hendrik Wade Bode, American engineer, 24 December, 1905-21 June, 1982.

$$Y(\omega) \sum_{n=0}^N a_n(j\omega)^n = X(j\omega) \sum_{m=0}^M b_m(j\omega)^m.$$

By (5.5), the system frequency response would then be found to be

$$H(j\omega) = \frac{Y(j\omega)}{X(j\omega)} = \frac{\sum_{m=0}^M b_m(j\omega)^m}{\sum_{n=0}^N a_n(j\omega)^n}. \quad (5.17)$$

Such a fast transition from the ODE in the time domain to the algebraic form in the frequency domain often substantially simplifies an analysis. In fact, instead of solving the ODE (5.16) for the impulse response, one can consider the ratio (5.17) of two power polynomials with a complex variable $j\omega$, representing the frequency response. The procedure is universal, however, in engineering practice it often becomes easier defining the frequency response by the methods of electric circuits.

Example 5.5. An LTI system is described with the ODE

$$y'''(t) + 0.2y''(t) - y(t) = 0.2x''(t) - x(t).$$

By the Fourier transform applied to both sides of the equation, we have

$$(j\omega)^3 Y(j\omega) + 0.2(j\omega)^2 Y(j\omega) - Y(j\omega) = 0.2(j\omega)^2 X(j\omega) - X(j\omega),$$

$$(0.2\omega^2 + 1 + j\omega^3)Y(j\omega) = (0.2\omega^2 + 1)X(j\omega).$$

and, by (5.5), the system frequency response appears to be

$$H(j\omega) = \frac{0.2\omega^2 + 1}{0.2\omega^2 + 1 + j\omega^3} = \operatorname{Re}H(j\omega) + j\operatorname{Im}H(j\omega),$$

where

$$\operatorname{Re}H(j\omega) = \frac{(0.2\omega^2 + 1)^2}{(0.2\omega^2 + 1)^2 + \omega^6},$$

$$\operatorname{Im}H(j\omega) = -\frac{\omega^3(0.2\omega^2 + 1)}{(0.2\omega^2 + 1)^2 + \omega^6}.$$

The magnitude and phase responses can now be readily described with, respectively,

$$|H(j\omega)| = \frac{0.2\omega^2 + 1}{\sqrt{(0.2\omega^2 + 1)^2 + \omega^6}},$$

$$\tan \varphi_H(\omega) = -\frac{\omega^3}{0.2\omega^2 + 1}.$$

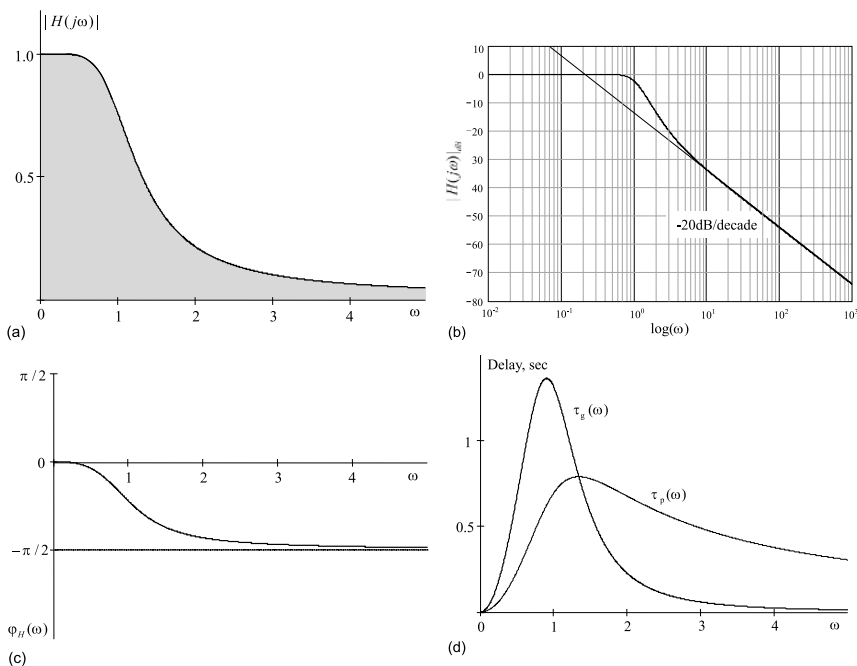


Fig. 5.2. Frequency response of an LTI system: (a) magnitude response, (b) Bode plot, (c) phase response, and (d) phase and group delays.

Fig. 5.2a illustrates $|H(j\omega)|$ in the positive frequency domain and Fig. 5.2b gives the relevant Bode plot. The phase response $\varphi_H(\omega)$ is sketched in Fig. 5.2c. It is seen that the magnitude response has the slope of -20dB/decade beyond the system bandwidth and that the phase response ranges from 0 to $-\pi/2$. \square

5.2.2 Phase Distortions

A typical duty of an input-to-output system is to alter the magnitude spectral density of an input signal, thereby providing the necessary spectral content in the output. In line with this, the output phase can also be changed by the phase response of a system to produce the so-called *phase distortions*. For some applications, violation of phase spectral density is not of importance and relevant errors are ignored. For some others, phase distortions can lead to errors in transmission of information, therefore are accounted. To evaluate phase distortions, two measures are commonly used: *phase delay* and *group delay*.

Phase Delay

An important characteristic of any LTI system is the *phase delay*, provided the definition:

Phase delay: The phase delay (in units of time) is a measure of how much each sinusoidal component of the input signal is delayed in time in the output signal of a system. \square

To find a quantitative measure for the phase delay, let us assume, following the definition, that the input is a harmonic signal $x(t) = A \cos(\omega_0 t + \phi_0)$, where A , ω_0 , and ϕ_0 are constant. Let an LTI system has at ω_0 the response $H(j\omega_0) = |H(j\omega_0)|e^{j\varphi_H(\omega_0)}$. If we present the input as

$$x(t) = A \cos(\omega_0 t + \phi_0) = \frac{1}{2} A e^{j(\omega_0 t + \phi_0)} + \frac{1}{2} A e^{-j(\omega_0 t + \phi_0)}$$

then the output, by the oddness of the phase response, will be defined as

$$\begin{aligned} y(t) &= \frac{1}{2} A H(j\omega_0) e^{j(\omega_0 t + \phi_0)} + \frac{1}{2} A H(j\omega_0) e^{-j(\omega_0 t + \phi_0)} \\ &= A |H(j\omega_0)| \cos[\omega_0 t + \varphi_H(\omega_0) + \phi_0] \\ &= A |H(j\omega_0)| \cos \left[\omega_0 \left(t + \frac{\varphi_H(\omega_0)}{\omega_0} \right) + \phi_0 \right] \\ &= A |H(j\omega_0)| \cos [\omega_0 (t - \tau_p) + \phi_0] . \end{aligned}$$

In this relation, obeying the definition, the frequency-dependent quantity

$$\tau_p(\omega_0) = -\frac{\varphi_H(\omega_0)}{\omega_0} \quad (5.18)$$

has a meaning of the phase delay (in units of time) in a harmonic signal at the frequency ω_0 . One thus infer that the phase delay is evaluated by the negative ratio of the system phase response at ω_0 and ω_0 .

Group Delay

In some cases, the measure of phase delay is not appropriate, and the other quantity called the *group delay* is used to characterize an LTI system, provided the definition:

Group delay: The group delay (in units of time) is a measure of how much a group of input signal components with neighboring close frequencies is delayed in time in the output signal of a system. \square

Let us now think that the input is a cosine carrier signal with a cosine envelope, $x(t) = A \cos \Omega t \cos \omega_0 t$, $\Omega \ll \omega_0$. For the sake of simplicity, we will let the system frequency response to have a unit magnitude in the observed frequency range, so $H(j\omega) = e^{j\varphi_H(\omega)}$ for $\omega_0 - \Omega \leq \omega \leq \omega_0 + \Omega$.

The output is therefore defined by

$$\begin{aligned} y(t) &= \frac{1}{2}A \cos[(\omega_0 - \Omega)t + \varphi_H(\omega_0 - \Omega)] \\ &\quad + \frac{1}{2}A \cos[(\omega_0 + \Omega)t + \varphi_H(\omega_0 + \Omega)] \\ &= A \cos \left[\omega_0 t + \frac{\varphi_H(\omega_0 + \Omega) + \varphi_H(\omega_0 - \Omega)}{2} \right] \\ &\quad \times \cos \left[\Omega t + \frac{\varphi_H(\omega_0 + \Omega) - \varphi_H(\omega_0 - \Omega)}{2} \right] \\ &= A \cos \left\{ \omega_0 \left[t + \frac{\varphi_H(\omega_0 + \Omega) + \varphi_H(\omega_0 - \Omega)}{2\omega_0} \right] \right\} \\ &\quad \times \cos \left\{ \Omega \left[t + \frac{\varphi_H(\omega_0 + \Omega) - \varphi_H(\omega_0 - \Omega)}{2\Omega} \right] \right\}. \end{aligned}$$

If we now allow $\varphi_H(\omega_0 + \Omega) + \varphi_H(\omega_0 - \Omega) \approx 2\varphi_H(\omega_0)$ and assign

$$\tau_p(\omega_0) = -\frac{\varphi_H(\omega_0 + \Omega) + \varphi_H(\omega_0 - \Omega)}{2\omega_0} \approx -\frac{\varphi_H(\omega_0)}{\omega_0}$$

to be the phase delay in the carrier signal, we then can also let

$$\tau_g(\omega_0) = -\frac{\varphi_H(\omega_0 + \Omega) - \varphi_H(\omega_0 - \Omega)}{2\Omega} \approx -\left. \frac{d\varphi_H(\omega)}{d\omega} \right|_{\omega=\omega_0}$$

to be a delay in the group of signals with neighboring frequencies around ω_0 .

It then follows that, obeying the definition, the quantity

$$\tau_g(\omega) = -\frac{d\varphi_H(\omega)}{d\omega} \tag{5.19}$$

plays a role of a delay in units of time of a group of signal's components with neighboring close frequencies. The group delay is hence evaluated by the negative derivative of the system phase response with respect to ω at ω_0 .

Example 5.6. The phase response of an LTI system is found in Example 5.5 to be

$$\varphi_H(\omega) = -\arctan \frac{\omega^3}{0.2\omega^2 + 1}.$$

By (5.18) and (5.19), the phase and group delays are evaluated at an arbitrary angular frequency ω with, respectively,

$$\tau_p(\omega) = \frac{1}{\omega} \arctan \frac{\omega^3}{0.2\omega^2 + 1},$$

$$\tau_g(\omega) = \frac{\omega^2(3 + 0.2\omega^2)}{(0.2\omega^2 + 1)^2 + \omega^6}.$$

Fig. 5.2d sketches both these functions. It is seen that the maximum of the group delay corresponds to the maximum rate of the phase response. However, the maxima of the phase and group delays do not coincide. Because a system in question is bandlimited (LP filter), the group delay is a more appropriate measure of phase distortions in this case. \square

5.2.3 Distortionless Transmission

In some cases, an LTI system is intended for transmitting and receiving signals without distortions. For distortionless transmission through an LTI system, it is required that the exact input signal waveform be reproduced at the output. Herewith, it is allowed for the signal amplitude to be gained and phase delayed in time.

Most generally, with distortionless transmission, the output is coupled with the input by the relation

$$y(t) = Kx(t - \tau_d) \quad (5.20)$$

where $K > 0$ is a constant positive-valued coefficient often called a *gain constant* and τ_d is the *time delay*. If we assume an arbitrary input waveform (Fig. 5.3a), then the undistorted output will be as in Fig. 5.3b. The signal is delayed in time on τ_d and its amplitude is gained with K .

By taking the Fourier transform (Appendix B) of both sides of (5.20), we provide

$$Y(j\omega) = Ke^{-j\tau_d\omega} X(j\omega). \quad (5.21)$$

The system frequency response hence attains the form of

$$H(j\omega) = \frac{Y(j\omega)}{X(j\omega)} = Ke^{-j\tau_d\omega} \quad (5.22)$$

and thus the magnitude and phase responses with distortionless transmission are, respectively,

$$|H(j\omega)| = K, \quad (5.23)$$

$$\varphi_H(\omega) = -\omega\tau_d. \quad (5.24)$$

A conclusion follows immediately: ideal distortionless transmission is achieved solely in noncausal LTI systems, which magnitude response is constant and phase response is linear over all frequencies.

The inverse Fourier transform applied to (5.22) produces (Appendix C)

$$h(t) = \mathcal{F}^{-1}H(j\omega) = K\mathcal{F}^{-1}e^{-j\tau_d\omega} = K\delta(t - \tau_d), \quad (5.25)$$

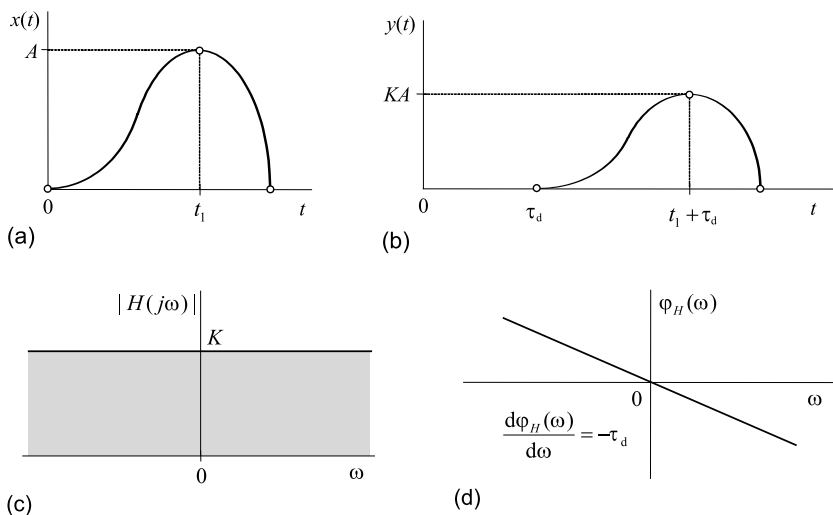


Fig. 5.3. Distortionless transmission: (a) input, (b) output, (c) uniform magnitude response of a system, and (d) linear phase response of a system.

indicating that the impulse response of an LTI system with distortionless transmission is delta-shaped at τ_d . It also follows that the phase and group delays associated with (5.24) are equal,

$$\tau_p = \tau_g = \tau_d.$$

On the other hand, the linear phase response can not obligatory be zero at a center of coordinates, $t = 0$. Most generally, one can consider $\varphi_H(\omega) = \varphi_0 - \omega\tau_d$. In this case, the phase delay is not constant over frequencies and tends toward infinity at $t = 0$. Contrary, the group delay still remains constant,

$$\tau_g = -\frac{d}{d\omega}(\varphi_0 - \tau_d\omega) = \tau_d.$$

The latter has an important practical meaning. In fact, because information is usually transmitted via the neighboring spectral components around the carrier, the linear phase response with an arbitrary initial phase φ_0 is also appropriate for distortionless transmission.

5.2.4 Filtering

One of the most important duties of electronic LTI systems is filtering.

Filtering: Filtering is said to be the process by which the amplitudes of some spectral components of an input signal are changed or even suppressed at the output of a system.

□

Because, by (5.5), spectral content of the output is affected by the frequency response, then any LTI system is actually a *filter* or a device that exhibits some sort of frequency-selective behavior. The following types of filters are commonly recognized.

All-pass filter. An *all-pass filter* is a device whose spectral magnitude response is unity over all frequencies. Fig. 5.3c illustrates the magnitude response of an all-pass filter, which phase response is linear (Fig. 5.3d). Therefore, an all-pass filter is the delay operator $e^{-j\omega\tau_d}$ itself. Its phase response as a function of ω is $-\omega\tau_d$ (5.24).

As one may observe, the amplitude of a signal is not changed by an all-pass filter that contradicts to the definition of filtering. Therefore an all-pass filter is not actually a filter in the applied sense. It is rather a delay-line.

Low-pass filter. A *low-pass filter* (LP filter) passes low frequencies and attenuates all other unwanted (high) frequencies. It is also sometimes called a *high-cut* filter, or *treble cut* filter, or even *hiss* filter.

A simplest LP filter is the RC circuit that consists of a resistor in series with the input signal path in conjunction with a capacitor in parallel with the output signal path. An example is an LP filter in an audio amplifier that would let through all signals below 3 KHz and suppress all others above 10 KHz.

An *ideal* LP filter is also called *perfect* LP filter and is specified with the rectangular shape of the frequency response,

$$H(j\omega) = \begin{cases} 1, & |\omega| \leq \omega_c \\ 0, & |\omega| > \omega_c \end{cases}, \quad (5.26)$$

where ω_c is a cut-off frequency. Fig. 5.4a shows the rectangular-shape magnitude response of this filter. The relevant impulse response is provided by taking the inverse Fourier transform of (5.25); that is,

$$h(t) = \frac{\omega_c}{\pi} \frac{\sin \omega_c t}{\omega_c t}. \quad (5.27)$$

High-pass filter. A *high-pass filter* (HP filter) passes high frequencies and attenuates unwanted low frequencies. Therefore, a HP filter is the opposite of an LP filter. The other term is a *low-cut* filter, or *bass-cut* filter, or *rumble* filter.

A simplest HP filter is the RC circuit that consists of a capacitor C in series with the input signal path in conjunction with a resistor R in parallel with the output signal path. For example, a HP filter with a cut-off frequency of $f_c = \omega_c/2\pi = 2$ MHz might be required for the antenna input to a receiver where AM Radio interference is proving troublesome. We thus will want to pass all frequencies above 2 MHz but attenuate those below 2 MHz.

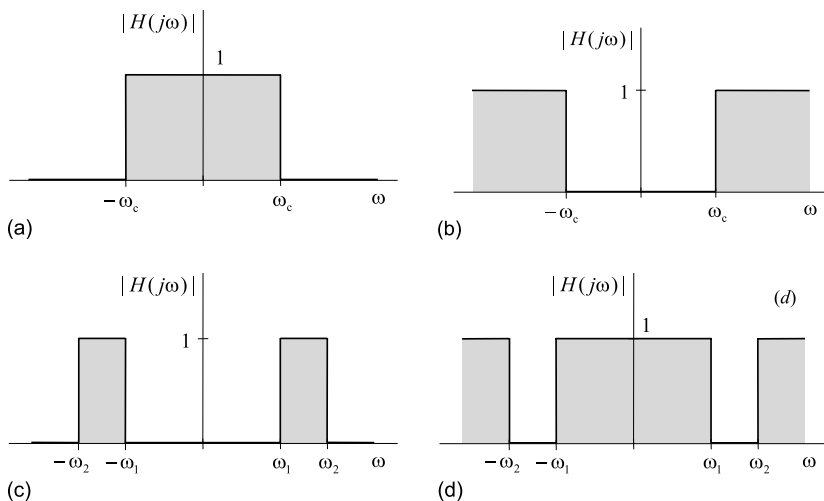


Fig. 5.4. Ideal LTI filters: (a) low-pass (LP), (b) high-pass (HP), (c) bandpass (BP), and (d) band-rejection (BR).

An *ideal* HP filter (or *perfect* HP filter) has a rectangular-shape frequency response

$$H(j\omega) = \begin{cases} 1, & |\omega| > \omega_c \\ 0, & |\omega| \leq \omega_c \end{cases}, \quad (5.28)$$

The magnitude response of an ideal HP filter is shown in Fig. 5.4b. Because (5.28) can be interpreted as a difference between the frequency responses of an all-pass filter and an LP filter, the impulse response of a HP filter can be found, by (5.27) and (5.25) with $\tau_d = 0$ and $K = 1$, to be

$$h(t) = \delta(t) - \frac{\omega_c \sin \omega_c t}{\pi \omega_c t}. \quad (5.29)$$

Band-pass filter. A *band-pass filter* (BP filter) lets through signal spectral components in a gap between two given cut-off frequencies. It can be created by a combination of an LP filter and a HP filter.

A simplest BP filter is the RLC circuit that consists of a capacitor C and inductance L in series with the input signal path in conjunction with a resistor R in parallel with the output signal path. An example is a radio receiver selective circuit (BP filter) that would let through all of the signals of the received station. All of the other signals of the neighboring stations have to be suppressed.

An *ideal* BP filter (or *perfect* BP filter) is performed with a rectangular-shape selective frequency response that is unity between two given cut-off frequencies, ω_{c1} and ω_{c2} , and is zero otherwise,

$$H(j\omega) = \begin{cases} 1, & -\omega_{c2} \leq \omega \leq -\omega_{c1} \quad \text{and} \quad \omega_{c1} \leq \omega \leq \omega_{c2} \\ 0, & \text{otherwise} \end{cases} . \quad (5.30)$$

Fig. 5.4c illustrates the magnitude response of an ideal BP filter. It is seen that (5.30) can be treated as a difference of the frequency responses of two ideal LP filters having the cut-off frequencies ω_{c2} and ω_{c1} , respectively. The relevant impulse response is therefore calculated, using (5.27), by

$$\begin{aligned} h(t) &= \frac{\omega_{c2}}{\pi} \frac{\sin \omega_{c2} t}{\omega_{c2} t} - \frac{\omega_{c1}}{\pi} \frac{\sin \omega_{c1} t}{\omega_{c1} t} \\ &= \frac{2\Omega \sin \Omega t}{\pi \Omega t} \cos \omega_0 t, \end{aligned} \quad (5.31)$$

where $\Omega = (\omega_{c2} - \omega_{c1})/2$ is an algebraic mean difference between two cut-off frequencies and

$$\omega_0 = \frac{\omega_{c1} + \omega_{c2}}{2} \quad (5.32)$$

is an algebraic mean cut-off frequency. We notice that in other cases the central frequency may be evaluated as the *geometric mean* by

$$\omega_0 = \sqrt{\omega_{c1}\omega_{c2}} . \quad (5.33)$$

However, both these simple measures, (5.32) and (5.33), may not be appropriate when the frequency response is not symmetric about ω_0 . Then the more common measures of a central frequency must be used (see Signals).

Band-rejection filter. In electronics, the *band-rejection filter* (BR filter) is the one that attenuates all frequencies between two given cut-off frequencies and passes all frequencies beyond this gap. It is also called a *band-stop* filter, or *band-elimination* filter, or *band-suppression* filter, or *notch* filter. The latter term is also used for a special kind of BR filters.

A simplest BP filter is the RLC circuit that consists of a resistor R in series with the input signal path in conjunction with a capacitor C and inductance (L) in parallel with the output signal path. For example, a BP filter would be used to protect a Radio receiver against interference from a nearby transmitter in the selected frequency range say 136-154 MHz or 152-175 MHz. The filter must be tuned to reject the interfering signal.

An *ideal* BR filter (or *perfect* BR filter) is the opposite of an ideal BP filter. As such, it is performed with the frequency response shown in Fig. 5.4d and described by

$$H(j\omega) = \begin{cases} 0, & -\omega_{c2} \leq \omega \leq -\omega_{c1} \quad \text{and} \quad \omega_{c1} \leq \omega \leq \omega_{c2} \\ 1, & \text{otherwise} \end{cases} . \quad (5.34)$$

The frequency response of an ideal BR filter may be combined by the frequency response of an ideal LP filter with the cut-off frequency ω_{c1} and

an ideal HP filter with the cut-off frequency $\omega_{c2} > \omega_{c1}$. The relevant impulse response is then readily provided, by (5.27) and (5.29), to be

$$\begin{aligned} h(t) &= \delta(t) - \left(\frac{\omega_{c2}}{\pi} \frac{\sin \omega_{c2}t}{\omega_{c2}t} - \frac{\omega_{c1}}{\pi} \frac{\sin \omega_{c1}t}{\omega_{c1}t} \right) \\ &= \delta(t) - \frac{2\Omega}{\pi} \frac{\sin \Omega t}{\Omega t} \cos \omega_0 t. \end{aligned} \quad (5.35)$$

Notch filter. A special kind of BR filters is called a *notch filter*. It is also known as a *band-stop* filter, *narrow band-pass* filter, or *T-notch* filter.

The filter is typically used when ω_{c2} and ω_{c1} are less than 1 to 2 decades apart (that is, ω_{c2} is less than 10 to 20 times the ω_{c1}). For example, an *anti-hum* filter would have $f_{c1} = \omega_{c1}/2\pi = 59$ Hz and $f_{c2} = \omega_{c2}/2\pi = 61$ Hz and an *anti-presence* filter is designed to have $f_{c1} = \omega_{c1}/2\pi = 1$ KHz and $f_{c2} = \omega_{c2}/2\pi = 4$ KHz.

As any other ‘ideal’ devices, all of the above-considered ideal filters are not realizable physically. That is because the sinc function in their impulse response requires infinite time, thus, the filter would need to predict the future. Even so, an ideal LP filter is used, for example, in the Nyquist-Kotelnikov-Shannon interpolation formula to reconstruct the continuous (analog) signal from the digital one (samples).

Therefore, in practice, selective filters are not ideal and do not attenuate frequencies just outside the desired frequency range completely. Instead, there is typically a smooth and quick decrease in transmitted frequency outside the band. This is known as the *roll-off*, and usually expressed in parts of dB/decade as in Fig. 5.2d, for example.

In some applied problems, the filter is intended to represent a desired (optimized) shape of the magnitude response that may not always be rectangular. Such filters are commonly called *optimal* filters. The phase response of an optimal filter is usually required to be linear, but not obligatorily.

As we observed before in Chapter 4, any LTI system (filter or other device) can be described in the time domain with ordinary differential equations (5.16). In Fourier analysis, the ODEs are translated to the frequency domain and investigated for the system frequency response (5.17). Below we consider two elementary LTI systems of the first and second orders.

5.2.5 LTI Systems of the First Order

The most general form of the ODE of an LTI system of the first order appears if to set $N = 1$ in (5.16). By $M \leq N$ that can be either 1 or 0, the equation becomes

$$a_1 \frac{d}{dt} y(t) + a_0 y = b_1 \frac{d}{dt} x(t) + b_0 x(t). \quad (5.36)$$

The Fourier transform applied to the both sides of (5.36) produces

$$j\omega a_1 Y(j\omega) + a_0 Y(j\omega) = j\omega b_1 X(j\omega) + b_0 X(j\omega) \quad (5.37)$$

that, by (5.5), instantly leads to the system frequency response

$$H(j\omega) = \frac{b_0 + j\omega b_1}{a_0 + j\omega a_1} = \frac{a_0 b_0 + a_1 b_1 \omega^2 + j\omega(a_0 b_1 - a_1 b_0)}{a_0^2 + \omega^2 a_1^2}. \quad (5.38)$$

The magnitude and phase responses associated with (5.38) are thus, respectively,

$$|H(j\omega)| = \frac{\sqrt{(a_0 b_0 + a_1 b_1 \omega^2)^2 + \omega^2 (a_0 b_1 - a_1 b_0)^2}}{a_0^2 + \omega^2 a_1^2}, \quad (5.39)$$

$$\tan \varphi_H(\omega) = \frac{\omega(a_0 b_1 - a_1 b_0)}{a_0 b_0 + a_1 b_1 \omega^2}. \quad (5.40)$$

As can be seen, $|H(j\omega)|$ has no special points (singularities and zeros) and thus (5.38) is a smooth function.

By $\varphi_H(\omega)$, the phase delay (5.18) and group delay (5.19) are defined to be, respectively,

$$\tau_p(\omega) = -\frac{1}{\omega} \arctan \frac{\omega(a_0 b_1 - a_1 b_0)}{a_0 b_0 + a_1 b_1 \omega^2}, \quad (5.41)$$

$$\tau_g(\omega) = -\frac{d\varphi_H(\omega)}{d\omega} = -\frac{(a_0 b_1 - a_1 b_0)(a_0 b_0 - a_1 b_1 \omega^2)}{(a_0 b_0 + a_1 b_1 \omega^2)^2 + \omega^2 (a_0 b_1 - a_1 b_0)^2}. \quad (5.42)$$

In electronic applications, a dynamic LTI system of the first order (5.36) is commonly represented with two simplest schemes of LP and HP filters.

Simplest LP Filters

Fig. 5.5 exhibits two electrical circuits of the most simple LP filters organized with series connections of a resistor R and capacitor C (Fig. 5.5a) and inductor L and resistor R (Fig. 5.5b).

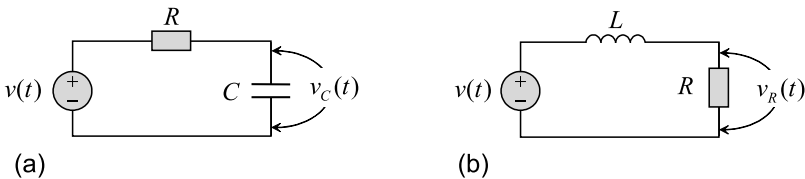


Fig. 5.5. Simplest LP filters: (a) RC and (b) RL.

The RC filter and RL filter are governed by the voltage $v(t)$ and described with the ODEs, respectively,

$$\frac{d}{dt}v_C + \frac{1}{RC}v_C = \frac{1}{RC}v, \quad (5.43)$$

$$\frac{d}{dt}v_R + \frac{R}{L}v_R = \frac{R}{L}v, \quad (5.44)$$

where the value

$$\frac{1}{RC} = \frac{R}{L} = 2\delta, \quad (5.45)$$

has a dimension of angular frequency and physical meaning of the filter cut-off frequency ω_c associated with the system bandwidth.

If we now assign $x(t) = v(t)$, $y(t) = v_C(t)$ or $y(t) = v_R(t)$, $a_1 = 1$, $a_0 = a$, $b_1 = 0$, $b_0 = b$, and think that $a = b$ may be either $1/RC$ or R/L , we arrive at a general ODE form of a simplest LP filter of the first order

$$y'(t) + ay(t) = bx(t),$$

earlier studied in the time domain.

The frequency response, magnitude response, phase response, phase delay, and group delay associated with this equation are readily provided, by (5.38)–(5.42), to be, respectively,

$$H(j\omega) = \frac{b}{a + j\omega}, \quad (5.46)$$

$$|H(j\omega)| = \frac{b}{\sqrt{a^2 + \omega^2}}, \quad (5.47)$$

$$\tan \varphi_H(\omega) = -\frac{\omega}{a}, \quad (5.48)$$

$$\tau_p(\omega) = \frac{1}{\omega} \arctan \frac{\omega}{a}, \quad (5.49)$$

$$\tau_g(\omega) = \frac{a}{a^2 + \omega^2}, \quad (5.50)$$

where $a = b = 2\delta$.

Alternatively, one can exploit the impedances of a capacitor and inductor, respectively,

$$x_C(j\omega) = \frac{1}{j\omega C}, \quad x_L(j\omega) = j\omega L \quad (5.51)$$

and straightforwardly write the frequency responses of the RC circuit and RL circuit as, respectively,

$$H(j\omega) = \frac{x_C}{R + x_C} = \frac{1/j\omega C}{R + 1/j\omega C},$$

$$H(j\omega) = \frac{R}{R + x_L} = \frac{R}{R + j\omega L}.$$

After simple transformations, both functions become (5.46).

Fig. 5.6 illustrates the frequency characteristics of a simplest LP filter. An analysis shows that attenuation of the magnitude response at the level

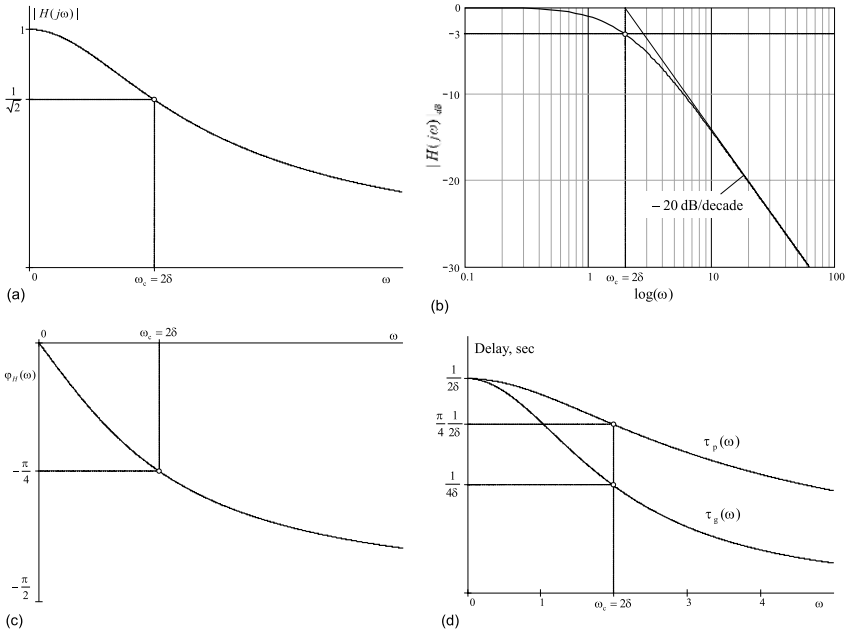


Fig. 5.6. Frequency characteristics of a simplest LP filter: (a) magnitude response, (b) Bode plot, (c) phase response, and (d) phase and group delays.

of $1/\sqrt{2}$ (Fig. 5.6a) or -3dB in the Bode plot (Fig. 5.6b) corresponds to the cut-off frequency $\omega_c = 2\delta$. Beyond the filter bandwidth, the frequency content attenuates with a slope of -20dB/decade . At ω_c , the phase attains a shift of $-\pi/4$ (Fig. 5.6c), the phase delay reduces from $1/2\delta$ to $\pi/8\delta$, and the group delay becomes twice smaller than at $\omega = 0$ (Fig. 5.6d). With ω increasing toward infinity, the magnitude response and both delays asymptotically approach zero, whereas the phase response approaches $-\pi/2$.

One thus can truly conclude that this simplest LTI system is not able to obtain neither a constant phase delay nor group delay and thus phase distortions will accompany the process.

Example 5.7. An LP filter (Fig. 5.5a) is loaded with the input resistor R_1 of a cascade included block. The frequency response of a loaded filter is thus defined by

$$H(j\omega) = \frac{\frac{R_1/j\omega C}{R_1+1/j\omega C}}{R + \frac{R_1/j\omega C}{R_1+1/j\omega C}} = \frac{R_1}{R + R_1 + j\omega CRR_1}.$$

The function can now be represented as

$$H(j\omega) = \frac{R_1}{R + R_1} \frac{1}{1 + j\omega CR_x} = k \frac{2\delta}{2\delta + j\omega},$$

where

$$k = \frac{R_1}{R + R_1}, \quad 2\delta = \frac{1}{CR_x}, \quad R_x = \frac{RR_1}{R + R_1}.$$

As it follows, the loaded filter can be represented with the frequency response (5.46) and functions shown in Fig. 5.6 if we account for an attenuation coefficient $k = R_1/(R + R_1)$ and set $2\delta = 1/CR_x$. \square

Simplest HP Filters

The other widely used representative of LTI systems of the first order is an HP filter. Fig. 5.7 gives two electrical schemes of the most simple HP filters composed by series connections of C and R (Fig. 5.7a) and R and L (Fig. 5.7b). The schemes are obtained from Fig. 5.5 by interchanging the components.

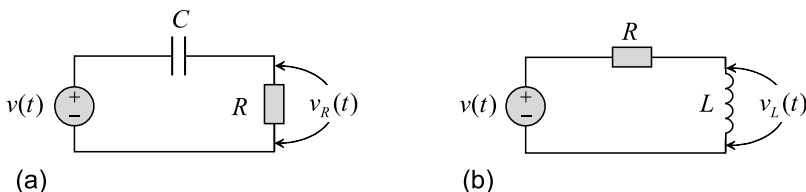


Fig. 5.7. Simplest HP filters: (a) RC and (b) RL.

The ODEs corresponding to Fig. 5.7a and 5.7b are readily derived to be, respectively,

$$\frac{d}{dt}v_R + \frac{1}{RC}v_R = \frac{d}{dt}v, \quad (5.52)$$

$$\frac{d}{dt}v_L + \frac{R}{L}v_L = \frac{d}{dt}v \quad (5.53)$$

and, in analogous to an LP filter, generalized by

$$y'(t) + ay(t) = x'(t), \quad (5.54)$$

where $a = 1/RC$ or $a = R/L$. In a like manner, by (5.38)–(5.42), the frequency response, magnitude response, phase response, phase delay, and group delay associated with (5.54) can be derived to be, respectively,

$$H(j\omega) = \frac{j\omega}{a + j\omega}, \quad (5.55)$$

$$|H(j\omega)| = \frac{\omega}{\sqrt{a^2 + \omega^2}}, \quad (5.56)$$

$$\tan \varphi_H(\omega) = \frac{a}{\omega}, \quad (5.57)$$

$$\tau_p(\omega) = -\frac{1}{\omega} \arctan \frac{a}{\omega}, \quad (5.58)$$

$$\tau_g(\omega) = -\frac{a}{a^2 + \omega^2}. \quad (5.59)$$

An illustration for all these functions is given in Fig. 5.8. It is seen that within the system bandwidth, $\omega > \omega_c = 2\delta$, the magnitude response varies from $1/\sqrt{2}$ to unity in Fig. 5.8a or from -3dB to 0dB in the Bode plot

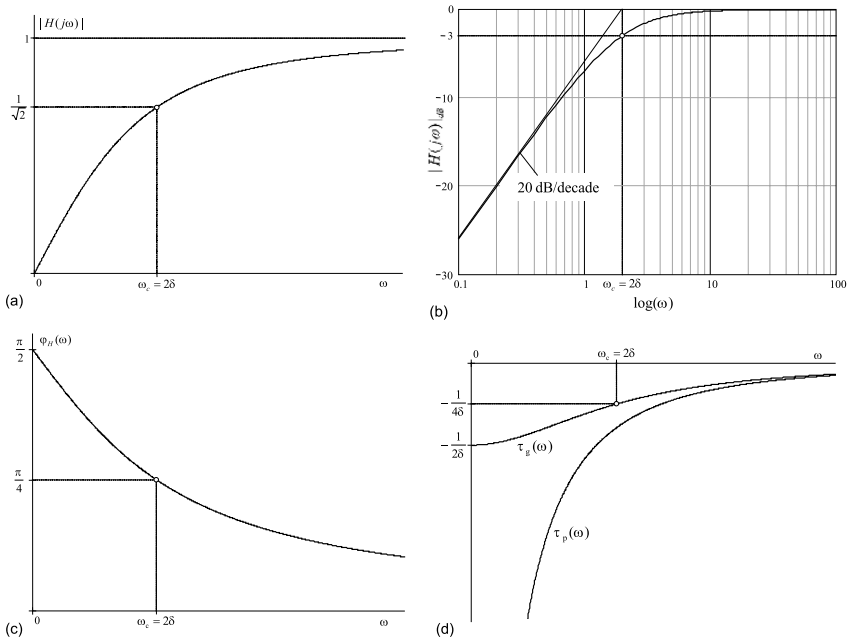


Fig. 5.8. Frequency characteristics of a simplest LP filter: (a) magnitude response, (b) Bode plot, (c) phase response, and (d) phase and group delays.

(Fig. 5.8b). Beyond the bandwidth, $\omega < \omega_c$, the frequency content attenuates with the slope of 20dB/decade. At $\omega = 0$, the phase acquires a shift of $\pi/2$ and, at ω_c , the value reduces to $\pi/4$ (Fig. 5.8c). It also follows that the group delay is equal to that, with its sign changed, featured to an LP filter (Fig. 5.4d). However, both these filters do not allow for a constant phase delay or group delay. Finally, the phase delay is not a proper measure of phase distortions for this kind of filters, once τ_p exhibits a singularity at $\omega = 0$.

Example 5.8. A simplest HP filter (Fig. 5.7b) is loaded with the input resistor R_1 of a cascade system. The frequency response of a loaded filter is therefore

$$H(j\omega) = \frac{\frac{R_1 j\omega L}{R_1 + j\omega L}}{R + \frac{R_1 j\omega L}{R_1 + j\omega L}} = k \frac{j\omega}{2\delta + j\omega},$$

where

$$k = \frac{R_1}{R + R_1}, \quad 2\delta = \frac{R_x}{L}, \quad R_x = \frac{RR_1}{R + R_1}.$$

This filter can be characterized with the frequency response (5.55) and functions shown in Fig. 5.8, if to account for an attenuation coefficient k and set $2\delta = R_x/L$. \square

5.2.6 LTI Systems of the Second Order

Second-order LTI systems are usually associated with a resonance frequency and some bandwidth around. They are used to increase sharpness of bandwidth's sides for different kinds of filters. Their most important property is an ability to select or suppress signals in the narrow frequency band. Because the gain of such systems becomes purely real at some frequency called *resonance frequency*, the second-order LTI system is often called *resonant system*. Two elementary resonant schemes are available: the *series resonant circuit* and *parallel resonant circuit*.

Series Resonant RLC Circuit

A simplest second-order LTI system has a main part as a series resonant RLC circuit that is a series connection of an inductance L , capacitance C , and resistance R as shown in Fig. 5.9.

The resonance of such a circuit occurs at a frequency ω_0 at which the inductive reactance $j\omega L$ and capacitive reactance $1/j\omega C$ are equal in magnitude but cancel each other because they are 180 degrees apart in phase. The sharp minimum in impedance which occurs is useful in tuning applications. The sharpness of the minimum depends on the value of R and is characterized by the quality factor Q of the circuit.

The complex impedance of a circuit (Fig. 5.9) can be written as

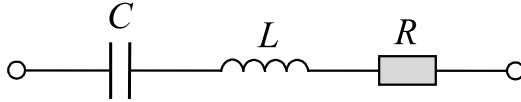


Fig. 5.9. Series resonant RLC circuit.

$$Z_s(j\omega) = R + j\omega L + \frac{1}{j\omega C}. \quad (5.60)$$

For the purposes of generalization, we need to introduce the resonance frequency $\omega_0 = 1/\sqrt{LC}$, bandwidth $2\delta = R/L$, quality factor $Q = \omega_0/2\delta$, and generalized detuning

$$\xi = Q \left(\frac{\omega}{\omega_0} - \frac{\omega_0}{\omega} \right) \Big|_{Q \gg 1} \cong 2Q \frac{\omega - \omega_0}{\omega_0}. \quad (5.61)$$

The quality factor of an RLC circuits is typically provided to be large, $Q \gg 1$. If so, then the value $\xi = 1$ means that a system is exactly a half bandwidth δ apart from ω_0 .

The complex impedance (5.60) can now be rewritten as

$$Z_s(j\xi) = |Z_s(j\xi)|e^{j\varphi_s(\xi)} = R(1 + j\xi), \quad (5.62)$$

having the total impedance and phase, respectively,

$$|Z_s(j\xi)| = R\sqrt{1 + \xi^2}, \quad (5.63)$$

$$\tan \varphi_s(\xi) = \xi. \quad (5.64)$$

A simple observation shows that, by $\xi = 0$, the circuit is at resonance, $\omega = \omega_0$, exhibiting a minimum impedance $Z_s(j\omega_0) = R$ that is real and zero phase $\varphi_s(\omega_0) = 0$. If $\xi \neq 0$ and increases, the total impedance becomes larger with the rate totally dependent on the quality factor. With $\xi < 0$, the phase ranges from $-\pi/2$ to 0 and, if $\xi > 0$, it behaves from 0 to $\pi/2$.

If such a circuit is driven by a voltage $x(t) = v(t)$, than the output $y(t)$ can be assigned to be a voltage induced on any of the components (typically on L or C). Therefore, there could not be found a universal scheme. Based upon a series resonant circuit, a second-order LTI system can appear in different configurations.

Example 5.9. Consider a simplest BR (or notch) filter shown in Fig. 5.10, in which the output is a voltage induced on both L and C .

The filter frequency response is defined by

$$H(j\omega) = \frac{j\omega L + 1/j\omega C}{R + j\omega L + 1/j\omega C}$$

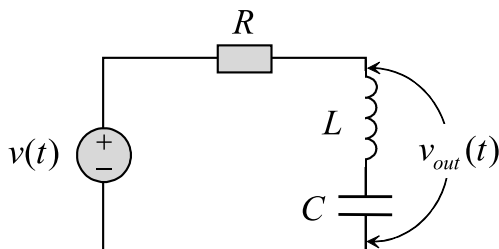


Fig. 5.10. Simplest BR filter.

and, in terms of the generalized detuning ξ , becomes

$$H(j\xi) = \frac{j\xi}{1 + j\xi}. \quad (5.65)$$

The filter is thus characterized with the following magnitude and phase responses, respectively,

$$|H(j\xi)| = \frac{|\xi|}{\sqrt{1 + \xi^2}}, \quad \tan \varphi_H(\xi) = \frac{1}{\xi}. \quad (5.66)$$

Fig. 5.11 illustrates (5.66). It follows that substituting $\xi = 0$ with $\omega = \omega_0$,

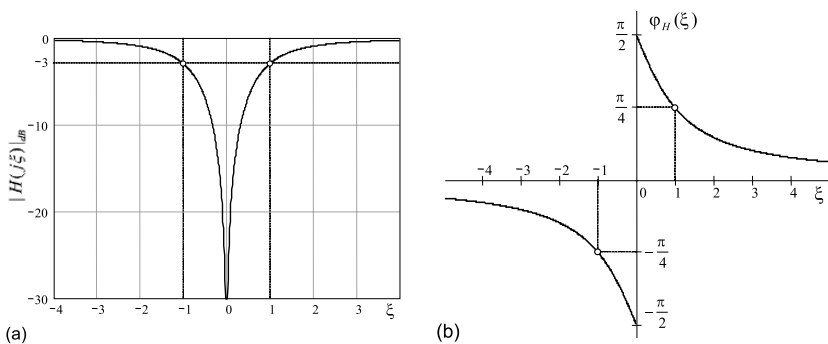


Fig. 5.11. Frequency response of a simplest BR filter: (a) magnitude and (b) phase.

needs substituting $\xi = \pm 1$ with $\omega_0 \pm \delta$. It is also seen that, by $\xi = 0$, the magnitude response is zero and the phase response has a singularity. The latter is due to the ideal elements L and C allowed for the filter model. Thus it is not the case to fit real measurements. To provide the more realistic responses, one needs accounting for the ohmic resistances of an inductor and capacitor. \square

Parallel Resonant Circuit

The other basic configuration of the second-order LTI systems comprises included in parallel the L , C , and R . This antipode of a series resonant circuit called the *parallel resonant circuit* (Fig. 5.12) has appeared to be incredibly useful in design of resonant amplifiers, channels, and tracts.

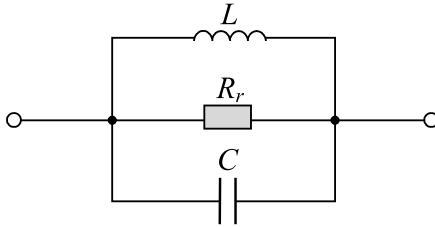


Fig. 5.12. Parallel resonant circuit.

The admittance of the parallel circuit is straightforwardly written as

$$\frac{1}{Z_p(j\omega)} = \frac{1}{R_r} + j\omega C + \frac{1}{j\omega L}. \quad (5.67)$$

If we substitute $R_r = Z_0 Q$, where $Z_0 = \sqrt{L/C}$ is the characteristic impedance, then the complex impedance can be obtained via the generalized detuning ξ (5.61) by a reciprocal of (5.67) as

$$Z_p(j\xi) = \frac{R_r}{1 + j\xi}. \quad (5.68)$$

The total impedance and phase are thus, respectively,

$$|Z_p(j\xi)| = \frac{R_r}{\sqrt{1 + \xi^2}}, \quad (5.69)$$

$$\varphi_p(\xi) = -\arctan \xi. \quad (5.70)$$

The bandwidth 2δ of a parallel circuit is ascertained in the same manner as for the series circuit. We measure the frequency span between two points around ω_0 , at which the impedance is reduced by the factor of $1/\sqrt{2}$. This span appears to be reduced by Q the resonance frequency ω_0 , i.e.,

$$2\delta = \frac{\omega_0}{Q}. \quad (5.71)$$

The value R_r of a parallel resonant circuit is substantially larger than that R of a series resonant circuit. It can be shown that R_r is a counterpart of a reciprocal of R such that infinite Q means infinite R_r and zero R .

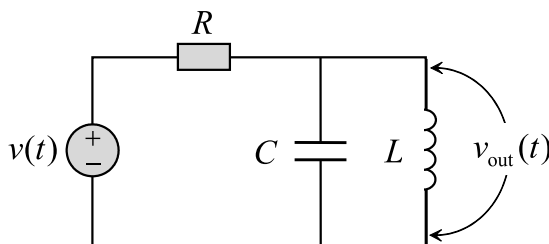


Fig. 5.13. Simplest BP filter.

Example 5.10. A simplest BP filter is designed as shown in Fig. 5.13.

Because neither C nor L is ideal (see remarks for Example 5.9), one can think that a parallel resonant circuit is loaded with some resistance R_r as in Fig. 5.12 to have a complex impedance $Z_p(j\xi)$ given by (5.68). The filter frequency response is then defined by

$$H(j\xi) = \frac{Z_p(j\xi)}{R + Z_p(j\xi)} = \frac{R_r}{R + R_r} \frac{1}{1 + j \frac{R}{R + R_r} \xi}.$$

An observation shows that if $R_r \gg R \rightarrow 0$, then $H(j\xi) \rightarrow 1$ and the filter loses an ability to process the input. In the other limiting case of $R \gg R_r$, the frequency response becomes $H(j\xi) = k/(1 + j\xi)$, where the gain k is extremely small, $k = R_r/(R + R_r) \ll 1$. The filter is thus inefficient.

In the matched case of $R = R_r$, the frequency response is calculated by

$$H(j\xi) = \frac{1}{2} \frac{1}{1 + j0.5\xi} \quad (5.72)$$

and we notice that the input is attenuated by the factor of 2 and the filter bandwidth becomes twice wider. The relevant magnitude and phase responses are, respectively,

$$|H(j\xi)| = \frac{1}{2\sqrt{1 + 0.25\xi^2}}, \quad \tan \varphi_H(\xi) = -\frac{\xi}{2}. \quad (5.73)$$

Fig. 5.14 sketches both these functions. □

An advantage of a parallel resonance circuit is that its large resistance R_r is well matched with a large resistance of the source of an electric current. For this reason, transistor resonant amplifiers are typically designed to have a parallel resonant circuit in a load.

Example 5.11. A narrowband LTI system is represented by a linear transistor resonant amplifier (Fig. 5.15a) combining the functions of gaining (transistor amplifier) and BP filtering (parallel resonant circuit).

A transistor amplifier converts the input voltage $v(t)$ to the electric current $i(t)$. To match the collector-emitter impedance of a transistor, its collector is partially connected to the parallel resonant circuit.

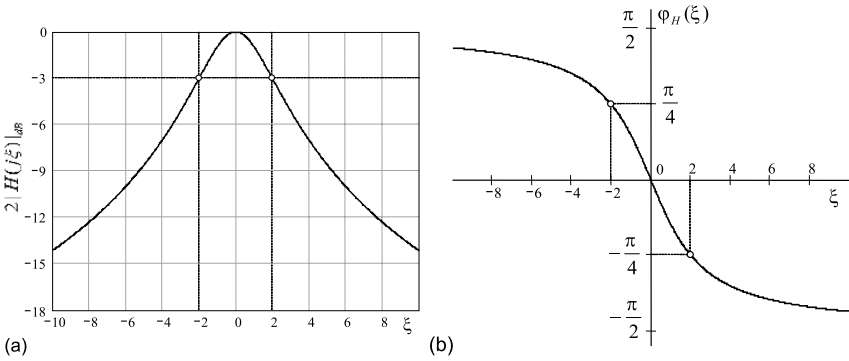


Fig. 5.14. Frequency response of a simplest BP filter: (a) magnitude and (b) phase.

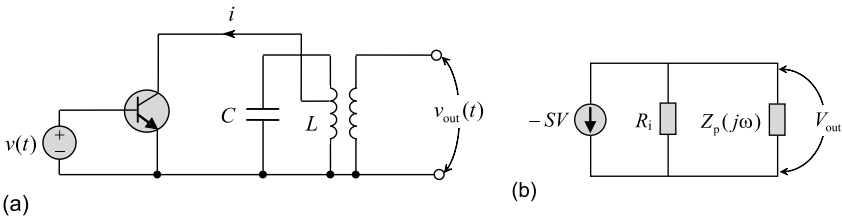


Fig. 5.15. Linear transistor resonant amplifier: (a) electrical equivalent scheme and (b) generalized equivalent scheme.

Equivalently, the scheme can be represented as in Fig. 5.15b. It is assumed that the harmonic input current has a complex amplitude $-SV$, where S is a transconductance of a transistor and V is a complex amplitude of a harmonic input voltage. The source of an electric current has an inner resistance R_i and the parallel resonant circuit is represented with the complex impedance $Z_p(j\omega)$ described by (5.68).

An equivalent impedance of the scheme is combined with the parallel connection of R_i and Z_p to be

$$Z_e(j\omega) = \frac{R_i Z_p}{R_i + Z_p}$$

that, invoking (5.68), transforms to

$$Z_e(j\xi) = \frac{R_e}{1 + j\xi\xi_e}, \tag{5.74}$$

where $R_e = R_i R_r / (R_i + R_r)$ and $\xi_e = \xi R_i / (R_i + R_r)$.

It can be shown that the value R_i reduces the quality factor of a parallel circuit so that it becomes

$$Q_e = \frac{QR_i}{R_i + R_r}.$$

The complex amplitude of an output voltage is now calculated by $V_{\text{out}} = -SZ_e V$ and the frequency response of an amplifier is thus

$$H(j\xi) = \frac{V_{\text{out}}}{V} = -SZ_e = -\frac{SR_e}{1 + j\xi_e} \quad (5.75)$$

producing the magnitude and phase responses, respectively,

$$|H(j\xi)| = \frac{SR_e}{\sqrt{1 + \xi_e^2}}, \quad \varphi_H(\xi) = \pi - \arctan \xi_e. \quad (5.76)$$

If an amplifier is matched with the resonant circuit by $R_i = R_r$, the magnitude and phase responses become, respectively,

$$|H(j\xi)| = \frac{SR_r}{2\sqrt{1 + 0.25\xi^2}}, \quad \varphi_H(\xi) = \pi - \arctan \frac{\xi}{2}. \quad (5.77)$$

As it is seen, the functions in (5.77) are consistent to those associated with a simplest BP filter (Example 5.10). \square

5.2.7 LTI Systems of High Orders

Simple structures of the first and second orders possess not enough capabilities to solve problems associated with high selectivity of signals. Mostly, it is because attenuation of spectral components beyond the bandwidth is not efficient in such systems. The problem may be solved by using several resonant circuits coupled properly. A cascade, however, suffers of instability. Therefore, a number of circuits typically does not exceed three. The effect rises dramatically by using piezoelectric structures, in which case both the high sides roll-off and system stability are achieved.

Amplifier with Two Coupled Resonant Circuits

A straightforward solution is to use a cascade of systems of low-orders (RC, RL, and/or RLC), thereby achieving the high side roll-off of the frequency response. An example is a resonant amplifier with two parallel resonant circuits coupled by a mutual inductance M as shown in Fig. 5.16a (or in Fig. 4.24).

A generalized equivalent scheme of this amplifier is shown in Fig. 5.16b. Here, two equal complex impedances $Z_p(j\omega)$ described by (5.68) as associated with two equal parallel resonant circuits, are coupled by means of an inductive impedance $Z_M(j\omega) = j\omega M$. It can be shown that the magnitude response of such a system is described by

$$|H(j\omega)| = \frac{k_1 K S R_e}{\sqrt{(1 + K^2 - \xi^2) + 4\xi^2}},$$

where, SR_e is as in (5.75), $0 < k_1 \leq 1$ is a coefficient indicating a power of inclusion of a transistor amplifier to the first resonant circuit and $K = MQ/L$

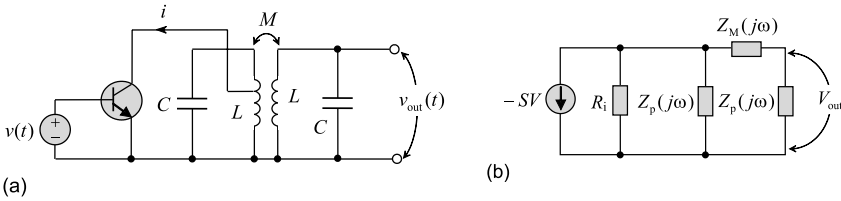


Fig. 5.16. Linear transistor resonant amplifier with two coupled resonant circuits: (a) electrical equivalent scheme and (b) generalized equivalent scheme.

is a coefficient of a mutual detuning of two resonant circuits. If $K = 1$, the magnitude response exhibits a flat part around the resonance frequency, $\xi = 0$. If a nonuniformity is allowed in the system bandwidth, then, by increasing K , the shape of $|H(j\omega)|$ can be obtained as shown in Fig. 5.17a.

Fig. 5.17b gives a surface plot of the magnitude response for small values of K . It is seen that, by $K = 0$, the amplifier gain is zero. When K is set to be unity, the gain also becomes unity at ω_0 . With greater values of K , the picture passes over sections shown in Fig. 5.17a.

Certainly, even with two coupled tuned circuits, rectangularity of the magnitude response is far from ideal. To increase the sides roll-off substantially, filters with active feedback are used. However, the problem arises of stability. The latter is overcome if piezoelectric resonators and filters are used.

5.2.8 Piezoelectric Structures

Selective properties of electronic systems are improved dramatically by using piezoelectric resonators, filters, and structures, which quality factor and operation stability can be achieved to be extremely high. Discovered by Pierre Curie² (with his brother Jacques) in 1880, the piezoelectric effect took several decades until it was finally used in 1921 by Cady³ to design first crystal resonators. Soon after, in 1923, Pierce⁴ designed the first quartz crystal oscillator and, in 1927, Marrison⁵ created the first quartz oscillator clock based on the works of Cady and Pierce.

Modern piezoelectric resonators and filters effectively exploit accuracy and precision of bulk acoustic waves (BAWs) and surface acoustic waves (SAWs) of the crystal media and surface, respectively. They can be organized with several units and even decades of elementary resonators.

² Pierre Curie, French chemist and physicist, 15 May 1859-19 April 1906.

³ Walter Guyton Cady, US scientist, 1874-1974.

⁴ George Washington Pierce, US physicist, 11 January 1872-25 August 1956.

⁵ Warren Marrison, US electrical engineer, 1896-1980.

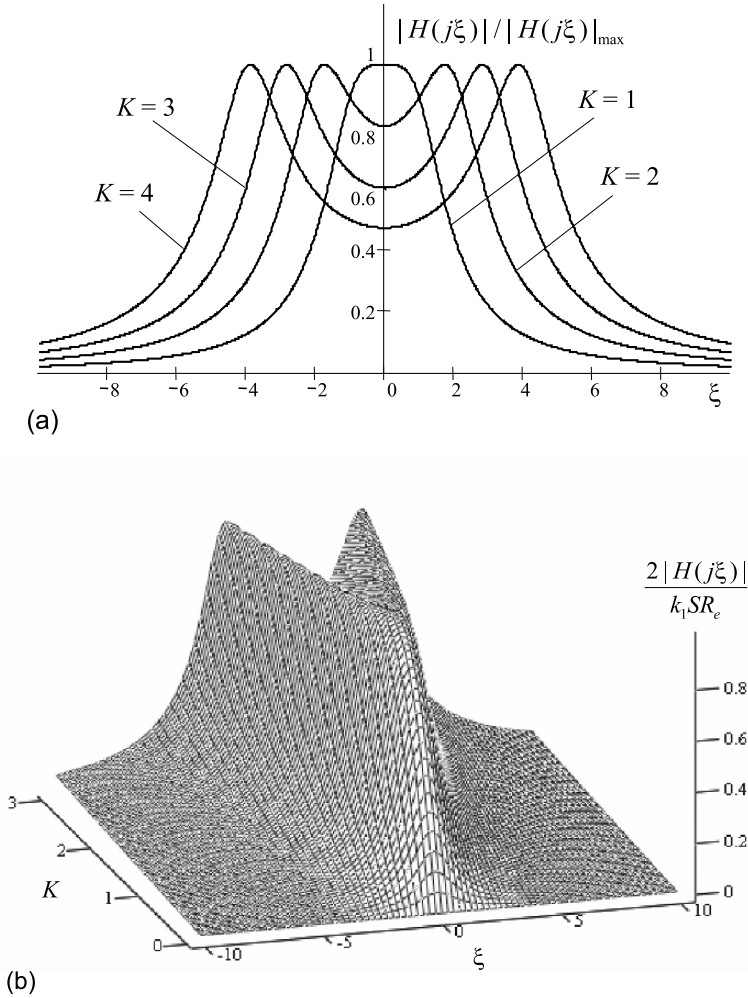


Fig. 5.17. Magnitude response of a two coupled resonant circuits: (a) by several values of K and (b) surface plot, by small values of K .

Piezoelectric Resonators

As electro-mechanical devices, *piezoelectric resonators* employ BAW vibrations featured to crystals. Nowadays, piezoelectric resonators are manufactured for watches (Fig. 5.18a), oscillators of different frequencies and applications (Fig. 5.18b), quartz crystal standards of frequency (Fig. 5.18c), sensors of various physical quantities, and for special applications.

Because waves in bulk media propagate in different directions, there are different kinds of BAW vibrations in any crystal resonator. Therefore, the

fundamental vibration is accompanied with a number of *spurious vibrations* often called *anharmonics*. In schemes, a piezoelectric resonator is imaged as in Fig. 5.18d. Its basic equivalent scheme comprises four principle components: motional inductance L_q , capacitance C_q , resistance R_q , and a static capacitance C_0 . Any of the ahnharmonic vibrations is commonly accounted for by an additional series resonance branch as shown in Fig. 5.18e.

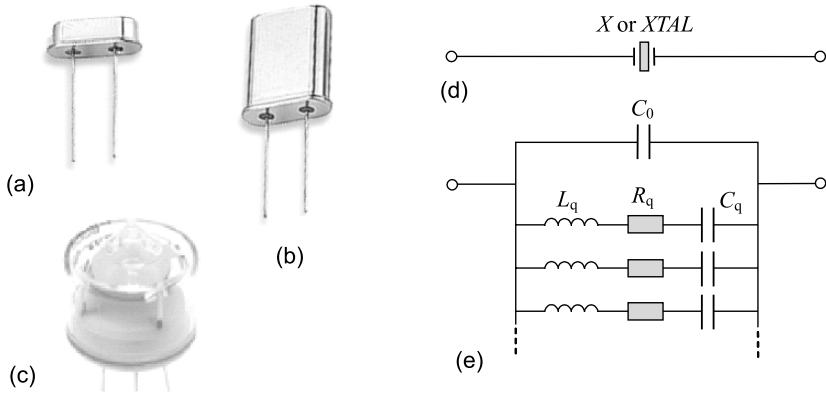


Fig. 5.18. Piezoelectric resonator: (a) for watches, (b), for oscillators, (c) precision, (d) schematic image, and (e) basic equivalent scheme.

For the fundamental vibration, the complex impedance of a resonator is specified by the relation

$$\begin{aligned} Z_r(j\omega) &= \frac{\left(j\omega L_q + \frac{1}{j\omega C_q} + R_q\right) \frac{1}{j\omega C_0}}{j\omega L_q + \frac{1}{j\omega C_q} + R_q + \frac{1}{j\omega C_0}} \\ &= |Z_r(j\omega)| e^{j\varphi_r(\omega)} = r_r(\omega) + jx_r(\omega) \end{aligned} \quad (5.78)$$

that can be represented in simpler forms if to introduce the resonator κ -factor, normalized frequency offset ν , and auxiliary coefficient $\alpha(\nu)$, respectively,

$$\kappa = R_q \omega C_0 > 0, \quad (5.79)$$

$$\nu = \frac{\omega - \omega_r}{\delta_r},$$

$$\alpha = \nu \left(1 + \frac{\nu}{4Q_r}\right) \left(1 + \frac{\nu}{2Q_r}\right)^{-1},$$

where $\omega_r^2 = \frac{1}{L_q C_q}$ is the resonator angular frequency, $2\delta_r = \frac{R_q}{L_q} = \frac{1}{Q_r^2 R_q C_q}$ is a resonator bandwidth, and $Q_r = \frac{\omega_r}{2\delta_r}$ is the quality factor.

By the above introduces quantities, the real part, imaginary part, total impedance, and phase of a resonator are described by, respectively,

$$r_r = R_q \frac{1}{(1 - \alpha\kappa)^2 + \kappa^2}, \quad (5.80)$$

$$x_r = R_q \frac{\alpha(1 - \alpha\kappa) - \kappa}{(1 - \alpha\kappa)^2 + \kappa^2}, \quad (5.81)$$

$$Z_r = R_q \frac{\sqrt{1 + [\alpha(1 - \alpha\kappa) - \kappa]^2}}{(1 - \alpha\kappa)^2 + \kappa^2}, \quad (5.82)$$

$$\tan \varphi_r = \alpha(1 - \alpha\kappa) - \kappa. \quad (5.83)$$

Fig. 5.19 shows (solid curves) typical spectral functions of an admittance $Y_r(j\omega) = Z_r^{-1}(j\omega)$ associated with the fundamental vibration of a piezoelectric resonator. It is seen that the maximum, $Y_r(j\omega_s) \cong R_q$, and minimum of $Y_r(j\omega)$

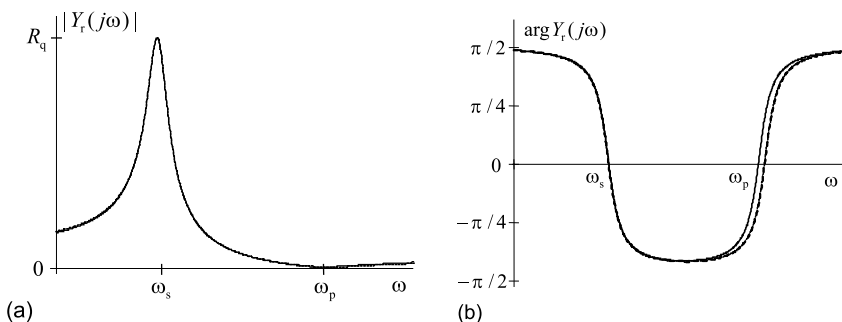


Fig. 5.19. Admittance of a piezoelectric resonator for $\kappa = 0.06$ and $Q = 100$, rigorous (solid) and approximate (dashed): (a) total and (b) phase.

correspond to the series and parallel resonance frequencies, respectively,

$$\omega_s \cong \frac{1}{\sqrt{L_q C_q}},$$

$$\omega_p \cong \omega_s \left(1 + \frac{C_q}{2C_0} \right).$$

The most important particular value of the κ -factor (5.79) is $\kappa_0 = R_q \omega_r C_0$. It can be shown that when $\kappa_0 > 0.5$, the phase never crosses zero that does not meet practical needs. Therefore, the κ -factor is commonly obtained such that $0 < \kappa_0 < 0.5$. We notice that a reciprocal of κ_0 is often called the *figure of merit*,

$$M_0 = \frac{1}{\kappa_0},$$

for which the relevant range of existence is $2 < M_0 < \infty$.

The quality factor of a crystal resonator is large, $Q > 10^4$. Therefore, by $Q \gg 1$, one can allow $\kappa \cong \kappa_0$ and $\alpha \cong \nu$, representing the spectral characteristics (5.80)-(5.83) in the interresonance gap by, respectively,

$$r_r = R_q \frac{1}{(1 - \nu\kappa_0)^2 + \kappa_0^2}, \tag{5.84}$$

$$x_r = R_q \frac{\nu(1 - \nu\kappa_0) - \kappa_0}{(1 - \nu\kappa_0)^2 + \kappa_0^2}, \tag{5.85}$$

$$Z_r = R_q \frac{\sqrt{1 + [\nu(1 - \nu\kappa_0) - \kappa_0]^2}}{(1 - \nu\kappa_0)^2 + \kappa_0^2}, \tag{5.86}$$

$$\tan \varphi_r = \nu(1 - \nu\kappa_0) - \kappa_0. \tag{5.87}$$

Dashed curves in Fig. 5.19 sketch approximate values of the total impedance and phase for $Q = 100$. It follows that, even by $Q = 100$, the difference between the relative curves is small. It almost vanishes when $Q > 10^4$.

Owing to highly stable structure of crystal media, the bandwidth of a crystal resonator can be achieved to be extremely narrow and the Q in best quartz crystal resonators of millions of units. That is, of course, of high applied importance for accurate and precise electronic systems.

BAW Piezoelectric Filters

Piezoelectric filters are used as signal processing devices allowing for high operation quality both in passband (minimum attenuation) and stopband (maximum attenuation). In such filters, owing to high quality factor, the transition region between the passband and stopband can be obtained to be extremely narrow. However, the constant group delay cannot be achieved and its deviation from the required value may cause troubles.

Two elementary configurations of piezoelectric filters are recognized. The ‘crystal’ can be placed either in the series arm (Fig. 5.20a) or shunt arm (Fig. 5.20b) of a ladder circuit. In each of these generalized schemes, the impedances Z_1 and Z_2 are intended to provide final adjustment of the frequency response and match the filter at the input and output. An additional

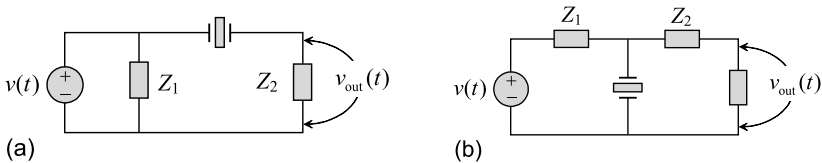


Fig. 5.20. Elementary ladder piezoelectric filters with a ‘crystal’: (a) in series arm and (b) in shunt arm.

capacitor may be included in series with a crystal to obtain a subtle correction of frequency.

Crystal ladder filters are widely used in SSB transmitters and CW receivers. However, they are not as perfect as the somewhat sophisticated lattice piezoelectric filter shown in Fig. 5.21. The lattice filter is fully symmetrical

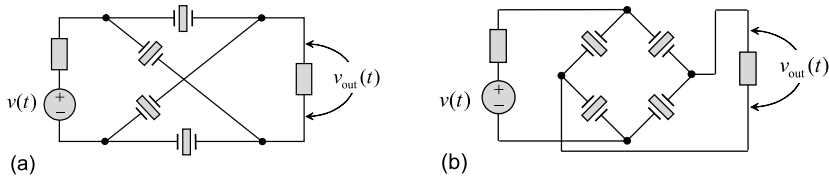


Fig. 5.21. Lattice piezoelectric filter: (a) basic and (b) redrawn as a bridge.

and balanced. Its bandwidth extends to more than twice the bandwidth of a corresponding ladder filter. In the stopband, the attenuation depends on the ratio of impedances of ‘crystals’ in the bridges. Overall, the frequency response of the lattice filter can be obtained to be highly symmetric about a center of the passband.

Any of the above-considered elementary schemes can be organized to structures in order to obtain small attenuation in the passband and efficient suppression beyond the bandwidth. Examples of the ladder filter structures are shown in Fig. 5.22. In the upper sideband (USB) structure (Fig. 5.22a), the

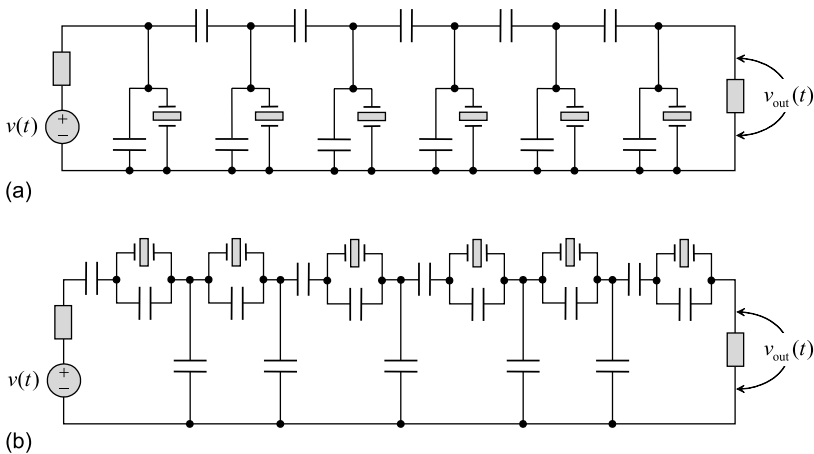


Fig. 5.22. Ladder piezoelectric filter structures: (a) upper sideband and (b) lower sideband.

filter passes signals with high frequencies and provides an efficient attenuation in the low frequency stopband. Contrary, the lower sideband (LSB) structure (Fig. 5.22b) allows through signals with low frequencies and efficiently suppresses components with high frequencies.

Examples of the frequency responses of USB and LSB ladder filter structures are shown in Fig. 5.23 with dashed and solid curves, respectively. If to

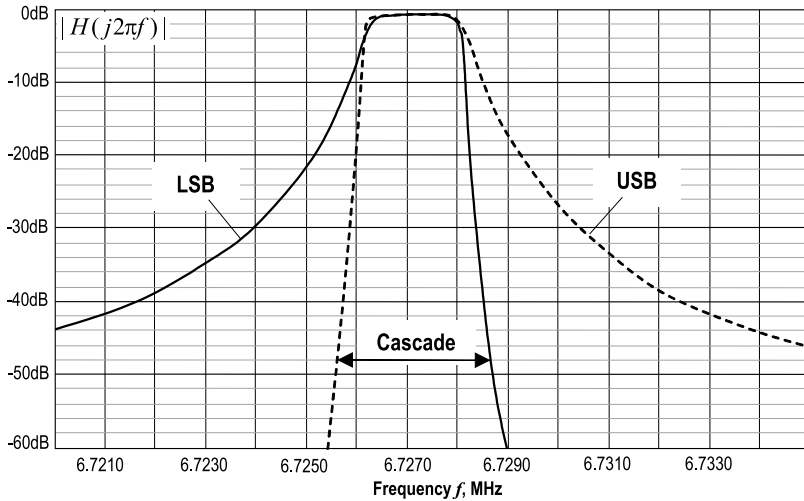


Fig. 5.23. Frequency response of a cascade of LSB and USB ladder piezoelectric structures.

include these structures in cascade, the resulting frequency response will possess a high-order of rectangularity in the extremely narrow band (Fig. 5.23).

SAW Devices

Surface acoustic wave (SAW) devices exploit properties of an acoustic wave traveling along the piezoelectric surface. The waves were discovered in 1887 by Lord Rayleigh and named for their discoverer. The first SAW devices based on the transduction of acoustic waves were made in 1965 for pulse compression radars and in the subsequent years there has been an explosion in their development. Nowadays, SAW devices are employed as filters, oscillators, transformers, and sensors covering applications ranging from professional radar and communications systems to consumer areas such as TV (SAW filters began replacing LC filters in TV-sets since 1985), pagers and mobile phones (since 1990). The world-wide production of different SAW devices stands at hundreds of millions annually.

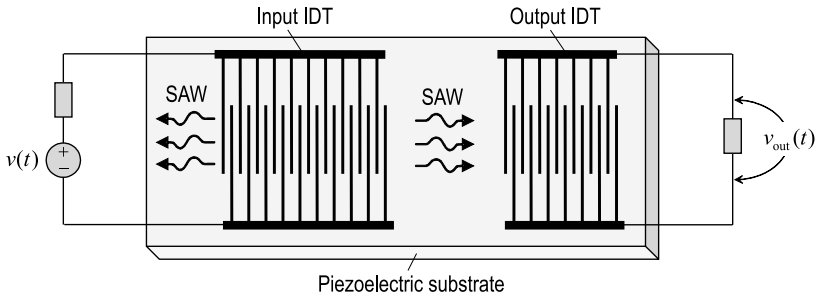


Fig. 5.24. Basic design of the SAW device.

A typical design of the SAW device is sketched in Fig. 5.24. The basic SAW device consists of two interdigital transducers (ITDs) placed on one of the surfaces of a piezoelectric substrate. The input ITD converts the electric signal $v(t)$ to the SAW and about a half of its energy propagates in opposite directions as shown in Fig. 5.24. While propagating, the SAW attenuates with about $6\text{dB}/\mu\text{s}$. The part of the SAW distributed toward the output IDT is reconverted, by this IDT, back to the electric signal. Other operation principles of the SAW device can easily be understood if it is mentioned that each IDT can be represented by a parallel resonant circuit of three elements: radial conductance (resistance), acoustic susceptance (inductance), and transducer capacitance (capacitance).

LTI SAW devices are manufactured with different configurations of evaporated elements. Their typical duties are time delaying, BP or BR filtering, and resonance.

A typical organization of the SAW delay line is shown in Fig. 5.25. Having a small propagation velocity ($3000\text{--}5000\text{ m/s}$) of the SAW, the design allows for time delay of microseconds with low attenuation in the radio frequency (RF) range up to gigahertz.

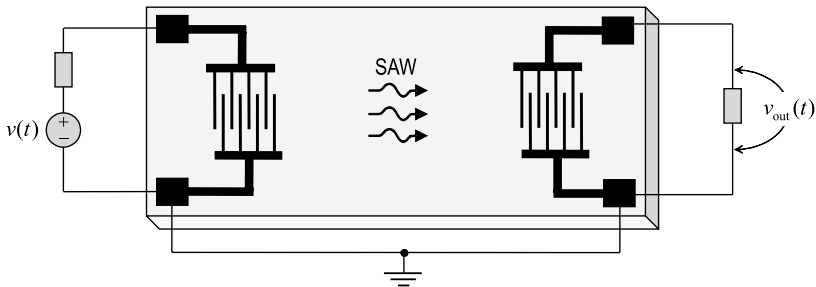


Fig. 5.25. SAW delay line.

In principle, the IDT can be designed to provide any required frequency response. This noble feature allows designing the SAW filters of different applications. A typical design of the BP one is shown in Fig. 5.26. The filter still

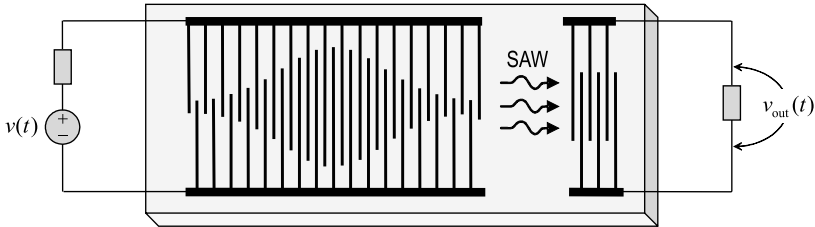


Fig. 5.26. SAW BP filter.

has two IDTs. Therefore, the required frequency response is formed by both IDTs. However, only the first IDT is usually manufactured to have a desired configuration as, for example, in Fig. 5.26. In spite of all the utterly useful properties demonstrated by the filter, there is an important disadvantage. Because of finite dimensions of the substrate truncate the ideal impulse response, unwanted in-band ripples appear along with the reduced out-of-band rejection.

Typically, SAW filters are designed to have the central frequency from 10 MHz to 2 GHz, transition bandwidth of 0.35 MHz to 1.5 MHz, insertion loss of < 3 dB to > 30 dB, passband amplitude ripple of ± 3 dB, and peak phase deviation of $\pm 3^\circ$.

A SAW device can serve a resonator if to make efforts in conserving the SAW energy in the IDT area. A typical design of the SAW resonator is shown in Fig. 5.27. A short IDT is placed at a center of the crystal substrate. To reflect the SAW back to the IDT with small dissipation, two distributed passive reflector banks (reflection gratings) of period $\lambda/4$ are closely placed to the left and right from the IDT. In best SAW resonators, the reflection coefficient is achieved more than 99% allowing for the quality factor of $Q \sim 10^4$.

The highly important property of the above considered BAW and SAW devices is that they can realize LTI systems of extremely high orders. Thus, the frequency response may be obtained of almost any reasonably desired shape. On the other hand, precision and accuracy featured to such devices requires special efforts in modeling. Therefore, the piezoelectric structures are commonly subject to the computer-aided design.

All of the LTI systems so far considered in this Chapter have been analyzed in the frames of Fourier analysis. A usefulness of the approach is that the system ODE of an arbitrary order is substituted with the ratio of two power polynomials with the variable $j\omega$ and the coefficients exactly equal to those in the ODE. This ratio, having a meaning of the frequency response, can also

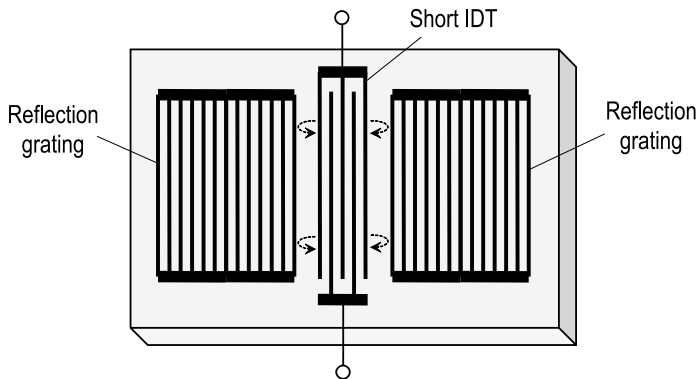


Fig. 5.27. SAW resonator.

be defined by the methods of linear circuits as we demonstrated above for systems of high-orders. Despite the certain engineering features, the Fourier method is not a suitable tool to investigate system stability. Whenever the latter is in question, the Laplace method is very often used being the most powerful in the transform domain.

5.3 Laplace Transform

The method by Laplace gives the other powerful technique to provide an analysis of LTI systems in the transform domain. The *Laplace transform* exists in two forms. The *bilateral* Laplace transform is a straightforward extension of the Fourier transform associated with non causal signals and systems. The *unilateral* Laplace transform relates to causal cases and is often used to solve the LTI system ODEs.

5.3.1 Bilateral Laplace Transform vs. Fourier Transform

To derive the bilateral Laplace transform, one can start with the familiar direct Fourier transform

$$X(j\omega) = \int_{-\infty}^{\infty} x(t)e^{-j\omega t} dt \quad (5.88)$$

applied to some signal $x(t)$ satisfying the Dirichlet conditions.

The transform (5.88) exploits the complex exponent function

$$e^{j\omega t} = \cos \omega t + j \sin \omega t \quad (5.89)$$

that is basic in the spectral analysis of signals. Real and imaginary components of (5.89) are shown in Fig. 5.28a. A generalization of the Fourier transform is achieved by using instead the general complex exponential function

$$e^{(\sigma+j\omega)t} = e^{\sigma t}(\cos \omega t + j \sin \omega t), \quad (5.90)$$

which real and imaginary parts are sketched in Fig. 5.28b for negative σ . The prime difference between two functions is that the envelope of $e^{j\omega t}$ is constant with time, whereas in $e^{(\sigma+j\omega)t}$ it becomes zero at infinity.

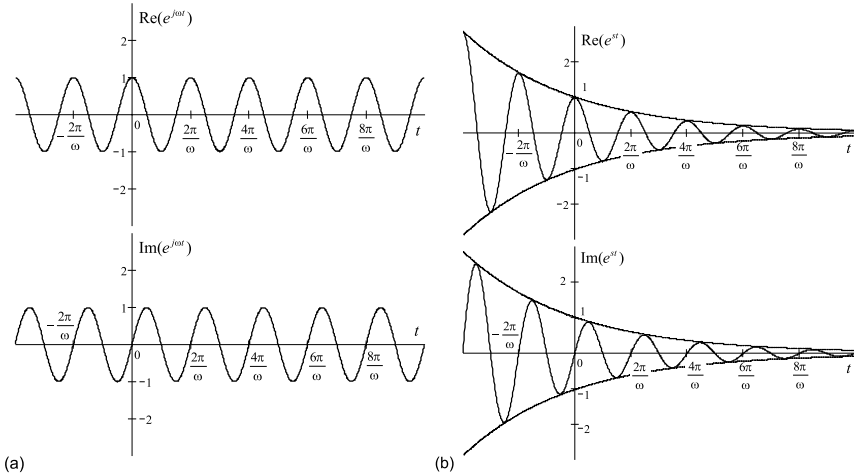


Fig. 5.28. Exponent functions: (a) complex (Fourier transform) and (b) general complex (Laplace transform).

Formally, we can rewrite (5.88) as

$$X(j\omega) = \int_{-\infty}^{\infty} x(t)e^{\sigma t}e^{-(\sigma+j\omega)t} dt,$$

introduce a new variable $s = \sigma + j\omega$, and go to the form of

$$X(j\omega) = \int_{-\infty}^{\infty} [x(t)e^{\sigma t}]e^{-st} dt,$$

meaning that

$$\mathcal{F}[x(t)] \triangleq X(j\omega) = \mathcal{L}[x(t)e^{\sigma t}],$$

where \mathcal{L} is newly introduced an integral operator. If we will think that $x(t) = x(t)e^{-\sigma t}$, we will arrive at the relation

$$\mathcal{F}[x(t)e^{-\sigma t}] = \mathcal{L}[x(t)] \triangleq X(s). \quad (5.91)$$

The function $X(s)$ in (5.91) is defined by the transform

$$X(s) \triangleq \mathcal{L}[x(t)] = \int_{-\infty}^{\infty} x(t)e^{-st} dt \quad (5.92)$$

known as the direct *bilateral Laplace transform* of $x(t)$.

Let us now apply the inverse Fourier transform to (5.91) and write

$$x(t)e^{-\sigma t} = \frac{1}{2\pi} \int_{-\infty}^{\infty} X(\sigma + j\omega)e^{j\omega t} d\omega.$$

By multiplying the both sides of this relation with $e^{\sigma t}$ and changing the variable, we arrive at the relation

$$x(t) \triangleq \mathcal{L}^{-1}[X(s)] = \frac{1}{2\pi j} \int_{\sigma-j\infty}^{\sigma+j\infty} X(s)e^{st} ds \quad (5.93)$$

called the inverse *bilateral Laplace transform* of $X(s)$. Accordingly, both (5.92) and (5.93) are said to be the bilinear Laplace transform pair.

The Laplace transform is denoted by

$$x(t) \stackrel{\mathcal{L}}{\Leftrightarrow} X(s),$$

where $X(s)$ is usually a rational function in s -plane

$$\begin{aligned} X(s) &= \frac{b_0 + b_1 s + \dots + b_M s^M}{a_0 + a_1 s + \dots + a_N s^N} \\ &= \frac{b_M (s - z_1)(s - z_2) \dots (s - z_M)}{a_N (s - p_1)(s - p_2) \dots (s - p_N)}. \end{aligned} \quad (5.94)$$

Here, M and N are positive integers and the coefficients a_i and b_j are real constants. The value M cannot exceed N in descriptions of real physical processes. If $N > M$, a ratio (5.94) is said to be the *proper* ratio. If $N \leq M$, it is the *improper* ratio.

In the Fourier transform, both $x(t)$ and $X(j\omega)$ are one-dimensional complex functions. In contrast, the Laplace transform $X(s)$ of $x(t)$ is a function defined over a two-dimensional complex plane, called s -plane, spanned by σ for the horizontal real axis and ω for the vertical imaginary axis. If $\sigma = 0$, the transforms are identical, so one-dimensional.

The roots z_i of the numerator tend $X(s)$ toward zero. Therefore, z_i are called *zeros* (or sometimes *nulls*) and indicated in the s -plane by cycles (“o”).

Contrary, the roots p_j of the denominator tend $X(s)$ toward infinity. Therefore, they are called the *poles* and indicated in the s -plane with crosses (“×”). The zeroes may lie inside and outside the region of convergence, whereas the poles cannot lie within this region, by the definition.

The magnitude function $|X(s)|$ can represent both nulls and poles by a surface plot. Fig. 5.29 shows an example of such a representation which benefit is in clarity featured to surface plots. A disadvantage is that $|X(s)|$ does not bear information about the region of convergence requiring an additional plot.

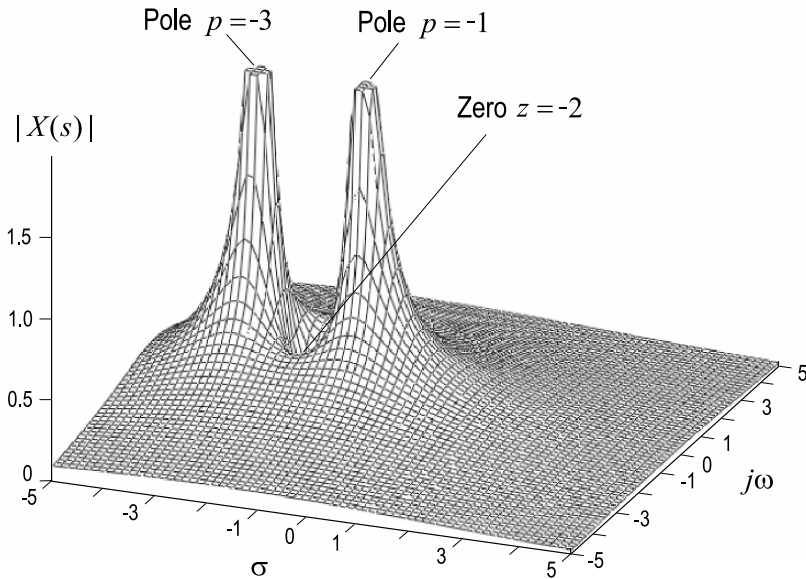


Fig. 5.29. Surface plot, by $|X(s)| = \left| \frac{s+2}{(s+1)(s+3)} \right|$.

5.3.2 Region of Convergence

Because the Laplace transform of $x(t)$ is the Fourier transform of $x(t)e^{-\sigma t}$, the former can be applied to a broader class of functions, including exponentially growing functions, satisfied the Dirichlet condition

$$\int_{-\infty}^{\infty} |x(t)e^{-\sigma t}| dt < \infty. \quad (5.95)$$

The set of values s for which (5.95) is true is called the *region of convergence* (ROC) of the function. The ROC of $X(s)$ is represented by strips

parallel to the $j\omega$ -axis in the s -plane. Such a representation also includes zeros and poles of $X(s)$ exhibiting the following properties:

Property 1: If $x(t)$ is absolutely integrable and of finite duration, then the ROC is the entire s -plane, since the Laplace transform is finite and $X(s)$ exists for any s . \square

Example 5.12. Consider a unit impulse $x(t) = \delta(t)$. By the sifting property of $\delta(t)$, the Laplace transform is defined to be

$$X(s) = \int_{-\infty}^{\infty} \delta(t)e^{-st} dt = e^{-s0} = 1.$$

The ROC thus occupies the entire s -plane without any zeros (and, of course, poles) as it is shown in Fig. 5.30a. \square

Property 2: If $x(t)$ is right-sided (i.e., exists with $t \geq 0$) and $\text{Re}[s] = a$ is in the ROC, then any s to the right of a (i.e., $\text{Re}[s] > a$) is also in the ROC. \square

Example 5.13. Given a signal $x(t) = e^{at}u(t)$, where a is arbitrary real. With $a > 0$, the Fourier transform of this function does not exist, since the Dirichlet conditions are not satisfied. Contrary, the Laplace transform is derived to be

$$\begin{aligned} X(s) &= \int_{-\infty}^{\infty} e^{at}u(t)e^{-st} dt = \int_0^{\infty} e^{-(s-a)t} dt = -\frac{1}{s-a}e^{-(s-a)t} \Big|_0^{\infty} \\ &= -\frac{1}{\sigma - a + j\omega}e^{-(\sigma-a)t}e^{-j\omega t} \Big|_0^{\infty}. \end{aligned}$$

The integral converges if only $\sigma > a$ and we have

$$X(s) = \frac{1}{s-a}, \quad \text{Re}(s) > a.$$

By $s = a$, the transform tends toward infinity, so there is a pole $p = a$. Fig. 5.30b sketches the ROC for this case. \square

Property 3: If $x(t)$ is left-sided (i.e., exists with $t \leq 0$) and $\text{Re}[s] = a$ is in the ROC, then any s to the left of a (i.e., $\text{Re}[s] < a$) is also in the ROC. \square

Example 5.14. Given a signal $x(t) = e^{at}u(-t)$, where a is arbitrary real. The Laplace transform integral

$$X(s) = \int_{-\infty}^0 e^{-(s-a)t} dt = -\frac{e^{-(s-a)t}e^{-j\omega t}}{\sigma - a + j\omega} \Big|_{-\infty}^0$$

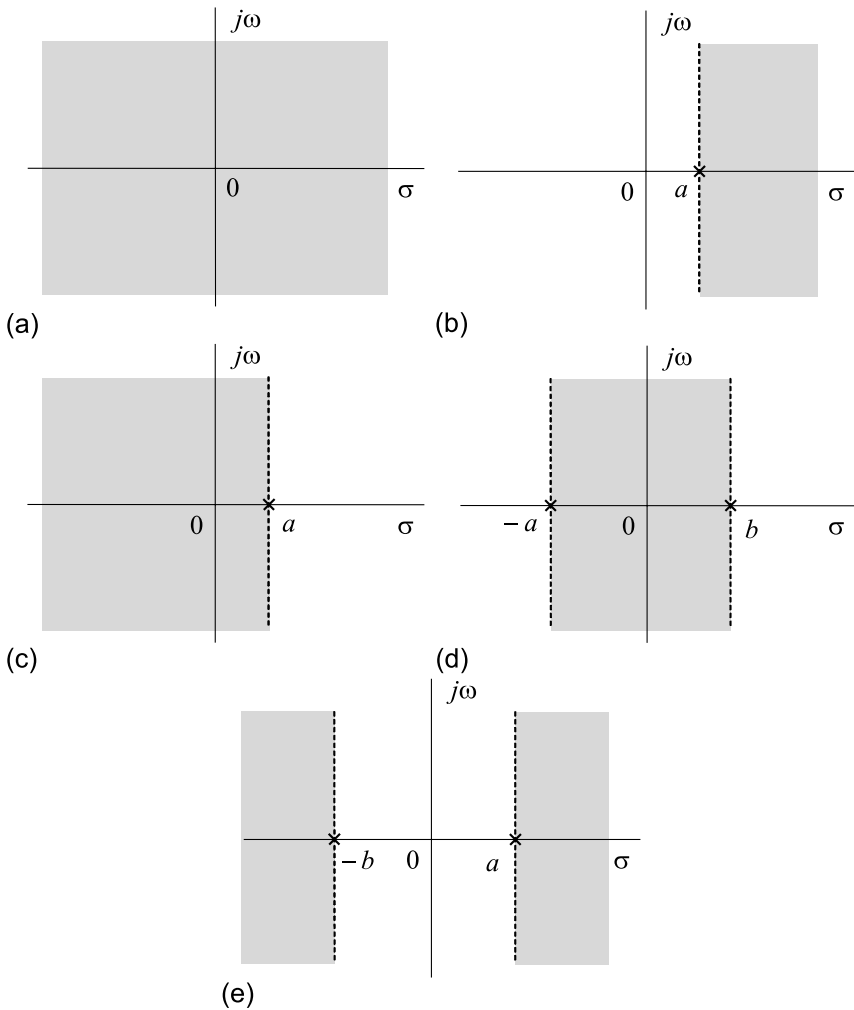


Fig. 5.30. ROCs of the Laplace transforms: (a) Example 5.12, (b) Example 5.13, (c) Example 5.14, (d) Example 5.15, (e) Example 5.16.

converges if $\sigma < a$ to produce

$$X(s) = \frac{1}{a - s}, \quad \text{Re}(s) < a,$$

with the pole $p = a$. Fig. 5.30c sketches the ROC for this case. □

Example 5.15. Given a signal $x(t) = -e^{-at}u(-t)$, where a is arbitrary real. The Laplace transform is

$$F(s) = \frac{1}{s - a}, \quad \text{Re}(s) < a,$$

having a pole $p = a$ and the same ROC as in Fig. 5.30c. \square

Property 4: If $x(t)$ is two-sided, then the ROC is the intersection of the two one-sided ROCs corresponding to the two one-sided components of $x(t)$. This intersection can be either a vertical strip or an empty set. \square

Example 5.16. Given a signal $x(t) = e^{-at}u(t) + e^{bt}u(-t)$, where $a > 0$ and $b > 0$. It follows, by Examples 5.13 and 5.14 that the ROC is a strip with two poles, $p_1 = -a$ and $p_2 = b$, as shown in Fig. 5.30d.

If we consider $x(t) = e^{at}u(t) + e^{-bt}u(-t)$, where $a > 0$ and $b > 0$, we arrive at the picture shown in Fig. 5.30e. \square

Property 5: A function $x(t)$ is absolutely integrable (satisfying the Dirichlet conditions and having the Fourier transform) if and only if the ROC of the corresponding Laplace transform $X(s)$ includes the imaginary axis, since $\text{Re}[s]=0$ and $s = j\omega$. \square

Example 5.17. Let us come back to Example 5.16. The ROC shown in Fig. 5.30d includes the imaginary axis and it can be shown that the relevant signal $x(t) = e^{-at}u(t) + e^{bt}u(-t)$, $a > 0$ and $b > 0$, is absolutely integrable. Contrary, the ROC in Fig. 5.30e does not contain the imaginary axis and the relevant function $x(t) = e^{at}u(t) + e^{-bt}u(-t)$, $a > 0$ and $b > 0$, does not satisfy the Dirichlet conditions, so is not absolutely integrable. \square

Observing Examples 5.13–5.15, we conclude that the same transform $1/(s - a)$ corresponds to different signals $e^{at}u(t)$ and $-e^{-at}u(-t)$. Yet, the same ROC $\text{Re}(s) < a$ fits different signals, $e^{at}u(-t)$ and $-e^{-at}u(-t)$. To explain these facts, one needs to remember the following fundamental property:

Fundamental property: In order for the bilateral Laplace transform $X(s)$ to be unique for each function $x(t)$, the ROC must be specified as part of the transform. \square

Overall, to represent $X(s)$ graphically, one can use either the $|X(s)|$ plot (Fig. 5.29) or ROC plot (Fig. 5.30). The latter is more preferable, because it bears a complete information about the transform, contrary to the former.

5.3.3 Properties of the Bilateral Laplace Transform

As any other transform, the Laplace transform demonstrates many useful properties allowing an efficient analysis of systems. In presenting these properties, we will think that the transform $X(s)$ of $x(t)$ is known and that the ROC depicted by R is known as well.

Time Shifting

Given a signal $x(t) \stackrel{\mathcal{L}}{\Leftrightarrow} X(s)$, $\text{ROC} = R$, and its shifted version $x_1(t) = x(t-t_0)$. The Laplace transform $X_1(s)$ of $x_1(t)$ is defined, by (5.92), as

$$X_1(s) = \int_{-\infty}^{\infty} x(t-t_0)e^{-st} dt, \quad \text{ROC} = R_1.$$

By changing a variable to $\theta = t - t_0$, we have

$$X_1(s) = \int_{-\infty}^{\infty} x(\theta)e^{-s(\theta+t_0)} d\theta = e^{-st_0} \int_{-\infty}^{\infty} x(\theta)e^{-s\theta} d\theta = e^{-st_0} X(s).$$

The *time shifting* property is thus ascertained by the following relationship and the same ROC as for $X(s)$:

$$x(t-t_0) \stackrel{\mathcal{L}}{\Leftrightarrow} e^{-st_0} X(s), \quad R_1 = R. \quad (5.96)$$

Example 5.18. A signal

$$x(t) = e^{at}u(t) \stackrel{\mathcal{L}}{\Leftrightarrow} X(s) = \frac{1}{s-a}, \quad \text{Re}(s) > a, \quad (5.97)$$

where a is arbitrary real, is shifted in time to be $x_1(t) = e^{a(t-t_0)}u(t-t_0)$. By (5.96), the Laplace transform $X_1(s)$ of $x_1(t)$ becomes

$$X_1(s) = \frac{e^{-st_0}}{s-a}, \quad \text{Re}(s) > a$$

and the inverse transformation readily leads to $x_1(s)$. □

Time Scaling

A pulse $x(t) \stackrel{\mathcal{L}}{\Leftrightarrow} F(s)$, $\text{ROC} = R$, is compressed (or stretched) in time to be $x_1(t) = x(\alpha t)$, where $\alpha > 0$. The Laplace transform $X_1(s)$ of $x_1(s)$ is

$$X_1(s) = \int_{-\infty}^{\infty} x(\alpha t)e^{-st} dt, \quad \text{ROC} = R_1.$$

By a new variable $\theta = \alpha t$ and $t = \theta/\alpha$ with $\alpha > 0$, we have

$$X_1(s) = \frac{1}{\alpha} \int_{-\infty}^{\infty} x(\theta)e^{-\frac{s}{\alpha}\theta} d\theta = \frac{1}{\alpha} X\left(\frac{s}{\alpha}\right), \quad R_1 = \alpha R,$$

where the ROC is scaled because of the scaling s/α in the transform. If $\alpha < 0$, a new variable $\theta = -\alpha t$ can be assigned leading to

$$\begin{aligned} X_1(s) &= \frac{1}{\alpha} \int_{\infty}^{-\infty} x(\theta) e^{-\frac{s}{\alpha}\theta} d\theta \\ &= -\frac{1}{\alpha} \int_{-\infty}^{\infty} x(\theta) e^{-\frac{s}{\alpha}\theta} d\theta = -\frac{1}{\alpha} X\left(\frac{s}{\alpha}\right), \quad R_1 = \alpha R. \end{aligned}$$

Thus, for arbitrary $\alpha \neq 0$, the following *scaling property* (also known as the *similarity theorem*) holds true:

$$x(\alpha t) \stackrel{\mathcal{L}}{\Leftrightarrow} \frac{1}{|\alpha|} X\left(\frac{s}{\alpha}\right), \quad R_1 = \alpha R. \quad (5.98)$$

Example 5.19. A signal (5.97) is scaled with $\alpha > 0$ to be $x_1(t) = e^{a\alpha t}u(\alpha t)$. By (5.88), the Laplace transform of the scaled signal is defined to be

$$F_1(s) = \frac{1}{s - a\alpha}, \quad \text{Re}(s) > \alpha a$$

and the inverse transform produces the origin. \square

Time Reversal

A signal $x(t) \stackrel{\mathcal{L}}{\Leftrightarrow} X(s)$, $\text{ROC} = R$, is presented in time reversal by $x_1(t) = x(-t)$. The Laplace transform $X_1(s)$ of $x_1(s)$ is given by

$$X_1(s) = \int_{-\infty}^{\infty} x(-t) e^{-st} dt, \quad \text{ROC} = R_1.$$

By a sign changed of time, we have

$$X_1(s) = - \int_{\infty}^{-\infty} x(t) e^{st} dt = \int_{-\infty}^{\infty} x(t) e^{-(-s)t} dt = X(-s)$$

and thus

$$x(-t) \stackrel{\mathcal{L}}{\Leftrightarrow} X(-s), \quad R_1 = -R, \quad (5.99)$$

meaning that time reversal of $x(t)$ produces a reversal of both σ axis and s axis in s -plane.

Example 5.20. A signal (5.97) is presented in time reversal by $x_1(t) = e^{-at}u(-t)$. By (5.98), the Laplace transform of the scaled function is

$$X_1(s) = -\frac{1}{s + a}, \quad \text{Re}(s) < a,$$

and the inverse transform leads to the origin. \square

Differentiation in Time

A signal $x(t) \stackrel{\mathcal{L}}{\Leftrightarrow} X(s)$, $\text{ROC} = R$, is differentiated in time to be $x_1 = dx(t)/dt$. To find the transform of $x_1(t)$, differentiate the both sides of (5.93) to have

$$\frac{dx(t)}{dt} = \frac{1}{2\pi j} \int_{\sigma-j\infty}^{\sigma+j\infty} [sF(s)]e^{st} ds.$$

It then follows straightforwardly that

$$\frac{dx(t)}{dt} \stackrel{\mathcal{L}}{\Leftrightarrow} sX(s), \quad R_1 \supset R. \quad (5.100)$$

Here R belongs to R_1 meaning that the ROC of the differentiated function is unchanged unless a cancellation (pole-zero) exists at $s = 0$.

Example 5.21. A unit impulse $x(t) = \delta(t) \stackrel{\mathcal{L}}{\Leftrightarrow} X(s) = 1$, $\text{R all } s$, is differentiated to be $x_1(t) = d\delta(t)/dt$. By (5.100), the transform of $x_1(t)$ becomes

$$F_1(s) = s, \quad \text{R all } s,$$

and the inverse transform leads to the origin. \square

Differentiation in the s Domain

A signal $x(t) \stackrel{\mathcal{L}}{\Leftrightarrow} X(s)$, $\text{ROC} = R$, is differentiated in the s domain to have a transform $X_1(s) = dX(s)/ds$. Differentiating (5.92) with respect to s yields

$$\frac{dX(s)}{ds} = \int_{-\infty}^{\infty} [-tx(t)]e^{-st} dt$$

and thus

$$-tx(t) \stackrel{\mathcal{L}}{\Leftrightarrow} \frac{dX(s)}{ds}, \quad R_1 = R. \quad (5.101)$$

Example 5.22. A unit impulse $x(t) = \delta(t) \stackrel{\mathcal{L}}{\Leftrightarrow} X(s) = 1$, $\text{R all } s$, is gained by t to be $x_1(s) = t\delta(t)$. By (5.101) and the sifting property of the δ -function, the transform of $x_1(t)$ is defined to be

$$X_1(s) = \frac{dX(s)}{ds} = \int_{-\infty}^{\infty} [-t\delta(t)]e^{-st} dt = 0e^{-s0} = 0, \quad \text{R all } s.$$

We arrive at the same result by differentiating $F(s) = 1$ with respect to s . \square

Integration in Time

A signal $x(t) \stackrel{\mathcal{L}}{\Leftrightarrow} X(s)$, $\text{ROC} = R$, is integrated in time to be

$$x_1(t) = \int_{-\infty}^t x(\theta) d\theta \stackrel{\mathcal{L}}{\Leftrightarrow} X_1(s).$$

By differentiating $x_1(t)$ and using (5.100), we have

$$x(t) = \frac{dx_1(t)}{dt} \stackrel{\mathcal{L}}{\Leftrightarrow} sX_1(s) = X(s)$$

and thus

$$\int_{-\infty}^t x(\theta) d\theta \stackrel{\mathcal{L}}{\Leftrightarrow} \frac{1}{s} X(s), \quad R_1 = R \cap [\text{Re}(s) > 0]. \quad (5.102)$$

The ROC R_1 follows from the possibility to have a pole at $s = 0$, by $1/s$.

Example 5.23. A signal

$$x(t) = e^{-at} u(t) \stackrel{\mathcal{L}}{\Leftrightarrow} X(s) = \frac{1}{s+a}, \quad \text{Re}(s) > -a,$$

$a > 0$, is integrated to be $x_1(t) = \frac{1}{a}(1 - e^{-at})u(t)$. By (5.92), we have

$$\begin{aligned} X_1(s) &= \frac{1}{a} \int_0^{\infty} (1 - e^{-at}) e^{-st} dt = \frac{1}{a} \int_0^{\infty} e^{-st} dt - \frac{1}{a} \int_0^{\infty} e^{-(s+a)t} dt \\ &= \frac{1}{as} - \frac{1}{a(s+a)} = \frac{1}{s(s+a)}, \quad [\text{Re}(s) > -a] \cap [\text{Re}(s) > 0]. \end{aligned}$$

Thus, $X_1(s) = \frac{1}{s} X(s)$ and the ROC is combined with two stripes, as claimed by (5.102). \square

Linearity

By the inherent property of linearity, if we have N signals,

$$x_i(t) \stackrel{\mathcal{L}}{\Leftrightarrow} X_i(s), \quad \text{ROC} = R_i,$$

where $i \in [1, N]$, then the transform of their addition is

$$\sum_{i=1}^N a_i x_i(t) \stackrel{\mathcal{L}}{\Leftrightarrow} \sum_{i=1}^N a_i X_i(s), \quad R_{\Sigma} \supset R_1 \cap R_2 \cap \dots \cap R_N. \quad (5.103)$$

The ROC R_{Σ} contains intersections between all of the particular ROCs as it is shown in Fig. 5.31 for two signals.

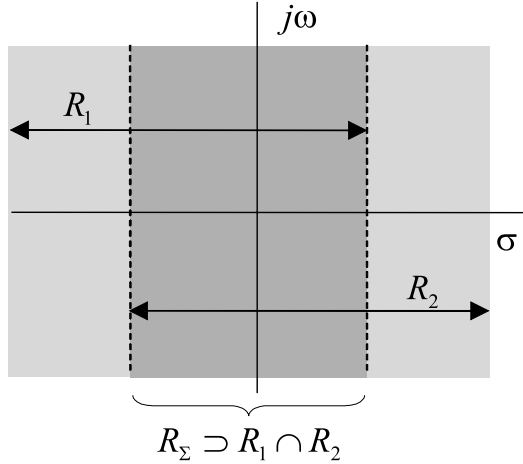


Fig. 5.31. ROC of an addition of two signals.

Example 5.24. A signal is composed by an additive sum of three truncated exponential subfunctions,

$$x(t) = e^{-2t}u(t) + 2e^{2t}u(-t) + e^{-t}u(t).$$

The transforms of the subfunctions are

$$x_1(t) = e^{-2t}u(t) \stackrel{\mathcal{L}}{\Leftrightarrow} X_1(s) = \frac{1}{s+2}, \quad \text{Re}(s) > -2,$$

$$x_2(t) = e^{2t}u(-t) \stackrel{\mathcal{L}}{\Leftrightarrow} X_2(s) = \frac{-1}{s-2}, \quad \text{Re}(s) < 2,$$

$$x_3(t) = e^{-t}u(t) \stackrel{\mathcal{L}}{\Leftrightarrow} X_3(s) = \frac{1}{s+1}, \quad \text{Re}(s) > -1.$$

By (5.103), the Laplace transform of a signal is defined to be

$$\begin{aligned} X(s) &= X_1(s) + 2X_2(s) + X_3(s) = \frac{1}{s+2} - \frac{2}{s-2} + \frac{1}{s+1} \\ &= \frac{-6(s + \frac{1}{3})}{(s+1)(s+2)(s-2)}, \quad -1 < \text{Re}(s) < 2. \end{aligned}$$

□

Example 5.25. A signal is given with

$$x(t) = Ae^{-a|t-\tau|}u(t),$$

where A and a are positive-values and τ is a time shift. A signal can be represented by an addition of three subfunctions,

$$x(t) = Ae^{a(t-\tau)}u(t) - Ae^{a(t-\tau)}u(t-\tau) + Ae^{-a(t-\tau)}u(t-\tau),$$

with known transform,

$$x_1(t) = e^{a(t-\tau)}u(t) \stackrel{\mathcal{L}}{\Leftrightarrow} X_1(s) = \frac{e^{-a\tau}}{s-a}, \quad \text{Re}(s) > a,$$

$$x_2(t) = e^{a(t-\tau)}u(t-\tau) \stackrel{\mathcal{L}}{\Leftrightarrow} X_2(s) = \frac{e^{-s\tau}}{s-a}, \quad \text{Re}(s) > a,$$

$$x_3(t) = e^{-a(t-\tau)}u(t-\tau) \stackrel{\mathcal{L}}{\Leftrightarrow} X_3(s) = \frac{e^{-s\tau}}{s+a}, \quad \text{Re}(s) > -a.$$

The transform of a signal is then defined, by (5.103), to be

$$\begin{aligned} X(s) &= A[X_1(s) + X_2(s) + X_3(s)] \\ &= A \frac{(s+a)e^{-a\tau} + 2se^{-s\tau}}{(s+a)(s-a)}, \quad \text{Re}(s) > a. \end{aligned}$$

□

Convolution in the Time Domain

This property is fundamental for the LTI systems description in the transform domain. Suppose the transforms of the input $x(t)$ and impulse response $h(t)$ of a system are known, respectively,

$$x(t) \stackrel{\mathcal{L}}{\Leftrightarrow} X(s), \quad \text{ROC} = R_x,$$

$$h(t) \stackrel{\mathcal{L}}{\Leftrightarrow} H(s), \quad \text{ROC} = R_h.$$

The output $y(t)$ is coupled with $x(t)$ via $h(t)$ by the convolution

$$y(t) = x(t) * h(t) = \int_{-\infty}^{\infty} x(\theta)h(t-\theta)d\theta.$$

By (5.92) applied to $y(t)$, we have

$$Y(s) = \int_{-\infty}^{\infty} \int_{-\infty}^{\infty} x(\theta)h(t-\theta)e^{-st}d\theta dt = \int_{-\infty}^{\infty} x(\theta) \left[\int_{-\infty}^{\infty} h(t-\theta)e^{-st}dt \right] d\theta$$

and then the time shift property (5.96) yields

$$Y(s) = \int_{-\infty}^{\infty} x(\theta)e^{-s\theta} H(s)d\theta = H(s) \int_{-\infty}^{\infty} x(\theta)e^{-s\theta} d\theta = H(s)X(s).$$

The latter relation means that

$$x(t) * h(t) \stackrel{\mathcal{L}}{\Leftrightarrow} X(s)H(s), \quad R_c \supset R_x \cap R_h, \quad (5.104)$$

where the ROC R_c contains an intersection of the ROCs of $X(s)$ and $H(s)$.

Example 5.26. Given a signal

$$x(t) = \delta(t) \stackrel{\mathcal{L}}{\Leftrightarrow} X(s) = 1$$

acting in the input of an LTI system having the impulse response, $a > 0$,

$$h(t) = e^{-at}u(t) \stackrel{\mathcal{L}}{\Leftrightarrow} H(s) = \frac{1}{s+a}, \quad \text{Re}(s) > -a.$$

The convolution and sifting property of the delta function yield the output

$$y(t) = x(t) * h(t) = \int_{-\infty}^{\infty} \delta(\theta)e^{-a(t-\theta)}u(t-\theta)d\theta = e^{-at}u(t)$$

that is equal to the impulse response. Thus

$$Y(s) = \frac{1}{s+a}, \quad \text{Re}(s) > -a.$$

By (5.104), we arrive at the same result straightforwardly. \square

Convolution in the Frequency Domain

Consider the transform of the product $x(t) = x_1(t)x_2(t)$ of two functions

$$x_1(t) \stackrel{\mathcal{L}}{\Leftrightarrow} X_1(s), \quad a_1 < \text{Re}(s) < b_1,$$

$$x_2(t) \stackrel{\mathcal{L}}{\Leftrightarrow} X_2(s), \quad a_2 < \text{Re}(s) < b_2,$$

We thus need evaluating the integral

$$X(s) = \int_{-\infty}^{\infty} x_1(t)x_2(t)e^{-st}dt.$$

Then substitute $x_2(t)$ with its inverse transform

$$x_2(t) = \frac{1}{2\pi j} \int_{\sigma-j\infty}^{\sigma+j\infty} X_2(s) e^{st} ds$$

and provide the transformations:

$$\begin{aligned} X(s) &= \frac{1}{2\pi j} \int_{-\infty}^{\infty} x_1(t) \left[\int_{\sigma-j\infty}^{\sigma+j\infty} X_2(s_1) e^{s_1 t} ds_1 \right] e^{-st} dt \\ &= \frac{1}{2\pi j} \int_{\sigma-j\infty}^{\sigma+j\infty} X_2(s_1) \left[\int_{-\infty}^{\infty} x_1(t) e^{-(s-s_1)t} dt \right] ds_1. \end{aligned}$$

Because the integral in brackets is the transform $X_1(s - s_1)$, we have

$$X(s) = \frac{1}{2\pi j} \int_{\sigma-j\infty}^{\sigma+j\infty} X_2(s_1) X_1(s - s_1) ds_1$$

that comprises the convolution in the transform domain, and thus

$$x_1(t)x_2(t) \stackrel{\mathcal{L}}{\Leftrightarrow} \frac{1}{2\pi j} X_1(s) * X_2(s), \quad a_1 + a_2 < \operatorname{Re}(s) < b_1 + b_2, \quad (5.105)$$

where, it can be shown, the ROC's lower and upper bounds are summed.

Modulation

Let us think that the following signal is known,

$$x(t) \stackrel{\mathcal{L}}{\Leftrightarrow} X(s), \quad a < \operatorname{Re}(s) < b,$$

and be interested of the transform $X_1(s)$ of the modulated signal $x_1(t) = e^{\alpha t} x(t)$. We then have

$$X_1(s) = \int_{-\infty}^{\infty} x(t) e^{\alpha t} e^{-st} dt = \int_{-\infty}^{\infty} x(t) e^{-(s-\alpha)t} dt$$

and thus

$$e^{\alpha t} x(t) \stackrel{\mathcal{L}}{\Leftrightarrow} X(s - \alpha), \quad a + \alpha < \operatorname{Re}(s) < b + \alpha. \quad (5.106)$$

We have considered, proved, and illustrated with examples many of the most common properties of the bilateral Laplace transform. These and some other properties are postponed to Appendix D. A common conclusion is that the bilateral Laplace transform, as a generalization of the Fourier transform, deals with both causal and noncausal signals and systems. Yet, it must be supplied with the ROC for the transform to be unique for each function.

5.3.4 System Characterization with Transfer Function

The convolution property of the Laplace transform gives us the rule (5.104) to investigate an LTI system in the transform domain, provided the definition:

Transfer function: The ratio of the Laplace transform $Y(s)$ of the output $y(t)$ and the Laplace transform $X(s)$ of the input $x(t)$ is the LTI system transfer function $H(s)$,

$$H(s) = \frac{Y(s)}{X(s)}. \quad (5.107)$$

□

An equivalent alternative definition is also valid for LTI systems:

Transfer function: The Laplace transform of the system impulse response $h(t)$ is the LTI system transfer function $H(s)$,

$$h(t) \stackrel{\mathcal{L}}{\Leftrightarrow} H(s)$$

□

So, the transfer function $H(s)$ completely characterizes an LTI system because the impulse response $h(t)$ completely characterizes the same system. The generalized structure of an LTI system in the transform domain is thus as in Fig. 5.32.

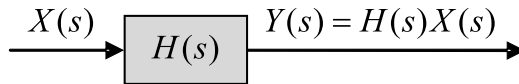


Fig. 5.32. Generalized structure of an LTI system in the transform domain.

Stability

To ascertain stability of an LTI system in the transform domain, we recall that the system is BIBO stable if and only if its impulse response function $h(t)$ is absolutely integrable; that is,

$$\int_{-\infty}^{\infty} |h(\tau)| d\tau \leq M < \infty.$$

Let us now consider the absolute value of the Laplace transform of the absolutely integrable $h(t)$ assuming that $s = j\omega$ (or $\sigma = 0$):

$$|H(j\omega)| = \left| \int_{-\infty}^{\infty} h(t)e^{-j\omega t} dt \right| \leq \int_{-\infty}^{\infty} |h(t)e^{-j\omega t}| dt$$

$$= \int_{-\infty}^{\infty} |h(t)|e^{-j\omega t} dt < \infty. \quad (5.108)$$

We thus have the only condition, meaning that an LTI system is stable if the ROC of its $H(s)$, by $\sigma = 0$, contains the imaginary axis $j\omega$.

Causality

The property of causality is usually associated with stability. The following typical cases are recognized.

Causal system. The ROC of $H(s)$ for the causal system must be right-hand placed (Property 2 of the ROC),

$$\operatorname{Re}(s) > a, \quad (5.109)$$

where a is real. By virtue of that, the ROC of a causal system is the region in the s -plane to the right of all the system poles. Example 5.27 and Fig. 5.33a give relevant illustrations, by $H_1(s)$ and $\operatorname{Re}(s) > -0.5$.

Noncausal system. If an LTI system is characterized with the impulse response $h(t) = \begin{cases} h(t) & t < 0 \\ 0 & t \geq 0 \end{cases}$, the system is noncausal. For such a system, the ROC of $H(s)$ is specified by

$$\operatorname{Re}(s) < a, \quad (5.110)$$

meaning that the region of the ROC is left-hand placed in the s -plane and all the system poles are to the right of this region. Example 5.25 and Fig. 5.33b illustrate this case, by $H_3(s)$ and $\operatorname{Re}(s) < 0.5$.

Stable and causal systems. If an LTI system is both causal and stable, all the poles of $H(s)$ must lie in the left half of the s -plane. Moreover, because of $\operatorname{Re}(s) > a$, all poles have negative real parts and, since the axis $j\omega$ is included in the ROC, the value of a must be negative, $a < 0$.

Example 5.27. Consider LTI systems represented with the transfer functions

$$H_1(s) = \frac{s-1}{(s+2)(s^2+2s+2)}, \quad \operatorname{Re}(s) > -0.5,$$

$$H_2(s) = \frac{s-1}{(s+2)(s^2+2s+2)}, \quad \operatorname{Re}(s) > 1,$$

$$H_3(s) = \frac{s+2}{(s-1)(s^2-2s+2)}, \quad \operatorname{Re}(s) < 0.5,$$

$$H_4(s) = \frac{s+2}{(s-1)(s^2-2s+2)}, \quad \operatorname{Re}(s) < -0.5.$$

The system $H_1(s)$ has a zero $z_1 = 1$ and three roots in the denominator: $s_1 = -2$, $s_2 = -1 + j$, and $s_3 = -1 - j$. Because the ROC includes the axis $j\omega$ and all of the poles lie to the left of the ROC, the system is both stable and causal (Fig. 5.33a).

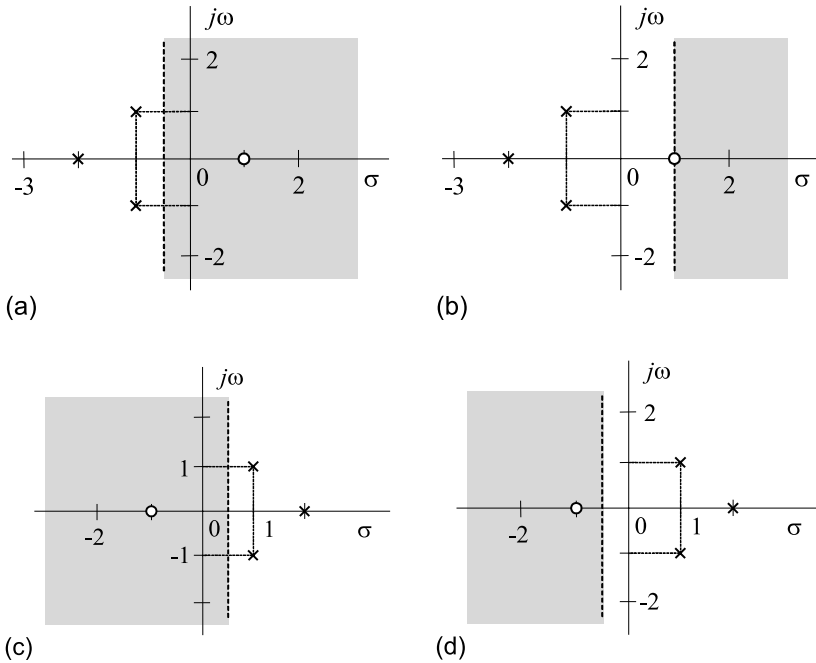


Fig. 5.33. LTI systems: (a) stable and causal, (b) unstable and causal, (c) stable and noncausal, and (d) unstable and noncausal.

The system $H_2(s)$ has the same roots as in $H_1(s)$. However, its ROC does not include the $j\omega$ axis and this causal system is thus unstable (Fig. 5.33b).

The system $H_3(s)$ is characterized with a zero $z_1 = -2$ and three poles, $p_1 = 1$, $p_2 = 1 + j$, and $p_3 = 1 - j$. Since the ROC includes the $j\omega$ axis and all of the poles lie to the right of the ROC, the system is both stable and noncausal (Fig. 5.33c).

The system $H_4(s)$ has the same roots as in $H_3(s)$. However, its ROC does not contain the $j\omega$ axis and the system is thus unstable and noncausal (Fig. 5.33d). \square

5.3.5 The Inverse Laplace Transform

It is now a proper place to say several words about the calculus of the inverse Laplace transform that was earlier formally defined by (5.93) as

$$x(t) \triangleq \mathcal{L}^{-1}[X(s)] = \frac{1}{2\pi j} \int_{v-j\infty}^{v+j\infty} X(s)e^{st} ds. \quad (5.111)$$

To calculate (5.111) properly, the real value v in the integral bounds must satisfy the condition for the ROC. For example, if $X(s)$ has the ROC $a < \operatorname{Re}(s) < b$, the value v must be chosen such that $a < v < b$. If v is set correctly, the inverse transform (5.111) can be applied to all forms of the transform function.

Typically, $X(s)$ is represented with a ratio of the polynomial functions (5.94). Irrespective of a number of zeros and poles in the transform, the methods of evaluating the integral in (5.111) remain actually the same. If one cannot represent $X(s)$ by the sum of simple functions placed to a Laplace transform table, the partial fraction expansion is used. The technique allows splitting $X(s)$ into fractions with known inverse transforms. To define unknown coefficients in fractions, the *cover-up* method is exploited.

Distinct Real Roots

Let us think that (5.94) is performed with $b_M = a_N = 1$ having distinct real roots. We then may represent this ratio as a sum of fractions,

$$\begin{aligned} F(s) &= \frac{(s - z_1)(s - z_2) \dots (s - z_M)}{(s - p_1)(s - p_2) \dots (s - p_N)} \\ &= \frac{\alpha_1}{s - p_1} + \frac{\alpha_2}{s - p_2} + \dots + \frac{\alpha_N}{s - p_N}, \end{aligned} \quad (5.112)$$

where the coefficients α_i , $i \in [1, N]$, are still unknown. By the cover-up method, α_i is predetermined to be

$$\alpha_i = (s - p_i)X(s)\Big|_{s=p_i} \quad (5.113)$$

and the problem is reduced to algebraic manipulations.

Example 5.28. The transfer function is represented by the sum of fractions,

$$H(s) = \frac{s + 1}{s(s + 2)} = \frac{\alpha_1}{s} + \frac{\alpha_2}{s + 2},$$

in which the coefficients, α_1 and α_2 , are unknown. By (5.113), we have

$$\begin{aligned} \alpha_1 &= s \frac{s + 1}{s(s + 2)} \Big|_{s=0} = \frac{1}{2}, \\ \alpha_2 &= (s + 2) \frac{s + 1}{s(s + 2)} \Big|_{s=-2} = \frac{1}{2}, \end{aligned}$$

and the transfer function becomes

$$H(s) = \frac{1}{2s} + \frac{1}{2(s+2)}.$$

A Laplace transform table (Appendix D) gives the impulse response

$$h(t) = \frac{1}{2}(1 + e^{-2t})u(t)$$

that can also be obtained by the inverse Laplace integral. \square

Repeated Real Roots

If $X(s)$ is performed with repeated real roots, containing factors of the form $(s - p_j)^n$, where n is integer, they say that p_j is the multiple pole of $X(s)$ with multiplicity n . In line with the terms associated with $i \in [1, N]$, $i \neq j$, an expansion of $X(s)$ will contain of terms caused by $i = j$,

$$\frac{\beta_1}{s - p_j} + \frac{\beta_2}{(s - p_j)^2} + \dots + \frac{\beta_n}{(s - p_j)^n}, \quad (5.114)$$

for which the coefficients β_l , $l \in [1, n]$, are commonly determined by

$$\beta_{n-i} = \frac{1}{i!} \left. \frac{d^i}{ds^i} [(s - p_j)^n X(s)] \right|_{s=p_j}. \quad (5.115)$$

Example 5.29. The transfer function is represented by the sum of fractions as

$$H(s) = \frac{s^2 + 1}{s^2(s+2)} = \frac{\alpha_1}{s+2} + \frac{\beta_1}{s} + \frac{\beta_2}{s^2},$$

where α_1 , β_1 , and β_2 are unknown. By the cover-up method we have

$$\alpha_1 = (s+2) \left. \frac{s^2 + 1}{s^2(s+2)} \right|_{s=-2} = \frac{5}{4},$$

$$\beta_2 = s^2 \left. \frac{s^2 + 1}{s^2(s+2)} \right|_{s=0} = \frac{1}{2}$$

and, by (5.115), the remaining coefficient is defined to be

$$\beta_1 = \frac{d}{ds} \left[s^2 \frac{s^2 + 1}{s^2(s+2)} \right] \Big|_{s=0} = -\frac{1}{4}.$$

The transfer function is thus represented with

$$H(s) = \frac{5}{4(s+2)} - \frac{1}{4s} + \frac{1}{2s^2}$$

that readily converts, by a table of the transforms, to the impulse response

$$h(t) = \frac{1}{4}(5e^{-2t} - 1 + 2t)u(t).$$

Note that the function can also be derived by (5.111) with, however, larger routine. \square

Complex Roots

When some roots occur to be complex conjugate, two approaches are used. Frequently, they agree with complex roots and use partial fraction expansion to find simpler forms. We can also expand $X(s)$ to fractions with the polynomials of order higher than one and find transforms in a table. So, for complex conjugate roots, one can follow the rule provided by (5.112) and (5.114).

Example 5.30. Given a transfer function

$$H(s) = \frac{A}{(s+2)(s^2+2s+2)} = \frac{\alpha_1}{s+2} + \frac{\beta_1 + \beta_2 s}{s^2+2s+2},$$

having in the denominator three roots: $s_1 = -2$, $s_2 = -1+j$, and $s_3 = -1-j$.

By the cover-up method, (5.113), the coefficient α_1 is defined to be

$$\alpha_1 = (s+2) \frac{A}{(s+2)(s^2+2s+2)} \Big|_{s=-2} = \frac{A}{2}.$$

To determine β_1 and β_2 , we apply the same approach and go to

$$\begin{aligned} (\beta_1 + \beta_2 s)|_{s=s_1} &= (s^2+2s+2) \frac{A}{(s+2)(s^2+2s+2)} \Big|_{s=s_1}, \\ \beta_1 - \beta_2 + j\beta_2 &= \frac{A}{-1+j+2} = \frac{A}{2} - j\frac{A}{2}. \end{aligned}$$

By comparing the terms in the left-hand and right-hand sides, we define

$$\beta_1 = 0, \quad \beta_2 = \frac{A}{2}.$$

Finally, by α_1 , β_1 , and β_2 , the transfer function $H(s)$ is found to be

$$H(s) = \frac{A}{2(s+2)} + \frac{As}{2(s^2+2s+2)}$$

and, by rearranging the terms, becomes

$$H(s) = \frac{A}{2} \left[\frac{1}{(s+1)^2+1} - \frac{s+1}{(s+1)^2+1} + \frac{1}{s+2} \right].$$

By a table of the transforms, $H(s)$ easily converts to the impulse response

$$h(t) = \frac{Ae^{-t}}{2} (\sin t - \cos t + e^{-t}) u(t).$$

Observe that $h(t)$ derived is absolutely integrable, because a multiplier e^{-t} approaches zero with time. Yet, the system is stable, since all the roots are placed in the second and third quadrants of the s -plane. \square

5.4 Unilateral Laplace transform

For causal signals and systems, the *unilateral* (or *one-sided* or *singly-infinite*) Laplace transform turns out to be more efficient. Because the transform deals with functions defined in positive time, (5.92) modifies to

$$X(s) \triangleq \mathcal{L}[x(t)] = \int_{0^-}^{\infty} x(t)e^{-st} dt, \quad (5.116)$$

being the Laplace transform of a causal signal $x(t)u(t)$.

The lower bound is chosen in (5.116) as “0⁻” to integrate the delta function and its derivatives. This means that a small (zero) amount of a nearest past is allowed for the transform. Sometimes, the bound is set as “0⁺” to avoid integrating the delta function.

Because (5.116) ignores $x(t)$ for $t < 0$, the ROC of any unilateral Laplace transform, by the Property 2 of the ROC, is always of the form $\text{Re}(s) > a$ and thus right-hand placed in the s -plane. For this reason, the ROC for (5.116) is often omitted and the transform is called just the Laplace transform.

5.4.1 Properties of the Unilateral Laplace Transform

Restricted to zero, the lower integration bound causes special properties of the unilateral Laplace transform associated with differentiation and integration. The other properties are common for both forms of the transform.

Differentiation in Time

Let us think that a causal $x(t)$ and its unilateral transform $X(s)$ are known. Then the transform $X_1(s)$ of $x_1(t) = dx(t)/dt$ is defined, by (5.116), as

$$X_1(s) = \int_{0^-}^{\infty} \frac{dx(t)}{dt} e^{-st} dt.$$

By differentiating by parts, we go to the relation

$$X_1(s) = x(t)e^{-st} \Big|_{0^-}^{\infty} + s \int_{0^-}^{\infty} x(t)e^{-st} dt$$

that produces $X_1(s) = -x(0^-) + sX(s)$, $\text{Re}(s) > 0$. The property of differentiation in time is thus stated by

$$\frac{dx(t)}{dt} \stackrel{\mathcal{L}}{\Leftrightarrow} sX(s) - x(0^-), \quad (5.117)$$

claiming that the unilateral Laplace transform is sensitive to the initial condition in a causal LTI system.

Example 5.31. An LTI system of the first order is represented with the ODE $y' + 2y = 0$, $y(0) = y_0$. By (5.117), the unilateral transform gives $sY(s) - y_0 + 2Y(s) = 0$ and

$$Y(s) = \frac{y_0}{s + 2}.$$

Using a table of the Laplace transforms, we arrive at

$$y(t) = y_0 e^{-2t}$$

avoiding solving the ODE in the time domain by traditional methods. \square

Double Differentiation in Time

Let us find the Laplace transform of the second time derivative of a signal $x(t)$, which $X(s)$ is known. By (5.117), the transform can be written as

$$\frac{dx^2(t)}{dt^2} = \frac{d}{dt} \frac{dx(t)}{dt} \stackrel{\mathcal{L}}{\Leftrightarrow} s[sX(s) - x(0^-)] - x'(0^-),$$

where $x'(0^-)$ is the value of the first time derivative of $x(t)$ and zero. The property is thus established by

$$\frac{dx^2(t)}{dt^2} \stackrel{\mathcal{L}}{\Leftrightarrow} s^2 X(s) - sx(0^-) - x'(0^-). \quad (5.118)$$

Example 5.32. An LTI system of the second order is represented with the ODE $y'' + 2y' + y = 0$, $y(0) = 0.5$, and $y'(0) = 1$.

By (5.117) and (5.118), the transform is written as

$$s^2 Y(s) - \frac{s}{2} - 1 + 2sY(s) - 1 + Y(s) = 0,$$

producing

$$Y(s) = \frac{1}{2} \frac{s + 4}{s^2 + 2s + 1} = \frac{s + 4}{2(s + 1)^2}.$$

For repeated roots, by (5.114) and (5.115), we can write

$$Y(s) = \frac{s + 4}{2(s + 1)^2} = \frac{\beta_1}{s + 1} + \frac{\beta_2}{(s + 1)^2}$$

and define the coefficients as

$$\beta_2 = (s+1)^2 \frac{s+4}{2(s+1)^2} \Big|_{s=-1} = \frac{3}{2},$$

$$\beta_1 = \frac{d}{ds} \left[(s+1)^2 \frac{s+4}{2(s+1)^2} \right] \Big|_{s=-1} = \frac{1}{2}.$$

The transform then attains the form

$$Y(s) = \frac{1}{2(s+1)} + \frac{3}{2(s+1)^2}$$

and, by a table of the transforms, we go to a solution

$$y(t) = \frac{1}{2}(1+3t)e^{-t},$$

without actually solving the ODE. □

Integration in Time

In causal systems, signals are integrated over finite bounds from 0 to t . They can also be integrated over the entire past history from $-\infty$ to t .

In the first case, if a causal signal $x(t) \stackrel{\mathcal{L}}{\Leftrightarrow} X(s)$ is known, of interest is evaluating the unilateral Laplace transform of the integral measure

$$x_1(t) = \int_{0^-}^t x(\theta) d\theta \tag{5.119}$$

that, alternatively, can be written as

$$x(t) = \frac{dx_1(t)}{dt}, \quad x_1(0^-) = 0. \tag{5.120}$$

If we apply the unilateral Laplace transform to (5.120), we arrive at

$$X(s) = sX_1(s) - x_1(0^-) = sX_1(s) \quad \text{or} \quad X_1(s) = \frac{1}{s}X(s)$$

that proves the property of integration in time:

$$\int_{0^-}^t x(\theta) d\theta \stackrel{\mathcal{L}}{\Leftrightarrow} \frac{1}{s}X(s). \tag{5.121}$$

In the second case, we can consider two integrals,

$$x_1(t) = \int_{-\infty}^t x(\theta) d\theta = \int_{-\infty}^{0^-} x(\theta) d\theta + \int_{0^-}^t x(\theta) d\theta. \quad (5.122)$$

By virtue of the fact that the integration from $-\infty$ to 0^- of any function produces a constant, say A , we arrive at the relevant property:

$$\int_{-\infty}^t x(\theta) d\theta \stackrel{\mathcal{L}}{\Leftrightarrow} \frac{1}{s}X(s) + \frac{1}{s}A, \quad A = \int_{-\infty}^{0^-} x(\theta) d\theta. \quad (5.123)$$

Example 5.33. An LTI system is described with the integral equation

$$y(t) + 2 \int_{-\infty}^t y(\theta) d\theta = 0, \quad \int_{-\infty}^{0^-} y(\theta) d\theta = 1.$$

The unilateral Laplace transform, by (5.123), produces

$$Y(s) + \frac{2}{s} + \frac{2}{s}Y(s) = 0$$

that becomes

$$Y(s) = -\frac{2}{s+2}$$

corresponding to the time-signal $y(t) = -2e^{-2t}$. □

Initial Value Theorem

Frequently, it needs evaluating an initial value $x(0^-)$ of $x(t)$ via the unilateral Laplace transform $X(s)$. To find this value, let us rewrite (5.117) as

$$\int_{0^-}^{\infty} \frac{dx(t)}{dt} e^{-st} dt = sX(s) - x(0^-)$$

and tend s to infinity,

$$\lim_{s \rightarrow \infty} \int_{0^-}^{\infty} \frac{dx(t)}{dt} e^{-st} dt = \lim_{s \rightarrow \infty} [sX(s) - x(0^-)].$$

Because $\lim_{s \rightarrow \infty} \int_{0^-}^{\infty} \frac{dx(t)}{dt} e^{-st} dt = 0$, we have

$$x(0^-) = \lim_{s \rightarrow \infty} sX(s) \quad (5.124)$$

that is stated by the final value theorem.

Example 5.34. Let us come back to Example 5.31, where we found that

$$y(t) = -2e^{-2t} \stackrel{\mathcal{L}}{\Leftrightarrow} Y(s) = -\frac{2}{s+2}.$$

An initial value of a signal is $y(0) = -2$. We go to the same result by the initial value theorem (5.124). Indeed, we can write

$$\lim_{s \rightarrow \infty} sY(s) = \lim_{s \rightarrow \infty} -s \frac{2}{s+2} = -2$$

getting the same result alternatively. \square

Final Value Theorem

In a like manner, one can find the value of $x(t)$ at infinity. Consider the limit

$$\lim_{s \rightarrow 0} \int_{0^-}^{\infty} \frac{dx(t)}{dt} e^{-st} dt = \lim_{s \rightarrow 0} [sX(s) - x(0^-)].$$

Providing the transformations, we have

$$\int_{0^-}^{\infty} \frac{dx(t)}{dt} dt = \int_{0^-}^{\infty} dx(t) = x(\infty) - x(0^-) = \lim_{s \rightarrow 0} [sX(s) - x(0^-)]$$

and arrive at the relation

$$x(\infty) = \lim_{s \rightarrow 0} sX(s) \tag{5.125}$$

that is stated by the final value theorem.

Example 5.35. Consider the transform found in Example 5.32,

$$y(t) = \frac{1}{2}(1+3t)e^{-t} \stackrel{\mathcal{L}}{\Leftrightarrow} Y(s) = \frac{1}{2(s+1)} + \frac{3}{2(s+1)^2}.$$

The final value $y(\infty)$ is ascertained, by (5.125), to be zero,

$$\lim_{s \rightarrow 0} sY(s) = \lim_{s \rightarrow 0} s \left[\frac{1}{2(s+1)} + \frac{3}{2(s+1)^2} \right] = 0.$$

We arrive at the same result, by considering the limit

$$\lim_{t \rightarrow \infty} x(t) = \lim_{t \rightarrow \infty} \frac{1}{2}(1+3t)e^{-t} = 0$$

that shows an alternative way to hit a target. \square

5.4.2 Laplace Transforms of Some Common Functions

Not only properties of the Laplace transform are of prime importance in solving applied problems. The transforms of some common and widely used functions often help reaching the goal in the shortest way. Below we observe the transforms of several common functions and the reader is referred to Appendix D, where the transform pairs of many others are gathered.

Dirac Delta function

The Laplace transform of the delta function $x(t) = \delta(t)$ is derived by using the sifting property of $\delta(t)$,

$$X(s) = \int_{0^-}^{\infty} \delta(t)e^{-st} dt = e^{-s0} = 1.$$

No restrictions to the ROC are produced and we have

$$\delta(t) \stackrel{\mathcal{L}}{\Leftrightarrow} 1, \quad \text{ROC is all } s. \quad (5.126)$$

Unit Step Function

For $x(t) = u(t)$, we have

$$X(s) = \int_{0^-}^{\infty} u(t)e^{-st} dt = \int_0^{\infty} e^{-st} dt = -\frac{1}{s}e^{-st} \Big|_0^{\infty}.$$

The integral converges only if $\text{Re}(s) > 0$ and thus

$$u(t) \stackrel{\mathcal{L}}{\Leftrightarrow} \frac{1}{s}, \quad \text{Re}(s) > 0. \quad (5.127)$$

Rectangular Pulse

Having $x(t) = u(t) - u(t - \tau)$, we use the time shift property and obtain

$$\begin{aligned} X(s) &= \int_{0^-}^{\infty} u(t)e^{-st} dt - \int_{0^-}^{\infty} u(t - \tau)e^{-st} dt \\ &= \frac{1}{s} \left(-e^{-st} \Big|_0^{\infty} + e^{-st} \Big|_{\tau}^{\infty} \right). \end{aligned}$$

The integrals converge if $\text{Re}(s) > 0$ and we have

$$u(t) - u(t - \tau) \stackrel{\mathcal{L}}{\Leftrightarrow} \frac{1}{s} (1 - e^{-s\tau}), \quad \text{Re}(s) > 0. \quad (5.128)$$

Truncated Exponential Function

The transform of $x(t) = e^{-at}u(t)$, where a is real, is defined by

$$\begin{aligned} X(s) &= \int_{0^-}^{\infty} e^{-at}u(t)e^{-st}dt = \int_0^{\infty} e^{-(s+a)t}dt \\ &= -\frac{1}{s+a}e^{-(s+a)t}\Big|_0^{\infty}. \end{aligned}$$

It is seen that the integrals converge if $\text{Re}(s) > -a$ and hence

$$e^{-at}u(t) \stackrel{\mathcal{L}}{\Leftrightarrow} \frac{1}{s+a}, \quad \text{Re}(s) > -a. \quad (5.129)$$

Truncated Sinusoid

Given a signal $x(t) = u(t) \sin \omega_0 t$. By Euler's formula, we have

$$\begin{aligned} X(s) &= \int_{0^-}^{\infty} u(t) \sin \omega_0 t e^{-st} dt = \int_0^{\infty} \frac{e^{j\omega_0 t} - e^{-j\omega_0 t}}{2j} e^{-st} dt \\ &= \frac{1}{2j} \int_0^{\infty} e^{-(s-j\omega_0)t} dt - \frac{1}{2j} \int_0^{\infty} e^{-(s+j\omega_0)t} dt \\ &= -\frac{1}{2j(s-j\omega_0)} e^{-(s-j\omega_0)t} \Big|_0^{\infty} + \frac{1}{2j(s+j\omega_0)} e^{-(s+j\omega_0)t} \Big|_0^{\infty}. \end{aligned}$$

Here, both integrals converge if $\text{Re}(s) > 0$. For this ROC, we have

$$X(s) = \frac{1}{2j(s-j\omega_0)} - \frac{1}{2j(s+j\omega_0)} = \frac{\omega_0}{s^2 + \omega_0^2}$$

and thus

$$u(t) \sin \omega_0 t \stackrel{\mathcal{L}}{\Leftrightarrow} \frac{\omega_0}{s^2 + \omega_0^2}, \quad \text{Re}(s) > 0. \quad (5.130)$$

Truncated Cosine Function

In a like manner, the transform of a causal cosine signal $x(t) = u(t) \cos \omega_0 t$ can be found to be

$$u(t) \cos \omega_0 t \stackrel{\mathcal{L}}{\Leftrightarrow} \frac{s}{s^2 + \omega_0^2}, \quad \text{Re}(s) > 0. \quad (5.131)$$

Finishing with examples, we notice again that the Laplace transforms of some other common functions are postponed to Appendix D.

5.5 Applications of Laplace transform

Owing to many splendid properties, the Laplace transform has found wide applications in a broad area of systems problems. The transform helps solving elegantly linear ODEs of systems and offers an incredibly useful tool for electrical circuits. LTI systems can efficiently be simulated in the transform domain by block diagrams. Finally, the state space model is easily analyzed, by the transform.

5.5.1 Solution of ODEs of LTI Systems

The most appreciable application of the Laplace transform is in solving the ODEs of LTI systems. To apply the transform to the N -order ODE, it first needs extending a property (5.117) to the multiple time derivative case. Comparing (5.117) and (5.118) one logically arrives at the rule

$$\begin{aligned} \frac{dx^n(t)}{dt^n} \stackrel{\mathcal{L}}{\Leftrightarrow} s^n X(s) - s^{n-1}x(0^-) - s^{n-2}x'(0^-) - \dots \\ - sx^{(n-2)}(0^-) - x^{(n-1)}(0^-). \end{aligned} \quad (5.132)$$

Now consider a familiar general ODE of an LTI system,

$$\sum_{n=0}^N a_n \frac{d^n}{dt^n} y(t) = \sum_{m=0}^M b_m \frac{d^m}{dt^m} x(t), \quad M \leq N. \quad (5.133)$$

If we think that the input is known, $x(t) \stackrel{\mathcal{L}}{\Leftrightarrow} X(s)$, the function $x(t)$ is multiply differentiable,

$$x(0) = x_0, \quad x'(0) = x'_0, \quad \dots, \quad x^{(M-1)}(0) = x_0^{(M-1)},$$

and all of the initial conditions are distinct,

$$y(0) = y_0, \quad y'(0) = y'_0, \quad \dots, \quad y^{(N-1)}(0) = y_0^{(N-1)},$$

we can apply the unilateral transform to (5.133), use (5.132), and write

$$\begin{aligned} \sum_{n=0}^N a_n \left[s^n Y(s) - s^{n-1}y(0^-) - \dots - sy^{(n-2)}(0^-) - y^{(n-1)}(0^-) \right] \\ = \sum_{m=0}^M b_m \left[s^m X(s) - s^{m-1}x(0^-) - \dots - sx^{(m-2)}(0^-) - x^{(m-1)}(0^-) \right]. \end{aligned}$$

The transform of $y(t)$ can now be expressed as

$$Y(s) = X(s) \frac{\sum_{m=0}^M b_m s^m}{\sum_{n=0}^N a_n s^n} + \frac{\sum_{n=0}^N a_n F_{1n}(s) - \sum_{m=0}^M b_m F_{2m}(s)}{\sum_{n=0}^N a_n s^n}, \quad (5.134)$$

where

$$F_{1n}(s) = s^{n-1}y(0^-) + \dots + sy^{(n-2)}(0^-) + y^{(n-1)}(0^-), \quad (5.135)$$

$$F_{2m}(s) = s^{m-1}x(0^-) + \dots + sx^{(m-2)}(0^-) + x^{(m-1)}(0^-). \quad (5.136)$$

As can be seen, the first term in the right-hand side of (5.134) is the bilateral transform of $y(t)$ and the remainder accounts for the initial conditions and time derivatives of the input. It is clear that the remainder is zero if all of the initial conditions and derivatives are zero. Defined $Y(s)$, a table of the Laplace transforms may serve finding an analytic expression for $y(t)$.

Below, we use the Laplace transform to analyze in detail familiar LTI systems of the first and second orders.

LTI system of the First Order

A SISO LTI system of the first order is described with the ODE

$$a_1 \frac{d}{dt}y(t) + a_0 y(t) = b_0 x(t). \quad (5.137)$$

Assuming that the initial condition $y(0^-) = y_0$ is known and the input $x(t) \stackrel{\mathcal{L}}{\Leftrightarrow} X(s)$ is known as well, we apply (5.117) and arrive at

$$a_1[sY(s) - y_0] + a_0 Y(s) = b_0 X(s) \quad (5.138)$$

that leads to the transform

$$Y(s) = \frac{b_0}{a_1 s + a_0} X(s) + \frac{y_0 a_1}{a_1 s + a_0}. \quad (5.139)$$

The next step is to substitute $X(s)$ and represent $Y(s)$ with forms that can be found in tables of the Laplace transforms. Below we find solutions of (5.139) for two test signals.

Unit impulse in the input. If the input is $x(t) = \delta(t) \stackrel{\mathcal{L}}{\Leftrightarrow} X(s) = 1$, the transform (5.139) becomes

$$Y(s) = \frac{y_0 + b_0/a_1}{s + a_0/a_1},$$

producing the output

$$y(t) = \left(y_0 + \frac{b_0}{a_1} \right) e^{-\frac{a_0}{a_1} t}. \quad (5.140)$$

By $y_0 = 0$, the system impulse response appears to be $h(t) = \frac{b_0}{a_1} e^{-\frac{a_0}{a_1} t}$.

Example 5.36. Consider a system $y' + 2y = 0$, $y(0) = y_0$, which solution is $y(t) = y_0 e^{-2t}$. Compared to (5.137), this equation has the coefficients $a_0 = 2$, $a_1 = 1$, and $b_0 = 0$. Instantly, by (5.140), we have a solution $y(t) = y_0 e^{-2t}$. \square

Unit step in the input. By $x(t) = u(t) \stackrel{\mathcal{L}}{\Leftrightarrow} X(s) = 1/s$, the transform (5.139) becomes

$$\begin{aligned} Y(s) &= \frac{b_0/a_1}{s(s + a_0/a_1)} + \frac{y_0}{s + a_0/a_1} \\ &= \frac{y_0 - b_0/a_0}{s + a_0/a_1} + \frac{b_0}{a_0 s} \end{aligned} \quad (5.141)$$

producing a solution

$$y(t) = y_0 e^{-\frac{a_0}{a_1}t} + \frac{b_0}{a_0} (1 - e^{-\frac{a_0}{a_1}t}). \quad (5.142)$$

The system step response $g(t) = \frac{b_0}{a_0} (1 - e^{-\frac{a_0}{a_1}t})$ appears if to set $y_0 = 0$.

Example 5.37. Given a system, described with the ODE $y' + 2y = x$, $y(0) = 0$, having the coefficients $a_0 = 2$, $a_1 = 1$, and $b_0 = 1$. For $x(t) = u(t)$, its step response, by (5.142), becomes $g(t) = 0.5(1 - e^{-2t})$. \square

LTI System of the Second Order

A SISO LTI system of the second order can be described with the ODE

$$a_2 \frac{d^2}{dt^2} y(t) + a_1 \frac{d}{dt} y(t) + a_0 y(t) = b_0 x(t). \quad (5.143)$$

For arbitrary initial conditions, $y(0^-) = y_0$ and $y'(0^-) = y'_0$, and known input $x(t) \stackrel{\mathcal{L}}{\Leftrightarrow} X(s)$, the transform applied to (5.143) yields

$$a_2 [s^2 Y(s) - s y_0 - y'_0] + a_1 [s Y(s) - y_0] + a_0 Y(s) = b_0 X(s). \quad (5.144)$$

From (5.144) one instantly derives

$$Y(s) = \frac{b_0}{a_2 s^2 + a_1 s + a_0} X(s) + \frac{a_2 y_0 s + a_2 y'_0 + a_1 y_0}{a_2 s^2 + a_1 s + a_0} \quad (5.145)$$

and, again, a shortest way to find a solution $y(t)$ for known $X(s)$ is to use a table of the Laplace transforms.

Let, for example, the input be delta-shaped, $x(t) = \delta(t)$, thus $X(s) = 1$. The transform (5.145) then attains the form

$$Y(s) = \frac{a_2 y_0 s + a_2 y'_0 + a_1 y_0 + b_0}{a_2 s^2 + a_1 s + a_0} = y_0 \frac{s + \lambda}{(s + \alpha)^2 + \beta^2}, \quad (5.146)$$

where

$$\alpha = \frac{a_1}{2a_2}, \quad \beta^2 = \frac{4a_0a_2 - a_1^2}{4a_2^2}, \quad \lambda = \frac{a_2y_0' + a_1y_0 + b_0}{a_2y_0}. \quad (5.147)$$

By a table of the Laplace transforms, the output is obtained to be

$$y(t) = y_0 e^{-\alpha t} \left(\cos \beta t + \frac{\lambda - \alpha}{\beta} \sin \beta t \right). \quad (5.148)$$

Example 5.38. Consider a system described by $y'' + 2y' + y = 0$, $y(0) = \frac{1}{2}$, with the coefficients $a_0 = 1$, $a_1 = 2$, $a_2 = 1$, and $b_0 = 0$. By (5.147), we have $\alpha = 1$, $\beta = 0$, and $\lambda = 4$. The solution then becomes that, $y(t) = \frac{1}{2}(1+3t)e^{-t}$, earlier found in Example 5.32 for the same system. \square

5.5.2 Application to Electric Circuits

The approach to solve ODEs of LTI systems using the Laplace transform is efficiently exploited in electric circuits. Here, first, all signals and memory operations are substituted with the Laplace transform equivalents. Then the terms are properly rearranged and a table of the transforms is used to produce time functions. This new equivalent form in the s domain needs to remember that all memory components are physical, thus their energy at some initial time $t = 0$ may not be zero. The unilateral Laplace transform is therefore the best candidate to solve the block of problems.

Electric Voltage and Current

Because both the electric voltage $v(t)$ and current $i(t)$ are commonly some time functions, they can be represented in the s domain with the relevant transforms, respectively,

$$v(t) \stackrel{\mathcal{L}}{\Leftrightarrow} V(s), \quad i(t) \stackrel{\mathcal{L}}{\Leftrightarrow} I(s) \quad (5.149)$$

and graphical images in both domains as shown in Fig. 5.34. Note that throughout the book we use equal images of $i(t)$ and $v(t)$ sources for the alternative and direct currents and voltages, respectively.

Resistor

The transform of a voltage $v(t) = Ri(t)$ induced on a resistor R by an electric current $i(t)$ can be represented in the s domain, by (5.149), as

$$v(t) = Ri(t) \stackrel{\mathcal{L}}{\Leftrightarrow} V(s) = RI(s). \quad (5.150)$$

and sketched graphically as in Fig. 5.34.

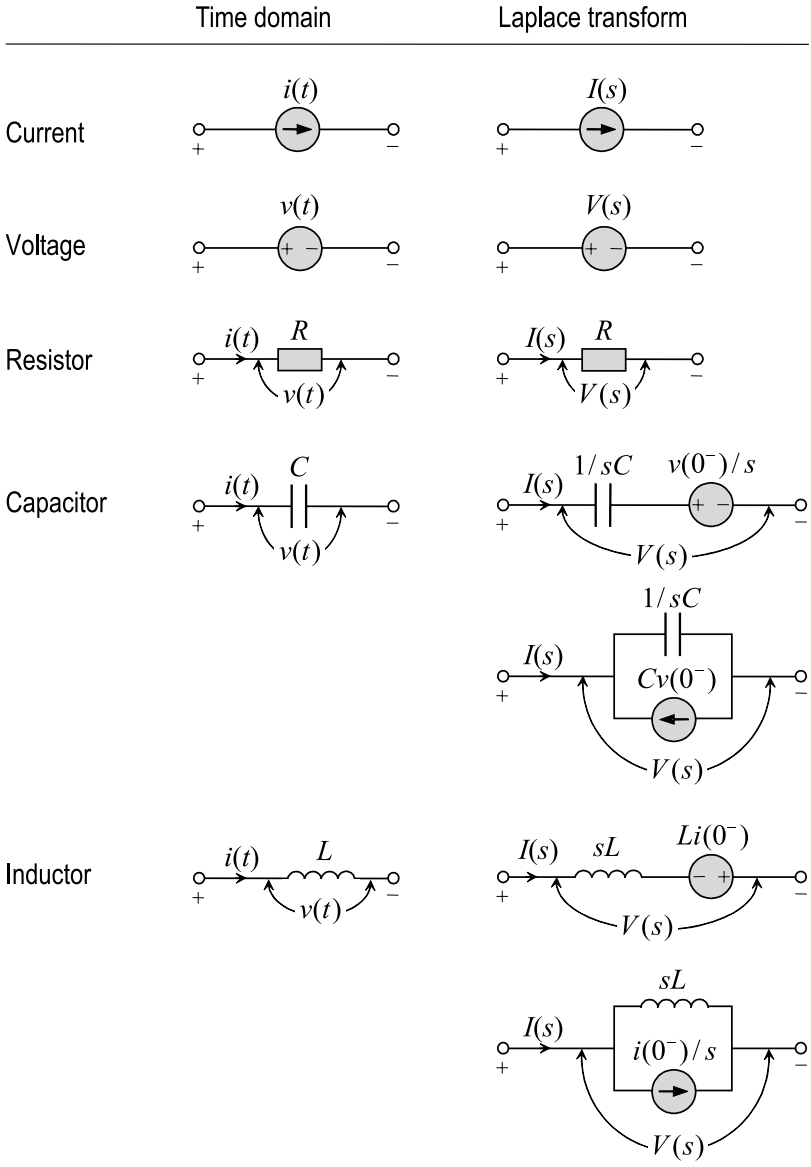


Fig. 5.34. Electric elements and their Laplace transform equivalents.

Capacitor

A voltage $v(t)$ induced on a constant capacitor C by an electric current $i(t)$ is given by the relation $v(t) = \frac{1}{C} \int_{-\infty}^t i(\tau) dt$. On the other hand, an electric current generated by the voltage through a capacitor is provided by $i(t) = Cdv(t)/dt$. By the properties of differentiation, (5.117), and integration, (5.123), we thus have two equal transforms

$$v(t) = \frac{1}{C} \int_{-\infty}^t i(\tau) d\tau \quad \Leftrightarrow \quad V(s) = \frac{1}{sC}I(s) + \frac{1}{s}v(0^-), \quad (5.151)$$

$$i(t) = C \frac{dv(t)}{dt} \quad \Leftrightarrow \quad I(s) = sCV(s) - Cv(0^-) \quad (5.152)$$

and two options (Fig. 5.34) in graphical representation.

Inductance

Reasoning similarly for an inductance L , we write

$$i(t) = \frac{1}{L} \int_{-\infty}^t v(t) dt \quad \Leftrightarrow \quad I(s) = \frac{1}{sL}V(s) + \frac{1}{s}i(0^-), \quad (5.153)$$

$$v(t) = L \frac{di(t)}{dt} \quad \Leftrightarrow \quad V(s) = sLI(s) - Li(0^-) \quad (5.154)$$

that is supported in Fig. 5.34 by graphical images.

RC and RL Circuits

Because of two different memory elements available, L and C , even a simplest electric circuit of the first order has two different schematic realizations.

RC circuit. Let us come back to a familiar LP filter organized with a resistor R and capacitor C (Fig. 5.5a). By Fig. 5.34, a representation of this circuit in the s domain becomes as in Fig. 5.35.

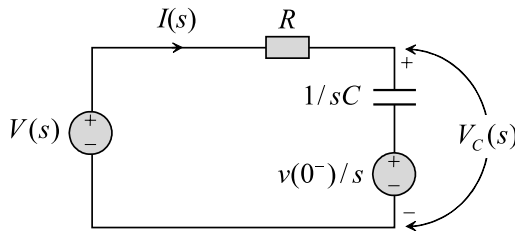


Fig. 5.35. Representation of an RC circuit in the s domain.

To describe the circuit, we first write an equality of voltages

$$V(s) = RI(s) + \frac{1}{sC}I(s) + \frac{1}{s}v_C(0^-) \quad (5.155)$$

that can further be rewritten for the electric current as

$$I(s) = \frac{1}{R} \frac{s}{s + 1/\tau_c} \left[V(s) - \frac{1}{s}v_C(0^-) \right], \quad (5.156)$$

where $\tau_c = RC$ is a time constant of the system.

By (5.156), the transform of a voltage induced on R is given by

$$V_R(s) = RI(s) = \frac{s}{s + 1/\tau_c} \left[V(s) - \frac{1}{s}v_C(0^-) \right] \quad (5.157)$$

and, by (5.151) and (5.156), the transform of a voltage on C becomes

$$\begin{aligned} V_C(s) &= I(s) \frac{1}{sC} + \frac{v_C(0^-)}{s} \\ &= \frac{1/\tau_c}{s + 1/\tau_c} \left[V(s) - \frac{1}{s}v_C(0^-) \right] + \frac{v_C(0^-)}{s}. \end{aligned} \quad (5.158)$$

So, the RC circuit is now fully represented in the s domain. Given the initial conditions, the functions can further be translated to the time domain, by a table of the Laplace transforms.

Example 5.39. Consider an RC circuit (Fig. 5.35), in which the input voltage is $v(t) = Vu(t) \stackrel{\mathcal{L}}{\Leftrightarrow} V(s) = V/s$.

By (5.156), the transform of an electric current can be found to be

$$I(s) = \frac{V - v_C(0^-)}{R} \frac{1}{s + 1/\tau_c} \quad (5.159)$$

that in the time domain becomes

$$i(t) = \frac{V - v_C(0^-)}{R} e^{-\frac{t}{\tau_c}}. \quad (5.160)$$

Instantly, we find the voltage induced on a resistor,

$$v_R(t) = Ri(t) = [V - v_C(0^-)]e^{-\frac{t}{\tau_c}}. \quad (5.161)$$

Substituting $V(s) = V/s$ to (5.158) gives

$$V_C(s) = [V - v_C(0^-)] \frac{1/\tau_c}{s(s + 1/\tau_c)} + \frac{v_C(0^-)}{s} \quad (5.162)$$

that has a counterpart in the time domain,

$$v_C(t) = [V - v_C(0^-)](1 - e^{-\frac{t}{\tau_c}})u(t) + v_C(0^-)u(t)$$

$$= V(1 - e^{-\frac{t}{\tau_c}})u(t) + v_C(0^-)e^{-\frac{t}{\tau_c}}u(t). \quad (5.163)$$

If we now set $V = 1$ and assume $v_C(0^-) = 0$, the function (5.163) becomes the system step response

$$g(t) = (1 - e^{-\frac{t}{\tau_c}})u(t), \quad (5.164)$$

earlier provided by (4.63) with $\tau_c = RC$. \square

RL circuit. The other electric circuit of the first order (Fig. 5.5b) comprises a resistor R and inductor L . By Fig. 5.34, its equivalent in the s domain is as shown in Fig. 5.36.

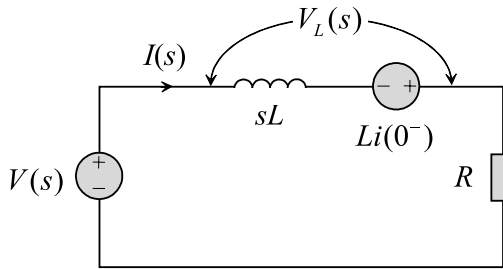


Fig. 5.36. Representation of an RL circuit in the s domain.

The voltage balance equation of the circuit can be written as

$$V(s) = (sL + R)I(s) - Li(0^-) \quad (5.165)$$

that allows finding the transforms of an electric current

$$I(s) = \frac{1}{L} \frac{1}{s + 1/\tau_c} [V(s) + Li(0^-)], \quad (5.166)$$

where $T = L/R$ is a time constant, and voltage induced on a resistor

$$V_R(s) = RI(s) = \frac{1/\tau_c}{s + 1/\tau_c} [V(s) + Li(0^-)]. \quad (5.167)$$

By (5.166), the transform of a voltage induced on L can be written as

$$\begin{aligned} V_L(s) &= I(s)sL - Li(0^-) \\ &= V(s) - \frac{1/\tau_c}{s + 1/\tau_c} [V(s) - Li(0^-)]. \end{aligned} \quad (5.168)$$

The circuit is thus exhaustively represented in the s domain and all of the functions can further be translated to the time domain by tables of the Laplace transforms.

Example 5.40. Given a system (Fig. 5.36) with the input voltage $v(t) = Ve^{-\alpha t}u(t) \stackrel{\mathcal{L}}{\Leftrightarrow} V(s) = \frac{V}{s+\alpha}$, $\alpha > 0$.

For the input given, the transform (5.166) of $i(t)$ becomes

$$I(s) = \frac{V}{L} \frac{1}{(s + 1/\tau_c)(s + \alpha)} + \frac{1}{s + 1/\tau_c} i(0^-) \quad (5.169)$$

corresponding, by a table of the Laplace transforms, to the time function

$$i(t) = \frac{V}{L} \frac{1}{\alpha - 1/\tau_c} \left(e^{-\frac{t}{\tau_c}} - e^{-\alpha t} \right) + i(0^-) e^{-\frac{t}{\tau_c}}. \quad (5.170)$$

The voltage induced on a resistor is thus

$$V_R(t) = V \frac{1/\tau_c}{\alpha - 1/\tau_c} \left(e^{-\frac{t}{\tau_c}} - e^{-\alpha t} \right) + i(0^-) e^{-\frac{t}{\tau_c}}. \quad (5.171)$$

By (5.168), the transform $V_L(s)$ is defined as

$$V_L(s) = \frac{V}{s + \alpha} - \frac{V/\tau_c}{(s + 1/\tau_c)(s + \alpha)} + \frac{L/\tau_c}{s + 1/\tau_c} i(0^-), \quad (5.172)$$

having a time domain presentation

$$v_L(t) = V \frac{\alpha}{\alpha - 1/\tau_c} e^{-\alpha t} u(t) - \left[V \frac{1/\tau_c}{\alpha - 1/\tau_c} - Ri(0^-) \right] e^{-\frac{t}{\tau_c}} u(t). \quad (5.173)$$

One can observe that all of the time functions were obtained here with a relatively lower burden, unlike a direct solution of the ODE. \square

Series Resonant RLC Circuit

Basic electric RLC circuits of the second order exist in two configurations. They typically exploit either a series or parallel connection.

By Fig. 5.34, a series RLC circuit is represented in the s domain as shown in Fig. 5.37. The voltage balance equation is written as

$$V(s) = I(s) \left(sL + \frac{1}{sC} + R \right) - Li(0^-) + \frac{1}{s} v_C(0^-)$$

and the transform of an electric current is readily expressed by

$$I(s) = \frac{1}{L} \frac{s}{s^2 + 2\delta s + \omega_0^2} \left[V(s) + Li(0^-) - \frac{1}{s} v_C(0^-) \right], \quad (5.174)$$

where $2\delta = R/L$ and $\omega_0^2 = 1/LC$. The transforms of voltages induced on the circuit components are

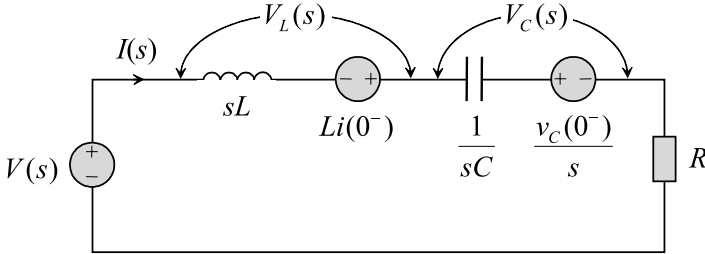


Fig. 5.37. Representation of a series RLC circuit in the s domain.

$$V_R(s) = \frac{2\delta s}{s^2 + 2\delta s + \omega_0^2} \left[V(s) + Li(0^-) - \frac{1}{s}v_C(0^-) \right], \quad (5.175)$$

$$V_L(s) = \frac{s^2}{s^2 + 2\delta s + \omega_0^2} \left[V(s) + Li(0^-) - \frac{1}{s}v_C(0^-) \right] - Li(0^-), \quad (5.176)$$

$$V_C(s) = \frac{\omega_0^2}{s^2 + 2\delta s + \omega_0^2} \left[V(s) + Li(0^-) - \frac{1}{s}v_C(0^-) \right] + \frac{v_C(0^-)}{s}. \quad (5.177)$$

Example 5.41. Given a system (Fig. 5.37) with the input $v(t) = Vu(t) \stackrel{\mathcal{L}}{\Leftrightarrow} V(s) = \frac{V}{s}$ and following components: $C = 0.5\text{F}$, $L = 1\text{H}$, $R = 2\Omega$, $i(0^-) = 0$, $V = 2\text{V}$, and $v_C(0^-) = 1\text{V}$. We thus have $\omega_0^2 = 2$ and $\delta = 1$.

For the parameters given, the transform (5.174) of $i(t)$ becomes

$$I(s) = \frac{1}{s^2 + 2s + 2} = \frac{1}{(s + 1)^2 + 1}$$

having a time representation $i(t) = e^{-t}u(t) \sin t$. Reasoning similarly, one can find time functions of each of the voltages in the circuit:

$$\begin{aligned} v_R(t) &= 2e^{-t}u(t) \sin t, \\ v_L(t) &= e^{-t}(\cos t - \sin t)u(t), \\ v_C(t) &= [2 - e^{-t}(\cos t + \sin t)]u(t). \end{aligned}$$

Fig. 5.38 illustrates all time functions associated with this circuit obtained by the Laplace transform equivalents. □

5.5.3 Block Diagram Presentation by the Laplace Transform

The other value of the Laplace transform is that we can efficiently simulate any LTI systems by block diagrams in a manner similar to the time domain.

The simulation by diagrams presumes starting with the system ODE

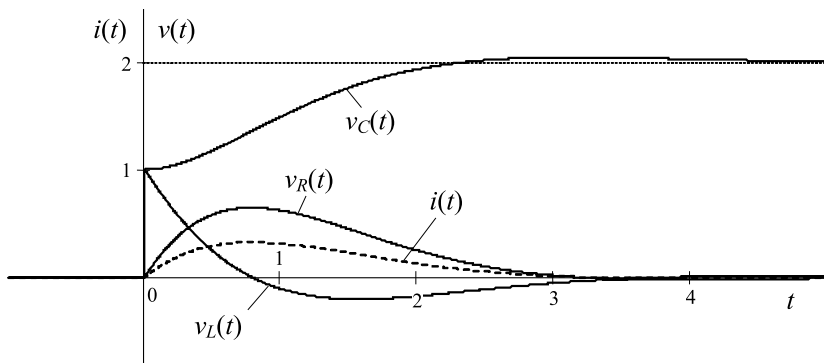


Fig. 5.38. Time functions of a series RLC circuits (Example 5.41).

$$\sum_{n=0}^N a_n \mathcal{D}^n y(t) = \sum_{m=0}^M b_m \mathcal{D}^m x(t), \quad (5.178)$$

where $\mathcal{D}^n \equiv d^n/dt^n$, $n \geq 1$, and $M \leq N$. The Laplace operator is applied to the both sides of (5.178) and, by zero initial conditions and $\mathcal{L}(\mathcal{D}) = s$, we obtain

$$Y(s) \sum_{n=0}^N a_n s^n = X(s) \sum_{m=0}^M b_m s^m \quad (5.179)$$

that allows representing the system transfer function as

$$H(s) = \frac{Y(s)}{X(s)} = \frac{\sum_{m=0}^M b_m s^m}{\sum_{n=0}^N a_n s^n}. \quad (5.180)$$

A representation of an LTI system in the s domain can now be made in two familiar direct (canonic) forms.

The First Direct Form

To arrive at the first direct form, one needs rewriting (5.179) for powers of a variable s . Without losing a generality, we set $a_N = 1$ and $M = N$ and write

$$\begin{aligned} & [a_0 Y(s) - b_0 X(s)] + s[a_1 Y(s) - b_1 X(s)] + \dots \\ & + s^{N-1}[a_{N-1} Y(s) - b_{N-1} X(s)] + s^N [Y(s) - b_N X(s)] = 0. \end{aligned} \quad (5.181)$$

Divided the both sided with s^N , (5.181) can be rewritten as

$$Y(s) = s^{-N}[b_0X(s) - a_0Y(s)] + s^{N-1}[b_1X(s) - a_1Y(s)] + \dots + s^{-1}[b_{N-1}X(s) - a_{N-1}Y(s)] + b_NX(s) \tag{5.182}$$

that allows us to sketch the first direct form of the diagrams as shown in Fig. 5.39. As well as in the time domain, the diagram is available in two forms.

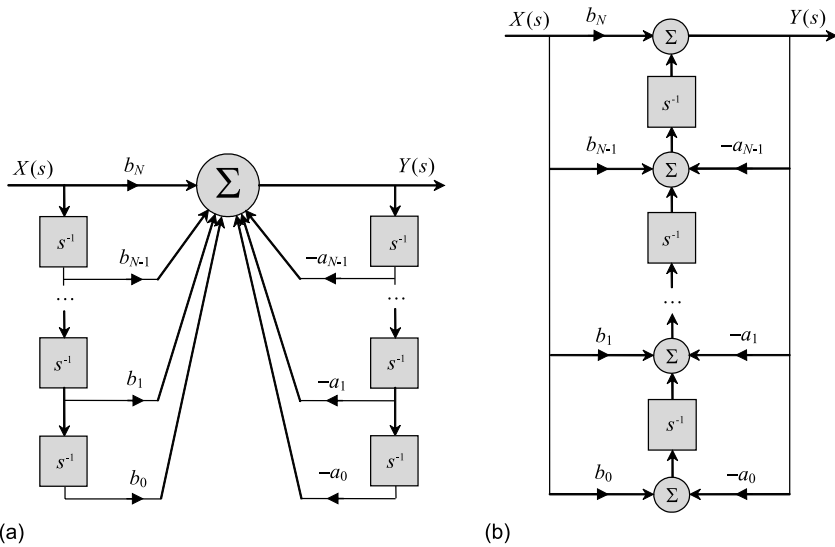


Fig. 5.39. The first direct form of block diagrams of LTI systems in the s domain: (a) addition efficient and (b) integration efficient.

It can be organized to be either addition efficient (Fig. 5.39a) or integration efficient (Fig. 5.39b). As can be seen, there is no substantial difference between the diagrams in the time and s domains. Integrators are merely substituted with the operators s^{-1} .

Example 5.42. A system is represented with the transfer function

$$H(s) = \frac{s - 3}{s^2 + 2s + 10}, \tag{5.183}$$

having the following coefficients in (5.180): $a_0 = 10$, $a_1 = 2$, $a_2 = 1$, $b_0 = -3$, and $b_1 = 1$. The first direct form of the diagram presentation of this system is shown in Fig. 5.40. □

The Second Direct Form

Similarly to the time domain, to sketch the second direct form of block diagrams in the s domain, we need substituting (5.179) with two relations:

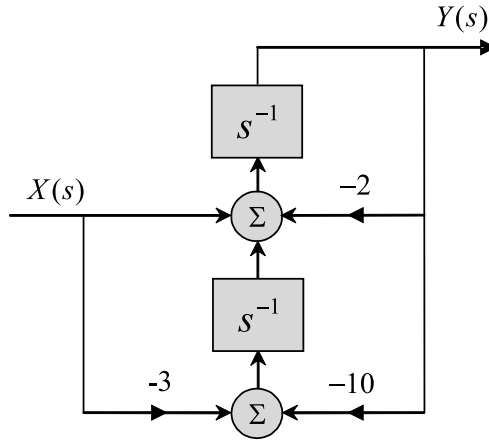


Fig. 5.40. The first direct form of block diagrams of a system (5.183).

$$Y(s) = \sum_{m=0}^M b_m s^m Z(s), \tag{5.184}$$

$$Z(s) = \left(\sum_{n=0}^N a_n s^n \right)^{-1} X(s). \tag{5.185}$$

The block diagram then appears straightforwardly to have two branches as shown in Fig. 5.41.

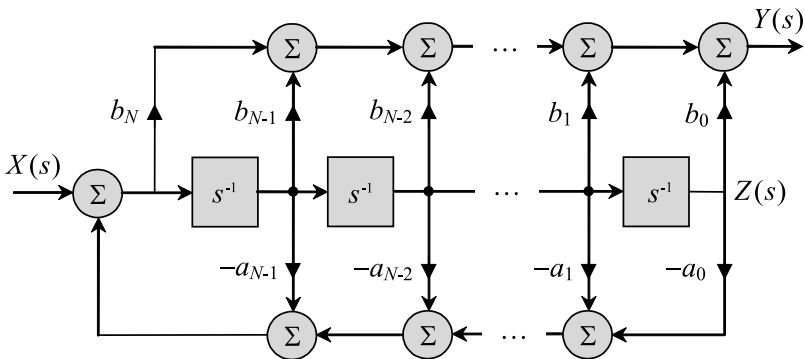


Fig. 5.41. The second direct form of block diagrams of LTI systems in the s domain.

Example 5.43. Consider an LTI system, which transfer function is given by (5.183). By known coefficients of the system ODE, the system is simulated with the diagram of the second direct form as shown in Fig. 5.42. \square

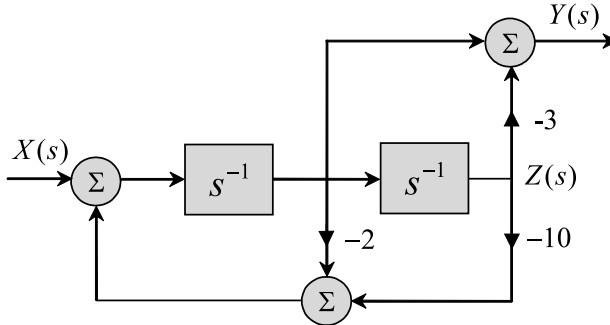


Fig. 5.42. The second direct form of block diagrams of a system (Example 5.43).

Let us notice that not only the first and second canonic forms are used in simulating LTI systems with block diagrams in the s domain. Albeit not commonly, some other kinds of diagrams may serve better. Nevertheless, it is commonly accepted that the above considered canonic solutions cover an overwhelming majority of practical needs.

5.5.4 State Space Analysis via Laplace Transform

One of the most impressive and utterly important properties of the Laplace transform is an ability to find the transfer function via the state space model of a system.

Let us recall that a general state space model, (4.125) and (4.126), of a MIMO system having k inputs, p outputs, and N state variables is given by

$$\mathbf{q}'(t) = \mathbf{A}\mathbf{q}(t) + \mathbf{B}\mathbf{x}(t), \tag{5.186}$$

$$\mathbf{y}(t) = \mathbf{C}\mathbf{q}(t) + \mathbf{D}\mathbf{x}(t), \tag{5.187}$$

where the $N \times 1$ state vector $\mathbf{q}(t)$ and its time derivative $\mathbf{q}'(t)$ are, respectively,

$$\mathbf{q}(t) = [q_1(t) \ q_2(t) \ \dots \ q_N(t)]^T, \tag{5.188}$$

$$\mathbf{q}'(t) = \frac{d}{dt}\mathbf{q}(t) = [q'_1(t) \ q'_2(t) \ \dots \ q'_N(t)]^T. \tag{5.189}$$

The $k \times 1$ input vector $\mathbf{x}(t)$ and $p \times 1$ output vector $\mathbf{y}(t)$ are, respectively,

$$\mathbf{x}(t) = [x_1(t) \ x_2(t) \ \dots \ x_k(t)]^T, \quad (5.190)$$

$$\mathbf{y}(t) = [y_1(t) \ y_2(t) \ \dots \ y_p(t)]^T. \quad (5.191)$$

The $N \times N$ system matrix \mathbf{A} and $p \times N$ observation matrix \mathbf{C} are given by (4.129). the $N \times k$ input matrix \mathbf{B} and $p \times k$ output matrix \mathbf{D} are performed with (4.130).

For zero initial conditions, we can apply the transform to (5.186) and write

$$s\mathbf{Q}(s) = \mathbf{A}\mathbf{Q}(s) + \mathbf{B}\mathbf{X}(s), \quad (5.192)$$

where $\mathbf{Q}(s)$ and $\mathbf{X}(s)$ are the Laplace transforms of $\mathbf{q}(t)$ and $\mathbf{x}(t)$, respectively. From (5.192) we have

$$\mathbf{Q}(s) = (s\mathbf{I} - \mathbf{A})^{-1}\mathbf{B}\mathbf{X}(s), \quad (5.193)$$

where \mathbf{I} is a proper unit matrix.

Applying the transform to (5.187) and substituting (5.193), we obtain

$$\mathbf{Y}(s) = [\mathbf{C}(s\mathbf{I} - \mathbf{A})^{-1}\mathbf{B} + \mathbf{D}]\mathbf{X}(s) \quad (5.194)$$

and thus the transfer function of a system is defined as

$$\mathbf{H}(s) = \mathbf{C}(s\mathbf{I} - \mathbf{A})^{-1}\mathbf{B} + \mathbf{D}. \quad (5.195)$$

The next step is seemingly obvious. One can represent (5.195) in a proper form, use a table of the Laplace transforms, and arrive at the system impulse response.

Example 5.44. A SISO LTI system is performed in state space with equations $\mathbf{q}'(t) = \mathbf{A}\mathbf{q}(t) + \mathbf{B}x(t)$ and $y(t) = \mathbf{C}\mathbf{q}(t)$, given the matrices

$$\mathbf{A} = \begin{bmatrix} -1 & 2 \\ 0 & -1 \end{bmatrix}, \quad \mathbf{B} = \begin{bmatrix} 0 \\ 1 \end{bmatrix}, \quad \mathbf{C} = [1 \ 1], \quad \mathbf{D} = [0].$$

To define the transfer function, we first determine the inverse matrix

$$\begin{aligned} (s\mathbf{I} - \mathbf{A})^{-1} &= \left(s \begin{bmatrix} 1 & 0 \\ 0 & 1 \end{bmatrix} - \begin{bmatrix} -1 & 2 \\ 0 & -1 \end{bmatrix} \right)^{-1} = \begin{bmatrix} s+1 & -2 \\ 0 & s+1 \end{bmatrix}^{-1} \\ &= \frac{1}{(s+1)^2 + 2} \begin{bmatrix} s+1 & 2 \\ 0 & s+1 \end{bmatrix}. \end{aligned}$$

Then substituting to (5.195) and providing the transformations yield

$$\begin{aligned} H(s) &= \frac{1}{(s+1)^2 + 2} [1 \ 1] \begin{bmatrix} s+1 & 2 \\ 0 & s+1 \end{bmatrix} \begin{bmatrix} 0 \\ 1 \end{bmatrix} \\ &= \frac{s+3}{(s+1)^2 + 2}. \end{aligned}$$

By a table of the Laplace transforms, we finally arrive at the system impulse response

$$h(t) = e^{-t}(\cos \sqrt{2}t + \sqrt{2} \sin \sqrt{2}t)u(t)$$

and notice that the result is obtained with a relatively low burden, unlike a direct solution in the time domain. \square

Overall, one can truly conclude that the transfer function of an LTI system can easily be derived via the state space model if all of the matrices are distinct. This conclusion is valid for both SISO and MIMO systems.

5.6 Stability Analysis of Feedback Systems

Ascertaining stability of LTI systems becomes of prime importance if the latter have any kinds of feedback. Systems with feedback play an important role in applications owing to their special properties. Typically, negative feedbacks allow for a substantial improvement of the characteristics of electronic systems. Positive feedbacks, in turn, make systems unstable. In the sequel, we shall show that, like in the time domain, stability of LTI systems can equivalently be ascertained in the s domain.

5.6.1 Transfer Function of Closed Systems

Most generally, an LTI system with feedback is represented as shown in Fig. 5.43.

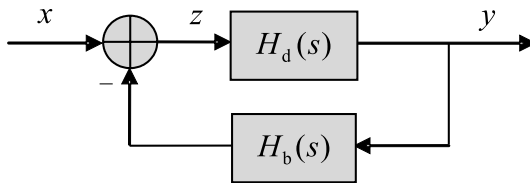


Fig. 5.43. Feedback LTI system.

The structure comprises two blocks. The forward path block with the transfer function $H_d(s)$ is the main part of a system. An auxiliary feedback branch with the transfer function $H_b(s)$ is placed over the main block connecting its output with the input. The feedback signal is subtracted from the input signal $x(t)$ to produce the input $z(t)$ for the main block. If the transforms $X(s)$ and $Y(s)$ of the input and output, respectively, are both known, the system equation can easily be written as

$$Y(s) = H_d(s)[X(s) - H_b(s)Y(s)] \quad (5.196)$$

producing the transfer function of a closed loop,

$$H(s) = \frac{Y(s)}{X(s)} = \frac{H_d(s)}{1 + H_b(s)H_d(s)}. \quad (5.197)$$

Observing (5.197), one can conclude that the transform domain properties of a closed loop system depend both on $H_d(s)$ and $H_b(s)$. This means that the properties of $H(s)$ can be varied in a wide range by changing the transfer function either of the main block or feedback. Therefore, of prime importance is what kind of feedback is organized, negative or positive.

Let us consider the system frequency response, by $s = j\omega$,

$$H(j\omega) = \frac{Y(j\omega)}{X(j\omega)} = \frac{H_d(j\omega)}{1 + H_b(j\omega)H_d(j\omega)}. \quad (5.198)$$

The key question is what is the value of the denominator. If at some frequency ω we have

$$|1 + H_b(j\omega)H_d(j\omega)| > 1, \quad (5.199)$$

the system magnitude response $H(j\omega)$ is reduced by feedback. Therefore, this kind of feedback is called *negative*. Note that in physiology and sometimes in control systems, negative feedback is called *homeostasis*. Contrary, if

$$|1 + H_b(j\omega)H_d(j\omega)| < 1, \quad (5.200)$$

the magnitude response $H(j\omega)$ increases owing to what is called *positive feedback*. Both negative and positive feedbacks are widely used in electronic blocks, tracts, and channels, although with different purposes.

Example 5.45 (Gain Stabilization). An amplifier with a uniform gain G_d in the required frequency range is designed to be marginally stable.

To increase stability, a uniform feedback $H_b(j\omega) = -G_b < 0$ is placed over the amplifier. By (5.198), we have

$$G = \frac{G_d}{1 + G_b G_d}$$

and, taking a derivative

$$\frac{\partial G}{\partial G_b} = \frac{1}{(1 + G_d G_b)^2} = \frac{G_d}{1 + G_b G_d} \frac{1}{(1 + G_d G_b) G_d} = \frac{G}{G_d (1 + G_d G_b)},$$

evaluate instability of a feedback amplifier by the relation

$$\frac{\partial G}{G} = \frac{1}{1 + G_d G_b} \frac{\partial G_d}{G_d}.$$

As can be seen, by $G_d G_b \gg 1$, the instability factor $\partial G/G$ and gain G are both reduced by the factor of $1 + G_d G_b$. The amplifier is thus no longer marginally stable. It is now rather Lyapunov stable. Obtained stability, the gain can further be increased by an auxiliary amplifier. \square

Example 5.46 (Suppression of Spurious Signals). An RF channel is composed with a cascade of two amplifiers, G_1 and G_2 . A spurious signal z acts in the input of the second amplifier as shown in Fig. 5.44. To suppress

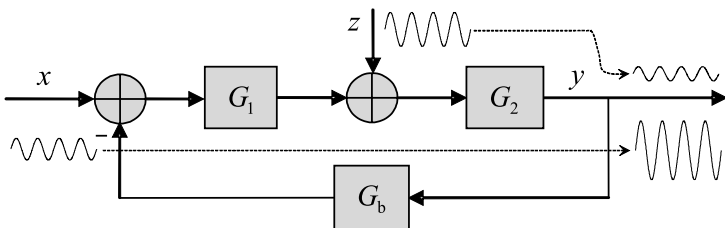


Fig. 5.44. Cascade feedback LTI system.

z , a feedback with a gain factor G_b is placed over the amplifier.

It can be shown that the feedback system gain is defined by

$$G = \frac{G_1 G_2}{1 + G_b G_1 G_2}$$

and the gain for the spurious signal z is calculated as

$$G_z = \frac{G_2}{1 + G_b G_1 G_2}.$$

Typically, amplification channels are designed such that $G_1 \gg G_2$. By virtue of that, a signal z is suppressed substantially at the output of a channel as it is sketched in Fig. 5.44. This trick is efficiently used in cascade amplifiers to lower a content of high harmonics in the output signal. Note that harmonics caused by nonlinearities often occur with large signals and gains. \square

Let us come back to (5.197). If the denominator is zero,

$$\Delta(s) = 1 + H_b(s)H_d(s) = 0, \quad (5.201)$$

a system has poles requiring investigations for stability. It is thus worth finding proper criteria of the Lyapunov stability in the s domain, directly via (5.201).

One already knows that, in order to ascertain stability of linear systems, the input must be zero-valued and autonomous equation investigated. If we let $X(j\omega) = 0$, then (5.196) becomes (5.201), meaning that it is the *characteristic*

equation. The latter may be represented with the n -degree polynomial having the roots s_1, s_2, \dots, s_n . By these roots, the output of an autonomous system can be performed in the time domain by a series of exponential solutions,

$$y(t) = a_1 e^{s_1 t} + a_2 e^{s_2 t} + \dots + a_n e^{s_n t}. \quad (5.202)$$

Analyzing (5.202), we inter that the series produces a finite value only if all of the roots s_1, s_2, \dots, s_n have negative real parts (then all the exponential functions converge). In other words, a system is stable if all of the roots of the characteristic equation are placed in the left part of a complex plane. If the roots that are unknown, stability can be ascertained directly via the characteristic equation polynomial if one tests a system by the Routh-Hurwitz or Nyquist stability criteria.

5.6.2 Routh-Hurwitz Criterion

Earlier, we used the criterion by Routh and Hurwitz (4.168) in the time domain. In order to apply it equally in the transform domain, let us represent the characteristic equation (5.201) with the n -degree polynomial

$$\Delta(s) = a_n s^n + a_{n-1} s^{n-1} + \dots + a_1 s + a_0 = 0, \quad (5.203)$$

in which all of the coefficients are real and roots are still unknown. Stability of a system can now be ascertained as follows, provided the definition:

Routh-Hurwitz criterion of stability: A system described with (5.203) is stable (all the roots lie in the left plane) if and only if the following quantities are *positive-valued*:

- All of the coefficients $a_i, i \in [0, n]$,
- Hurwitz determinant

$$D_{n-1} = \begin{vmatrix} a_{n-1} & a_n & 0 & 0 & \dots & 0 & 0 \\ a_{n-3} & a_{n-2} & a_{n-1} & a_n & \dots & 0 & 0 \\ a_{n-5} & a_{n-4} & a_{n-3} & a_{n-2} & \dots & 0 & 0 \\ \vdots & \vdots & \vdots & \vdots & \ddots & \vdots & \vdots \\ 0 & 0 & 0 & 0 & \dots & a_0 & a_1 \end{vmatrix},$$

- All principle minors of the Hurwitz determinant

$$\left| a_{n-1} \right|, \quad \begin{vmatrix} a_{n-1} & a_n \\ a_{n-3} & a_{n-2} \end{vmatrix}, \quad \begin{vmatrix} a_{n-1} & a_n & 0 \\ a_{n-3} & a_{n-2} & a_{n-1} \\ a_{n-5} & a_{n-4} & a_{n-3} \end{vmatrix}, \quad \dots$$

□

Example 5.47. A closed loop system is represented with the characteristic equation $s^3 + 3s^2 + 6s + 2 = 0$. The test for stability by the Routh-Hurwitz criterion is as follows. The first test is positive, because all the coefficients are positive. The second test is also positive, because the Hurwitz determinant is positive,

$$\begin{vmatrix} 3 & 1 \\ 2 & 6 \end{vmatrix} = 18 - 2 = 16 > 0.$$

The only principle minor here is positive, $3 > 0$, thus the third test is positive as well. Because all three tests are positive, the system is stable. \square

5.6.3 Nyquist Criterion

The other test for stability is provided in the frequency domain by the *Nyquist*⁶ *criterion* known from 1932. The criterion is based on the Cauchy⁷ “Principle of Argument” from complex analysis. By applying this criterion to the open loop system transfer function

$$\Lambda(s) = H_d(s)H_b(s), \quad (5.204)$$

it becomes possible getting information about stability of the closed loop, provided the definition:

Nyquist criterion of stability: A system is asymptotically stable if the Nyquist plot of $\Lambda(s)$ does not encircle the point $-1 + 0i$ in the complex plane in the clockwise direction. \square

It follows that the Nyquist criterion applied to the frequency response of an open loop ascertains stability of a closed loop. Why does it become possible? No magic, just the poles of $\Delta(s)$ (5.191) are contributed by the poles of $\Lambda(s)$ (5.204). From the plot of magnitude $|\Lambda(j\omega)|$ vs. phase $\varphi(\omega)$ or real part $\text{Re}\Lambda(j\omega)$ vs. imaginary part $\text{Im}\Lambda(j\omega)$ as ω varies from negative infinity to positive infinity, the number of unstable poles can be determined. Additionally, we can realize how “close” the closed loop system is to becoming unstable.

Example 5.48. Given an LP transistor amplifier with the transfer function

$$H_d(s) = \frac{2}{1 + s\tau},$$

where $\tau = 10\text{sec}$. The output and input are coupled directly, $H_b(s) = 1$, therefore the open loop transfer function is $\Lambda(s) = H_d(s)$. By $s = j\omega$, the frequency response of an open loop is calculated as

⁶ Harry Nyquist, Swedish born, US physicist, 7 February 1889–4 April 1976

⁷ Augustin Louis Cauchy, French mathematician, 21 August 1789–23 May 1857.

$$A(j\omega) = \frac{2}{\sqrt{1 + \omega^2\tau^2}} e^{-j \arctan(\omega\tau)},$$

having the real and imaginary parts, respectively,

$$\operatorname{Re}A(j\omega) = \frac{2}{1 + \omega^2\tau^2} \quad \text{and} \quad \operatorname{Im}A(j\omega) = \frac{2\omega\tau}{1 + \omega^2\tau^2}.$$

The corresponding Nyquist plot is shown in Fig. 5.45a. Because the plot does not encircle the point $-1 + 0i$, the amplifier is stable. □

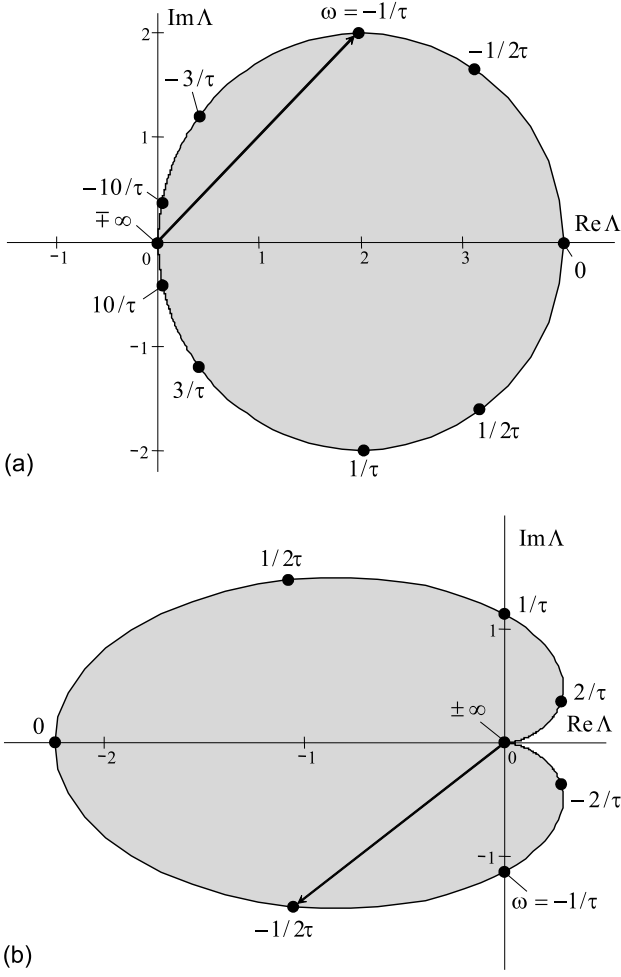


Fig. 5.45. Nyquist plots: (a) Example 5.48 and (b) Example 5.49.

Example 5.49. An amplifier with the transfer function

$$H_d(s) = \frac{1.5}{1 + s\tau},$$

where $\tau = 10\text{sec}$, is closed with the feedback inverting amplifier having the transfer function $H_b(s) = -H_d(s)$. The open loop transfer function is thus

$$A(s) = H_d(s)H_b(s) = -\frac{1.5^2}{(1 + s\tau)^2}$$

and the associated frequency response is given by

$$A(j\omega) = \frac{1.5^2}{1 + \omega^2\tau^2} e^{j(\pi - 2 \arctan \omega\tau)}.$$

Fig. 5.45b sketches the relevant Nyquist plot. The curve encircles a point $-1 + 0i$ and the amplifier is thus unstable. Indeed, the inverting amplifier makes the feedback positive that cause instability. \square

5.6.4 Gain and Phase Stability Margins

The other value of the Nyquist stability criterion is that it allows determining the relative degree of system stability by producing the so-called *gain* and *phase stability margins*. The margins tell us how far the given system is from the instability region that is needed, for example, for frequency domain controller design techniques.

The *gain margin* Gm is the factor by which one evaluates how lesser (in dB) the system open loop gain is than the critical (instability) value (0 dB),

$$\text{Gm} = 20 \log \frac{1}{|H_d(j\omega_{cp})H_b(j\omega_{cp})|} [\text{dB}]. \quad (5.205)$$

The frequency at which Gm is evaluated is the *phase crossover frequency* ω_{cp} , calculated by

$$\arg[H_d(j\omega_{cp})H_b(j\omega_{cp})] = \pi. \quad (5.206)$$

The *phase margin* Pm, in radian, is defined as the amount by which the phase of $A(j\omega)$ exceeds π when $|A(j\omega)| = 1$,

$$\text{Pm} = \pi + \arg[H_d(j\omega_{cg})H_b(j\omega_{cg})], \quad (5.207)$$

and the frequency at which Pm is evaluated is the *gain crossover frequency* ω_{cg} , calculated by

$$|H_d(j\omega_{cg})H_b(j\omega_{cg})| = 1. \quad (5.208)$$

The most transparent way to evaluate Gm and Pm offers the Bode plots (Fig. 5.46a). With a bit larger burden, the margins can be evaluated via the

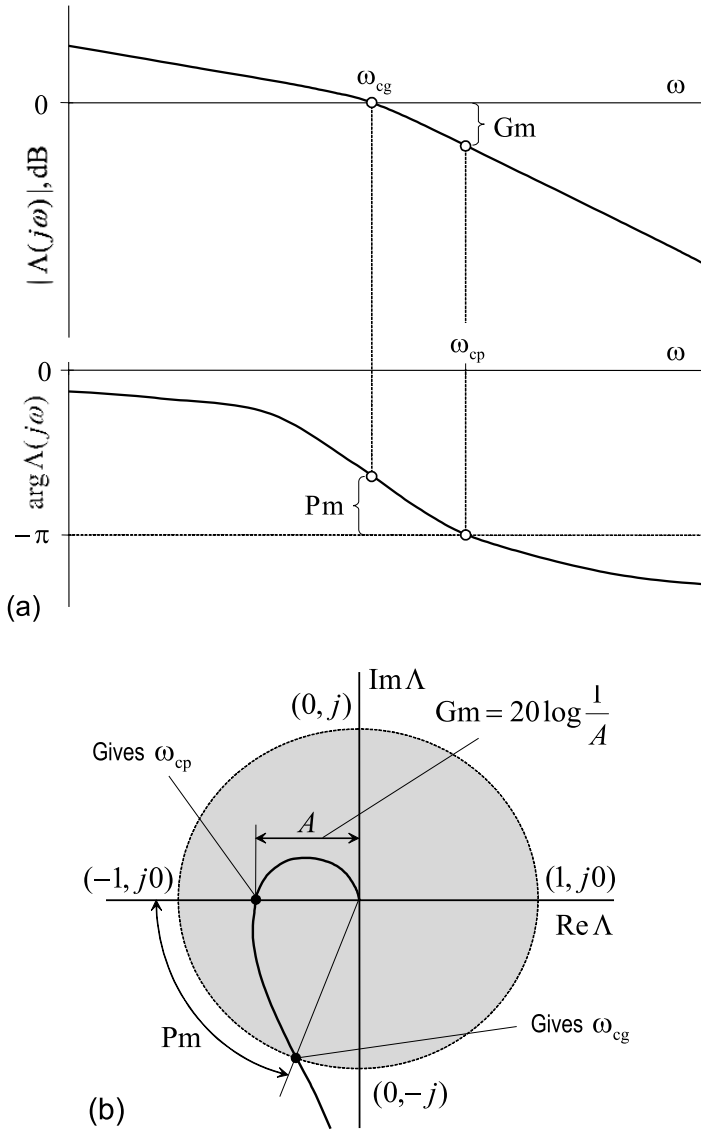


Fig. 5.46. Gain (G_m) and phase (P_m) stability margins: (a) via the Bode plots and (b) via the Nyquist plot.

Nyquist plot (Fig. 5.46b). In both cases, it is enough considering only positive frequencies obeying the following rule: A system is stable if $G_m > 0$, it stays at a bound of stability by $G_m = 0$, and it is unstable when $G_m < 0$.

Example 5.50. An LTI channel is composed by a cascade of two amplifiers. The first amplifier inverts a signal with the transfer function $H_1(j\omega) = \frac{-1}{1+j\omega\tau}$ and the second one, $H_2(j\omega) = \frac{G_0}{1+j\omega\tau}$, has a gain G_0 that can be adjusted. An ideal integrator feedback, $H_b(j\omega) = \frac{1}{j\omega}$, is placed over the channel so that the open loop gain is

$$A(j\omega) = \frac{G_0}{j\omega(1+j\omega\tau)^2}.$$

The crossover frequencies as well as the gain and phase stability margins calculated for $G_0 = 1$, $G_0 = 2$, and $G_0 = 3$ are postponed to Tab. 5.1. The relevant Bode and Nyquist plots are shown in Fig. 5.47.

Table 5.1. Stability parameters of a system (Example 5.50)

Gain	ω_{cp}	ω_{cg}	Gm,dB	Pm,rad
$G_0 = 1$	1	0.682	6.021	0.373
$G_0 = 2$	1	1	0	0
$G_0 = 3$	1	1.241	-3.522	-0.193

As can be seen (Fig. 5.47a), “stability resources” with $G_0 = 1$ are about $G_m = 6\text{dB}$ and $P_m = 10.7^\circ$. With $G_0 = 2$, the system stays at the bound of stability, $G_m = P_m = 0$. If $G_0 = 3$, there is a “lack of stability” evaluated by $G_m = -3.5\text{dB}$ and $P_m = -5.5^\circ$.

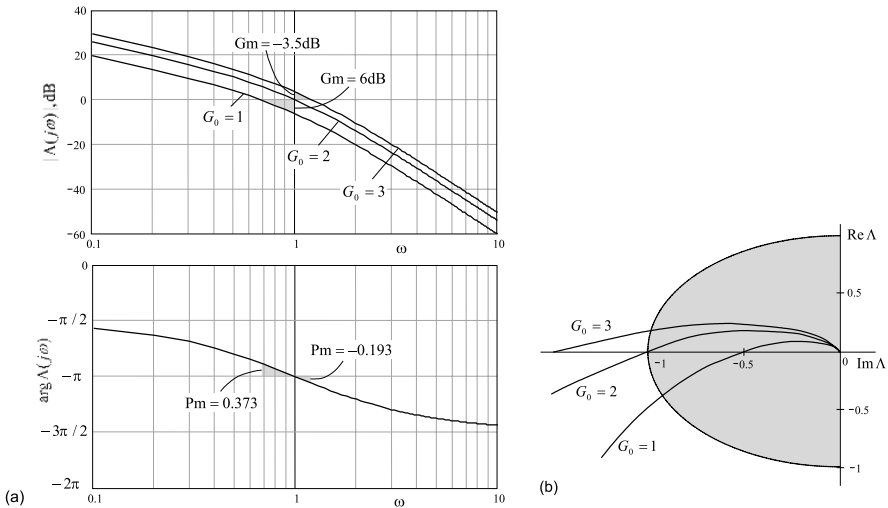


Fig. 5.47. Gain (G_m) and phase (P_m) stability margins: (a) Bode plots and (b) Nyquist plot.

In turn, the Nyquist plot (Fig. 5.47b) shows that the point $(-1, j0)$ is encircled by $G_0 = 3$ (system is unstable), not encircled by $G_0 = 1$ (system is stable), and the case of $G_0 = 2$ is intermediate. \square

5.6.5 Bandwidth Correction by Feedback

The widely used property of feedback is its ability to correct the bandwidth of a system. The effect occurs owing to dissipation or insertion of some amount of energy that results, respectively, in contraction or extension of the bandwidth. The effect is exploited, for example, in *high-quality audio coding*.

To demonstrate such facilities of feedback, let us consider an LP amplifier with the frequency response $H_a(j\omega)$ such that $H_a(j0) = G_0$. If we place over a feedback with the uniform gain G_b , the resulting frequency response at zero will be

$$H(j\omega) = \frac{H_a(j\omega)}{1 + G_b H_a(j\omega)}. \quad (5.209)$$

We may now substitute $H_a(j\omega) = A(\omega) + jB(\omega)$ and the relation becomes

$$H(j\omega) = \frac{H_a(j\omega)}{1 + G_b A(\omega) + jG_b B(\omega)},$$

meaning that the real part of the denominator is changed and so is the cut-off frequency of the bandwidth. Because the feedback gain may be either negative or positive, the bandwidth is either extended or contracted, respectively.

Bandwidth Flattering and Correction

Consider a simplest inverting LP amplifier with the frequency response

$$H_a(j\omega) = \frac{-G_0}{1 + j\omega\tau},$$

where a gain G_0 is constant. By the feedback inserted with a gain G_b , the frequency response and the relevant magnitude response of a closed loop can be found to be, respectively,

$$\begin{aligned} H(j\omega) &= \frac{-G_0}{1 + G_b G_0 + j\omega\tau}, \\ |H(j\omega)| &= \frac{G_0}{\sqrt{(1 + G_b G_0)^2 + \omega^2 \tau^2}}. \end{aligned} \quad (5.210)$$

Fig. 5.48a sketches the Bode plots of $|H(j\omega)|$ for several values of the open loop gain $G_b G_0$. Fig. 5.48b gives a picture for the output additionally gained with $1 + G_b G_0$.

In the first case (Fig. 5.48a), positive values of $G_b G_0$ cause flattering of the frequency response simultaneously with decreasing the gain factor. In turn,

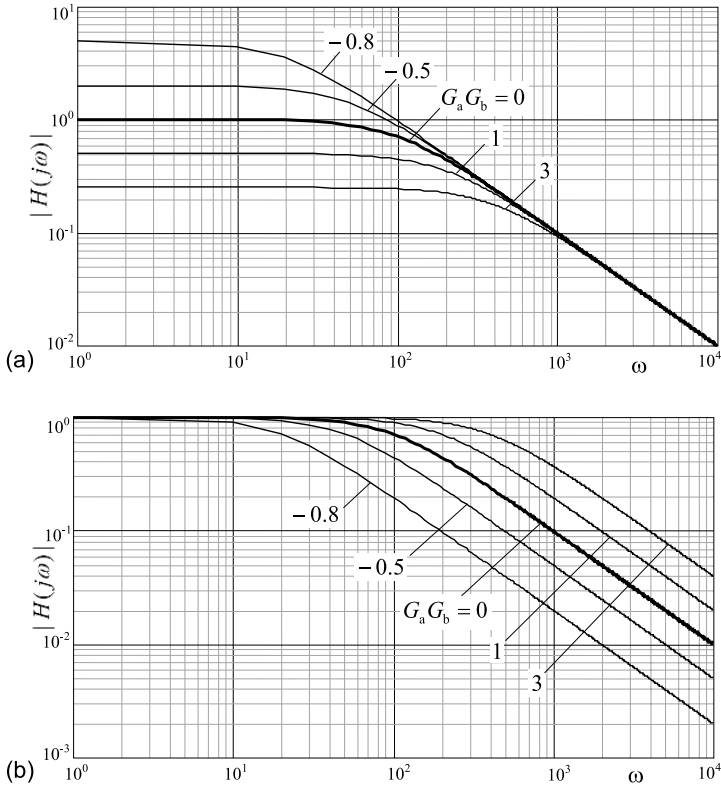


Fig. 5.48. Bode plot of the magnitude response of an amplifier with feedback for $\tau = 10^{-2}$ sec: (a) original and (b) gained with $1 + G_b G_0$.

negative values of $G_b G_0$ produce an opposite effect. To realize what happens with the bandwidth, by changing $G_b G_0$, let us scale each curve with $1 + G_b G_0$. This makes the gain unity at zero for all values of $G_b G_0$ and we see that the bandwidth is extended by the positive feedback and contracted by negative. Following (5.210), the cut-off frequency is defined at the level of $1/\sqrt{2}$ by

$$\omega_c = \frac{1}{\tau}(1 + G_b G_0),$$

allowing evaluating G_b for the required bandwidth.

The simplest way to organize a negative feedback implies including a resistor to the collector branch of a transistor amplifier as shown in Fig. 5.49. Here increase in the input voltage V_{in} causes increase in the emitter current. The latter induces an additional amount of the feedback voltage V_b on a resistor R_b . Consequently, the base-emitter voltage $V_{in} - V_b$ becomes lower and the feedback is thus negative.

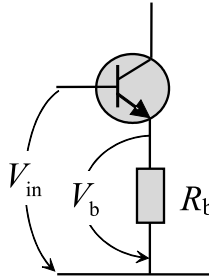


Fig. 5.49. Negative feedback in a transistor amplifier.

Regenerative Amplification

Nowadays, *regenerative amplification* is used widely in nanosecond and femtosecond techniques. To explain the operation principle, let us consider a resonant inverting amplifier performed with the response

$$H_a(j\omega) = \frac{H_a(j0)}{1 + j(\omega - \omega_0)\tau}, \quad (5.211)$$

where $H_a(j0) = -G_0$, $\tau = 2Q/\omega_0$ is the time constant, ω_0 is the resonance frequency, and Q is the quality factor. A positive feedback loop with a uniform gain G_b is placed over the amplifier so that the resulting frequency response becomes

$$H(j\omega) = \frac{H_a(j\omega)}{1 + G_b H_a(j\omega)} = \frac{-G_0}{1 - G_b G_0 + j(\omega - \omega_0)\tau}. \quad (5.212)$$

An influence of the feedback gain G_b is illustrated in Fig. 5.50a. It is seen that, by $G_b > 0$, the gain increases around ω_0 , where the feedback is most efficient. Increasing in the gain results in increasing in the quality factor. Indeed, if we scale each curve with $1 - G_b G_0$, the frequency response acquires a constant gain G_0 at ω_0 for all G_b and we watch for narrowing the bandwidth, by $G_b > 0$, as shown in Fig. 5.50b.

An example of the regenerative amplifier is shown in Fig. 5.51. Here an amount of the voltage taken from the parallel resonant circuit is induced to the input via the mutual inductance M . In such a way, a positive feedback is organized.

Certainly, regenerative amplification is a very simple way to increase the gain and reduce the bandwidth of a resonance amplifier. Nevertheless, it is not the one that is widely used. The fact is that every amplifier with positive feedback is addicted to self excitation when, even occasionally and by external factors, the open loop gain tends toward unity, $G_0 G_b \rightarrow 1$. The amplifier then becomes unstable and its duties can no longer be fulfilled.

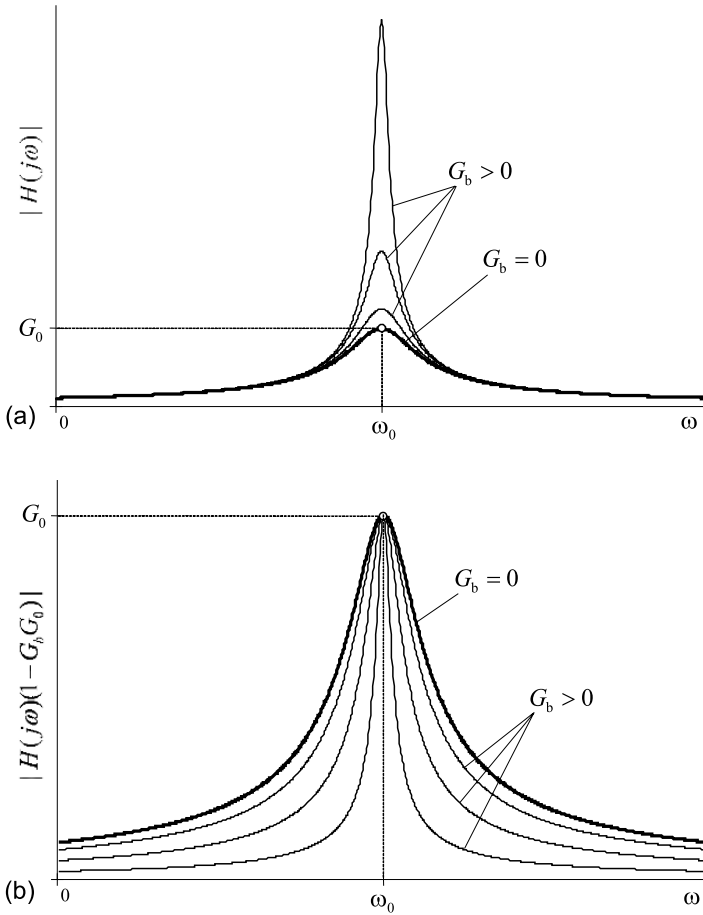


Fig. 5.50. Magnitude response of a regenerative amplifier: (a) original and (b) gained with $1 - G_b G_0$.

Delay Feedback Systems

At high frequencies, system feedbacks often almost ideally delay signals. A time delay τ_0 can also be inserted intentionally to attach some useful properties to a system. A system with a delay in the feedback is called the *delay feedback system* and the delay feedback system can be represented by the block diagram as shown in Fig. 5.52.

An ideal delay feedback is usually modeled at a frequency ω with the frequency response $H_\tau(\omega) = e^{-j\omega\tau_0}$. In view of that, the frequency response and magnitude response of the delay feedback system become, respectively,

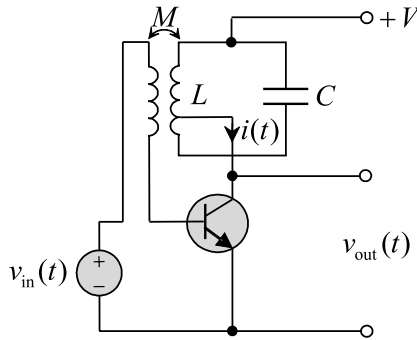


Fig. 5.51. Regenerative amplifier.

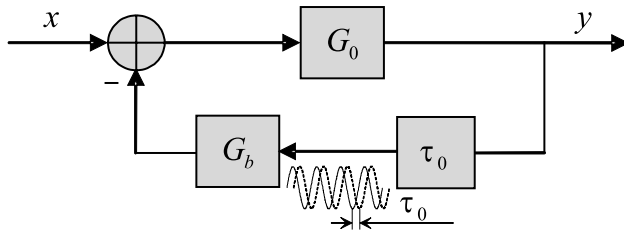


Fig. 5.52. Delay feedback system.

$$H(j\omega) = \frac{G_0}{1 + G_b G_0 e^{-j\omega\tau_0}} \tag{5.213}$$

$$|H(j\omega)| = \frac{G_0}{\sqrt{1 + 2G_b G_0 \cos \omega\tau_0 + G_b^2 G_0^2}} \tag{5.214}$$

Owing to a periodic cosine function in the denominator, the response $H(j\omega)$ is also periodically repeated with the frequency step $\Omega = 2\pi/\tau_0$ as shown in Fig. 5.53. As it is seen, the magnitude tends toward infinity by $G_b G_0 \rightarrow 1$ with $\cos \omega\tau_0 = -1$ that causes instability.

We notice that a great deal of applications of delayed feedback systems is associated namely with their ability to have periodic frequency responses. Such systems can possess chaotic attractors with extremely high dimension, even if only a few physical degrees of freedom are involved. Delayed feedback allows designing multifrequency oscillators and watch for the noise-induced resonances and bifurcations. Also, special robust methods are developed for controlling delay feedback systems with bounded uncertainty.

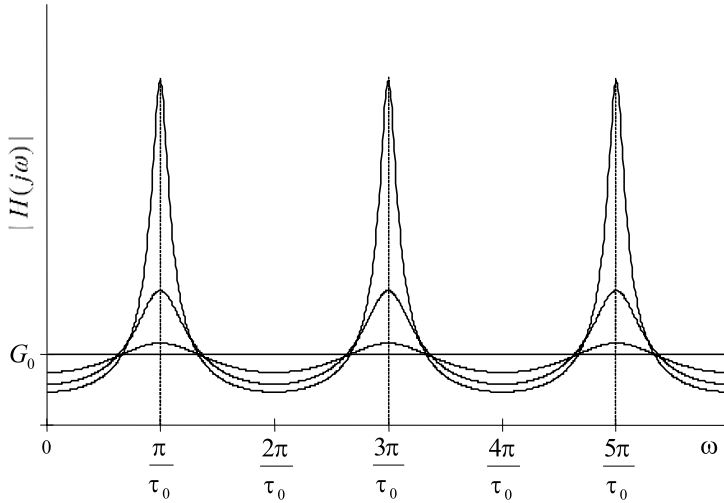


Fig. 5.53. Periodic magnitude response of a delay feedback system.

5.7 Selective Filter Approximations

Except for optimal filters, the filter magnitude response is typically, desirable to have a rectangular (“ideal”) shape implying an abrupt transition between the passband and the stopband or the infinitely steep roll-off slope. Practically, such a magnitude response cannot be obtained and they search for an approximation that still meets the requirements. Commonly, the approximation is supposed to be the best if a compromise is found between the following filter parameters: the filter order n , roll-off rate (in dB per decade or dB per octave), attenuation rate near the cut-off frequency ω_c , monotonicity over all frequencies, passband ripple, and stopband ripple.

To find and implement practically the best approximation, a number of standard filter characteristics have been defined and described in special engineering books. Below, we observe in brief the most widely used continuous-time filters of high orders, such as Butterworth and Chebyshev. These filters are represented in the transform and frequency domains and can be described in state space.

5.7.1 Butterworth Filter

Among all other continuous-time (analog) filters, the arbitrary order filter designed by Butterworth⁸ in 1930 has a maximally flat (without ripple) frequency response in the passband and monotonically rolls off towards zero

⁸ Stephen Butterworth, British engineer.

beyond the bandwidth (in the stopband). As any other first-order filter, the first-order Butterworth one has a roll-off slope of -20 dB per decade. A second-order Butterworth filter rolls off with -40 dB per decade, a third-order with -60 dB, and so on.

The transfer function of an n -order LP Butterworth filter is given with

$$H(s) = \frac{G_0}{\prod_{k=1}^n (s - p_k)}, \quad (5.215)$$

where the poles

$$p_k = e^{j\pi(\frac{1}{2} + \frac{2k-1}{2n})}, \quad k = 1, 2, \dots, n \quad (5.216)$$

are entirely placed in the left plane and G_0 is a constant gain. It is seen that (5.215) has no roots in the numerator and thus no zeros.

For the transfer function (5.215), the square magnitude response of a normalized filter having the cut-off frequency $\omega_c = 1$ rad/sec and $G_0 = 1$ is defined by

$$|H(j\omega)|^2 = \frac{1}{1 + \omega^{2n}}. \quad (5.217)$$

Equivalently, in the s domain, (5.217) can be rewritten as

$$H(s)H(-s) = \frac{1}{1 + (-s^2)^n}. \quad (5.218)$$

Properties of the Butterworth filter are completely defined by (5.217):

- The filter has only poles, because all of its zeros are placed at infinity.
- At $\omega = 1$ rad/s, the filter gain is $|H(j\omega_c)| = 1/\sqrt{2}$, i.e. the magnitude response rolls off by 3 dB.
- The filter order n fully defines its frequency response.

Design of the Butterworth filter implies calculating the only parameter that is the filter order n . Given the cut-off frequency ω_c and an auxiliary frequency ω_a at which an attenuation parameter is A , the filter order is calculated by

$$n = \frac{\log(A^2 - 1)}{2 \log(\omega_a/\omega_c)}. \quad (5.219)$$

Example 5.51 (Butterworth LP filter). Let the Butterworth LP filter be designed to have a cut-off frequency $f_c = 60$ Hz (-3 dB) and an auxiliary frequency $f_a = 120$ Hz (-66 dB).

Calculate $1/A = 10^{66/20} = 0.0005$ and $f_a/f_c = \omega_a/\omega_c = 2$. By (5.219), we have $n = 10.99$ and let $n = 11$. By (5.215), (5.216), and $G_0 = 1$, calculate the filter transfer function.

The filter is characterized with 11 poles, all of which lie in the left plane as shown in Fig. 5.54. The magnitude response, phase response, and group delay of this filter are sketched in Fig. 5.55. Observing Fig. 5.55, one can infer

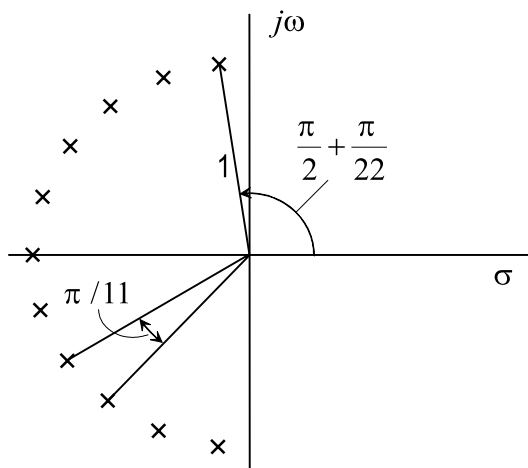


Fig. 5.54. Poles of an 11-order Butterworth LP filter.

that, in line with a nice flatness in the passband, the filter phase is not linear. Therefore, the group delay is not constant. \square

To find a practical solution for the Butterworth approximation (to design the filter), there have been proposed a number of different filter topologies. Of importance is that the proposed filter circuits differ only in the values of the components, but not in their connections.

One of the most widely used topology was proposed by Cauer⁹. The Butterworth filter of a given order n calculated by (5.219) can be designed using the Cauer first form shown in Fig. 5.56. The capacitances and inductances for the normalized filter are given by

$$C_k = 2 \sin \frac{2k-1}{2n} \pi, \quad k \text{ is odd}, \quad (5.220)$$

$$L_k = 2 \sin \frac{2k-1}{2n} \pi, \quad k \text{ is even}. \quad (5.221)$$

Example 5.52 (Design of the Butterworth LP filter). The Butterworth LP filter is required to have an order $n = 5$. By (5.220) and (5.221), the components of the normalized filter (Fig. 5.56) are calculated to be $C_1 = C_5 = 0.618$ F, $C_3 = 2$ F, and $L_2 = L_4 = 1.618$ H. \square

⁹ Wilhelm Cauer, German mathematician and scientist, 24 June 1900-22 April 1945.

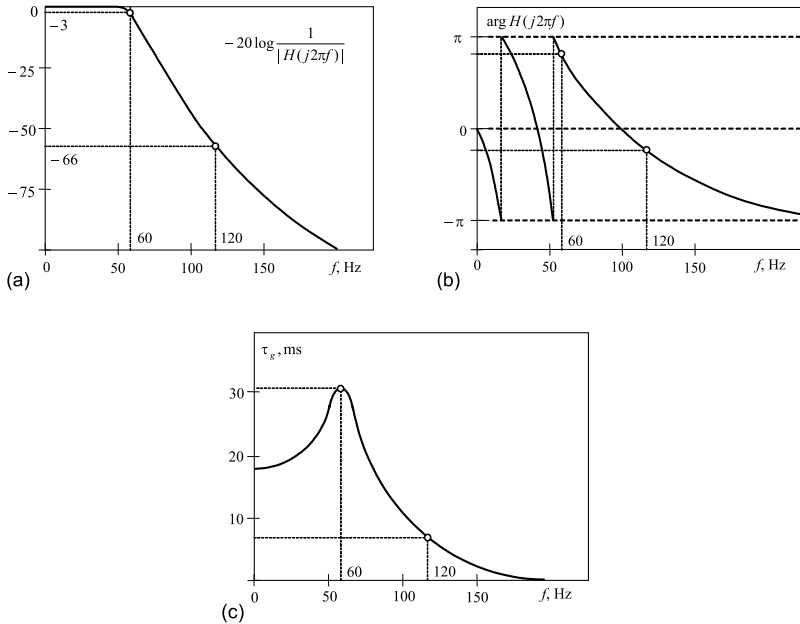


Fig. 5.55. Frequency response of an 11-order Butterworth LP filter (Example 5.51): (a) magnitude, (b) phase mod 2π , and (c) group delay.

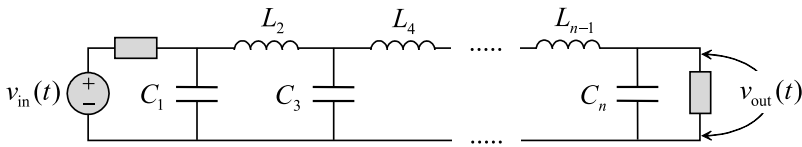


Fig. 5.56. The first form Cauer's topology of the Butterworth filter.

5.7.2 Chebyshev Filter

A special feature of the Chebyshev filter is that it minimizes the error caused by ripple in the passband. The filter is named in honor of Chebyshev because the filter frequency response is derived from Chebyshev polynomials. This type of filter has a much steeper monotonous roll-off. However, ripple appears in passband that makes it unsuitable for audio systems, for example. The filter is preferable for applications in which the passband includes only one frequency, e.g., the derivation of a sine wave from a square wave, by filtering out the harmonics. Two types of Chebyshev filters are commonly recognized.

Type I Chebyshev Filter

The transfer function of the type I Chebyshev filter is defined by (5.215) with poles specified by

$$p_k = \sigma_k + j\mu_k, \tag{5.222}$$

where

$$\begin{aligned} \sigma_k &= -\frac{\gamma - \gamma^{-1}}{2} \sin \frac{(2k - 1)\pi}{2n}, \\ \mu_k &= \frac{\gamma + \gamma^{-1}}{2} \cos \frac{(2k - 1)\pi}{2n}, \\ \gamma &= \left(\frac{1 + \sqrt{1 + \varepsilon^2}}{\varepsilon} \right)^{1/n}, \end{aligned}$$

and ε is the ripple factor.

The magnitude response of a normalized type I Chebyshev filter, $\omega_c = 1$, is defined as

$$|H(j\omega)| = \frac{1}{1 + \varepsilon^2 T_n^2(\omega)}, \tag{5.223}$$

where $T_n(\omega)$ is an n -order Chebyshev polynomial

$$T_n(\omega) = \begin{cases} \cos(n \arccos \omega), & |\omega| \leq 1 \\ \cosh(n \operatorname{arccosh} \omega), & |\omega| > 1 \end{cases} \tag{5.224}$$

and the order n is calculated by

$$n = \frac{\log \left(\sqrt{(A^2 - 1)/\varepsilon^2} + \sqrt{(A^2 - 1)/\varepsilon^2 - 1} \right)}{\log \left(\omega_a/\omega_c + \sqrt{\omega_a^2/\omega_c^2 - 1} \right)}, \tag{5.225}$$

where we allowed for an arbitrary cut-off frequency ω_c and auxiliary frequency $\omega_a > \omega_c$. Fig. 5.57a shows a typical magnitude response of the type I Chebyshev filter for odd n . It is seen that the ripple has equal amplitudes over the passband. The error in the passband is thus $1/(1 + \varepsilon^2)$.

Type II Chebyshev Filter

The type II Chebyshev filter has both zeros and poles. Therefore, its transfer function is represented with a general relation

$$H(s) = G_0 \frac{\prod_{k=1}^m (s - z_k)}{\prod_{k=1}^n (s - p_k)}, \tag{5.226}$$

where all of the zeros are purely imaginary corresponding to the points

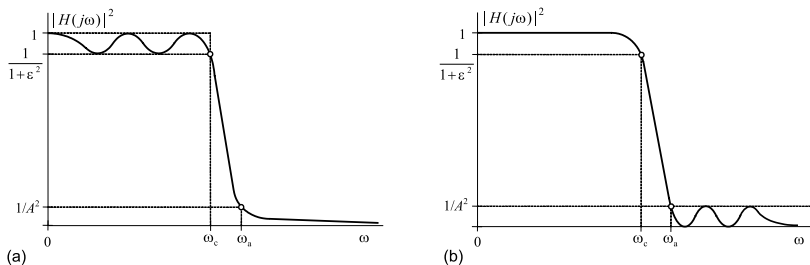


Fig. 5.57. Two types of the Chebyshev filter for odd order n : (a) ripple in bandpass and (b) ripple in stopband.

$$z_k = j\omega_a \left(\cos \frac{2k-1}{2n} \pi \right)^{-1}, \quad k = 1, 2, \dots, n, \quad (5.227)$$

and the poles are defined by (5.222) if to substitute

$$\sigma_k = \omega_a \frac{\alpha_k}{\alpha_k^2 + \beta_k^2}, \quad \mu_k = -\omega_a \frac{\beta_k}{\alpha_k^2 + \beta_k^2},$$

where

$$\alpha_k = -\frac{\gamma - \gamma^{-1}}{2} \sin \frac{(2k-1)\pi}{2n},$$

$$\beta_k = \frac{\gamma + \gamma^{-1}}{2} \cos \frac{(2k-1)\pi}{2n},$$

and $\gamma = (A + \sqrt{A^2 - 1})^{1/n}$.

The magnitude response of the type II Chebyshev filter is defined by

$$|H(j\omega)|^2 = \frac{1}{1 + \varepsilon^2 T_n^2(\frac{\omega_a}{\omega_c}) / T_n^2(\frac{\omega_a}{\omega_c \omega})}, \quad (5.228)$$

where the Chebyshev polynomial is given by (5.224) and the filter order is calculated by (5.225). Fig. 5.57b sketches a typical magnitude response of the type II Chebyshev filter for odd n . As can be seen, the response is flat in the passband and ripples appear in the stopband with a maximum amplitude at the level of $1/A$.

Overall, as follows, each type of Chebyshev filters is completely specified with a given ω_c by any of the following parameters:

- Filter order n .
- Ripple factor ε .
- Frequency $\omega_a > \omega_c$ at which an attenuation parameter A must be given.
- Attenuation parameter A corresponding to ω_a .

Example 5.53 (Chebyshev LP filter). The Chebyshev LP filter is designed for $f_c = 60\text{Hz}$ (-2 dB) and $f_a = 80\text{Hz}$ (-66 dB).

From an equality $-2 = 20 \log \frac{1}{\sqrt{1+\varepsilon^2}}$, we determine $\varepsilon = 0.764$ and an equality $-66 = 20 \log \frac{1}{A}$ yields $A = 1995$. By (5.225), the filter order is calculated as $n = 10.762$ and we let $n = 11$.

The frequency response of the type I filter is shown in Fig. 5.58. Inherently,

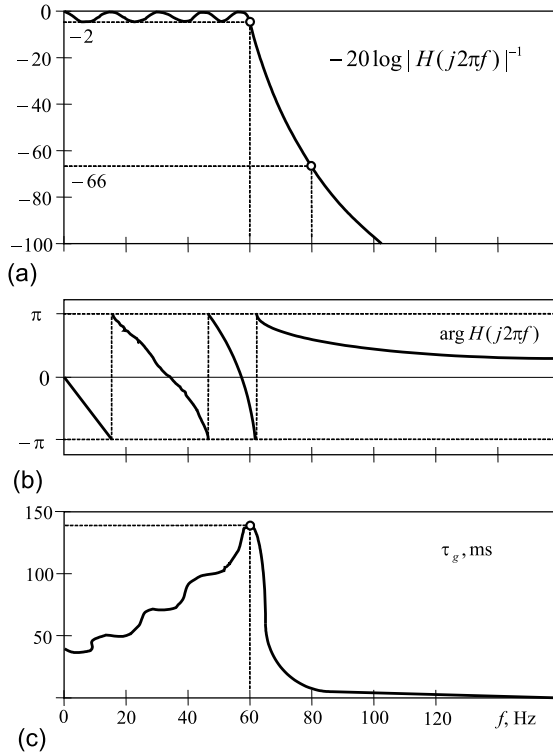


Fig. 5.58. Frequency response of an 11-order Chebyshev LP filter of type I (Example 5.53): (a) magnitude, (b) phase mod 2π , and (c) group delay.

the ripple appears in the passband with a maximum amplitude corresponding to -2 dB . Beyond the passband, the magnitude response (Fig. 5.58a) rolls off monotonously. Like the case of Butterworth filters, here the phase response (Fig. 5.58b) is not linear causing the group delay to be not constant (Fig. 5.58c) with a maximum delay of about 140 ms at the cut-off frequency.

Fig. 5.59 illustrates the frequency response of the type II filter. Just on the contrary, here the ripple appears in the magnitude response (Fig. 5.59a) in the stopband with a maximum amplitude corresponding to -66 dB . Within the passband, the magnitude response is flat. The phase response (Fig. 5.59b)

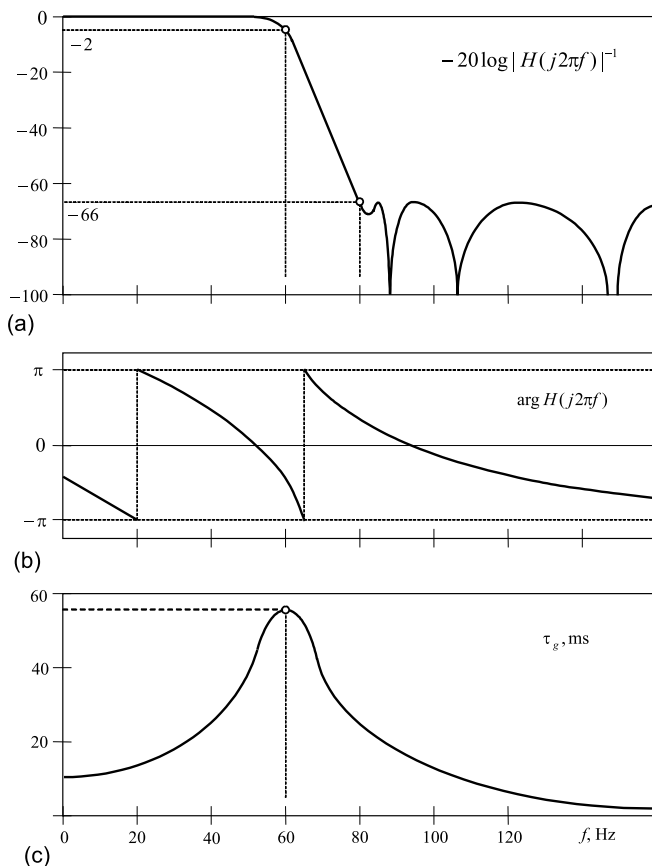


Fig. 5.59. Frequency response of an 11-order Chebyshev LP filter of type II (Example 5.53): (a) magnitude, (b) phase mod 2π , and (c) group delay.

is still not linear. Therefore, the group delay (Fig. 5.59c) ranges from zero up to decades of ms with a maximum value of about 55 ms at the cut-off frequency. \square

As well as the Butterworth filter, the Chebyshev one of n -order can be implemented practically for the given ripple factor ε , bandwidth, and roll-off beyond. Engineering methodologies to design LC and RC Chebyshev filters of type I and II can be found in a number of books devoted to analog filters design. These books give also an opportunity to design filters based on the Bessel, elliptic, and some other useful approximations.

In this Chapter we considered basic methods of LTI systems description in the frequency (ω) domain and transform ($s = \sigma + j\omega$) domain associated, respectively, with Fourier analysis and Laplace analysis. Even though the

transform domain and time domain are equivalent for LTI systems, in many cases namely the transform allows solving problems with low burden.

5.8 Summary

In the transform domain, LTI systems are analyzed using the Fourier and Laplace transforms via the frequency response and transfer function, respectively. The following fundamental canons serve in the transform domains:

- The LTI system frequency response is
 - The response to $e^{j\omega t}$.
 - The Fourier transform of the impulse response $h(t)$.
 - The ratio of the Fourier transforms of the output and input.
- As a complex function, the frequency response is specified with the magnitude and phase responses.
- A transmission is distortionless, if the input is scaled and delayed.
- The phase delay is evaluated by the negative ratio of the phase response to the angular frequency.
- The group delay is evaluated by the negative derivative of the phase response with respect to the angular frequency.
- Filtering is the process, by which the amplitudes of some spectral components of the input are changed or even suppressed.
- The Laplace transform is a generalization of the Fourier transform for the complex frequency. It may be bilateral and unilateral.
- In order for the Laplace transform to be unique for each function, the region of convergence must be specified as part of the transform.
- The system transfer function is
 - The ratio of the Laplace transforms of the output and input.
 - The Laplace transform of the impulse response $h(t)$.
- A closed loop system is stable if all of the roots of the characteristic equation have negative real part (lie in the left part of the complex plane).
- The gain and phase stability margins determine the relative degree of system stability.
- Negative feedback reduces the gain and expands the bandwidth of a system. Positive feedback increases the gain and contracts the bandwidth.

5.9 Problems

5.1. Find simple words to explain why the LTI systems can equivalently be represented in the time and frequency domains. How does this property relate to the inherent property of linearity of LTI systems?

5.2. Analyze electronic systems briefly described in Chapter 1 and explain which system may better be analyzed in the time domain and which in the frequency domain.

5.3 (Frequency response). An LTI system is represented with the following impulse response. Define the frequency response of a system.

1. $h(t) = e^{-at}u(t), a > 0$
2. $h(t) = e^{-3t}u(t) \sin t$
3. $h(t) = Au(t) - Au(t - \tau)$
4. $h(t) = e^{3t}u(-t)$
5. $h(t) = Au(t) - 2Au(t - \tau) + Au(t - 2\tau)$
6. $h(t) = e^{-2|t|}$
7. $h(t) = a \left(1 - \frac{t}{\tau}\right) [u(t) - u(t - \tau)]$
8. $h(t) = |t - 1|e^{-|t|}$
9. $h(t) = a \frac{t}{\tau} [u(t) - u(t - \tau)]$
10. $h(t) = \delta(t) + e^{-t}u(t)$
11. $h(t) = a \frac{\sin b|t|}{|t|}, a > 0, b > 0$

5.4. Derive and investigate the magnitude and phase responses of an LTI system, which frequency response is specified in Problem 5.1.

5.5. The input and output signals of an LTI system are given below, $x(t)$ and $y(t)$, respectively. Define the frequency response $H(j\omega)$ of a system

- | | |
|--|--|
| 1. $x(t) = u(t)$ | $y(t) = te^{-2t}u(t)$ |
| 2. $x(t) = u(t)$ | $y(t) = t^2e^{-t}u(t)$ |
| 3. $x(t) = e^{-t}u(t)$ | $y(t) = u(t)$ |
| 4. $x(t) = u(t) - e^{-2t}u(t - \tau)$ | $y(t) = e^{-2t}u(t)$ |
| 5. $x(t) = a \frac{t}{\tau} [u(t) - u(t - \tau)]$ | $y(t) = a[u(t) - u(t - \tau)]$ |
| 6. $x(t) = a \left(1 - \frac{t}{\tau}\right) [u(t) - u(t - \tau)]$ | $y(t) = a \frac{t}{\tau} [u(t) - u(t - \tau)]$ |

5.6. An LTI system is represented with the impulse response shown in Fig. 5.60. Define the frequency response of a system. Derive and plot its magnitude and phase responses.

5.7. An LTI system is given with the following spectral densities of its input and output, $X(j\omega)$ and $Y(j\omega)$, respectively. Define the frequency response of a system. Draw plots of the magnitude and phase responses

- | | |
|---|---|
| 1. $X(j\omega) = \frac{2}{1+j\omega}$ | $Y(j\omega) = \frac{1}{(1+j\omega)^2}$ |
| 2. $X(j\omega) = \frac{1}{1+j\omega} + \frac{1}{1-j\omega}$ | $Y(j\omega) = \frac{1}{1+j\omega}$ |
| 3. $X(j\omega) = k \frac{\sin \omega\tau}{\omega}$ | $Y(j\omega) = \frac{A}{1-j\omega}$ |
| 4. $X(j\omega) = \frac{1}{(1+j\omega)(1-2j\omega)^2}$ | $Y(j\omega) = \frac{1}{2(1+j\omega)^2}$ |
| 5. $X(j\omega) = A[u(\omega) - u(\omega - \omega_c)]$ | $Y(j\omega) = B[u(\omega - 0.5\omega_c) - u(\omega - 0.8\omega_c)]$ |
| 6. $X(j\omega) = k_1 \frac{\sin \omega\tau}{\omega} \frac{\sin \omega\tau/2}{\omega}$ | $Y(j\omega) = k_2 \frac{\sin^2 \omega\tau}{\omega^2}$ |

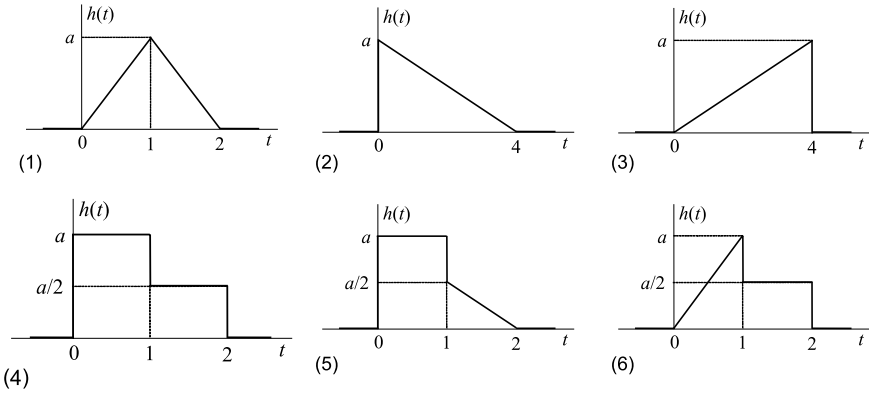


Fig. 5.60. Impulse response of a system.

5.8. A LTI system is given with the ODE

1. $3y''' + \sum_{m=1}^2 b_m \frac{d^m x}{dt^m} - 4y' + y = 2x, b_2 = 2, b_1 = 1$
2. $ay'' + by' + cy = dx'' - ex'$
3. $2 \frac{d^2 x}{dt^2} + 4x + y = 2 \frac{d^3 y}{dt^3} + 4 \frac{dx}{dt}$
4. $4(\int y dt - x') = 3(y' - x)$
5. $a_2 y'' - b_0 x - a_1 y' - b_1 x' = 0$
6. $2y'' - 3 \int y dt = 2x' - x$
7. $2 \frac{d^2 y}{dt^2} + x + 2y = 2 \frac{d^3 y}{dt^3} + 4 \frac{dx}{dt}$

Define the frequency response of a system. Draw and analyze the magnitude and phase responses.

5.9. Show the Bode plot of the magnitude response found in Problem 5.7. Determine the function slopes, in dB/decade, in different regions.

5.10. Explain why the linear and constant phase and group delays are preferable for systems. Give examples of systems, in which the nonzero and nonlinear phase and group delays may cause substantial errors.

5.11. Define the phase and group delays of an LTI system, which frequency response is found in Problem 5.8.

5.12 (Filtering). An LTI system is given with the frequency response associated with the ODE (Problem 5.8). Define the magnitude response. What kind of filters (LP, HP, BP, or BR) represents this response?

5.13. An LTI filter is designed to have the following frequency response. Define the impulse response of a filter.

$$1. H(j\omega) = \begin{cases} 1, & 0 \leq \omega \leq \omega_c \quad \text{and} \quad 2\omega_c \leq \omega \leq 3\omega_c \\ 0, & \text{otherwise} \end{cases}$$

2. $H(j\omega) = \begin{cases} a \left(1 - \frac{|\omega|}{\omega_c}\right), & \omega \leq |\omega_c| \\ 0, & \text{otherwise} \end{cases}$
3. $H(j\omega) = \begin{cases} 2A, & 0 \leq \omega < 0.5\omega_c \\ A, & 0.5\omega_c \leq \omega \leq \omega_c \\ 0, & \text{otherwise} \end{cases}$
4. $H(j\omega) = Ae^{-a|\omega|}$
5. $H(j\omega) = A \frac{\sin a\omega}{\omega}$

In the last case, use the duality property of the Fourier transform.

5.14. An AM signal $x(t) = A_0(1 + 0.25 \cos 0.1\omega_0 t) \cos \omega_0 t$ passes through an LTI filter with the following frequency response. Determine the amplitudes of the spectral components in the input and output of the filter.

1. LP filter: $H(j\omega) = \frac{1}{1+j\omega/\omega_0}$
2. HP filter: $H(j\omega) = \frac{j\omega/\omega_0}{1+j\omega/\omega_0}$
3. BR filter: $H(j\omega) = \frac{j\xi(\omega)}{1+j\xi(\omega)}$, $\xi = 4(\omega - \omega_0)/\omega_0$
4. BP filter: $H(j\omega) = \frac{1}{1+j\xi(\omega)}$, $\xi = 4(\omega - \omega_0)/\omega_0$

5.15 (Systems of the first order). An LTI system of the first order is given with an electrical equivalent (Fig. 5.61). Define the frequency response of the system.

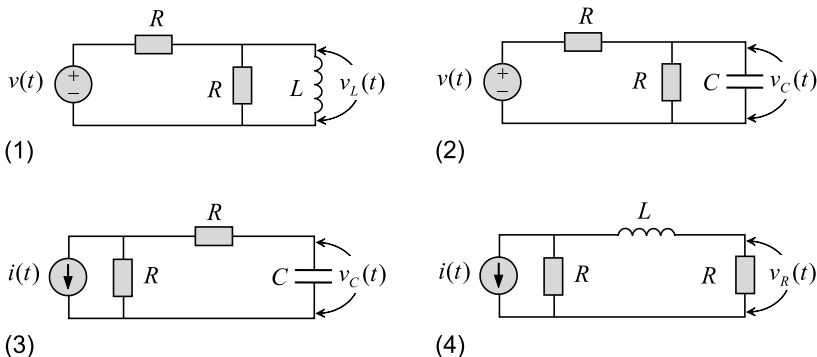


Fig. 5.61. Systems of the first order.

5.16. Define the magnitude response of a system given in Problem 5.15. What kind of filters represents this system. Show the Bode plot and determine the cut-off frequency.

5.17. Define the phase response of a system given in Problem 5.15. Evaluate the phase and group delays.

5.18 (Systems of the second order). An electrical system of the second order is given with the scheme shown in Fig. 5.62. Define the frequency response of the system.

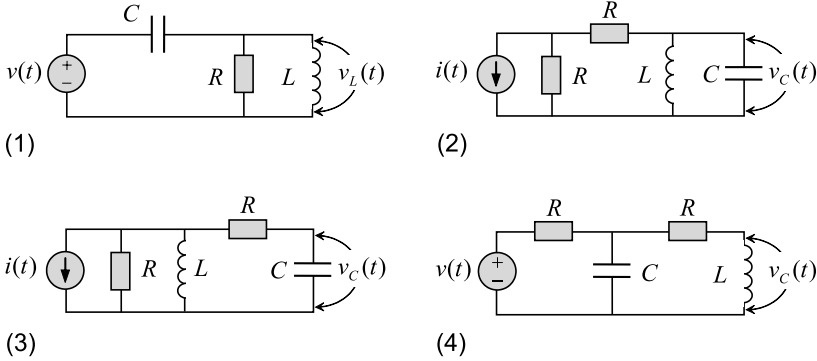


Fig. 5.62. Systems of the second order.

5.19 (Laplace transform). Define the transfer function of a system represented with the impulse response (Problem 5.3). Determine the region of convergence for each Laplace transform. Characterize causality of a system.

5.20. Given the input and output (Problem 5.5), define the transfer function of a system and ascertain its stability.

5.21. An LTI system is represented with the ODE (Problem 5.8). Assuming zero initial conditions and using the properties of the Laplace transform, define the transfer function of a system and the relevant ROC.

5.22. An LTI system is represented with the following transfer function. Find the zeros and poles. Ascertain stability and causality.

$$1. H_1(s) = \frac{(s+1)(s-3)}{(s^2+2s-1)(s+3)}, \quad \text{Re}(s) > -0.5$$

$$2. H_2(s) = \frac{s-1}{(s+2)(s-5)(s+6)}, \quad \text{Re}(s) > 1$$

$$3. H_3(s) = \frac{s+4}{s^2-s-2} + \frac{1}{s+1}, \quad \text{Re}(s) < 0.5$$

$$4. H_4(s) = \frac{1}{s-1} + \frac{2}{s+2} + \frac{1}{s+3}, \quad \text{Re}(s) < -0.5$$

5.23. Using the cover-up method, represent the transfer functions given in Problem 5.22 (items 1–3) in the simple forms (as in item 4) placed to a table of the Laplace transforms.

5.24. The zeros and poles of the LTI system transfer function are placed on the ROC as shown in Fig. 5.63. Which system is stable and which is not? Which is causal and which is not?

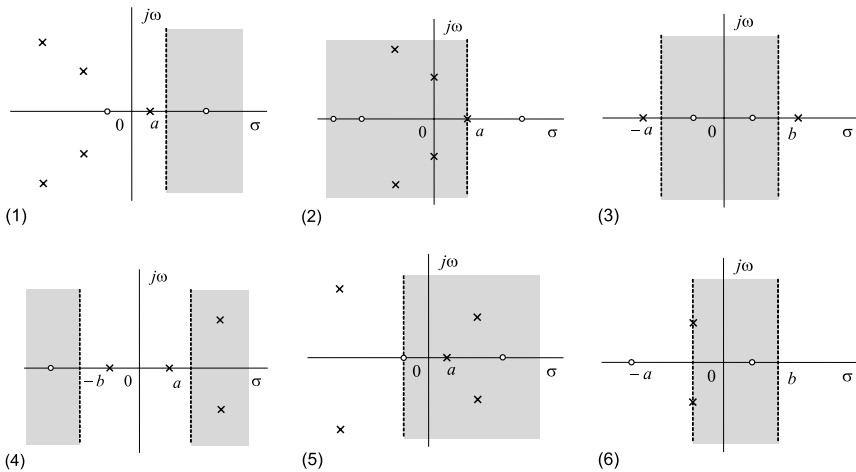


Fig. 5.63. ROCs of systems with known poles and zeros.

5.25 (Solving ODEs with the Laplace transform). An LTI system is given with the ODE $y' + 0.1y = 2x'$, $y(0) = 1$. Solve this equation using the Laplace method.

5.26. Assuming arbitrary initial conditions and using the unilateral Laplace transform, solve the ODE of an LTI system given in Problem 5.8.

5.27. Show the Laplace domain equivalent of electric circuits given in Fig. 5.61 and Fig. 5.62. Write an equation of the circuit in the Laplace form. Use a table of the Laplace transforms and go to the time function.

5.28 (Block diagrams). Represent the system ODE (Problem 5.8) in the first and second direct forms of diagrams in the s domain.

5.29 (State space model in the s domain). The state space model of a system, $\mathbf{q}'(t) = \mathbf{A}\mathbf{q}(t) + \mathbf{B}\mathbf{x}(t)$ and $\mathbf{y}(t) = \mathbf{C}\mathbf{q}(t) + \mathbf{D}\mathbf{x}(t)$, is given with the following matrices. Define the transfer function of a system

1. $\mathbf{A} = \begin{bmatrix} 2 & 4 \\ 0 & 2 \end{bmatrix}$, $\mathbf{B} = \begin{bmatrix} 0 \\ 2 \end{bmatrix}$, $\mathbf{C} = [1 \ 0]$, $\mathbf{D} = [0]$.
2. $\mathbf{A} = \begin{bmatrix} -1 & 0 \\ 0 & -1 \end{bmatrix}$, $\mathbf{B} = \begin{bmatrix} 1 & 0 \\ 0 & 1 \end{bmatrix}$, $\mathbf{C} = \begin{bmatrix} 1 & 0 \\ 0 & 1 \end{bmatrix}$, $\mathbf{D} = \begin{bmatrix} -1 & 0 \\ 0 & -1 \end{bmatrix}$.

In the case of a MIMO system (item 2), solve the problem for every input-to-output pair.

5.30 (Stability of closed loop systems). A feedback with the transfer function $H_b = 1/s$ is placed over the system given in Problem 5.22. Ascertain stability of the system by the Routh-Hurwitz test.

5.31. Test the system given in Problem 5.30 by the Nyquist criterion of stability.

5.32. Define the gain and phase stability margins of systems described in Problem 5.30.

5.33 (Selective filters approximations). An LP filter is required with the cut-off frequency $f_c = 11$ kHz at -1 dB and additional frequency $f_a = 12$ kHz at -60 dB. Determine the Butterworth filter order and Chebyshev filter order.

5.34. A 5-order Butterworth LP filter is used with a cut-off frequency $f_c = 1$ MHz at -1 dB. Determine the roll-off slope and attenuation (in dB) at $f_a = 1.5f_c$.

5.35. Solve Problem 5.34 for the 5-order Chebyshev LP filter having ripple -1 dB in the passband and a cut-off frequency $f_c = 100$ kHz.

Linear Time-Varying Systems

6.1 Introduction

Any linear system represented with the time-dependent operator $\mathcal{O}(t)$ demonstrates different properties at least at two different time instances. A system of this type is called *linear time-varying* (LTV) or *time-variant* and its $p \times 1$ output and $k \times 1$ input are coupled by the $p \times k$ time-varying operator matrix $\mathbf{O}(t)$ as follows

$$\mathbf{y}(t) = \mathbf{O}(t)\mathbf{x}(t). \quad (6.1)$$

Actually, any real physical system is time-varying at least owing to the flicker noise in its components and environmental influence (e.g. thermal) making the operator variable. In some applications, it is allowed to ignore such a nuisance dependency as being insignificant. In another ones, the effect results in substantial violations of system's characteristics. Moreover, it can be generated artificially to attach some special properties to systems. Examples are the linear parametric amplifier with its ability to remove spectral components from one frequency region to another and tracking filter following with time the carrier frequency (or phase) of the input.

Since the system operator $\mathcal{O}(t)$ is time-varying, of prime importance is to realize how the variations result in the output. On the other hand, it is often desirable to find a proper LTV operator to obtain the required characteristics of a system. In both cases, the problem is directly coupled with stability of a solution, which investigation occupies an important place in the theory of LTV systems.

6.2 Time-varying Impulse Response and General Convolution

Because an LTV system is still linear, we could try representing it with the convolution. The latter, however, must be modified for the inherent time-

dependency in the operator $\mathcal{O}(t)$ causing the system impulse response to be time-varying as well.

For the sake of simplicity, we start with a SISO LTV system, which output $y(t)$, by (6.1), is coupled with the input $x(t)$ by

$$y(t) = \mathcal{O}(t)x(t). \quad (6.2)$$

Let us think that the input is shaped with the delta function $\delta(t)$ acting at some arbitrary time θ . Since, by the definition, the response of an LTI system to $\delta(t - \theta)$ is its impulse response $h(t - \theta)$, then it is in order supposing that the response of an LTV system to $\delta(t - \theta)$ is its time-varying impulse response $h(t, \theta)$. We therefore can rewrite (6.2) as

$$h(t, \theta) = \mathcal{O}(t)\delta(t - \theta), \quad (6.3)$$

noticing that $h(t, \theta)$ cannot commonly be a function of $t - \theta$, like for LTI systems. It certainly must be a more sophisticated function of t and θ .

We can now exploit an identity

$$x(t) = \int_{-\infty}^{\infty} x(\theta)\delta(t - \theta) d\theta, \quad (6.4)$$

apply the operator $\mathcal{O}(t)$ to both its sides, and, by (6.2) and (6.3), write

$$y(t) = \mathcal{O}(t) \int_{-\infty}^{\infty} x(\theta)\delta(t - \theta) d\theta = \int_{-\infty}^{\infty} x(\theta)\mathcal{O}(t)\delta(t - \theta) d\theta = \int_{-\infty}^{\infty} x(\theta)h(t, \theta) d\theta.$$

The convolution for SISO LTV systems has thus the form of

$$y(t) = x(t) * h(t, \theta) = \int_{-\infty}^{\infty} x(\theta)h(t, \theta) d\theta. \quad (6.5)$$

Relation (6.5) is called the *general convolution* or *general superposition integral*. Analogously to LTI systems, it is readily extended to SIMO, MISO, and MIMO LTV systems.

The term “general” suggests that (6.5) is applicable for both LTI and LTV systems. To verify, let us suppose that the system operator is time-invariant. For any time shift τ , we hence can write $h(t, \theta) = h(t - \tau, \theta - \tau)$. By $\tau = \theta$, one goes to $h(t, \theta) = h(t - \theta, 0)$. For LTI systems, the second variable “0” is meaningless, and we arrive at the familiar convolution integral (4.4),

$$y(t) = \int_{-\infty}^{\infty} x(\theta)h(t - \theta, 0) d\theta = \int_{-\infty}^{\infty} x(\theta)h(t - \theta) d\theta. \quad (6.6)$$

A verification of (6.6) is straightforward. If one lets $x(\theta) = \delta(\theta)$ and thus, by the definition, $y(t) = h(t)$, an equality of both sides is guaranteed by the sifting property of the delta function.

In a like manner, one can verify (6.5). Indeed, by letting $x(\theta) = \delta(\theta - \tau)$ and substituting $y(t) = h(t, \tau)$, where τ is any time shift, we obtain an equality $h(t, \tau) = h(t, \tau)$, provided the definition:

Time-varying impulse response: The response of a system at time t to the unit impulse at time θ is the LTV system time-varying impulse response $h(t, \theta)$.

□

The realizability constraint for the time-varying impulse response is a zero value $h(t, \theta) = 0$ for $t < \theta$. Therefore, the output (6.5) is commonly expressed, by changing a variable to $\tau = t - \theta$, in two equal forms of

$$y(t) = \int_{-\infty}^t x(\theta)h(t, \theta) d\theta = \int_0^{\infty} x(t - \tau)h(t, t - \tau) d\tau. \quad (6.7)$$

Example 6.1. An LP filter with a modulated bandwidth $a(t) = (1 + \alpha \cos \Omega t)$ is described by the ODE

$$y' + a(t)y = b(t)x, \quad (6.8)$$

having $b(t) = a(t)$ and a zero initial condition, $y(0) = 0$. By (4.54), a general solution of (6.8) is given as

$$y(t) = e^{-\int_0^t a(\tau) d\tau} \int_0^t b(\tau)x(\tau)e^{\int_0^{\tau} a(\tau_1) d\tau_1} d\tau \quad (6.9)$$

$$= e^{-t - \frac{\alpha}{\Omega} \sin \Omega t} \int_0^t (1 + \alpha \cos \Omega \tau)x(\tau)e^{\tau + \frac{\alpha}{\Omega} \sin \Omega \tau} d\tau. \quad (6.10)$$

The time-varying impulse response is provided, by $x(t) = \delta(t - \theta)$, to be

$$h(t, \theta) = (1 + \alpha \cos \Omega \theta)e^{-(t-\theta)} e^{-\frac{\alpha}{\Omega}(\sin \Omega t - \sin \Omega \theta)} u(t - \theta). \quad (6.11)$$

It is seen that, by $\alpha = 0$, the response (6.11) degenerates to $h(t, \theta) = e^{-(t-\theta)} u(t - \theta)$ as associated with the unmodulated filter. If we further shift both time variables on θ , the response becomes $h(t - \theta, \theta - \theta) = e^{-(t-\theta-\theta+\theta)}$, or $h(t - \theta) = e^{-(t-\theta)} u(t - \theta)$ or, by $\theta = 0$, $h(t) = e^{-t} u(t)$, corresponding to the LTI filter. □

Example 6.2. Given a SISO LTV system (LP filter) described by (6.8) with $a(t) = 2t$, $b(t) = 1$, and a zero initial condition $y(0) = 0$. The solution (6.9) readily produces

$$y(t) = e^{-t^2} \int_0^t x(\tau) e^{\tau^2} d\tau \quad (6.12)$$

leading, by $x(t) = \delta(t - \theta)$, to the time-varying impulse response

$$h(t, \theta) = e^{-(t^2 - \theta^2)} u(t - \theta). \quad (6.13)$$

To get an ultimate assurance that the system is LTV, we allow a time shift τ to the power of the exponential function in (6.13), $(t + \tau)^2 - (\theta + \tau)^2 = (t^2 - \theta^2) + 2\tau(t - \theta)$. Once τ causes an additional time-function $2\tau(t - \theta)$, the system is time-varying and thus $h(t, \theta) \neq h(t - \theta)$. Fig. 6.1a sketches (6.13) as a bi-time surface plot and Fig. 6.1b gives sections for several values of θ .

It is neatly seen (Fig. 6.1b) that the impulse response narrows as θ increases and that its peak value lies at unity. A phenomenon has a clear physical explanation. Recall that the coefficient $a(t) = 2t$ represents, in (6.8), the bandwidth of a system and that the wider bandwidth, the narrower the impulse response. Since $a(t)$ increases with time, the impulse response ought to compress possessing a zero-width at infinity. Namely this tendency is seen in Fig. 6.1, by increasing θ . \square

Example 6.3. An LTV system (Example 6.2) is described with the impulse response (6.13). The input is $x(t) = u(t)$. Therefore, by (6.7) and an identity $\int_0^x e^{a^2 t^2} dt = \frac{\sqrt{\pi}}{2a} \operatorname{erfi}(ax)$, where $\operatorname{erfi}(x)$ is an imaginary error function, the output is defined as

$$y(t) = \int_0^t e^{-(t^2 - \theta^2)} d\theta = e^{-t^2} \int_0^t e^{\theta^2} d\theta = \frac{\sqrt{\pi}}{2} e^{-t^2} \operatorname{erfi}(t). \quad (6.14)$$

On the other hand, a general solution (6.9) transforms, by $x(t) = u(t)$, to $y(t) = e^{-t^2} \int_0^t e^{\tau^2} d\tau$ that is identical to (6.14). \square

6.2.1 Modified Time-varying Impulse Response

Two inconveniences arise in applications of the time-varying impulse response $h(t, \theta)$. First, the realizability constraint $t < \theta$ involves two variables. Second, the Fourier transform of $h(t, \theta)$ is not the frequency response of an LTV system. To circumvent, Kailath¹ proposed to modify $h(t, \theta)$ in two forms by

¹ Thomas Kailath, Indian-born US mathematician, 7 June 1935-

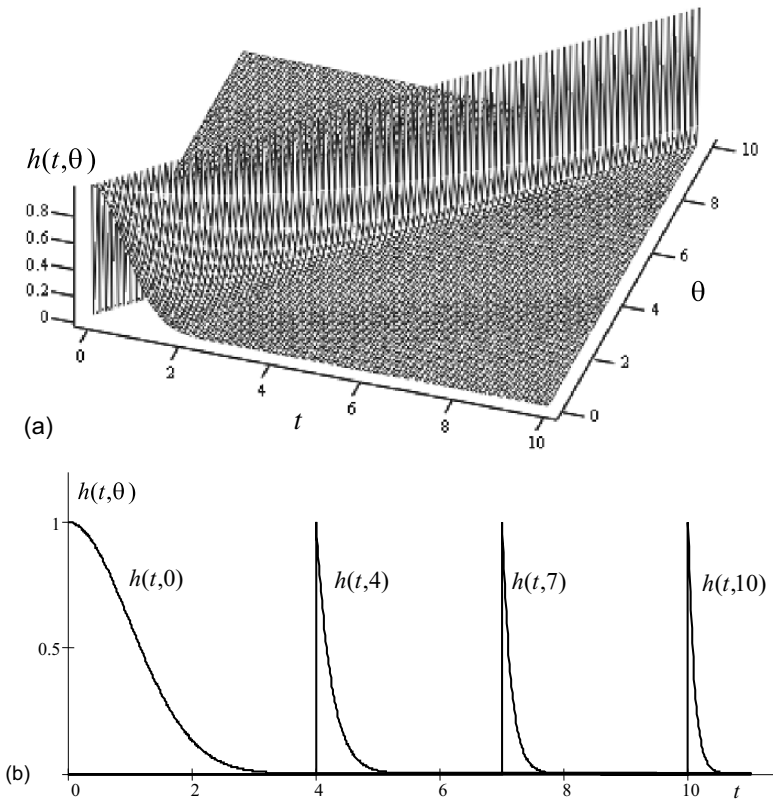


Fig. 6.1. Time-varying impulse response (6.13): (a) bi-time presentation and (b) sections for fixed values of θ .

changing the variables. One of those forms has gained currency in the time-varying communications channels and can be useful in other applications. Below we present this form as the *modified* time-varying impulse response.

Let us change the variables in $h(t, \theta)$ based on the relation $t - \theta = \tau$. If we substitute t with τ and θ with t , we arrive at a new function $\bar{h}(\tau, t)$, provided the definition:

The modified time-varying impulse response: The response of a system at time t to the unit impulse at time $t - \tau$ is the LTV system modified impulse response $\bar{h}(\tau, t)$.

□

In other words, $\bar{h}(\tau, t)$ is a response measured at t to the unit impulse applied τ seconds ago. The realizability constraint for the modified response involves only one variable τ , namely the constraint is a zero value $\bar{h}(\tau, t) = 0$ for $\tau < 0$. This predetermines the convolution to be

$$y(t) = \int_{-\infty}^t \bar{h}(t-\theta, t)x(\theta)d\theta = \int_0^{\infty} \bar{h}(\tau, t)x(t-\tau)d\tau. \quad (6.15)$$

The obvious relations between the time-varying impulse response and its modified version are thus the following

$$\begin{aligned} h(t, \theta) &= \bar{h}(t-\theta, t), \\ \bar{h}(\tau, t) &= h(t, t-\tau), \end{aligned} \quad (6.16)$$

where, by Kailath, t is a current time corresponding to instant of observation, θ corresponds to instant of the unit impulse in the input, and τ corresponds to age of input.

Example 6.4. An LTV system is represented with the time-varying impulse response (6.13). By (6.16), the modified response is readily derived to be

$$\bar{h}(\tau, t) = h(t, t-\tau) = e^{-(2t-\tau)\tau}u(\tau). \quad (6.17)$$

Fig. 6.2a shows the bi-time (two-dimensional) presentation of (6.17) and Fig. 6.2b sketches several section of the surface plot for small values of τ .

Observing Fig. 6.2, one can infer that the modified function (6.17) tends toward infinity at $t = 0$, by increasing τ , and approaches zero with time t , except for the case when $\tau = 0$. Recall that the response $h(t, \theta)$ (6.13) does not exceed unity in the allowed range of θ and t (Fig. 6.1) that makes it more preferable from the computational point of view. \square

It can be shown, by the transformation of time variables, that the convolution forms, (6.7) and (6.15), are coupled by the relations:

$$\begin{aligned} y(t) &= \int_{-\infty}^t h(t, \theta)x(\theta)d\theta = \int_0^{\infty} h(t, t-\tau)x(t-\tau)d\tau \\ &= \int_{-\infty}^t \bar{h}(t-\theta, t)x(\theta)d\theta = \int_0^{\infty} \bar{h}(\tau, t)x(t-\tau)d\tau. \end{aligned} \quad (6.18)$$

Example 6.5. An LTV system is specified with the responses (6.13) and (6.17). Although with different variables, the response of a system to the unit step $x(t) = u(t)$ is equivalently defined, by (6.18), to be

$$\begin{aligned} y(t) &= \int_0^{\infty} e^{-[t^2-(t-\theta)^2]}u(\theta)u(t-\theta)d\theta = \int_t^{\infty} e^{-2t\theta+\theta^2}d\theta \\ &= \int_0^{\infty} e^{-(2t-\tau)\tau}u(\tau)u(t-\tau)d\tau = \int_t^{\infty} e^{-2t\tau+\tau^2}d\tau, \end{aligned}$$

meaning that two definitions are equal. \square

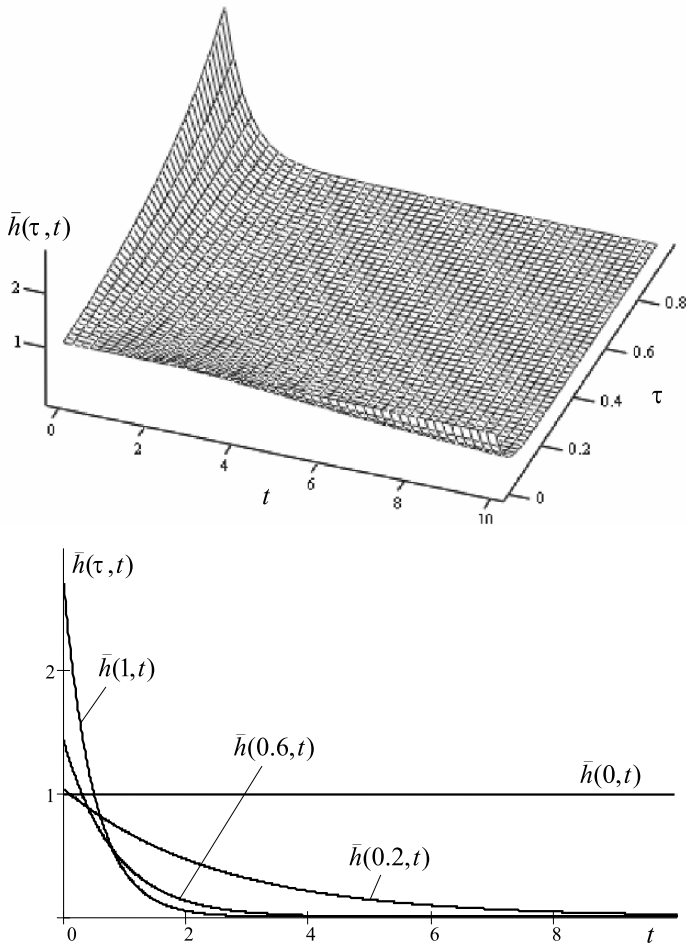


Fig. 6.2. Modified impulse response (6.17): (a) bi-time presentation and (b) sections for fixed values of τ .

Range of Existence for Impulse Responses

Here is the place to outline and compare the ranges of existence for the time-varying and modified time-varying impulse responses as shown in Fig. 6.3. By the bi-variable constraint, the response $h(t, \theta)$ does not equal zero in the shadowed section in Fig. 6.3a, when $t \geq \theta$. In the case of $\bar{h}(\tau, t)$, we need setting τ nonnegative. By this constraint, the modified response exists for all nonnegative values, $\tau \geq 0$, in the shadowed section in Fig. 6.3b. Because $\bar{h}(\tau, t)$ is constrained by only one variable τ , it certainly possesses more

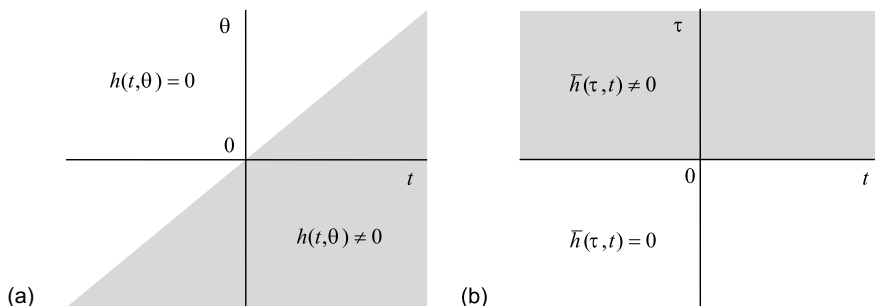


Fig. 6.3. Range of existence of the time-varying impulse response: (a) $h(t, \theta)$ and (b) $\bar{h}(\tau, t)$.

engineering features. One, however, needs to remember that $\bar{h}(\tau, t)$ is defined in a somewhat artificial way, contrary to $h(t, \theta)$.

6.2.2 Time-varying Frequency Response

If $h(t, \theta)$ satisfies the Dirichlet conditions, it can be represented in the frequency domain by the Fourier transform. Unfortunately, the transform does not produce the LTV system frequency response, because the input unit impulse is shifted on θ with respect to the response time t , unlike the LTI systems case. We thus need starting with the basic definition:

Frequency response: The ratio of the system response to the complex exponential signal $x(t) = e^{j\omega t}$ and $e^{j\omega t}$ is the LTV system time-varying frequency response,

$$H(j\omega, t) = \frac{\text{Response to } e^{j\omega t}}{e^{j\omega t}}. \quad (6.19)$$

□

From (6.19) we have

$$y(t) = \text{Response to } e^{j\omega t} = H(j\omega, t)e^{j\omega t} = \mathcal{O}(t)e^{j\omega t} \quad (6.20)$$

and conclude that, unlike the LTI systems case, the frequency response of an LTV system changes with time.

Example 6.6. Consider an LTV system (6.8) with the input $x(t) = e^{j\omega t}$ and zero initial condition $y(0) = 0$. By (6.20), its output is specified by $y(t) = H(j\omega, t)e^{j\omega t}$. Substituting $x(t)$ and $y(t)$ to (6.8) yields the ODE

$$H' + [j\omega + a(t)]H = b(t),$$

which general solution, by (6.9), is given as

$$H(j\omega, t) = e^{-\int_0^t [j\omega + a(\tau)] d\tau} \int_0^t b(\tau) e^{\int_0^\tau [j\omega + a(\tau_1)] d\tau_1} d\tau.$$

For the coefficients $a(t) = 2t$ and $b(t) = 1$ (Example 6.2), by an identity $\int e^{-(ax^2+bx+c)} dx = \frac{1}{2} \sqrt{\frac{\pi}{a}} e^{\frac{b^2-4ac}{4a}} \operatorname{erf}\left(x\sqrt{a} + \frac{b}{2\sqrt{a}}\right)$, the solution becomes

$$\begin{aligned} H(j\omega, t) &= e^{-j\omega t - t^2} \int_0^t e^{j\omega\tau + \tau^2} d\tau \\ &= -j \frac{\sqrt{\pi}}{2} e^{-j\omega t - t^2 + \frac{\omega^2}{4}} \left[\operatorname{erf}\left(jt - \frac{\omega}{2}\right) + \operatorname{erf}\left(\frac{\omega}{2}\right) \right]. \end{aligned} \tag{6.21}$$

Fig. 6.4 illustrates the magnitude response associated with (6.21). It is seen (Fig. 6.4a) that, by $t = 0$, the response is zero for all frequencies. This is because the integration range is zero with $t = 0$. The case of $t = 0$ is thus isolated. With $t \approx 1$, the response is brightly pronounced. Further increase in t and ω forces $|H(j\omega, t)|$ to approach zero that is neatly seen in the sections (Fig. 6.4b and c). \square

Let us now find a correspondence between $h(t, \theta)$ and $H(j\omega, t)$. To translate $h(t, \theta)$ to the frequency domain, we employ the convolution (6.5), suppose that the input is $x(t) = e^{j\omega t}$ and therefore $y(t) = H(j\omega, t)e^{j\omega t}$. After simple manipulations, using (6.19), we arrive at a pair of the transformations

$$H(j\omega, t) = \int_{-\infty}^{\infty} h(t, \theta) e^{-j\omega(t-\theta)} d\theta, \tag{6.22}$$

$$h(t, \theta) = \frac{1}{2\pi} \int_{-\infty}^{\infty} H(j\omega, t) e^{j\omega(t-\theta)} d\omega \tag{6.23}$$

that was first shown by Zadeh². As can be seen, (6.22) and (6.23) are not the Fourier transform pair. However, for a time variable t , the Fourier transform can be applied regarding the “slow” system frequency Ω . This leads to the spectral function

$$H(\theta, j\Omega) = \int_{-\infty}^{\infty} h(t, \theta) e^{-j\Omega t} dt = \int_{\theta}^{\infty} h(t, \theta) e^{-j\Omega t} dt. \tag{6.24}$$

Of practical importance also is the *two-dimensional frequency response* or *bi-frequency response* produced by the Fourier transform of (6.22),

² Lotfi Asker Zadeh, US mathematician and computer scientist, 4 February 1921-.

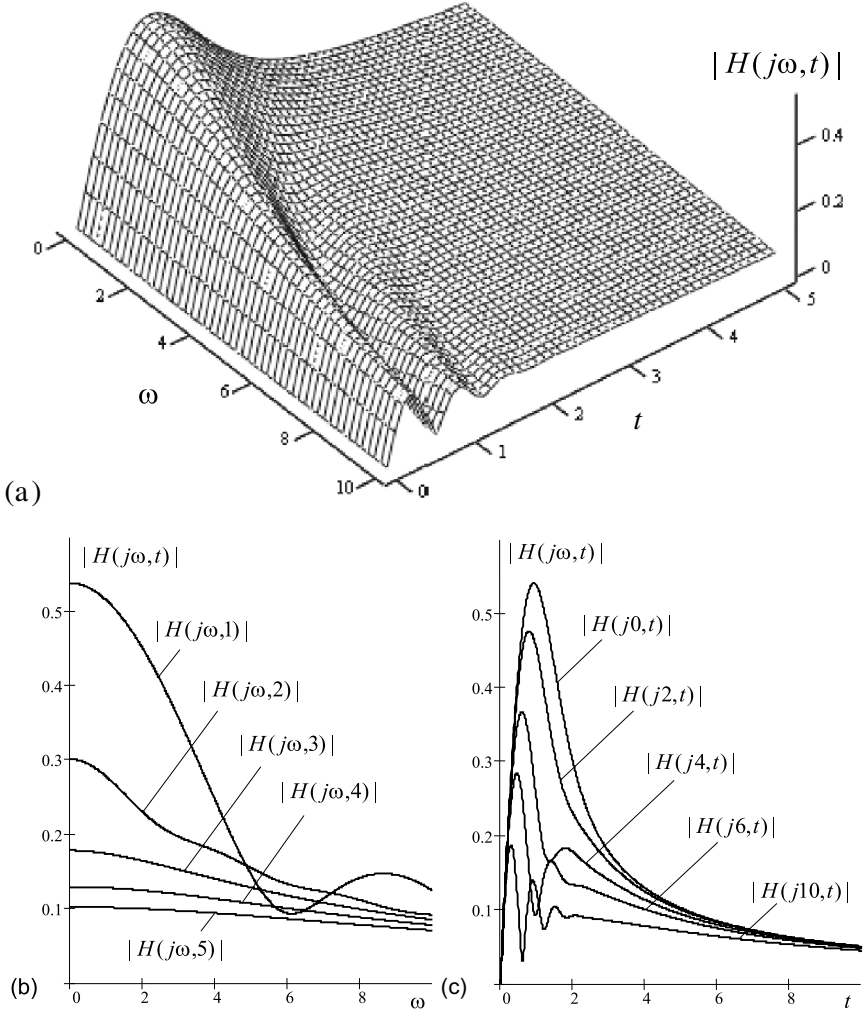


Fig. 6.4. Magnitude time-varying response associated with (6.21): (a) frequency-time presentation, (b) sections for several t , and (c) sections for several ω .

$$H(j\omega, j\Omega) = \int_{-\infty}^{\infty} H(j\omega, t)e^{-j\Omega t} dt. \tag{6.25}$$

Certainly, the inverse Fourier transform can be applied to (6.24) and (6.25) to produce $h(t, \theta)$ and $H(j\omega, t)$, respectively.

Example 6.7. For the impulse response (6.13), the frequency response is defined, by (6.22), to be

$$H(j\omega, t) = \int_0^t e^{-(t^2-\theta^2)} e^{-j\omega(t-\theta)} d\theta = e^{-j\omega t - t^2} \int_0^t e^{j\omega\theta + \theta^2} d\theta$$

that contains the same integral as in (6.21) and is thus identical to (6.21). The spectral function (6.24) is defined in a like manner to be

$$H(\theta, j\Omega) = \frac{\sqrt{\pi}}{2} e^{\theta^2 - \frac{\Omega^2}{4}} \left[1 - \operatorname{erf} \left(\theta + j \frac{\Omega}{2} \right) \right].$$

The bi-frequency response $H(j\omega, j\Omega)$ (6.25) does not have a simple closed form in this case. We therefore calculate this function numerically.

For the illustrative purposes, Fig. 6.5 shows the two-dimensional pictures of $|H(\theta, j\Omega)|$ (Fig. 6.5a) and $|H(j\omega, j\Omega)|$ (Fig. 6.5b). It is seen (Fig. 6.5a) that, by tending θ toward infinity, the LP filter loses an ability to be a filter, since its frequency response becomes uniform with zero magnitude. The same tendency is seen in Fig. 6.5b. Increasing Ω results in flattening the frequency response and lowering its magnitude down to zero. \square

Example 6.8. An LTV system channel is characterized by the time-varying impulse response $h(t, \theta) = \delta(t - \tau_0 - \theta) e^{j\Omega_0 t} u(t - \theta)$, where τ_0 is a time delay and Ω_0 is a Doppler shift. By (6.22), (6.24), and (6.25), the representation of a channel in the frequency domain is provided with, respectively

$$H(j\omega, t) = \int_{-\infty}^t \delta(t - \tau_0 - \theta) e^{j\Omega_0 t} e^{-j\omega(t-\theta)} d\theta = e^{-j\omega\tau_0} e^{j\Omega_0 t}, \quad (6.26)$$

$$H(\theta, j\Omega) = \int_{\theta}^{\infty} \delta(t - \tau_0 - \theta) e^{j\Omega_0 t} e^{-j\Omega t} dt = e^{-j(\Omega - \Omega_0)(\tau_0 + \theta)}, \quad (6.27)$$

$$H(j\omega, j\Omega) = \int_{-\infty}^{\infty} e^{-j\omega\tau_0} e^{j\Omega_0 t} e^{-j\Omega t} dt = 2\pi e^{-j\omega\tau_0} \delta(\Omega - \Omega_0). \quad (6.28)$$

Here we used the familiar sifting property of the delta function (Appendix A) and an identity $\int_{-\infty}^{\infty} e^{\pm j(\omega - \omega_0)t} dt = 2\pi\delta(\omega - \omega_0)$. \square

Let us come back to the transformations (6.22) and (6.23). Simple manipulations with the variables, $\tau = t - \theta$, lead to the relations

$$H(j\omega, t) = \int_{-\infty}^{\infty} h(t, t - \tau) e^{-j\omega\tau} d\tau$$

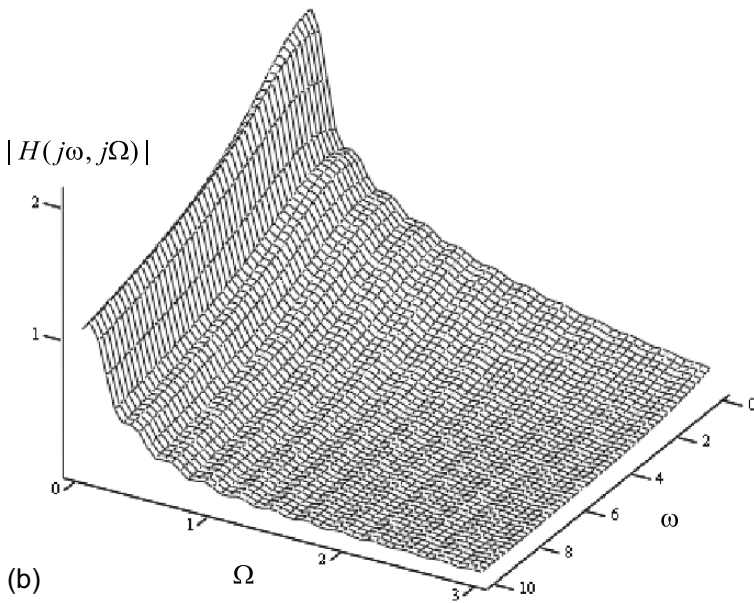
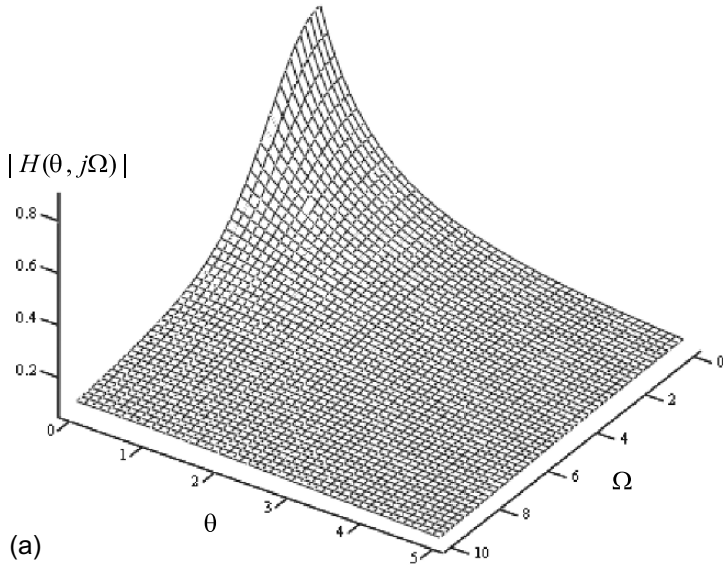


Fig. 6.5. Time-varying magnitude responses (Example 6.7): (a) $|H(\theta, j\Omega)|$ and (b) $|H(j\omega, j\Omega)|$.

$$= \int_{-\infty}^{\infty} \bar{h}(\tau, t) e^{-j\omega\tau} d\tau = \bar{H}(j\omega, t), \quad (6.29)$$

$$\begin{aligned} h(t, t - \tau) &= \frac{1}{2\pi} \int_{-\infty}^{\infty} H(j\omega, t) e^{j\omega\tau} d\omega \\ &= \frac{1}{2\pi} \int_{-\infty}^{\infty} \bar{H}(j\omega, t) e^{j\omega\tau} d\omega = \bar{h}(\tau, t), \end{aligned} \quad (6.30)$$

producing a noble identity

$$\bar{H}(j\omega, t) = H(j\omega, t). \quad (6.31)$$

An important meaning of (6.29) and (6.30) is that the Fourier transform of $\bar{h}(\tau, t)$ over τ is the frequency response $H(j\omega, t)$ of an LTV system.

In line with (6.24) and (6.25), the so-called *spread function* or *Doppler-delay spread function* and bi-frequency response of a system are also used. Both these functions are specified by the Fourier transform applied to $\bar{h}(\tau, t)$, respectively,

$$\bar{H}(\tau, j\Omega) = \int_{-\infty}^{\infty} \bar{h}(\tau, t) e^{-j\Omega t} dt, \quad (6.32)$$

$$\bar{H}(j\omega, j\Omega) = \int_{-\infty}^{\infty} \bar{H}(j\omega, t) e^{-j\Omega t} dt. \quad (6.33)$$

From (6.31) and (6.33), the other noble identity can be found,

$$\bar{H}(j\omega, j\Omega) = H(j\omega, j\Omega). \quad (6.34)$$

However, the transformation of variables shows that $\bar{H}(\tau, j\Omega) \neq H(\theta, j\Omega)$.

Example 6.9. By an identity (6.16), we transfer from $h(t, \theta) = \delta(t - \tau_0 - \theta) e^{j\Omega_0 t} u(t - \theta)$ (Example 6.8) to the modified impulse response $\bar{h}(\tau, t) = \delta(\tau - \tau_0) e^{j\Omega_0 t} u(\tau)$. Thereafter, the transform produces

$$\bar{H}(j\omega, t) = \int_0^{\infty} \delta(\tau - \tau_0) e^{j\Omega_0 t} e^{-j\omega\tau} d\tau = e^{-j\omega\tau_0} e^{j\Omega_0 t}, \quad (6.35)$$

$$\bar{H}(\tau, j\Omega) = \int_{-\infty}^{\infty} \delta(\tau - \tau_0) e^{j\Omega_0 t} e^{-j\Omega t} dt = 2\pi \delta(\tau - \tau_0) \delta(\Omega - \Omega_0), \quad (6.36)$$

$$\bar{H}(j\omega, j\Omega) = \int_{-\infty}^{\infty} e^{-j\omega\tau_0} e^{j\Omega_0 t} e^{-j\Omega t} dt = 2\pi e^{-j\omega\tau_0} \delta(\Omega - \Omega_0). \quad (6.37)$$

Comparing these results to (6.26)–(6.28), one infers that (6.35) is equal to (6.26), (6.37) is identical to (6.28), but (6.36) and (6.27) do not fit each other. \square

So, we can now sketch the most principle features of the impulse responses, $h(t, \theta)$ and $\bar{h}(\tau, t)$:

- $h(t, \theta)$ is the strong time-varying impulse response (advantage) having two-variables constraint (disadvantage) and being not the Fourier transform of the frequency response (disadvantage). \square
- $\bar{h}(\tau, t)$ is an artificial modified version of $h(t, \theta)$ (disadvantage) having one-variable constraint (advantage) and being the Fourier transform of the frequency response (advantage). \square

Both $h(t, \theta)$ and $\bar{h}(\tau, t)$ can be used equivalently and the choice typically depends on what the application area is. It turns out, for example, that the modified function $\bar{h}(\tau, t)$ is more preferable for describing the time-varying communications channels.

Range of Existence for Frequency Responses

For the illustrative purposes, in the above examples we showed the frequency responses implying positive variables. Most generally, the range of existence of the frequency responses in the whole range of variables can be sketched as in Fig. 6.6. By the constraint $h(t, \theta) = 0$ if $t < \theta$, the response $H(j\omega, t)$ is not zero only if $t \geq \theta$ (Fig. 6.6a). Two other responses, $H(\theta, j\Omega)$ and $H(j\omega, j\Omega)$, are unconstrained as shown in Fig. 6.6b and Fig. 6.6c, respectively. Unconstrained also are the modified responses $\bar{H}(j\omega, t)$ and $\bar{H}(j\omega, j\Omega)$ as shown in Fig. 6.6d and Fig. 6.6f, respectively. However, the response $\bar{h}(\tau, j\Omega)$, by the constrain $\bar{h}(\tau, t) = 0$ if $\tau < 0$, inherently exists only when $\tau \geq 0$ (Fig. 6.6e).

6.2.3 Time-varying Transfer Function

The representation of an LTV system by the standard transfer function is commonly not possible. That is because the standard transfer function is specified by the ratio of the Laplace transform of the output and Laplace transform of the input and thus cannot be time-varying. However, if an LTV system changes with time slowly, the transfer function can be defined with no large error similarly to the transfer function of an LTI system.

An example is a tracking filter, which coefficients vary with time in the control loop. If such a filter is of the second order, its general ODE can be written as

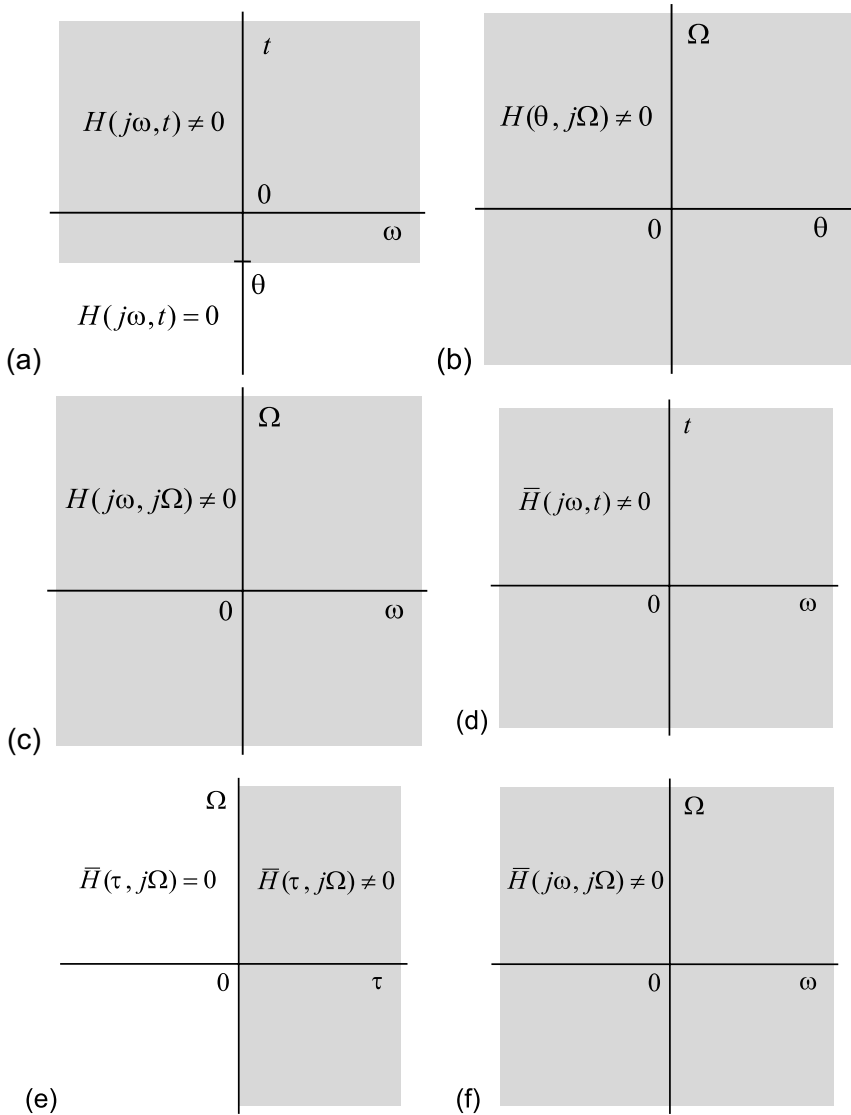


Fig. 6.6. Range of existence for the frequency responses: (a) $H(j\omega, t)$, (b) $H(\theta, j\Omega)$, (c) $H(j\omega, j\Omega)$, (d) $\bar{H}(j\omega, t)$, (e) $\bar{H}(\tau, j\Omega)$, and (f) $\bar{H}(j\omega, j\Omega)$.

$$y'' + a(t)y' + b(t)y = c(t)x.$$

Supposing that the coefficients $a(t)$, $b(t)$, and $c(t)$ of a filter are changed with time slowly; that is the spectral contents of all of the coefficients occupy the frequency range narrower (or even much narrower) than the system band-

width, the Laplace transform is applied straightforwardly, yielding the time varying transfer function

$$H(s, t) = \frac{c(t)}{s^2 + a(t)s + b(t)},$$

in which t must be perceived as a “constant” coefficient. Then the Laplace transform theory of LTI systems can be applied.

6.2.4 Classification of LTV Systems

So, we are now aware of how to represent an LTV system in the time domain with the time-varying impulse response and in the frequency domain by the time-varying frequency response. This allows us to classify LTV systems. Most generally, a classification can be provided with regards to how close time changes in the system operator relate to time changes in signals.

Linear Asynchronously Time-varying Systems

If the LTV system operator varies by some reason without any relation to the input and output of a system, the latter can be said to be linear *asynchronously* time-varying (LATV). Namely this kind of system is traditionally associated with LTV systems. Here, an a priori description of $h(t, \theta)$ is obligatory, because the impulse response takes values independently on the signals. An example is an LP filter, whose parameter (i.e., value C of a capacitor) changes with time owing to variations in the ambient temperature. Fig. 6.7a illustrates such a case. Supposing that the start point $t = 0$ of a system time scale is set arbitrary for θ , we watch for different shapes of the impulse response depending on θ .

Linear Synchronously Time-varying Systems

Contrary, if changes in the system operator exactly follow changes in signals, the system can be said to be linear *synchronously* time-varying (LSTV). An example is the same LP filter, which capacitance C is varied with time by the amplitude of the input signal. In view of that, the impulse response of the filter will also undergo changes. To illustrate these changes qualitatively, we sketch in Fig. 6.7b the “deformed” (bold) and “linear” (dashed) impulse responses. It is seemingly obvious that under such conditions the “deformed” response remains the same irrespective of the start point $t = 0$ in the system time scale.

The LSTV system is potentially not self-sufficient and can be represented by another systems. Let us illustrate this state considering a simplest system of the first order $y' + a(t)y = x$.

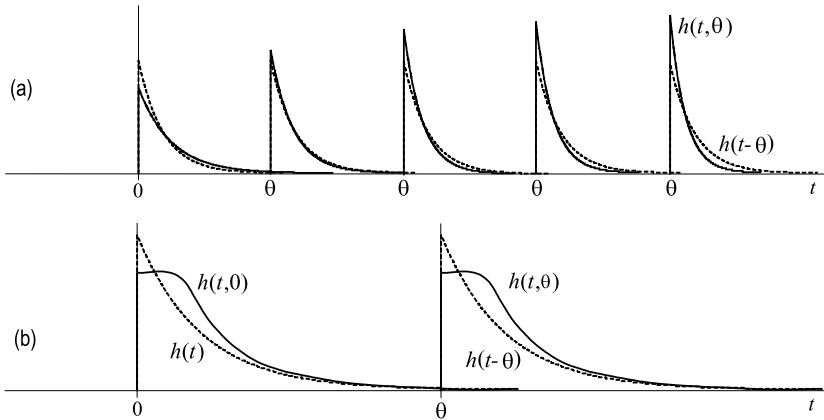


Fig. 6.7. Impulse responses of a linear system: (a) LATV and (b) LSTV. Dashed curves represent relevant LTI systems.

- If $a(t)$ is representable via the input and thus $a(t) = a[x(t)]$, the system can be said to be degenerate LTV. If $a(t) = a[t, x(t)]$, the system is LTV. □
- If $a(t)$ is a function of the output such that $a(t) = a[y(t)]$, the system becomes NTI. If $a(t) = a[t, y(t)]$, it is an NTV system. □

Example 6.10. Given an LTV system represented with the ODE

$$y' + a(t)y = x.$$

If $a(t)$ is specified to be $a(t) = a_0 + x(t)$, the equation becomes $y' + a_0y + xy = x$ and the system is degenerate LTV. With $a(t) = a_0(t) + x(t)$, the equation is written as $y' + a_0(t)y + xy = x$ describing the LTV system. By $a(t) = a_0 + y$, we get $y' + a_0y + y^2 = x$ that corresponds to the NTI system. Finally, supposing $a(t) = a_0(t) + y$, we arrive at $y' + a_0(t)y + y^2 = x$ that is the NTV system. □

Linear Periodically Time-varying Systems

LTV systems can undergo periodic time-variations, meaning that some parameter $a(t)$ changes with period T and thus $a(t) = a(t + nT)$, $n = 1, 2, \dots$. Such systems have found wide applications mostly owing to an ability of transforming and removing spectral components of input signals. A system with periodic variations is termed *linear periodically time-varying* (LPTV) or *linear parametric time-varying* (LPTV).

6.3 Properties of LTV Systems

Because an LTV system is still linear, it demonstrates some features of LTI systems, however, disagrees with some others, associated with time changes. The most important properties of LTV systems are observed below.

6.3.1 Linearity

The term “linear” suggests that an LTV system satisfies the conditions of *distributivity* and *homogeneity*.

Distributivity

Featured to LTI systems, this property is supported by the *superposition principle*. If a signal $x(t)$ goes through a parallel connection of N SISO LTV subsystems, then the output can be calculated as

$$x(t) * \sum_{i=1}^N h_i(t, \theta) = \sum_{i=1}^N [x(t) * h_i(t, \theta)] . \quad (6.38)$$

In the other case, if an input is composed by the sum of several subsignals, then the output can be provided by

$$\left(\sum_{i=1}^N x_i(t) \right) * h(t, \theta) = \sum_{i=1}^N [x_i(t) * h(t, \theta)] . \quad (6.39)$$

Example 6.11. An LTV system is composed with two included in parallel identical subsystems with the impulse responses $h_1(t, \theta) = h_2(t, \theta) = e^{-(t^2 - \theta^2)} u(t - \theta)$. The input is a unit step $x(t) = u(t)$, for which the output of the first subsystem is given by (6.14),

$$y_1(t) = \frac{\sqrt{\pi}}{2} e^{-t^2} \operatorname{erfi}(t) u(t) . \quad (6.40)$$

The second subsystem produces the same result and we thus have

$$y(t) = y_1(t) + y_2(t) = 2y_1(t) = \sqrt{\pi} e^{-t^2} \operatorname{erfi}(t) u(t) .$$

By (6.38), one can first get summed the impulse responses to have $h(t) = h_1(t) + h_2(t) = 2e^{-(t^2 - \theta^2)} u(t - \theta)$ and then arrive at the above provided result by the general convolution. \square

Homogeneity

If one of the functions, $x(t)$ or $h(t, \theta)$, is gained with a constant a , then, by the *homogeneity* property, we have

$$x(t) * [ah(t, \theta)] = ax(t) * h(t, \theta) . \quad (6.41)$$

6.3.2 Non-commutativity

Contrary to LTI systems, the time-varying linear operator is potentially non-commuting. This property was verified before, when we introduced to (6.5) a new variable $\tau = t - \theta$ with $\theta = t - \tau$ and $d\theta = -d\tau$,

$$\begin{aligned} y(t) &= \int_{-\infty}^{\infty} x(\theta)h(t, \theta)d\theta = - \int_{\infty+t}^{-\infty+t} x(t - \tau)h(t, t - \tau)d\tau \\ &= \int_{-\infty}^{\infty} h(t, t - \tau)x(t - \tau)d\tau. \end{aligned} \quad (6.42)$$

Everything would be fine, if $h(t, t - \tau) = h[t - (t - \tau)] = h(\tau)$. Unfortunately, the latter commonly does not hold true for LTV systems, and the convolution thus commonly does not commute,

$$y(t) = x(t) * h(t, \theta) \neq h(t, \theta) * x(t). \quad (6.43)$$

However, if the impulse response at t occurs to be equal to that at 2τ , we can substitute $h(t, t - \tau) = h(t, \tau)$, and the convolution commutes.

6.3.3 Associativity

Let the input $x(t)$ pass through the cascade of two SISO LTV subsystems with the time-varying impulse responses $h_1(t, \theta)$ and $h_2(t, \theta)$. By the associativity property, the output can be calculated in the same time scale in two ways:

$$y(t) = [x(t) * h_1(t, \theta)] * h_2(t, \theta) = x(t) * [h_1(t, \theta) * h_2(t, \theta)]. \quad (6.44)$$

Indeed, if we obtain two results separately as

$$\begin{aligned} [x(t) * h_1(t, \theta)] * h_2(t, \theta) &= \int_{-\infty}^{\infty} [x(\tau_1) * h_1(\tau_1, \theta)]h_2(t, \tau_1)d\tau_1 \\ &= \int_{-\infty}^{\infty} \int_{-\infty}^{\infty} x(\tau_2)h_1(\tau_1, \tau_2)h_2(t, \tau_1)d\tau_1d\tau_2, \end{aligned} \quad (6.45)$$

$$\begin{aligned} x(t) * [h_1(t, \theta) * h_2(t, \theta)] &= \int_{-\infty}^{\infty} x(\tau_3)[h_1(t, \tau_3) * h_2(t, \tau_3)]d\tau_3 \\ &= \int_{-\infty}^{\infty} \int_{-\infty}^{\infty} x(\tau_3)h_1(\tau_4, \tau_3)h_2(t, \tau_4)d\tau_3d\tau_4 \end{aligned} \quad (6.46)$$

and then change in (6.46) τ_3 to τ_2 and τ_4 to τ_1 , we transfer from (6.46) to (6.45) and the proof is complete.

Example 6.12. A cascade LTV system is composed with two subsystems having equal impulse responses, $h_1(t, \theta) = h_2(t, \theta) = e^{-(t^2 - \theta^2)} u(t - \theta)$. The input is a unit step, $x(t) = u(t)$.

Because the output of the first subsystem is provided, by (6.14), as

$$y_1(t) = \frac{\sqrt{\pi}}{2} e^{-t^2} u(t) \operatorname{erfi}(t),$$

the output of the second system is found by the general convolution to be

$$\begin{aligned} y(t) &= \int_{-\infty}^{\infty} y_1(\theta) h_2(t, \theta) d\theta = \int_{-\infty}^{\infty} \frac{\sqrt{\pi}}{2} e^{-\theta^2} u(\theta) \operatorname{erfi}(\theta) e^{-(t^2 - \theta^2)} u(t - \theta) d\theta \\ &= \frac{\sqrt{\pi}}{2} e^{-t^2} \int_0^t \operatorname{erfi}(\theta) d\theta. \end{aligned} \quad (6.47)$$

Alternatively, one can first define the impulse response of the cascade,

$$\begin{aligned} h(t, \theta) &= \int_{-\infty}^{\infty} h(\tau, \theta) h(t, \tau) d\tau = \int_{-\infty}^{\infty} e^{-(\tau^2 - \theta^2)} u(\tau - \theta) e^{-(t^2 - \tau^2)} u(t - \tau) d\tau \\ &= u(t - \theta) \int_{\theta}^t e^{-x(\tau^2 - \theta^2)} e^{-(t^2 - \tau^2)} d\tau = (t - \theta) e^{-(t^2 - \theta^2)} u(t - \theta). \end{aligned} \quad (6.48)$$

Then the general convolution yields the output

$$\begin{aligned} y(t) &= \int_{-\infty}^{\infty} u(\theta) h(t, \theta) d\theta = \int_0^{\infty} (t - \theta) e^{-(t^2 - \theta^2)} u(t - \theta) d\theta \\ &= \int_0^t (t - \theta) e^{-(t^2 - \theta^2)} d\theta = t e^{-t^2} \int_0^t e^{\theta^2} d\theta - e^{-t^2} \int_0^t \theta e^{\theta^2} d\theta. \end{aligned}$$

Here, the first integral is represented by $\frac{\sqrt{\pi}}{2} \operatorname{erfi}(t)$ and the second one can be rewritten as $\frac{1}{2} \int_0^t \frac{d}{d\theta} e^{\theta^2} d\theta = \frac{1}{2} e^{\theta^2} \Big|_0^t = \frac{1}{2} (e^{t^2} - 1)$. The output hence becomes

$$y(t) = \frac{\sqrt{\pi}}{2} t e^{-t^2} \operatorname{erfi}(t) - \frac{1}{2} (1 - e^{-t^2}). \quad (6.49)$$

The same result appears if we substitute in (6.47) $\operatorname{erfi}(x) = -i \operatorname{erf}(ix)$ and use an identity $\int \operatorname{erf}(ax) dx = x \operatorname{erf}(ax) + \frac{1}{a\sqrt{\pi}} e^{-a^2 x^2}$. Fig. 6.8 illustrates graphically two options in providing the output. \square

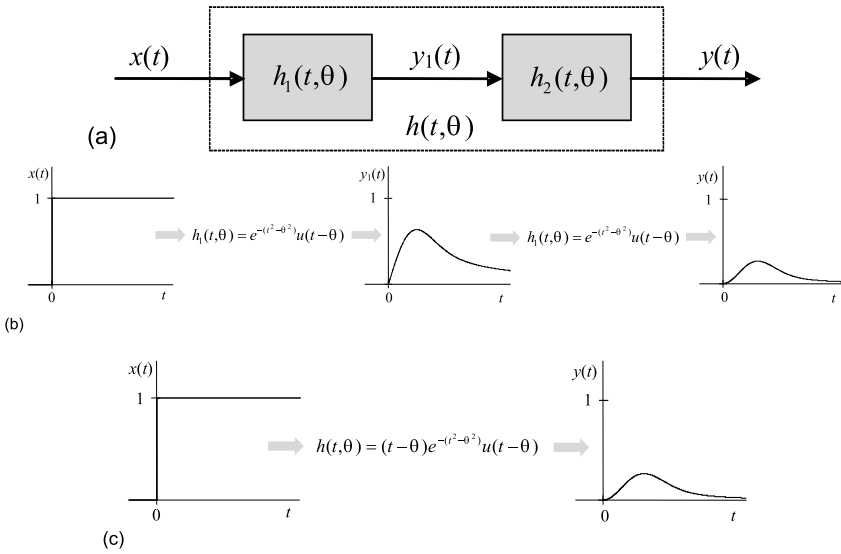


Fig. 6.8. An LTV system: (a) cascade, (b) calculus by $[x(t) * h_1(t, \theta)] * h_2(t, \theta)$, and (c) calculus by $x(t) * [h_1(t, \theta) * h_2(t, \theta)]$.

6.3.4 Inconvertibility of Impulse and Step Responses

An important feature of an LTV system is that its time-varying impulse response and time-varying step response are potentially inconvertible. A verification can be obtained by considering a SISO LTV system described with the ODE of the first order $y' + a(t)y = x$, which solution is given by (6.9). If we set $x(t) = \delta(t - \theta)$ to (6.9), we go, by the sifting property of $\delta(t)$, to the time-varying impulse response

$$\begin{aligned}
 h(t, \theta) &= e^{-\int_0^t a(\tau) d\tau} \int_0^t \delta(\tau - \theta) e^{\int_0^\tau a(\tau_1) d\tau_1} d\tau \\
 &= e^{-\int_\theta^t a(\tau) d\tau} u(t - \theta).
 \end{aligned} \tag{6.50}$$

Reasoning similarly, we suppose that $x(t) = u(t - \theta)$, and then (6.9) ought to produce the time-varying step-response

$$\begin{aligned}
 g(t, \theta) &= e^{-\int_0^t a(\tau) d\tau} \int_0^t u(\tau - \theta) e^{\int_0^\tau a(\tau_1) d\tau_1} d\tau \\
 &= e^{-\int_\theta^t a(\tau) d\tau} u(t - \theta) \int_\theta^t e^{\int_\theta^\tau a(\tau_1) d\tau_1} d\tau.
 \end{aligned} \tag{6.51}$$

Implying a convertibility of $h(t, \theta)$ and $g(t, \theta)$, we integrate (6.50) and equate the result to (6.51) that leads, by $t \geq \theta$, to the relation

$$e^{-\int_{\theta}^t a(\tau) d\tau} \int_{\theta}^t e^{\int_{\theta}^{\tau} a(\tau_1) d\tau_1} d\tau = \int_{\theta}^t e^{-\int_{\theta}^{\tau} a(\tau_1) d\tau_1} d\tau.$$

Let us now suppose that integrating $a(t)$ yields a linear term at and some time-dependent function $f(t)$. Thus, we write

$$e^{-at+a\theta-f(t)+f(\theta)} \int_{\theta}^t e^{a\tau-a\theta+f(\tau)-f(\theta)} d\tau = \int_{\theta}^t e^{-a\tau+a\theta-f(\tau)+f(\theta)} d\tau,$$

$$e^{-at-f(t)} \int_{\theta}^t e^{a\tau+f(\tau)} d\tau = e^{a\theta+f(\theta)} \int_{\theta}^t e^{-a\tau-f(\tau)} d\tau.$$

Setting aside a trivial solution associated with $a = 0$ and $f(t) = 0$, we deduce that the above equality is valid if $f(t) = 0$ and $\theta = 0$ that fits only LTI systems.

So, for LTV systems, we basically have two inequalities,

$$g(t, \theta) \neq \int_0^t h(t, \theta) dt \quad \text{and} \quad h(t, \theta) \neq \frac{d}{dt} g(t, \theta), \quad (6.52)$$

meaning that the time-varying impulse and step responses are commonly inconvertible.

Example 6.13. An LTV system is described by $y' + a(t)y = x$ with $a(t) = (t + 2)/(t + 1)$. Its time-varying impulse response is defined, by (6.50), to be

$$h(t, \theta) = e^{-\int_{\theta}^t a(\tau) d\tau} u(t - \theta) = e^{-\int_{\theta}^t (1 + \frac{1}{\tau+1}) d\tau} u(t - \theta)$$

$$= e^{-(t-\theta) - \ln(t+1) + \ln(\theta+1)} u(t - \theta) = \frac{\theta + 1}{t + 1} e^{-(t-\theta)} u(t - \theta). \quad (6.53)$$

By (6.51) and an identity $\int x e^{\alpha x} dx = e^{\alpha x} (\frac{x}{\alpha} - \frac{1}{\alpha^2})$, the time-varying step-response can be found as

$$g(t, \theta) = e^{-\int_{\theta}^t a(\tau) d\tau} u(t - \theta) \int_{\theta}^{\tau} e^{\int_{\theta}^{\tau_1} a(\tau_1) d\tau_1} d\tau$$

$$= \frac{\theta + 1}{t + 1} e^{-t+\theta} u(t - \theta) \int_{\theta}^{\tau} \frac{\tau + 1}{\theta + 1} e^{\tau-\theta} d\tau = \frac{e^{-t}}{t + 1} u(t - \theta) \int_{\theta}^{\tau} (\tau + 1) e^{\tau} d\tau$$

$$= \frac{t - \theta e^{-(t-\theta)}}{t+1} u(t-\theta). \quad (6.54)$$

Now observe that differentiating $g(t, \theta)$ (6.54) with respect to t does not produce $h(t, \theta)$ performed by (6.53). The responses are thus inconvertible. \square

6.3.5 BIBO Stability

Being a generalized function, the time-varying impulse response gives an idea about stability of an LTV system over time. Most generally, an LTV system is BIBO stable if for every bounded input the output is also bounded. For SISO LTV systems, the necessary and sufficient condition for BIBO stability is that there exists a finite value of the the integral,

$$\int_{t_0}^t |h(t, \theta)| d\theta \leq M < \infty, \quad (6.55)$$

where M is finite and $t > t_0$ takes any value exceeding an initial time t_0 .

Example 6.14. Consider a system represented with the time-varying impulse response (6.53). The BIBO stability of a system is ascertained by (6.55) if to use a familiar identity $\int x e^{\alpha x} dx = e^{\alpha x} \left(\frac{x}{\alpha} - \frac{1}{\alpha^2} \right)$ and provide the integration,

$$\begin{aligned} \int_{t_0}^t \frac{\theta+1}{t+1} e^{-(t-\theta)} u(t-\theta) d\theta &= \frac{e^{-t}}{t+1} \int_{t_0}^t (\theta+1) e^{\theta} d\theta \\ &= \frac{1}{t+1} \left[t - t_0 e^{-(t-t_0)} \right]. \end{aligned} \quad (6.56)$$

For $t > t_0$, the integral value ranges from zero to unity and the system is thus BIBO stable. \square

6.4 Representation by Differential Equations

Similarly to LTI systems, any LTV system can be represented with the ODE of some order N . In contrast, at least one of the coefficients of the ODE is time-varying. Most generally, the ODE of an LTV system can be written as

$$\sum_{n=0}^N a_n(t) \frac{d^n}{dt^n} y(t) = \sum_{m=0}^M b_m(t) \frac{d^m}{dt^m} x(t), \quad (6.57)$$

where $N \geq M$ is the realizability constraint guaranteeing not using the future points in the calculus. If we introduce two operators

$$\mathcal{O}_y(\mathcal{D}, t) = \sum_{n=0}^N a_n(t) \mathcal{D}^n \quad \text{and} \quad \mathcal{O}_x(\mathcal{D}, t) = \sum_{m=0}^M b_m(t) \mathcal{D}^m,$$

where $\mathcal{D} \triangleq d/dt$, then the ODE can be rewritten as

$$\mathcal{O}_y(\mathcal{D}, t)y(t) = \mathcal{O}_x(\mathcal{D}, t)x(t). \quad (6.58)$$

If we further let $x(t) = \delta(t - \theta)$, then the time-varying impulse response $h(t, \theta)$ of the system will be specified by the relation

$$\mathcal{O}_y(\mathcal{D}, t)h(t, \theta) = \mathcal{O}_x(\mathcal{D}, t)\delta(t - \theta). \quad (6.59)$$

On the other hand, letting $x(t) = e^{j\omega t}$ and hereby defining $y(t) = H(j\omega, t)e^{j\omega t}$ yield a relation

$$\mathcal{O}_y(\mathcal{D}, t)H(j\omega, t)e^{j\omega t} = \mathcal{O}_x(\mathcal{D}, t)e^{j\omega t}$$

that can be reduced to the more convenient form proposed by Zadeh,

$$\mathcal{O}_y(\mathcal{D} + j\omega, t)H(j\omega, t) = \mathcal{O}_x(j\omega, t). \quad (6.60)$$

To solve (6.59) and (6.60), one needs to remember that $h(t, \theta)$ and $H(j\omega, t)$ are coupled by a pair of the transformations, (6.22) and (6.23). We notice that the relevant solutions depend on $a_n(t)$ and $b_n(t)$ and can not obligatorily have simple (or even any) analytical forms. If it is the case, numerical analysis or simulation by the block diagrams could be more efficient that we shall show in the sequel. Now in order is to consider in detail the familiar first order ODE with time-varying coefficients.

6.4.1 LTV System of the First Order

Earlier, in Chapters 4 and 5, we investigated an LTI system of the first order represented with the ODE having constant coefficients. For time-varying $a(t)$ and $b(t)$, the ODE becomes

$$\frac{d}{dt}y(t) + a(t)y(t) = b(t)x(t) \quad (6.61)$$

or (6.58), if we specify the operators as

$$\mathcal{O}_y = \mathcal{D} + a(t) \quad \text{and} \quad \mathcal{O}_x = b(t). \quad (6.62)$$

By multiplying (6.61) with the integration factor $e^{\int a(t)dt}$ and reasoning similarly to the relevant ODE (4.53) having constant coefficients, we arrive at the general solution

$$y(t) = e^{-\int_{t_0}^t a(\tau)d\tau} \left[\int_{t_0}^t b(\tau)x(\tau)e^{\int_{t_0}^{\tau} a(\tau_1)d\tau_1} d\tau + y_0 \right], \quad (6.63)$$

where $y_0 = y(t_0)$. Because the coefficient $b(t)$ gains only the input $x(t)$, its influence can be controlled, e.g., by predistortions in $x(t)$. The other coefficient $a(t)$ predefines dynamics and stability of the system, thereby playing a key role in the solution of its ODE.

Example 6.15. An LTV system is described by (6.61) with $a(t) = x(t) = u(t) \cos t$, $b(t) = 1$, and zero initial condition $y(0) = 0$. The general solution (6.63) produces

$$\begin{aligned} y(t) &= e^{-\int_0^t \cos \tau d\tau} \int_0^t e^{\int_0^\tau \cos \tau_1 d\tau_1} \cos \tau d\tau = e^{-\sin t} \int_0^t e^{\sin \tau} \cos \tau d\tau \\ &= e^{-\sin t} \int_0^t e^{\sin \tau} d \sin \tau = e^{-\sin t} e^{\sin \tau} \Big|_0^t = e^{-\sin t} (e^{\sin t} - 1) u(t). \\ &= (1 - e^{-\sin t}) u(t). \end{aligned} \tag{6.64}$$

Fig. 6.9 illustrates $x(t)$ and $y(t)$ and one concludes that the output $y(t)$ is not absolutely monochromatic owing to the harmonically changing coefficient $a(t)$. This means that the LTV system is able to produce new spectral com-

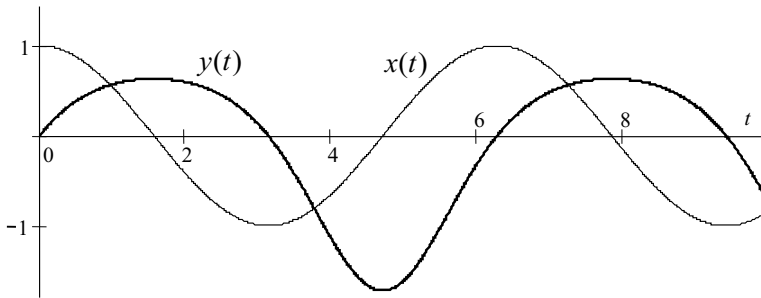


Fig. 6.9. Input $x(t)$ and output $y(t)$ of the LTV system (Example 6.15).

ponents at the output similarly to NTI systems that we shall discuss in the sequel. \square

Response to Unit Impulse

If we let $x(t) = \delta(t - \theta)$ and set $y(0) = 0$, the output (6.63) would be the time-varying impulse response $h(t, \theta)$.

Most generally, we can allow $y(0) = y_0 \neq 0$ and write

$$\begin{aligned}
y(t, \theta) &= e^{-\int_0^t a(\tau) d\tau} \left[\int_0^t \delta(\tau - \theta) b(\tau) e^{\int_0^\tau a(\tau_1) d\tau_1} d\tau + y_0 \right] u(t) \\
&= y_0 e^{-\int_0^t a(\tau) d\tau} u(t) + e^{-\int_0^t a(\tau) d\tau} u(t) \int_0^t \delta(\tau - \theta) b(\tau) e^{\int_0^\tau a(\tau_1) d\tau_1} d\tau \\
&= y_0 e^{-\int_0^t a(\tau) d\tau} u(t) + b(\theta) e^{-\int_\theta^t a(\tau) d\tau} u(t - \theta), \tag{6.65}
\end{aligned}$$

where the first term represents the time-varying homogenous solution starting at $t = 0$. The last term contributes to the time-varying forced solution starting at $t = \theta$, so this is the time-varying system impulse response $h(t, \theta)$,

$$h(t, \theta) = b(\theta) e^{-\int_\theta^t a(\tau) d\tau} u(t - \theta).$$

Example 6.16. Consider a system (6.61) with an initial condition $y_0 = 1$ having the coefficients $a(t) = 2t$ and $b(t) = -e^{-t^2}$. By (6.63), the system response to the unit impulse is defined as

$$\begin{aligned}
y(t, \theta) &= e^{-t^2} u(t) - e^{-\theta^2} e^{-(t^2 - \theta^2)} u(t - \theta) \\
&= e^{-t^2} [u(t) - u(t - \theta)] \tag{6.66}
\end{aligned}$$

that is the doubly-truncated Gaussian pulse. Function (6.66) approaches zero owing to the rapidly decaying coefficient $b(t)$. \square

Response to Unit Step

If we let the input signal $x(t)$ of a relaxed system $y(0) = 0$ to be the unit step $u(t - \theta)$ acting at θ , a solution (6.63) would be treated as the time-varying system step response $g(t, \theta)$.

Most generally, we can imply $y(t) = y_0 \neq 0$, and write a solution as

$$\begin{aligned}
y(t, \theta) &= e^{-\int_0^t a(\tau) d\tau} \left[\int_0^t b(\tau) u(\tau - \theta) e^{\int_0^\tau a(\tau_1) d\tau_1} d\tau + y_0 \right] u(t) \\
&= y_0 e^{-\int_0^t a(\tau) d\tau} u(t) + e^{-\int_0^t a(\tau) d\tau} \int_0^t b(\tau) u(\tau - \theta) e^{\int_0^\tau a(\tau_1) d\tau_1} d\tau \\
&= y_0 e^{-\int_0^t a(\tau) d\tau} u(t) + e^{-\int_0^t a(\tau) d\tau} u(t - \theta) \int_\theta^t b(\tau) e^{\int_0^\tau a(\tau_1) d\tau_1} d\tau. \tag{6.67}
\end{aligned}$$

Inherently, (6.67) comprises the homogenous solution (the first term) and the forced solution (the last term). The step response $g(t, \theta)$ is associated solely with the forced solution, so that we have

$$g(t, \theta) = e^{-\int_0^t a(\tau) d\tau} u(t - \theta) \int_{\theta}^t b(\tau) e^{\int_0^{\tau} a(\tau_1) d\tau_1} d\tau.$$

Example 6.17. An LTV system is performed with $a(t) = 2t$, $b(t) = -e^{-t^2}$, and $y_0 = 1$ (Example 6.16). By (6.67), the response of a system to $u(t - \theta)$ is easily defined to be

$$y(t, \theta) = e^{-t^2} [u(t) - (t - \theta)u(t - \theta)]. \quad (6.68)$$

Observe that, by $\theta > t$, (6.66) and (6.68) become identical and independent on θ . \square

Time-varying Frequency Response

Employing (6.60) with the operators (6.62), we arrive at the ODE

$$\begin{aligned} [\mathcal{D} + j\omega + a(t)]H(j\omega, t) &= b(t), \\ H' + [j\omega + a(t)]H &= b(t), \end{aligned}$$

which solution is provided by (6.63) to be

$$\begin{aligned} H(j\omega, t) &= e^{-\int_0^t [j\omega + a(\tau)] d\tau} \int_0^t b(\tau) e^{\int_0^{\tau} [j\omega + a(\tau_1)] d\tau_1} d\tau, \\ &= e^{-j\omega t} e^{-\int_0^t a(\tau) d\tau} \int_0^t b(\tau) e^{j\omega\tau} e^{\int_0^{\tau} a(\tau_1) d\tau_1} d\tau. \end{aligned} \quad (6.69)$$

We notice that for particular functions $a(t)$ and $b(t)$, the relation (6.69) was applied in Example 6.6.

6.4.2 Application to Electrical Circuits

A specific representation of time-varying electrical circuits as LTV systems exploits the fundamental relations for the electric current and voltage associated with an electric resistance, capacitance and inductance. The relations appear from the physical analysis of energy bearers in each of these components. In fact, dynamic properties of time-varying a capacitance are associated with the time-varying electric charge and an inductance with magnetic flux. Therefore, rigorously, the ODEs of electrical circuits must be written and solved for the electric charge and magnetic flux, to fit physical processes.

Time-varying Resistance

A time-varying resistance $R(t)$ is still memoryless, therefore the relations for the electric current $i_R(t)$ and induced voltage $v_R(t)$ remain those specified for its time-invariant analog,

$$i_R(t) = \frac{1}{R(t)}v_R(t), \quad (6.70)$$

$$v_R(t) = R(t)i_R(t). \quad (6.71)$$

Time-varying Capacitance

A capacitor is evaluated by a measure of the amount of electric charge stored (or separated) for a given electric potential. This amount is usually defined as the total electric charge Q placed on the object divided by the potential V of the object: $C = Q/V$. The unit of capacitance is the “farad” (F) in honor of Michael Faraday³.

To define the relations for the time-varying capacitance, one needs to recall that the electric current $i_C(t)$ through the capacitor is calculated by the speed of change of the charge $Q(t)$ on its plates. This means the following

$$i_C(t) = \frac{dQ}{dt} = \frac{dQ}{dv_C} \frac{dv_C}{dt} = C(t) \frac{dv_C}{dt}, \quad (6.72)$$

$$v_C(t) = \int_{-\infty}^t \frac{i_C(\tau)}{C(\tau)} d\tau. \quad (6.73)$$

Example 6.18. Consider an electrical RC circuit represented by a closed loop of $R(t)$, $C(t)$, and a source of voltage $v(t)$.

For the electric current $i = Q' = dQ/dt$, the voltage balance, using (6.72) and (6.73), is obtained by the relation

$$RQ' + \int_{-\infty}^t \frac{Q'}{C} d\tau = v,$$

which differentiation and consequent rearranging the terms leads to the ODE of the second order for the electric charge,

$$Q'' + \left(\frac{R'}{R} + \frac{1}{RC} \right) Q' = \frac{1}{R} v'.$$

Specifying an electric current by $i = v_R/R$, we go to the first order ODE for the voltage v_R induced on a resistance,

³ Michael Faraday, British chemist and physicist, 22 September 1791–25 August 25 1867.

$$v'_R + \frac{1}{RC}v_R = v'. \quad (6.74)$$

If we define the current, by (6.72), as $i = Cv'_C$, the voltage balance equation becomes $RCv'_C + v_C = v$, meaning that the system can be modeled by the ODE of the first order

$$v'_C + \frac{1}{RC}v_C = \frac{1}{RC}v. \quad (6.75)$$

Apparently, solutions of all these equations depend on the functions of $C(t)$ and $R(t)$. \square

Time-varying Inductance

An inductor is evaluated by a measure of the amount of magnetic flux Φ produced for a given electric current i . The inductance is defined as $L = \Phi/i_L$ and evaluated in henry, H. The term “inductance” was introduced to the text in 1886 by Oliver Heaviside⁴ and the dimension “henry” is used in honor of the physicist Heinrich Lenz⁵. This definition relates, strictly speaking, to self-inductance, because the magnetic field is created solely by the conductor that carries the current.

If an inductor is time-varying, one can consider $\Phi(t) = L(t)i_L(t)$, differentiate this relation, account for $\Phi' = \frac{d\Phi}{dt} = v_L$, and arrive at the basic relations

$$v_L(t) = \frac{d}{dt}L(t)i_L(t) = L'(t)i_L(t) + L(t)i'(t), \quad (6.76)$$

$$i_L(t) = \frac{1}{L(t)} \int_{-\infty}^t v_L(\tau) d\tau. \quad (6.77)$$

Example 6.19. Consider a closed loop of a series connection of R , C , $L(t)$, and $v(t)$. For the electric current $i = \Phi/L$, the voltage balance equation

$$R\frac{\Phi}{L} + \Phi' + \int_{-\infty}^t \frac{1}{C} \frac{\Phi}{L} dt$$

produces the ODE of the second order for the magnetic flux

$$\Phi'' + \frac{R}{C}\Phi' + \left(\frac{1}{LC} - \frac{RL'}{L^2} \right) \Phi = v'.$$

⁴ Oliver Heaviside, English electrical engineer, mathematician, and physicist, 18 May 1850–3 February 1925.

⁵ Heinrich Friedrich Emil Lenz, Baltic German physicist, 12 February 1804–10 February 1865.

In a like manner, the ODE for the voltages induced, for example, on a resistor R is defined to be

$$v_R'' + \left(\frac{R}{L} + 2\frac{L'}{L} \right) v_R' + \left(\frac{1}{LC} + \frac{L''}{L} \right) v_R = \frac{R}{L} v'. \quad (6.78)$$

It is seen that variations in $L(t)$ affect both the system bandwidth $2\delta(t)$ that, by $L = \text{const}$, becomes a familiar $2\delta = R/L$,

$$2\delta(t) = \left(\frac{R}{L} + 2\frac{L'}{L} \right) \Big|_{L=\text{const}} = \frac{R}{L},$$

and the system resonance frequency $\omega_0(t)$ that also tends to $\omega_0 = 1/\sqrt{LC}$, by L becoming constant,

$$\omega_0^2(t) = \left(\frac{1}{LC} + \frac{L''}{L} \right) \Big|_{L=\text{const}} = \frac{1}{LC}.$$

□

Two typical situations with LTV electrical circuits are usually met. In the first block of problems, the components vary periodically and some special methods are used to solve the ODEs. In the other one, the components change with time slowly, so that all of their time-derivatives are almost zero and such systems can be considered to be quasi LTI.

6.4.3 Block Diagrams

Like for LTI systems, simulation of LTV systems in the time domain can also be provided by block diagrams with all the benefit of such a representation. However, not all forms of diagrams are suitable for LTV systems.

Similarly, translation starts with the generalized ODE of an LTV system

$$\sum_{n=0}^N a_n(t) \frac{d^n}{dt^n} y(t) = \sum_{m=0}^N b_m(t) \frac{d^m}{dt^m} x(t), \quad (6.79)$$

in which, without losing generality, each batch is bounded with N .

The next steps forward are those exploited for LTI systems. By the operator $\mathcal{D}^n \triangleq d^n/dt^n$, $n \geq 1$, equation (6.79) becomes

$$\sum_{n=0}^N a_n(t) \mathcal{D}^n y(t) = \sum_{m=0}^N b_m(t) \mathcal{D}^m x(t), \quad (6.80)$$

allowing for two familiar canonic forms of the block diagrams, namely the *first direct form* and *second direct form*, even in particular cases.

The First Direct Form

To come up with the first direct form, we use the inverse operator $\mathcal{D}^{-1} \triangleq \int_{-\infty}^t$, multiply both sides of (6.80) with \mathcal{D}^{-N} , suppose $a_N = 1$, and rewrite the equation as

$$\begin{aligned}
 y(t) &= - \sum_{n=0}^{N-1} \mathcal{D}^{-N} a_n(t) \mathcal{D}^n y(t) + \sum_{m=0}^N \mathcal{D}^{-N} b_m(t) \mathcal{D}^m x(t) \\
 &= \sum_{n=0}^{N-1} \mathcal{D}^{-N} [-a_n(t) \mathcal{D}^n y(t) + b_n(t) \mathcal{D}^n x(t)] + \mathcal{D}^{-N} b_N(t) \mathcal{D}^N x(t) \quad (6.81)
 \end{aligned}$$

that can also be rewritten as

$$\begin{aligned}
 y(t) &= \mathcal{D}^{-N} [b_0(t)x(t) - a_0(t)y(t)] \\
 &\quad + \mathcal{D}^{-N} [b_1(t)\mathcal{D}x(t) - a_1(t)\mathcal{D}y(t)] + \dots \\
 &\quad + \mathcal{D}^{-N} [b_{N-1}(t)\mathcal{D}^{N-1}x(t) - a_{N-1}(t)\mathcal{D}^{N-1}y(t)] + \mathcal{D}^{-N} b_N(t)\mathcal{D}^N x(t). \quad (6.82)
 \end{aligned}$$

A simulation of (6.82) with a block diagram is shown in Fig. 6.10a. The principle point to notice is that the input must multiply be differentiable. Therefore, the N -order time derivative of the input, $x^{(N)}(t) = \mathcal{D}^N x(t)$ serves

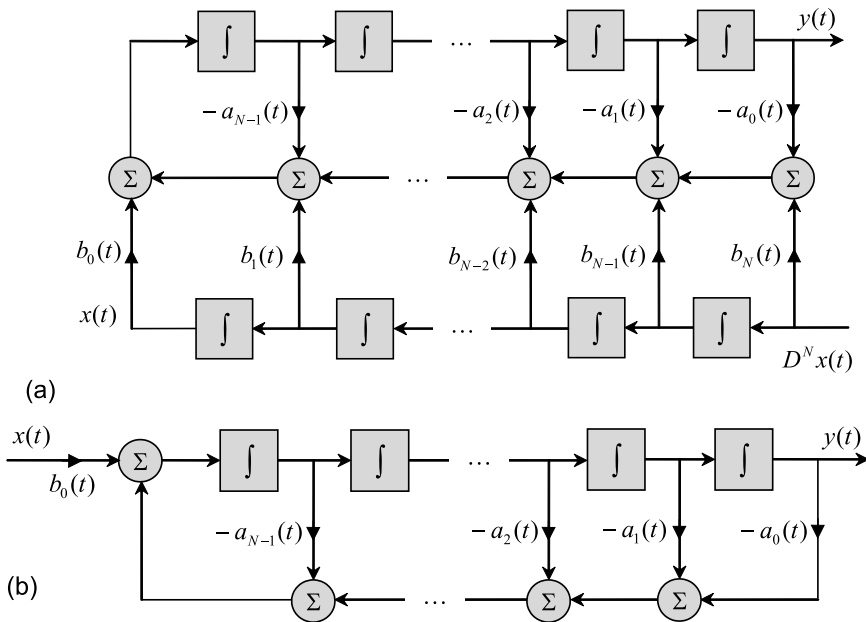


Fig. 6.10. The first direct form of diagrams of LTV systems: (a) $M = N$ and (b) $M = 0$.

actually as an input for the block diagram. Certainly, this is a disadvantage of the first form that is not peculiar to its particular realization, by $M = 0$. This disadvantage can also be overcome if the ODE (6.79) can be rewritten in the form of

$$\sum_{n=0}^N \frac{d^n}{dt^n} c_n(t) y(t) = \sum_{m=0}^N \frac{d^m}{dt^m} d_m(t) y(t),$$

where $c_n(t)$ and $d_m(t)$ are some time-varying coefficients. The reader is encouraged to build the block diagram of the first direct form for this case.

A Particular Case of $M = 0$

In the important particular case of $M = 0$, when no one time derivative of the input is involved to the model, equation (6.79) degenerates to

$$\sum_{n=0}^N a_n(t) \frac{d^n}{dt^n} y(t) = b_0(t) x(t) \quad (6.83)$$

and the first direct form originates from

$$y(t) = \mathcal{D}^{-N} [b_0(t)x(t) - a_0(t)y(t) - a_1(t)\mathcal{D}y(t) - a_2(t)\mathcal{D}^2y(t) - \dots - a_{N-1}(t)\mathcal{D}^{N-1}y(t)]. \quad (6.84)$$

Accordingly, the block diagram becomes as shown in Fig. 6.10b and we deduce that the algorithm represents a direct transformation of $x(t)$ to $y(t)$ with time-varying coefficients $a_n(t)$ and $b_0(t)$, unlike the case of (6.81).

Example 6.20. An LTV system of the second order is given with the ODE

$$y'' + 2ty' + 3 \cos(t)y = 2 \sin(t)x - tx'. \quad (6.85)$$

In the standard form (6.79), the equation becomes

$$\sum_{n=0}^2 a_n(t) \frac{d^n}{dt^n} y(t) = \sum_{m=0}^1 b_m(t) \frac{d^m}{dt^m} x(t),$$

where the coefficients are specified as $a_0 = 3 \cos(t)$, $a_1 = 2t$, $a_2 = 1$, $b_0 = 2 \sin(t)$, and $b_1 = -t$. By virtue of that, the block diagram (Fig. 6.10a) attains the form shown in Fig. 6.11a. As it is seen, the first-time derivative of an input is necessary to simulate a system properly. If a differentiator is available, the structure modifies to that shown in Fig. 6.11b. \square

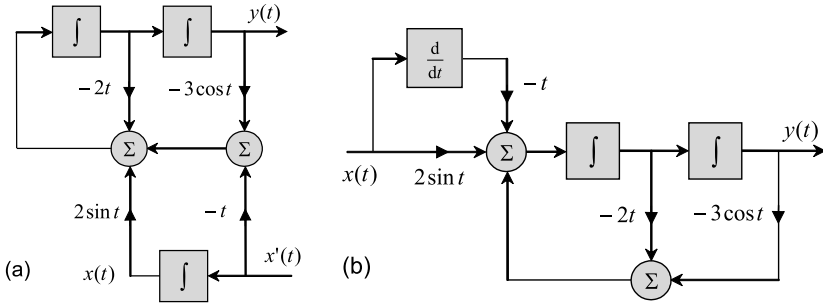


Fig. 6.11. Block diagrams of the first direct form of a system (Example 6.20): (a) standard structure and (b) involving a differentiator.

The Second Direct Form For $M = 0$

The second direct form cannot commonly be applied to the general ODE (6.79). However, it can be used in a particular case of $M = 0$ and constant b_0 . If that is the case, then, similarly to LTI systems, one can represent (6.79) by

$$\left(\sum_{n=0}^N a_n(t) \mathcal{D}^n \right) y(t) = b_0 x(t),$$

and then transform it to

$$\left(\sum_{n=0}^N a_n(t) \mathcal{D}^n \right) \frac{y(t)}{b_0} = x(t).$$

Assigning an additional function $q(t)$ allows for two equations

$$\left(\sum_{n=0}^N a_n(t) \mathcal{D}^n \right) q(t) = x(t),$$

$$y(t) = b_0 q(t).$$

Thereafter, by multiplying the first of the above equations with \mathcal{D}^{-N} and setting $a_N = 1$, we arrive at

$$q(t) = - \sum_{n=0}^{N-1} \mathcal{D}^{-N} a_n(t) \mathcal{D}^n q(t) + \mathcal{D}^{-N} x(t),$$

$$y(t) = b_0 q(t). \tag{6.86}$$

The block diagram associated with (6.86) is shown in Fig. 6.12. Similarly to Fig. 6.10b, this diagram does not involve time-derivatives of the input and

is thus a straightforward simulation of the output via the input with time-varying coefficients. One can also infer that, by $b_0 = 1$, the first and second direct forms become identical.

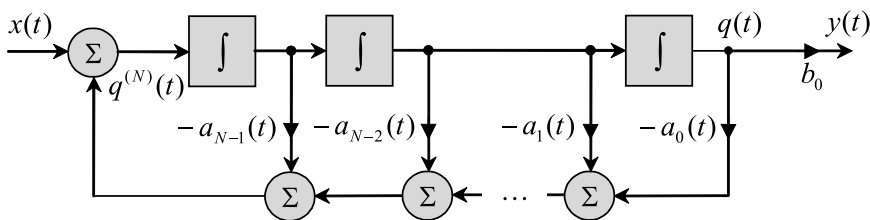


Fig. 6.12. The second direct form of diagrams of LTV systems.

Example 6.21. Consider an LTV system, described in Example 6.20 with the ODE $y'' + 2ty' + 3 \cos(t)y = b_0x$. In the second direct form (6.86), this ODE is rewritten as

$$q'' + 2tq' + 3 \cos(t)q = x,$$

$$y = b_0q.$$

By these equations, the diagram (Fig. 6.12) becomes as shown in Fig. 6.13.

□

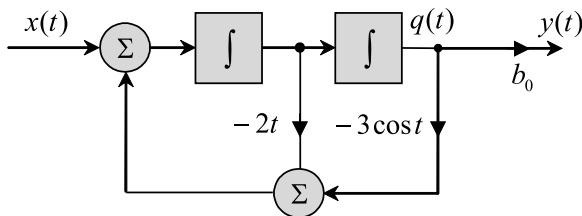


Fig. 6.13. The second direct form of diagrams of a system (Example 6.21).

Overall, we conclude like the case of LTI systems, the first and second direct forms of block diagrams can serve as an efficient tool to simulate LTV systems, even in particular cases.

We can now continue with representing LTV systems in state space, noticing that state space modeling occupies an important place in the theory of such systems owing to transparency and universality.

6.5 State Space Representation

Among other approaches, state space modeling seems to be the most universal and powerful to represent LTV systems. Below, we first show a particular state space model translated from Fig. 6.12 and proceed with the general analysis of LTV systems in state space.

6.5.1 State Space Model via the Second Direct Form for $M = 0$

Let us come back to the block diagram shown in Fig. 6.12. To transfer to state space, we assign the output of each of the integrators to be the system state variable and arrive, similarly to LTI systems, at the equations

$$\begin{aligned}
 q_1'(t) &= q_2(t), \\
 q_2'(t) &= q_3(t), \\
 &\vdots \\
 q_{N-1}'(t) &= q_N(t), \\
 q_N'(t) &= -a_{N-1}(t)q_N(t) - a_{N-2}(t)q_{N-1}(t) - \dots - a_0(t)q_1(t) + x(t), \\
 y(t) &= b_0q_1(t).
 \end{aligned} \tag{6.87}$$

In matrix forms, (6.87) is represented with the state and observation equations, respectively,

$$\begin{bmatrix} q_1'(t) \\ q_2'(t) \\ \vdots \\ q_{N-1}'(t) \\ q_N'(t) \end{bmatrix} = \begin{bmatrix} 0 & 1 & 0 & \dots & 0 \\ 0 & 0 & 1 & & 0 \\ \vdots & \vdots & & \ddots & \vdots \\ 0 & 0 & 0 & & 1 \\ -a_0(t) & -a_1(t) & -a_2(t) & \dots & -a_{N-1}(t) \end{bmatrix} \begin{bmatrix} q_1(t) \\ q_2(t) \\ \vdots \\ q_{N-1}(t) \\ q_N(t) \end{bmatrix} + \begin{bmatrix} 0 \\ 0 \\ \vdots \\ 0 \\ 1 \end{bmatrix} x(t), \tag{6.88}$$

$$y(t) = [b_0 \quad 0 \quad \dots \quad 0] \begin{bmatrix} q_1(t) \\ q_2(t) \\ \vdots \\ q_N(t) \end{bmatrix}, \tag{6.89}$$

which, in compact forms, can be written as, respectively,

$$\mathbf{q}'(t) = \mathbf{A}(t)\mathbf{q}(t) + \mathbf{B}x(t), \tag{6.90}$$

$$y(t) = \mathbf{C}\mathbf{q}(t) + \mathbf{D}x(t), \tag{6.91}$$

where the $N \times N$ system matrix is specified by

$$\mathbf{A}(t) = \begin{bmatrix} 0 & 1 & 0 & \dots & 0 \\ 0 & 0 & 1 & & 0 \\ \vdots & \vdots & & \ddots & \vdots \\ 0 & 0 & 0 & & 1 \\ -a_0(t) & -a_1(t) & -a_2(t) & \dots & -a_{N-1}(t) \end{bmatrix}, \quad (6.92)$$

the $N \times 1$ input matrix is given by

$$\mathbf{B} = [0 \ 0 \ \dots \ 0 \ 1]^T, \quad (6.93)$$

the $1 \times N$ observation (or measurement) matrix is described by

$$\mathbf{C} = [b_0 \ 0 \ \dots \ 0] \quad (6.94)$$

and, finally, the 1×1 output matrix is nilpotent,

$$\mathbf{D} = [0]. \quad (6.95)$$

As it is seen, here only $A(t)$ is time-varying.

Example 6.22. An LTV system is governed by the ODE with the coefficients $a_0 = 2$, $a_1 = t$, $a_2 = 4$, $a_3 = 2$, and $b_0 = 4$. To transfer to state space, it first needs dividing the equation by the factor of 2 to get $a_3 = 1$. The new coefficients then become $a_0 = 1$, $a_1 = t/2$, $a_2 = 2$, $a_3 = 1$, and $b_0 = 2$. The state space model, (6.90) and (6.91), is easily described now with the following matrices:

$$\mathbf{A}(t) = \begin{bmatrix} 0 & 1 & 0 \\ 0 & 0 & 1 \\ -1 & -\frac{t}{2} & -2 \end{bmatrix}, \quad \mathbf{B} = \begin{bmatrix} 0 \\ 0 \\ 1 \end{bmatrix}, \quad \mathbf{C} = [2 \ 0 \ 0], \quad \mathbf{D} = [0].$$

As can be seen, $\mathbf{A}(t)$ is time-varying, whereas \mathbf{B} and \mathbf{C} are time-invariant. \square

6.5.2 Block Diagram Representation

In a manner similar to LTI systems, LTV systems can be simulated in state space with the block diagram as that shown in Fig. 4.22. The diagram simulating (6.90) and (6.91) with all time-varying coefficients is shown in Fig. 6.14. In the sequel, it will be obvious that this diagram is equivalently valid for both SISO and MIMO LTV systems.

A Particular Case of $M = 0$

Because $M = 0$ implies $b_N = 0$, the system is performed in state space with the equations

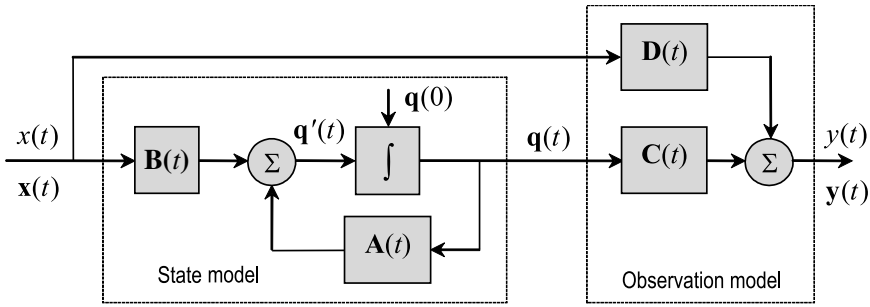


Fig. 6.14. Block diagram representation of LTV systems in state space.

$$\mathbf{q}'(t) = \mathbf{A}(t)\mathbf{q}(t) + \mathbf{B}(t)x(t), \tag{6.96}$$

$$y(t) = \mathbf{C}(t)\mathbf{q}(t), \tag{6.97}$$

in which, for example, the matrices $\mathbf{A}(t)$, $\mathbf{B}(t)$, and $\mathbf{C}(t)$ are given by (6.92), (6.93), and (6.94), respectively.

Having $b_N = 0$, the system is simulated with the diagram shown in Fig. 6.15, in which the branch associated with the nilpotent matrix \mathbf{D} is omitted. Like the LTI system case, this diagram is valid for any $M < N$.

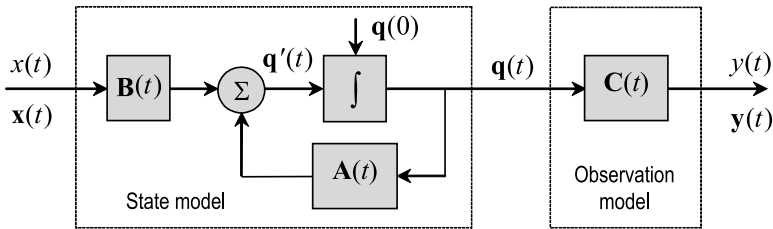


Fig. 6.15. Block diagram representation of LTV systems in state space with $M < N$.

Example 6.23. An LTV system represents a series RLC circuit with a variable resonant frequency. The system equation is given by

$$v_C''(t) + 2\delta v_C'(t) + \omega_0^2(t)v_C(t) = \omega_0^2(t)v(t), \tag{6.98}$$

where $v(t)$ is an input and $v_c(t)$ is an output. The coefficients of the ODE (6.79) are described here as $a_0(t) = \omega_0^2(t)$, $a_1 = 2\delta$, and $b_0(t) = \omega_0^2(t)$. The state space model, (6.96) and (6.97), represents this system with the matrices

$$\mathbf{A}(t) = \begin{bmatrix} 0 & 1 \\ -\omega_0^2(t) & -2\delta \end{bmatrix}, \quad \mathbf{B} = \begin{bmatrix} 0 \\ 1 \end{bmatrix}, \quad \mathbf{C}(t) = [\omega_0^2(t) \ 0].$$

□

MIMO LTV Systems in State Space

Representation of MIMO LTV systems in state space has no substantial peculiarities and is provided as for LTI systems. One merely needs modifying equations (4.125) and (4.126) for time-varying matrices and write

$$\mathbf{q}'(t) = \mathbf{A}(t)\mathbf{q}(t) + \mathbf{B}(t)\mathbf{x}(t), \quad (6.99)$$

$$\mathbf{y}(t) = \mathbf{C}(t)\mathbf{q}(t) + \mathbf{D}(t)\mathbf{x}(t), \quad (6.100)$$

where $q(t)$ and $q'(t)$ are described by (4.103) and (4.104), respectively. The $k \times 1$ vector of a multiple input $\mathbf{x}(t)$ and $p \times 1$ vector of a multiple output $\mathbf{y}(t)$ are given by, respectively,

$$\mathbf{x}(t) = [x_1(t) \ x_2(t) \ \dots \ x_k(t)]^T, \quad (6.101)$$

$$\mathbf{y}(t) = [y_1(t) \ y_2(t) \ \dots \ y_p(t)]^T, \quad (6.102)$$

the $N \times N$ system matrix $\mathbf{A}(t)$ and $p \times N$ observation matrix $\mathbf{C}(t)$ are described with, respectively,

$$\mathbf{A}(t) = \begin{bmatrix} a_{11}(t) & a_{12}(t) & \dots & a_{1N}(t) \\ a_{21}(t) & a_{22}(t) & \dots & a_{2N}(t) \\ \vdots & \vdots & \ddots & \vdots \\ a_{N1}(t) & a_{N2}(t) & \dots & a_{NN}(t) \end{bmatrix}, \quad \mathbf{C}(t) = \begin{bmatrix} c_{11}(t) & c_{12}(t) & \dots & c_{1N}(t) \\ c_{21}(t) & c_{22}(t) & \dots & c_{2N}(t) \\ \vdots & \vdots & \ddots & \vdots \\ c_{p1}(t) & c_{p2}(t) & \dots & c_{pN}(t) \end{bmatrix}, \quad (6.103)$$

and the $N \times k$ input matrix $\mathbf{B}(t)$ and $p \times k$ output matrix $\mathbf{D}(t)$ are, respectively,

$$\mathbf{B}(t) = \begin{bmatrix} b_{11}(t) & b_{12}(t) & \dots & b_{1k}(t) \\ b_{21}(t) & b_{22}(t) & \dots & b_{2k}(t) \\ \vdots & \vdots & \ddots & \vdots \\ b_{N1}(t) & b_{N2}(t) & \dots & b_{Nk}(t) \end{bmatrix}, \quad \mathbf{D}(t) = \begin{bmatrix} d_{11}(t) & d_{12}(t) & \dots & d_{1k}(t) \\ d_{21}(t) & d_{22}(t) & \dots & d_{2k}(t) \\ \vdots & \vdots & \ddots & \vdots \\ d_{p1}(t) & d_{p2}(t) & \dots & d_{pk}(t) \end{bmatrix}. \quad (6.104)$$

Most generally, all of these matrices are supposed to be time-varying.

It follows that simulation of both SISO and MIMO LTV systems is provided by the same universal block diagram shown in Fig. 6.14 for $M = N$ and in Fig. 6.15 for $M < N$. The choice of $x(t)$ or $\mathbf{x}(t)$ and $y(t)$ or $\mathbf{y}(t)$ depends on what kind of LTV systems is simulated: SISO, SIMO, MISO, or MIMO.

6.5.3 Solution of State Space Equations

When we deal with LTI systems in state space, a lucky trick to come up with a solution to the state space equations is to use the integration factor $e^{-\mathbf{A}t}$, in

which, inherently, the matrix \mathbf{A} is time-invariant. For the time-varying $\mathbf{A}(t)$, an instant desire may arise for solving an equation with the more common factor $e^{-\int_{t_0}^t \mathbf{A}(\tau) d\tau}$. Indeed, multiplying both sides of (6.99) with this factor leads to

$$e^{-\int_{t_0}^t \mathbf{A}(\tau) d\tau} \mathbf{q}'(t) - e^{-\int_{t_0}^t \mathbf{A}(\tau) d\tau} \mathbf{A}(t) \mathbf{q}(t) = e^{-\int_{t_0}^t \mathbf{A}(\tau) d\tau} \mathbf{B}(t) \mathbf{x}(t)$$

and a lucky case will be to write an exact ODE

$$\left[e^{-\int_{t_0}^t \mathbf{A}(\tau) d\tau} \mathbf{q}(t) \right]' = e^{-\int_{t_0}^t \mathbf{A}(\tau) d\tau} \mathbf{B}(t) \mathbf{x}(t)$$

and solve it in a regular way. The time derivative of $e^{-\int_{t_0}^t \mathbf{A}(\tau) d\tau}$, however, commonly does not produce the necessary relation. In fact, it can easily be verified, by some particular example, that

$$\frac{d}{dt} e^{-\int_{t_0}^t \mathbf{A}(\tau) d\tau} \neq -e^{-\int_{t_0}^t \mathbf{A}(\tau) d\tau} \mathbf{A}(t) \neq -\mathbf{A}(t) e^{-\int_{t_0}^t \mathbf{A}(\tau) d\tau}$$

and we thus need finding another approach to solve (6.99).

Let us then start with the homogenous ODE

$$\mathbf{q}'(t) = \mathbf{A}(t) \mathbf{q}(t), \quad (6.105)$$

supposing that at least one of the components of $\mathbf{A}(t)$ is time-varying.

It is known from the matrix theory that if $\mathbf{A}(t)$ is continuous with $t \geq t_0$, then a solution of (6.105) with the initial condition $\mathbf{q}(t_0)$ exists for $t \geq t_0$, is unique, and can be written as

$$\mathbf{q}(t) = \mathbf{Q}(t) \mathbf{q}(t_0), \quad (6.106)$$

where $\mathbf{Q}(t)$ satisfies the differential equation

$$\mathbf{Q}'(t) = \mathbf{A}(t) \mathbf{Q}(t), \quad \mathbf{Q}(t_0) = \mathbf{I}, \quad (6.107)$$

and is called the *fundamental matrix*. Because any initial conditions could be chosen to solve (6.107), the fundamental matrix $\mathbf{Q}(t)$, for the time-varying matrix $\mathbf{A}(t)$, is not unique, exhibiting the following important properties:

- *Dimensions.* It is the $N \times N$ square matrix. \square
- *Nonsingularity.* It is nonsingular for all t . Otherwise, $\mathbf{Q}(t)$ does not satisfy (6.106) and, in particular, cannot be a unit matrix \mathbf{I} at t_0 as claimed by an equality $\mathbf{q}(t_0) = \mathbf{Q}(t_0)\mathbf{q}(t_0)$, meaning that $\mathbf{q}(t_0) = \mathbf{I}\mathbf{q}(t_0)$. \square

To determine $\mathbf{Q}(t)$, a common way is to consider some initial state $\mathbf{q}_n(t_0)$, $n = 1, 2, \dots, N$, for which (6.105) produces a unique solution $\mathbf{q}_n(t)$, $n = 1, 2, \dots, N$. All N particular solutions $\mathbf{q}_n(t)$ can be united to the $N \times N$ matrix $\mathbf{Q}(t) = [\mathbf{q}_1(t) \ \mathbf{q}_2(t) \ \dots \ \mathbf{q}_N(t)]$. Because every $\mathbf{q}_n(t)$ satisfies (6.105), the matrix $\mathbf{Q}(t)$ determined in such a way satisfies (6.106).

Example 6.24. An LTV system is described with the homogenous equation (6.105) as

$$\begin{bmatrix} q_1'(t) \\ q_2'(t) \end{bmatrix} = \begin{bmatrix} 0 & t \\ 0 & 0 \end{bmatrix} \begin{bmatrix} q_1(t) \\ q_2(t) \end{bmatrix}$$

having initial conditions $q_1(0)$ and $q_2(0)$. Equivalently, we can write

$$q_1'(t) = tq_2(t) \quad \text{and} \quad q_2'(t) = 0.$$

The second equation has an obvious solution $q_2(t) = q_2(0)$ and thus the first equation is solved by

$$q_1(t) = \int_0^t \tau q_2(\tau) d\tau + q_1(0) = q_2(0) \int_0^t \tau d\tau + q_1(0) = \frac{t^2}{2} q_2(0) + q_1(0).$$

Voluntary, one may suppose that $q_1(0) = 0$ and $q_2(0) = 1$. The first particular solution will then be defined by

$$\mathbf{q}_1(0) = \begin{bmatrix} 0 \\ 1 \end{bmatrix} \quad \text{and} \quad \mathbf{q}_1(t) = \begin{bmatrix} t^2/2 \\ 1 \end{bmatrix}.$$

If we allow, for example, $q_1(0) = 3$ and $q_2(0) = 1$, we can find the second particular solution

$$\mathbf{q}_2(0) = \begin{bmatrix} 3 \\ 1 \end{bmatrix} \quad \text{and} \quad \mathbf{q}_2(t) = \begin{bmatrix} \frac{t^2}{2} + 3 \\ 1 \end{bmatrix}.$$

The fundamental matrix can now be filled as

$$\mathbf{Q}(t) = [\mathbf{q}_1(t) \ \mathbf{q}_2(t)] = \begin{bmatrix} \frac{t^2}{2} & \frac{t^2}{2} + 3 \\ 1 & 1 \end{bmatrix}. \quad (6.108)$$

\square

Let us come back to the inhomogeneous equation (6.105). Following the Lagrange method of variation, we could try finding a solution in the form of $\mathbf{q}(t) = \mathbf{Q}(t)\mathbf{u}(t)$, where $\mathbf{Q}(t)$ satisfies (6.107) and $\mathbf{u}(t)$ is still some unknown function of the same class. Substituting to (6.99) yields

$$\mathbf{Q}'\mathbf{u} + \mathbf{Q}\mathbf{u}' = \mathbf{A}\mathbf{Q}\mathbf{u} + \mathbf{B}\mathbf{x}.$$

By (6.107), we have $\mathbf{Q}'\mathbf{u} = \mathbf{A}\mathbf{Q}\mathbf{u}$ and the above identity becomes

$$\mathbf{Q}\mathbf{u}' = \mathbf{B}\mathbf{x} \quad \text{or} \quad \mathbf{u}' = \mathbf{Q}^{-1}\mathbf{B}\mathbf{x}, \quad (6.109)$$

having a solution, by $\mathbf{u}(t_0) = \mathbf{Q}^{-1}(t_0)\mathbf{q}(t_0)$,

$$\begin{aligned} \mathbf{u}(t) &= \mathbf{u}(t_0) + \int_{t_0}^t \mathbf{Q}^{-1}(\tau)\mathbf{B}(\tau)\mathbf{x}(\tau)d\tau \\ &= \mathbf{Q}^{-1}(t_0)\mathbf{q}(t_0) + \int_{t_0}^t \mathbf{Q}^{-1}(\tau)\mathbf{B}(\tau)\mathbf{x}(\tau)d\tau. \end{aligned} \quad (6.110)$$

A general solution of (6.99), by $\mathbf{q}(t) = \mathbf{Q}(t)\mathbf{u}(t)$ and (6.110), can now be found to be

$$\begin{aligned} \mathbf{q}(t) &= \mathbf{Q}(t)\mathbf{Q}^{-1}(t_0)\mathbf{q}(t_0) + \int_{t_0}^t \mathbf{Q}(t)\mathbf{Q}^{-1}(\tau)\mathbf{B}(\tau)\mathbf{x}(\tau)d\tau \\ &= \Phi(t, t_0)\mathbf{q}(t_0) + \int_{t_0}^t \Phi(t, \tau)\mathbf{B}(\tau)\mathbf{x}(\tau)d\tau, \end{aligned} \quad (6.111)$$

where the function

$$\Phi(t, \theta) = \mathbf{Q}(t)\mathbf{Q}^{-1}(\theta) \quad (6.112)$$

is called the *state transition matrix* owing to an ability of predetermining a transition of the system state vector $\mathbf{q}(t)$ from θ to t . We notice that, by zero input $\mathbf{x}(t) = 0$, (6.111) becomes homogenous,

$$\mathbf{q}(t) = \Phi(t, t_0)\mathbf{q}(t_0). \quad (6.113)$$

Example 6.25. Consider a system (Example 6.24) represented with the fundamental matrix (6.108), which determinant calculates

$$|\mathbf{Q}(t)| = \begin{vmatrix} \frac{t^2}{2} & \frac{t^2}{2} + 3 \\ 1 & 1 \end{vmatrix} = -3$$

and thus the matrix is nonsingular. The inverse matrix $\mathbf{Q}^{-1}(t)$ is defined by

$$\mathbf{Q}^{-1}(t) = \begin{bmatrix} -\frac{1}{3} \frac{t^2}{6} + 1 \\ \frac{1}{3} & -\frac{t^2}{6} \end{bmatrix}$$

specifying the state transition matrix

$$\Phi(t, \theta) = \mathbf{Q}(t)\mathbf{Q}^{-1}(\theta) = \begin{bmatrix} \frac{t^2}{2} & \frac{t^2}{2} + 3 \\ 1 & 1 \end{bmatrix} \begin{bmatrix} -\frac{1}{3} \frac{\theta^2}{6} + 1 \\ \frac{1}{3} & -\frac{\theta^2}{6} \end{bmatrix} = \begin{bmatrix} 1 & \frac{t^2 - \theta^2}{2} \\ 0 & 1 \end{bmatrix}. \quad (6.114)$$

□

By substituting (6.111) to the observation equation (6.100), we finally arrive at the solution for the system output

$$\mathbf{y}(t) = \mathbf{C}(t)\Phi(t, t_0)\mathbf{q}(t_0) + \mathbf{C}(t) \int_{t_0}^t \Phi(t, \tau)\mathbf{B}(\tau)\mathbf{x}(\tau)d\tau + \mathbf{D}(t)\mathbf{x}(t), \quad (6.115)$$

in which the last term vanishes if $M < N$. The next steps in transforming (6.115) can be facilitated by using properties of the state transition matrix $\Phi(t, \theta)$ that we observe below.

Properties of the State Transition Matrix

Because the state transition matrix $\Phi(t, \theta)$ is formed, by (6.112), with a nonsingular fundamental matrix $\mathbf{Q}(t)$ and its inverse version, several important properties of $\Phi(t, \theta)$ can be observed:

- For equal time variables $t = \theta$ and, in particular, for the initial condition $t = t_0$, the matrix is unit,

$$\Phi(\theta, \theta) = \Phi(t_0, t_0) = \mathbf{I}. \quad (6.116)$$

□

- The matrix is a unique solution of the ODE

$$\Phi'(t, \theta) = \mathbf{A}(t)\Phi(t, \theta) \quad (6.117)$$

with the initial condition $\Phi(\theta, \theta) = \mathbf{I}$. This fact follows behind the substitution of $\Phi(t, \theta) = \mathbf{Q}(t)\mathbf{Q}^{-1}(\theta)$. Merely observe that $\mathbf{Q}^{-1}(\theta)$ does not depend on t and thus (6.117) degenerates to (6.107). □

- Invertibility:

$$\Phi^{-1}(t, \theta) = [\mathbf{Q}(t)\mathbf{Q}^{-1}(\theta)]^{-1} = \mathbf{Q}(\theta)\mathbf{Q}^{-1}(t) = \Phi(\theta, t). \quad (6.118)$$

□

- Decomposition:

$$\begin{aligned}\Phi(t, \theta) &= \mathbf{Q}(t)\mathbf{Q}^{-1}(\theta) = \mathbf{Q}(t)\mathbf{Q}^{-1}(\theta_1)\mathbf{Q}(\theta_1)\mathbf{Q}^{-1}(\theta) \\ &= \Phi(t, \theta_1)\Phi(\theta_1, \theta).\end{aligned}\quad (6.119)$$

The rule (6.119) is applicable to any t , θ , and θ_1 . Moreover, it can be extended to an infinite number of subfunctions such that

$$\Phi(t, \theta) = \Phi(t, \theta_1)\Phi(\theta_1, \theta_2) \dots \Phi(\theta_k, \theta). \quad (6.120)$$

□

- If $\mathbf{A}(t)$ is diagonal, it demonstrates a commutative property

$$\mathbf{A}(t) \left(\int_{\theta}^t \mathbf{A}(\tau) d\tau \right) = \left(\int_{\theta}^t \mathbf{A}(\tau) d\tau \right) \mathbf{A}(t)$$

for any t and θ . Owing to this, the state transition matrix can be found as a reciprocal of the integration factor,

$$\Phi(t, \theta) = e^{\int_{\theta}^t \mathbf{A}(\tau) d\tau} = \sum_{n=0}^{\infty} \frac{1}{n!} \left(\int_{\theta}^t \mathbf{A}(\tau) d\tau \right)^n. \quad (6.121)$$

□

6.5.4 System Impulse Response in State Space

If $\mathbf{q}(t_0) = \mathbf{0}$, the output (6.115) allows us now to derive the time-varying impulse response of an LTV system. We notice that, sometimes, the impulse response is also called the *zero-state* impulse response. By the sifting property of the delta function, we can equivalently write

$$\mathbf{y}(t) = \mathbf{C}(t) \int_{t_0}^t \Phi(t, \theta) \mathbf{B}(\theta) \mathbf{x}(\theta) d\theta + \mathbf{D}(t) \mathbf{x}(t) \quad (6.122)$$

$$= \int_{t_0}^t [\mathbf{C}(t) \Phi(t, \theta) \mathbf{B}(\theta) + \mathbf{D}(\theta) \delta(t - \theta)] \mathbf{x}(\theta) d\theta. \quad (6.123)$$

Equation (6.123) can further be transformed to

$$\mathbf{y}(t) = \int_{t_0}^t \mathbf{H}(t, \theta) \mathbf{x}(\theta) d\theta, \quad (6.124)$$

where

$$\begin{aligned}\mathbf{H}(t, \theta) &= \mathbf{C}(t)\Phi(t, \theta)\mathbf{B}(\theta) + \mathbf{D}(\theta)\delta(t - \theta) \\ &= \mathbf{C}(t)\mathbf{Q}(t)\mathbf{Q}^{-1}(\theta)\mathbf{B}(\theta) + \mathbf{D}(\theta)\delta(t - \theta).\end{aligned}\quad (6.125)$$

Because (6.124) is nothing more than the general convolution for MIMO LTV systems, the function (6.125) is nothing less than the impulse response matrix of a MIMO LTV system.

Example 6.26. A MIMO LTV system is described by (6.99) and (6.100) with the following matrices

$$\mathbf{A}(t) = \begin{bmatrix} 0 & t \\ 0 & 0 \end{bmatrix}, \quad \mathbf{B} = \begin{bmatrix} 0 & 1 \\ 1 & 0 \end{bmatrix}, \quad \mathbf{C} = \begin{bmatrix} 1 & -\frac{t^2}{2} \\ 1 & 0 \end{bmatrix}, \quad \mathbf{D} = [0].$$

Given $\mathbf{A}(t)$, the state transition matrix $\Phi(t, \theta)$ is defined by (6.114). By virtue of (6.125), the time-varying impulse response matrix is determined as

$$\begin{aligned}\mathbf{H}(t, \theta) &= \mathbf{C}(t)\Phi(t, \theta)\mathbf{B}, \\ \begin{bmatrix} h_{11}(t, \theta) & h_{12}(t, \theta) \\ h_{21}(t, \theta) & h_{22}(t, \theta) \end{bmatrix} &= \begin{bmatrix} 1 & -\frac{t^2}{2} \\ 1 & 0 \end{bmatrix} \begin{bmatrix} 1 & \frac{t^2 - \theta^2}{2} \\ 0 & 1 \end{bmatrix} \begin{bmatrix} 0 & 1 \\ 1 & 0 \end{bmatrix} = \begin{bmatrix} -\frac{\theta^2}{2} & 1 \\ \frac{t^2 - \theta^2}{2} & 1 \end{bmatrix}.\end{aligned}$$

The system is thus specified with the following time-varying impulse responses

$$\begin{aligned}h_{11}(t, \theta) &= -\frac{\theta^2}{2}u(t - \theta), \quad h_{21}(t, \theta) = \frac{1}{2}(t^2 - \theta^2)u(t - \theta), \\ h_{12}(t, \theta) &= h_{22}(t, \theta) = u(t - \theta).\end{aligned}$$

□

Example 6.27. A SISO LTV system is represented in state space by (6.99) and (6.100) with the matrices

$$\mathbf{A}(t) = \begin{bmatrix} 0 & 0 \\ 0 & 0 \end{bmatrix}, \quad \mathbf{B} = \begin{bmatrix} -te^{-at} \\ e^{-at} \end{bmatrix}, \quad \mathbf{C} = [e^{at} \quad te^{at}], \quad \mathbf{D} = [0].$$

For $\mathbf{A}(t)$ having zero components, solutions of the homogenous equations, $q_1'(t) = 0$ and $q_2'(t) = 0$, produce, respectively, $q_1(t) = q_1(0)$ and $q_2(t) = q_2(0)$. For some voluntarily assigned initial conditions, one therefore can let

$$\mathbf{q}_1(0) = \mathbf{q}_1(t) = \begin{bmatrix} 0 \\ 1 \end{bmatrix} \quad \text{and} \quad \mathbf{q}_2(0) = \mathbf{q}_2(t) = \begin{bmatrix} 1 \\ 1 \end{bmatrix}.$$

The time-invariant fundamental matrix thus obeys

$$\mathbf{Q} = \begin{bmatrix} 0 & 1 \\ 1 & 1 \end{bmatrix}, \quad \mathbf{Q}^{-1} = \begin{bmatrix} -1 & 1 \\ 1 & 0 \end{bmatrix}.$$

By (6.112), the state transition matrix becomes identity,

$$\Phi = \begin{bmatrix} 1 & 0 \\ 0 & 1 \end{bmatrix}, \quad (6.126)$$

and the time-varying impulse response can be determined, by (6.125), as

$$\begin{aligned} h(t, \theta) &= \mathbf{C}(t)\Phi\mathbf{B}(\theta) \\ &= [e^{at} \quad te^{at}] \begin{bmatrix} 1 & 0 \\ 0 & 1 \end{bmatrix} \begin{bmatrix} -\theta e^{-a\theta} \\ e^{-a\theta} \end{bmatrix} = e^{a(t-\theta)}(t-\theta)u(t-\theta). \end{aligned}$$

□

6.5.5 BIBO Stability of MIMO LTV Systems

Formerly, we mentioned that a SISO system is BIBO stable if the value M in (6.55) is finite. For MIMO systems having the time-varying impulse response matrix $\mathbf{H}(t, \theta)$, the necessary and sufficient condition for BIBO stability modifies to

$$\int_{t_0}^t \|\mathbf{H}(t, \theta)\| d\theta \leq M < \infty, \quad (6.127)$$

where $t \geq t_0$ and $\|\mathbf{H}(t, \theta)\|$ is a norm of $\mathbf{H}(t, \theta)$. It is allowed to apply any norm. Most frequently, however, they employ the H_∞ -norm,

$$\|\mathbf{H}\|_\infty = \max_t |\mathbf{H}(t)|, \quad (6.128)$$

as most “reliable”, because it characterizes the maximum of the absolute value (peak value) of the function,

Let us recall that the LTV system impulse response matrix $\mathbf{H}(t, \theta)$ is described by (6.125). The condition for BIBO stability associated with this function is obtained by (6.127). Additionally, if the input is bounded, (6.125) brings forward one more claim

$$\|\mathbf{D}(t)\| < \infty. \quad (6.129)$$

It can be shown that (6.127) and (6.129) are most general to ascertain BIBO stability of LTV systems.

The other widely used approach implies analyzing the familiar homogenous equation (6.113). Apparently, the system states will be bounded if and only if the norm of $\Phi(t, t_0)$ is finite,

$$\|\Phi(t, t_0)\| < \infty. \quad (6.130)$$

If it is the case, the system is said to be *marginally stable*. This definition coincides with the other sign of stability. The system is *asymptotically stable*

if and only if the response excited by any bounded input is also bounded and approaches zero at infinity. Thus, for the asymptotically stable system, along with (6.130) the following condition must also be satisfied,

$$\|\Phi(t, t_0)\|_{t \rightarrow \infty} \rightarrow 0. \quad (6.131)$$

Example 6.28. An LTV system (Example 6.25) is represented with the state transition matrix

$$\Phi(t, \theta) = \begin{bmatrix} 1 & \frac{t^2 - \theta^2}{2} \\ 0 & 1 \end{bmatrix}.$$

The norm $\|\Phi(t, \theta)\|$ can be regarded as the maximum “magnification” capability of $\Phi(t, \theta)$. For the initial time $\theta = 0$, the “12” component of $\Phi(t, \theta)$ grows quadratically and becomes infinity at $t = \infty$. Therefore, a system is neither marginally stable, because (6.130) is not satisfied, nor asymptotically stable, because (6.131) is not satisfied. \square

Example 6.29. The state transition matrix (6.126) of a system (Example 6.27) is time-invariant and identity,

$$\Phi = \begin{bmatrix} 1 & 0 \\ 0 & 1 \end{bmatrix}.$$

This system is thus marginally stable, because (6.130) is satisfied. However, it is not asymptotically stable, because (6.131) can never be obeyed. \square

We notice that several other criteria of stability used in the theory of LTV systems can be found in special books.

6.5.6 Controllability

An important characteristic of any system is its controllability. By the definition, an LTV linear system described by (6.99) and (6.100) is completely controllable on the finite time interval $[t_0, t_1]$ if for any initial state $\mathbf{q}(t_0)$ there may be found an input $\mathbf{x}(t)$ to transfer the system to the other given state $\mathbf{q}(t_1)$. Without loss in generality, we can let $\mathbf{q}(t_0) = 0$ and write a general solution (6.111) as

$$\mathbf{q}(t) = \int_{t_0}^t \Phi(t, \theta) \mathbf{B}(\theta) \mathbf{x}(\theta) d\theta. \quad (6.132)$$

Now assume that there is some nonzero vector ϱ of the same dimensions as $\mathbf{q}(t)$. The system will be controllable if the projection of the system state on this vector can be set arbitrary. To find the relevant condition, we multiply both sides of (6.132) with ϱ^T and go to

$$\begin{aligned} \varrho^T \mathbf{q}(t) &= \varrho^T \int_{t_0}^t \Phi(t, \theta) \mathbf{B}(\theta) \mathbf{x}(\theta) d\theta = \int_{t_0}^t \varrho^T \Phi(t, \theta) \mathbf{B}(\theta) \mathbf{x}(\theta) d\theta \\ &= \int_{t_0}^t [\mathbf{B}^T(\theta) \Phi^T(t, \theta) \varrho]^T \mathbf{x}(\theta) d\theta = \int_{t_0}^t \mathbf{z}_t^T(\theta) \mathbf{x}(\theta) d\theta, \end{aligned} \quad (6.133)$$

where a newly introduced vector is

$$\mathbf{z}_t(\theta) = \mathbf{B}^T(\theta) \Phi^T(t, \theta) \varrho. \quad (6.134)$$

Because the input can be assigned arbitrary, we can let $\mathbf{x}(\theta) = \gamma \mathbf{z}_t(\theta)$, where γ is some nonzero constant. For such an input, (6.133) transforms to

$$\varrho^T \mathbf{q}(t) = \int_{t_0}^t \mathbf{z}_t^T(\theta) \mathbf{x}(\theta) d\theta = \gamma \int_{t_0}^t \mathbf{z}_t^T(\theta) \mathbf{z}_t(\theta) d\theta = \gamma \int_{t_0}^t \|\mathbf{z}_t(\theta)\|^2 d\theta, \quad (6.135)$$

where the value $\|\mathbf{z}_t(\theta)\|$ denotes the length of a vector $\mathbf{z}_t(\theta)$.

If the product (6.135) is zero for any input, $\varrho^T \mathbf{q}(t) = 0$, the system is certainly uncontrollable. The latter means that, for any θ from t_0 to t , we have

$$\mathbf{B}^T(\theta) \Phi^T(t, \theta) \varrho = 0, \quad (6.136)$$

meaning that, for the nonzero ϱ , the columns of $\mathbf{B}^T(\theta) \Phi^T(t, \theta)$ must be linearly dependent. If the columns are linearly independent, the only solution of (6.136) will be provided with $\varrho = 0$ that is a contradiction.

We hence have a sign of LTV system controllability: The LTV system is controllable if the columns of $\mathbf{B}^T(\theta) \Phi^T(t, \theta)$ are linearly independent for $t \geq t_0$.

Example 6.30. Consider an LTV system (Example 6.27), which input and state transition matrices are given by, respectively,

$$\mathbf{B}(\theta) = \begin{bmatrix} -\theta e^{-a\theta} \\ e^{-a\theta} \end{bmatrix}, \quad \Phi = \begin{bmatrix} 1 & 0 \\ 0 & 1 \end{bmatrix}.$$

The matrix $\mathbf{B}^T(\theta) \Phi^T$ calculates

$$\mathbf{B}^T(\theta) \Phi^T = [-\theta e^{-a\theta} \ e^{-a\theta}] \begin{bmatrix} 1 & 0 \\ 0 & 1 \end{bmatrix} = [-\theta e^{-a\theta} \ e^{-a\theta}],$$

indicating that the columns are linearly independent. The system is thus controllable.

We arrive at the same conclusion even intuitively. In fact, for the matrices given (Example 6.27), the states of a system are defined as $q_1'(t) = -te^{-at}x(t)$ and $q_2'(t) = e^{-at}x(t)$. Because every state directly depends on the input $x(t)$, the system is controllable. \square

6.5.7 Observability

An LTV system described in state space by (6.99) and (6.100) is *completely observable* on the finite time interval $[t_0, t_1]$ if for any t_0 an initial state $\mathbf{q}(t_0)$ can be determined from observation of the output $\mathbf{y}(t)$ over this interval with the input $\mathbf{x}(t)$ known over the same interval.

To find a condition for the LTV system to be observable, let us rewrite a solution (6.115) as

$$\mathbf{C}(t)\Phi(t, t_0)\mathbf{q}(t_0) = \mathbf{y}(t) - \mathbf{C}(t) \int_{t_0}^t \Phi(t, \theta)\mathbf{B}(\theta)\mathbf{x}(\theta)d\theta - \mathbf{D}(t)\mathbf{x}(t) \quad (6.137)$$

and solve it at the interval from t_0 to t for the initial state $\mathbf{q}(t_0)$. If it is soluble for $\mathbf{q}(t_0)$, the system is observable.

To obtain the necessary solution, we multiply both sides of (6.137) with $[\mathbf{C}(t)\Phi(t, t_0)]^{-1}$ and the condition for the system to be observable appears instantly. An LTV system is observable if for any $\beta \neq 0$ the vector $\mathbf{C}(t)\Phi(t, t_0)\beta$ is not identically zero for all $t \geq t_0$.

Example 6.31. Evaluate observability of the system considered in Example 6.27. By the matrices given, the vector $\mathbf{C}(t)\Phi(t, t_0)\beta$ is defined as

$$\mathbf{C}(t)\Phi(t, t_0)\beta = \begin{bmatrix} e^{at} & te^{at} \end{bmatrix} \begin{bmatrix} 1 & 0 \\ 0 & 1 \end{bmatrix} \beta = \begin{bmatrix} \beta e^{at} & t\beta e^{at} \end{bmatrix}$$

and, it follows, can never be identically zero if $\beta \neq 0$. The system is thus observable. But it is not absolutely observable with $t_0 = 0$, in view of the fact that its component “12” becomes zero at $t = 0$. We confirm this conclusion by analyzing the observation equation (6.100) with the matrices given in Example 6.27. In fact, because $y(t) = q_1(t)e^{at} + q_2(t)te^{at}$, the initial first state is observable via the output with $q_1(0) = y(0)$ and the initial second state $q_2(0)$ is not observable. \square

6.6 Linear Periodically Time-varying Systems

Linear periodically time-varying (LPTV) systems play a tremendous role in solving a great deal of electronic problems. Utilizing such systems, it becomes possible to remove spectra of signals from one region to another, modulate, detect, and amplify signals, excite passive circuits, etc. In spite of an applied significance, the problem of finding periodic solutions of ODEs with time-varying coefficients describing periodic systems is still far from simple engineering solutions and distinct receipts. In this section, we bring forward many engineering solutions and discuss fundamentals of the most general Floquet’s theory of LPTV systems.

6.6.1 Basic Foundations

To catch the difference between periodic and non-periodic versions of LTV systems, it is in order to consider a simplest linear ODE of the first order with a time-varying coefficient $a(t)$,

$$y'(t) = a(t)x(t). \quad (6.138)$$

Let us apply the Fourier transform to both its sides. By the properties of the Fourier transform (Appendix C), we get

$$j\omega Y(j\omega) = \frac{1}{2\pi} A(j\omega) * X(j\omega) = \frac{1}{2\pi} \int_{-\infty}^{\infty} A(j\omega_1) X(j\omega - j\omega_1) d\omega_1, \quad (6.139)$$

where $Y(j\omega)$, $A(j\omega)$, and $X(j\omega)$ are the transforms of $y(t)$, $a(t)$, and $x(t)$, respectively. The ODE is thus transformed to the integral equation that commonly gives no preference.

A situation changes cardinally when $a(t)$ becomes periodic. In fact, for $a(t) = a(t + T)$, where T is period of repetition, one can extend $a(t)$ to the Fourier series

$$a(t) = \sum_{k=-\infty}^{\infty} C_k e^{jk\Omega t}, \quad (6.140)$$

where $\Omega = 2\pi/T$ is an angular frequency associated with T and the coefficient C_k is provided by

$$C_k = \frac{1}{T} \int_{-T/2}^{T/2} a(t) e^{-jk\Omega t} dt. \quad (6.141)$$

Now we can find the Fourier transform of (6.140),

$$A(j\omega) = 2\pi \sum_{k=-\infty}^{\infty} C_k \delta(\omega - k\Omega), \quad (6.142)$$

and substitute (6.142) to (6.139). The transformation produces

$$\begin{aligned} j\omega Y(j\omega) &= \frac{1}{2\pi} \int_{-\infty}^{\infty} A(j\omega_1) X(j\omega - j\omega_1) d\omega_1 \\ &= \int_{-\infty}^{\infty} \sum_{k=-\infty}^{\infty} C_k \delta(\omega_1 - k\Omega) X(j\omega - j\omega_1) d\omega_1 \end{aligned}$$

$$\begin{aligned}
&= \sum_{k=-\infty}^{\infty} C_k \int_{-\infty}^{\infty} \delta(\omega_1 - k\Omega) X(j\omega - j\omega_1) d\omega_1 \\
&= \sum_{k=-\infty}^{\infty} C_k X(j\omega - jk\Omega), \tag{6.143}
\end{aligned}$$

allowing us to represent the spectral density $Y(j\omega)$ of the output via the spectral density $X(j\omega)$ of the input as in the following,

$$Y(j\omega) = \frac{1}{j\omega} \sum_{k=-\infty}^{\infty} C_k X(j\omega - jk\Omega). \tag{6.144}$$

A solution (6.144) for an LPTV system (6.138) is thus found in the frequency domain. A simple observation shows that the spectral content of the output is enriched with new components caused by the k -order harmonics of a periodically varying input. The latter represents one of the most recognized properties of LPTV systems.

6.6.2 Floquet's Theory

Any LPTV system demonstrates a very important feature that is the time-varying coefficients act as auxiliary sources of energy. This auxiliary resource is exploited widely. However, an accompanying problem arises of stability occupying a central place in the theory of periodic systems.

In the most general terms, the conditions for an LPTV system to be stable as well as solutions in state space were mathematically given by Floquet⁶. After many decades apart, recognizing a theoretical and applied significance of this mathematical work, the approach was called the Floquet theory. Its basis is in the transformation of the LPTV system into the LTI system through the Lyapunov transformation of variables. If one follows this transformation, then stability of the original periodic system can be ascertained from the relevant LTI system.

Floquet's Theorem

We have already shown that stability of a system described in state space can be ascertained for $t \geq t_0$ by considering only the homogenous equation

$$\mathbf{q}'(t) = \mathbf{A}(t)\mathbf{q}(t) \tag{6.145}$$

with known initial condition $\mathbf{q}(t_0)$.

Now let us think that the matrix $\mathbf{A}(t)$ is continuous, bounded, and periodic with period T , namely $\mathbf{A}(t) = \mathbf{A}(t+T)$. We can suppose that the fundamental

⁶ Achille Marie Gaston Floquet, French mathematician, 15 December 1847-7 October 1920.

matrix $\mathbf{Q}(t)$ is defined and thus the state transition matrix $\Phi(t, t_0)$ is distinct as well.

For periodic $\mathbf{A}(t)$, the *Floquet theorem* argues the following.

1. The state transition matrix $\Phi(t, t_0)$ is periodic for all t and t_0

$$\Phi(t, t_0) = \Phi(t + T, t_0 + T). \quad (6.146)$$

To prove, put $\tau = t - T$, then $\frac{d}{d\tau}\mathbf{q} = \mathbf{A}(\tau + T)\mathbf{q} = \mathbf{A}(\tau)\mathbf{q}$. Thus, $\Phi(t + T, t_0 + T)$ is also a fundamental matrix.

2. There exists a nonsingular matrix $\mathbf{P}(t, t_0)$, satisfying $\mathbf{P}(t, t_0) = \mathbf{P}(t + T, t_0)$ and $\mathbf{P}(t_0, t_0) = \mathbf{I}$, and a constant square matrix \mathbf{F} such that

$$\Phi(t, t_0) = \mathbf{P}(t, t_0)e^{\mathbf{F}(t-t_0)}. \quad (6.147)$$

In fact, because the fundamental matrices $\Phi(t, t_0)$ and $\Phi(t + T, t_0 + T)$ are linearly dependent even with unit coefficients as in (6.146), there exists a nonsingular matrix \mathbf{F}_1 (known as the *monodromy matrix*) such that

$$\Phi(t + T, t_0) = \Phi(t, t_0)\mathbf{F}_1 \quad (6.148)$$

and a constant matrix \mathbf{F} such that

$$\mathbf{F}_1 = e^{\mathbf{F}T} \quad \text{and} \quad \mathbf{F} = \frac{1}{T} \ln \mathbf{F}_1. \quad (6.149)$$

We can now rewrite (6.147) as

$$\mathbf{P}(t, t_0) = \Phi(t, t_0)e^{-\mathbf{F}(t-t_0)}, \quad (6.150)$$

put $\tau = t - T$, let for simplicity $t_0 = 0$, and show that $\mathbf{P}(t, 0) \equiv \mathbf{P}(t)$ is T -periodic:

$$\begin{aligned} \mathbf{P}(\tau + T) &= \Phi(\tau + T)e^{-\mathbf{F}(\tau+T)} = \Phi(\tau)\mathbf{F}_1e^{-\mathbf{F}(\tau+T)} \\ &= \Phi(\tau)e^{\mathbf{F}T}e^{-\mathbf{F}(\tau+T)} = \Phi(\tau)e^{-\mathbf{F}\tau} = \mathbf{P}(\tau). \end{aligned}$$

3. The Lyapunov substitution of a variable,

$$\mathbf{q}(t) = \mathbf{P}(t, t_0)\mathbf{z}(t), \quad (6.151)$$

transforms an LPTV system (6.145) to the LTI system

$$\mathbf{z}'(t) = \mathbf{F}\mathbf{z}(t) \quad (6.152)$$

for $t \geq t_0$ and initial condition $\mathbf{z}(t_0) = \mathbf{q}(t_0)$. To verify, we differentiate (6.150) for $t_0 = 0$, employ the above-given relations, and arrive at

$$\begin{aligned} \mathbf{P}'(t) &= \Phi'(t)e^{-\mathbf{F}t} - \Phi(t)e^{-\mathbf{F}t}\mathbf{F} = \mathbf{A}(t)\Phi(t)e^{-\mathbf{F}t} - \mathbf{P}(t)\mathbf{F} \\ &= \mathbf{A}(t)\mathbf{P}(t) - \mathbf{P}(t)\mathbf{F}. \end{aligned} \quad (6.153)$$

On the other hand, differentiating (6.151) yields

$$\mathbf{q}'(t) = \mathbf{P}'(t)\mathbf{z}(t) + \mathbf{P}(t)\mathbf{z}'(t)$$

and, by (6.145) and (6.151), we have

$$\begin{aligned}\mathbf{A}(t)\mathbf{q}(t) &= \mathbf{P}'(t)\mathbf{z}(t) + \mathbf{P}(t)\mathbf{z}'(t), \\ \mathbf{A}(t)\mathbf{P}(t)\mathbf{z}(t) &= \mathbf{P}'(t)\mathbf{z}(t) + \mathbf{P}(t)\mathbf{z}'(t)\end{aligned}$$

that gives

$$\mathbf{z}'(t) = \mathbf{P}^{-1}(t)[\mathbf{A}(t)\mathbf{P}(t) - \mathbf{P}'(t)]\mathbf{z}(t). \quad (6.154)$$

By (6.153), (6.154) becomes (6.152) and the verification is complete.

Characteristic Exponents and Multipliers

Substituting (6.149) to (6.148) and representing the state transition matrices via the fundamental solutions allow us now to derive the time-invariant matrix \mathbf{F} . First, by the transformations,

$$\begin{aligned}\Phi(t+T, t_0) &= \Phi(t, t_0)e^{\mathbf{F}T}, \\ e^{\mathbf{F}T} &= \Phi^{-1}(t, t_0)\Phi(t+T, t_0)\end{aligned}$$

we go to

$$e^{\mathbf{F}T} = \mathbf{Q}(t_0)\mathbf{Q}^{-1}(t)\mathbf{Q}(t+T)\mathbf{Q}^{-1}(t_0),$$

It can be shown that, in line with (6.148), the following relation holds true, $\mathbf{Q}(t+T) = \mathbf{Q}(t)e^{\mathbf{F}T}$, and we arrive at

$$\begin{aligned}e^{\mathbf{F}T} &= \mathbf{Q}(t_0)\mathbf{Q}^{-1}(t)\mathbf{Q}(t)e^{\mathbf{F}T}\mathbf{Q}^{-1}(t_0) \\ &= \mathbf{Q}(t_0+T)\mathbf{Q}^{-1}(t_0) \\ &= \Phi(t_0+T, t_0).\end{aligned} \quad (6.155)$$

The latter means that \mathbf{F} is defined via the state transition matrix,

$$\mathbf{F} = \frac{1}{T} \ln \Phi(t_0+T, t_0). \quad (6.156)$$

If (6.156) occurs to be complex, a real matrix can be obtained from

$$\mathbf{F} = \frac{1}{2T} \ln \Phi(t_0+2T, t_0), \quad (6.157)$$

because any T -periodic function is also $2T$ -periodic.

In the Floquet theory, the eigenvalues λ_k of \mathbf{F} are said to be the *Floquet exponents* or *characteristic exponents*. The real parts of λ_k are also the *Lyapunov exponents*. The eigenvalues η_k of $\Phi(t_0+T, t_0)$ are called the *characteristic multipliers*. Finally, the relation

$$\eta_k = e^{\lambda_k T} \quad (6.158)$$

establishes the correspondence between λ_k and η_k .

Stability of LPTV systems

Floquet's theory brings forward the following criteria for the linear periodic system to be stable:

- The system is exponentially stable if
 - all eigenvalues of \mathbf{F} have negative real parts, □
 - all eigenvalues of $\Phi(t_0 + T, t_0)$ have magnitudes less than unity. □
- A zero solution of the system is
 - asymptotically stable if all Lyapunov exponents are negative, □
 - Lyapunov stable if the Lyapunov exponents are nonpositive. □

Otherwise, the system is unstable.

Example 6.32. An LPTV system is represented in state space by the following homogenous equation

$$\begin{bmatrix} q_1' \\ q_2' \end{bmatrix} = \begin{bmatrix} 0 & \cos t \\ 0 & 0 \end{bmatrix} \begin{bmatrix} q_1 \\ q_2 \end{bmatrix} \quad (6.159)$$

with initial conditions $q_1(0)$ and $q_2(0)$ and period $T = 2\pi$.

Equivalently, the system is described with two equations: $q_1' = q_2 \cos t$ and $q_2' = 0$. The second equation leads to the obvious solution $q_2(t) = q_2(0)$. A solution of the first equation is provided by

$$\begin{aligned} q_1(t) &= \int_0^t q_2(\tau) \cos \tau \, d\tau + q_1(0) = q_2(0) \int_0^t \cos \tau \, d\tau + q_1(0) \\ &= q_2(0) \sin t + q_1(0). \end{aligned} \quad (6.160)$$

For the initial conditions $q_1(0) = 0$ and $q_2(0) = 1$, solutions become, respectively, $q_1(t) = \sin t$ and $q_2(t) = 1$. Setting $q_1(0) = 1$ and $q_2(0) = 1$, we have, respectively, $q_1(t) = 1 + \sin t$ and $q_2(t) = 1$.

The fundamental matrix and its inverse version can now be written as

$$\mathbf{Q}(t) = \begin{bmatrix} \sin t & 1 + \sin t \\ 1 & 1 \end{bmatrix}, \quad \mathbf{Q}^{-1}(t) = \begin{bmatrix} -1 & 1 + \sin t \\ 1 & -\sin t \end{bmatrix}, \quad (6.161)$$

producing the state transition matrix

$$\Phi(t, \tau) = \mathbf{Q}(t)\mathbf{Q}^{-1}(\tau) = \begin{bmatrix} 1 & \sin t - \sin \tau \\ 0 & 1 \end{bmatrix}. \quad (6.162)$$

In accordance with (6.156), to investigate stability of this system, one needs to describe the matrix $\Phi(T, 0)$. It can be shown that the matrix is identity,

$$\Phi(T, 0) = \begin{bmatrix} 1 & 0 \\ 0 & 1 \end{bmatrix}$$

having unit eigenvalues (characteristic multipliers) $\eta_1 = \eta_2 = 1$. By (6.158), both characteristic exponents are zero here, $\lambda_1 = \lambda_2 = 0$.

Following the definitions of stability, one infers that the system is not exponentially stable, because the real $\lambda_{1,2}$ are nonnegative and $\eta_{1,2}$ are not less than unity. A zero solution is also unstable for the same reasons. However, the system is Lyapunov stable, because both λ_1 and λ_2 are zero (non-positive).

One can arrive at the same conclusions by analyzing a solution (6.160). Indeed, at $t \rightarrow \infty$, the solution still oscillates and, thus, is unstable in the above senses. At $t = 0$, it is constant and, hence, Lyapunov stable. \square

On the whole, the main difficulties with applications of Floquet's theory are in determination of the fundamental matrix and state transition matrix. For complex systems, it may become a problem.

6.6.3 Frequency Transformation

One of the classical applications of LPTV systems can be found in the superheterodyne receiver, in which a spectral content of the modulated signal is removed without any change in the modulation law from the carrier frequency ω_c to some other frequency ω_i called the *intermediate frequency* (IF) (usually $\omega_i < \omega_c$ and ω_i is constant). This is what we call the *frequency transformation* because ω_c is transformed to ω_i .

A structure of the superheterodyne receiver is shown in Fig. 6.16. The

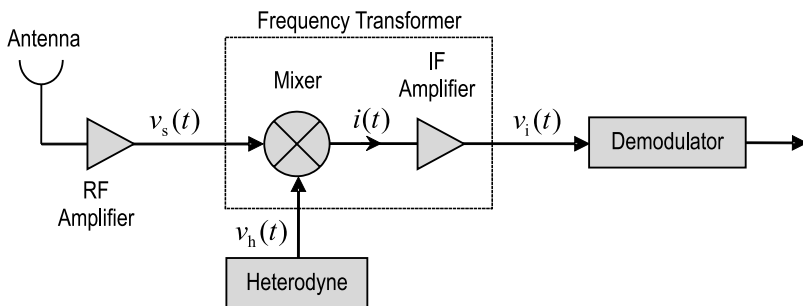


Fig. 6.16. Superheterodyne receiver.

basic idea is to multiply the RF signal $v_s(t)$ with the time-varying periodic voltage (coefficient) $v_h(t)$ generated by a local oscillator (heterodyne), enrich the spectrum of the electric current $i(t)$ as in (6.144), and then filter by the IF amplifier only the components at the intermediate frequency ω_i . The voltage $v_i(t)$ is then demodulated to produce the message signal at the output of the receiver.

Let us consider the operation principle of such an LPTV system in detail based on the electric scheme of the frequency transformer shown in Fig. 6.17a. The voltage $v_h(t)$ causes a periodic change of the transconductance slope

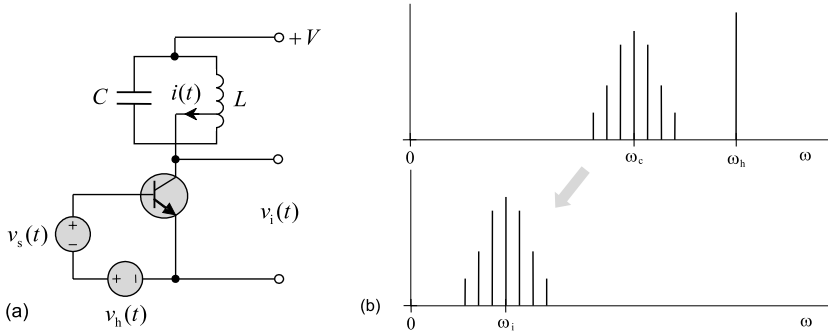


Fig. 6.17. Frequency transformer: (a) scheme and (b) frequency diagram.

$g_m(t)$ of a transistor. Because the characteristic of a transistor is nonlinear, the time-varying transconductance slope can be expanded to the harmonic Fourier series and we have

$$g_m(t) = g_{m0} + g_{m1} \cos \omega_h t + g_{m2} \cos 2\omega_h t + \dots \tag{6.163}$$

If the input voltage represents, for example, an AM signal

$$v_s(t) = V_s(1 + \mu \cos \Omega t) \cos \omega_c t, \tag{6.164}$$

where μ is the modulation factor, V_s is a constant amplitude, and Ω is an angular modulation frequency, the electric current $i(t)$ produced by the transistor can be written as

$$i(t) = g_m(t)v_s(t),$$

where $v_s(t)$ is the input, $i(t)$ is the output, and $g_m(t)$ plays the role of a time-varying coefficient. Substituting (6.163) and (6.164) leads to

$$\begin{aligned} i(t) &= V_s(1 + \mu \cos \Omega t) \cos \omega_c t \\ &\times [g_{m0} + g_{m1} \cos \omega_h t + g_{m2} \cos 2\omega_h t + \dots] \\ &= V_s(1 + \mu \cos \Omega t) \\ &\times \left[g_{m0} \cos \omega_c t + \frac{1}{2}g_{m1} \cos(\omega_h - \omega_c)t + \frac{1}{2}g_{m1} \cos(\omega_h + \omega_c)t \right. \\ &\left. + \frac{1}{2}g_{m2} \cos(2\omega_h - \omega_c)t + \frac{1}{2}g_{m2} \cos(2\omega_h + \omega_c)t + \dots \right]. \end{aligned} \tag{6.165}$$

If to choose the intermediate frequency to be $\omega_i = |\omega_h - \omega_c|$ and tune the IF amplifier to this frequency with a proper gain, then the output voltage can be obtained to be

$$v_i(t) = V_s(1 + \mu \cos \Omega t) \cos \omega_i t. \quad (6.166)$$

As can be inferred, the spectral content of the input signal (6.164) is merely removed in (6.166) to the intermediate frequency ω_i with the fully saved modulation law, as shown in Fig. 6.17b.

6.6.4 Parametric Modulation

Using mixers allows the creation of different kinds of *parametric modulators* exploited in communications: amplitude, phase, and frequency. The basic structure of a parametric modulator is given in Fig. 6.18.

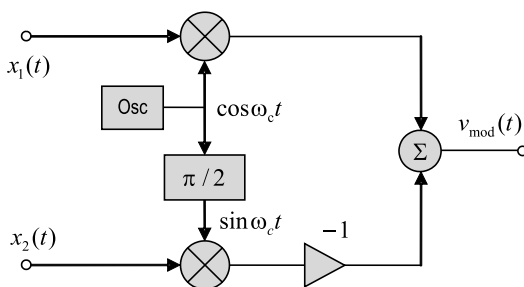


Fig. 6.18. Basic structure of a parametric modulator.

The LPTV system (Fig. 6.18) has two inputs, $x_1(t)$ and $x_2(t)$, bearing a message and one output $y(t) = v_{\text{mod}}(t)$. The functions $x_1(t)$ and $x_2(t)$ are multiplied in two mixers by periodically time-varying the coefficients, $\cos \omega_c t$ and $\sin \omega_c t$, shifted on $\pi/2$. The product of the second mixture is inverted with the coefficient -1 . Two products are then added to produce the modulated output

$$\begin{aligned} y(t) &= x_1(t) \cos \omega_c t - x_2(t) \sin \omega_c t \\ &= \sqrt{x_1^2(t) + x_2^2(t)} \cos[\omega_c t + \psi(t)], \end{aligned} \quad (6.167)$$

where $\tan \psi(t) = x_2(t)/x_1(t)$. In the matrix form, (6.167) represents a memoryless system with

$$y(t) = \mathbf{C}(t)\mathbf{x}(t), \quad (6.168)$$

where $\mathbf{C} = [\cos \omega_c t \quad -\sin \omega_c t]$ and $\mathbf{x}(t) = [x_1(t) \quad x_2(t)]^T$.

If $x_2(t) = 0$, the output becomes an AM signal $v_{AM}(t) = x_1(t) \cos \omega_c t$. This function can further be added to the carrier signal with a unit amplitude that yields the standard form of an AM signal $v_{AM}(t) = [1 + x_1(t)] \cos \omega_c t$. Otherwise, with $x_2(t) \neq 0$, the output is either FM or PM. A combined modulation such as AM-FM or AM-PM can also be provided by this structure.

6.6.5 Synchronous Detection

The principle of the frequency transformation utilized to the superheterodyne receiver is efficiently used in the *synchronous detection* of RF signals as an example of *parametric demodulation*. The scheme of a synchronous detector is shown in Fig. 6.19.

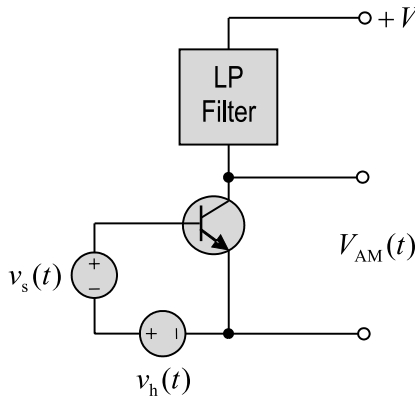


Fig. 6.19. Scheme of synchronous detection.

To grasp the essence of the synchronous detection, one may suppose an AM signal

$$v_s(t) = V_s(1 + \mu \cos \Omega t) \cos(\omega_c t + \vartheta_0) \quad (6.169)$$

and think that the heterodyne generates a signal $v_h(t)$ exactly of the carrier frequency, $\omega_h = \omega_c$. The time-varying transconductance slope (6.163) will therefore be periodically changed with the carrier frequency,

$$g_m(t) = g_{m0} + g_{m1} \cos \omega_c t + g_{m2} \cos 2\omega_c t + \dots \quad (6.170)$$

By virtue of (6.170), the electric (collector) current of the frequency transformer will vary as

$$i(t) = V_s(1 + \mu \cos \Omega t) \cos(\omega_c t + \vartheta_0)$$

$$\begin{aligned}
& \times [g_{m0} + g_{m1} \cos \omega_c t + g_{m2} \cos 2\omega_c t + \dots] \\
= & V_s(1 + \mu \cos \Omega t) \left[g_{m0} \cos(\omega_c t + \vartheta_0) + \frac{1}{2} g_{m1} \cos \vartheta_0 \right. \\
& \left. + \frac{1}{2} g_{m1} \cos(2\omega_c t + \vartheta_0) + \dots \right]. \tag{6.171}
\end{aligned}$$

It is not hard to observe that the spectral content of (6.171) includes low-frequency components representing the message signal. By an LP filter, the output of the detector becomes

$$V_{AM}(t) = \frac{1}{2} V_s g_{m1} (1 + \mu \cos \Omega t) \cos \vartheta_0. \tag{6.172}$$

As it follows, the synchronous detector is sensitive to the phase angle ϑ_0 between two signals. The best choice of course is $\vartheta_0 = 0$ and if $\vartheta_0 = \pi/2$ the output is merely absent. We notice that such a high dependence on ϑ_0 can play a positive role when it is exploited in meters to indicate the phase differences between two coherent signals.

More sophisticated structures of synchronous detection utilize the phase locked loop (PLL). In the basic structure (Fig. 6.20a), the PLL tracks the phase ϑ_0 of the input signal at the carrier frequency ω_c . The PLL output is

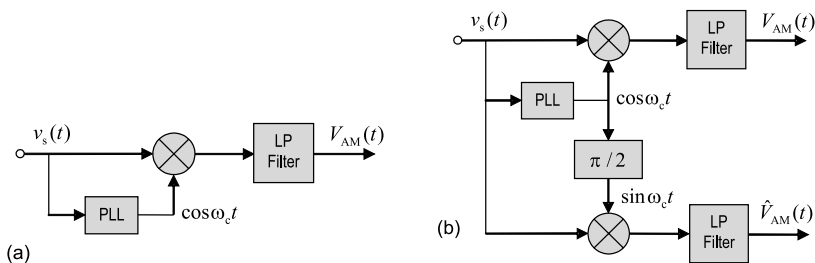


Fig. 6.20. Structures of synchronous detection: (a) basic and (b) with quadrature channels.

then formed as $v_{PLL} = \cos(\omega_c t + \vartheta_0)$ and a mixer produces

$$\begin{aligned}
v_m(t) &= V_s(1 + \mu \cos \Omega t) \cos(\omega_c t + \vartheta_0) \cos(\omega_c t + \vartheta_0) \\
&= \frac{1}{2} V_s(1 + \mu \cos \Omega t) + \frac{1}{2} V_s(1 + \mu \cos \Omega t) \cos(2\omega_c t + 2\vartheta_0). \tag{6.173}
\end{aligned}$$

If an LP filter has a gain factor of 2, the output becomes exactly equal to the message signal

$$V_{AM}(t) = V_s(1 + \mu \cos \Omega t). \tag{6.174}$$

The second structure shown in Fig. 6.20b is sophisticated with the quadrature channel, in which the PLL output is shifted in phase to $\pi/2$. In view of that, the output of an auxiliary mixer produces

$$\begin{aligned}\hat{v}_M(t) &= V_s(1 + \mu \cos \Omega t) \cos(\omega_c t + \vartheta_0) \sin(\omega_c t + \vartheta_0) \\ &= \frac{1}{2} V_s(1 + \mu \cos \Omega t) \sin(2\omega_c t + 2\vartheta_0).\end{aligned}\quad (6.175)$$

If the PLL tracks the carrier phase precisely and an LP filter is used with the gain factor of 2, the output of the quadrature channel is identically zero, $\hat{V}_{AM} = 0$. If it is not the case, this channel produces some amount of energy indicating errors in synchronous detection.

6.6.6 Linear Parametric Excitation

There is an important practical application of LPTV systems associated with parametric excitation. The effect occurs when the energy of a modulating signal is added, under the certain circumstances, to the signal energy.

Historical roots of parametric excitation are in the works of Faraday who noticed in 1831 that, in the crispations (ruffled surface waves) observed in a wine glass excited to “sing”, oscillations of one frequency may be excited by forces of double the frequency. Melde⁷, in 1859, generated parametric oscillations in a string by employing a tuning fork to periodically vary the tension at twice the resonance frequency of the string. Parametric oscillations in general were first treated by Rayleigh in 1883 and 1887.

Below, we first observe a physical occurrence of the effect in electronic resonant circuits. We then discuss a linear parametric oscillator and special features of parametric excitation in LPTV systems.

Excitation of Linear Resonant Circuits

Let us consider a closed series resonant circuit without a source of energy as shown in Fig. 6.21. Because R dissipates energy, the amplitude of oscillations in this circuit inherently attenuates with time starting at some initial value.

A situation changes if a capacitor C is modulated. To show that oscillations could be protected from attenuation, sustained, and even developed, we let the modulating function to be a rectangular pulse train. A capacitor thus changes its value abruptly from $C_0 - \Delta C$ to $C_0 + \Delta C$ around a mean value C_0 with an increment ΔC as shown in Fig. 6.22a.

To figure out a physical picture, we shall think that, by the modulating signal, the plates of a capacitor are merely moved together and apart, thereby increasing and reducing a capacitance, respectively. The voltage v_C induced on a capacitor is coupled with the electric charge Q by the relation $v_C = Q/C$, in

⁷ Franz Melde, German physicist, 11 March 1832-17 March 1901.

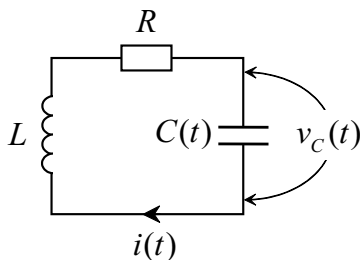


Fig. 6.21. Linear resonant circuit with a modulated capacitor.

which Q , as an energy bearer, cannot change instantly. In view of that, when we switch a capacitance, we also instantly change v_C .

The modulation process can now be organized as follows. Let us move the plates together at the moments, when $v_C(t)$ reaches extrema (minimum and maximum) and apart when it crosses zero. By such manipulations, the amplitude of v_C will jump, at extrema, as shown in Fig. 6.22b. With time, the amplitude will increase more and more and we watch for the effect termed the *parametric excitation* or *parametric pumping* of linear systems. It is also known as the *parametric resonance*.

It follows from the physical picture sketched that, to excite the circuit parametrically, the modulating signal must be synchronized in phase with the oscillating voltage and that the modulating frequency must be twice the oscillations frequency $f_0 = 1/2\pi\sqrt{LC_0}$.

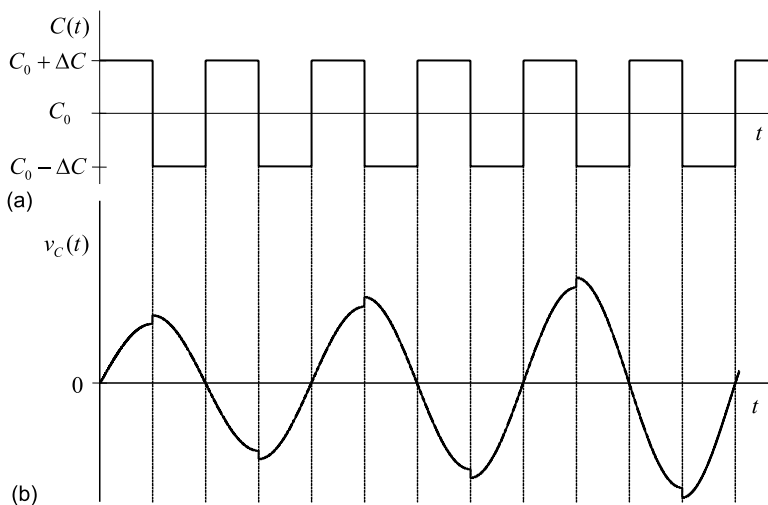


Fig. 6.22. Parametric excitation of a resonant circuit: (a) modulating signal and (b) voltage induced on a capacitor.

6.6.7 Linear Parametric Oscillator. Mathieu's Equation

It turns out that the effect of parametric excitation of the loop (Fig. 6.21) still occurs if to substitute the rectangular modulating train with the harmonic wave. This agrees with what we know as the *harmonic pumping*.

For the electric current $i(t)$, the ODE of the circuit is written as

$$L \frac{di}{dt} + Ri + \int \frac{idt}{C(t)} = 0. \quad (6.176)$$

If to substitute $i(t) = \frac{dQ(t)}{dt}$, (6.176) becomes

$$Q(t)'' + 2\delta Q(t)' + \frac{1}{LC(t)}Q(t) = 0, \quad (6.177)$$

where the system bandwidth $2\delta = \frac{R}{L}$ is typically much smaller than the angular frequency $\omega(t) = 1/\sqrt{LC(t)}$.

Let us now suppose that a capacitor is modulated harmonically,

$$C(t) = C_0(1 + \mu \cos \omega_p t), \quad (6.178)$$

around the mean value C_0 with some frequency ω_p and small modulation factor $\mu \ll 1$. The frequency of oscillations can then be found as

$$\omega_0^2(t) = \frac{1}{LC(t)} \approx \omega_0^2(1 - \mu \cos \omega_p t),$$

where $\omega_0 = \frac{1}{\sqrt{LC_0}}$ is the mean natural oscillation frequency. In view of that, the equation (6.177) becomes

$$q'' + 2\delta q' + \omega_0^2(1 - \mu \cos \omega_p t)q = 0 \quad (6.179)$$

and its solution bears all the properties of a system associated with oscillations and stability. It is seen that the ODE is linear and time-varying representing the so-called *linear oscillator*. In this "oscillator," the frequency is modulated, whereas the bandwidth becomes unaltered.

In state space, (6.179) is equivalently represented with $\mathbf{q}' = \mathbf{A}(t)\mathbf{q}$ or

$$\begin{bmatrix} q_1' \\ q_2' \end{bmatrix} = \begin{bmatrix} 0 & 1 \\ -\omega_0^2(1 - \mu \cos \omega_p t) & -2\delta \end{bmatrix} \begin{bmatrix} q_1 \\ q_2 \end{bmatrix} \quad (6.180)$$

and we can alternatively write, assigning $y = q_1$ and $z = q_2$,

$$\begin{aligned} y' &= z = P(y, z), \\ z' &= -\omega_0^2(1 - \mu \cos \omega_p t)y - 2\delta z = Q(y, z). \end{aligned}$$

The nonzero value $P'_y + Q'_z = -2\delta \neq 0$ means that, by Bendixson's criterion (3.16), the system has no periodic orbit inside the finite bounds. So, the oscillations can either develop or attenuate.

Example 6.33. Consider an LPTV system (6.180) with $\omega_0 = 10$ rad/s, $\omega_p = 2\omega_0$, and the quality factor of 2.5. Three typical behaviors of the system, by $y(0) = 0$ and $z(0) = 1$, are sketched in Fig. 6.23 for the attenuating ($\mu < \mu_{cr}$), near stationary ($\mu = \mu_{cr}$), and developing ($\mu > \mu_{cr}$) oscillations. The critical value of the modulating factor was found numerically to be $\mu_{cr} \cong 0.8845$. The modulating function is represented by $v(t) = \mu \cos \omega_p t$.

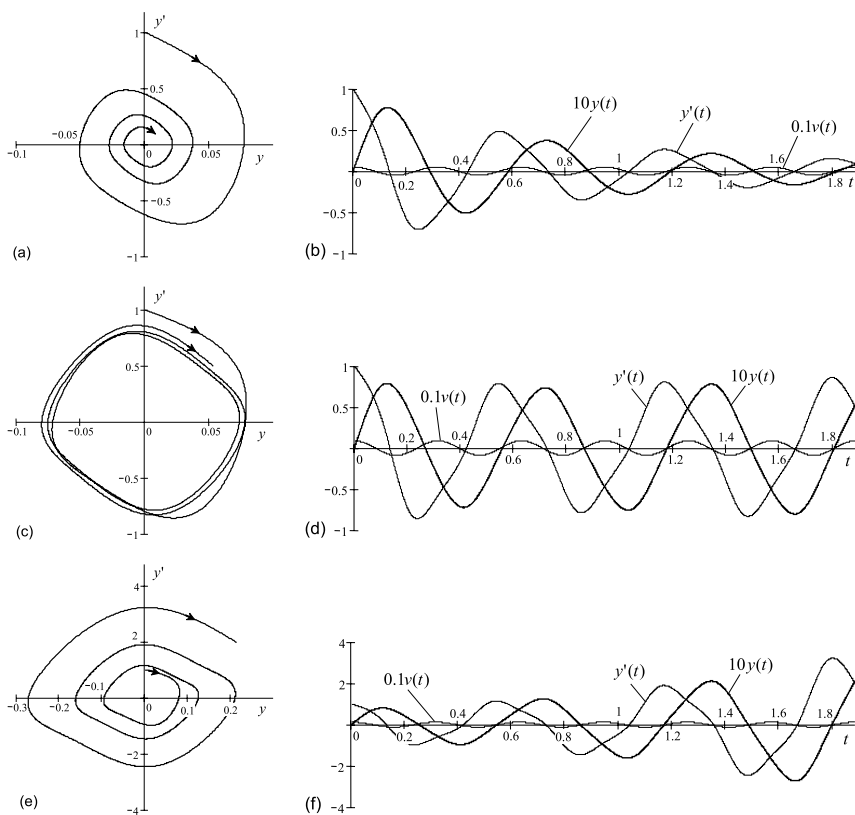


Fig. 6.23. Oscillations in an LPTV system (6.180): (a) and (b) attenuation with $\mu = 0.5$, (c) and (d) near steady state with $\mu = 8845$, and (e) and (f) development with $\mu = 1.2$.

It is seen that oscillations and their time derivatives are not purely harmonic. A solution of (6.180) is thus represented with the Fourier series composed of harmonics of the fundamental frequency ω_0 . \square

Mathieu's Equation

If to neglect the dissipation (second) term, $2\delta = 0$, and introduce a new variable $\zeta = \omega_p t/2$, then (6.179) can be generalized in the form of

$$\frac{d^2 q}{d\zeta^2} + (a - 2b \cos 2\zeta)q = 0, \quad (6.181)$$

where $a = 4\frac{\omega_0^2}{\omega_p^2}$ and $b = 2\mu\frac{\omega_0^2}{\omega_p^2}$. This equation is known as the Mathieu⁸ equation being a special case of Hill's⁹ equation. In state space, (6.181) reads

$$\begin{bmatrix} q_1' \\ q_2' \end{bmatrix} = \begin{bmatrix} 0 & 1 \\ -a + 2b \cos 2\zeta & 0 \end{bmatrix} \begin{bmatrix} q_1 \\ q_2 \end{bmatrix}. \quad (6.182)$$

Because the matrix $\mathbf{A}(t)$ in (6.182) is periodic, we can apply the Floquet's theory and investigate this system for stability. In accordance with Floquet, (6.182) has solutions, which for a proper value of the characteristic exponent λ , satisfy the equation

$$q(\zeta + \pi) = e^{2\pi\lambda} q(\zeta).$$

Stability of a solution is entirely defined by λ . The solution is periodic if $e^{2\pi\lambda} = 1$ and it is semiperiodic when $e^{2\pi\lambda} = -1$. By that reason, the relevant real value of λ is called the *periodic eigenvalue* or *semiperiodic eigenvalue*.

On the other hand, here we have

$$q_1' = y' = z = P(y, z),$$

$$q_2' = z' = -\omega_0^2(1 - \mu \cos \omega_p t)y = Q(y, z),$$

producing $P_y' + Q_z' = 0$. By the Bendixson's criterion (3.16), the Mathieu oscillator has thus a periodic orbit inside the finite bounds and that is independently on the modulation term.

The theory of Mathieu's equation (6.181) is well developed via the special Mathieu functions $C(a, b, \varsigma)$ and $S(a, b, \varsigma)$ representing the even and odd solutions, respectively. The functions can be found in special books, however, their rigorous forms have not enough engineering features. Moreover, neglected the dissipation term 2δ , the solution does not fully fit practical needs in electronic systems, especially when the quality factor is low. We notice that some special features of this solution can be studied by the method of harmonic balance that we discuss below.

⁸ Emile Lonard Mathieu, French mathematician, 15 May 1835-19 October 1890.

⁹ George William Hill, American mathematician, 3 March 1838-16 April 1914.

Solution by the Method of Harmonic Balance

Consider an equation (6.179) under the condition that $2\delta \ll \omega_0$. In the view of a high quality factor, $\omega_0/2\delta \gg 1$, the amplitude of the oscillating solution cannot change substantially during the period of oscillations. Moreover, by Floquet's theorem, it is periodic. Therefore, in the first-order approximation, we can discard all high harmonics and think that a solution is harmonic.

Now recall that the pumping frequency ω_p must be twice ω_0 . However, ω_p is variable, so that one may suppose that $\omega_p = 2\omega_0 + \Delta$, where Δ represents a small frequency offset. If so, then the system frequency is $\omega = \omega_0 + \frac{\Delta}{2}$.

Under such assumptions, a solution of (6.179) can approximately be found in the harmonic form of

$$q(t) = A \cos \omega t + B \sin \omega t, \quad (6.183)$$

where the amplitudes $A(t)$ and $B(t)$ are time-varying functions. After taking the first and second time derivatives of (6.183), we write

$$q'(t) = A' \cos \omega t - A\omega \sin \omega t + B' \sin \omega t + B\omega \cos \omega t, \quad (6.184)$$

$$\begin{aligned} q''(t) = & A'' \cos \omega t - 2A'\omega \sin \omega t - A\omega^2 \cos \omega t + B'' \sin \omega t \\ & + 2B'\omega \cos \omega t - B\omega^2 \sin \omega t. \end{aligned} \quad (6.185)$$

Substituting (6.183)–(6.185) to (6.179), equating the amplitudes of $\cos \omega t$ and $\sin \omega t$, and neglecting the small values, $A'' \sim 2\delta A' \ll \omega_0^2 A$ and $B'' \sim 2\delta B' \ll \omega_0^2 B$, leads to the differential equations

$$A' + \delta A = -\frac{1}{2} \left(\Delta - \frac{\mu\omega_0}{2} \right), \quad (6.186)$$

$$B' + \delta B = \frac{1}{2} \left(\Delta + \frac{\mu\omega_0}{2} \right). \quad (6.187)$$

Solutions of (6.186) and (6.187) are given by $A = \alpha e^{\lambda t}$ and $B = \beta e^{\lambda t}$ that leads to the algebraic equations

$$\begin{aligned} (\lambda + \delta)\alpha + \frac{1}{2} \left(\Delta - \frac{\mu\omega_0}{2} \right) \beta &= 0, \\ \frac{1}{2} \left(\Delta + \frac{\mu\omega_0}{2} \right) \alpha - (\lambda + \delta)\beta &= 0. \end{aligned} \quad (6.188)$$

A nontrivial (not zero) solution of (6.188) is provided by zero determinant that gives two eigenvalues

$$\lambda_{1,2} = -\delta \pm \frac{1}{2} \sqrt{\left(\frac{\mu\omega_0}{2} \right)^2 - \Delta^2}.$$

Excitation is possible solely by positive λ , so that, further on, we will be interested in the value

$$\lambda = -\delta + \frac{1}{2}\sqrt{\left(\frac{\mu\omega_0}{2}\right)^2 - \Delta^2} \quad (6.189)$$

that, by exact tuning, $\Delta = 0$, becomes $\lambda = -\delta + \frac{\mu\omega_0}{4}$.

Of interest is an unstable region outlined by values of the modulation factor μ for which the offset Δ yields positive eigenvalues. If we solve (6.189) for $\mu(\Delta)$ and plot it, the picture for different quality factors Q will look like in Fig. 6.24.

An analysis shows that a system with large Q is highly addicted to excitation even by insignificant (noise) levels of μ . On the other hand, lowering Q results in increase in the excitation threshold that reaches $\mu = 0.5$ with $Q = 4$.

In the above analysis, we were concerned only with the first zone of a possible parametric excitation around the resonant frequency ω_0 . In a like manner, other excitation regions associated with harmonics of ω_0 can be outlined, although with the increased transformation burden and difficulties.

To increase the accuracy in determining the excitation regions, the series (6.183) must involve high harmonics. If to provide the necessary transformations and find the regions, the picture will no longer be symmetric as in Fig. 6.24. It will be as shown in Fig. 6.25 for several neighboring regions sketched in terms of the Mathieu equation (6.181).

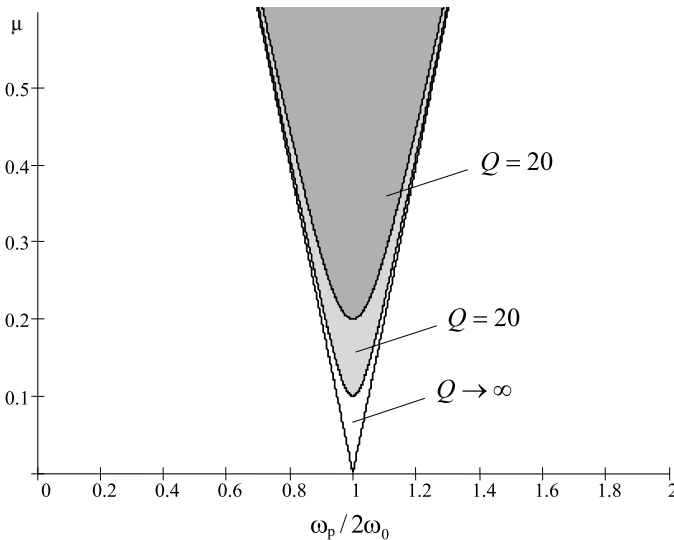


Fig. 6.24. Excitation regions (shadowed) for a linear oscillator (6.179), by different quality factors Q .

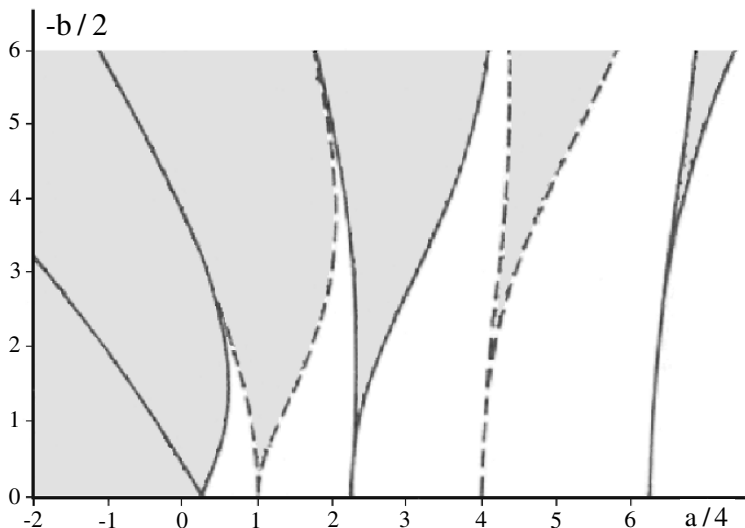


Fig. 6.25. Excitation regions corresponding to Mathieu's equation: dash bounded are for period T and sold bounded for $2T$.

Frequency Dividers

An alternative application of parametrical excitation can be found in frequency dividers having the division factor of 2, 4, \dots . The relevant LPTV system is organized so that the input plays the role of the pumping signal with the frequency ω_p . In turn, oscillations taken from the resonant circuit at the frequency $\omega_p/2$, $\omega_p/4$, \dots go to the output. Properly obtained the modulation factor μ , the structure is able to generate the output with almost the constant amplitude and frequency divided. An example of such a signal is given in Fig. 6.23c and Fig. 6.23d. Note that a BP filter must be included in cascade to pass through only the component with the divided frequency.

6.6.8 Parametric Amplification

The other benefit of “pumping” is in its ability to obtain *parametric amplification*. The relevant LPTV system is designed without active components (transistors) and thus has a very low-noise level. That makes “pumping” challenging to amplify small signals in wireless channels, by using the energy from the pumping action. Parametric amplifiers with a variable-capacitance main-oscillator semiconductor diode are used in radar tracking and communications Earth stations, Earth satellite stations, and deep-space stations.

The principle of parametric amplification is illustrated by the electrical circuit shown in Fig. 6.26a. Here, the input signal $v_{in}(t)$ with the frequency ω drives the circuit with the resonance frequency ω_0 . A capacitor $C(t)$ is

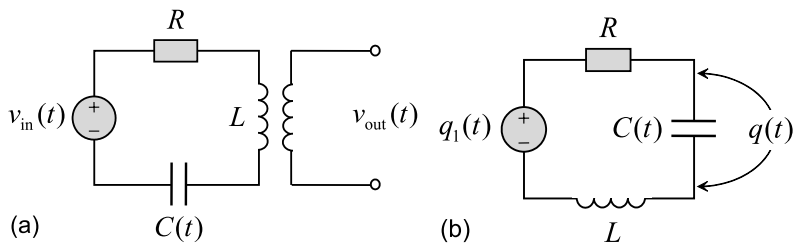


Fig. 6.26. Parametric amplifier circuits: (a) electrical and (b) equivalent.

modulated with the pumping frequency $\omega_p = 2\omega_0$ and the output voltage is typically taken from the inductor L .

To come up with the idea of parametric amplification, let us observe again a passive circuit shown in Fig. 6.21 and modify it for the driving charge $Q_1(t) = Q_M e^{j\omega t}$, where Q_M is a peak charge value, as shown in Fig. 6.26b. We thus write an equation

$$Q(t)'' + 2\delta Q(t)' + \omega_0^2(1 - \mu \cos \omega_p t)Q(t) = q_M e^{j\omega t}. \quad (6.190)$$

To find a solution of (6.190) by the familiar method of harmonica balance, one first needs to observe its possible spectral components, once there are three frequencies. The principle point is that an interaction of the modulating signal with $\omega_p = 2\omega_0$ and the system signal with ω produces a spectral component with the frequency $\omega_i = \omega_p - \omega = 2\omega_0 - \omega$ called the *idle* frequency. In the sequel, it will become obvious that namely ω_i plays a role of a positive feedback increasing the amplitude of oscillations.

In the first order approximation, since ω is not obligatorily equal to ω_0 , we can find a steady-state solution of (6.190) as composed of two harmonic waves,

$$Q(t) = Ae^{j\omega t} + Be^{j\omega_i t}, \quad (6.191)$$

where A and B are constants. The first and second time derivatives of (6.191) are provided by

$$Q'(t) = j\omega Ae^{j\omega t} + j\omega_i Be^{j\omega_i t}, \quad (6.192)$$

$$Q''(t) = -\omega^2 Ae^{j\omega t} - \omega_i^2 Be^{j\omega_i t}. \quad (6.193)$$

By representing $\cos \omega_p t$ with Euler's formula, accounting for (6.191)–(6.193), neglecting harmonics and sums of all frequencies, and taking into account that $\omega - \omega_p = \omega_i$ and $\omega_i - \omega_p = \omega$, we transform (6.190) to

$$\begin{aligned} -\omega^2 Ae^{j\omega t} - \omega_i^2 Be^{j\omega_i t} + 2j\delta\omega Ae^{j\omega t} + 2j\delta\omega_i Be^{j\omega_i t} + \omega_0^2 Ae^{j\omega t} + \omega_0^2 Be^{j\omega_i t} \\ - \frac{\mu}{2}\omega_0^2 Ae^{j\omega_i t} - \frac{\mu}{2}\omega_0^2 Be^{j\omega t} = q_M e^{j\omega t}. \end{aligned}$$

If we further equate to zero the amplitudes of the relevant exponential functions and substitute $\omega_0^2 - \omega^2 \cong 2\omega_0\Omega$, where $\Omega = \omega_0 - \omega$, we arrive at the algebraic equations

$$\begin{aligned} A(\Omega + j\delta) + \frac{\mu\omega_0}{4}B &= \frac{q_M}{2\omega_0}, \\ B(\Omega + j\delta) + \frac{\mu\omega_0}{4}A &= 0, \end{aligned}$$

whose solutions are

$$A = \frac{q_M}{2\omega_0} \frac{\Omega + j\delta}{(\Omega + j\delta)^2 + (\mu\omega_0/4)^2}, \quad (6.194)$$

$$B = \frac{q_M m}{8} \frac{1}{(\Omega + j\delta)^2 + (\mu\omega_0/4)^2}. \quad (6.195)$$

The amplifier complex gain at Ω can now be defined by the ratio

$$\begin{aligned} G(\Omega) &= \frac{A(\Omega)}{A(0)} = \frac{(\Omega + j\delta)^2}{(\Omega + j\delta)^2 + (\mu\omega_0/4)^2} \\ &= \frac{1}{1 + \left[\frac{\mu\omega_0}{4(\Omega + j\delta)} \right]^2} \end{aligned} \quad (6.196)$$

exhibiting a maximum at $\Omega = 0$,

$$G_{\max} = \frac{1}{1 - \left(\frac{\mu Q}{2} \right)^2}, \quad (6.197)$$

where $Q = \omega_0/2\delta$ is the system quality factor. A simple observation shows that the modulation factor μ must be less than $2/Q$. Otherwise, by $m = 2/Q$, the system becomes unstable, since G_{\max} goes toward infinity. If to take the latter into account and assign normalized the detuning $\nu = \Omega/\delta$ and modulation factor $\alpha = \mu Q/2$, the complex gain (6.196) can be generalized to be

$$G(\nu, \alpha) = \frac{(\nu + j)^2}{(\nu + j)^2 + \alpha^2}. \quad (6.198)$$

Fig. 6.27 sketches the total gain $|G(\nu, \alpha)|$ in a wide range of detunings, $-0.5 \leq \nu \leq 0.5$, for the allowed factor $0 < \alpha < 1$. Observing Fig. 6.27, one infers that the input signal is gained by the factor of more than 10 if $0.95 \leq \alpha < 1$ and $|\nu| \leq 0.02$.

The most general conclusion following behind our examination of LTV systems is that such systems are able to produce effects featured to both LTI and NTI systems. In fact, although an LTV system is still linear, it produces harmonics of the input in the output that is a fundamental feature of nonlinear systems. Therefore, LTV systems have a wide range of applications in electronics.

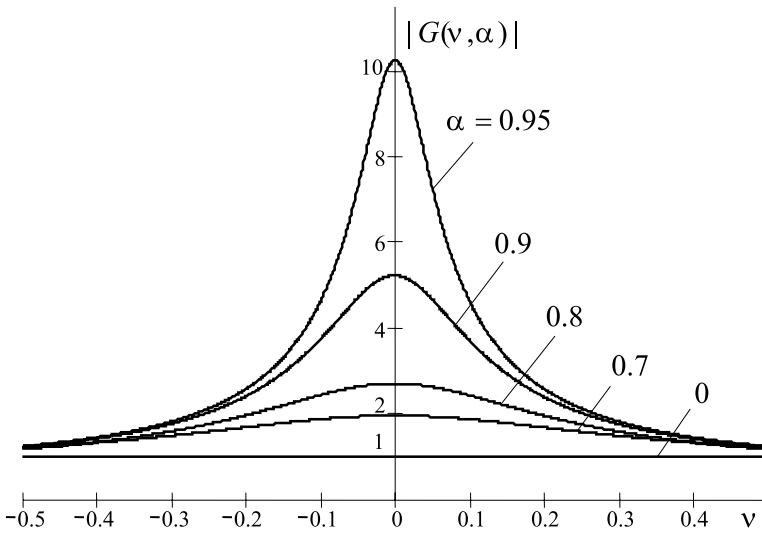


Fig. 6.27. Total gain $|G(\nu, \alpha)|$ of a parametric amplifier.

6.7 Summary

All major properties of LTV systems are entirely coupled with time-variations in their parameters. The theory of such system has the following basic foundations:

- A linear system that provides transformations with a time-varying operator is the LTV system.
- The response of a system at time t to the unit impulse at time θ is the LTV system time-varying impulse response $h(t, \theta)$.
- The response of a system at time t to the unit impulse at time $t - \tau$ is the LTV system modified time-varying impulse response $\bar{h}(\tau, t)$.
- The frequency response of an LTV system is coupled by the Fourier transform with $\bar{h}(\tau, t)$ and it is not the Fourier transform of $h(t, \theta)$.
- An LTV system demonstrates the properties of linearity (distributivity and homogeneity) and associativity. Its operator commonly is non-commuting.
- The time-varying impulse and step responses are commonly not convertible by differentiation and integration.
- The first direct form of block diagrams of LTV systems involves time derivatives of the input.
- The second direct form of block diagrams of LTV systems appears in a particular case of $M = 0$ and constant b_0 .

- A solution of the time-varying state space equations is provided via the fundamental matrix and state transition matrix.
- A solution of the LPTV system can be represented in the frequency domain by the Fourier series.
- The Floquet's theory is universal for LPTV systems represented in state space.
- Stability of LPTV systems in state space is evaluated via the Floquet's exponents and characteristic multipliers.
- Frequency transformation, parametric modulation, and synchronous detection exploit an ability of LPTV systems to remove frequency spectra from one region to another.
- Parametric excitation and amplification is provided by LPTV systems when the energy of a modulated parameter is added with the signal energy.

6.8 Problems

6.1. Observe different electronic systems (communications, radars, positioning, control, etc.) given in Chapter 1. Find subblocks in these systems that seem to be time-varying.

6.2. Based on the ODE $y' + a(t)y = b(t)x$, find simple words to explain the difference between LTI and LTV systems. Provide explanations in the time and frequency domains.

6.3 (Time-varying impulse response). Give a simple graphical illustration for the time-varying impulse response $h(t, \theta)$ and its modified version $\bar{h}(\tau, t)$. Explain how to transfer from $h(t, \theta)$ to $\bar{h}(\tau, t)$ and from $\bar{h}(\tau, t)$ to $h(t, \theta)$.

6.4. An LTV system is represented with the time-varying impulse response

1. $h(t, \theta) = \frac{\theta+1}{t+1} e^{-(t-\theta)} u(t-\theta)$
2. $h(t, \theta) = \delta(t-\theta-\theta_0)$
3. $h(t, \theta) = \delta(t-\theta) e^{j\omega_0 t}$
4. $h(t, \theta) = (1 + \alpha \cos \Omega\theta) e^{-(t-\theta)} e^{-\frac{\alpha}{\Omega}(\sin \Omega t - \sin \Omega\theta)} u(t-\theta)$

Involving the necessary constraint, show the plot of the response. By changing variables, translate the response to the modified form $\bar{h}(\tau, t)$. Sketch the plot of the modified response.

6.5. An LTV system is represented with the modified time-varying impulse response

1. $\bar{h}(\tau, t) = \sqrt{|a_0|} \delta[b_0 - a_0\tau - (1 - a_0)t]$

2. $\bar{h}(\tau, t) = \delta(\tau - \tau_0)e^{j\omega_0 t}$
3. $\bar{h}(\tau, t) = e^{-\tau} e^{-\frac{\alpha}{\Omega} \sin \Omega t} u(\tau)$
4. $\bar{h}(\tau, t) = e^{-a(\cos \Omega \tau - \sin \Omega t)} e^{-b(t-\tau)} \cos \Omega \tau u(\tau)$

Involving the necessary constraint, show the plot of the response. By changing variables, translate the response to $h(t, \theta)$. Sketch the plot of $h(t, \theta)$.

6.6 (Frequency response). An LTV system is given with the following differential equation. Assuming the input to be $x = e^{j\omega t}$ and the output to be $y(t) = H(j\omega, t)e^{j\omega t}$, define the time-varying frequency response of a system.

1. $y' + 2ty = 2tx$
2. $y' + y = 2tx'$
3. $y' + 2ty = te^{-j\omega t}x$
4. $y' + 2ty = t^2e^{-j\omega t}x'$

6.7. Define the bi-frequency response of an LTV system given in Problem 6.6. Investigate this response numerically. Make a conclusion about the bandwidth of a time-varying system.

6.8. Define the frequency responses $H(j\omega, t)$, $H(\theta, j\Omega)$, and $H(j\omega, j\Omega)$ of an LTV system represented with the impulse response (Problem 6.4). Investigate these responses numerically.

6.9. Solve Problem 6.8 for the frequency responses $\bar{H}(j\omega, t)$, $\bar{H}(\theta, j\Omega)$, and $\bar{H}(j\omega, j\Omega)$ via the modified impulse response (Problem 6.5).

6.10 (BIBO stability). Ascertain BIBO stability of an LTV system via the impulse response given in Problems 6.4 and 6.5.

6.11. Realize, whether LTV systems described with the impulse responses (6.11) and (6.13) are BIBO stable or not.

6.12 (Differential equations presentation). Given three systems described with the ODE (6.57). In the first system, one of the coefficients is sensitive to the ambient temperature. In the second one, several coefficients are stabilized in the control loop. The third system is designed with the precision components. Which system can be modeled as LTV and which as LTI?

6.13. An LTV system is represented with the ODE (Problem 6.6). Define the system time-varying impulse and step responses.

6.14 (Application to electrical circuits). Given an electrical circuit of the first order with a time-varying component (Fig. 6.28). Write the ODE of this circuit: 1) for the electric charge or magnetic flux and 2) for the voltage induced on a component indicated. Define the impulse response, step response, and frequency response of this circuit with respect to the voltage.

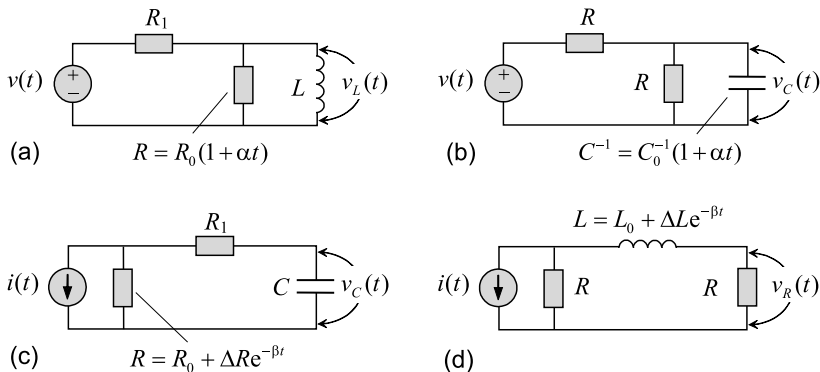


Fig. 6.28. Electric circuits with time-varying components.

6.15. An LTV system of the second order is represented by the electric circuit (Fig. 6.29). Write the ODE of the system, assuming that the variable component is: 1) R , 2) C , 3) L , 4) R and L , 5) L and C , 6) R and C , 7) R , C , and L .

6.16. Describe the circuit shown in Fig. 6.29 with the ODE:

1. Fig. 6.29a: For the electric charge $Q(t)$ on a capacitor $C(t)$ with R and L constant.
2. Fig. 6.29b: For the magnetic flux $\Phi(t)$ on an inductor $L(t)$ with R and C constant.
3. Fig. 6.29c: For the electric charge $Q(t)$ on a capacitor $C(t)$ with R and L constant.
4. Fig. 6.29d: For the magnetic flux $\Phi(t)$ on an inductor $L(t)$ with R and C constant.

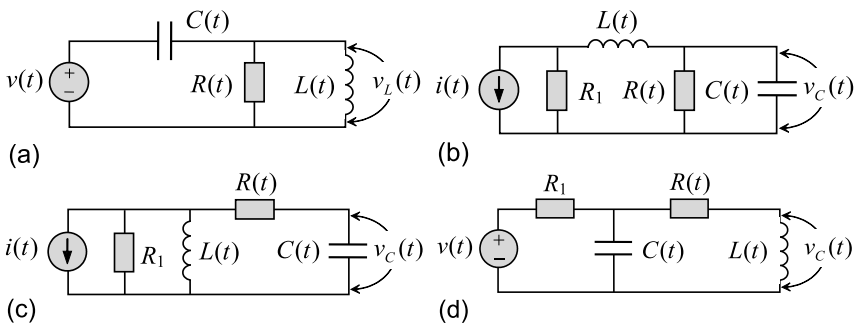


Fig. 6.29. Electric circuits with time-varying components.

6.17 (Block diagrams). Represent an LTV system given in Problem 6.6 with the block diagrams of the first and second direct forms. For the second direct form, represent the right-hand side of the ODE as b_0x , where b_0 is constant.

6.18. An LTV system is given with the ODE

1. $ay'' + b(t)y' + cy = dx'' - e(t)x'$
2. $\int y dt - 4y' + 2ty = -x$
3. $2y''' - 3\cos(t)y = 2x'' - \sin(t)x$
4. $y'' + \int y dt - 2ty' = \sum_{m=0}^1 b_m \frac{d^m x}{dt^m}$, $b_0 = 2\cos t$, $b_1 = 1$
5. $x = \int y' dt + ty'$
6. $2\frac{d^2x}{dt^2} + 4tx + e^{-2t}y = 2\frac{d^3y}{dt^3} + 4\frac{dx}{dt}$
7. $4(y'' - tx) = 3(e^{-t}y' - x'')$
8. $e^{-4t}x' + \int x dt - 2ty' = \int y dt - 2y''$
9. $a_2y'' - b_0(t)x - a_1(t)y' - b_1x' = 0$
10. $2ty + \int x dt - 2e^{-3t}y' = \int \int y dt dt$
11. $3ty'' + 2 \int y dt = 2t^2x$
12. $\sum_{n=0}^1 a_n \frac{d^n y}{dt^n} = 3e^t x + \int x dt - 2y'$, $a_0 = 2e^{2t}$, $a_1 = \cos t$
13. $\sum_{n=0}^1 a_n \frac{d^n y}{dt^n} + 2 \int x dt = \sum_{m=0}^1 b_m \frac{d^m x}{dt^m} + 2e^t y + \int y dt$,
 $a_0 = 2$, $a_1 = 1$, $b_0 = 2$, $b_1 = 1$
14. $3y''' + \sum_{m=1}^2 b_m \frac{d^m x}{dt^m} - 4y' + (1 + t^2)y = 2x$, $b_2 = 2\cos t$, $b_1 = 1$
15. $tx + \int x dt - 2y' = \sum_{m=0}^1 b_m \frac{d^m x}{dt^m}$, $b_0 = 2$, $b_1 = \sin t$
16. $2\frac{d^2y}{dt^2} + tx + 2e^t y = 2\frac{d^3y}{dt^3} + 4\frac{dx}{dt}$

Represent the system in the first and second direct forms of block diagrams. If a system cannot be represented in the second direct form, substitute the right-hand side of the ODE transformed to (6.79) with b_0x , where b_0 is constant.

6.19 (State space presentation). Represent an LTV system given in Problem 6.18 in state space.

6.20. Verify that the following fundamental and state transition matrices, respectively,

$$\mathbf{Q}(t) = e^{-t} \begin{bmatrix} 1 & 0 \\ t^2 & 1 \end{bmatrix} \quad \text{and} \quad \mathbf{\Phi}(t, \theta) = e^{-(t-\theta)} \begin{bmatrix} 1 & 0 \\ \frac{t^2 - \theta^2}{2} & 1 \end{bmatrix},$$

correspond to the system matrix $\mathbf{A}(t) = \begin{bmatrix} -1 & 0 \\ t & -1 \end{bmatrix}$.

6.21. An LTV system is represented in state space with the following system matrix. Define the fundamental matrix and state transition matrix of the system.

$$\begin{aligned} 1. \mathbf{A}(t) &= \begin{bmatrix} -1 & t \\ 0 & 0 \end{bmatrix} \\ 2. \mathbf{A}(t) &= \begin{bmatrix} -1 & 0 \\ t^2 & -1 \end{bmatrix} \\ 3. \mathbf{A}(t) &= \begin{bmatrix} -1 & t \\ 0 & -1 \end{bmatrix} \\ 4. \mathbf{A}(t) &= \begin{bmatrix} -1 & t^3 \\ 0 & 0 \end{bmatrix} \end{aligned}$$

By using the property (6.116), verify that the state transition matrix derived is correct.

6.22. Ascertain BIBO stability of an LTV system represented with the state transition matrix derived in Problem 6.21.

6.23. Evaluate controllability and observability of an LTV system given in Problem 6.6.

6.24 (Linear periodically time-varying systems). An LPTV system is represented with the following system matrix. Define the state transition matrix of the system.

$$\begin{aligned} 1. \mathbf{A}(t) &= \begin{bmatrix} -1 \cos t \\ 0 & 0 \end{bmatrix} \\ 2. \mathbf{A}(t) &= \begin{bmatrix} -1 & 0 \\ \sin t & -1 \end{bmatrix} \\ 3. \mathbf{A}(t) &= \begin{bmatrix} -1 \cos t \\ 0 & -1 \end{bmatrix} \\ 4. \mathbf{A}(t) &= \begin{bmatrix} -1 \sin t \\ 0 & 0 \end{bmatrix} \end{aligned}$$

6.25. By the Floquet's theory, determine the Floquet's exponents and characteristic multipliers for the LTV system described with the matrices given in Problem 6.24. Ascertain stability of the system.

6.26 (Parametric systems). Analyze the operation principle of the heterodyne receiver. The frequency ω_c of a received signal may be transformed to the intermediate frequency ω_i in two ways: $\omega_i = \omega_c - \omega_h$ and $\omega_i = \omega_h - \omega_c$. Which way is more preferable and why?

6.27. Parametric modulation implies using the quadrature signals, $\cos \omega_c$ and $\sin \omega_c$ (Fig. 6.18). Give mathematical and graphical explanations for the modulation error if the second signal is not exactly shifted on $\pi/2$ and is $\sin(\omega_c t + \phi)$.

6.28. Provide a similar error analysis (as in Problem 6.27) for the synchronous detection (Fig. 6.20b).

6.29. Assume that a source of energy is absent in Fig. 6.29; that is the source of voltage is closed and the source of current is switched-off. A capacitor is modulated as $C^{-1}(t) = C_0^{-1}(1 - \alpha \cos \Omega t)$ and all other components are constant. Write the ODE of this system and transfer to the form (6.179). Similarly to Fig. 6.23, investigate behavior and stability of this system numerically.

6.30. Consider a system shown in Fig. 6.29. Write the ODE for the modulated capacitance $C^{-1}(t) = C_0^{-1}(1 - \alpha \cos \omega_p t)$ and all other components constant. Find a solution of the ODE by the method of harmonic balance. Define the conditions for parametric excitation in the system.

Nonlinear Time Invariant Systems

7.1 Introduction

Not all electronic problems can be solved by linear systems. Many capabilities possess the nonlinear ones, which output and input are coupled nonlinearly. Even if the problem is soluble with an LTV system, the nonlinear device does it usually with a simpler structure; in some cases just with several units.

If a nonlinearity does not undergo any changes with time, the system is *nonlinear time-invariant* (NTI). In control systems, nonlinearity is typically required of the certain shape and can even be synthesized. To design quadratic and logarithmic amplifiers, semiconductor components are used providing the necessary characteristics. In many cases, piecewise nonlinearities meet practical needs. Let us add that, in all electronic systems, natural spurious nonlinearities occur owing to saturation.

In SISO NTI systems, the input $y(t)$ and output $x(t)$ are coupled by the nonlinear time-invariant operator $\mathcal{O}(x)$,

$$y(t) = \mathcal{O}(x)x(t) \equiv \mathcal{O}[x(t)]x(t), \quad (7.1)$$

that can be represented by the nonlinear ODE, integro-differential equation, or integral equation. To study dynamics and stability, the qualitative methods are used universally. Rigorous analytical solutions of nonlinear problems are usually available only in particular cases. On the other hand, in the overwhelming majority of practical situations, of importance are solutions for harmonics of the input. In view of that, different variations of the methods of averaging and linearization are used rendering a tremendous influence on the engineering theory of nonlinear systems.

Our discussion of linear systems was started with the convolution and differential equation, so with memory (dynamic) solutions. This is because the memoryless linear system is nothing more than a time-invariant or time-varying gain. In memoryless nonlinear systems, the gain depends on the signal, therefore such systems need special investigations. If a nonlinear system is

memory, the gain inherently changes with time taking different values for the same signal.

Fig. 7.1 sketches a typical picture explaining how memory affects the output of an NTI system. Suppose that the input-to-output dependence $y[x(t)]$

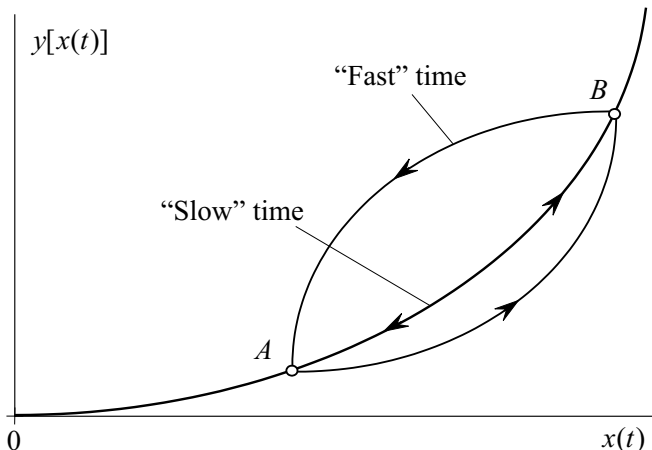


Fig. 7.1. The memory effect in nonlinear systems: “slow” time corresponds to memoryless systems (no hysteresis) and “fast” time to memory systems (with hysteresis).

is nonlinear. If $x(t)$ changes with time slowly, a circular transition from the point A to B would trace along the same trajectory (“Slow” time). With fast changes, any dynamic system inherently demonstrates inertia and the transitions from A to B and back to A do not coincide in trajectories (“Fast” time). The effect is called *hysteresis*. The negative appearance of hysteresis is that the input produces two values of the output with coordinates dependent on the input rate.

Of course, the terms “slow” and “fast” are conditional in a sense. Conventionally, one may think that if the spectrum of an input signal corresponds to the “slow” time of a system, then the latter is memoryless (negligible hysteresis). Having no memory, a system is described by $y(x)$ that does not involve time t as a variable. Otherwise, a system is memory, $y[x(t)]$ or (7.1).

7.2 Memoryless Systems

If a SISO NTI system is memoryless, its input is coupled with the output by the operator (7.1) losing a variable t such that

$$y = \mathcal{O}(x)x = y(x). \quad (7.2)$$

Typically, a nonlinearity $y(x)$ is defined analytically and then synthesized to attach some required properties to a system. An example is a feedback gain that is usually nonlinear of a certain shape to solve the control problem with highest efficiency. Frequently, natural nonlinearities of electronic units are used. In such cases, the function $y(x)$ is measured at discrete points and then approximated with a reasonable accuracy.

Below, we observe several methods most widely used for approximation, interpolation, and extrapolation in NTI memoryless systems.

7.2.1 Lagrange Interpolation

The Lagrange method is a classical technique of finding an order polynomial $y(x)$ which passes through measured points. The formula published by Lagrange in 1795 was earlier found by Waring¹ in 1779 and soon after rediscovered by Euler in 1783. Therefore, it is also called Waring-Lagrange interpolation or, rarely, Waring-Euler-Lagrange interpolation.

The Lagrange interpolation is performed as follows. Let a function $y(x)$ be given at $m + 1$ discrete points called *knots* as $y(x_n)$, $n = 0, 1, \dots, m$. Then the following unique order m polynomial interpolates the function between these points by

$$L_m(x) = \sum_{i=0}^m y(x_i) l_{mi}(x), \quad (7.3)$$

where

$$l_{mi}(x) = \prod_{k=0, k \neq i}^m \frac{x - x_k}{x_i - x_k} \\ = \frac{(x - x_0)(x - x_1) \dots (x - x_{i-1})(x - x_{i+1}) \dots (x - x_m)}{(x_i - x_0)(x_i - x_1) \dots (x_i - x_{i-1})(x_i - x_{i+1}) \dots (x_i - x_m)} \quad (7.4)$$

is an elementary n -order polynomial satisfying the condition of

$$l_{mi}(t_n) = \begin{cases} 1 & \text{if } n = i \\ 0 & \text{if } n \neq i \end{cases} \quad (7.5)$$

A simple observation shows that the numerator of the right-hand side of (7.4) has zeros at all of the points except the k th and that the denominator here is a constant playing a role of a normalizing coefficient to satisfy (7.5). To find the coefficients of the interpolating polynomial (7.3), it needs solving the equations system of order polynomials that is usually provided via the Vandermonde² matrix.

¹ Edward Waring, English mathematician, 1736–15 August 1798.

² Alexandre-Thophile Vandermonde, French mathematician, 28 February 1735–1 January 1796.

Example 7.1. The nonlinearity is measured at discrete points x_n , $n = 0, 1, \dots, 5$ with a constant step of $x_n - x_{n-1} = 1$ to possess the values of $y(x_0) = 0$, $y(x_1) = 2.256$, $y(x_2) = 3.494$, $y(x_3) = 4.174$, $y(x_4) = 4.546$, and $y(x_5) = 4.751$. The Lagrange interpolation (7.3) applied to these samples produces a polynomial

$$y(x) = 2.989x - 0.872x^2 + 0.156x^3 - 0.016x^4 + 7.791 \times 10^{-4}x^5. \quad (7.6)$$

Fig. 7.2 demonstrates that (7.6) gives exact interpolation at each of the measured points and is still accurate in extrapolating to the nearest future. However, the polynomial order is large having not enough applied features.

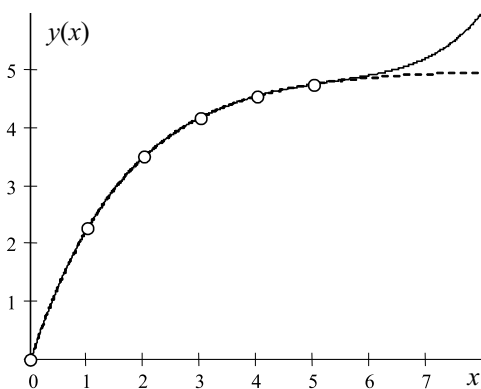


Fig. 7.2. Interpolation of measured points: Lagrange interpolation (bold) and physical formula (7.7) (dashed).

On the other hand, the measurements fit a physical process described by

$$y(x) = 5(1 - e^{-0.6x}) \quad (7.7)$$

that corresponds to a dashed line in Fig. 7.2. This example neatly demonstrates that a physical law can be superior to approximation, whenever the law is available. \square

Overall, Lagrange interpolation is fairly useful, but its usefulness is not so doubtless. In fact, a long interpolation order polynomial is not practicable. Moreover, constructing the $(m + 1)$ -order polynomial $y_{m+1}(x)$ we fully lose information about the lower order polynomial $y_m(x)$. The latter disadvantage is circumvented in the Newton interpolation formula.

7.2.2 Newton Method

An interpolation polynomial in the Newton form is also called Newton's divided differences interpolation polynomial because of its coefficients are cal-

culated using divided differences. Again, we deal here with the function $y(x)$ that is given at $m + 1$ knots as $y(x_n)$, $n = 0, 1, \dots, m$.

The values

$$y(x_n, x_{n+1}) = \frac{y(x_{n+1}) - y(x_n)}{x_{n+1} - x_n}$$

are called the *divided differences* of the first order. The ones of the second order are defined by

$$y(x_n, x_{n+1}, x_{n+2}) = \frac{y(x_{n+1}, x_{n+2}) - y(x_n, x_{n+1})}{x_{n+2} - x_n}$$

and then those of an arbitrary $k \geq 2$ order are performed as

$$y(x_n, x_{n+1}, \dots, x_{n+k}) = \frac{y(x_{n+1}, \dots, x_{n+k}) - y(x_n, \dots, x_{n+k-1})}{x_{n+k} - x_n}. \quad (7.8)$$

Utilizing (7.8), the Newton interpolation polynomial finally becomes

$$\begin{aligned} P_m(t) = & y(x_0) + y(x_0, x_1)(x - x_0) + y(x_0, x_1, x_2)(x - x_0)(x - x_1) + \dots \\ & + y(x_0, \dots, x_m)(x - x_0) \dots (x - x_{m-1}). \end{aligned} \quad (7.9)$$

The value $\varepsilon_m = |y(x) - P_m(x)|$ represents the interpolation error or the rest interpolation term that is the same as in the Lagrange form. Usually, the approximate relation $y(x) - P_m(x) \approx P_{m+1}(x) - P_m(x)$ is used to estimate the interpolation error by

$$\varepsilon_m \cong |P_{m+1}(x) - P_m(x)|. \quad (7.10)$$

It can be shown that Newton's method gives the same result as that by the Lagrange method (one is encouraged to solve the problem in Example 7.1 employing the Newton approach). There is, however, one important difference between two these forms. It follows from the definition of the divided differences that new data points can be added to the data set to create a new interpolation polynomial without recalculation the old coefficients. Hence, when a data point changes one usually does not have to recalculate all coefficients. Furthermore, if a time-step is constant, the calculation of the divided differences becomes significantly easier. Therefore the Newton form is usually preferred over the Lagrange one. In fact, adding a new sample, the Lagrange polynomial has to be recalculated fully, whereas the Newton form requires only an addition calculated for this new term.

7.2.3 Splines

Both Lagrange and Newton interpolations give unsatisfactory long approximating formulas on the interval $x \in [a, b]$ if a number of knots is large.

Moreover, with a high degree of interpolation, the computational errors and divergency of the interpolation process increase.

Another mathematical tool termed “splines” refers to a wide class of functions that are used to interpolate and/or smooth the measured nonlinearity only between neighboring points. The spline functions $S(x)$ are therefore finite dimensional in nature, being represented by the small degree polynomials, stable, and have a good convergence.

The first mathematical reference to splines was given in the 1946 by Schoenberg³, who used the word “spline” in connection with smooth, piecewise polynomial approximation. Thereafter, many efforts were done to find the most appropriate interpolating polynomials. Nowadays, it is accepted that one of the most efficient approximations is provided by cubic splines that fit a third-degree polynomial through two points so as to achieve a certain slope at one of the points. There are also used Bezier’s⁴ splines which interpolate a set of points using smooth curves and do not necessarily pass through the points. The Bernstein⁵ polynomial that is a linear combination of Bernstein basis polynomials is the other opportunity for interpolation.

A spline is a piecewise polynomial function determined on $x \in [a, b]$ of $m + 1$ knots, $a = x_0 < x_1 < \dots < x_{m-1} < x_m = b$, via the polynomial pieces as follows

$$S(x) = \begin{cases} P_1(x), & x_0 \leq x < x_1 \\ P_2(x), & x_1 \leq x < x_2 \\ \vdots & \vdots \\ P_m(x), & x_{m-1} \leq x \leq x_m \end{cases} \quad (7.11)$$

Accordingly, the vector $\mathbf{x} = [x_1, x_2, \dots, x_m]$ of the points is called a *knot vector*. If the knots are equidistantly distributed in the interval $[a, b]$, the spline is *uniform* and it is *non-uniform* otherwise.

If the polynomial pieces on the subintervals between two neighboring points all have degree at most n , then the spline is said to be of order $n + 1$ or degree $\leq n$. Fig. 7.3 gives examples of interpolation by splines of the zeroth (a) and first (b) degrees. We notice that the first degree interpolation by splines is achieved with the Lagrange formula.

Interpolation by splines of the zeroth and first degrees faces no problem in describing the elementary polynomial pieces. However, for the degrees $n \geq 2$, additional conditions should be assigned to define the unique coefficients for the polynomials. Such conditions make the spline to be of *smoothness*, meaning that the two pieces P_{i-1} and P_i share common derivative values from the derivative of order 0 (the function value) up through the derivative of order r_i . A vector $\mathbf{r} = [r_1, r_2, \dots, r_{m-1}]$ such that the spline has smoothness at

³ Isaac Jacob Schoenberg, Romanian born scientist, 21 April 1903–21 February 1990.

⁴ Pierre Étienne Bézier, French engineer, 1 September 1910–25 November 1999.

⁵ Sergei Bernstein, Ukrainian mathematician, 5 March 1880–26 October 1968.

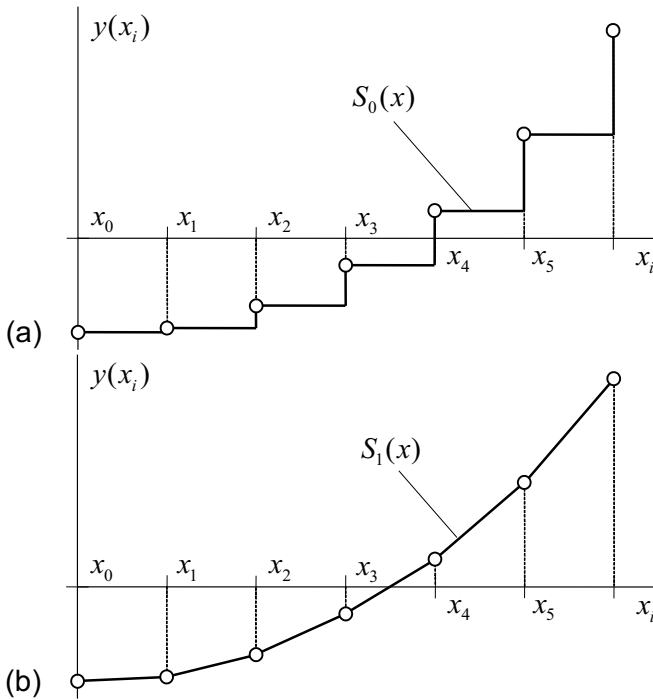


Fig. 7.3. Interpolation by splines: (a) degree 0 and (b) degree 1.

x_i for $1 \leq i \leq m - 1$ is called a smoothness vector for the spline. In other words, the pieces would have the same values and derivatives in the points from the second to last but one. Embedded smoothness, the spline space is commonly denoted by $S_n^r(\mathbf{x})$. Below, we demonstrate the effect of smoothness in examining the most popular cubic splines.

Cubic Splines

Owing to some important special features, the cubic splines have found most wide applications in engineering practice. The cubic spline interpolation within the interval $x \in [a, b]$ gives the formula that satisfies the following *interpolation conditions*:

- On each subinterval $x_{i-1} \leq x \leq x_i$, $i = 1, 2, \dots, m$, the function $S(x)$ is represented, by (7.11), with a polynomial of the third degree.

$$P_i(x) = a_i + b_i(x - x_i) + \frac{c_i}{2}(x - x_i)^2 + \frac{d_i}{6}(x - x_i)^3, \quad (7.12)$$

where a_i , b_i , c_i , and d_i are the coefficients to be determined for the given measurement $y(x_i)$, $i \in [0, m]$. \square

- The function $S(x)$ and its first and second derivatives are continuous on $[a, b]$ that is satisfied by the conditions

$$\begin{aligned} P_i(x_i) &= P_{i+1}(x_i), \quad i \in [1, m - 1], \\ P'_i(x_i) &= P'_{i+1}(x_i), \quad i \in [1, m - 1], \\ P''_i(x_i) &= P''_{i+1}(x_i), \quad i \in [1, m - 1]. \end{aligned}$$

□

- At each knot, the interpolation function equals exactly to the measurement, $S(x) = y(x_i) = y_i, i = 0, 1, \dots, m$. □

It can easily be shown, by taken the derivatives of (7.12) with respect to x , the coefficients of the polynomial are defined by

$$a_i = P_i(x_i), \quad b_i = P'_i(x_i), \quad c_i = P''_i(x_i), \quad d_i = P'''_i(x_i). \tag{7.13}$$

From (7.12) and the third interpolation condition one instantly defines

$$a_i = y_i, \quad i \in [0, m]. \tag{7.14}$$

From the rest of the interpolation conditions, there can be found an equation specifying the coefficients c_i ,

$$\begin{aligned} \Delta_i c_{i-1} + 2(\Delta_i + \Delta_{i+1})c_i + \Delta_{i+1}c_{i+1} &= 6 \left(\frac{y_{i+1} - y_i}{\Delta_{i+1}} - \frac{y_i - y_{i-1}}{\Delta_i} \right), \\ i &\in [1, m - 1], \end{aligned} \tag{7.15}$$

where $\Delta_i = x_i - x_{i-1}$ is a variable sample step between measurements. The coefficients c_0 and c_m are set arbitrary to obtain the necessary trend of the interpolating polynomial beyond the interval $[a, b]$. If $c_0 = c_m = 0$, the interpolation polynomial behaves linearly beyond the interval $[a, b]$ that is associated with the so-called *natural cubic spline*.

In the matrix form, (7.15) becomes

$$\begin{bmatrix} u_1 & \Delta_2 & 0 & 0 & \dots & 0 & 0 & 0 \\ \Delta_2 & u_2 & \Delta_3 & 0 & \dots & 0 & 0 & 0 \\ 0 & \Delta_3 & u_3 & \Delta_4 & & 0 & 0 & 0 \\ \vdots & & \ddots & \ddots & \ddots & & \vdots & \vdots \\ 0 & 0 & 0 & 0 & & u_{m-3} & \Delta_{m-2} & 0 \\ 0 & 0 & 0 & 0 & \dots & \Delta_{m-2} & u_{m-2} & \Delta_{m-1} \\ 0 & 0 & 0 & 0 & \dots & 0 & \Delta_{m-1} & u_{m-1} \end{bmatrix} \begin{bmatrix} c_1 \\ c_2 \\ c_3 \\ \vdots \\ c_{m-3} \\ c_{m-2} \\ c_{m-1} \end{bmatrix} = \begin{bmatrix} v_1 \\ v_2 \\ v_3 \\ \vdots \\ v_{m-3} \\ v_{m-2} \\ v_{m-1} \end{bmatrix}, \tag{7.16}$$

where the $(m - 1) \times (m - 1)$ matrix is tridiagonal and the functions u_i and v_i are given by, respectively,

$$u_i = 2(\Delta_i + \Delta_{i+1}), \quad (7.17)$$

$$v_i = 6 \left(\frac{y_{i+1} - y_i}{\Delta_{i+1}} - \frac{y_i - y_{i-1}}{\Delta_i} \right). \quad (7.18)$$

Determined c_i , the rest of the coefficients in (7.12) are calculated, for $i \in [1, m]$, with the functions

$$d_i = \frac{1}{\Delta_i}(c_i - c_{i-1}), \quad (7.19)$$

$$b_i = \frac{\Delta_i}{2}c_i - \frac{\Delta_i^2}{6}d_i + \frac{1}{\Delta_i}(y_i - y_{i-1}). \quad (7.20)$$

Example 7.2. The ampere-voltage characteristic $I(V)$ of a semiconductor tunnel diode was measured from 0 to 7 volts with the step of 1 volt for the values $I = 0, 1.98, 3.01, 2.02, 0.99, 1.99, 4.02$ and 6.97 (in amperes). The characteristic was then interpolated by (7.11) with the cubic splines (7.12). By (7.14), the coefficient a_i was equated to y_i . The coefficients c_i were determined for $i \in [1, 6]$ by (7.16)–(7.18), and then d_i and b_i were calculated, respectively, by (7.19) and (7.20). The interpolating curve is shown in Fig. 7.4. \square

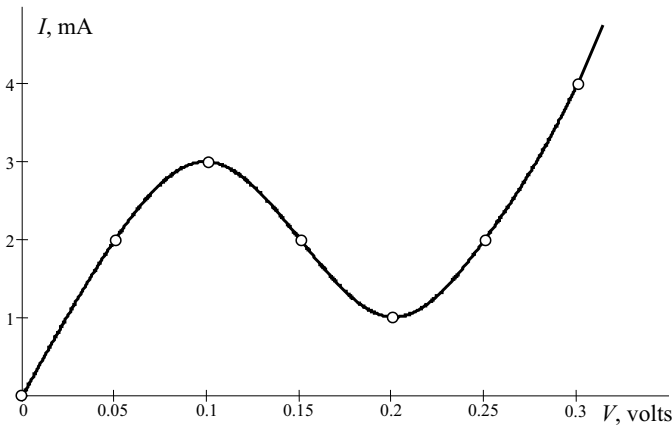


Fig. 7.4. The ampere-voltage characteristic of a semiconductor tunnel diode interpolated by cubic splines.

7.2.4 Exponential Approximation

It is well-known from the operation of semiconductor diodes that the electric current I is coupled with the applied electric voltage V by the relation

$$I(V) = I_0 \left(e^{\frac{V}{V_T}} - 1 \right), \quad V > 0, \quad (7.21)$$

where I_0 is a feedback current of saturation and V_T is a temperature potential that, for the silicon devices with the temperature of 300 K, is about 25×10^{-3} volts.

The dependence (7.21) is often used to describe nonlinear phenomena in semiconductor electrical systems. The approximation is quite accurate if the electric current does not exceed several milliamperes. With larger values, (7.21) evolves to a straight line which slope is mostly associated with the real resistance of a semiconductor body.

7.2.5 Taylor Series Expansion

Frequently, owing to complexity, an actual nonlinearity of a memoryless system cannot be used straightforwardly in models. The problem then arises how to find an appropriate and reasonably accurate approximate function. If we recall that a system typically operates in some bounds, the nonlinear input-to-output dependence $y(x)$ can be expanded to the Taylor series around some operation point x_0 ,

$$\begin{aligned} y(x) = & y(x_0) + \left. \frac{\partial y(x)}{\partial x} \right|_{x=x_0} (x - x_0) + \frac{1}{2} \left. \frac{\partial^2 y(x)}{\partial x^2} \right|_{x=x_0} (x - x_0)^2 \\ & + \dots + \frac{1}{k!} \left. \frac{\partial^k y(x)}{\partial x^k} \right|_{x=x_0} (x - x_0)^k + \dots \end{aligned} \quad (7.22)$$

Such an expansion has several important advantages. We can save only two first terms in the right-hand side and thereby linearize the nonlinearity around x_0 . Such a way is now commonly accepted whenever a linearization is needed. Accounting for more terms from (7.22) allows substituting a real function with, for example, quadratic or cubic approximations. Therefore, the Taylor series is accepted as the most common and universal tool to describe and approximate memoryless NTI systems.

Example 7.3. A semiconductor diode described by (7.21) operates in the vicinity of an operation point $V = 0.4$ volts. By the Taylor series (7.22), the function is approximated at the given point with a linear ($k = 1$), quadratic ($k = 2$), and cubic ($k = 3$) polynomials. The results of approximation are shown in Fig. 7.5.

As can be seen, all three approximating curves are of high accuracy in the region closely surrounding a point $V = 0.4$ volts. Beyond this region, better results are achieved, of course, with quadratic and cubic approximations. \square

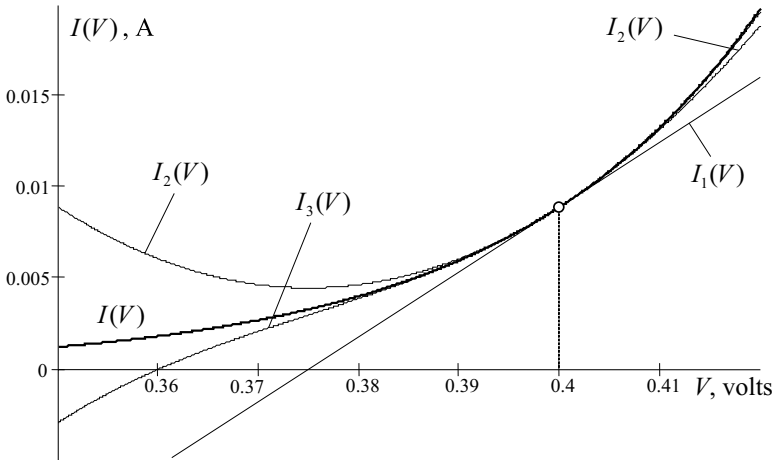


Fig. 7.5. Approximation of the ampere-voltage characteristic of a semiconductor diode with the Taylor series around the point $V = 0.4$ volts.

7.2.6 Linearization Techniques

Technical linearization of NTI memoryless systems implies using some auxiliary nonlinear blocks to make the system linear. Among a variety of linearization techniques, the feedforward and feedback linearizations as well as nonlinear predistortion of signals are most popular.

Feedforward Linearization

In the *feedforward linearization* (Fig. 7.6a), the nonlinear distortions of a signal $y_1 = \mathcal{O}_1(x)x$ produced by the main amplifier A_1 are compensated by the signal $y_2 = \mathcal{O}_2(x)x$ of an auxiliary amplifier A_2 . The resulting system is assumed to be linear and such that

$$y = \mathcal{O}_1(x)x - \mathcal{O}_2(x)x = ax + b, \quad (7.23)$$

where a and b are some constant values. In the other structures, the distortion can first be extracted, then amplified, and finally subtracted from the output.

Feedback Linearization

Another technique is known as the *feedback linearization* (Fig. 7.6b). By the functions $y = \mathcal{O}_1(x_1)x_1$ of a main nonlinear amplifier A_1 and the nonlinear function $x_2 = \mathcal{O}_2(y)y$ of an auxiliary amplifier A_2 , the system equation is written as

$$y = \mathcal{O}_1(x)[x - \mathcal{O}_2(y)y], \quad (7.24)$$

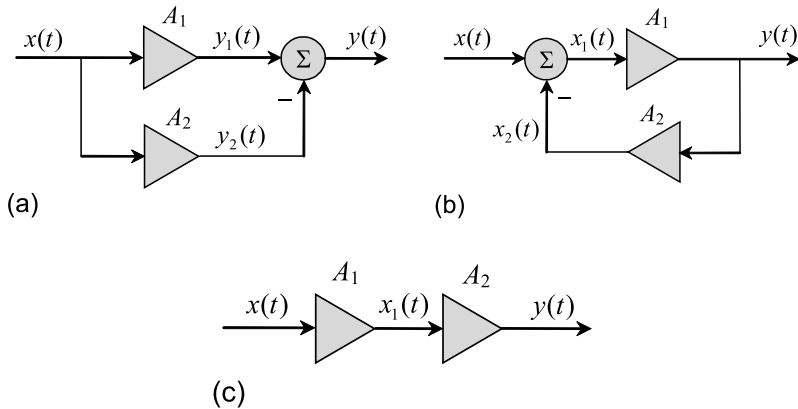


Fig. 7.6. Linearization techniques: (a) feedforward, (b) feedback, and (c) with predistortions.

where an operator $\mathcal{O}_2(y)$ is chosen such that the system becomes linear, $y = ax + b$.

Nonlinear Predistortion

Efficient linearization can be achieved by the so-called *predistortions*. The relevant cascade system is shown in Fig. 7.6c, in which the input signal is intentionally predistorted by an auxiliary amplifier A_1 to compensate distortions of a main amplifier A_2 . The cascade thus becomes linear if the operator $\mathcal{O}_1(x)$ is chosen such that

$$y = \mathcal{O}_2(x_1)[\mathcal{O}_1(x)x] = ax + b. \tag{7.25}$$

At this point, we finish an analysis of principle foundations of memoryless NTI systems and start discussing how memory affects the model and what are the methods of describing NTI memory systems. Following the tradition, we continue with a presentation of the Volterra series method that extends the convolution approach to the nonlinear systems.

7.3 Representation of Memory Systems by Volterra Series

In systems with memory, the output depends not solely on the input, but also on its rate that results in a hysteresis loop (Fig. 7.1). In view of that, the methods for memoryless systems become inappropriate and the general operator (7.1) is applied.

To represent a SISO NTI memory system with some functions, an operator $\mathcal{O}(x)$ can be expanded to the Taylor series (7.22) that formally yields

$$\begin{aligned} y(t) &= \mathcal{O}(x)x(t) \\ &= \{\mathcal{V}_0[x(t)] + \mathcal{V}_1[x(t)] + \dots + \mathcal{V}_n[x(t)] + \dots\}x(t) = \mathcal{V}[x(t)]x(t), \end{aligned} \quad (7.26)$$

where \mathcal{V}_n is some newly introduced the degree n nonlinear operator. In this expansion, \mathcal{V}_0 is associated with the constant term, \mathcal{V}_1 with linear term, \mathcal{V}_2 with quadratic term, and so on. A significance of these new operators will become clear very soon.

The method of determining the degree n operator \mathcal{V}_n was proposed by Volterra and is now commonly referred to as the *Volterra series method* or *functional method*. In accordance with the approach, a system is considered to be nonlinear and memory either being governed by the operator \mathcal{V} called the *Volterra operator*. By virtue of the fact that the method exploits the Taylor expansion, the Volterra series is also often called the Taylor series with memory.

In the Volterra approach, the series (7.26) is performed as

$$y(t) = h_0 + \sum_{n=1}^{\infty} \int_{-\infty}^{\infty} \dots \int_{-\infty}^{\infty} h_n(\theta_1, \dots, \theta_n) x(t - \theta_1) \dots x(t - \theta_n) d\theta_1 \dots d\theta_n, \quad (7.27)$$

where $h_n(\theta_1, \dots, \theta_n)$ is called the degree n *Volterra kernel*. In view of similarity with the LTI systems, (7.27) is often referred to as the *generalized convolution*. For the Volterra kernel of degree n , the generalized convolution is depicted as

$$\begin{aligned} &h_n(\theta_1, \dots, \theta_n) * x(t) \\ &= \int_{-\infty}^{\infty} \dots \int_{-\infty}^{\infty} h_n(\theta_1, \dots, \theta_n) x(t - \theta_1) \dots x(t - \theta_n) d\theta_1 \dots d\theta_n. \end{aligned} \quad (7.28)$$

A direct comparison of (7.26) and (7.27) allows specifying the terms of the series, using (7.28), as in the following.

The term associated with $n = 0$,

$$\mathcal{V}_0 x(t) = h_0, \quad (7.29)$$

is a constant corresponding to the system output with zero input. The second term of degree $n = 1$ is linear,

$$\mathcal{V}_1 x(t) = \int_{-\infty}^{\infty} h_1(\theta_1) x(t - \theta_1) d\theta_1, \quad (7.30)$$

representing a convolution. In this sense, the Vilterra kernel $h_1(t)$ is nothing more than the impulse response $h(t)$ of a linearized NTI system.

The higher degree terms are defined, by (7.28), in a like manner. For example, the quadratic and cubic nonlinearities are associated with, respectively,

$$\mathcal{V}_2 x(t) = \int_{-\infty}^{\infty} \int_{-\infty}^{\infty} h_2(\theta_1, \theta_2) x(t - \theta_1) x(t - \theta_2) d\theta_1 d\theta_2, \quad (7.31)$$

$$\mathcal{V}_3 x(t) = \int_{-\infty}^{\infty} \int_{-\infty}^{\infty} \int_{-\infty}^{\infty} h_3(\theta_1, \theta_2, \theta_3) x(t - \theta_1) x(t - \theta_2) x(t - \theta_3) d\theta_1 d\theta_2 d\theta_3. \quad (7.32)$$

It follows from what was observed that, like any LTI system that is exhaustively characterized by the impulse response, any NTI system described by the Volterra series is exhaustively characterized by the Volterra kernels. Does it mean that any NTI memory system can exhaustively be described by the Volterra series? The answer is both “Yes” and “Not”. On the one hand, (7.27) is certainly a general model of any NTI system. On the other hand, application of (7.27) instantly faces three problems:

- How to determine and measure the Volterra kernels? □
- How to transfer from the system ODE to the Volterra series? □
- Because the terms in the Volterra series are not orthogonal, they must be identified all at once. □

In order to avoid raising strong solutions in this book to the above-listed problems (the reader can open a book by Rugh or other special books), in the sequel we shall apply the approach to some particular NTI problems. Before continuing with applications, it is worth observing a simple example demonstrating a typical engineering approach to NTI memory systems.

7.3.1 A Noble Example

Let us consider the well-known simplest resonant transistor amplifier (Fig. 7.7a) and think, for simplicity, that the collector current $i(t)$ depends quadratically on the emitter-base input voltage $v_{in}(t)$.

Whenever such a system is encountered, we typically analyze it via the equivalent scheme shown in Fig. 7.1b. Even intuitively, one decomposes the scheme to the memoryless (or static) nonlinear part (transistor) and memory (or dynamic) linear part (resonant circuit). Why do we act in such a manner? Because it is much easier to analyze any nonlinearity if it is memoryless. In fact, having $v_{in}(t) = \cos \omega t$ and a quadratic nonlinearity, we can write

$$i(t) = av_{in}^2(t) = a \cos^2 \omega t = \frac{a}{2} + \frac{a}{2} \cos 2\omega t. \quad (7.33)$$

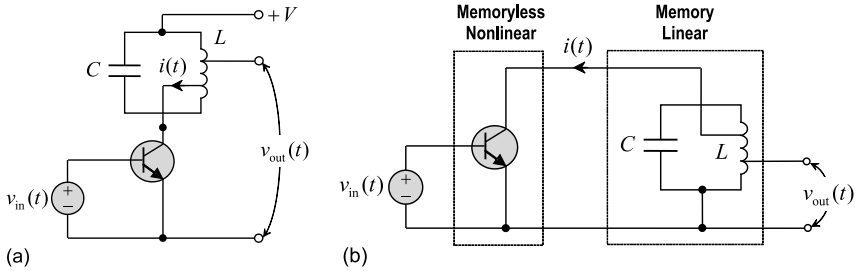


Fig. 7.7. Resonant amplifier: (a) electrical scheme and (b) equivalent scheme.

A resonant circuit tuned to 2ω produces the output voltage $v_{out}(t) = \frac{1}{2}ak \cos 2\omega t$, where $k < 1$. In this amplifier, the input is removed to the twice frequency ω with the gain factor $ak/2$.

This noble example neatly demonstrates that in order to analyze an NTI memory system in the simplest way, one first needs to split a system into the memoryless nonlinear and memory linear parts. On the ground of that, two basic structures of NTI systems appear, namely the Hammerstein and Wiener systems.

7.3.2 Hammerstein and Wiener Systems

Two basic cascade interconnections of memoryless NTI and memory LTI subblocks are recognized. The Hammerstein system (Fig. 7.8a) is a nonlinear-to-linear structure. Its example is represented by the scheme shown in Fig. 7.7b. Another model, linear-to-nonlinear, shown in Fig. 7.8b was investigated by Wiener. It follows that the Wiener model would fit the scheme (Fig. 7.7b) if to include a resonant circuit in the input of a transistor amplifier.

The lucky principle of separation resulting in the Hammerstein and Wiener models is effectively exploited in the Volterra series method. We verify this fact below by two useful examples.

Example 7.4. A SISO NTI system is performed with the ODE

$$y' + 2ay - 2b\sqrt{y}x = 0, \quad y \geq 0 \tag{7.34}$$

and zero initial condition $y(0) = 0$. Substituting $y = y_1^2$ leads to the linear ODE and nonlinear algebraic equations, respectively,

$$y_1' + ay_1 = bx, \quad y = y_1^2. \tag{7.35}$$

By (4.55), a general solution of the first equation is written as

$$y_1(t) = be^{-at} \int_0^t x(\tau)e^{a\tau} d\tau,$$

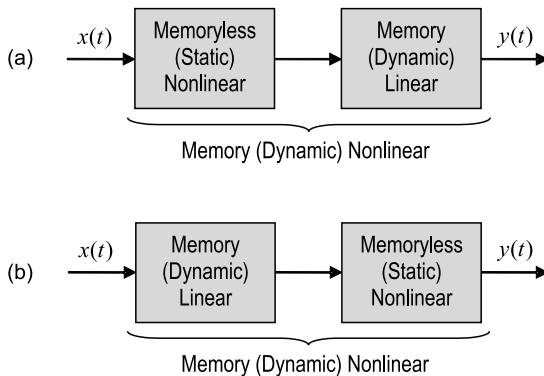


Fig. 7.8. Generalized models of NTI systems: (a) Hammerstein and (b) Wiener.

producing, by $x(t) = \delta(t)$, the impulse response $h(t) = be^{-at}u(t)$. A linear dynamic part of the system is thus represented with the convolution

$$y_1(t) = \int_{-\infty}^{\infty} h(\theta)x(t - \theta)d\theta.$$

The second equation in (7.35) completes the input-to-output relation by

$$y(t) = y_1^2(t) = \int_{-\infty}^{\infty} \int_{-\infty}^{\infty} h_2(\theta_1, \theta_2)x(t - \theta_1)x(t - \theta_2)d\theta_1d\theta_2, \quad (7.36)$$

where

$$h_2(\theta_1, \theta_2) = h(\theta_1)h(\theta_2) = b^2e^{-a(\theta_1+\theta_2)}u(\theta_1)u(\theta_2) \quad (7.37)$$

is the degree $n = 2$ Volterra kernel. A system (7.34) is hence described by the Volterra operator \mathcal{V}_2 (7.31) and simulated with the Wiener model (Fig. 7.8b) as shown in Fig. 7.9.

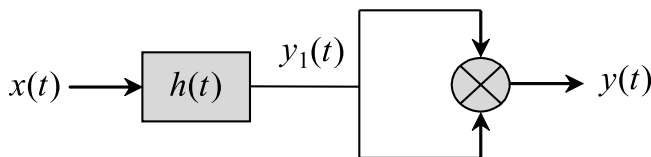


Fig. 7.9. The Wiener model of a system (Example 7.4).

The step response of a system is defined, by $x(t) = u(t)$, (7.36), and (7.37), to be

$$\begin{aligned}
 g(t) &= b^2 \int_{-\infty}^{\infty} \int_{-\infty}^{\infty} e^{-a(\theta_1+\theta_2)} u(\theta_1) u(\theta_2) u(t-\theta_1) u(t-\theta_2) d\theta_1 d\theta_2 \\
 &= b^2 \int_{-\infty}^{\infty} e^{-a\theta_1} u(\theta_1) u(t-\theta_1) d\theta_1 \int_{-\infty}^{\infty} e^{-a\theta_2} u(\theta_2) u(t-\theta_2) d\theta_2 \\
 &= b^2 \int_0^t e^{-a\theta_1} d\theta_1 \int_0^t e^{-a\theta_2} d\theta_2 = \frac{b^2}{a^2} (1 - e^{-at})^2 u(t). \quad (7.38)
 \end{aligned}$$

It can easily be verified that the impulse and step responses of this system are not coupled by the integral and differential relations. \square

Example 7.5. An NTI system is represented with the block diagram shown in Fig. 7.10.

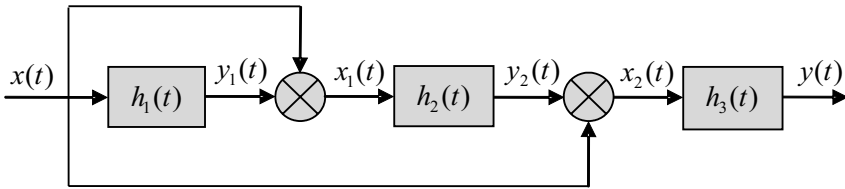


Fig. 7.10. Block diagram of an NTI system.

By the commutative property of the convolution, the system equation can be derived, step-by-step, as in the following:

$$\begin{aligned}
 y_1(t) &= \int_{-\infty}^{\infty} h_1(t - \tau_1) x(\tau_1) d\tau_1, \\
 x_1(t) &= \int_{-\infty}^{\infty} h_1(t - \tau_1) x(\tau_1) d\tau_1 x(t), \\
 y_2(t) &= \int_{-\infty}^{\infty} h_2(t - \tau_2) x_1(\tau_2) d\tau_2 \\
 &= \int_{-\infty}^{\infty} \int_{-\infty}^{\infty} h_2(t - \tau_2) h_1(\tau_2 - \tau_1) x(\tau_1) x(\tau_2) d\tau_1 d\tau_2,
 \end{aligned}$$

$$\begin{aligned}
 x_2(t) &= \int_{-\infty}^{\infty} \int_{-\infty}^{\infty} h_2(t - \tau_2) h_1(\tau_2 - \tau_1) x(\tau_1) x(\tau_2) d\tau_1 d\tau_2 x(t), \\
 y(t) &= \int_{-\infty}^{\infty} h_3(t - \tau_3) x_2(\tau_3) d\tau_3, \\
 &= \int_{-\infty}^{\infty} \int_{-\infty}^{\infty} \int_{-\infty}^{\infty} h_3(t - \tau_3) h_2(t - \tau_2) h_1(\tau_2 - \tau_1) x(\tau_1) x(\tau_2) x(\tau_3) d\tau_1 d\tau_2 d\tau_3, \quad (7.39)
 \end{aligned}$$

If to introduce new variables $\theta_1 = t - \tau_1$, $\theta_2 = t - \tau_2$, and $\theta_3 = t - \tau_3$, then (7.39) can be transformed to the familiar form (7.32),

$$y(t) = \int_{-\infty}^{\infty} \int_{-\infty}^{\infty} \int_{-\infty}^{\infty} h_3(\theta_1, \theta_2, \theta_3) x(t - \theta_1) x(t - \theta_2) x(t - \theta_3) d\theta_1 d\theta_2 d\theta_3, \quad (7.40)$$

where $h_3(\theta_1, \theta_2, \theta_3) = h_1(\theta_1 - \theta_2) h_2(\theta_2) h_3(\theta_3)$ is the degree $n = 3$ Volterra kernel. \square

Like the convolution of LTI systems, the generalized convolution of NTI systems is often used in different forms and applied to a variety of interconnections of nonlinear and linear subsystems as shown, for example, in Example 7.5. To provide an analysis in the most efficient and shortest way, it is worth knowing the properties of the Volterra operator.

7.3.3 Properties of the Volterra Operator

In this section, we observe several the most common properties of the Volterra operator bearing in mind that many others can be found in special and rather mathematical books.

Commutativity

Consider the Volterra series (7.27). Because an NTI system is time-invariant, we can change variables to $\tau_1 = t - \theta_1$, $\tau_2 = t - \theta_2$, \dots , $\tau_n = t - \theta_n$ and write

$$y(t) = h_0 + \sum_{n=1}^{\infty} \int_{-\infty}^{\infty} \dots \int_{-\infty}^{\infty} h_n(t - \tau_1, \dots, t - \tau_n) x(\tau_1) \dots x(\tau_n) d\tau_1 \dots d\tau_n, \quad (7.41)$$

where $h_n(t - \tau_1, \dots, t - \tau_n) = h_n(t, \tau_1, \dots, \tau_n)$ is still the Volterra kernel of degree n .

For time-invariant systems, one is allowed to set the current time arbitrary. Thus $h_n(t, \tau_1, \dots, \tau_n) = h_n(0, \tau_1, \dots, \tau_n)$ or, by dropping “0”, it is just

$$h_n(t, \tau_1, \dots, \tau_n) = h_n(\tau_1, \dots, \tau_n). \quad (7.42)$$

The latter means commutativity of the generalized convolution, namely

$$\begin{aligned} y(t) &= h_n(\theta_1, \dots, \theta_n) * x(t) \\ &= x(t) * h_n(\theta_1, \dots, \theta_n). \end{aligned} \quad (7.43)$$

Example 7.6. Consider a square amplifier represented with the block diagram shown in Fig. 7.9. By the commutative property of the convolution, one can write the system equation as follows

$$\begin{aligned} y(t) &= \left[\int_{-\infty}^{\infty} h(t - \tau)x(\tau)d\tau \right]^2 \\ &= \int_{-\infty}^{\infty} \int_{-\infty}^{\infty} h(t - \tau_1)h(t - \tau_2)x(\tau_1)x(\tau_2)d\tau_1d\tau_2. \end{aligned}$$

By changing variables, $\theta_1 = t - \tau_1$ and $\theta_2 = t - \tau_2$, and using (7.42), the input-to-output relation becomes (7.36) comprising the Volterra kernel (7.37). \square

Non-distributivity

Contrary to LTI systems, the operator of NTI systems does not demonstrate an ability to distribute. That means that

$$\mathcal{V} \sum_{i=1}^m x_i(t) \neq \sum_{i=1}^m \mathcal{V}x_i(t). \quad (7.44)$$

The simplest case of two signals, the following inequality commonly exists

$$\mathcal{V}[x_1(t) + x_2(t)] \neq \mathcal{V}x_1(t) + \mathcal{V}x_2(t). \quad (7.45)$$

Example 7.7. Given a system represented by the degree $n = 2$ Volterra kernel $h_2(\theta_1, \theta_2) = e^{-a(\theta_1 + \theta_2)}u(\theta_1)u(\theta_2)$.

Let the Volterra operator act on each of the signals, $x_1(t) = e^{-bt}u(t)$ and $x_2(t) = e^{-ct}u(t)$, separately producing two subsignals, $y_1(t)$ and $y_2(t)$, respectively,

$$y_1(t) = \int_{-\infty}^{\infty} \int_{-\infty}^{\infty} e^{-a(\theta_1 + \theta_2)}u(\theta_1)u(\theta_2)e^{-b(t - \theta_1)}u(t - \theta_1)e^{-b(t - \theta_2)}u(t - \theta_2)d\theta_1d\theta_2$$

$$\begin{aligned}
&= \int_0^t \int_0^t e^{-a(\theta_1+\theta_2)} e^{-b(t-\theta_1)} e^{-b(t-\theta_2)} d\theta_1 d\theta_2 \\
&= e^{-2bt} \int_0^t e^{-(a-b)\theta_1} d\theta_1 \int_0^t e^{-(a-b)\theta_2} d\theta_2 = \frac{(e^{-bt} - e^{-at})^2}{(a-b)^2} u(t), \quad (7.46)
\end{aligned}$$

$$y_2(t) = \frac{(e^{-ct} - e^{-at})^2}{(a-c)^2} u(t). \quad (7.47)$$

The subsignals $y_1(t)$ and $y_2(t)$ are added to produce the output

$$z_1(t) = y_1(t) + y_2(t) = \frac{(e^{-bt} - e^{-at})^2}{(a-b)^2} u(t) + \frac{(e^{-ct} - e^{-at})^2}{(a-c)^2} u(t). \quad (7.48)$$

Now, let us allow the Volterra operator to act on the sum of two signals, $x_1(t) + x_2(t)$. This yields

$$\begin{aligned}
z_2(t) &= \int_0^t \int_0^t e^{-a(\theta_1+\theta_2)} [e^{-b(t-\theta_1)} + e^{-c(t-\theta_1)}] \\
&\quad \times [e^{-b(t-\theta_2)} + e^{-c(t-\theta_2)}] d\theta_1 d\theta_2 \\
&= z_1(t) + e^{-(b+c)t} \int_0^t \int_0^t e^{-a(\theta_1+\theta_2)} (e^{b\theta_1} e^{c\theta_2} + e^{c\theta_1} e^{b\theta_2}) d\theta_1 d\theta_2, \quad (7.49)
\end{aligned}$$

where $z_1(t)$ is specified by (7.48). Because the integral remainder in the right-hand side of (7.49) is not zero for $t > 0$, we have $z_1(t) \neq z_2(t)$. Hence, the system does not distribute and (7.45) holds true. \square

Homogeneity

Scaling a signal $x(t)$ [actually, each of n subsignals in (7.27)] with some constant a is equivalent to the multiplication of $h_n(\theta_1, \dots, \theta_n)$ with a^n . This property of *homogeneity* follows directly from an analysis of (7.27). The property results in two forms of the generalized convolution:

$$[ah_n(\theta_1, \dots, \theta_n)] * x(t) = h_n(\theta_1, \dots, \theta_n) * [a^{1/n}x(t)], \quad (7.50)$$

$$[a^n h_n(\theta_1, \dots, \theta_n)] * x(t) = h_n(\theta_1, \dots, \theta_n) * [ax(t)]. \quad (7.51)$$

Stationarity

The property of *stationarity* or familiar time shifting is inherent for any NTI system. It means that the system performance is not changed with time, because the operator \mathcal{V} is time-invariant. In view of that, any time shift τ induced to the operator (7.27) does not affect the operator itself and hence

$$\begin{aligned} y(t - \tau) &= \mathcal{V}[x(t - \tau)]x(t - \tau) \\ &= h_0 + \sum_{n=1}^{\infty} \int_{-\infty}^{\infty} \dots \int_{-\infty}^{\infty} h_n(\theta_1, \dots, \theta_n) x(t - \tau - \theta_1) \dots x(t - \tau - \theta_n) d\theta_1 \dots d\theta_n. \end{aligned} \quad (7.52)$$

Any nonlinear system that does not fit this property belongs to the class of NTV systems.

Example 7.8. Consider an NTI system described by (7.46). Introduce a time shift τ and write

$$y(t - \tau) = \frac{[e^{-b(t-\tau)} - e^{-a(t-\tau)}]^2}{(a - b)^2} u(t - \tau).$$

Now change a variable by $t_1 = t - \tau$ and infer that the result is exactly (7.46) written in a new time t_1 ,

$$y(t_1) = \frac{(e^{-bt_1} - e^{-at_1})^2}{(a - b)^2} u(t_1). \quad (7.53)$$

Since no one coefficient in (7.53) depends on time, the system is stationary or time-invariant. \square

Causality

In its most general form, the Volterra operator (7.27) implies integration over the infinite bounds and hence fits the cases of both *causal* and *noncausal* signals and systems. If a signal or/and system is *causal*, some or all bounds become finite.

Causal systems. Recall that a system is *causal* if its output $y(t)$ at an arbitrary time instant t_1 depends on only its input $x(t)$ for $t_1 \geq t$. This means that a causal system does not respond to any input event until that event actually occurs. Because the Volterra kernels are akin to the impulse responses, they do not exist in negative time and (7.27) thus becomes

$$y(t) = h_0 + \sum_{n=1}^{\infty} \int_0^{\infty} \dots \int_0^{\infty} h_n(\theta_1, \dots, \theta_n) x(t - \theta_1) \dots x(t - \theta_n) d\theta_1 \dots d\theta_n. \quad (7.54)$$

Causal signals. By the definition, causal signals do not exist in negative time. Thus, all auxiliary variables θ cannot exceed the current time t and we have

$$y(t) = h_0 + \sum_{n=1}^{\infty} \int_{-\infty}^t \dots \int_{-\infty}^t h_n(\theta_1, \dots, \theta_n) x(t - \theta_1) \dots x(t - \theta_n) d\theta_1 \dots d\theta_n. \quad (7.55)$$

Both causal systems and signals. In the real physical world, both systems and signals are causal, therefore, the lower and upper integration bounds are both restricted that yields

$$y(t) = h_0 + \sum_{n=1}^{\infty} \int_0^t \dots \int_0^t h_n(\theta_1, \dots, \theta_n) x(t - \theta_1) \dots x(t - \theta_n) d\theta_1 \dots d\theta_n. \quad (7.56)$$

Example 7.7 exploits (7.56) and one can find many other relevant examples, whenever causal signals and/or systems are of concern.

Stability

In a manner similar to LTI systems, to ascertain BIBO stability of NTI systems, the absolute values of Volterra kernels must be examined for absolute integration. By virtue of the finite value

$$\int_{-\infty}^{\infty} \dots \int_{-\infty}^{\infty} |h_n(\theta_1, \dots, \theta_n)| d\theta_1 \dots d\theta_n \leq M < \infty, \quad (7.57)$$

the system described with the Volterra kernel $h_n(\theta_1, \dots, \theta_n)$ is said to be BIBO stable.

Example 7.9. Consider an NTI system represented with the degree $n = 2$ Volterra kernel (7.37). To ascertain BIBO stability of the system, we evaluate the integral

$$\begin{aligned} & b^2 \int_{-\infty}^{\infty} \int_{-\infty}^{\infty} \left| e^{-a(\theta_1 + \theta_2)} u(\theta_1) u(\theta_2) \right| d\theta_1 d\theta_2 \\ &= b^2 \int_0^{\infty} \int_0^{\infty} e^{-a(\theta_1 + \theta_2)} d\theta_1 d\theta_2 = \frac{b^2}{a^2}. \end{aligned}$$

If the coefficients of the Volterra kernel are such that $b^2/a^2 < \infty$, the system is BIBO stable. Otherwise, it is BIBO unstable. \square

7.3.4 Wiener approach

One of the weaknesses of the Volterra approach is that the terms in the series are not orthogonal and therefore must be identified all at once. To orthogonalize the series, Wiener proposed a solution now known as the *Wiener method*. The method is based on a simulation of the NTI memory system in the special manner via the functional Volterra series with the Brownian motion in the input.

Similarly to the Volterra approach, in the Wiener method, an NTI system is represented with the series

$$\begin{aligned}
 y(t) &= \mathcal{W}[x(t)]x(t) \\
 &= \mathcal{W}_0[k_0, x(t)] + \mathcal{W}_1[k_1, x(t)] + \dots + \mathcal{W}_n[k_n, x(t)] + \dots, \tag{7.58}
 \end{aligned}$$

where \mathcal{W}_n is the degree n Wiener operator and k_n is the *Wiener kernel* that is *symmetric*. Presenting the Wiener method in brief without digging the mathematical justification (the reader is referred to a book by Rugh and other special books), we notice that (7.58) is equivalently represented with

$$\begin{aligned}
 y(t) &= k_0 + \sum_{n=1}^{\infty} \sum_{i=0}^{[n/2]} \frac{(-1)^i n! A^i}{2^i (n-2i)! i!} \\
 &\times \int_{-\infty}^{\infty} \dots \int_{-\infty}^{\infty} k_n(\theta_1, \dots, \theta_{n-2i}, \lambda_1, \lambda_1, \dots, \lambda_i, \lambda_i) \\
 &d\lambda_1 \dots d\lambda_i x(t - \theta_1) \dots x(t - \theta_{n-2i}) d\theta_1 \dots d\theta_{n-2i}, \tag{7.59}
 \end{aligned}$$

where A is an intensity of the real, stationary, zero mean, and white Gaussian noise. Yet, $[n/2] \leq n/2$ means the greatest integer.

It can be shown, by comparing (7.58) and (7.59), that the degree n Wiener operator $\mathcal{W}_n[k_n, x(t)]$ is the degree n polynomial specified via the symmetric Wiener kernel $k_n(\theta_1, \dots, \theta_n)$ such that

$$\mathcal{W}_0[k_0, x(t)] = k_0, \tag{7.60}$$

$$\mathcal{W}_1[k_1, x(t)] = \int_{-\infty}^{\infty} k_1(\theta) x(t - \theta) d\theta, \tag{7.61}$$

$$\begin{aligned}
 \mathcal{W}_2[k_2, x(t)] &= \int_{-\infty}^{\infty} \int_{-\infty}^{\infty} k_2(\theta_1, \theta_2) x(t - \theta_1) x(t - \theta_2) d\theta_1 d\theta_2 \\
 &- A \int_{-\infty}^{\infty} k_2(\theta, \theta) d\theta, \tag{7.62}
 \end{aligned}$$

$$\begin{aligned} \mathcal{W}_3[k_3, x(t)] &= \int_{-\infty}^{\infty} k_3(\theta_1, \theta_2, \theta_3) x(t - \theta_1) x(t - \theta_2) x(t - \theta_3) d\theta_1 d\theta_2 d\theta_3 \\ &\quad - 3A \int_{-\infty}^{\infty} k_3(\theta_1, \theta_1, \theta) x(t - \theta) d\theta_1 d\theta. \end{aligned} \tag{7.63}$$

The higher degree kernels are defined in a like manner.

By the essence of the approach, the Wiener kernels are derived from the system structure not in such a straightforward way as the Volterra ones. Therefore, if one needs representing an NTI system with the Wiener kernels, the latter might be defined by the symmetric Volterra kernels, provided the relationship

$$\begin{aligned} k_N(\theta_1, \dots, \theta_N) &= \sum_{l=0}^{\infty} \frac{(N + 2l)! A^l}{N! l! 2^l} \\ &\times \int_{-\infty}^{\infty} h_{(N+2l)}(\theta_1, \dots, \theta_N, \lambda_1, \lambda_1, \dots, \lambda_l, \lambda_l) d\lambda_1 \dots d\lambda_l. \end{aligned} \tag{7.64}$$

Example 7.10. An NTI system is represented in Fig. 7.11 with a diagram. A linear block is described with the impulse response $h(t) = \frac{1}{\tau_c} e^{-\frac{t}{\tau_c}} u(t)$ and the nonlinear memoryless nonlinearity is cubic.

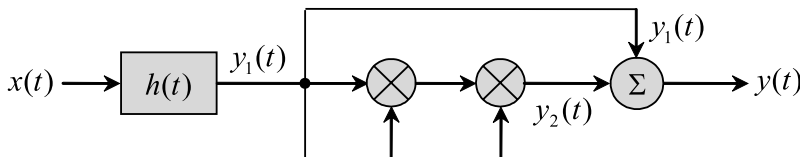


Fig. 7.11. NTI system with a cubic nonlinearity.

For the noncausal signal $x(t)$, the inner functions, $y_1(t)$ and $y_2(t)$, are defined by, respectively,

$$\begin{aligned} y_1(t) &= \int_0^{\infty} h(\theta) x(t - \theta) d\theta, \\ y_2(t) &= \int_0^{\infty} \int_0^{\infty} \int_0^{\infty} h(\theta_1) h(\theta_2) h(\theta_3) x(t - \theta_1) x(t - \theta_2) x(t - \theta_3) d\theta_1 d\theta_2 d\theta_3, \end{aligned}$$

predetermining the output to be

$$y(t) = \int_0^{\infty} h_1(\theta_1)x(t - \theta_1)d\theta_1 + \int_0^{\infty} \int_0^{\infty} \int_0^{\infty} h_3(\theta_1, \theta_2, \theta_3)x(t - \theta_1)x(t - \theta_2)x(t - \theta_3)d\theta_1d\theta_2d\theta_3, \quad (7.65)$$

where the Volterra kernels, $h_1(\theta_1)$ and $h_3(\theta_1, \theta_2, \theta_3)$, are given by, respectively,

$$h_1(\theta) = \frac{1}{\tau_c} e^{-\frac{\theta}{\tau_c}} u(\theta), \quad (7.66)$$

$$h_3(\theta_1, \theta_2, \theta_3) = \frac{1}{\tau_c^3} e^{-\frac{\theta_1 + \theta_2 + \theta_3}{\tau_c}} u(\theta_1)u(\theta_2)u(\theta_3). \quad (7.67)$$

It can be shown, using (7.64), (7.66), and (7.67), that the system is described with the two Wiener kernels

$$k_1(\theta) = \frac{1}{\tau_c} \left(1 + \frac{3A}{2} \right) e^{-\frac{\theta}{\tau_c}} u(\theta), \quad (7.68)$$

$$k_3(\theta_1, \theta_2, \theta_3) = h_3(\theta_1, \theta_2, \theta_3). \quad (7.69)$$

One can infer that, by $A = 0$, the degree $n = 1$ Wiener kernel (7.68) degenerates to the degree $n = 1$ Volterra kernel (7.63), $k_1(\theta) = h_1(\theta)$. By virtue of that, orthogonalization of the Volterra series (7.65) by the Wiener kernels is achieved only with a nonzero intensity of the induced white Gaussian noise. \square

We notice that, in line with the Volterra and Wiener approaches, some other methods are used, for example, the Fliess generating power series. Overall, in spite of their general forms for any NTI system, the Volterra, Wiener, and other available series methods allow for satisfactory modeling if systems have weak and, desirably, symmetric nonlinearities. Otherwise, one encounters at least two problems typically associated with long series:

- With a large number of the terms (large degree n), the model becomes cumbersome losing engineering features. \square
- The Gibbs⁶ phenomenon (see Signals) accompanies the model if a sharp nonlinearity is described with the finite degree series. \square

Of applied important also is that the series expansion allows providing an analysis of NTI systems in the transform domain that we discuss below.

⁶ Josiah Willard Gibbs, US theoretical physicist and chemist, 11 February 1839–28 April 1903.

7.4 Representation in the Transform Domain

Observing (7.27), one can deduce that the generalized convolution can be investigated in the transform domain if to employ the multivariate Fourier and Laplace transforms. In fact, the degree $n = 0$ Volterra operator that is a constant is specified in the transform domain by the delta function and the degree $n = 1$ operator by the product of the linearized system transfer function and transform of the input.

To define the transforms of the higher degree Volterra operators, we first need to extend the definition of the transform to the multivariate function. The two-variable forms of the Fourier transform were already used in descriptions of LTV systems. Now, let us focus our attention on the most general multivariate Laplace transform.

Supposing a multivariate function (signal or kernel) $f(t_1, \dots, t_n)$ of n variables t_1, \dots, t_n , the direct and inverse Laplace transforms of f are defined by, respectively,

$$\begin{aligned} F(s_1, \dots, s_n) &= \mathcal{L}f(t_1, \dots, t_n) \\ &= \int_{-\infty}^{\infty} \dots \int_{-\infty}^{\infty} f(t_1, \dots, t_n) e^{-s_1 t_1} \dots e^{-s_n t_n} dt_1 \dots dt_n, \\ \text{ROC} &\in [R_1, \dots, R_n], \end{aligned} \quad (7.70)$$

$$\begin{aligned} f(t_1, \dots, t_n) &= \mathcal{L}^{-1}F(s_1, \dots, s_n) \\ &= \frac{1}{(2\pi j)^n} \int_{\sigma_n - j\infty}^{\sigma_n + j\infty} \dots \int_{\sigma_1 - j\infty}^{\sigma_1 + j\infty} F(s_1, \dots, s_n) e^{s_1 t_1} \dots e^{s_n t_n} ds_1 \dots ds_n, \end{aligned} \quad (7.71)$$

where $s_i = \sigma_i + j\omega_i$, $i \in [1, n]$, is the Laplace variable. It is assumed that the region of convergence ROC is specified for every Laplace variable s_1, \dots, s_n by R_1, \dots, R_n , respectively. In particular cases, the reader can ascertain the ROCs (whenever necessary) invoking the basic properties of the Laplace transform given in Chapter 5 and Appendix D. Below, we observe the most critical properties of the multivariate Laplace transform.

7.4.1 Properties of the Multivariate Laplace Transform

Let us think that we have two or more multivariate functions f_1, \dots, f_m of the same class as $f(t_1, \dots, t_n)$ with different numbers of variables and known transforms $f_i(t_1, \dots, t_n) \stackrel{\mathcal{L}}{\Leftrightarrow} F_i(s_1, \dots, s_n)$, $i \in [1, m]$. The following properties of the Laplace transform can be applied to such functions.

Distributivity

Given f_i , then the following obvious *distributivity* property holds true

$$\mathcal{L} \sum_{i=1}^m f_i(t_1, \dots, t_n) = \sum_{i=1}^m \mathcal{L} f_i(t_1, \dots, t_n). \quad (7.72)$$

Homogeneity

Scaling f_i with a constant α is equivalent to scaling F_i with the same α . This property is known as *homogeneity*. United with (7.72), the property results in

$$\sum_{i=1}^m a_i f_i(t_1, \dots, t_n) \stackrel{\mathcal{L}}{\Leftrightarrow} \sum_{i=1}^m a_i F_i(s_1, \dots, s_n), \quad (7.73)$$

reminding us that both distributivity and homogeneity imply *linearity*.

Example 7.11. The degree $n = 2$ Volterra system is represented with the kernel $h_2(\theta_1, \theta_2) = 2e^{-2\theta_1}u(\theta_1) - 3e^{-3\theta_2}u(\theta_2)$. By the property of linearity, the two-variable transfer function of the system is defined to be

$$\begin{aligned} H_2(s_1, s_2) &= \mathcal{L}h_2(\theta_1, \theta_2) = \mathcal{L}[2e^{-2\theta_1}u(\theta_1) - 3e^{-3\theta_2}u(\theta_2)] \\ &= 2\mathcal{L}e^{-2\theta_1}u(\theta_1) - 3\mathcal{L}e^{-3\theta_2}u(\theta_2) \\ &= 2 \int_0^{\infty} e^{-(s_1+2)\theta_1} d\theta_1 - 3 \int_0^{\infty} e^{-(s_2+3)\theta_2} d\theta_2 \\ &= \frac{2s_2 - 3s_1 + 1}{(s_1 + 2)(s_2 + 3)}, \quad \text{Re}(s_1) > -2, \quad \text{Re}(s_2) > -3. \end{aligned} \quad (7.74)$$

□

Time Shifting

If every time variable t_1, \dots, t_n of a function $f(t_1, \dots, t_n)$ is individually shifted on τ_1, \dots, τ_n , respectively, then the transform of the shifted function is defined by

$$\mathcal{L}f(t_1 - \tau_1, \dots, t_n - \tau_n) = F(s_1, \dots, s_n)e^{-s_1\tau_1 - \dots - s_n\tau_n}. \quad (7.75)$$

Reminiscent of the single-variable case, the proof of (7.75) is readily provided by changing variables.

Example 7.12. The Volterra kernel of degree $n = 2$ is given by

$$h_2(\theta_1 - \tau_1, \theta_2) = 2e^{-2(\theta_1 - \tau_1)}u(\theta_1 - \tau_1) - 3e^{-3\theta_2}u(\theta_2).$$

By the time-shifting property (7.75) and the transform (7.70), the transfer function of the system is defined to be

$$\begin{aligned} H_2(s_1, s_2) &= -\frac{2}{s_1 + 2}e^{-s_1\tau_1} + \frac{3}{s_2 + 3} \\ &= \frac{3(s_1 + 2) - 2(s_2 + 3)e^{-s_1\tau_2}}{(s_1 + 2)(s_2 + 3)}, \quad \text{Re}(s_1) > -2, \quad \text{Re}(s_2) > -3. \end{aligned} \quad (7.76)$$

□

Product Transform

Assume we have a function $f(t_1, \dots, t_n)$ that is represented by the product of two subfunctions. If subfunctions are given with different variables, $f(t_1, \dots, t_n) = f_1(t_1, \dots, t_k)f_2(t_{k+1}, \dots, t_n)$, thus non-overlapped in time, the transform of f is given by

$$F(s_1, \dots, s_n) = F_1(s_1, \dots, s_k)F_2(s_{k+1}, \dots, s_n). \quad (7.77)$$

In a case of the same variables, $f(t_1, \dots, t_n) = f_1(t_1, \dots, t_n)f_2(t_1, \dots, t_n)$, the transform is represented with the convolution

$$F(s_1, \dots, s_n) = \frac{1}{(2\pi j)^n} \int_{\sigma-j\infty}^{\sigma+j\infty} F_1(s_1 - v_1, \dots, s_n - v_n)F_2(v_1, \dots, v_n)dv_1 \dots dv_n. \quad (7.78)$$

Example 7.13. A system is represented with the degree $n = 2$ Volterra kernel $h_2(\theta_1, \theta_2) = e^{-2(\theta_1 + \theta_2)}u(\theta_1)u(\theta_2)$. The kernel can be rewritten as $h_2(\theta_1, \theta_2) = e^{-2\theta_1}u(\theta_1)e^{-2\theta_2}u(\theta_2) = f_1(\theta_1)f_2(\theta_2)$ and the property (7.77) can be applied too. As a result, we have

$$\begin{aligned} F(s_1) &= \mathcal{L}e^{-2\theta_1}u(\theta_1) = \frac{1}{s_1 + 2}, \\ F(s_2) &= \mathcal{L}e^{-2\theta_2}u(\theta_2) = \frac{1}{s_2 + 2}. \end{aligned}$$

The transfer function of the system is thus defined by

$$H(s_1, s_2) = F_1(s_1)F_2(s_2) = \frac{1}{(s_1 + 2)(s_2 + 2)}. \quad (7.79)$$

□

Convolution Transform

If a function f is represented by the convolution, two important cases can be distinguished. When $f(t_1, \dots, t_n) = f_1(t_1) * f_2(t_1, \dots, t_n)$, the transform produces

$$F(s_1, \dots, s_n) = F_1(s_1 + \dots + s_n)F_2(s_1, \dots, s_n). \quad (7.80)$$

In the case of an n -fold convolution, $f(t_1, \dots, t_n) = f_1(t_1, \dots, t_n) * f_2(t_1, \dots, t_n)$, the transform is found in a manner similar to a single variable,

$$F(s_1, \dots, s_n) = F_1(s_1, \dots, s_n)F_2(s_1, \dots, s_n). \quad (7.81)$$

7.4.2 Laplace Transform of the Volterra Series

We now know enough properties to find the Laplace transform of the Volterra series (7.27) and, thereby, translate an NTI system to the transform domain.

An application of the Laplace transform to the Volterra series needs some care. To emphasize the special feature of such transformations, let us consider the degree n Volterra system

$$y(t) = \int_{-\infty}^{\infty} \dots \int_{-\infty}^{\infty} h_n(\theta_1, \dots, \theta_n)x(t - \theta_1) \dots x(t - \theta_n)d\theta_1 \dots d\theta_n. \quad (7.82)$$

As can be seen, the transform of the output $y(t)$ is one-variable, $y(s)$. In turn, the integrand in the right-hand side consists of a multivariate kernel h_n and thus the relevant transform would be a function of n variables s_1, \dots, s_n . To overcome this obvious discrepancy, it is in order to reassign the output as follows

$$y(t) = y(t_1, \dots, t_n)|_{t_1=\dots=t_n=t} \triangleq y(t, \dots, t). \quad (7.83)$$

Actually, nothing has changed. We just substituted a single-variable output with the multivariate output having equal variables. On the other hand, it allows matching the transforms of both sides of (7.82) and write

$$\begin{aligned} \mathcal{L}y_n(t) &= \mathcal{L}y_n(t_1, \dots, t_n) = Y_n(s_1, \dots, s_n) \\ &= \mathcal{L} \int_{-\infty}^{\infty} \dots \int_{-\infty}^{\infty} h_n(\theta_1, \dots, \theta_n)x(t - \theta_1) \dots x(t - \theta_n)d\theta_1 \dots d\theta_n, \end{aligned} \quad (7.84)$$

where $t = t_1 = \dots = t_n$.

By the properties (7.77) and (7.81), (7.84) instantly becomes

$$Y_n(s_1, \dots, s_n) = H(s_1, \dots, s_n)X(s_1) \dots X(s_n), \quad (7.85)$$

where $H(s_1, \dots, s_n) = \mathcal{L}h_n(\theta_1, \dots, \theta_n)$ is the *multivariate transfer function* also called the degree n *Laplace domain kernel*, or, by $s = j\omega$, *frequency domain kernel* of an NTI system. Here, $X(s_i)$, $i \in [1, n]$, is the transform of the input in the relevant scale. Now, both sides of (7.85) are matched in variables.

A generalized structure of the degree n Volterra system is shown in Fig. 7.12. Note that the multivariate transform of the input is composed, by

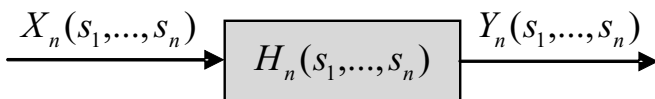


Fig. 7.12. Generalized structure of the degree n Volterra system.

(7.85), with the single variable transforms having different Laplace variables, $X_n(s_1, \dots, s_n) = X(s_1) \dots X(s_n)$.

Example 7.14. A unit step pulse acts in the input of an NTI system, $x(t) = u(t)$. A system is represented with the degree $n = 2$ Volterra kernel $h_2(\theta_1, \theta_2) = e^{-2(\theta_1+\theta_2)}u(\theta_1)u(\theta_2)$.

Using (7.82) and (7.83), the output can be represented as

$$\begin{aligned}
 y(t_1, t_2) &= \int_{-\infty}^{\infty} \int_{-\infty}^{\infty} e^{-2(\theta_1+\theta_2)}u(\theta_1)u(\theta_2)u(t_1 - \theta_1)u(t_2 - \theta_2)d\theta_1d\theta_2 \\
 &= \int_0^{t_1} \int_0^{t_2} e^{-2(\theta_1+\theta_2)}d\theta_1d\theta_2 = \frac{1}{4} (1 - e^{-2t_1}) (1 - e^{-2t_2}) u(t_1)u(t_2) \quad (7.86)
 \end{aligned}$$

and, by $t_1 = t_2 = t$, (7.86) becomes

$$y(t) = \frac{1}{4} (1 - e^{-2t})^2 u(t). \quad (7.87)$$

The transfer function (7.79) of this system is found in Example 7.13. Because of $\mathcal{L}u(t) = 1/s$, the Laplace transform of the output becomes, by (7.85),

$$Y(s_1, s_2) = \frac{1}{s_1s_2(s_1 + 2)(s_2 + 2)}. \quad (7.88)$$

To be absolutely sure that (7.88) corresponds to (7.87), we recall that $t_1 = t_2 = t$, apply the inverse Laplace transform to (7.87), and find

$$y(t) = \frac{1}{(2\pi j)^2} \int_{\sigma-j\infty}^{\sigma+j\infty} Y(s_1, s_2)e^{-s_1t_1-s_2t_2}ds_1ds_2$$

$$= \left[\frac{1}{2\pi j} \int_{\sigma-j\infty}^{\sigma+j\infty} \frac{e^{st}}{s(s+2)} ds \right]^2 = \left[\mathcal{L}^{-1} \frac{1}{s(s+2)} \right]^2.$$

Now take $\frac{1}{(s-a)(s-b)} \xleftrightarrow{\mathcal{L}} \frac{1}{a-b} (e^{at} - e^{bt})$ from a table of the Laplace transforms (Appendix D) and set $b = 0$ and $a = -2$. After simple manipulations, we arrive at (7.87) and the verification is complete. \square

7.4.3 System Representation in the Transform Domain

The fundamental relation (7.85) and basic structure shown in Fig. 7.12 allow representing different NTI systems in the transform domain by block diagrams. Typically, of interest are two kinds of cascade interconnections observed below.

When the degree n NTI system follows by an LTI system, the structure becomes as in Fig. 7.13a, for which the multivariate kernel h_{1n} is defined by the convolution as

$$\begin{aligned} h_{1n}(t_1, \dots, t_n) &= h(t) * h_n(t_1, \dots, t_n) \\ &= \int_{-\infty}^{\infty} h(\theta) h_n(t_1 - \theta, \dots, t_n - \theta) d\theta. \end{aligned} \tag{7.89}$$

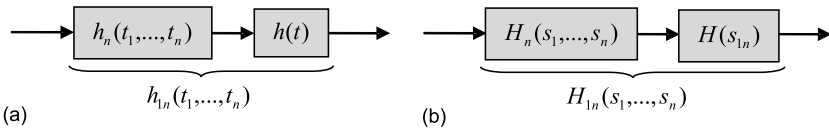


Fig. 7.13. Cascade of NTI and LTI systems: (a) time domain and (b) transform domain.

By (7.80), the transform of (7.89) can be written as

$$H(s_1, \dots, s_n) = H_n(s_1, \dots, s_n) H(s_1 + \dots + s_n) \tag{7.90}$$

and represented by the diagram as in Fig. 7.13b, where $s_{1n} = s_1 + \dots + s_n$.

In the second possible case, an LTI system follows by an NTI system (Fig. 7.14a) and the resulting kernel h_{2n} is defined by the convolution as

$$h_{2n}(t_1, \dots, t_n) = \int_{-\infty}^{\infty} \dots \int_{-\infty}^{\infty} h_n(\theta_1, \dots, \theta_n) h(t_1 - \theta_1) \dots h(t_n - \theta_n) d\theta_1 \dots d\theta_n. \tag{7.91}$$

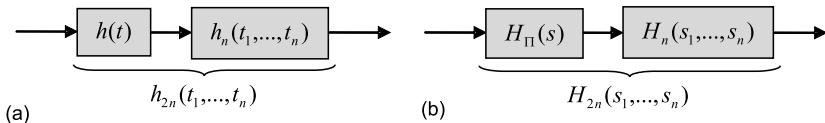


Fig. 7.14. Cascade of LTI and NTI systems: (a) time domain and (b) transform domain.

By (7.77) and (7.81), the transform of (7.91) can easily be defined to be

$$H_{2n}(s_1, \dots, s_n) = H(s_1) \dots H(s_n) H_n(s_1, \dots, s_n). \tag{7.92}$$

A structural representation of (7.92) is given in Fig. 7.14b, where we assigned $H_{II}(s) = H(s_1)H(s_2) \dots H(s_n)$.

Below, we observe a typical example demonstrating an efficiency of (7.90) and (7.92) in finding the transfer function of an NTI system.

Example 7.15. Consider an NTI system organized as in Fig. 7.15a. To define the transfer function, the structure can be represented in different equivalent forms shown in Figs. 7.15b-d. Respectively, the transfer function can also be found in different ways.

A linear part of the system following by the multiplier can be represented as in Fig. 7.15b with two branched having the transform domain kernels $H_1(s)H_2(s)$ and $H_1(s)H_3(s)$. A part following by $H_4(s)$ can now be described by the transform $F_1(s_1, s_2) = H_1(s_1)H_2(s_1)H_1(s_2)H_3(s_2)$. By (7.90), the transfer function of the system becomes

$$H_2(s_1, s_2) = H_1(s_1)H_1(s_2)H_2(s_1)H_3(s_2)H_4(s_1 + s_2). \tag{7.93}$$

The system can be split into NTI (left) and LTI (right) subsystems as shown in Fig. 7.15c. Then $F_1(s_1, s_2)$ is defined in a manner identical to that used for Fig. 7.15b and we arrive at the same transfer function (7.93).

One can also split the system into two parts as in Fig. 7.15d and, first, consider the right block (dashed). By (7.90), the transform domain kernel of this subsystem is provided to be $F_2(s_1, s_2) = H_2(s_1)H_3(s_2)H_4(s_1 + s_2)$ and, by (7.92), we have the same transfer function (7.93) of the whole system. \square

Example 7.16. An NTI system is represented with the transfer function

$$H_3(s_1, s_2, s_3) = \frac{1}{s_2} \left[\frac{1}{s_1(1 + s_1 + s_2)} + \frac{1}{s_3(1 + s_2 + s_3)} \right]. \tag{7.94}$$

To restore the diagram associated with (7.94), we first notice that each of the terms composing $H_3(s_1, s_2, s_3)$ consists of the transform domain kernel dependent on the sum of the Laplace variables. This means that the system

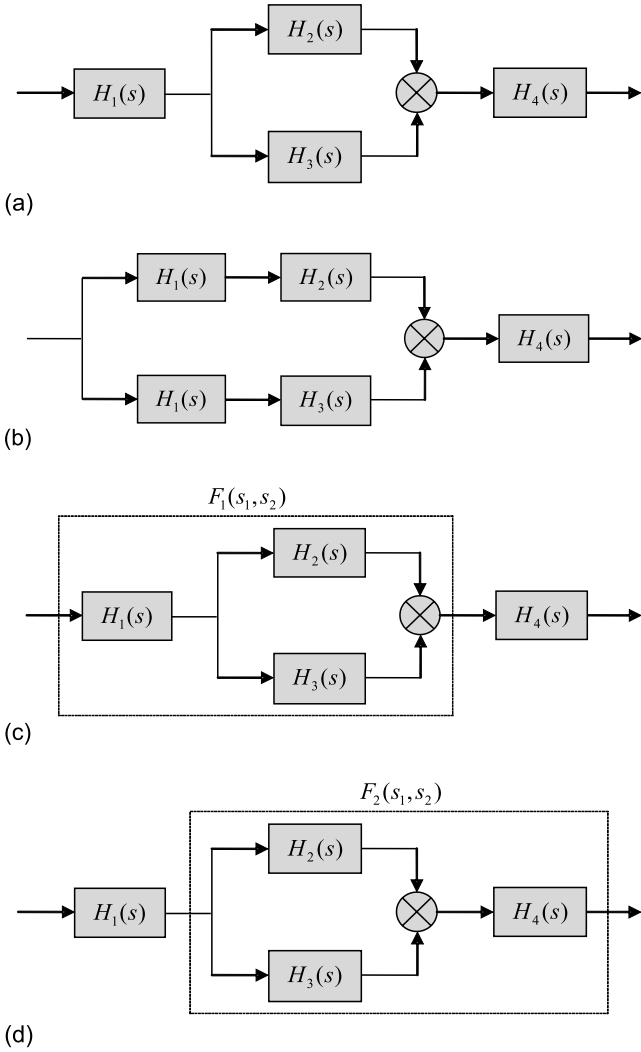


Fig. 7.15. Equivalent forms of block diagrams of an NTI system.

is represented with two subsystems shown in Fig. 7.15b. The block diagram of the system thus becomes as in Fig. 7.16.

It can easily be verified that the kernels

$$H_1(s) = H_2(s) = H_3(s) = \frac{1}{s},$$

$$H_4(s) = H_5(s) = \frac{1}{1+s}$$

of the diagram (Fig. 7.16) exactly fit the transfer function (7.94). □

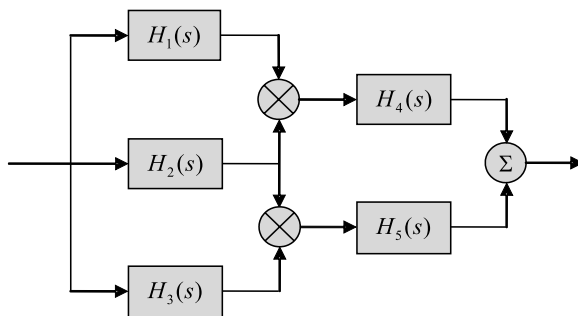


Fig. 7.16. Block diagram of an NTI system (7.94).

7.5 Approximation by Describing Functions

To continue with our description of the input-to-output NTI systems, we remind the reader that the Volterra series method becomes low efficient if non-linearity is sharp. A competitive approximate engineering approach is known as the *describing function* (DF) method produced by the classical method of equivalent linearization. Reminiscent of the familiar harmonic balance, the method is applicable for both memory and memoryless systems.

7.5.1 System Representation with Describing Functions

The basic idea of the DF method is illustrated in Fig. 7.17. Assume we have an arbitrary input $x(t)$ passing through an NTI system to produce the output $y(t)$ (Fig. 7.17a). The DF methods suggests expanding $x(t)$ to the series of subsignals $x_1(t), \dots, x_m(t)$. For these subsignals, the impulse responses $h_1(t), \dots, h_m(t)$ are found to produce the suboutputs $y_1(t), \dots, y_m(t)$, respectively. All suboutputs are added to yield an approximate output $y_a(t)$. By this, an NTI system is linearized as shown in Fig. 7.17b. In order for $y_a(t)$ to be closer to the real signal $y(t)$, all impulse responses are searched in the sense of the minimum mean square error.

Basically, any basis of subsignals $x_i(t)$, $i \in [1, m]$, can be used being not obligatory orthogonal. Electronic systems, however, are usually associated with the 2π -periodicity. Therefore, they are typically interested in an expansion of a signal $x(t)$ to the Fourier series.

A great deal of practical problems are solved by accounting in the signal $x(t)$ only the first (or fundamental) harmonic. If $x(t)$ is substituted with a harmonic wave (cosine or sine) with the amplitude r , then the first harmonic of the output can be found as the complex amplitude $c_1 e^{-j\psi_1}$. The relevant gain of such a linearized system is evaluated by the ratio of the amplitudes

$$N(r, j\omega) = \frac{c_1}{r} e^{-j\psi_1} \quad (7.95)$$

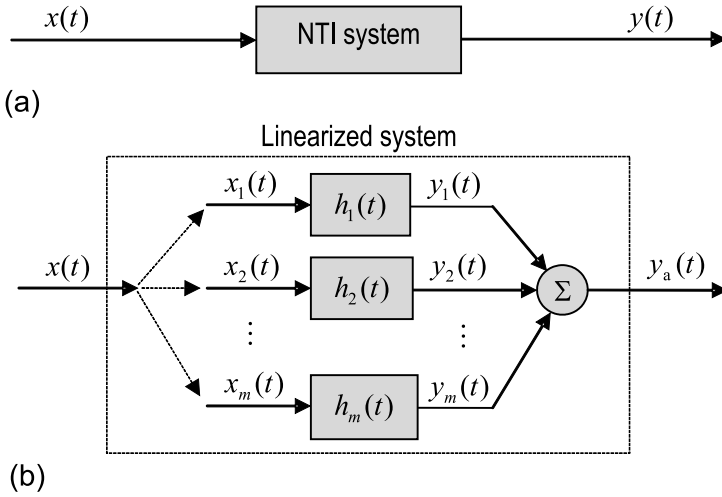


Fig. 7.17. NTI system: (a) general structure and (b) linearized by the DF method.

called the *describing function*. The function (7.95) is thus kind of frequency response of a linearized system and the system response to the harmonic input is hence evaluated by $y(t) = N(r, j\omega)x(t)$.

Such a simplification, like other attempts of linearization, does not seem to be useful for subtle NTI structures. Instead, the approach allows solving many problems in open and closed NTI systems, such as predicting limit cycles, that makes the DF method useful in engineering practice. Extensive investigations of the method were provided by Gelb and Velde.

Cosine Input Signal

Suppose we have a SISO NTI system with the cosine input

$$x(t) = r \cos \omega t = r e^{-j0} \cos \omega t. \tag{7.96}$$

By van der Pol's variables, (2.90) and (2.91), the output associated with (7.96) for an arbitrary general nonlinearity $y(x, x')$ can be performed as

$$y(t) = \mathcal{O}(x)x(t) = y(x, x') = y(r \cos \omega t, -r\omega \sin \omega t). \tag{7.97}$$

Formally, we can expand (7.97) to the Fourier series

$$y(r \cos \omega t, -r\omega \sin \omega t) = \sum_{k=1}^{\infty} c_k \cos(k\omega t - \Psi_k) \tag{7.98}$$

that, saving only the first harmonic, gives

$$y(r \cos \omega t, -r\omega \sin \omega t) \cong c_1 \cos(\omega t - \Psi_1). \quad (7.99)$$

By multiplying (7.99) with $\cos \omega t$ or $\sin \omega t$ and thereafter averaging the product over ωt from $-\pi$ to π , we arrive at two equations, respectively,

$$c_1 \cos \Psi_1 = \frac{1}{\pi} \int_{-\pi}^{\pi} y(r \cos \omega t, -r\omega \sin \omega t) \cos \omega t \, d\omega t, \quad (7.100)$$

$$c_1 \sin \Psi_1 = \frac{1}{\pi} \int_{-\pi}^{\pi} y(r \cos \omega t, -r\omega \sin \omega t) \sin \omega t \, d\omega t. \quad (7.101)$$

The complex amplitude of the output can now be found by multiplying (7.101) with $-j$ and then summing (7.100) and (7.101) that gives

$$c_1 e^{-j\Psi_1} = \frac{1}{\pi} \int_{-\pi}^{\pi} y(r \cos \omega t, -r\omega \sin \omega t) e^{-j\omega t} \, d\omega t. \quad (7.102)$$

In virtue of (7.99) and (7.102), the linearized system produces the following output

$$y(t) = c_1 e^{-j\Psi_1} \cos \omega t. \quad (7.103)$$

By (7.95), the DF for the cosine input can now be defined as

$$N(r, j\omega) = \frac{1}{\pi r} \int_{-\pi}^{\pi} y(r \cos \omega t, -r\omega \sin \omega t) e^{-j\omega t} \, d\omega t \quad (7.104)$$

or, if a system lost memory, by

$$N(r) = \frac{1}{\pi r} \int_{-\pi}^{\pi} y(r \cos \omega t) e^{-j\omega t} \, d\omega t. \quad (7.105)$$

Finally, the output of a linearized system is described by

$$y(t) = N(r, j\omega)x(t), \quad (7.106)$$

where $N(r, j\omega)$ is predefined either by (7.105) or (7.106).

Example 7.17 (Relay System). Given a memoryless relay system with a nonlinearity described by $y(x) = Au(x) - Au(-x)$. For the cosine input $x(t) = r \cos \omega t$, the output is a periodic rectangular pulse train (Fig. 7.18).

By (7.105), the DF is obtained to be

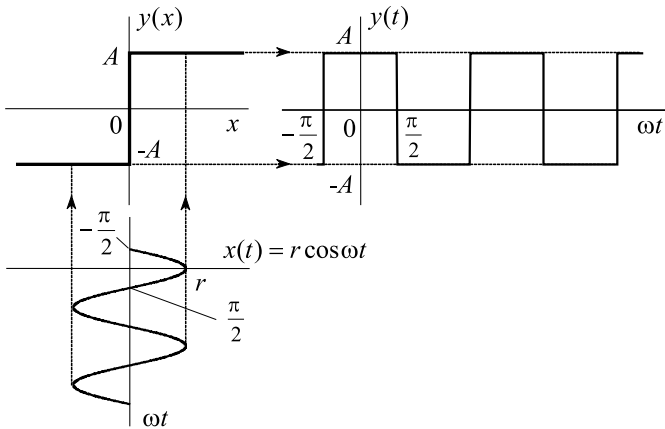


Fig. 7.18. Signal transformation in a relay memoryless system.

$$\begin{aligned}
 N(r) &= \frac{1}{\pi r} \int_{-\pi}^{\pi} y(r \cos \omega t) e^{-j\omega t} d\omega t \\
 &= \frac{A}{\pi r} \left(\int_{-\pi/2}^{\pi/2} e^{-j\omega t} d\omega t - \int_{\pi/2}^{3\pi/2} e^{-j\omega t} d\omega t \right) = \frac{4A}{\pi r}. \tag{7.107}
 \end{aligned}$$

□

Example 7.18 (Backlash). Consider a memory NTI system, which nonlinearity is represented with the hysteresis loop called the *backlash*. When the nonlinearity restricts the amplitude of a cosine input, $r > A$, the signals are formed as in Fig. 7.19.

To define the DF, one needs determining the values of phases, corresponding to points at which the piecewise nonlinearity changes in the direct and back ways. In doing so, we assign $y_1 = a(x + \delta)$ and $y_2 = a(x - \delta)$ to be the backward and toward linear branches of a backlash, respectively.

The phase ϕ_1 is defined by an equality $y_1 = a(x_1 + \delta) = A$ that gives $x_1 = (A - a\delta)/a$. Equating the value of x_1 to $r \cos \phi_1$ yields

$$\phi_1 = \arccos \frac{A - a\delta}{ar}. \tag{7.108}$$

Reasoning similarly, the reminding phases are determined to be

$$\phi_2 = \arccos \frac{-A - a\delta}{ar}, \tag{7.109}$$

$$\phi_3 = 2\pi - \arccos \frac{-A + a\delta}{ar}, \tag{7.110}$$

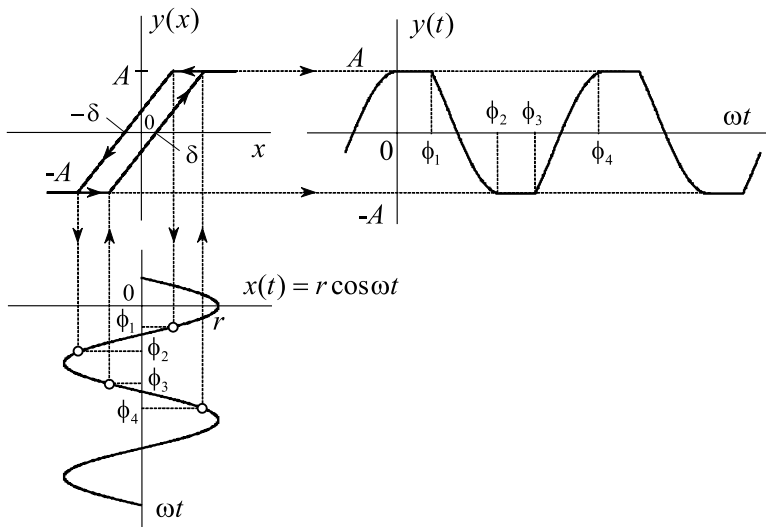


Fig. 7.19. Signal transformation in a backlash memory system.

$$\phi_4 = 2\pi - \arccos \frac{A + a\delta}{ar} . \tag{7.111}$$

The DF is now defined, by (7.104), as in the following,

$$\begin{aligned} N(r, j\omega) &= \frac{A}{\pi r} \int_0^{\phi_1} e^{-j\omega t} d\omega t - \frac{A}{\pi r} \int_{\phi_2}^{\phi_3} e^{-j\omega t} d\omega t + \frac{A}{\pi r} \int_{\phi_4}^{2\pi} e^{-j\omega t} d\omega t \\ &+ \frac{a}{\pi r} \int_{\phi_1}^{\phi_2} (r \cos \omega t + \delta) e^{-j\omega t} d\omega t + \frac{a}{\pi r} \int_{\phi_3}^{\phi_4} (r \cos \omega t - \delta) e^{-j\omega t} d\omega t \\ &= j \frac{A - a\delta}{\pi r} (e^{-j\phi_1} - e^{-j\phi_3}) + j \frac{A + a\delta}{\pi r} (e^{-j\phi_2} - e^{-j\phi_4}) \\ &+ \frac{a}{2\pi} (\phi_2 - \phi_1 - \phi_3 + \phi_4) + j \frac{a}{4\pi} (e^{-2j\phi_2} - e^{-2j\phi_1} - e^{-2j\phi_3} + e^{-2j\phi_4}) \\ &= \frac{a}{2} \left[f \left(\frac{A}{ar} + \frac{\delta}{r} \right) + f \left(\frac{A}{ar} - \frac{\delta}{r} \right) \right] - j \frac{4A\delta}{\pi r^2} , \end{aligned} \tag{7.112}$$

where an auxiliary function is

$$f(u) = \begin{cases} -1 & \text{if } u < -1 \\ \frac{2}{\pi} (a \sin u + u\sqrt{1-u^2}) & \text{if } |u| \leq 1 \\ 1 & \text{if } u > 1 \end{cases} . \tag{7.113}$$

Fig. 7.20 illustrates $x(t)$, $y(t)$, and $y_a(t)$ for $a = 1$ and $\delta = 0.5$.

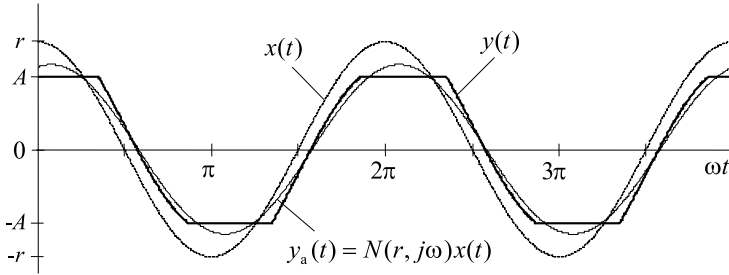


Fig. 7.20. Signals in a backlash memory system.

Observing Fig. 7.20 and comparing $x(t)$ with $y(t)$ and $y_a(t)$, one can indicate the effect of phase delay associated with system's memory. Depending on δ , the effect becomes more or less brightly pronounced. By $\delta = 0$, all signals coincide in phase. The latter case having its own applied significance is examined below. \square

Example 7.19 (Saturation). A particular case of the backlash system with $\delta = 0$ describes the saturation effect in linear memoryless systems. In view of $\delta = 0$, the transformation of signals is obtained as in Fig. 7.21.

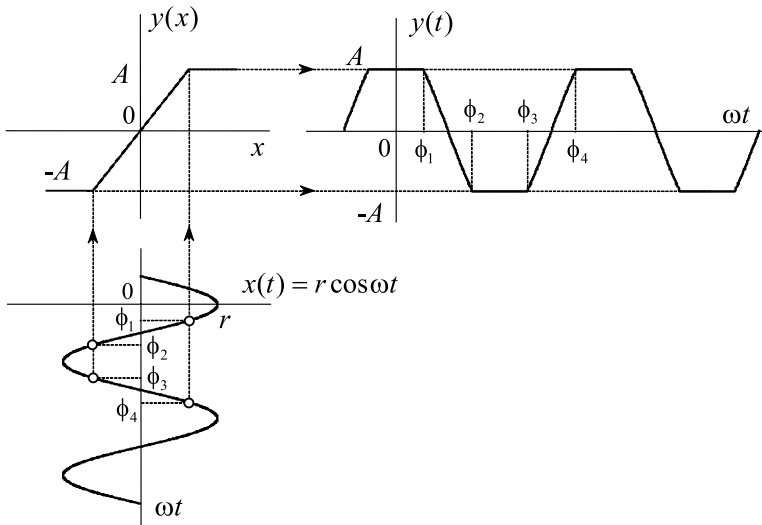


Fig. 7.21. Signal transformation in a memoryless system with saturation.

As it follows from Fig. 7.21, the DF $N(r)$ can be derived by (7.105) if we integrate from 0 to π involving two angles $\phi_1 = \arccos \frac{A}{ar}$ and $\phi_2 = \pi - \phi_1$.

That leads to

$$\begin{aligned}
 N(r) &= \frac{2A}{\pi r} \int_0^{\phi_1} e^{-j\omega t} d\omega t - \frac{2A}{\pi r} \int_{\phi_2}^{\pi} e^{-j\omega t} d\omega t \\
 &\quad + \frac{2a}{\pi} \int_{\phi_1}^{\phi_2} \cos \omega t e^{-j\omega t} d\omega t \\
 &= \frac{4A}{\pi r} \sin \phi_1 + \frac{a}{\pi} (\pi - 2\phi_1 - \sin 2\phi_1). \tag{7.114}
 \end{aligned}$$

The signals $x(t)$, $y(t)$, and $y_a(t)$ are shown Fig. 7.22 for $a = 1$. Contrary

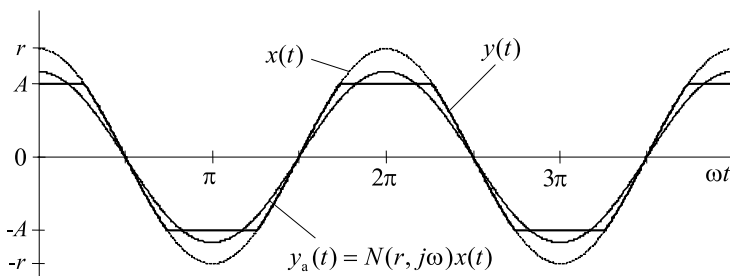


Fig. 7.22. Signals in a memoryless system with saturation.

to Fig. 7.20, no phase shift occurs here between the signals. The only easily seen effect is produced by saturation at the level of $\pm A$. \square

Sinusoidal Input Signal

Let us now suppose that the input is sinusoidal,

$$x(t) = r \sin \omega t = r e^{-j0} \sin \omega t, \tag{7.115}$$

and describe the output by

$$y(t) = \mathcal{O}(x)x(t) = y(r \sin \omega t, r\omega \cos \omega t). \tag{7.116}$$

Similarly to the cosine input, one can expand (7.116) to the Fourier series

$$y(r \sin \omega t, r\omega \cos \omega t) = \sum_{k=1}^{\infty} c_k \sin(k\omega t - \Psi_k) \tag{7.117}$$

and derive the DF for the memory and memoryless cases to be, respectively,

$$N(r, j\omega) = \frac{j}{\pi r} \int_{-\pi}^{\pi} y(r \sin \omega t, r\omega \cos \omega t) e^{-j\omega t} d\omega t, \quad (7.118)$$

$$N(r) = \frac{j}{\pi r} \int_{-\pi}^{\pi} y(r \sin \omega t) e^{-j\omega t} d\omega t. \quad (7.119)$$

As can be seen, (7.118) and (7.119) associated with the sinusoidal input differ from (7.104) and (7.105), respectively, corresponding to the cosine input. This does not mean, however, that the final expressions for $N(r, j\omega)$ and $N(r)$ also differ for the cosine and sinusoidal inputs.

Example 7.20 (Relay System). Consider the familiar relay system (Fig. 7.18) allowing for the sinusoidal input. By (7.119), the DF is defined to be

$$\begin{aligned} N(r) &= \frac{j}{\pi r} \int_{-\pi}^{\pi} y(r \sin \omega t) e^{-j\omega t} d\omega t \\ &= \frac{Aj}{\pi r} \left(\int_0^{\pi} e^{-j\omega t} d\omega t - \int_{\pi}^{2\pi} e^{-j\omega t} d\omega t \right) = \frac{4A}{\pi r}. \end{aligned} \quad (7.120)$$

One infers that the DF (7.120), derived for the sinusoidal input is exactly that (7.107) derived for the cosine input. \square

Example 7.21 (Dead Zone). Consider a nonlinear unit with a dead zone in a gap of $\pm\delta$ at zero. For the sinusoidal input with the amplitude $r > \delta$, the signal is transformed as in Fig. 7.23 with the angles $\phi_1 = \arcsin \frac{\delta}{r}$, $\phi_2 = \pi - \phi_1$, $\phi_3 = \pi + \phi_1$, and $\phi_4 = 2\pi - \phi_1$.

By (7.119), similarly to Example 7.18, the DF is derived to be

$$N(r) = \frac{a}{\pi} \left(\pi - 2\phi_1 - \frac{2\delta}{r} \sqrt{1 - \frac{\delta^2}{r^2}} \right). \quad (7.121)$$

\square

We notice that the DF method, as a product of equivalent linearization, can be applied whenever the NTI (memory or memoryless) system needs to be analyzed for harmonic inputs. It can also be applied for combined harmonic signal (bi-harmonic, etc.). To pass through the transformation routine with a minimum burden, the following properties of the DFs are usually used.

7.5.2 Properties of Describing Functions

The necessity of observing the properties of described functions arises, at least, from the fact that the general relations for DFs associated with cosine and sine inputs are different, whereas for particular nonlinearities they are equal.

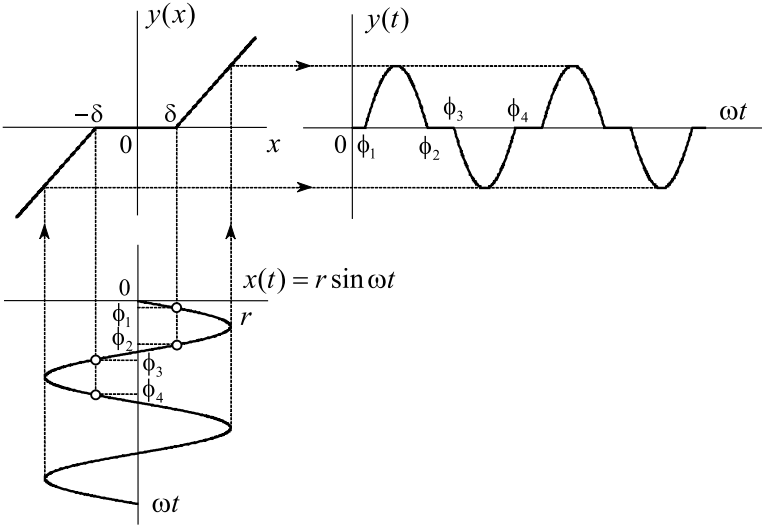


Fig. 7.23. Signal transformation in a memoryless system with a dead zone.

Uniqueness

Consider a general nonlinearity $y(x, x')$. The DF for a sinusoidal input is provided by (7.118). Substituting $\sin \omega t = \cos(\omega t - \frac{\pi}{2})$, we go to

$$N(r, j\omega) = \frac{j}{\pi r} \int_{2\pi} y \left[r \cos \left(\omega t - \frac{\pi}{2} \right), -r\omega \sin \left(\omega t - \frac{\pi}{2} \right) \right] e^{-j\omega t} d\omega t .$$

By changing a variable, $\psi = \omega t - \frac{\pi}{2}$, the relation becomes

$$\begin{aligned} N(r, j\omega) &= \frac{j}{\pi r} \int_{2\pi} y(r \cos \psi, -r\omega \sin \psi) e^{-j\frac{\pi}{2}} e^{-j\psi} d\psi \\ &= \frac{1}{\pi r} \int_{2\pi} y(r \cos \psi, -r\omega \sin \psi) e^{-j\psi} d\psi \end{aligned} \tag{7.122}$$

that is exactly (7.104) derived for the cosine signal. This means that the DF is unique for the given nonlinear function. The uniqueness suggests that the relation to derive the DF depends on the phase shift in the harmonic input and that the DF itself does not depend on this shift. The property is supported by Examples 7.17 and 7.20.

We notice that, for the reason of uniqueness of the DF, the input is often chosen to be sinusoidal.

Complexity

The DF of a generalized memory system is a complex function. As such, it can be represented as

$$N(r, j\omega) = N_a(r, \omega) + jN_r(r, \omega), \quad (7.123)$$

where the real component $N_a(r, \omega)$ and imaginary component $N_r(r, \omega)$ are defined as follows. Consider (7.118) and substitute the exponential function with the Euler formula, $e^{-j\omega t} = \cos \omega t - j \sin \omega t$. It gives

$$\begin{aligned} N(r, j\omega) &= \frac{j}{\pi r} \int_{-\pi}^{\pi} y(r \sin \omega t, r\omega \cos \omega t) \cos \omega t \, d\omega t \\ &+ \frac{1}{\pi r} \int_{-\pi}^{\pi} y(r \sin \omega t, r\omega \cos \omega t) \sin \omega t \, d\omega t = N_a(r, \omega) + jN_r(r, \omega) \end{aligned} \quad (7.124)$$

and thus

$$N_a(r, \omega) = \frac{1}{\pi r} \int_{-\pi}^{\pi} y(r \sin \omega t, r\omega \cos \omega t) \sin \omega t \, d\omega t, \quad (7.125)$$

$$N_r(r, \omega) = \frac{1}{\pi r} \int_{-\pi}^{\pi} y(r \sin \omega t, r\omega \cos \omega t) \cos \omega t \, d\omega t. \quad (7.126)$$

The real DF (7.125) produces the output that coincides in phase with the input. Therefore, it is called the *in-phase gain*. In turn, (7.126) is said to be the *quadrature phase gain*, because the output is shifted on $\pi/2$ for the input.

Alternatively, (7.123) can be expressed in the polar coordinates as

$$N(r, j\omega) = \rho(r, \omega) e^{j\varphi(r, \omega)}, \quad (7.127)$$

where the radius and phase are specified by, respectively,

$$\rho(r, \omega) = \sqrt{N_a^2(r, \omega) + N_r^2(r, \omega)}, \quad (7.128)$$

$$\tan \varphi(r, \omega) = \frac{N_r(r, \omega)}{N_a(r, \omega)}. \quad (7.129)$$

Knowing $\rho(r, \omega)$ and $\varphi(r, \omega)$, one can define the in-phase and quadrature phase gains by, respectively,

$$N_a(r, \omega) = \rho(r, \omega) \cos \varphi(r, \omega), \quad (7.130)$$

$$N_r(r, \omega) = \rho(r, \omega) \sin \varphi(r, \omega). \quad (7.131)$$

Example 7.22. A memory NTI system is represented with the DF (7.112). The real and imaginary components of the DF are, respectively,

$$N_a(r, \omega) = \frac{a}{2} \left[f \left(\frac{A}{ar} + \frac{\delta}{r} \right) + f \left(\frac{A}{ar} - \frac{\delta}{r} \right) \right],$$

$$N_r(r, \omega) = -\frac{4A\delta}{\pi r^2},$$

where an auxiliary function f is defined by (7.113). \square

Memoryless Nonlinearity

Consider the DF for a general memoryless nonlinearity (7.119). For a sinusoidal input, the output is expanded to the sinusoidal Fourier series. Because the integration of the product $(\sin n\omega t) \cos \omega t$, where n is integer, over ωt from $-\pi$ to π produces zero we have two equal forms of $N(r)$,

$$\begin{aligned} N(r) &= \frac{j}{\pi r} \int_{-\pi}^{\pi} y(r \sin \omega t) e^{-j\omega t} d\omega t \\ &= \frac{1}{\pi r} \int_{-\pi}^{\pi} y(r \sin \omega t) \sin \omega t d\omega t = N_a(r), \end{aligned} \quad (7.132)$$

meaning that $N(r)$ is a real function.

Memoryless Odd Nonlinearity

If an NTI system is memoryless and nonlinearity is odd, $y(x) = -y(-x)$, the DF is calculated for the restricted bounds as

$$N(r) = \frac{2j}{\pi r} \int_0^{\pi} y(r \sin \omega t) e^{-j\omega t} d\omega t. \quad (7.133)$$

In fact, for a general memoryless nonlinearity (7.119), we can write

$$\begin{aligned} N(r) &= \frac{j}{\pi r} \int_{-\pi}^0 y(r \sin \omega t) e^{-j\omega t} d\omega t + \frac{j}{\pi r} \int_0^{\pi} y(r \sin \omega t) e^{-j\omega t} d\omega t \\ &= N_1(r) + N_2(r) \end{aligned}$$

Inducing a phase shift π and recalling that $y(x) = -y(-x)$, we rewrite the first integral as

$$\begin{aligned} N_1(r) &= \frac{j}{\pi r} \int_{-\pi}^0 y(r \sin \omega t) e^{-j\omega t} d\omega t \\ &= \frac{j}{\pi r} \int_{-\pi+\pi}^{\pi} y[r \sin(\omega t - \pi)] e^{j\pi} e^{-j\omega t} d(\omega t - \pi) \end{aligned}$$

$$= -\frac{j}{\pi r} \int_0^{\pi} y(-r \sin \omega t) e^{-j\omega t} d\omega t = \frac{j}{\pi r} \int_0^{\pi} y(r \sin \omega t) e^{-j\omega t} d\omega t$$

that is equal to the second integral $N_2(r)$ and we arrive at (7.133). This property was exploited in Example 7.19.

In view of (7.132), we also have

$$N(r) = \frac{2}{\pi r} \int_{-\pi/2}^{\pi/2} y(r \sin \omega t) \sin \omega t d\omega t. \quad (7.134)$$

Since the integrand in (7.134) is a function symmetric about zero, (7.134) can also be calculated by

$$N(r) = \frac{4}{\pi r} \int_0^{\pi/2} y(r \sin \omega t) \sin \omega t d\omega t. \quad (7.135)$$

So, for the memoryless odd nonlinearity, three equal forms of $N(r)$ are available, namely those provided by (7.133)–(7.135).

Example 7.23. Consider a memoryless system with an odd nonlinearity $y(x) = x^3$. By (7.119), the DF is defined to be

$$\begin{aligned} N(r) &= \frac{jr^2}{\pi} \int_{-\pi}^{\pi} \sin^3 \omega t e^{-j\omega t} d\omega t \\ &= \frac{jr^2}{\pi} \int_{-\pi}^{\pi} \sin^3 \omega t \cos \omega t d\omega t + \frac{r^2}{\pi} \int_{-\pi}^{\pi} \sin^4 \omega t d\omega t \\ &= \frac{r^2}{\pi} \int_{-\pi}^{\pi} \sin^4 \omega t d\omega t = \frac{r^2}{\pi} \left. \frac{3}{8} d\omega t \right|_{-\pi}^{\pi} = \frac{3r^2}{4}. \end{aligned} \quad (7.136)$$

Alternatively, one can follow (7.133)–(7.135). Observe that different integral forms lead to the same result (7.136). \square

Overall, the DF method is a very convenient and useful tool to solve a great deal of nonlinear problems. As a product of equivalent linearization, it is essentially a unified approach to linearize an NTI system in steady-state and define the frequency response. In this regard, the method is more practicable than the Volterra approach. On the other hand, the DF is inappropriate in transient and becomes almost useless, when an exact shape of an output is of concern. If so, the Volterra series and presentation by differential equations have no alternative.

7.6 Description by Differential Equations

Representation of NTI systems with ODEs is usually achieved in the most short form. Most generally, a SISO NTI system is performed with the N -order nonlinear ODE that for the highest order time derivative of the output $y(t)$ can be written as

$$\frac{d^N y}{dt^N} = f \left(y, \frac{dy}{dt}, \dots, \frac{d^{N-1}y}{dt^{N-1}}, x, \frac{dx}{dt}, \dots, \frac{d^M x}{dt^M} \right), \quad (7.137)$$

where $M \leq N$. Because the nonlinear function f in the right-hand side can be arbitrary, the general solution of (7.137) cannot be found. This lamentable peculiarity of nonlinear ODEs is so strong that, even for the particular forms, not every equation can be solved analytically. Therefore, the qualitative methods are used widely to sketch a picture associated with the system dynamics.

On the other hand, not every nonlinear ODE needs to be solved exactly. In a great deal of engineering problems, of interest is a certain spectral content of $y(t)$, rather than its full spectrum. Examples may be found in systems with both weak and strong nonlinearities. Moreover, nonlinearity is often formed intentionally to produce or gain one spectral component and suppress others.

By virtue of the fact that an exact solution is typically hard to find and often unnecessary for applications, many efforts have been made for centuries to find and develop the approximate methods. After discussing an exact solution of the Bernoulli⁷ nonlinear ODE of the first order, we shall observe the most widely used approximate methods.

7.6.1 System of the First Order (Bernoulli's Equation)

Among a variety of NTI systems of the first order, are many closed loop representatives described by the Bernoulli equation. The equation allows investigating both weak and sharp nonlinearities.

Before discussing the nonlinear case, let us consider an LTI system described by

$$y' + ay = bx, \quad (7.138)$$

where a and b are some constants. We can suppose that the input $x(t)$ is coupled with the output $y(t)$, by the nonlinear feedback, as $x(t) = y^\alpha(t)$, where $\alpha \neq 1$ is real. The closed loop is thus described with the nonlinear ODE

$$y' + ay = by^\alpha \quad (7.139)$$

known as the *Bernoulli equation*.

⁷ Jacob (Jacques) Bernoulli, Swiss mathematician, 27 December 1654–16 August 1705.

An exact solution of (7.139) can be found by changing a variable, $u = y^{1-\alpha}$, that transforms (7.139) to the linear ODE

$$u' + cu = d, \quad (7.140)$$

where $c = a(1 - \alpha)$ and $d = b(1 - \alpha)$. Using the standard trick with the integration factor (Chapter 4), further integrating from t_0 to t , and thereafter returning to the original variable yield

$$\begin{aligned} y(t) &= {}^{1-\alpha} \sqrt{e^{-a(1-\alpha)(t-t_0)} \left[b(1-\alpha) \int_{t_0}^t e^{a(1-\alpha)(\tau-t_0)} d\tau + C \right]} \\ &= {}^{1-\alpha} \sqrt{\frac{b}{a} + \left(C - \frac{b}{a} \right) e^{-a(1-\alpha)(t-t_0)}}, \end{aligned} \quad (7.141)$$

where a constant C is determined by the initial condition $y(t_0) = y_0$ at t_0 to be $C = y_0^{1-\alpha}$. A simple observation shows that the solution starts with y_0 at t_0 and can either converge or diverge depending on the coefficients.

Example 7.24. Consider an NTI system described by the Bernoulli ODE (7.139) with $a = 2$, $b = 1$, and $\alpha = 3$,

$$y' + 2y = y^3. \quad (7.142)$$

The initial condition is $y_0 = y(t_0)$. By (7.141), the solution becomes

$$y(t) = y_0 \sqrt{\frac{e^{-2t}}{1 - 2y_0^2(1 - e^{-2t})}}. \quad (7.143)$$

It is seen that, by $t = t_0$, the function starts with $y(t_0) = y_0$ and, by $t \rightarrow \infty$, tends toward zero asymptotically. The system is thus stable. \square

7.6.2 Linearization of Nonlinear ODEs

When an NTI system is exploited around some operation point, its linearization is very useful to ascertain stability. Linearization is also very often applied for weak annoying nonlinearities caused by undesirable factors.

A complete linearized picture appears if we apply the Taylor expansion to the right-hand side of (7.137) at some operation point x_0, y_0 and save only constant and linear terms. If all of the n -order time derivatives at this point are known, $y'_0, y''_0, \dots, y_0^{(N-1)}, x'_0, x''_0, \dots, x_0^{(M)}$, a linearized equation becomes

$$\tilde{y}^{(N)}(t) = \left. \frac{\partial f}{\partial y} \right|_0 \tilde{y}(t) + \left. \frac{\partial f}{\partial y'} \right|_0 \tilde{y}'(t) + \dots + \left. \frac{\partial f}{\partial y^{(N-1)}} \right|_0 \tilde{y}^{(N-1)}(t) + \dots$$

$$+ \left. \frac{\partial f}{\partial x} \right|_0 \tilde{x}(t) + \left. \frac{\partial f}{\partial x'} \right|_0 \tilde{x}'(t) + \dots + \left. \frac{\partial f}{\partial x^{(M)}} \right|_0 \tilde{x}^{(M)}(t), \quad (7.144)$$

where we used the following assignments:

$$\begin{aligned} \left. \frac{\partial f}{\partial \text{var}} \right|_0 &\triangleq \left. \frac{\partial f}{\partial \text{var}} \right|_{x=x_0, y=y_0, x^{(m)}=x_0^{(m)}, y^{(n)}=y_0^{(n)}}, n \in [1, N-1], m \in [1, M], \\ \tilde{y} &= y - y_0, \quad \tilde{y}' = y' - y'_0, \quad \dots, \quad \tilde{y}^{(N)} = y^{(N)} - y_0^{(N)}, \\ \tilde{x} &= x - x_0, \quad \tilde{x}' = x' - x'_0, \quad \dots, \quad \tilde{x}^{(M)} = x^{(M)} - x_0^{(M)}. \end{aligned} \quad (7.145)$$

Let us add that, from the standpoint of accuracy, all increments in (7.145) must be small enough.

If we substitute all of the derivatives in (7.144) with the coefficients

$$\tilde{a}_0 = \left. \frac{\partial f}{\partial y} \right|_0, \quad \tilde{b}_0 = \left. \frac{\partial f}{\partial x} \right|_0, \quad \tilde{a}_n = \left. \frac{\partial f}{\partial y^{(n)}} \right|_0, \quad \tilde{b}_m = \left. \frac{\partial f}{\partial x^{(m)}} \right|_0, \quad (7.146)$$

we arrive at the other form of the linearized ODE

$$\begin{aligned} \tilde{y}^{(N)}(t) &= \tilde{a}_0 \tilde{y}(t) + \tilde{a}_1 \tilde{y}'(t) + \dots + \tilde{a}_{N-1} \tilde{y}^{(N-1)}(t) + \dots \\ &\quad + \tilde{b}_0 \tilde{x}(t) + \tilde{b}_1 \tilde{x}'(t) + \dots + \tilde{b}_M \tilde{x}^{(M)}(t). \end{aligned} \quad (7.147)$$

A linear ODE (7.147) can be solved by the standard methods allowing for ascertaining stability of an NTI system at a given point. With this aim, (7.147) is often translated to state space.

Example 7.25. Consider a familiar Bernoulli ODE (7.139) at the point $y(t_0) = y_0$. By (7.144) and (7.145), the linearized equation becomes

$$\tilde{y}' = - (a - \alpha b y_0^{\alpha-1}) \tilde{y} \quad (7.148)$$

and can be rewritten as

$$y' = -a y_0 + b y_0^\alpha - (a - \alpha b y_0^{\alpha-1}) (y - y_0). \quad (7.149)$$

The effect of linearization is easily traced on a phase plane of y' and y . Fig. 7.24 represents (7.139) for $a = 2$, $b = 1$, and $\alpha = 3$, by (7.142). A linear function (7.149) is placed here at three different points depicted by circles. As can be seen, there is no large error in modeling the NTI system with straight lines in a small vicinity of the operation point.

For the coefficients given, (7.149) becomes

$$\tilde{y}' = - (2 - 3y_0^2) \tilde{y}, \quad (7.150)$$

having a solution

$$\tilde{y}(t) = y_0 e^{-(2-3y_0^2)t}. \quad (7.151)$$

A comparison of (7.143) and (7.151) shows that the functions trace along different trajectories with time. However, their limiting values with $t = t_0$ and $t = \infty$ are the same. \square

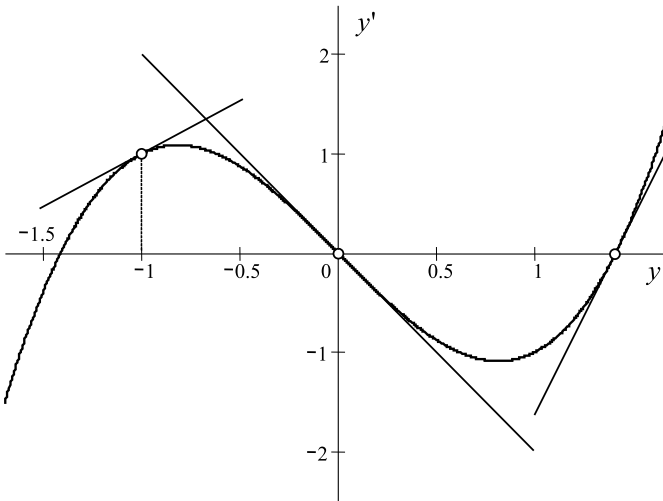


Fig. 7.24. Linearization of an NTI system (7.142) in phase plane.

Example 7.26 (Linearized Van der Pol's Oscillator). Given the nonlinear oscillator equation by van der Pol,

$$y'' + \omega_0^2 y = \epsilon(1 - y^2)y'. \quad (7.152)$$

At the form (7.137), the nonlinear function is specified by $f(y, y') = -\omega_0^2 y + \epsilon(1 - y^2)y'$. By (7.144) and (7.145), a linearized version of (7.152) is provided to be

$$\tilde{y}'' + (\omega_0^2 + 2\epsilon y_0 z_0)\tilde{y} = \epsilon(1 - y_0^2)\tilde{y}', \quad (7.153)$$

where y_0 and z_0 are coordinates of the operation point. The linearization effect here is reminiscent of that considered in Example 7.25. \square

It seems now obvious that the general solution of the NTI system ODE (7.137) does not exist for arbitrary nonlinearity. Moreover, many nonlinear electronic problems do not imply finding such solutions and rely rather on approximate results. In view of that, below we examine several typical NTI systems illustrating applications of the approximate methods observed in Chapter 2.

7.6.3 Nonlinear Piezoelectric Filter

A typical nuisance effect in electronic systems is a dependance of some components on the electric power. In many cases, the effect can be neglected. For selective circuits, however, it may become crucial if the frequency response is

“deformed” substantially. An example is a familiar piezoelectric crystal resonator (Chapter 5) used nowadays universally whenever accurate and precise selectivity and oscillations are needed.

An electric scheme of a piezoelectric filter is shown in Fig. 7.25a. The fundamental frequency of a resonator is due to the series resonance branch composed with the equivalent motional inductance L_1 , resistance R_1 , and capacitance C_1 . In parallel, a static capacitance C_0 is included producing the parallel resonance, which frequency is typically much far from the resonator bandwidth.

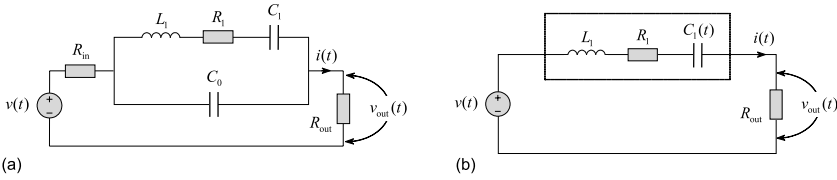


Fig. 7.25. Piezoelectric filter scheme: (a) basic and (b) simplified.

An important peculiarity of a piezoelectric resonator is that, with high drive levels, all its equivalent parameters depend on the power of a piezoelectric current $i(t)$. The effect is termed the *drive level dependence* (DLD).

To illustrate the nonlinear DLD effect, we shall examine a simplified scheme (Fig. 7.25b) represented with a series resonant branch, which capacitance C_1 depends on the power of a piezoelectric current as

$$C_1(t) = C_{10}[1 - \beta i^2(t)], \tag{7.154}$$

where C_{10} is a value of C_1 with normal drive levels, β is a DLD coefficient, and the DLD effect is small, $|\beta i^2(t)| \ll 1$. It is supposed that the input and output are matched with the resonator, $R_{in} = R_{out} = R_1$.

The motion equation for the voltage $v_{out}(t)$ induced on R_{out} is written as

$$\begin{aligned} \frac{L_1}{R_{out}} \frac{dv_{out}}{dt} + \frac{R_1 + R_{out}}{R_{out}} v_{out} + \frac{1}{R_{out}} \int \frac{v_{out}}{C_1(t)} dt &= v, \\ v''_{out} + 2\frac{R_1}{L_1} v'_{out} + \frac{1}{C_1 L_1} v_{out} &= \frac{R_1}{L_1} v'. \end{aligned} \tag{7.155}$$

Substituting (7.154) and recalling that $|\beta i^2(t)| \ll 1$, we write

$$v''_{out} + 4\delta v'_{out} + \omega_0^2 \left(1 + \frac{\beta}{R_1^2} v_{out}^2 \right) v_{out} = 2\delta v', \tag{7.156}$$

where $2\delta = R_1/L_1$ is the resonator bandwidth and $\omega_0 = 1/\sqrt{L_1 C_{10}}$ is the resonance frequency with normal drive levels. Finally, we arrive at the formalized nonlinear ODE

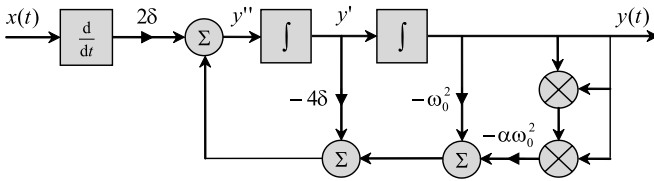


Fig. 7.26. Block diagram simulation of (7.157).

$$y'' + 4\delta y' + \omega_0^2(1 + \alpha y^2)y = 2\delta x', \tag{7.157}$$

where $\alpha = \beta/R_1^2$, $x = v$ is the input, and $y = v_{\text{out}}$ is the output. The block diagram simulation of (7.157) is shown in Fig. 7.26.

By virtue of the high quality factor of a piezoelectric filter, $Q = \omega_0/2\delta \gg 1$, the investigations of (7.157) can be provided by the method of harmonic balance. For the harmonic input $x(t) = V \cos \omega t$, a periodic solution of (7.157) can be written as

$$y(t) = A \cos(\omega t + \psi), \tag{7.158}$$

where, in the view of nonlinearity, the amplitude $A(\omega)$ and phase $\psi(\omega)$ are functions of the current frequency. Dropping the high-order harmonics, the nonlinear term in (7.157) becomes

$$y^3(t) \cong \frac{3}{4}A^3 \cos(\omega t + \psi) \tag{7.159}$$

allowing for a linearization and representation of (7.157) by

$$y'' + 4\delta y' + \omega_A^2 y = -2\delta\omega V \sin \omega t, \tag{7.160}$$

where $\omega_A^2 = \omega_0^2 (1 + \frac{3}{4}\beta A^2)$ is the DLD frequency.

Substituting the following functions to (7.160)

$$y = A \cos \psi \cos \omega t - A \sin \psi \sin \omega t,$$

$$y' = -A\omega \cos \psi \sin \omega t - A\omega \sin \psi \cos \omega t,$$

$$y'' = -A\omega^2 \cos \psi \cos \omega t + A\omega^2 \sin \psi \sin \omega t$$

and equating the terms with $\cos \omega t$ and $\sin \omega t$ leads to the equations

$$(\omega^2 - \omega_A^2) \cos \psi + 4\delta\omega \sin \psi = 0, \tag{7.161}$$

$$4\delta\omega A \cos \psi - A(\omega^2 - \omega_A^2) \sin \psi = 2\delta\omega V. \tag{7.162}$$

The first equation (7.161) produces $\tan \psi = \frac{\omega^2 - \omega_A^2}{4\delta\omega}$ that can be accounted in the second one (7.162) and we have the solutions

$$A = \frac{2\delta\omega V}{\sqrt{(\omega^2 - \omega_A^2)^2 + 16\delta^2\omega^2}}, \quad (7.163)$$

$$\tan \psi = -\frac{\omega^2 - \omega_0^2}{4\delta\omega} + \frac{\omega_0^2}{4\delta\omega} \frac{3}{4} \beta A^2. \quad (7.164)$$

Assigning the fractional detuning $\Delta = (\omega - \omega_0)/\omega_0$ and allowing $\omega + \omega_0 \cong 2\omega_0$, we arrive at the relations for the magnitude response $|H(j\Delta)| = A(\Delta)/V$ and phase response $\psi(\Delta)$ of the nonlinear piezoelectric filter, respectively,

$$|H(j\Delta)| = \frac{1}{2\sqrt{1 + Q^2 \left(\Delta - \frac{3}{8}\beta V^2 |H(j\Delta)|^2\right)^2}}, \quad (7.165)$$

$$\psi(\Delta) = -\arctan Q \left(\Delta - \frac{3}{8}\beta V^2 |H(j\Delta)|^2 \right). \quad (7.166)$$

As can be seen, the algebraic equation (7.165) is cubic regarding $|H(j\Delta)|^2$ and quadratic for Δ^2 . For Δ^2 , it thus can be rewritten as

$$\Delta^2 - \frac{3}{4}\beta V^2 H^2 \Delta + \frac{9}{64}\beta^2 V^4 H^4 + \frac{4H^2 - 1}{4H^2 Q^2} = 0 \quad (7.167)$$

that has a solution

$$\Delta_{1,2} = \frac{3}{8}\beta V^2 H^2 \pm \frac{\sqrt{1 - 4H^2}}{2HQ}. \quad (7.168)$$

The magnitude and phase responses can now be plotted. In doing so, we change $|H(j\Delta)|$ from 0 up to some reasonable value and find, by (7.168), the relevant detunings $\Delta_{1,2}$. Thereafter, the phase response (7.166) is calculated for $|H(j\Delta)|$ and $\Delta_{1,2}$ and we show both responses in Fig. 7.27. It is seen that increasing the DLD coefficient β results in “deforming” the magnitude response so that the resonance frequency becomes larger (Fig. 7.27a). This effect is neatly traced in the phase response (Fig. 7.27b). As can be seen, the zero phase associated with a peak value of the magnitude response shifts toward higher frequencies, by increasing β .

If the DLD effect occurs, the filter may no longer fulfil the requirements. Let us observe what can happen following Fig. 7.28. Suppose we move along the frequency response from the left to the right. When we reach a point A , the response jumps to a point B . If to turn back, the function jumps from C to D . The frequency response has thus a “dead zone” bounded by the points A, B, C , and D . Owing to a hysteresis loop, the output will contain of spectral components either on the level between D and A or B and C . The signal will be “flaking” and filtering will no longer be properly obtained. On the other hand, the effect may be used in special kinds of modulation and binary coding.

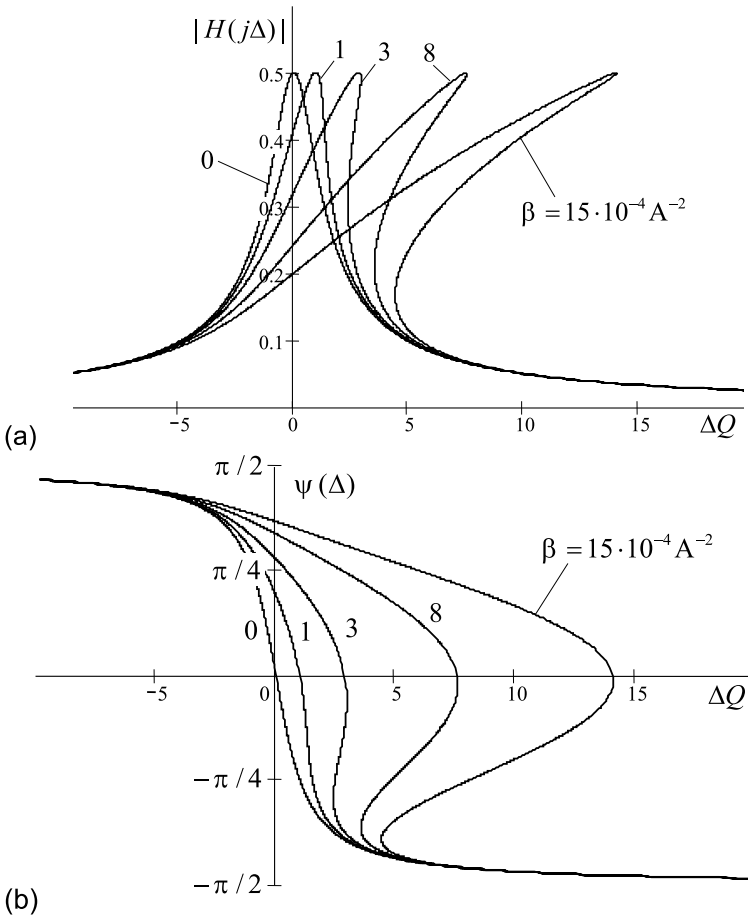


Fig. 7.27. Frequency response of a nonlinear piezoelectric filter: (a) magnitude and (b) phase.

7.6.4 Harmonic Oscillator

A classical representative of NTI systems is a harmonic oscillator. The device is inherently nonlinear, because, if it is linear, oscillations have no stable limit cycle. An equivalent scheme of a transistor oscillator is shown in Fig. 7.29. The resonant circuit is composed with L , R , and C . The output voltage $v(t)$ induced on the capacitor C governs the collector current $i(t)$ of a nonlinear transistor. In turn, the current $i(t)$ induces the voltage on the feedback inductance L_1 that via the mutual inductance M induces the feedback voltage on L . By the feedback, the dissipated energy is compensated and the steady state oscillations become available. The nonlinear dependence $i(v)$ is chosen such that an equilibrium in the closed loop occurs at some given level.

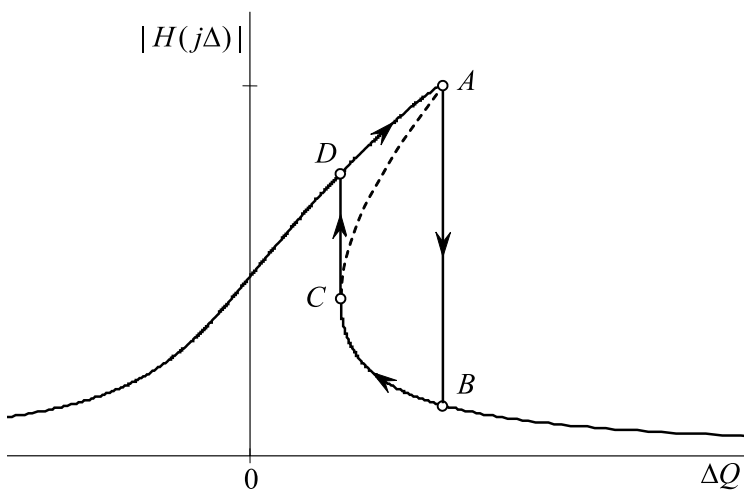


Fig. 7.28. Nonlinear effect in the magnitude response of a piezoelectric filter.

The voltage balance equation can be written as

$$L \frac{di_c}{dt} + Ri_c + \frac{1}{C} \int i_c(t) dt = M \frac{di}{dt}$$

that, by $i_c = C \frac{dv}{dt}$, becomes

$$v'' + 2\delta v' + \omega_0^2 v = \omega_0^2 M \frac{di}{dt}, \tag{7.169}$$

where $2\delta = R/L$ and $\omega_0^2 = 1/LC$.

The first time derivative of $i(t)$ can be represented by

$$\frac{di}{dt} = \frac{di}{dv} \frac{dv}{dt} = S(v)v', \tag{7.170}$$

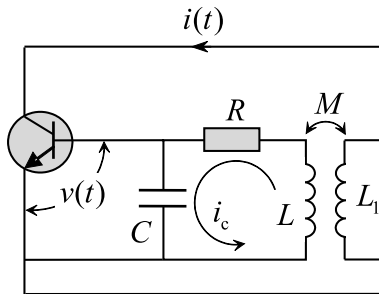


Fig. 7.29. Harmonic transistor oscillator.

where $S(v) = di/dv$ is a memoryless sensitivity of the collector current $i(t)$ to $v(t)$. By (7.170), the ODE (7.169) attains the form

$$v'' + [2\delta - \omega_0^2 MS(v)] v' + \omega_0^2 v = 0. \quad (7.171)$$

Traditionally assigning $y = v$, we formally rewrite (7.171) as

$$y'' + 2\delta_1 y' + \omega_0^2 y = 0, \quad (7.172)$$

where $2\delta_1(y) = 2\delta - \omega_0^2 MS(y)$ is the bandwidth of a closed loop. In the first order approximation, the solution of (7.172) can be written as

$$y(t) = A_0 e^{-\delta_1 t} \cos(\omega_1 t + \vartheta_0), \quad (7.173)$$

where A_0 and ϑ_0 are some constant amplitude and phase dependent on the initial conditions. The oscillator frequency is defined by

$$\omega_1^2 = \omega_0^2 - \delta_1^2. \quad (7.174)$$

By the high quality factor, $Q = \omega_0/2\delta \gg 1$, it is typical to think that $\omega_1 \cong \omega_0$. At the steady state, the solution (7.173) therefore becomes $y(t) = A_0 \cos(\omega_0 t + \vartheta_0)$, if we recall that the losses at the equilibrium are compensated fully, thus $\delta_1 = 0$, and the steady state is reached at infinity, $t \rightarrow \infty$.

Let us now take a more precise look at (7.172) recalling that $S(v)$ is nonlinear. Actually, namely this nonlinearity is responsible for the limit cycle at equilibrium. For the sake of simplicity, we restrict our analysis with the typically implied cubic polynomial $i = av - bv^3$ that produces $S(v) = a - 3bv^2$. The nonlinear bandwidth $2\delta_1$ can therefore be rewritten as

$$2\delta_1(y) = 2\delta - \omega_0^2 Ma + \omega_0^2 Mbv^2.$$

In terms of the feedback coefficient $k = M/L_1$, characteristic resistance $\rho = \sqrt{L/C}$, and quality factor $Q = \omega_0/2\delta$, the bandwidth is evaluated by

$$2\delta_1(y) = -2\delta(Qk\rho a - 1) \left(1 - \frac{Qk\rho b}{Qk\rho a - 1} y^2 \right) = -2\delta_e(1 - \alpha y^2),$$

where $2\delta_e = 2\delta(Qk\rho a - 1)$ is an equivalent bandwidth and $\alpha = Qk\rho/(Qk\rho a - 1)$. The nonlinear ODE (7.171) thus becomes

$$y'' - 2\delta_e(1 - \alpha y^2)y' + \omega_0^2 y = 0. \quad (7.175)$$

At the first moment after the power supply is switched on, the amplitude of oscillations is very small. We thus have $\alpha y^2 \ll 1$, meaning that the second term in (7.175) is negative. Consequently, the energy coming from the feedback overcompensates the dissipated energy and oscillations develop. The amplitude rises up to the value associated with $\alpha y^2 = 1$. At this point, the

second term in (7.175) disappears and the system behaves along a limit cycle with the frequency ω_0 .

It can be shown that, by a new variable $z = \sqrt{\alpha}y$ and $\epsilon = 2\delta_e$, the oscillator becomes van der Pol's (2.89),

$$y'' + \omega_0^2 y = \epsilon(1 - y^2)y',$$

and we remind the reader that investigations of the van der Pol oscillator were provided in different aspects in Section 2.5.2 and Examples 2.20–2.25, 2.27, 3.1, 3.12, and 7.26.

7.6.5 Biharmonic Oscillatory System

A capability of a nonlinearity to create a single limit cycle is not the only one that is used. If an oscillatory system comprises two or more resonant circuits, a certain type of nonlinearity is able to create more than one limit cycle. Under the certain circumstances, an oscillator may thus become *biharmonic* or even *multiharmonic* (or *multifrequency*). An example is an oscillatory system with a crystal resonator, whose bulk piezoelectric structure is inherently multimodal.

To analyze the principle of biharmonic excitation, let us consider a simple scheme comprising two series resonant circuits as shown in Fig. 7.30. Typically, the bandwidths of the branches are not overlapped and the resonant circuits are therefore not coupled with each other. The current $i = i_1 + i_2$ induces a voltage v_{in} on the input resistor R_{in} . A nonlinear feedback with the gain $G(v_{in})$ transfers v_{in} to the output. By v_{out} , the dissipated energy is compensated making possible for oscillations to be in steady state. A key point is the nonlinearity of the gain G . In the sequel, we shall show that only with the certain coefficients of this nonlinearity two stable limit cycles may be created, thereby allowing for biharmonic oscillations.

The loop can be described by two equations of motion regarding the currents i_1 and i_2 ,

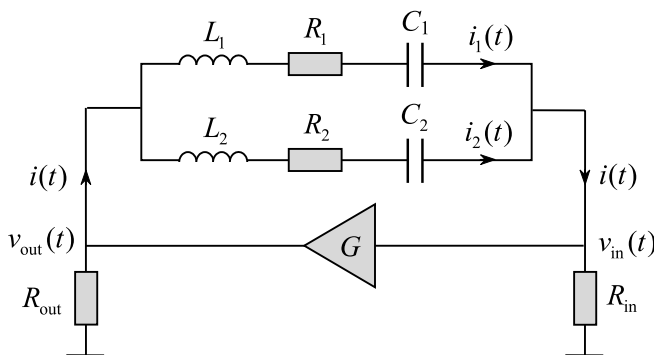


Fig. 7.30. Biresonant oscillatory system.

$$L_1 \frac{di_1}{dt} + (R_1 + R_{in})i_1 + \frac{1}{C_1} \int i_1 dt = v_{1out}, \quad (7.176)$$

$$L_2 \frac{di_2}{dt} + (R_2 + R_{in})i_2 + \frac{1}{C_2} \int i_2 dt = v_{2out}, \quad (7.177)$$

where v_{1out} and v_{2out} are voltages induced on R_{out} regarding the signals with the frequencies $\omega_1 = 1/\sqrt{L_1 C_1}$ and $\omega_2 = 1/\sqrt{L_2 C_2}$, respectively. The voltages v_{1out} and v_{2out} are coupled with v_{in} by the nonlinear gain G as follows:

$$G(v_{in}) = G(v_1 + v_2) = v_{1out} + v_{2out} + \dots,$$

where $v_1 = R_{in} i_1$ and $v_2 = R_{in} i_2$. Equations (7.176) and (7.177) can now be rewritten as

$$v_1'' + 2\delta_1^* v_1' + \omega_1^2 v_1 = \frac{R_{in}}{L_1} v_{1out}, \quad (7.178)$$

$$v_2'' + 2\delta_2^* v_2' + \omega_2^2 v_2 = \frac{R_{in}}{L_2} v_{2out}, \quad (7.179)$$

where $2\delta_1^* = 2\delta_1 + R_{in}/L_1$, $2\delta_2^* = 2\delta_2 + R_{in}/L_2$, $2\delta_1 = R_1/L_1$, $2\delta_2 = R_2/L_2$, and $v_{in} = v_1 + v_2$.

To investigate limit cycles, the nonlinear gain may be approximated with the 5-order polynomial as

$$G(v_{in}) = a(v_1 + v_2) + b(v_1 + v_2)^3 - c(v_1 + v_2)^5, \quad (7.180)$$

$$G'(v_{in}) = [a + 3b(v_1 + v_2)^2 - 5c(v_1 + v_2)^4](v_1' + v_2'), \quad (7.181)$$

where a , b , and c some constant coefficients.

Let us now examine stability of biharmonic oscillations. To find the relevant conditions and investigate the special points in phase plane, we rewrite (7.180) and (7.181) as follows

$$v_1'' + \omega_1^2 v_1 = \epsilon_1 f_1(v_1, v_1', v_2, v_2'). \quad (7.182)$$

$$v_2'' + \omega_2^2 v_2 = \epsilon_2 f_2(v_1, v_1', v_2, v_2'), \quad (7.183)$$

where $\epsilon_1 = 2\delta_1$, $\epsilon_2 = 2\delta_2$, and the nonlinear functions are defined by

$$f_1 = -\frac{v_1'}{1 - k_1} + \frac{k_1}{1 - k_1} [a + 3b(v_1 + v_2)^2 - 5c(v_1 + v_2)^4] (v_1' + v_2'), \quad (7.184)$$

$$f_2 = -\frac{v_2'}{1 - k_2} + \frac{k_2}{1 - k_2} [a + 3b(v_1 + v_2)^2 - 5c(v_1 + v_2)^4] (v_1' + v_2'), \quad (7.185)$$

where $k_1 = R_{in}/(R_1 + R_{in})$ and $k_2 = R_{in}/(R_2 + R_{in})$ are the feedback coefficients of the first and second branches, respectively.

By the van der Pol solutions,

$$\begin{aligned} v_1 &= r_1 \cos(\omega_1 t + \varphi_1) = r_1 \cos \psi_1, \\ v'_1 &= -r_1 \omega_1 \sin(\omega_1 t + \varphi_1) = -r_1 \omega_1 \sin \psi_1, \\ v_2 &= r_2 \cos(\omega_2 t + \varphi_2) = r_2 \cos \psi_2, \\ v'_2 &= -r_2 \omega_2 \sin(\omega_2 t + \varphi_2) = -r_2 \omega_2 \sin \psi_2, \end{aligned}$$

and the Krylov and Bogoliubov method, the amplitudes r_1 and r_2 of oscillations are defined to be

$$r'_1 = \epsilon_1 A_{11}(r_1, r_2), \tag{7.186}$$

$$r'_2 = \epsilon_2 A_{12}(r_1, r_2), \tag{7.187}$$

where, in view of two variables, the values of A_{11} and A_{12} are determined by double averaging over periods of oscillations with the frequencies ω_1 and ω_2 ,

$$\begin{aligned} A_{11}(r_1, r_2) &= -\frac{1}{4\pi^2\omega_1} \int_0^{2\pi} \int_0^{2\pi} f_1(r_1 \cos \psi_1, -r_1 \omega_1 \sin \psi_1, r_2 \cos \psi_2, -r_2 \omega_2 \sin \psi_2) \\ &\quad \times \sin \psi_1 \, d\psi_1 \, d\psi_2, \end{aligned} \tag{7.188}$$

$$\begin{aligned} A_{12}(r_1, r_2) &= -\frac{1}{4\pi^2\omega_2} \int_0^{2\pi} \int_0^{2\pi} f_2(r_1 \cos \psi_1, -r_1 \omega_1 \sin \psi_1, r_2 \cos \psi_2, -r_2 \omega_2 \sin \psi_2) \\ &\quad \times \sin \psi_2 \, d\psi_1 \, d\psi_2, \end{aligned} \tag{7.189}$$

where f_1 and f_2 are defined by (7.184) and (7.185), respectively. After the routine integration (the reader is encouraged to use a symbolic block of the applied software such as Mathcad and Matlab), equations (7.186) and (7.187) attain the forms of, respectively,

$$r'_1 = -\frac{\mu_1 \gamma r_1}{\tau_1(1 - k_1)} [\alpha_1 + \beta(r_1^2 + 2r_2^2) + r_1^4 + 3r_2^4 + 6r_1^2 r_2^2], \tag{7.190}$$

$$r'_2 = -\frac{\mu_2 \gamma r_2}{\tau_2(1 - k_2)} [\alpha_2 + \beta(r_2^2 + 2r_1^2) + r_2^4 + 3r_1^4 + 6r_2^2 r_1^2], \tag{7.191}$$

where $\tau_{1,2} = 1/\delta_{1,2}$ is the time constant of the relevant branch, $k_{1,2} = R_{in}/(R_{1,2} + R_{in})$, $\mu_{1,2} = ak_{1,2}$ is a closed loop gain, $\alpha_{1,2} = (1 - \mu_{1,2})/\gamma\mu_{1,2}$, $\beta = -24b/5c$, and $\gamma = 5c/8a$.

Being difficult to solve analytically in the time domain, (7.190) and (7.191) can completely be investigated in phase plane, by the phase trajectories

$$\begin{aligned} \frac{dr_1}{dr_2} &= \frac{\tau_2(1 - k_2) P(r_1, r_2)}{\tau_1(1 - k_1) Q(r_1, r_2)} \\ &= \frac{\tau_2(1 - k_2) \mu_1 r_1 [\alpha_1 + \beta(r_1^2 + 2r_2^2) + r_1^4 + 3r_2^4 + 6r_1^2 r_2^2]}{\tau_1(1 - k_1) \mu_2 r_2 [\alpha_2 + \beta(r_2^2 + 2r_1^2) + r_2^4 + 3r_1^4 + 6r_2^2 r_1^2]}. \end{aligned} \quad (7.192)$$

We commence an investigation, by ascertaining stability at zero.

Stability at Zero

To ascertain stability at a zero excitation point, $r_1 = 0$ and $r_2 = 0$, we write the characteristic equation of (7.192),

$$\lambda^2 + r_x \lambda + q_x = 0, \quad (7.193)$$

in which the coefficients r_x and q_x are predetermined by

$$r_x = -[P'_1(0, 0) + Q'_2(0, 0)], \quad (7.194)$$

$$q_x = \begin{vmatrix} P'_1(0, 0) & P'_2(0, 0) \\ Q'_1(0, 0) & Q'_2(0, 0) \end{vmatrix}, \quad (7.195)$$

where $P'_1(0, 0) = \left. \frac{\partial P}{\partial r_1} \right|_{r_1, r_2=0}$, $P'_2(0, 0) = \left. \frac{\partial P}{\partial r_2} \right|_{r_1, r_2=0}$, $Q'_1(0, 0) = \left. \frac{\partial Q}{\partial r_1} \right|_{r_1, r_2=0}$, and $Q'_2(0, 0) = \left. \frac{\partial Q}{\partial r_2} \right|_{r_1, r_2=0}$. After the transformations, we have

$$r_x = 2 - a(k_1 + k_2), \quad q_x = (ak_1 - 1)(ak_2 - 1). \quad (7.196)$$

For the system to be stable in the sense of Lyapunov, the real parts of the roots of (7.193) must be negative. This is only possible if r_x and q_x are positive. Additionally, to ascertain whether a fixed point is spirals or node, it needs investigating the bound of the determinant $D = r_x^2 - 4q_x = 0$. In view of that, we have three equations to study:

$$(r_x = 0) : \quad 2 - a(k_1 + k_2) = 0, \quad (7.197)$$

$$(q_x = 0) : \quad (ak_1 - 1)(ak_2 - 1) = 0, \quad (7.198)$$

$$(D = 0) : \quad (k_1 - k_2)^2 = 0. \quad (7.199)$$

By Fig. 3.1 and (7.197)–(7.199), stability of a fixed point in the range of the possible values $0 \leq k_{1,2} \leq 1$ is ascertained as shown in Fig. 7.31. When both coefficients are small, $k_1 < 1/a$ and $k_2 < 1/a$, no one resonant circuit can be excited, because the feedback is insufficient. The fixed point is thus a stable node. If $k_1 > 1/a$ and $k_2 > 1/a$, the system can be excited at two frequencies, ω_1 and ω_2 , and the point is an unstable node. Whenever a system is designed such that either $k_1 > 1/a$ and $k_2 < 1/a$ or vice versa, the fixed point is saddle.

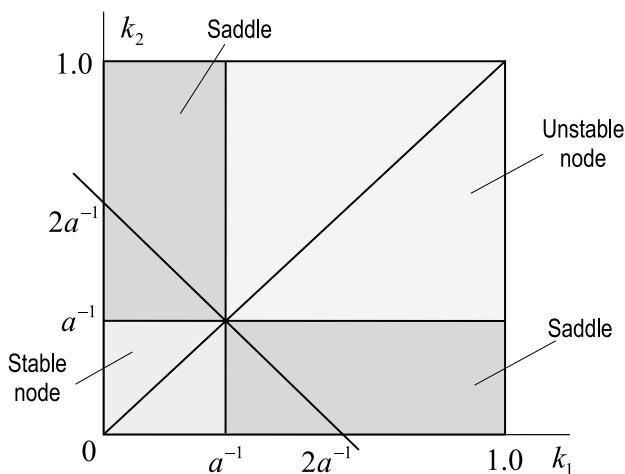


Fig. 7.31. Stability of a fixed point at zero, by (7.197)–(7.199).

Phase Portrait

All fixed points in phase plane are defined by investigating the cross points of the curves

$$P(r_1, r_2) = 0, \quad Q(r_1, r_2) = 0, \tag{7.200}$$

described by (7.192). Depending on the coefficients of the nonlinearity, several oscillation modes are available. Topological pictures corresponding to each of these modes are shown in Fig. 7.32. Several bifurcations are watched in phase plane if to change the coefficients $\alpha_1, \alpha_2, \beta, k_1,$ and k_2 . Because $\alpha_1, \alpha_2,$ and β are defined via the coefficients $a, b,$ and c , the phase portraits can be separated as in the following.

For the symmetric resonant system, $k_1 = k_2$, the picture (Fig. 7.32a) is obtained with

$$c < \frac{9k}{5(1 - \mu_1)} b^2. \tag{7.201}$$

Under the condition (7.201) and with small amplitudes (quasi linear system), both branches are excited simultaneously. It is a typical *soft excitation* similar to van der Pol’s oscillator. With larger amplitudes, the nonlinearity allows for the development of one of the modes and attenuating the other one. Such a process is known as *modes competition*. Depending on the initial conditions, the limit cycle is formed here only for one of the frequencies.

The next portrait (Fig. 7.32b) occurs if the coefficient c is set such that

$$\frac{9k}{5(1 - \mu_1)} b^2 < c < \frac{81k}{25(1 - \mu_1)} b^2. \tag{7.202}$$

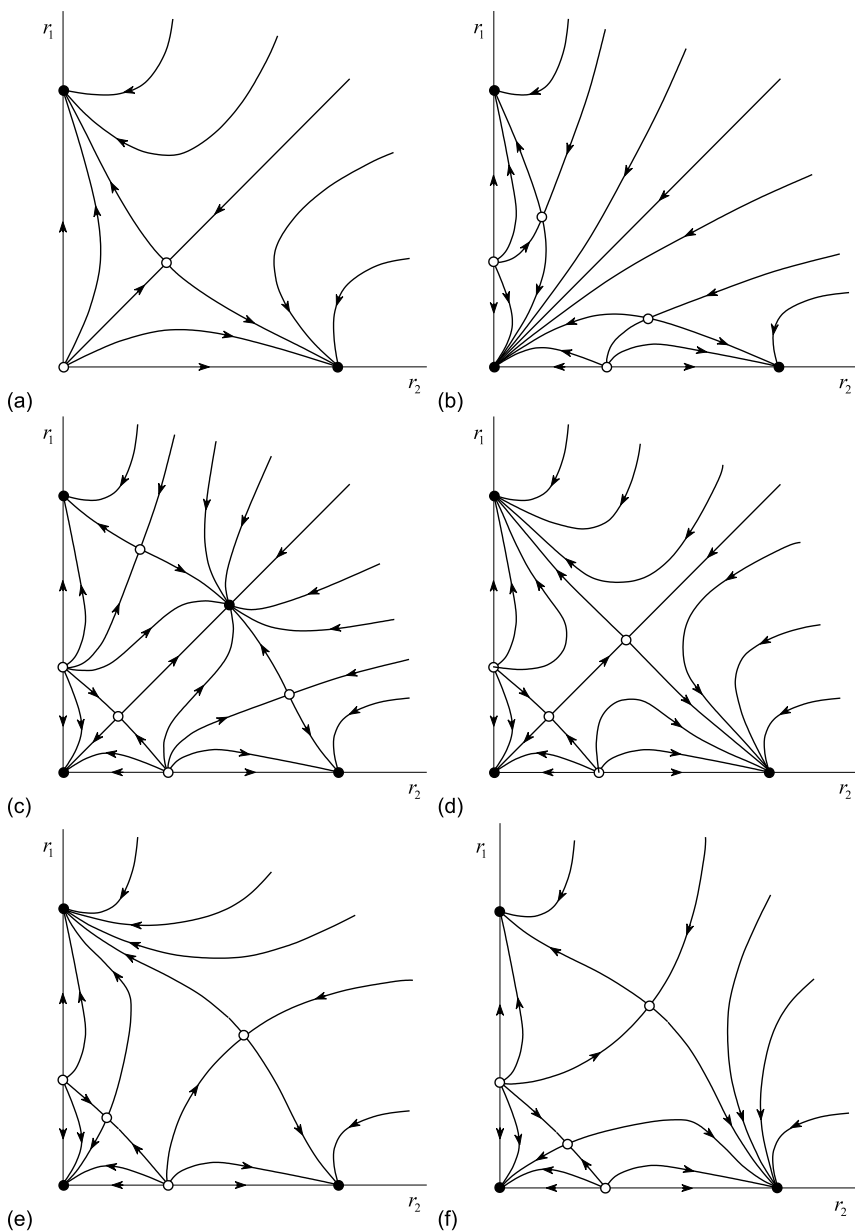


Fig. 7.32. Phase portraits of the biharmonic oscillatory system: (a) soft excitation, by (7.201), (b) hard excitation, by (7.202), (c) biharmonic mode, by (7.203), (d) hard excitation, by (7.204), (e) break of a biharmonic mode, by $k_1 > k_2$, and (f) break of a biharmonic mode, by $k_1 < k_2$.

With zero amplitudes, the excitation conditions are not satisfied here neither for the first circuit nor for second. Only with large initial amplitudes, one of the branches can be excited. In the oscillators theory, such a process is termed *hard excitation*.

An oscillator becomes biharmonic (Fig. 7.32c) if

$$\frac{81k}{25(1-\mu_1)}b^2 < c < \frac{18k}{5(1-\mu_1)}b^2. \quad (7.203)$$

The system is characterized here with two stable limit cycles, meaning that the structure generates in the steady state two signals with equal amplitudes and different frequencies ω_1 and ω_2 . The necessary condition for oscillations to be biharmonic is the hard excitation. Most generally, this means that if an oscillator is excited softly, then one should not expect generating a multifrequency signal. However, if the process with soft excitation will further satisfy (7.203), the biharmonic signal will be available at the steady state. Namely such a trick with the conditions changed during the transient is widely used in applications to create bifrequency and even multifrequency oscillators.

One more portrait occurs as in Fig. 7.32d if $k_1 = k_2$ is obtained by

$$\frac{18k}{5(1-\mu_1)}b^2 < c. \quad (7.204)$$

The topology is akin to Fig. 7.32a if to implement the hard excitation region discussed above.

Because the resonant branches can dissipate energy with different rates and thus the more realistic situation is when $k_1 \neq k_2$, of importance is to investigate how unequal coefficients affect the biharmonic mode. Fig. 7.32e demonstrates what happens if k_1 exceeds k_2 by only several percent. Fig. 7.32f sketches an inverse picture. It follows that, under the condition of $k_1 \neq k_2$, the system can lose an ability to be biharmonic. This means that the branch with a larger feedback coefficient acquires more chances for excitation.

7.6.6 Synchronized Harmonic Oscillator

With any necessity for the communication or other system to operate permanently in a common time scale with other systems, a local oscillator is disciplined in phase for the reference signal. A solution implies inducing a synchronizing voltage $v_s(t) = V_s \cos \omega_s t$, where V_s is a constant amplitude and ω_s is a reference frequency, to a local oscillator as shown in Fig. 7.33.

Similarly to (7.169), the nonlinear ODE of a loop is written as

$$v'' + 2\delta v' + \omega_0^2 v = \omega_0^2 V_s \cos \omega_s t + \omega_0^2 M \frac{di}{dt}, \quad (7.205)$$

allowing us to investigate stability of a synchronization mode.

Following (7.170) and introducing the nonlinear sensitivity $S(v) = di/dv$, we go from (7.205) to

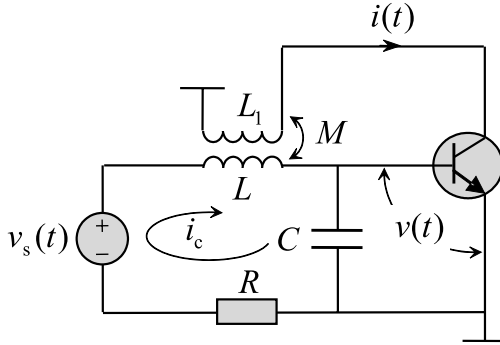


Fig. 7.33. Synchronized harmonic oscillator.

$$v'' + (2\delta - \omega_0^2 MS)v' + \omega_0^2 v = \omega_0^2 V_s \cos \omega_s t. \tag{7.206}$$

If we further normalize the time scale, $\tau = \omega_s t$, and traditionally assign $y = v$ to be the output, we can rewrite (7.206) as follows

$$y''_\tau + 2\eta(y)y'_\tau + \zeta^2 y = \lambda \cos \tau, \tag{7.207}$$

where $y'_\tau = dy/d\tau$, $y''_\tau = d^2y/d\tau^2$, $2\eta = [2\delta - \omega_0^2 MS(y)]/\omega_s$ is the bandwidth, $\zeta^2 = \omega_0^2/\omega_s^2$, and $\lambda = V_s \zeta^2$.

For a typically high quality factor, $Q = \omega_0/2\delta \gg 1$, a solution of (7.207) may be found by the method of averaging. In doing so, it is in order first representing an equation in the traditional form of

$$y''_\tau + y = \varepsilon f(y, y'_\tau, \tau), \tag{7.208}$$

where $\varepsilon = 1/Q$ and

$$f = \zeta(\omega_0 MQS - 1)y' + Q(1 - \zeta^2)y + V_s Q \zeta^2 \cos \tau. \tag{7.209}$$

We now approximate $i(t)$ with an incomplete odd cubic polynomial $i = av - bv^3$, where a and b are constant coefficients properly predetermined to obtain soft excitation. That gives $S(v) = a - 3bv^2$ and (7.209) becomes

$$f = \zeta[\omega_0 MQ(a - 3by^2) - 1]y' + Q(1 - \zeta^2)y + V_s Q \zeta^2 \cos \tau. \tag{7.210}$$

By the van der Pol solutions, $y = r \cos \psi = r \cos(\tau + \vartheta)$ and $y' = -r \sin \psi = -r \sin(\tau + \vartheta)$, and Krylov-Bogoliubov method, (7.208) can be represented, in the first order approximation, with two equations

$$\frac{dr}{d\tau} = r'_\tau = \varepsilon A_1(r, \vartheta), \tag{7.211}$$

$$\frac{d\psi}{d\tau} = \psi'_\tau = 1 + \varepsilon B_1(r, \vartheta), \quad (7.212)$$

where the functions $A_1(r, \vartheta)$ and $B_1(r, \vartheta)$ are defined by, respectively,

$$A_1(r, \vartheta) = -\frac{1}{2\pi} \int_0^{2\pi} f(r \cos \psi, -r \sin \psi, \psi - \vartheta) \sin \psi \, d\psi, \quad (7.213)$$

$$B_1(r, \vartheta) = -\frac{1}{2\pi r} \int_0^{2\pi} f(r \cos \psi, -r \sin \psi, \psi - \vartheta) \cos \psi \, d\psi. \quad (7.214)$$

Substituting (7.210) to (7.213) and (7.214) and rewriting (7.212) for the phase ϑ , we arrive at the equations for the amplitude and phase of oscillations, respectively,

$$r'_\tau = -\frac{r\zeta}{2} \left(\frac{1}{Q} - \omega_0 M a + \frac{3}{4} \omega_0 M b r^2 \right) - \frac{V_s \zeta^2}{2} \sin \vartheta, \quad (7.215)$$

$$\vartheta'_\tau = -\frac{1}{2}(1 - \zeta^2) - \frac{V_s}{2r} \zeta^2 \cos \vartheta. \quad (7.216)$$

In the form given, (7.215) is hard to analyze. A simplification can be obtained by introducing the steady state amplitude r_0 associated with the absence of a synchronizing signal, $V_s = 0$. For $r'_\tau = 0$ and $V_s = 0$, (7.215) gives

$$\frac{1}{Q} - \omega_0 M a + \frac{3}{4} \omega_0 M b r_0^2 = 0$$

yielding

$$r_0 = \sqrt{\frac{4(\omega_0 Q M a - 1)}{3Q\omega_0 M b}}. \quad (7.217)$$

Using (7.217), equations (7.215) and (7.214) can be rewritten in the following most general forms,

$$\varrho'_\tau = \frac{\mu}{2} (1 - \varrho^2) \varrho - \frac{\kappa}{2} \sin \vartheta, \quad (7.218)$$

$$\vartheta'_\tau = -\frac{\xi}{2} - \frac{\kappa}{2\varrho} \cos \vartheta, \quad (7.219)$$

where $\varrho = r/r_0$, $\mu = \zeta \left(\omega_0 M a - \frac{1}{Q} \right)$, $\kappa = V_s \zeta^2 / r_0$, and $\xi = 1 - \zeta^2$. Equations (7.218) and (7.219) allows us to analyze what happens with the amplitude, phase, and frequency of oscillations if the amplitude and frequency of a synchronizing signal is changed.

Magnitude Response

The effect of synchronization is typically of interest in steady state. Therefore, by $r'_\tau = 0$ and $\vartheta'_\tau = 0$, we rewrite (7.218) and (7.219) as follows, respectively,

$$\mu(1 - \varrho^2)\varrho = \kappa \sin \vartheta, \quad (7.220)$$

$$-\xi\varrho = \kappa \cos \vartheta. \quad (7.221)$$

By squaring both sides of (7.220) and (7.221) and thereafter examining the sum of these squares, we arrive at

$$\varrho^2 [(1 - \varrho^2)^2 + \alpha^2] = \eta^2, \quad (7.222)$$

where $\alpha(\xi) = \xi/\mu$ and $\eta = \kappa/\mu$. A solution of (7.222) represents the magnitude response $\varrho(\alpha)$ of a system. It is easily seen that (7.222) is cubic regarding ϱ^2 and quadratic for α . In the latter case, a direct solution is

$$\alpha_{1,2} = \pm \sqrt{\frac{\eta^2}{\varrho^2} - (1 - \varrho^2)^2}, \quad (7.223)$$

allowing us to restore a full picture.

The bounds $\alpha_0 = \pm\eta$ of the synchronization region are easily defined by $\varrho = 1$. A maximum value ϱ_{\max} of ϱ corresponds to $\alpha = 0$ and is derived by solving for ϱ^2 the cubic equation $\varrho^6 - 2\varrho^4 + \varrho^2 = \eta^2$. Also, this equation specifies the other possible values of ϱ lying below ϱ_{\max} and associated with different amplitudes of a synchronizing signal. The magnitude response of such an NTI system is shown in Fig. 7.34 for several values of η around unity.

As we noticed above, the synchronization region is bounded with $\alpha < |\eta|$. Within this range, by $\eta > 1$, the energy of a synchronizing signal dominates and the oscillator is fully disciplined. The magnitude response is shaped here to be almost that associated with a resonant circuit of the second order.

With $\eta = 1$, the oscillator is still well disciplined. However, owing to the energy of a synchronizing signal, the magnitude response tends to be more flat within the synchronization region having sharper sides.

The picture changes cardinally by $\eta < 1$. The energy of an input is still enough to discipline an oscillator within the synchronization region. However, it is too small beyond the bounds $\pm\eta$. Accordingly, the magnitude response tends to be almost rectangular with $\eta = 0.5$. It then becomes horseshoe, by $\eta = 0.385$. With lower values of η , the response is represented with three levels associated with the ellipsoid shaped around $\varrho = 1$ and an almost flat pedestal. To answer on the question which level is stable and which is not, one needs to study stability of forced oscillations.

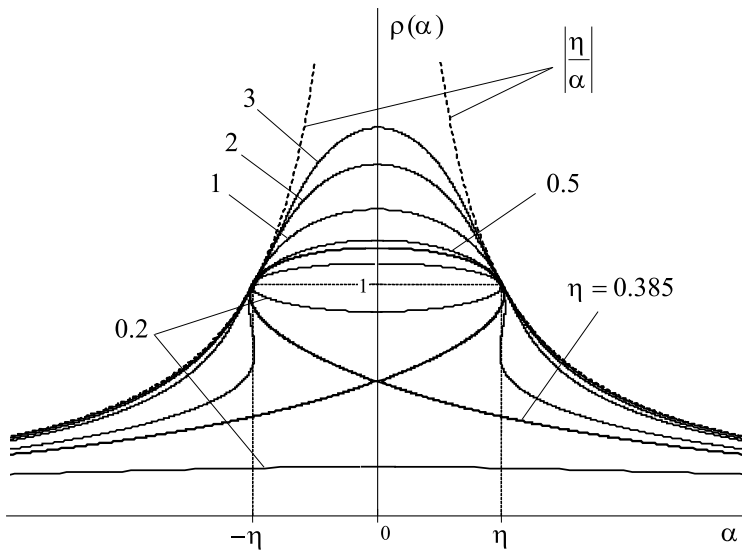


Fig. 7.34. Magnitude response of a synchronized harmonic oscillator.

Stability of Forced Oscillations

To ascertain stability of a synchronized oscillator, one needs to investigate its linearized version at an arbitrary steady state point shown in Fig. 7.34. In doing so, it is first in order to rewrite (7.218) and (7.219) as

$$\varrho'_\tau = \frac{\mu}{2} (1 - \varrho^2) \varrho - \frac{\kappa}{2} \sin \vartheta = P(\varrho, \vartheta), \tag{7.224}$$

$$\vartheta'_\tau = -\frac{\xi}{2} - \frac{\kappa}{2\varrho} \cos \vartheta = Q(\varrho, \vartheta), \tag{7.225}$$

and find the coefficients (3.9) of the Jacobian matrix (3.8) at some steady state point ϱ_s and ϑ_s . This gives

$$a = P'_\varrho(\varrho_s, \vartheta_s) = \frac{\mu}{2} (1 - 3\varrho_s^2), \quad b = P'_\vartheta(\varrho_s, \vartheta_s) = -\frac{\kappa}{2} \cos \vartheta_s,$$

$$c = Q'_\varrho(\varrho_s, \vartheta_s) = \frac{\kappa}{2\varrho_s^2} \cos \vartheta_s, \quad d = Q'_\vartheta(\varrho_s, \vartheta_s) = \frac{\kappa}{2\varrho_s} \sin \vartheta_s.$$

The relevant characteristic equation is written as

$$\begin{vmatrix} a - \lambda & b \\ c & d - \lambda \end{vmatrix} = \lambda^2 + \sigma\lambda + \Delta = 0,$$

where the coefficients are determined by

$$\sigma = -\mu(1 - 2\varrho_s^2), \tag{7.226}$$

$$\Delta = \frac{\mu^2}{4} [(1 - 3\rho_s^2)(1 - \rho_s^2) + \alpha^2] . \tag{7.227}$$

By these values, a solution of the characteristic equation is given as

$$\frac{2\lambda}{\mu} = (1 - 2\rho_s^2) \pm \sqrt{\rho_s^4 - \alpha^2} . \tag{7.228}$$

Using (7.226) and (7.227) and following Fig. 3.1, we separate the fixed points as shown in Fig. 7.35. With $\sigma^2 - 4\Delta < 0$, that is $\rho_s < \sqrt{\alpha}$, the roots

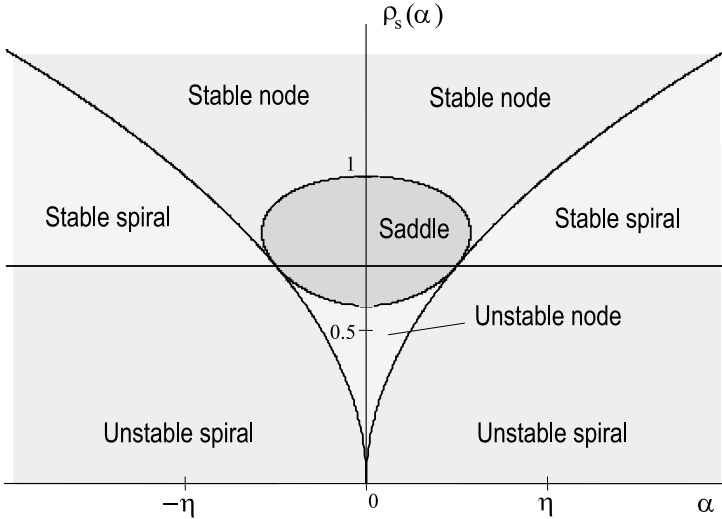


Fig. 7.35. Fixed points of a system in the plane ρ_s, α .

are complex and the point is spiral. If $\sigma > 0$ or $\rho_s > \frac{1}{\sqrt{2}}$, spiral is stable and, by $\sigma < 0$ or $\rho_s < \frac{1}{\sqrt{2}}$, it is unstable. If $\sigma = 0$ or ρ_s exactly equals to $1/\sqrt{2}$, the spiral degenerates to a center.

The condition $\Delta = 0$ is satisfied by an ellipsoidal equation

$$\frac{1}{3} - 3 \left(\rho_s^2 - \frac{2}{3} \right)^2 = \alpha^2$$

that allows us to examine the rest of the points. If $\sigma^2 - 4\Delta > 0$ and $\Delta > 0$ that is $\rho_s > \sqrt{\alpha}$ and $|\alpha| > \sqrt{\frac{1}{3} - 3 \left(\rho_s^2 - \frac{2}{3} \right)^2}$, respectively, the point is node. The node is stable if $\sigma > 0$ or $\rho_s > \frac{1}{\sqrt{2}}$ and it is unstable if $\sigma < 0$ or $\rho_s < \frac{1}{\sqrt{2}}$. Finally, with $\Delta < 0$ or $|\alpha| < \sqrt{\frac{1}{3} - 3 \left(\rho_s^2 - \frac{2}{3} \right)^2}$, the point is saddle.

Phase Synchronization

We finish our analysis with ascertaining stability of phase synchronization and frequency disciplining. Note that namely two of these characteristics are of prime importance in synchronized oscillators.

Let us come back to (7.219) and consider this phase equation in real time $t = \tau/\omega_s$. If we represents ξ by

$$\xi = 1 - \frac{\omega_0^2}{\omega_s^2} = \frac{(\omega_s - \omega_0)(\omega_s + \omega_0)}{\omega_s^2} \cong -\frac{2\Omega_0}{\omega_s},$$

where $\Omega_0 = \omega_0 - \omega_s$, (7.219) can be rewritten as

$$\vartheta' = \Omega_0 - \Omega \cos \vartheta \tag{7.229}$$

and, by changing a variable to $\varphi = \theta - \frac{\pi}{2}$, may be substituted with

$$\varphi' = \Omega_0 - \Omega \sin \varphi \tag{7.230}$$

that often is more convenient to use in an analysis of phase systems.

To ascertain stability of synchronization, we first consider a limiting case of $\omega_s = \omega_0$. This case means $\Omega_0 = 0$ and hence (7.230) degenerates to $\varphi' = -\Omega \sin \varphi$. For the near zero initial phase, a linearized ODE becomes $\varphi' = -\Omega\varphi$. Because Ω is always positive, a solution of (7.230) with $\Omega_0 = 0$ is zero at steady state and synchronization is stable. Moreover, it can be shown that synchronization is stable for an arbitrary initial phase.

If we allow $0 < \Omega_0 \leq \Omega$, a solution of (7.230) would still be stable (zero at infinity), because of the negative right side. The synchronization region is hence bounded with $|\Omega_0| \leq \Omega$ that is consistent with the bounds $|\alpha| \leq \eta$ in the magnitude response.

In the other limiting case, one may suppose that $\Omega_0 \gg \Omega$ and consider instead an ODE $\varphi' = \Omega_0$, which solution, commencing with zero, is $\varphi = \Omega_0 t$. The relevant asymptotic value of a synchronized frequency is therefore calculated by $\Omega_s^* = \Omega_0$. Fig. 7.36 depicts the asymptotic level by a dashed straight line.

To define transitions of Ω_s from zero at $\Omega_0 = \pm\Omega$ to the asymptotic line $\Omega_s^* = \Omega_0$ beyond the synchronization region, one first needs to observe that the relevant solution of (7.230) oscillates with period T_c owing to the harmonic function in the right-hand side. To find T_c , we rewrite (7.230) in the integral form

$$\int_{\varphi_0}^{\varphi} \frac{dx}{\Omega_0 - \Omega \sin x} = t_0 - t \tag{7.231}$$

that, by $\varphi_0 = 0$, $\varphi = 2\pi$, $t_0 = 0$, and $t = T_c$, yields

$$T_c = \int_0^{2\pi} \frac{dx}{\Omega_0 - \Omega \sin x}. \quad (7.232)$$

Solved (7.230) for $\varphi(t)$, the frequency associated with oscillations in φ is calculated by $\Omega_s^* = \frac{d\varphi}{dt}$. Finally, averaging Ω_s^* over T_c given by (7.232) produces the frequency synchronized beyond the synchronization region,

$$\Omega_s = \frac{1}{T_c} \int_0^{T_c} \Omega_s^*(t) dt = \frac{1}{T_c} [\varphi(T_c) - \varphi(0)]. \quad (7.233)$$

Fig. 7.36 sketches $\Omega_s(\Omega_0)$ defined numerically in the whole range of Ω_0 . One can observe that the effect of synchronization is strong with $|\Omega_0| < \Omega$ and still is partly saved with $|\Omega_0| > \Omega$.

Despite the direct approximate investigation of nonlinear ODEs of NTI systems sketches a complete picture of the system dynamics in phase plane, in many cases it becomes more convenient to solve the problem in state space. Moreover, state space offers solutions for several most general applied structures of NTI systems. Therefore, we proceed below with the state space analysis of NTI systems.

7.7 State Space Representation

A special feature of state space is an ability of performing any ODE of any order with the ODEs of the first order. Exploiting this facility, the state space representation is often used when an NTI system is of high order and generalization of a solution is required.

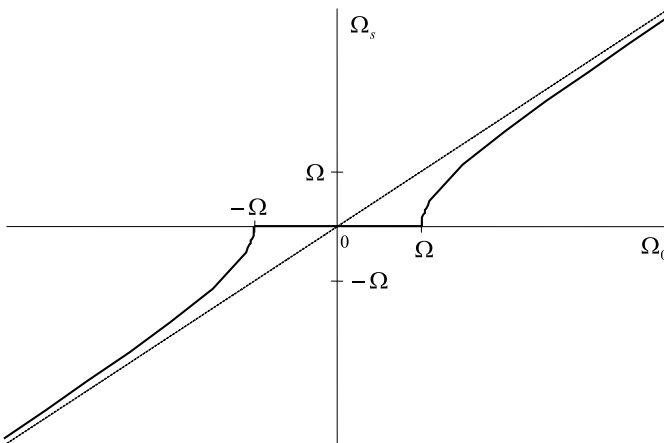


Fig. 7.36. Disciplining of frequency in a synchronized oscillator.

Most generally, an NTI system is performed in state space with

$$\mathbf{q}'(t) = \Psi[\mathbf{q}(t), \mathbf{x}(t)], \quad (7.234)$$

$$\mathbf{y}(t) = \Upsilon[\mathbf{q}(t), \mathbf{x}(t)], \quad (7.235)$$

where Ψ and Υ are some nonlinear vector functions. As well as the general nonlinear ODE (7.137), these equations cannot be solved, until the nonlinear functions Ψ and Υ are specified. And even though they are given, solutions can be found only for some particular cases.

Example 7.27. An NTI system is performed with the ODE

$$y''' + 3y''y - 2y' + y^3 = 3x^2. \quad (7.236)$$

To represent a system in state space, we assign the state variables $q_1 = y$, $q_2 = y' = q_1'$, and $q_3 = y'' = q_2'$, and find $q_3' = -3q_2q_1 + 2q_2 - q_1^3 + 3x^2$. The state space nonlinear model of a system is now performed by

$$\mathbf{q}'(t) = \mathbf{A}[\mathbf{q}(t)]\mathbf{q}(t) + \mathbf{B}[\mathbf{x}(t)]x(t), \quad (7.237)$$

$$y(t) = \mathbf{C}\mathbf{q}(t), \quad (7.238)$$

where

$$\mathbf{q} = \begin{bmatrix} q_1 \\ q_2 \\ q_3 \end{bmatrix}, \quad \mathbf{A} = \begin{bmatrix} 0 & 1 & 0 \\ 0 & 0 & 1 \\ -q_1^2 & 2 & -3q_1 \end{bmatrix}, \quad \mathbf{B} = \begin{bmatrix} 0 \\ 0 \\ 3x \end{bmatrix}, \quad \mathbf{C} = [1 \ 0 \ 0].$$

We notice that (7.237) and (7.238) cannot be solved in a manner similar to any linear ODE, in which both \mathbf{A} and \mathbf{B} contain only constant components and depend neither on state variables nor on signals. Typically, such equations are studied in phase plane. \square

7.7.1 Linearization of State Space Model

When stability of an NTI system needs to be ascertained at some point, the state space model is often linearized. Linearization is based on the construction of the tangent space and provided similarly to the nonlinear ODE.

To come up with the linearization to (7.234) and (7.235), let us examine a system in a vicinity of the point \mathbf{y}_0 , \mathbf{x}_0 corresponding to the state \mathbf{q}_0 and its time derivative \mathbf{q}'_0 . The actual system state, input, and output can then be defined by, respectively,

$$\mathbf{q}(t) = \mathbf{q}_0(t) + \tilde{\mathbf{q}}(t), \quad (7.239)$$

$$\mathbf{x}(t) = \mathbf{x}_0(t) + \tilde{\mathbf{x}}(t), \quad (7.240)$$

$$\mathbf{y}(t) = \mathbf{y}_0(t) + \tilde{\mathbf{y}}(t), \quad (7.241)$$

where $\tilde{\mathbf{q}}(t)$, $\tilde{\mathbf{x}}(t)$, and $\tilde{\mathbf{y}}(t)$ are small time varying increments. By (7.239)–(7.241), the state space model, (7.234) and (7.235), is rewritten as

$$\mathbf{q}'_0(t) + \tilde{\mathbf{q}}'(t) = \Psi[\mathbf{q}_0(t) + \tilde{\mathbf{q}}(t), \mathbf{x}_0(t) + \tilde{\mathbf{x}}(t)], \quad (7.242)$$

$$\mathbf{y}_0(t) + \tilde{\mathbf{y}}(t) = \Upsilon[\mathbf{q}_0(t) + \tilde{\mathbf{q}}(t), \mathbf{x}_0(t) + \tilde{\mathbf{x}}(t)]. \quad (7.243)$$

The right-hand sides of (7.242) and (7.243) can now be expanded to the Taylor series. If to save only the constant and linear terms, we arrive at the linearized equations

$$\tilde{\mathbf{q}}'(t) = \mathbf{A}\tilde{\mathbf{q}}(t) + \mathbf{B}\tilde{\mathbf{x}}(t), \quad (7.244)$$

$$\tilde{\mathbf{y}}(t) = \mathbf{C}\tilde{\mathbf{q}}(t) + \mathbf{D}\tilde{\mathbf{x}}(t), \quad (7.245)$$

in which the Jacobian matrices are determined as

$$\mathbf{A} = \left. \frac{\partial \Psi}{\partial \mathbf{q}} \right|_0, \quad \mathbf{B} = \left. \frac{\partial \Psi}{\partial \mathbf{x}} \right|_0, \quad \mathbf{C} = \left. \frac{\partial \Upsilon}{\partial \mathbf{q}} \right|_0, \quad \mathbf{D} = \left. \frac{\partial \Upsilon}{\partial \mathbf{x}} \right|_0, \quad (7.246)$$

where Ψ and Υ are taken from (7.242) and (7.243), respectively, and the condition “0” means that all functions are taken at \mathbf{x}_0 , \mathbf{y}_0 , and \mathbf{q}_0 .

Example 7.28. An NTI system is represented in state space by the ODEs

$$q'_1 = q_2,$$

$$q'_2 = -3q_1 - 2q_3^2 + x_1,$$

$$q'_3 = -q_1q_2 - 4q_3 + 2x_2.$$

The inputs are $x_1 = 0.5$ and $x_2 = 1$.

To ascertain stability of this system, substitute $x_1 = 0.5$ and $x_2 = 1$ to the system equations, set all of the time derivatives to zero, and solve the remaining algebraic equations. The only steady-state point is $\mathbf{q}_0 = [0 \ 0 \ \frac{1}{2}]^T$. At this point, by (7.246), the linearized state equation (7.244) is represented with the system and input matrices, respectively,

$$\mathbf{A} = \begin{bmatrix} 0 & 1 & 0 \\ -3 & 0 & -2 \\ 0 & 0 & -4 \end{bmatrix} \quad \text{and} \quad \mathbf{B} = \begin{bmatrix} 0 \\ 1 \\ 2 \end{bmatrix}.$$

The matrix \mathbf{A} is characterized with the characteristic polynomial

$$\lambda^3 + 4\lambda^2 + 3\lambda + 12 = 0$$

having three roots: $\lambda_1 = -4$, $\lambda_2 = j1.732$, and $\lambda_3 = -j1.732$. Because one of the roots is real and negative and two others have zero real parts, the system is stable in the sense of Lyapuniov and it is not asymptotically stable. \square

As can be inferred, the general model (7.234) and (7.235) has not enough applied features. Therefore, several more simple but soluble and practicable forms have been investigated for decades. The necessity of using simplified models follows, as a minimum, from Fig. 7.7, in which the NTI system (Fig. 7.7a) is split into the memoryless NTI (Fig. 7.7b) and memory LTI subsystems. It then has appeared that two models, namely the Hammerstein (Fig. 7.8a) and Wiener (Fig. 7.8b), as well as their cascade, series, or feedback interconnections are capable of representing a great deal of real nonlinear systems and channels with sufficient accuracy and without losing functionality. Such a simulating structure was called the *Wiener-Hammerstein system* and the latter often arises in the black box approach to identification of nonlinear systems.

It what follows, we observe the most principle features of open and feedback NTI systems utilizing Hammerstein and Wiener subsystems.

7.7.2 Hammerstein System

The familiar Hammerstein model is used in applications for blind identification of uncertain nonlinear channels and networks, modeling of power amplifiers and controlled oscillators, design of the Hammerstein-type equalizers, etc.

The basic SISO structure of such a model is represented with the memoryless NTI subsystem following by the memory LTI subsystem as shown in Fig. 7.37a. A nonlinearity is depicted here by $f(\cdot)$ and a linear block is described with the transfer function $H(s)$.

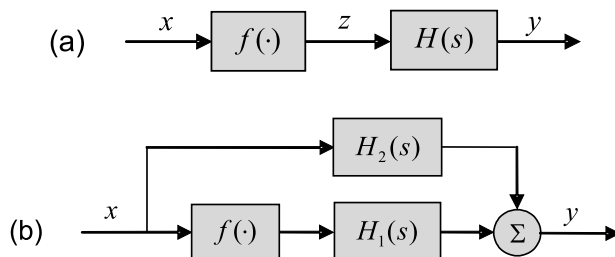


Fig. 7.37. Hammerstein system: (a) basic and (b) generalized.

The modified Hammerstein system often called *generalized* consists of two branches (Fig. 7.37b). The basic branch fulfils the traditional function. In parallel, an LTI branch with the transfer function $H_2(s)$ is included.

As follows from an analysis of the basic Hammerstein system, the input $x(t)$ is first preprocessed by a nonlinear block $f(\cdot)$ to produce a signal $z(t)$. The latter is thereafter transformed by a linear block to yield the output $y(t)$. In state space, this system is typically described with the equations

$$\begin{aligned}
 \mathbf{q}'(t) &= \mathbf{A}\mathbf{q}(t) + \mathbf{B}z(t), \\
 y(t) &= \mathbf{C}\mathbf{q}(t), \\
 z(t) &= f[x(t)],
 \end{aligned}
 \tag{7.247}$$

where the dimensions of the state vector \mathbf{q} depend on the order of the LTI subsystem. Stability of the Hammerstein system is guaranteed if the function $f(x)$ is bounded, $|z(t)| \leq M < \infty$, \mathbf{B} and \mathbf{C} have finite components, and the matrix \mathbf{A} is Hurwitz.

By (4.175), a solution of (7.247) is given as

$$y(t) = \mathbf{C}\Phi(t, t_0)\mathbf{q}(t_0) + \mathbf{C} \int_{t_0}^t \Phi(t, \theta)\mathbf{B}f[x(\theta)]d\theta,
 \tag{7.248}$$

where $\Phi(t, \tau) = e^{\mathbf{A}(t-\tau)}$ is the state transition matrix. Alternatively, by (5.194), the transform of the output is calculated for the known transform $z(t) \xleftrightarrow{\mathcal{L}} Z(s) = \mathcal{L}f[x(t)]$ as

$$\mathbf{Y}(s) = \mathbf{C}(s\mathbf{I} - \mathbf{A})^{-1}\mathbf{B}Z(s),
 \tag{7.249}$$

yielding the transfer function of a linear subblock $\mathbf{H}(s) = \mathbf{C}(s\mathbf{I} - \mathbf{A})^{-1}\mathbf{B}$.

It is of importance that a solution of the state space equations (7.247) can also be performed in the Volterra series form. Yet, for some particular cases, the describing functions are applied to linearize nonlinearity.

Example 7.29 (Asynchronous Demodulator of AM Signal). Consider the simplest asynchronous demodulator of AM signal modeled by the Hammerstein system. The classical scheme (Fig. 7.38) comprises a rectifier diode and an RC filter to track the envelope of an input signal.

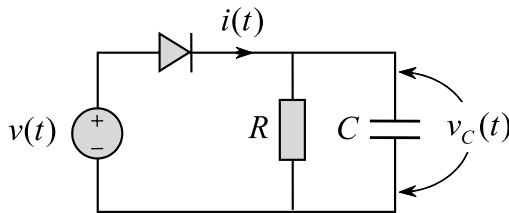


Fig. 7.38. Asynchronous demodulator of AM signal.

Assigning $x(t) = v(t)$, $q(t) = y(t) = v_C(t)$, and $z(t) = i(t)$, and approximating the electric current $i(t)$ of a diode by (7.21) allows us to represent the scheme in state space as

$$\begin{aligned} q'(t) &= Aq(t) + Bz(t), \\ y(t) &= |C|q(t), \\ z(t) &= I_0 \left(e^{\frac{x(t)}{V_T}} - 1 \right), \end{aligned}$$

where $A = -\frac{1}{RC}$, $B = \frac{1}{C}$, and $C = [1]$. By (7.248), the output becomes

$$y(t) = y_0 e^{-\frac{t}{RC}} + \frac{I_0}{C} e^{-\frac{t}{RC}} \int_0^t e^{\frac{\theta}{RC}} \left[e^{\frac{x(\theta)}{V_T}} - 1 \right] d\theta, \quad (7.250)$$

where $y_0 = y(0)$. A typical waveform of a demodulated AM signal restored by (7.250) is shown in Fig. 7.39. Even a quick look at the picture leads to the

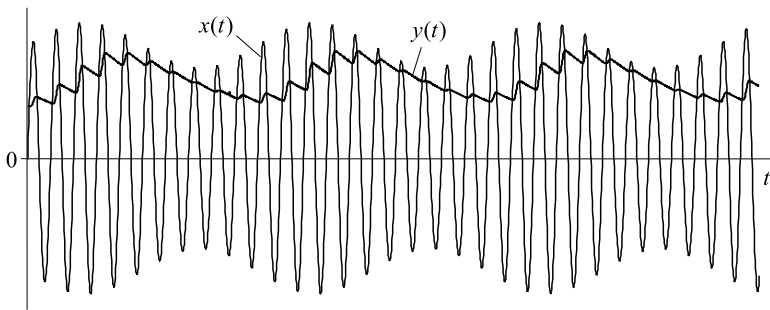


Fig. 7.39. Asynchronous demodulation: $x(t)$ is AM signal and $y(t)$ is demodulated envelope, by (7.250).

conclusion that the restored signal $y(t)$ fits physical imaginations about the demodulation process. We notice that in the more sophisticated asynchronous demodulators the phase shift between $y(t)$ and the envelope of $x(t)$ is almost negligible. □

Example 7.30 (Power Amplifier). Consider a scheme (Fig. 7.40) intended for power amplification.

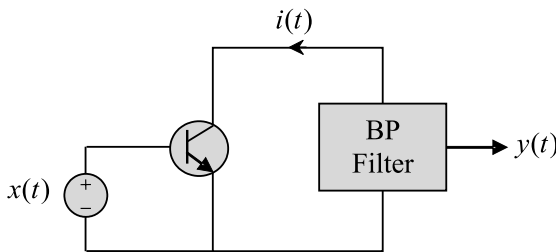


Fig. 7.40. Power amplifier.

The input signal is performed by a sum of two harmonic signals, $x(t) = \alpha \cos \omega_1 t + \cos \omega_2 t$. A transistor amplifier with a gain factor G is designed such that its collector current is in cubic dependence on the input voltage. The input voltage of a BP filter can therefore be written as $z(t) = Gx^3(t)$. The spectral content of $z(t)$ is as follows,

$$\begin{aligned} \frac{1}{G}z(t) &= (\alpha \cos \omega_1 t + \cos \omega_2 t)^3 \\ &= \frac{3\alpha}{2} \left(\frac{\alpha^2}{2} + 1 \right) \cos \omega_1 t + \frac{3}{4} (2\alpha^2 + 1) \cos \omega_2 t + \frac{\alpha^3}{4} \cos 3\omega_1 t \\ &\quad + \frac{1}{4} \cos 3\omega_2 t + \frac{3\alpha}{4} \cos(\omega_1 t + \omega_2 t) + \frac{3\alpha}{4} \cos(\omega_1 t - \omega_2 t) \\ &\quad + \frac{3\alpha^2}{4} \cos(2\omega_1 t + \omega_2 t) + \frac{3\alpha^2}{4} \cos(2\omega_1 t - \omega_2 t). \end{aligned}$$

The BP filter tuned to the frequency $2\omega_1 - \omega_2$ with a peak gain a forms the output voltage $y(t) = \frac{3}{4}Ga\alpha^2 \cos(2\omega_1 t - \omega_2 t)$ that is proportional to the power α^2 of a signal $\alpha \cos \omega_1 t$ removed to the frequency $2\omega_1 - \omega_2$.

The scheme is the Hammerstein system that is represented in state space with (7.247), where $z(t) = Gx^3(t)$, and solutions (7.248) and (7.249). \square

7.7.3 Wiener System

Another widely used idealization of NTI systems is the familiar *Wiener system* shown in Fig. 7.41. Here, the memory LTI subsystem with the transfer function

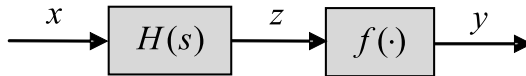


Fig. 7.41. Wiener system.

$H(s)$ follows by the memoryless NTI subsystem described by the nonlinear function $f(\cdot)$.

In state space, the SISO Wiener system can be represented as

$$\begin{aligned} \mathbf{q}'(t) &= \mathbf{A}\mathbf{q}(t) + \mathbf{B}x(t), \\ z(t) &= \mathbf{C}\mathbf{q}(t), \\ y(t) &= f[z(t)], \end{aligned} \tag{7.251}$$

where the dimensions of the state vector \mathbf{q} depend on the order of the LTI subsystem and $f(\cdot)$ is any nonlinear function. Like the Hammerstein system,

stability of the Wiener system is guaranteed by the bounded function $f(\cdot)$, $|y(t)| \leq M < \infty$, and Hurwitz matrix \mathbf{A} , if \mathbf{B} and \mathbf{C} have finite components.

By (4.175), a solution of (7.251) can be written as

$$y(t) = f \left[\mathbf{C}\Phi(t, t_0)\mathbf{q}(t_0) + \mathbf{C} \int_{t_0}^t \Phi(t, \theta)\mathbf{B}x(\theta)d\theta \right]. \quad (7.252)$$

In applications of the Wiener model, the main problem arises of identifying the nonlinearity and coefficients of (7.251) and (7.252) to fit an uncertain system with a reasonable accuracy.

Example 7.31 (Radio Frequency Transformer). Consider a basic nonlinear structure (Fig. 7.42) called the *radio frequency transformer* intended to transform the spectrum of an input signal. A classical application of such a

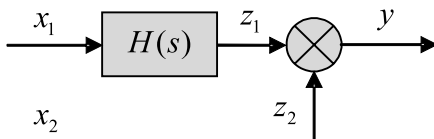


Fig. 7.42. Radio frequency transformer.

transformer can be found in the heterodyne receiver. Here a received signal $x_1(t)$ passes through the linear selective circuit with the transfer function $H(s)$ to produce an informative signal $z_1(t)$. Thereafter, $z_1(t)$ is mixed with the reference harmonic signal $z_2(t) = x_2(t)$. The nonlinear product $y(t) = z_1(t)z_2(t)$ consists of the components at the difference and sum frequencies. The low frequency components at the intermediate frequency are further used to produce the audio signal.

In state space, such a Wiener system is described with

$$\begin{aligned} \mathbf{q}'(t) &= \mathbf{A}\mathbf{q}(t) + [1 \ 0] \begin{bmatrix} x_1 \\ x_2 \end{bmatrix}, \\ \mathbf{z}(t) &= \begin{bmatrix} z_1 \\ z_2 \end{bmatrix} = \mathbf{C}\mathbf{q}(t), \\ y(t) &= \frac{1}{2}\mathbf{z}^T(t)\mathbf{S}\mathbf{z}(t), \end{aligned}$$

where $z_2 = x_2$ and $\mathbf{S} = \begin{bmatrix} 0 & 1 \\ 1 & 0 \end{bmatrix}$. By a solution of the linear part

$$\mathbf{z}(t) = \mathbf{C}\Phi(t, t_0)\mathbf{q}(t_0) + \mathbf{C} \int_{t_0}^t \Phi(t, \theta)\mathbf{B}x(\theta)d\theta$$

and zero initial conditions, the output becomes

$$y(t) = \left[\mathbf{C} \int_{t_0}^t \Phi(t, \theta) \mathbf{B} x(\theta) d\theta \right]^T \mathbf{S} \left[\mathbf{C} \int_{t_0}^t \Phi(t, \theta) \mathbf{B} x(\theta) d\theta \right].$$

□

7.7.4 Cascade Hammerstein and Wiener Systems

Frequently, cascade interconnections of Hammerstein and Wiener systems are used to simulate a whole system and not only its part. Different structures are exploited. The Hammerstein-Wiener system (Fig. 7.43a) fits, for example, a simple radio receiver. In turn, the Wiener-Hammerstein system (Fig. 7.43b) models well corrective predistortion and/or postdistortion in power amplification.

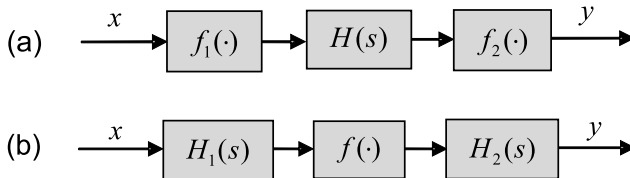


Fig. 7.43. Cascade NTI systems: (a) Hammerstein-Wiener and (b) Wiener-Hammerstein.

Example 7.32 (Coherent Receiver). The Wiener-Hammerstein system well models the coherent receiver (Fig. 7.44) intended to form the in-phase I and quadrature phase Q components from the received signal $x_1(t) = 2A \cos[\omega_0 t - \phi(t)]$, in which the phase $\phi(t)$ is informative.

A received signal $x_1(t)$ passes through the selective BP filter to the mixers as $z_1(t) = 2 \cos[\omega_0 t - \phi(t)]$. In the first mixer, a signal $z_1(t)$ is multiplied with the cosine signal $x_2(t) = z_2(t) = \cos \omega_0 t$ and in the second one with the sine signal $x_3(t) = z_3(t) = \sin \omega_0 t$. Accordingly, two signals are formed

$$\begin{aligned} v_1(t) &= 2 \cos[\omega_0 t - \phi(t)] \cos \omega_0 t = \\ &= \cos[2\omega_0 t - \phi(t)] + \cos \phi(t), \\ v_2(t) &= 2 \cos[\omega_0 t - \phi(t)] \sin \omega_0 t = \\ &= \sin[2\omega_0 t - \phi(t)] + \sin \phi(t). \end{aligned}$$

At the outputs of LP filters having unit gain factors, we thus have two quadrature components,

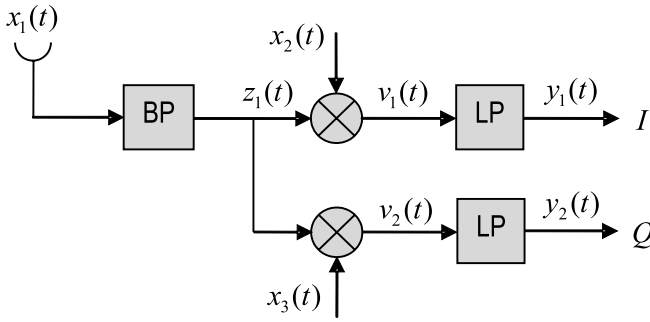


Fig. 7.44. Coherent receiver.

$$I(t) = y_1(t) = \cos \varphi(t),$$

$$Q(t) = y_2(t) = \sin \varphi(t).$$

Using $I(t)$ and $Q(t)$, the phase is readily restored by $\tan \varphi(t) = Q/I$.

In state space, the receiver is performed by the equations

$$\mathbf{q}' = \mathbf{A}\mathbf{q} + [1 \ 0 \ 0] \mathbf{x},$$

$$z_1 = \mathbf{C}\mathbf{q},$$

$$\mathbf{v} = \begin{bmatrix} \mathbf{z}^T \mathbf{S}_1 \mathbf{S}_2 \mathbf{x} \\ \mathbf{z}^T \mathbf{S}_3 \mathbf{x} \end{bmatrix},$$

$$\mathbf{q}'_1 = \mathbf{A}_1 \mathbf{q}_1 + [1 \ 0] \mathbf{v},$$

$$\mathbf{q}'_2 = \mathbf{A}_2 \mathbf{q}_2 + [0 \ 1] \mathbf{v},$$

$$\mathbf{y} = \begin{bmatrix} I \\ Q \end{bmatrix} = \begin{bmatrix} y_1 \\ y_2 \end{bmatrix} = \begin{bmatrix} \mathbf{C}_1 \mathbf{q}_1 \\ \mathbf{C}_2 \mathbf{q}_2 \end{bmatrix},$$

where $\mathbf{q}(t) = \begin{bmatrix} q_1(t) \\ q_2(t) \\ q_3(t) \end{bmatrix}$, $\mathbf{x}(t) = \begin{bmatrix} x_1(t) \\ \cos \omega_0 t \\ \sin \omega_0 t \end{bmatrix}$, $\mathbf{z}(t) = \begin{bmatrix} z_1(t) \\ \cos \omega_0 t \\ \sin \omega_0 t \end{bmatrix}$, $\mathbf{S}_1 = \begin{bmatrix} 0 & 0 & 1 \\ 0 & 1 & 0 \end{bmatrix}$,

$\mathbf{S}_2 = \begin{bmatrix} 0 & 1 \\ 0 & 0 \\ 0 & 0 \end{bmatrix}$, and $\mathbf{S}_3 = \begin{bmatrix} 0 & 0 & 1 \\ 0 & 0 & 0 \\ 0 & 0 & 0 \end{bmatrix}$.

Here \mathbf{A} , \mathbf{A}_1 , \mathbf{A}_2 , \mathbf{C} , \mathbf{C}_1 , and \mathbf{C}_2 are the matrices describing the linear filters. □

7.7.5 Closed Loop Systems

In modeling nonlinear systems, two closed loops are used as originating from the Hammerstein and Wiener systems (Fig. 7.45). The Wiener-based closed loop is also referred to as the Lure's system. In some cases, the loops are interchangeable. Basically, each of these loops can be designed with positive or negative feedback. Because the feedback can change the picture cardinally, an investigation of stability in such structures occupies an important place.

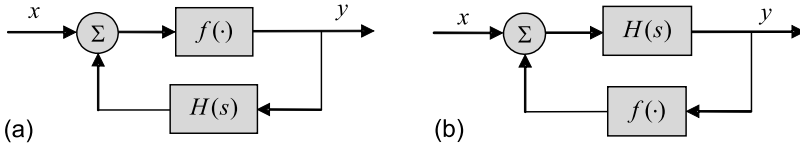


Fig. 7.45. Closed loop systems: (a) Hammerstein-based and (b) Wiener-based (Lur'e system).

Popov's and Circle Criteria of Stability

To ascertain stability of closed loops (Fig. 7.45), one can try using the second Lyapunov method. It turns out, however, that the Lyapunov approach is too general. Therefore a number of efforts were made for decades to find some more engineering tool. With time, the currency have gained two criteria: *Popov's* and *circle*.

Popov's criterion: An autonomous closed loop Lur'e system is asymptotically stable if

- Its LTI part is stable (has no right-hand plane singularities).
- Its memoryless NTI feedback is bounded, satisfied

$$f(0) = 0 \quad \text{and} \quad 0 < \frac{f(y)}{y} < M < \infty, \quad y \neq 0.$$

- There exists a constant α such that

$$(1 + \alpha s)H(s) + \frac{1}{M}$$

is a positive real function: it has no poles with positive real parts, the poles with zero real parts are simple and have positive real residues, and $\text{Re}H(j\omega) \geq 0$ for all ω .

□

In accordance with the Popov's criterion, the function $f(\cdot)$ must trace within the sector bounded by the line My and abscissa axis as shown in Fig. 7.46a.

The other useful engineering criterion is called the *circle criterion* that is a modification of Popov's criterion for the lower bound of nonlinearity. The circle criterion follows from the works of Sandberg and Zames. Therefore it is also often called *Sandberg's circle criterion* or *Zames's circle criterion*.

Circle (Sandberg-Zames) criterion: An autonomous closed-loop Lure's system is globally asymptotically stable if

- Its LTI part is stable (\mathbf{A} is Hurwitz), controllable, and observable.
- Its memoryless NTI feedback is bounded, satisfied

$$f(0) = 0 \quad \text{and} \quad M_2 < \frac{f(y)}{y} < M_1 < \infty, \quad y \neq 0.$$

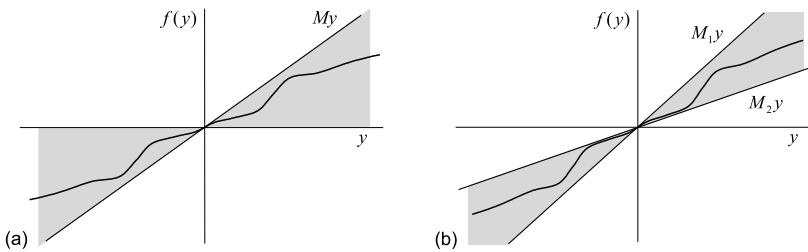


Fig. 7.46. Bounded nonlinearity criteria: (a) Popov's and (b) circle.

- The plot of $H(j\omega)$ in the complex plane $U = \text{Re}H(j\omega)$ and $V = \text{Im}H(j\omega)$ does not touch or encircle the circular region $R(M_1, M_2)$:

$$R(M_2, M_1 \neq 0) :$$

$$M_1 M_2 \left[\left(U + \frac{1}{2M_2} + \frac{1}{2M_1} \right)^2 + V^2 - \frac{1}{4} \left(\frac{1}{M_2} - \frac{1}{M_1} \right) \right] \leq 0,$$

$$R(M_2 = 0, M_1 \neq 0) : U \leq -\frac{1}{M_1},$$

$$R(M_1 = 0, M_2 \neq 0) : U \geq -\frac{1}{M_2}.$$

□

Unlike Popov's criterion, the circle one claims the function $f(\cdot)$ to trace within the sector bounded by two lines M_1y and M_2y as shown in Fig. 7.46b. The circle criterion also states that if the Nyquist plot of $H(j\omega)$ does not touch or intersect the circular region $R(M_1, M_2)$, then the system is absolutely stable.

Hammerstein-based Closed Loop System

The Hammerstein-based model (Fig. 7.45a) represents a memoryless NTI system with a memory LTI system in the feedback. If the feedback is positive, it can be a familiar harmonic oscillator. An example of a system with the negative feedback is the frequency control loop of the voltage-controlled crystal oscillator (VCXO). Here the controlling voltage steers the frequency via the nonlinear memoryless diode-varactor. The frequency offset is then measured by a linear resonance circuit for the reference frequency to produce a feedback voltage. When the VCXO frequency is exactly equal to the reference frequency, the feedback voltage is $x(t)$ and the control voltage is zero.

In state space, a SISO closed loop (Fig. 7.45a) is represented with

$$\mathbf{q}'(t) = \mathbf{A}\mathbf{q} + \mathbf{B}y(t),$$

$$\begin{aligned}v(t) &= \mathbf{C}\mathbf{q}, \\y(t) &= f[x(t) + v(t)].\end{aligned}\tag{7.253}$$

The state equation can also be written in the compact form as

$$\mathbf{q}'(t) = \mathbf{A}\mathbf{q} + \mathbf{B}f[\mathbf{C}\mathbf{q} + x(t)]$$

and the Popov's criterion of stability can be applied as for Lure's system that we consider below.

Lur's System

Another closed loop control originated from the Wiener system is known as the *Lur's system*. The structure of this loop is shown in Fig. 7.45b. The system has found applications in secure communications owing to its ability to generate chaotic signals with external synchronization. Examples of chaotic Lur's systems are Chua's circuit, n-scroll circuits, and cellular neural networks consisting of chaotic cells that reveal hyperchaotic behavior.

In state space, the SISO Lur's system (Fig. 7.45b) is given by the equations

$$\begin{aligned}\mathbf{q}'(t) &= \mathbf{A}\mathbf{q}(t) + \mathbf{B}v(t), \\y(t) &= \mathbf{C}\mathbf{q}(t), \\v(t) &= x(t) + f(y)\end{aligned}\tag{7.254}$$

allowing for representing the state equation in the following compact form

$$\mathbf{q}'(t) = \mathbf{A}\mathbf{q}(t) + \mathbf{B}\{x(t) + f[\mathbf{C}\mathbf{q}(t)]\}.$$

Example 7.33 (Chua's circuit). Consider the Chua's circuit representing the autonomous chaotic Lur'e system ($x = 0$) in state space (7.254) with the equations

$$\begin{bmatrix} q_1'(t) \\ q_2'(t) \\ q_3'(t) \end{bmatrix} = \begin{bmatrix} -am_1 & a & 0 \\ 1 & -1 & 1 \\ 0 & -b & 0 \end{bmatrix} \begin{bmatrix} q_1(t) \\ q_2(t) \\ q_3(t) \end{bmatrix} + \begin{bmatrix} -a(m_0 - m_1) \\ 0 \\ 0 \end{bmatrix} f(q_1),$$

$$y(t) = [1 \ 0 \ 0] \begin{bmatrix} q_1(t) \\ q_2(t) \\ q_3(t) \end{bmatrix},$$

$$f(q_1) = \frac{1}{2}(|q_1 + 1| - |q_1 - 1|).$$

In order to obtain the double scroll attractor, the coefficients of the equations are chosen such that $a = 9$, $b = 14.286$, $m_0 = -\frac{1}{7}$, and $m_1 = \frac{2}{7}$. It can easily be verified that the nonlinearity $f(q_1)$ is bounded within the sector

$[0, 1]$. However, the matrix \mathbf{A} is not Hurwitz having a simple pole $s = 3.942$ in the right plane. This Lur'e system does not satisfy neither Popov's nor circle conditions and hence is unstable.

Solutions of the equations for the initial values $q_1(0) = 1$, $q_2(0) = 0$, and $q_3(0) = 0$ are shown in Fig. 7.47. At the first glance, no periodicity could be

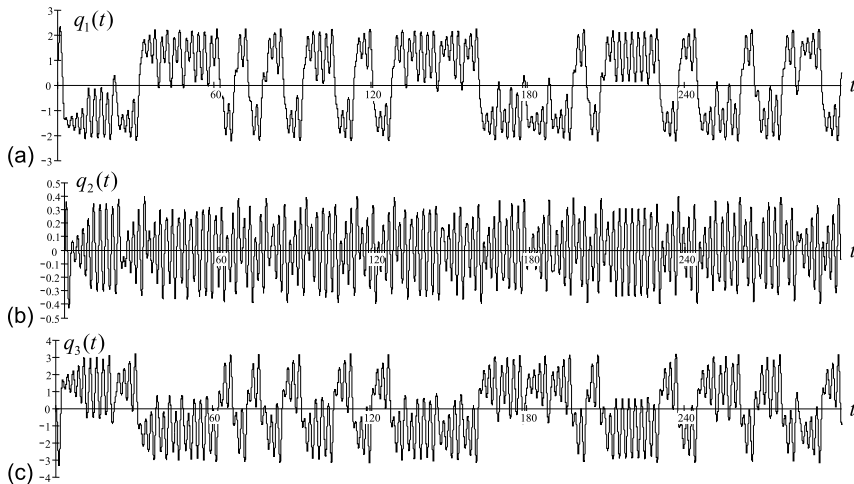


Fig. 7.47. Solutions of Chua's equations for $q_1(0) = 1$, $q_2(0) = 0$, and $q_3(0) = 0$: (a) $q_1(t)$, (b) $q_2(t)$, and (c) $q_3(t)$.

fixed in dynamics of the state variables.

More precisely, the double scroll picture can be watched in phase plane of different states as shown in Fig. 7.48. As easily seen, the circuit trajectory traces periodically about two centers of attraction. Such a pseudo random effect is used in secure communications. It is important to notice that, by the properly set coefficients, the circuit allows for the n -scroll attractor. However, in applications, stability of the multi-scroll picture requires obtaining the values of the coefficients with high accuracy and precision under the operation conditions. \square

7.7.6 Phase Locked Loop

We finish our analysis of NTI systems in state space with a brief presentation of the so-called *phase locked loop* (PLL). This closed-loop system has found wide applications in carrier phase and frequency tracking, symbol (bit) synchronization, clock and data recovery, demodulation and modulation, frequency synthesis and translation, frequency dividers, noise shaping, etc. The technique was first described in 1932 by Bellescise in a paper "La réception Synchrone" published in the French journal "Onde Electrique". Thereafter,

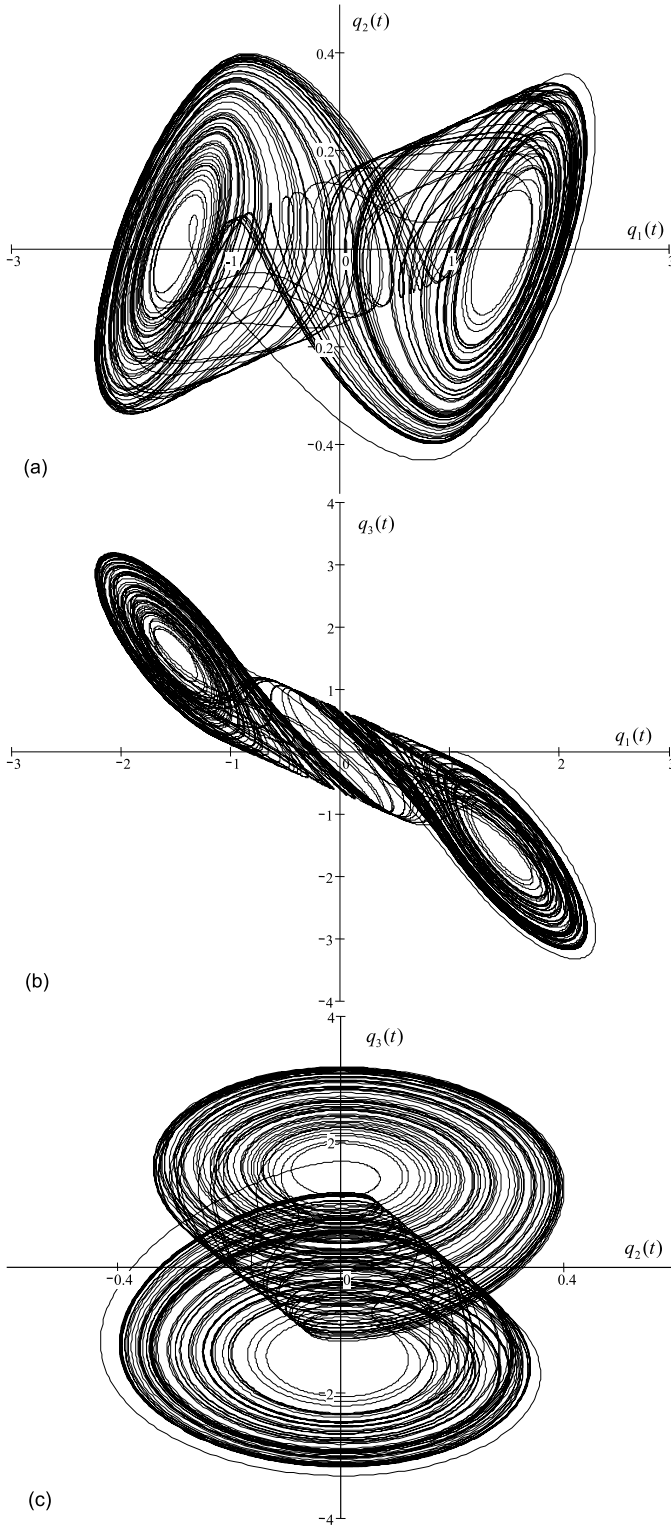


Fig. 7.48. Double scroll of Chua's circuit in the phase plane of: (a) $q_2(t)$ and $q_1(t)$, (b) $q_3(t)$ and $q_1(t)$, and (c) $q_3(t)$ and $q_2(t)$.

an enormous number of papers and books was devoted to its investigation by different methods.

Having a LP filter of an arbitrary order as a main memory component, the loop may be analyzed in the time and transform domains having the most general presentation in state space. Basic operation principle of the PLL is illustrated in Fig. 7.49.

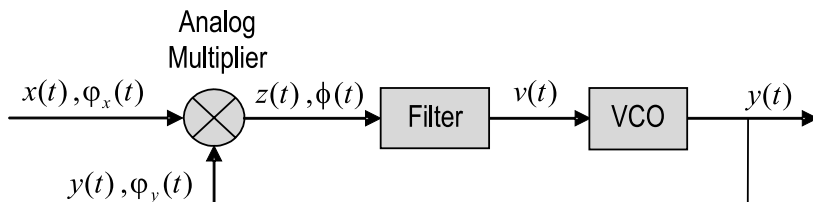


Fig. 7.49. Phase-locked loop.

A local voltage-controlled oscillator (VCO) generates a signal

$$y(t) = \sqrt{2}A_y \sin \varphi_y(t), \quad (7.255)$$

where A_y is a constant amplitude and $\varphi_y(t) = \omega_{os}t + \psi_y(t)$ is the time-varying phase. Here ω_{os} is the initial oscillator frequency.

Generally, it is supposed that neither ω_{os} nor $\psi_y(t)$ meet the requirements and must be disciplined by the reference input signal

$$x(t) = \sqrt{2}A_x \cos \varphi_x(t), \quad (7.256)$$

where A_x is constant and $\varphi_x(t) = \omega_r t + \psi_r(t)$. Here ω_r is the reference frequency and $\psi_r(t)$ is the reference (generally, time-varying) phase.

In the analog multiplier (phase detector), the signals (7.255) and (7.256) are mixed to produce

$$z(t) = k_{PD}A_xA_y \sin(\varphi_x - \varphi_y) + k_{PD}A_xA_y \sin(\varphi_x + \varphi_y),$$

where k_{PD} is the gain of the multiplier. The low-frequency component is then filtered. Therefore, $z(t)$ may be written as

$$z(t) = k_{PD}A_xA_y \sin \phi(t), \quad (7.257)$$

where the phase angle

$$\phi(t) = \varphi_x(t) - \varphi_y(t) \quad (7.258)$$

represents the instantaneous phase error in the loop and called the *closed loop phase error*.

An LP filter provides filtering the low frequency components at the output of the multiplier. The filter order can be arbitrary. In view of that, its input and output are coupled by the linear time-invariant operator

$$v(t) = \mathcal{O}z(t) \quad (7.259)$$

that, equivalently, can be written in the following traditional forms of

$$\sum_{n=0}^N a_n \frac{d^n}{dt^n} v(t) = \sum_{m=0}^M b_m \frac{d^m}{dt^m} z(t), \quad (7.260)$$

$$V(s) = \frac{\sum_{m=0}^M b_m s^m}{\sum_{n=0}^N a_n s^n} Z(s), \quad (7.261)$$

$$v(t) = \int_0^t z(\theta) h(t - \theta) d\theta, \quad (7.262)$$

where all the coefficients, a_n , $n \in [0, N]$ and b_m , $m \in [0, M]$, $M \leq N$, are constants, $V(s)$ and $Z(s)$ are the Laplace transforms of $v(t)$ and $z(t)$, respectively, and $h(t)$ is the impulse response of the filter.

The frequency control characteristic of a local oscillator is typically nonlinear. It is known from the PLL theory that namely this nonlinearity allows for shortening the phase transient during synchronization. In our case, for the sake of simplicity, we are going to model a local oscillator with an ideal integrator as

$$\psi_y(t) = K_{os} \int v(t) d\theta,$$

where K_{os} is the gain of the oscillator control input, and

$$\psi'_y(t) = K_{os} v(t). \quad (7.263)$$

The next step presumes considering an equation $\phi' = \varphi'_r - \varphi'_y$, substitute for above-defined functions and write the dynamic equation of the PLL,

$$\begin{aligned} \phi' &= \varphi'_r - \varphi'_y = \omega_r - \omega_{os} + \psi'_r - \psi'_y \\ &= \Delta_0 + \psi'_r - K_{os} v(t) = \Delta_0 + \psi'_r - K_{os} \mathcal{O}z(t) \\ &= \Delta_0 - G\mathcal{O} \sin \phi + \psi'_r, \end{aligned} \quad (7.264)$$

where $\Delta_0 = \omega_r - \omega_{os}$ is the frequency shift between the reference and local oscillators and $G = K_{os} k_{PD} A_x A_y$ is the *closed loop gain*. We notice that in the simplified PLL model, it can be supposed that $\omega_r = \omega_{os}$ and $\Delta_0 = 0$.

Under such assumptions and by assigning in (7.260) the left-hand side and right-hand side ODE operators to be, respectively,

$$\mathcal{O}_1 \equiv \sum_{n=0}^N a_n \frac{d^n}{dt^n} \quad \text{and} \quad \mathcal{O}_2 \equiv \sum_{m=0}^M b_m \frac{d^m}{dt^m},$$

and, to represent a general operator \mathcal{O} in (7.264), we finally arrive at the generalized equation of the PLL

$$\mathcal{O}_1[\phi' - \psi'_r - \Delta_0] = -G\mathcal{O}_2[\sin \phi] \quad (7.265)$$

that can be investigated in different domains and various forms for the operators given, \mathcal{O}_1 and \mathcal{O}_2 .

Example 7.34 (PLLs of low orders). If an LP filter is assumed to have a uniform frequency response, we have $\mathcal{O}_1 = \mathcal{O}_2 = 1$ and the PLL equation attains the simplest form of

$$\phi' + G \sin \phi = \psi'_r + \Delta_0. \quad (7.266)$$

When $\mathcal{O}_1 = a_0 + \frac{d}{dt}$ and $\mathcal{O}_2 = 1$, the equation becomes

$$\phi'' + a_0\phi' + G \sin \phi = \psi''_r + a_0\psi'_r + a_0\Delta_0. \quad (7.267)$$

For the filter designed such that $\mathcal{O}_1 = a_0 + \frac{d}{dt}$ and $\mathcal{O}_2 = 1 + \frac{d}{dt}$, the PLL equation is written as

$$\phi'' + (a_0 + G \cos \phi)\phi' + G \sin \phi = \psi''_r + a_0\psi'_r + a_0\Delta_0. \quad (7.268)$$

We notice that (7.268) describes a wide class of phase systems, including the classical pendulum and Josephson⁸ junction. Readers can find extensive investigations of these equations in many books devoted to PLLs. \square

Allowing for $a_N = 1$ and $N = M$, (7.265) can be represented in state space. In doing so, we first rewrite (7.265) as follows

$$\sum_{n=0}^N \frac{d^n}{dt^n} (a_n\phi' + Gb_n \sin \phi) = \sum_{n=0}^N a_n \frac{d^n}{dt^n} (\psi'_r + \Delta_0)$$

and assign the state variables

$$q_1 = \phi, \quad q_2 = \phi' = q'_1, \quad \dots, \quad q_N = \phi^{(N-1)} = q'_{N-1}, \quad q_{(N+1)} = \phi^{(N)} = q'_N,$$

$$\begin{aligned} q'_{N+1} &= \phi^{(N+1)} = -a_0\phi' - a_1\phi'' - \dots - a_{N-1}\phi^{(N)} \\ &- Gb_0 \sin \phi - Gb_1\phi' \cos \phi + Gb_2\phi'' \sin \phi + \dots + b_N \sin^{(N)} \phi \\ &= -a_0q_2 - a_1q_3 - \dots - a_{N-1}q_{N+1} \\ &- Gb_0 \sin q_1 - gb_1q_2 \cos q_1 + Gb_2q_3 \sin q_1 + \dots + Gb_N \sin^{(N)} q_1. \end{aligned}$$

⁸ Brian D. Josephson, British physicist, 4 January 1940–.

In the PLL, the input signal is associated with the initial frequency offset Δ_0 and dynamic frequency drift ψ'_r . If we let

$$x_1 = \psi'_r + \Delta_0, \quad x_2 = x'_1 = \psi''_r, \quad \dots, \quad x_N = x'_{N-1} = \psi^{(N)}_r,$$

the state space model of the PLL will be formed by

$$\begin{bmatrix} q'_1(t) \\ q'_2(t) \\ \vdots \\ q'_N \\ q'_{N+1} \end{bmatrix} = \mathbf{A}[\mathbf{q}(t)] \begin{bmatrix} q_1(t) \\ q_2(t) \\ \vdots \\ q_N \\ q_{N+1} \end{bmatrix} + \begin{bmatrix} 0 & 0 & \dots & 0 & 0 \\ 0 & 0 & \dots & 0 & 0 \\ \vdots & \vdots & & \ddots & \\ 0 & 0 & \dots & 0 & 0 \\ a_0 & a_1 & \dots & a_{N-1} & 1 \end{bmatrix} \begin{bmatrix} x_1(t) \\ x_2(t) \\ \vdots \\ x_{N-1}(t) \\ x_N(t) \end{bmatrix} \quad (7.269)$$

$$y(t) = \phi(t) = [1 \ 0 \ \dots \ 0 \ 0] \begin{bmatrix} q_1(t) \\ q_2(t) \\ \vdots \\ q_N(t) \\ q_{N+1}(t) \end{bmatrix}, \quad (7.270)$$

where the nonlinear system matrix is specified by

$$\mathbf{A}[\mathbf{q}(t)] = \begin{bmatrix} 0 & 1 & 0 & \dots & 0 \\ 0 & 0 & 1 & \dots & 0 \\ \vdots & \vdots & & \ddots & \\ 0 & 0 & 0 & \dots & 1 \\ A_{N+1,1} & A_{N+1,2} & A_{N+1,3} & \dots & A_{N+1,N+1} \end{bmatrix} \quad (7.271)$$

with the components

$$\begin{aligned} A_{N+1,1} &= -Gb_0 \frac{\sin q_1}{q_1}, \\ A_{N+1,2} &= -a_0 - Gb_1 \cos q_1, \\ A_{N+1,3} &= -a_1 + Gb_2 \sin q_1, \\ &\vdots \\ A_{N+1,N+1} &= -a_{N-1} + Gb_N \frac{\sin^{(N)} q_1}{q_{N+1}}. \end{aligned}$$

Example 7.35. Consider the PLL differential equation (7.268). By $y = q_1 = \phi$, $q_2 = \phi' = q'_1$, $q'_2 = -(a_0 + G \cos q_1)q_2 - G \sin q_1$, $x_1 = \psi'_r + \Delta_0$, and $x_2 = \psi''_r$, the PLL is represented in state space with

$$\begin{bmatrix} q'_1(t) \\ q'_2(t) \end{bmatrix} = \mathbf{A}[\mathbf{q}(t)] \begin{bmatrix} q_1(t) \\ q_2(t) \end{bmatrix} + \begin{bmatrix} 0 & 0 \\ a_0 & 1 \end{bmatrix} \begin{bmatrix} x_1(t) \\ x_2(t) \end{bmatrix},$$

$$y(t) = [1 \ 0] \begin{bmatrix} q_1(t) \\ q_2(t) \end{bmatrix},$$

where the nonlinear system matrix is specified by

$$\mathbf{A}[\mathbf{q}(t)] = \begin{bmatrix} 0 & 1 \\ -G \frac{\sin q_1}{q_1} & -(a_0 + G \cos q_1) \end{bmatrix}.$$

It is seen that at the equilibrium point of zero loop error, $q_1 = 0$, the system matrix becomes linear, $\mathbf{A} = \begin{bmatrix} 0 & 1 \\ -G & -(a_0 + G) \end{bmatrix}$, with negative components A_{21} and A_{22} . As one remembers, such a system is Lyapunov stable. \square

In this chapter, we observed the most common methods of NTI systems analysis in the time and transform domains. An analysis is supplied with the most typical examples. The reader must keep in mind that selection of the methods is dictated by engineering needs, to mean that accuracy must be sufficient and calculus short. With any necessity of describing the input-to-output NTI system and restoring the exact output, the ODE or Volterra method is usually used. If approximation is allowed, the describing functions could be in order. If a system is closed, the amplitude and phase of possible oscillations are typically of prime interest. Here, the approximate methods based on averaging and linearization commonly solve the block of questions satisfactory. A special place occupy the methods of ascertaining stability of the solutions.

7.8 Summary

Contrary to linear systems, the NTI ones are typically much harder to analyze. Here the qualitative and even approximate methods are often the only tools to find proper solutions. In dealing with NTI systems, the reader must remember the following fundamentals:

- A system that provides nonlinear transformations with a time-invariant operator is the NTI system.
- For every new measured point, the Lagrange interpolation polynomial must be recalculated fully, whereas the Newton one needs determining only an addition for this point.
- Splines represent a wide class of functions intended to interpolate or/and smooth the measured memoryless nonlinearity between neighboring points.
- The Taylor series is used universally to linearize or represent the memoryless nonlinearity around some operation point.
- The Volterra series describes a memory system in the time domain via the Volterra kernels and generalized convolution. It is also called the Taylor series with memory.

- The Wiener series is akin to the Volterra series. The terms in the Wiener series are orthogonalized.
- The multivariate Laplace transform represents an NTI system in the transform domain via the Volterra series.
- The describing function is akin to the frequency response of an NTI system equivalently linearized for the harmonic input.
- The nonlinear ODE describing an NTI system has typically no general solution. Therefore, the qualitative methods are widely used to investigate stability and dynamics in phase plane.
- Any NTI system can be represented in state space. To ascertain stability of a system, the state space model is linearized at a given point and the characteristic equation associated with the system matrix is investigated.

7.9 Problems

7.1. Explain in simple words the difference between the LTI and NTI systems. Bring examples of both systems taken from the operation principles of the most common systems given in Chapter 1.

7.2. Both the LTV and NTI systems are able to transform the spectral content of the input. In view of that, what actually is the difference between two of these systems? Bring graphical illustration.

7.3 (interpolation). Explain the difference between the Lagrange and Newton interpolations. Which approach is more preferable for flexible measurements with a variable number of the points?

7.4. The nonlinearity of a memoryless system is measured at discrete points with a constant step $\Delta x = x_{i+1} - x_i$, $i = 1, 2, \dots$. The measurements are postponed to Table 7.1. Interpolate the function with the Lagrange formulae. Repeat interpolation with the Newton formulae. Compare the results.

7.5. Interpolate the nonlinearity (Table 7.1) with the cubic splines allowing for a linear behavior beyond the measurement region.

7.6 (Volterra series). A SISO NTI system is represented with the ODE

$$y'' + \left(\frac{y'}{y} + 1 \right) y' + y = \frac{x}{y}.$$

By an auxiliary variable $z = y^2$, separate the system into the LTI memory and NTI memoryless parts. Represent the system with the Volterra kernels and sketch the block diagram.

7.7. Resolve Problem 7.6 for the following ODEs and auxiliary functions:

1. $y' + y = xy^{-2}$, $z = y^3$

Table 7.1. Memoryless nonlinearity measured at discrete points

No	y_1	y_2	y_3	y_4	y_5	y_6	y_7	y_8	y_9
1	0	0.785	1.107	1.249	1.326	1.373	1.406	1.429	1.446
2	1.111	0.651	-0.305	-0.879	-0.543	0.395	1.071	-	-
3	-2	-1	0	1	2	1	0	-1	-2
4	0.632	0	-0.233	-0.318	-0.35	-0.361	-0.366	-	-
5	-0.6	-0.4	-0.2	0	-0.8	-0.6	-0.4	-0.2	0
6	-2	2	14	34	62	98	142	194	254
7	1	-0.5	-1	-0.5	1	3.5	7	11.5	17
8	-1	-1	-1	-0.5	0	0.5	1	1	1
9	-0.5	1	5.5	13	23.5	37	53.5	73	95.5
10	0	0	0	1	1	1	-	-	-

2. $y''' + 3\frac{y'}{y}y'' + y^2 = \frac{x}{y}$, $z = y^2$
3. $y'' - \frac{y'^2}{2y} - \frac{x}{\sqrt{y}} = -1$, $z = \sqrt{y}$
4. $y' + y - \frac{x}{\sqrt{y}} = 0$, $z = y^{\frac{3}{2}}$

7.8. An NTI system is represented with the block diagram shown in Fig. 7.50. Find the Volterra kernel of the system.

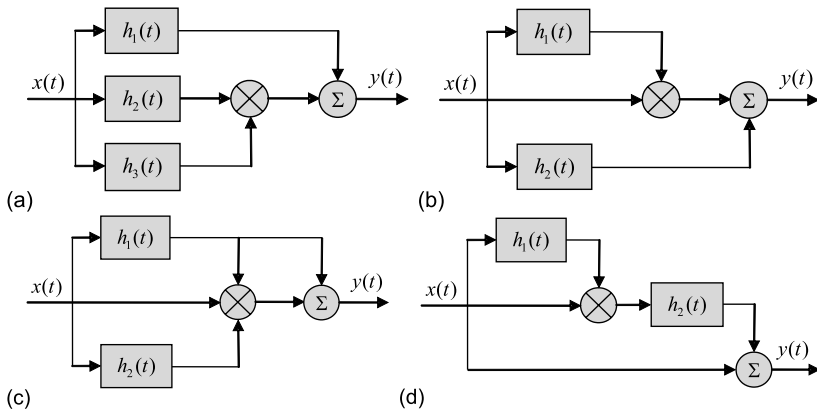


Fig. 7.50. Structures of NTI systems.

7.9. Based on the Volterra kernel derived in Problem 7.7, ascertain stability of the system.

7.10. Using the Volterra kernels derived in Problem 7.8, define the Wiener kernels of the system diagrammed in Fig. 7.50.

7.11 (Transform domain). Verify that the system performed by the Volterra kernel $h_2(\theta_1, \theta_2) = \theta_1(1 - e^{-\theta_2})u(\theta_1)u(\theta_2)$ is represented in the transform domain with the two-variate transfer function $H_2(s_1, s_2) = \frac{1}{s_1^2 s_2 (s_2 + 1)}$.

7.12. An NTI system is represented with the following Volterra kernels. Define the multivariate transfer function of the system.

1. $h_2(\theta_1, \theta_2) = e^{-\theta_1} (e^{-3\theta_2} - e^{-\theta_2}) u(\theta_1)u(\theta_2)$
2. $h_3(\theta_1, \theta_2, \theta_3) = e^{-\theta_1 - \theta_3} (1 - e^{-\theta_2}) u(\theta_1)u(\theta_2)u(\theta_3)$
3. $h_2(\theta_1, \theta_2) = e^{-\theta_1} u(\theta_1 - \theta_2)$
4. $h_2(\theta_1, \theta_2) = \theta_1 u(\theta_1) - (\theta_1 - \theta_2)u(\theta_2 - \theta_1)u(\theta_1)$

7.13. Verify that the two-variable transfer function $H_2(s_1, s_2) = \frac{1}{s_1 s_2 (s_1 + s_2)}$ corresponds to the Volterra kernel $h_2(\theta_1, \theta_2) = \theta_2 u(\theta_1)u(\theta_2) - (\theta_2 - \theta_1)u(\theta_2 - \theta_1) - \theta_1 u(\theta_1)$.

7.14. An NTI system is given with the multivariate transfer function. Using the multivariate inverse Laplace transform, define the Volterra kernel of the system.

1. $H_2(s_1, s_2) = \frac{2}{s_1 s_2 (s_1 + s_2 + 3)}$
2. $H_2(s_1, s_2) = \frac{3}{s_1 (s_1 + s_2) (s_1 + s_2 + 1)}$
3. $H_3(s_1, s_2, s_3) = \frac{1}{(s_1 + 1)(s_2 + 2)(s_3 + 1)}$
4. $H_3(s_1, s_2) = \frac{1}{(s_1 + 1)(s_2 + 1)(s_1 + s_2 + 2)}$

7.15. Using different forms of the cascade interconnections in the transform domain, define the multivariate transfer function of a system diagrammed in Fig. 7.51.

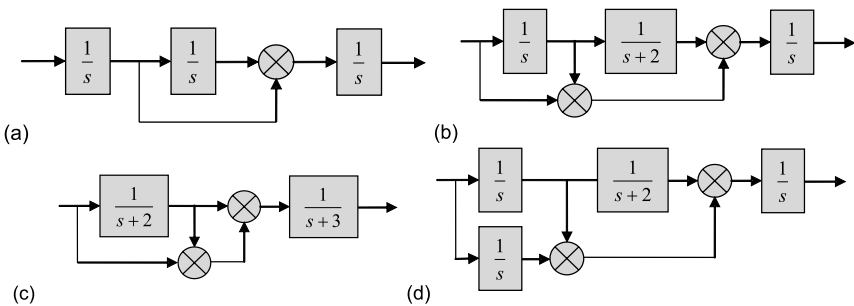


Fig. 7.51. Structures of NTI systems.

7.16 (Describing Functions). Verify that the memoryless nonlinearity $y(x) = -Au(x + \delta) + 2Au(x) - Au(x - \delta)$ with the input signal $x(t) = r \sin \psi$, $r > A$, is represented with the describing function $N(r) = \frac{4A}{\pi r} \left(1 - \sqrt{1 - \frac{\delta^2}{r^2}} \right)$.

7.17. A memoryless NTI system has the following nonlinear characteristic. Define the DF of a system.

1. $y(x) = x|x|$
2. $y(x) = x^{1/3}$
3. $y(x) = x^a$
4. $y(x) = x^3|x|$

7.18. The memory NTI system is represented with a piecewise nonlinear characteristic sketched in Fig. 7.52. Define the DF of the system for the sinusoidal input $x(t) = r \sin \psi$ with an arbitrary amplitude r .

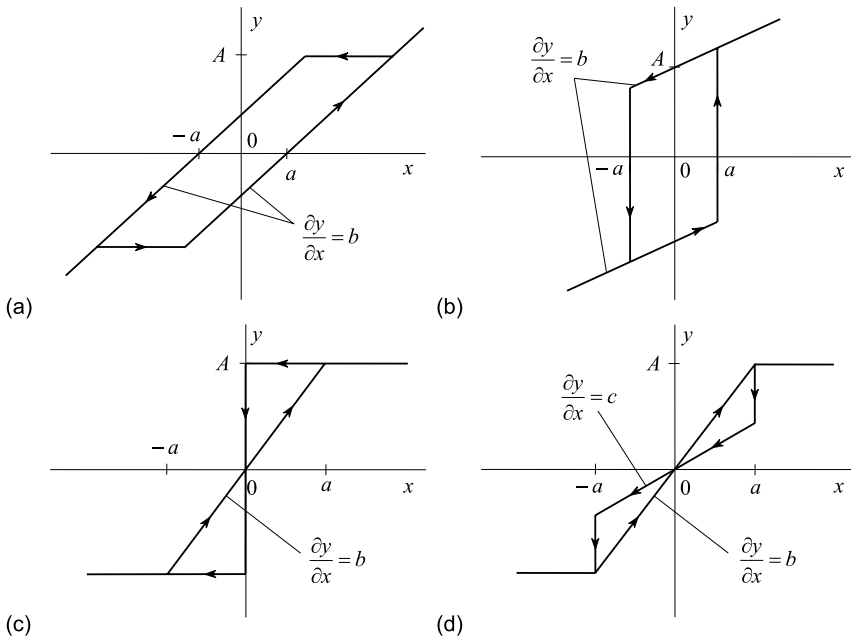


Fig. 7.52. Nonlinear memory characteristics of NTI systems.

7.19. Solve Problem 7.18 for the cosine input $x(t) = r \cos \psi$ with an arbitrary amplitude r . Compare the result to the sinusoidal input.

7.20 (Differential Equation). At an arbitrary operation point, linearize an NTI system represented in Problem 7.7 with the nonlinear ODE.

7.21. An oscillator is described by the following nonlinear ODE. Determine the fixed points. Linearize this equation at an arbitrary point.

1. $y'' - 2\delta \left(1 - \mu \frac{y'^2}{\omega^2}\right) y' + \omega^2 y = 0$

2. $y'' - 2\delta(1 - \mu|y|)y' + \omega^2y = 0$
3. $y'' - 2\delta(1 + ay - by^2)y' + \omega^2y = 0$
4. $y'' - 2\delta(1 + ay^2 - by^4)y' + \omega^2y = 0$

7.22 (State Space Presentation). The following nonlinear ODE represents a system. Translate this equation to the state space. Find fixed points and investigate the system in phase plane.

1. $y'' + y'y^2 - y^3 = x^2$
2. $y^{(4)} - 3y''' + y'y^2 - y^3 = 2x^2$
3. $y''' + (1 - 4y^2)y' - y^3 = 3x^3$
4. $(2y'' + y')(y^2 - y^3) = 2x^2$

7.23. Give a simple explanation to the fact that the linearized nonlinear ODE allows ascertaining stability of an NTI system at the point of linearization.

7.24. An oscillator (Problem 7.21) is described in state space with the following equations. Linearize these equations and investigate stability at the fixed points via the characteristic equation.

1. $y' = -\omega z, \quad z' = \omega y + \epsilon(1 - \mu z^2)z$
2. $y' = -\omega z, \quad z' = \omega y + \epsilon(1 - \mu|y|)z$
3. $y' = -\omega z, \quad z' = \omega y + \epsilon(1 + ay - by^2)z$
4. $y' = -\omega z, \quad z' = \omega y + \epsilon(1 + ay^2 - by^4)z$

7.25 (Stability). Ascertain stability of the system (Problem 7.21) by the Popov's and circle criteria.

7.26. Consider an NTI system in state space (Problem 7.24) and ascertain its Lyapunov stability. Compare the result to that obtained by the Popov's and circle criteria.

Nonlinear Time Varying Systems

8.1 Introduction

Any serious electronics engineer can say that systems (linear or nonlinear) are inherently time-varying, at least because of physical fluctuations in units (systems with fluctuations fall to the class of *stochastic systems*). For example, electronic oscillators often imply adjusting frequency (or phase) for the reference source to obtain the necessary quality of the output signal. On the other hand, real physical units composing oscillators undergo natural changes with time owing to flicker noises, environment, and aging. Under such circumstances, the oscillator frequency, phase, and even amplitude undergo time-changes and an oscillator being a nonlinear system becomes also time-variant.

Other examples can be found in nonlinear time-varying communication channels and channel equalizers, trajectory tracking control, adaptive nonlinear controllers, noise constellation systems, fixed-architecture controller synthesis for systems with input-to-output time-varying nonlinearities, autonomous systems with time-varying gains, nonlinear state estimation feedback controllers for uncertain systems, stabilization of nonholonomic systems by time-varying feedback, nonlinear amplifiers, oscillators with time-varying nonlinearities, etc.

These and many other relevant examples explain the essence of the term *nonlinear time-varying* (NTV). In fact, if a nonlinear system undergoes time-changes caused by different sources (natural and artificial) then it is an NTV system also sometimes called *nonautonomous nonlinear*.

The input $x(t)$ and output $y(t)$ of a SISO NTV system are coupled by the nonlinear time-varying operator $\mathcal{O}(x, t)$,

$$y(t) = \mathcal{O}[x(t), t]x(t) \equiv \mathcal{O}(x, t)x(t), \quad (8.1)$$

dependent on both the input and time. If a system (8.1) is closed loop, the operator depends on the output and time.

For NTV systems, the operator $\mathcal{O}(x, t)$ can be the ODE, integro-differential equation, and integral equation. It can also be represented by the Volterra and Wiener kernels and performed in state space. The qualitative methods are usually not efficient here, although they are applied to systems with slowly changing parameters and when time t exists as a coefficient. Averaging and linearization are the most widely used techniques for NTV systems. If a nonlinear system (oscillator) is modulated with time periodically, the modulation functions method can be used. The state space analysis is basic for several important classes of NTV systems, especially when a system is closed loop and control. Here, the time-varying open and closed Hammerstein and Wiener systems along with their interconnections (series, parallel, and feedback) help solving a great deal of electronic problems.

Traditionally, we observe below the most common rigorous and approximate methods related to different classes of NTV systems.

8.2 Memoryless Time-varying Nonlinearities

Time-varying nonlinearities without memory are used in nonlinear amplifiers, noise constellation devices, oscillators to transfer from soft to hard excitation, adaptive nonlinear controllers, tracking control, etc. In each of these applications, the basic idea is to design an NTV structure with the separated the memoryless NTV part playing a critical role in the system performance. The nonlinearity is then varied with time following the control function to attach the necessary properties to the system. In many cases, namely this approach allows optimizing NTV systems within a stable operation range.

Typically, the nonlinearity is changed with time in three ways:

- By removing the operation point, □
- By adjusting the shape at a given operation point, □
- By switching. □

Which way is most efficient depends on what kind of problems is under consideration.

8.2.1 Bias Voltage Control

One of the most common methods of controlling the memoryless nonlinearity in electronic systems implies changing the bias voltage in semiconductor devices (transistors and diodes). It can be changed automatically with typically the exponential law after a system is energized. It can also be varied by an external signal adapting a system to operation conditions. In transistor NTV systems, control of nonlinearities is often provided similarly to the heterodyne receivers and synchronous detectors; namely, the control voltage is included in series to the input signal. By this, the bias voltage is controlled and nonlinearity varied.

Two bias schemes are used as shown in Fig. 8.1. In the first case (Fig. 8.1a), the necessary base-emitter voltage corresponding to the required bias and nonlinearity is obtained after a capacitor C is fully charged. This scheme represents what is called the *automatic bias voltage control*. In the second

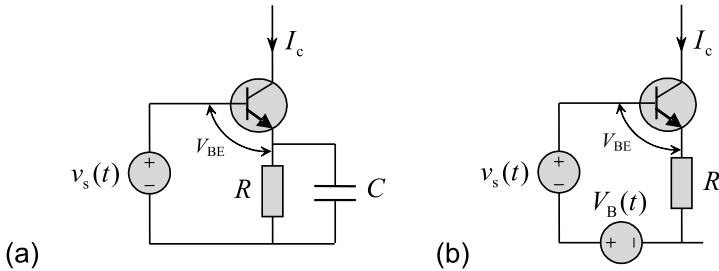


Fig. 8.1. Bias voltage control in a transistor amplifier: (a) internal (automatic) and (b) external (forced).

scheme (Fig. 8.1b), the bias voltage control is accomplished permanently via the time-varying voltage $V_B(t)$ that is known as the *external bias voltage control*. By $V_B(t)$, an amplifier is able to pass over the classes A, AB, and B to the class C, so from the linear regime (class A) and weak nonlinearity (class AB) to strong nonlinearity (classes B and C).

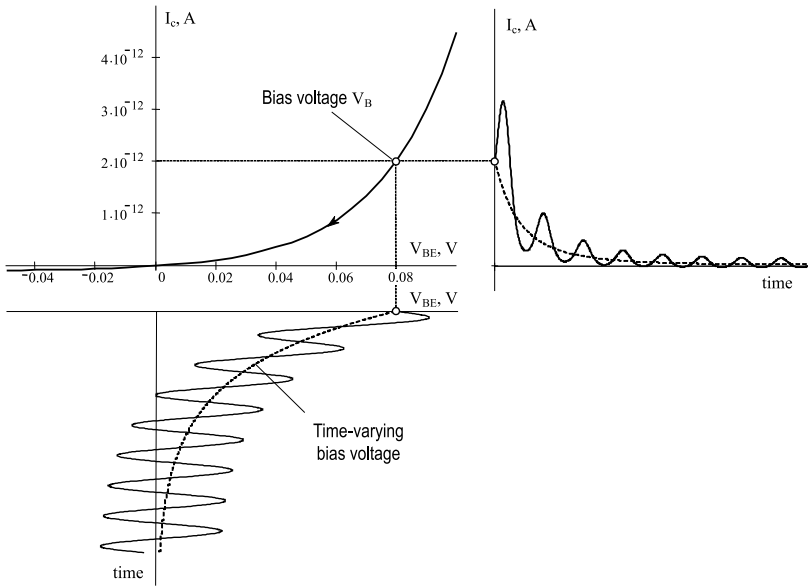
Fig. 8.2 illustrates the effect caused by time-varying bias voltage in a memoryless NPN transistor amplifier (Fig. 8.1a), which nonlinear collector current I_c is described with

$$I_c = \alpha I_{ES} \left(e^{\frac{V_{BE}}{V_T}} - 1 \right), \quad (8.2)$$

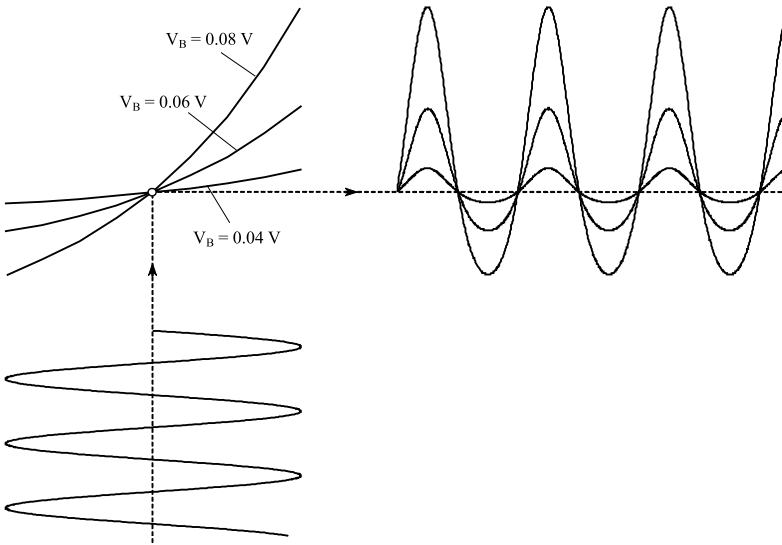
where, typically, $\alpha = 0.98$ is the common base forward short circuit current gain, $I_{ES} = 10^{-13} \text{A}$ is the reverse saturation current of the base-emitter diode, and $V_T = 26 \text{mV}$ is the thermal voltage.

After the scheme is energized, a capacitor C is charged by the emitter current exponentially and so reduced with time is the bias voltage V_B . With such a trace of the bias, the harmonic input signal is mapped to the collector current as shown in Fig. 8.2a. As can be seen, I_c changes with time substantially varying the nonlinearity. The effect seems more illustrative if to reduce all signals to the fixed point as in Fig. 8.2b. By different bias voltages, an alternative collector current acquires different amplitudes. With large input amplitudes and zero bias, the scheme becomes almost an ideal limiter owing to a near zero current with the negative input signal.

In another scheme is organized as in Fig. 8.1b, the nonlinearity can be varied harmonically and the alternative collector current thus modulated. This



(a)



(b)

Fig. 8.2. Memoryless time-varying nonlinearity: (a) automatically controlled and (b) about the operation point.

solution was already observed, allowing for linearization, when we described the heterodyne receiver and synchronous detector as LTV systems.

8.2.2 Interpolation of Time-varying Memoryless Nonlinearities

Any interpolation technique (Lagrange, Newton, splines, etc.) is applicable for memoryless NTV systems and subblocks as related to some fixed time instant. The interpolation formula is then represented in the matrix form or even in a more complicated multivariate form.

An example is a semiconductor device, which nonlinear characteristic is affected by temperature. For the system to operate properly, the characteristic should be measured at fixed values of temperature, then interpolated and described as two-dimensional. If to do so, the effect of temperature can be compensated with time using a sensor of temperature.

Having no special peculiarities against the common approach, time-varying interpolation is rather an extension to NTV systems. The reader, if necessary, can provide a multidimensional interpolation without difficulties. Otherwise, special books must be used.

8.2.3 Taylor Series Expansion for Time-varying Characteristics

A memoryless nonlinearity of an NTV system can be expanded to the Taylor series as follows. If the operation point x_0 is fixed and the nonlinearity $y(x, t)$ is time-variant, the Taylor expansion (7.22) is applied assuming t to be a constant,

$$y(x, t) = y(x_0) + \left. \frac{\partial y(x, t)}{\partial x} \right|_{x=x_0} (x - x_0) + \frac{1}{2} \left. \frac{\partial^2 y(x, t)}{\partial x^2} \right|_{x=x_0} (x - x_0)^2 + \dots + \frac{1}{k!} \left. \frac{\partial^k y(x, t)}{\partial x^k} \right|_{x=x_0} (x - x_0)^k + \dots \quad (8.3)$$

The other feasible case is when $y(x)$ is fixed, but an operation point $x_0(t)$ varies with time. An example is a time-varying bias voltage as shown in Fig. 8.2a. Here, the Taylor expansion gives

$$y(x) = y[x_0(t)] + \left. \frac{\partial y(x)}{\partial x} \right|_{x=x_0(t)} [x - x_0(t)] + \frac{1}{2} \left. \frac{\partial^2 y(x)}{\partial x^2} \right|_{x=x_0(t)} [x - x_0(t)]^2 + \dots + \frac{1}{k!} \left. \frac{\partial^k y(x)}{\partial x^k} \right|_{x=x_0(t)} [x - x_0(t)]^k + \dots \quad (8.4)$$

As can be seen, $y(x)$ is not affected by time in (8.4). The effect of time-varying nonlinearity is achieved at the operation point by varying $x_0(t)$ as demonstrated in Fig. 8.2b.

Most generally, the memoryless nonlinearity can be expanded both in variable and time in the neighborhood of some flexible point $x_0(t_0)$. The Taylor series expansion thus becomes two-dimensional and the nonlinear function $y(x, t)$ is represented with

$$\begin{aligned}
 y(x, t) = & y(x_0, t_0) + \left[\frac{\partial}{\partial x} \Big|_0 (x - x_0) + \frac{\partial}{\partial t} \Big|_0 (t - t_0) \right] y(x, t) \\
 & + \frac{1}{2!} \left[\frac{\partial}{\partial x} \Big|_0 (x - x_0) + \frac{\partial}{\partial t} \Big|_0 (t - t_0) \right]^2 y(x, t) \\
 & + \dots + \frac{1}{k!} \left[\frac{\partial}{\partial x} \Big|_0 (x - x_0) + \frac{\partial}{\partial t} \Big|_0 (t - t_0) \right]^k y(x, t) + \dots, \quad (8.5)
 \end{aligned}$$

where the notion “0” means $x = x_0$ and $t = t_0$ and an application of k to the operator $\partial/\partial x$ is equivalent to $\partial^k/\partial x^k$.

As well as in NTI systems without memory, application of the Taylor series expansion to memoryless NTV systems has several important advantages. The system is linearized at $x_0(t_0)$ by saving only the constant and linear terms in the series. By accounting for quadratic and/or cubic terms, in many cases it becomes possible simulating nonlinear systems with sufficient accuracy or at least without losing principle features.

Example 8.1. A time-varying feedback nonlinearity for a controller is required of the function

$$x(y, t) = \left(1 - \frac{1}{2} \cos t \right) \arctan(y + \sin t),$$

which surface plot is shown in Fig. 8.3a.

The system is linearized with the Taylor series (8.5) in the neighborhood of a point (y_0, t_0) as

$$\begin{aligned}
 x(y, t) \cong & \left(1 - \frac{1}{2} \cos t_0 \right) \arctan(y_0 + \sin t_0) \\
 & + \frac{1 - 0.5 \cos t_0}{1 + (y_0 + \sin t_0)^2} (y - y_0) \\
 & + \left[\frac{1 - 0.5 \cos t_0}{1 + (y_0 + \sin t_0)^2} + \frac{1}{2} \sin(t_0) \arctan(y_0 + \sin t_0) \right] (t - t_0).
 \end{aligned}$$

The nonlinearity is sketched in Fig. 8.3b for $t = 0$ and in Fig. 8.3c for $t = 1.5$. Tangent lines are found at $y_0 = 0$ by the Taylor linear expansion. As can be seen, the time-varying linearization provides for an accurate approximation at a fixed point. \square

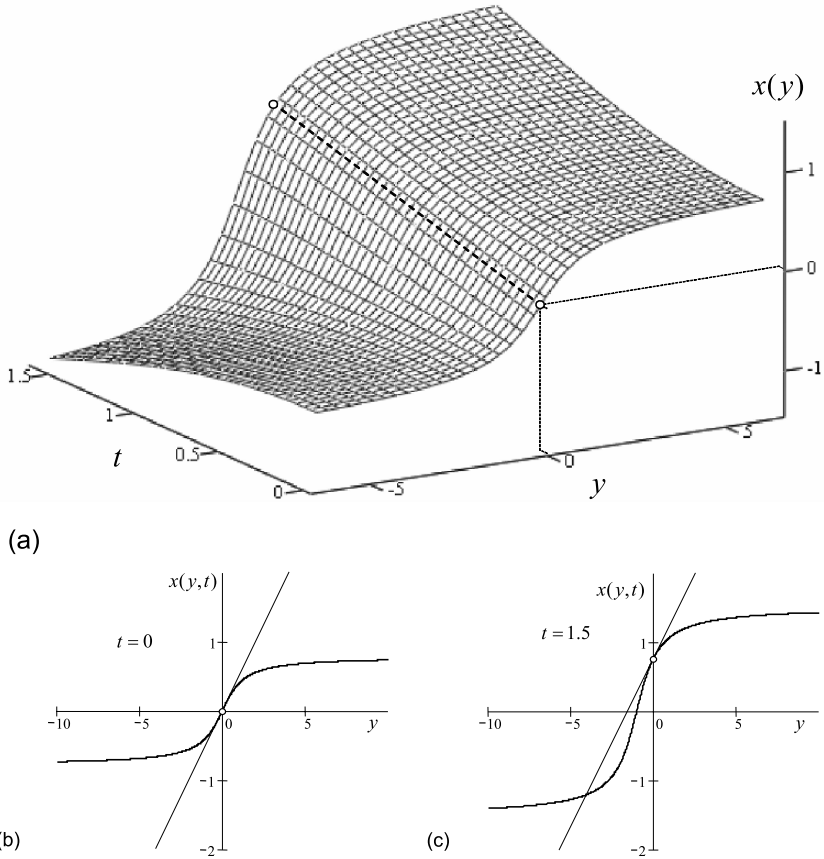


Fig. 8.3. A time-varying feedback nonlinearity $x(y, t)$: (a) two-variable plot, (b) $x(y, 0)$, and (c) $x(y, 1.5)$. Straight lines are due to the Taylor linear expansion.

8.3 Volterra Series Expansion

In line with the convolution for LTI systems that is extended in its general form to LTV systems, the Volterra approach for NTI systems can be extended to NTV systems. The key point is to substitute the degree n time-invariant Volterra kernel $h_n(\tau_1, \dots, \tau_n)$ with the degree n time-varying kernel $h_n(t, \tau_1, \dots, \tau_n)$ and investigate properties of the latter.

The time-varying Volterra series have found applications in modeling nonlinear channels, controlled oscillators, periodically switched nonlinear circuits, track-and-hold sampling mixers, etc. The series can universally be used with any other necessity to describe nonlinear systems with variable coefficients and desirably weak nonlinearities.

To represent an NTV system with the time-varying Volterra series, it first needs to expand the operator $\mathcal{O}(x, t)$ to the Taylor series,

$$\begin{aligned} y(t) &= \mathcal{O}(x, t)x(t) \\ &= \{\mathcal{V}_0[x(t), t] + \mathcal{V}_1[x(t), t] + \dots + \mathcal{V}_n[x(t), t] + \dots\} x(t) = \mathcal{V}[x(t), t]x(t), \end{aligned} \quad (8.6)$$

where \mathcal{V}_n is the degree n nonlinear time-varying operator. Similarly to LTV systems, the Volterra series can be represented in the time-varying form as

$$y(t) = h_0 + \sum_{n=1}^{\infty} \int_{-\infty}^{\infty} \dots \int_{-\infty}^{\infty} h_n(t, \theta_1, \dots, \theta_n) x(\theta_1) \dots x(\theta_n) d\theta_1 \dots d\theta_n, \quad (8.7)$$

where the time-varying Volterra kernel $h_n(t, \theta_1, \dots, \theta_n)$ is defined by the time-varying linear and nonlinear parts of a system. Like the LTV system case, it is implied that $h_n(t, \theta_1, \dots, \theta_n)$ does not equal to zero only if $\theta_i > t$, $i \in [1, n]$. For the degree n time-varying Volterra kernel $h_n(t, \theta_1, \dots, \theta_n)$, the generalized convolution becomes

$$y(t) = \mathcal{V}_n[x(t), t] = x(t) * h_n(t, \theta_1, \dots, \theta_n), \quad (8.8)$$

specifying the following components for (8.6). The term associated with $n = 0$ is still a constant corresponding to the system output with zero input at t

$$\mathcal{V}_0 x(t) = h_0. \quad (8.9)$$

The degree $n = 1$ linear term is defined by

$$\mathcal{V}_1 x(t) = \int_{-\infty}^{\infty} h_1(t, \theta_1) x(\theta_1) d\theta_1, \quad (8.10)$$

representing the general convolution of a linearized system. It is clear that all of the properties of the general convolution (Chapter 6) are conserved by (8.10). Likewise, one can find the terms of higher degrees. For quadratic and cubic nonlinearities we thus have, respectively,

$$\mathcal{V}_2 x(t) = \int_{-\infty}^{\infty} \int_{-\infty}^{\infty} h_2(t, \theta_1, \theta_2) x(\theta_1) x(\theta_2) d\theta_1 d\theta_2, \quad (8.11)$$

$$\mathcal{V}_3 x(t) = \int_{-\infty}^{\infty} \int_{-\infty}^{\infty} \int_{-\infty}^{\infty} h_3(t, \theta_1, \theta_2, \theta_3) x(\theta_1) x(\theta_2) x(\theta_3) d\theta_1 d\theta_2 d\theta_3. \quad (8.12)$$

By such a universal technique (8.7), any NTV system can be represented with the Volterra series having time-varying kernels. The approach, however,

inherits all major problems of the time-invariant series expansion. In fact, we need to know exactly how to measure the time-varying Volterra kernels and how to transfer from the system time-varying ODE to the time-varying series. Let us notice that these and some other relevant problems are still under theoretical investigations.

Example 8.2. An NTV system is organized as shown in Fig. 8.4 by a cascade of the BP filter having the time-varying impulse response $h_1(t, \theta)$, square amplifier, and LP filter with the impulse response $h_2(t)$. The time-varying

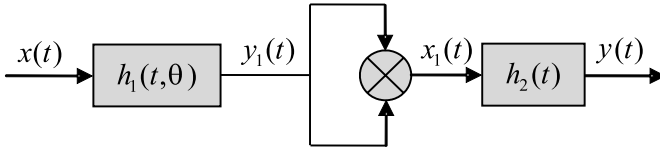


Fig. 8.4. An NTV system.

BP filter has a controlled central frequency to track the carrier of a received signal. A square amplifier produces a constant value proportional to the power of a carrier signal. This value is filtered with an LP filter.

The system can be represented with the following signals,

$$\begin{aligned}
 y_1(t) &= \int_{-\infty}^{\infty} h_1(t, \theta_1)x(\theta_1)d\theta_1, \\
 x_1(t) &= \int_{-\infty}^{\infty} \int_{-\infty}^{\infty} h_1(t, \theta_1)h_1(t, \theta_2)x(\theta_1)x(\theta_2)d\theta_1d\theta_2, \\
 y(t) &= \int_{-\infty}^{\infty} h_2(t - \theta_3) \int_{-\infty}^{\infty} \int_{-\infty}^{\infty} h_1(\theta_3, \theta_1)h_1(\theta_3, \theta_2)x(\theta_1)x(\theta_2)d\theta_1d\theta_2d\theta_3, \\
 &= \int_{-\infty}^{\infty} \int_{-\infty}^{\infty} \int_{-\infty}^{\infty} h_3(t, \theta_1, \theta_2, \theta_3)x(\theta_1)x(\theta_2)d\theta_1d\theta_2d\theta_3,
 \end{aligned}$$

where

$$h_3(t, \theta_1, \theta_2, \theta_3) = h_1(\theta_3, \theta_1)h_1(\theta_3, \theta_2)h_2(t - \theta_3)$$

is the third-degree time-varying Volterra kernel of a system. □

Example 8.3. An NTV system is represented with the diagram shown in Fig. 8.5. Here an LP filter with a modulated bandwidth $2\delta(t) = (1 + \alpha \cos \Omega t)$, where α is a modulation factor and Ω is a modulation frequency, is described by the time-varying impulse response

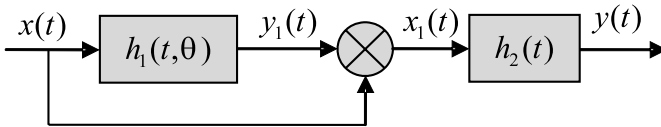


Fig. 8.5. An NTV system.

$$h_1(t, \theta) = (1 + \alpha \cos \Omega\theta)e^{-(t-\theta)}e^{-\frac{\alpha}{T}(\sin \Omega t - \sin \Omega\theta)}u(t - \theta). \quad (8.13)$$

An LP filter is characterized with the impulse response $h_2(t) = e^{-t}u(t)$.

It can easily be verified that the system is represented with the relation

$$\begin{aligned} y(t) &= \int_{-\infty}^{\infty} \int_{-\infty}^{\infty} h_2(t - \theta_2)h_1(\theta_2, \theta_1)x(\theta_1)x(\theta_2)d\theta_1d\theta_2 \\ &= \int_{-\infty}^{\infty} \int_{-\infty}^{\infty} h_2(t, \theta_1, \theta_2)x(\theta_1)x(\theta_2) d\theta_1d\theta_2, \end{aligned}$$

where the second degree time-varying Volterra kernel is given by

$$\begin{aligned} h_2(t, \theta_1, \theta_2) &= h_1(\theta_2, \theta_1)h_2(t - \theta_2) \\ &= (1 + \alpha \cos \Omega\theta_1)e^{-(\theta_2-\theta_1)}e^{-\frac{\alpha}{T}(\sin \Omega\theta_2 - \sin \Omega\theta_1)}u(\theta_2 - \theta_1)e^{-(t-\theta_2)}u(t - \theta_2) \\ &= (1 + \alpha \cos \Omega\theta_1)e^{-(t-\theta_1)}e^{-\frac{\alpha}{T}(\sin \Omega\theta_2 - \sin \Omega\theta_1)}u(\theta_2 - \theta_1)u(t - \theta_2). \end{aligned} \quad (8.14)$$

By (8.14), the output signal becomes

$$y(t) = e^{-t} \int_{-\infty}^t e^{-\frac{\alpha}{T} \sin \Omega\theta_2}x(\theta_2) \int_{-\infty}^{\theta_2} (1 + \alpha \cos \Omega\theta_1)e^{\theta_1 + \frac{\alpha}{T} \sin \Omega\theta_1}x(\theta_1) d\theta_1d\theta_2 \quad (8.15)$$

and we notice that, for causal input $x(t)$, the lower bounds in (8.15) must be substituted with zero. □

8.3.1 Properties of the Time-varying Volterra Operator

When a nonlinear system becomes time-varying, the Volterra operator loses many of the useful properties featured to its counterpart applied to NTI systems. In what follows, we observe the most typical properties of the time-varying Volterra operator.

Non-commutativity

The time-varying Volterra kernels commonly does not commute, because time t cannot be set arbitrary. This also means that the NTV operator does not commute and we commonly have

$$h_n(t, \theta_1, \dots, \theta_n) * x(t) \neq x(t) * h_n(t, \theta_1, \dots, \theta_n). \quad (8.16)$$

Example 8.4. A signal goes through the time-varying LP filter having the impulse response $h(t, \theta) = e^{-(t^2 - \theta^2)} u(t - \theta)$. The output of the filter is then squared to evaluate the signal power.

The output of a system is coupled with the input by the relation

$$\begin{aligned} y(t) &= \int_{-\infty}^{\infty} \int_{-\infty}^{\infty} h(t, \theta_1) h(t, \theta_2) x(\theta_1) x(\theta_2) d\theta_1 d\theta_2 \\ &= \int_{-\infty}^{\infty} \int_{-\infty}^{\infty} e^{-2t^2} e^{\theta_1^2 + \theta_2^2} u(t - \theta_1) u(t - \theta_2) x(\theta_1) x(\theta_2) d\theta_1 d\theta_2. \end{aligned} \quad (8.17)$$

By changing the variables to $\tau_1 = t - \theta_1$ and $\tau_2 = t - \theta_2$, we arrive at

$$y(t) = \int_{-\infty}^{\infty} \int_{-\infty}^{\infty} e^{-2t(\tau_1 + \tau_2)} e^{\tau_1^2 + \tau_2^2} u(\tau_1) u(\tau_2) x(t - \tau_1) x(t - \tau_2) d\tau_1 d\tau_2. \quad (8.18)$$

A comparison of the exponential functions in the integrands of (8.17) and (8.18) shows that their forms do not fit linear transformations. Therefore, the Volterra operator (8.17) does not commute. \square

Non-distributivity

Because the operator of an NTI system does not demonstrate an ability to distribute (Chapter 7), the operator of an NTV system does not do it as well. This inherent property is supported by Example 7.7 if to substitute one of the time-variables, θ_1 or θ_2 , with the current time t .

Homogeneity

Homogeneity featured to NTI systems is luckily saved in NTV structures. The property means that the product of a signal $x(t)$ and some real a equivalently results in the multiplication of $h_n(t, \theta_1, \dots, \theta_n)$ with a^n ,

$$[ah_n(t, \theta_1, \dots, \theta_n)] * x(t) = h_n(t, \theta_1, \dots, \theta_n) * [a^{1/n} x(t)], \quad (8.19)$$

$$[a^n h_n(t, \theta_1, \dots, \theta_n)] * x(t) = h_n(t, \theta_1, \dots, \theta_n) * [ax(t)], \quad (8.20)$$

where an integer n corresponds to the Volterra operator degree.

Nonstationarity

It is seemingly obvious that nonstationarity is inherent property of NTV systems, because the operator is time-varying. In other words, an arbitrary time shift $\pm t_0$ commonly changes the kernel, so that we have an inequality

$$h_n(t \pm t_0, \theta_1, \dots, \theta_n) \neq h_n(t, \theta_1, \dots, \theta_n). \quad (8.21)$$

Most generally, if a system satisfies (8.21), then it belongs to the class of time-varying systems.

Causality

Similarly to other types of systems, the time-varying Volterra operator (8.7) can be modified for causal and/or noncausal signals and systems.

- **Causal systems.** If an NTV system is causal, its response at t_1 is zero if $t \leq t_1$. In view of that and similarly to (6.7), the expansion becomes

$$y(t) = h_0 + \sum_{n=1-\infty}^{\infty} \int_{-\infty}^t \dots \int_{-\infty}^t h_n(t, \theta_1, \dots, \theta_n) x(\theta_1) \dots x(\theta_n) d\theta_1 \dots d\theta_n. \quad (8.22)$$

□

- **Causal signals.** When a signal does not exist in negative time, all variables τ_i , $i \in [1, n]$ cannot lie below zero and we have

$$y(t) = h_0 + \sum_{n=1}^{\infty} \int_0^{\infty} \dots \int_0^{\infty} h_n(t, \theta_1, \dots, \theta_n) x(\theta_1) \dots x(\theta_n) d\theta_1 \dots d\theta_n. \quad (8.23)$$

□

- **Causal both systems and signals.** If signals and systems are both real, so causal, the expansion possesses finite bounds and we have

$$y(t) = h_0 + \sum_{n=1}^{\infty} \int_0^t \dots \int_0^t h_n(t, \theta_1, \dots, \theta_n) x(\theta_1) \dots x(\theta_n) d\theta_1 \dots d\theta_n, \quad (8.24)$$

Namely (8.24) is commonly applied to real physical signals and systems.

□

Stability

Similarly to other systems, BIBO stability of NTV systems is ascertained by evaluating the total resources via the Volterra kernels. The finite value

$$\int_{-\infty}^t \dots \int_{-\infty}^t |h_n(t, \theta_1, \dots, \theta_n)| d\theta_1 \dots d\theta_n \leq M < \infty \quad (8.25)$$

valid for all t assures that a causal NTV system described with the time-varying Volterra kernel $h_n(t, \theta_1, \dots, \theta_n)$ is BIBO stable.

Example 8.5. A time-varying nonlinear channel is characterized with the degree $n = 2$ Volterra kernel

$$h_2(t, \theta_1, \theta_2) = \delta(t - \tau_0 - \theta_2) e^{-(t^2 + \theta_1^2)} u(t - \theta_1) u(\theta_1), \quad (8.26)$$

where τ_0 is some constant time delay. Total resources of the channel are evaluated by (8.25) to be

$$\begin{aligned} & \int_{-\infty}^t \int_{-\infty}^t |h_n(t, \theta_1, \theta_2)| d\theta_1 d\theta_2 \\ &= \int_{-\infty}^t \int_{-\infty}^t |\delta(t - \tau_0 - \theta_2) e^{-(t^2 + \theta_1^2)} u(t - \theta_1) u(\theta_1)| d\theta_1 d\theta_2 \\ &= \int_0^t e^{-(t^2 + \theta_1^2)} d\theta_1 = e^{-t^2} \int_0^t e^{-\theta_1^2} d\theta_1 \\ &= \frac{\sqrt{\pi}}{2} e^{-t^2} \operatorname{erf}(t) < 0.38 \quad \text{for } t \geq 0. \end{aligned}$$

In the view of a finite value produced for all $t \geq 0$, the channel is characterized as BIBO stable. \square

8.3.2 Representation in the Frequency Domain

There are a lot of applications requiring an NTV system performance in the frequency domain. A classical example is an oscillator, which amplitude and phase power spectral densities are extended by the flicker noise.

Following the transforms (6.22) and (6.23), the n -degree time-varying Volterra kernel can be represented in the frequency domain and returned back as follows,

$$H_n(j\omega_1, \dots, j\omega_n, t)$$

$$= \int_{-\infty}^{\infty} \dots \int_{-\infty}^{\infty} h_n(t, \theta_1, \dots, \theta_n) e^{-j\omega_1(t-\theta_1)} \dots e^{-j\omega_n(t-\theta_n)} d\theta_1 \dots d\theta_n, \quad (8.27)$$

$$h_n(t, \theta_1, \dots, \theta_n)$$

$$= \frac{1}{(2\pi)^n} \int_{-\infty}^{\infty} H_n(j\omega_1, \dots, j\omega_n, t) e^{j\omega_1(t-\theta_1)} \dots e^{j\omega_n(t-\theta_n)} d\omega_1 \dots d\omega_n \quad (8.28)$$

and we remind the reader that this pair is not the Fourier transform.

The multifrequency response $H_n(j\omega_1, \dots, j\omega_n, t)$ associated with the degree n Volterra kernel is also called in different applications the *multivariate system function*, or the *multifrequency system function*, or the *multifrequency network function*.

Example 8.6. Consider a SISO NTV system represented with the ODE

$$y' + 2y - 2e^{-t}\sqrt{y}x = 0, \quad (8.29)$$

and zero initial condition $y(0) = 0$. The system can be substituted with the Wiener model (Fig. 7.8b) having a time-varying dynamic part as follows

$$y_1' + y_1 = e^{-t}x, \quad y = y_1^2. \quad (8.30)$$

The system diagram is shown in Fig. 8.6.

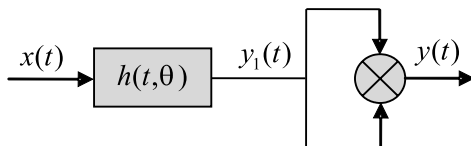


Fig. 8.6. Wiener model of a system (8.29).

A direct solution of the first equation in (8.30),

$$y_1(t) = e^{-t} \int_0^t e^{-\tau} x(\tau) e^{\tau} d\tau,$$

allows us finding the time-varying impulse response of the LTV part. Substituting $x(t) = \delta(t - \theta)$ and using the sifting property of the delta function (Appendix A) yields

$$h(t, \theta) = e^{-t} \int_0^t e^{-\tau} \delta(\tau - \theta) e^{\tau} d\tau = e^{-t} u(t - \theta). \quad (8.31)$$

By the second equation in (8.30) and the convolution rule, the second degree Volterra kernel describing the system becomes

$$h_2(t, \theta_1, \theta_2) = h(t, \theta_1)h(t, \theta_2) = e^{-2t}u(t - \theta_1)u(t - \theta_2). \quad (8.32)$$

If we now apply (8.27) to (8.32), the bi-frequency response representing (8.29) in the frequency domain can be found as

$$\begin{aligned} H_2(j\omega_1, j\omega_2, t) &= \int_{-\infty}^{\infty} \int_{-\infty}^{\infty} e^{-2t}u(t - \theta_1)u(t - \theta_2)e^{-j\omega_1(t-\theta_1)}e^{-j\omega_2(t-\theta_2)}d\theta_1d\theta_2 \\ &= \int_0^t \int_0^t e^{-2t}e^{-j\omega_1(t-\theta_1)}e^{-j\omega_2(t-\theta_2)}d\theta_1d\theta_2 \\ &= \frac{e^{-2t}}{j\omega_1j\omega_2}e^{-j(\omega_1+\omega_2)t}(e^{j\omega_1t} - 1)(e^{j\omega_2t} - 1) \\ &= \frac{e^{-2t}}{j\omega_1j\omega_2}(1 - e^{-j\omega_1t})(1 - e^{-j\omega_2t}). \end{aligned} \quad (8.33)$$

Here, we took into consideration the range of existence $0 \leq \theta \leq t$ of the time-varying impulse response.

Alternatively, one can apply the general convolution to (8.31) and first find the time-varying frequency response of a linear part,

$$\begin{aligned} H(j\omega, t) &= \int_{-\infty}^{\infty} e^{-t}u(t - \theta)e^{-j\omega(t-\theta)}d\theta \\ &= e^{-t} \int_0^t e^{-j\omega(t-\theta)}d\theta = \frac{e^{-t}}{j\omega}(1 - e^{-j\omega t}). \end{aligned} \quad (8.34)$$

Because the kernel (8.32) is the product of the time-varying impulse responses, the product transform rule (7.77) can be applied to (8.34). Consequently, we arrive at (8.33) having verified the validity of (8.27).

Let us now think that the input is $x(t) = e^{j\omega t}$. The output of a linear part is thus $y_1(t) = H(j\omega, t)e^{j\omega t}$. Substituting to the first equation in (8.29) yields an equation

$$H' + (1 + j\omega)H = e^{-t},$$

which direct solution produces a familiar result (8.34). The output of a total system is then calculated by the second equation in (8.30) as

$$y(t) = H(j\omega_1, t)H(j\omega_2, t)e^{j\omega_1 t}e^{j\omega_2 t} = H_2(j\omega_1, j\omega_2, t)e^{j\omega_1 t}e^{j\omega_2 t}$$

and we infer that the bi-frequency system function is defined by

$$H_2(j\omega_1, j\omega_2, t) = \frac{\text{Response to } e^{j\omega t}}{e^{j\omega_1 t}e^{j\omega_2 t}} \quad (8.35)$$

giving us the rule reminiscent of that applied to linear systems. \square

Observing (8.35), one can truly deduce that the multi-frequency system function of an NTV system described by the n -degree Volterra kernel $h_n(t, \theta_1, \dots, \theta_n)$ is defined by

$$H_2(j\omega_1, \dots, j\omega_n, t) = \frac{\text{Response to } e^{j\omega t}}{e^{j\omega_1 t} \dots e^{j\omega_n t}}. \quad (8.36)$$

\square

Similarly to LTV systems, the multiple spectral function of an NTV system is coupled with the kernel $h_n(t, \theta_1, \dots, \theta_n)$ by the Fourier transform applied to time t and the “slow” system frequency Ω ,

$$H(\theta_1, \dots, \theta_n, j\Omega) = \int_{-\infty}^{\infty} h(t, \theta_1, \dots, \theta_n) e^{-j\Omega t} dt, \quad (8.37)$$

$$h(t, \theta_1, \dots, \theta_n) = \frac{1}{2\pi} \int_{-\infty}^{\infty} H(\theta_1, \dots, \theta_n, j\Omega) e^{j\Omega t} d\Omega. \quad (8.38)$$

Finally, the Fourier transform couples the total multi-frequency system function with $H_n(j\omega_1, \dots, j\omega_n, t)$ by a pair

$$H(j\omega_1, \dots, j\omega_n, j\Omega) = \int_{-\infty}^{\infty} H(j\omega_1, \dots, j\omega_n, t) e^{-j\Omega t} dt, \quad (8.39)$$

$$H(j\omega_1, \dots, j\omega_n, t) = \frac{1}{2\pi} \int_{-\infty}^{\infty} H(j\omega_1, \dots, j\omega_n, j\Omega) e^{j\Omega t} d\Omega. \quad (8.40)$$

Example 8.7. Let us come back to a system (Example 8.6) described with the degree $n = 2$ Volterra kernel (8.32) and bi-frequency system function (8.33). By (8.36), the multiple spectral function is defined as

$$\begin{aligned} H(\theta_1, \theta_2, j\Omega) &= \int_{-\infty}^{\infty} e^{-2t} u(t - \theta_1) u(t - \theta_2) e^{-j\Omega t} dt \\ &= \int_{\max \theta}^{\infty} e^{-(2+j\Omega)t} dt = \frac{1}{2+j\Omega} e^{-(2+j\Omega) \max \theta}, \end{aligned}$$

where $\max \theta$ means a bigger value of θ_1 and θ_2 such that

$$H(\theta_1, \theta_2, j\Omega) = \begin{cases} \frac{1}{2+j\Omega} e^{-(2+j\Omega)\theta_1}, & \theta_1 > \theta_2 \\ \frac{1}{2+j\Omega} e^{-(2+j\Omega)\theta_2}, & \theta_2 > \theta_1 \end{cases}. \quad (8.41)$$

The total function is defined by (8.39),

$$H(j\omega_1, j\omega_2, j\Omega) = \int_0^{\infty} \frac{e^{-2t}}{j\omega_1 j\omega_2} (1 - e^{-j\omega_1 t}) (1 - e^{-j\omega_2 t}) e^{-j\Omega t} dt,$$

where the lower integral bound is inherently zero, by the range of existence for causal systems. After the transformations, we have

$$H(j\omega_1, j\omega_2, j\Omega) = \frac{1}{j\omega_1 j\omega_2} \left[\frac{1}{2+j\Omega} - \frac{1}{2+j(\Omega+\omega_2)} - \frac{1}{2+j(\Omega+\omega_1)} + \frac{1}{2+j(\Omega+\omega_1+\omega_2)} \right] \quad (8.42)$$

that allows us to investigate the system in the domain of three frequencies, ω_1 , ω_2 , and Ω . \square

8.3.3 Representation in the Transform Domain

As well as for LTV systems, the transfer function representation is generally not possible for NTV systems. However, the transform domain theory can be applied if the coefficients of NTI systems are slowly changed with time. More precisely, it means that spectral contents of all of the time-varying coefficients must occupy the frequency region narrower (or even much more narrower) than the system bandwidth. If so, the Laplace transform is applied straightforwardly, yielding the time varying transfer function, in which t is assumed to be a constant. We notice that, straightly speaking, such a system is rather NTI possessing all major properties of the latter. Studying such systems, one must think that the properties are valid for all $t \geq t_0$, where t_0 is an initial time.

8.4 Description by Differential Equations

Many NTV electronic systems are originally described by the finite order nonlinear ODEs with time-variant coefficients using the theory of electrical circuits. Most generally, a SISO NTV system can be performed with the N -order nonlinear time-varying ODE

$$\frac{d^N y}{dt^N} = f\left(y, \frac{dy}{dt}, \dots, \frac{d^{N-1}y}{dt^{N-1}}, x, \frac{dx}{dt}, \dots, \frac{d^M x}{dt^M}, t\right), \quad (8.43)$$

where $M \leq N$. An obvious problem with a solution of (8.43) arises similarly to its time-invariant counterpart. If the nonlinear function $f(\cdot, t)$ is not distinct and changes with time arbitrary, a solution of (8.43) is not available. In view of that, they used to consider instead simplified ODEs fitting principle features of systems.

In a manner similar to NTI systems, the simplified forms of nonlinear time-varying ODEs are investigated for stability and principle system characteristics under the constraints imposed by time-variations. Below we observe several typical NTV systems of the first and second orders.

8.4.1 Systems of the First Order

The first order NTV systems are used, for example, in dynamic noise reduction (DNR) as the voltage controlled filters. Typically, such an LP filter tracks dynamics of the input signal and so reduces the audio bandwidth of the signal path at such times as the full bandwidth is not required, with a consequent reduction in high frequency noise.

Most generally, the ODE of the first order SISO NTV system with the input $x(t)$ and output $y(t)$ can be written as

$$y' = f(y, x, t), \quad (8.44)$$

where a nonlinear time-varying function $f(\cdot, t)$ can be arbitrary. A general solution of (8.44) is such that starting from the initial point $y(t_0)$ at t_0 the output changes as

$$y(t) = y(t_0) + \int_{t_0}^t f(y, x, \tau) d\tau. \quad (8.45)$$

Note that further transformations of (8.45) are possible only for some particular cases of $f(\cdot, t)$.

A general form of the relevant closed system is written as

$$y' = f(y, t) \quad (8.46)$$

and its solution is obtained by (8.45) if we substitute $x(t)$ with $x(y, t)$.

Example 8.8 (Voltage Controlled LP Filter). Consider a simple LP filter, which cut-off frequency is voltage controlled via a nonlinear capacitor of a semiconductor diode varactor (Fig. 8.7). The effect of “nuisance parameters” is caused here by inherent nonlinearity of a diode.

The capacitance of a varactor is calculated by

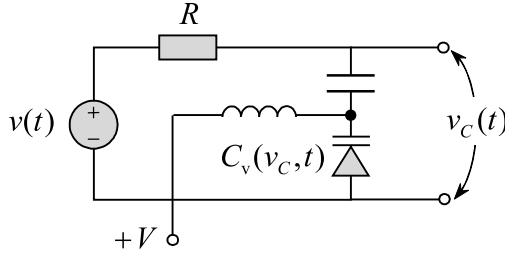


Fig. 8.7. Simplest voltage controlled LP filter.

$$C_v = S \sqrt{\frac{\varepsilon \varepsilon_0 e N}{8\pi(U + \varphi_t)}} = \frac{C_{v0}}{(1 + U/\varphi_t)^\gamma}, \tag{8.47}$$

where S is the area of the p - n transition, ε is the relative dielectric constant (permittivity) of a semiconductor, ε_0 is vacuum permittivity, e is the electron charge ($1.6 \times 10^{-19}\text{C}$), $N = 3 \times 10^{21}\text{m}^{-3}$, φ_t is the contact (Volta¹) potential difference in small fractions of a volt, and U is an applied voltage. The coefficient γ is usually about 1/2. A capacitance value associated with $U = 0$ is $C_{v0} = S(\varepsilon \varepsilon_0 e N / 8\pi \varphi_t)^{-\gamma}$.

The nonlinear time-varying ODE of the filter can be written as

$$v'_C + \frac{1}{RC_v(v_C, t)}v_C = \frac{1}{RC_v(v_C, t)}v$$

that, by (8.47), becomes

$$y' + \frac{1}{RS} \sqrt{\frac{8\pi(\bar{y} + V + \varphi_t)}{\varepsilon \varepsilon_0 e N}} y = \frac{1}{RS} \sqrt{\frac{8\pi(\bar{y} + V + \varphi_t)}{\varepsilon \varepsilon_0 e N}} x, \tag{8.48}$$

where \bar{y} is a rectified input voltage acting on a varactor. Equations like (8.48) are hard to solve and solutions commonly do not exist in closed forms.

In the particular case, the time-varying frequency response can be found if the inverse voltage V is allowed such that $V \gg \bar{y}$ and $V \gg \varphi_t$. We thus arrive at a linearized ODE

$$y' + a(t)y = a(t)x,$$

where $a(t) = \frac{1}{RS} \sqrt{\frac{8\pi V(t)}{\varepsilon \varepsilon_0 e N}}$. Substituting $x(t) = e^{j\omega t}$ and $y(t) = H(j\omega, t)e^{j\omega t}$ leads to the equation

¹ Alessandro Giuseppe Antonio Anastasio Volta, Italian physicist, 18 February 1745–5 March, 1827.

$$H' + [j\omega + a(t)]H = a(t),$$

which general solution is

$$H(j\omega, t) = e^{-\int_{-\infty}^t [j\omega + a(\tau)]d\tau} \int_{-\infty}^t a(\tau) e^{\int_{-\infty}^{\tau} [j\omega + a(\tau_1)]d\tau_1} d\tau.$$

If we further consider a typical situation when the width of the spectral density of $V(t)$ is narrower than the filter bandwidth, the coefficient $a(t)$ can be allowed to be constant in the integrals and we obtain the time-varying frequency response

$$H(j\omega, t) = a(t) e^{-[j\omega + a(t)]t} \int_{-\infty}^t e^{[j\omega + a(\tau_1)]\tau} d\tau = \frac{a(t)}{a(t) + j\omega}. \quad (8.49)$$

Because the coefficient $a(t)$ is time-variant, the cut-off frequency of the filter is also varied with time by $V(t)$. As we mentioned above, this effect is used, for example, in dynamic noise reduction. \square

Bernoulli's Time-varying Differential Equation

Among a variety of nonlinear ODEs, there is the one of the first order with time-varying coefficients investigated long ago by Bernoulli and, nowadays, widely used to solve dynamic problems in electronics. In particular, it fits the amplitude processes in oscillators.

The most general form of Bernoulli's time-varying ODE is

$$y' + a(t)y = b(t)y^n, \quad (8.50)$$

where $a(t)$ and $b(t)$ are some time-variant coefficients and the initial condition is $y(t_0) = y_0$. Earlier, we considered this equation having constant coefficients (7.139). The approach to solve (8.50) remains the same and we bring the final solution for $n \neq 1$,

$$y(t) = \left[\frac{(1-n) \int_{t_0}^t e^{(1-n) \int_{t_0}^{t_1} a(t_2) dt_2} b(t_1) dt_1 + C}{e^{(1-n) \int_{t_0}^t a(t_1) dt_1}} \right]^{\frac{1}{1-n}}, \quad (8.51)$$

where $C = y_0^{1-n}$ is predetermined by the initial condition $y(t_0) = y_0$. The solution starts with y_0 at t_0 and can either converge or diverge depending on the coefficients $a(t)$ and $b(t)$. Below, we exploit (8.51) to investigate the amplitude transient in the voltage controlled oscillator.

8.4.2 Voltage Controlled Oscillator

A typical example of NTV systems of the second order is the *voltage controlled oscillator*, whose frequency is slowly varied with time by an external synchronizing reference source. An oscillator is inherently nonlinear and variations of its frequency are provided in the steady state.

A simplified equivalent scheme of a transistor oscillator is shown in Fig. 8.8. A parallel resonant circuit comprises an inductance L , resistance R , ca-

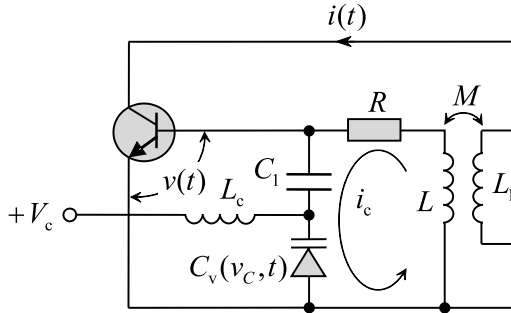


Fig. 8.8. Voltage controlled transistor oscillator.

pacitance C_1 , and voltage controlled capacitance C_v of a varactor. The control signal $+V_c$ obtains the necessary positive voltage on C_v . The voltage $v(t)$ governs the collector current $i(t)$ of a nonlinear transistor. The current $i(t)$, in turn, induces the voltage on the feedback inductance L_1 and the feedback is organized via the mutual inductance M .

The voltage balance in the resonant circuit is obtained with

$$L \frac{di_c}{dt} + Ri_c + \int \frac{1}{C(t)} i_c(t) dt = M \frac{di}{dt},$$

where $C(t) = C_1 C_v(t) / [C_1 + C_v(t)]$ is a time-variant capacitance of the circuit and $i(t)$ is a nonlinear collector current governed by $v(t)$.

By substituting $i_c = C(t) \frac{dv}{dt} = C(t)v'$ and $\frac{di}{dt} = S(v)v'$, where $S(v)$ is a sensitivity of $i(t)$ to $v(t)$, the equation becomes

$$L \frac{d}{dt} C(t) \frac{dv}{dt} + [RC(t) - MS(v)] \frac{dv}{dt} + v = 0$$

and we arrive at the standard form (2.123) for NTV systems with slowly changing parameters, namely at

$$[m(\tau)y']' + k(\tau)y = \epsilon f(\tau, y, y'), \tag{8.52}$$

where $y(t) = v(t)$, $m(\tau) = LC(\tau)$, $k(\tau) = 1$, $\epsilon = 1/Q$. Q is the quality factor,

$$f = -Q[RC(\tau) - MS(y)]y',$$

and $\tau = \epsilon t$ is a “slow” time. The model presumes that the coefficient $m(\tau) \neq 0$ is differentiable (analytical) on the observable time interval that is typically satisfied in real physical systems.

In the first order approximation a solution of (8.52) can be written as

$$y = r \cos \psi, \quad (8.53)$$

where the amplitude and phase are given by, respectively,

$$r' = \epsilon A_1(\tau, r), \quad (8.54)$$

$$\psi' = \omega_0(\tau) + \epsilon B_1(\tau, r). \quad (8.55)$$

The oscillator frequency is calculated by

$$\omega_0^2(\tau) = \frac{k(\tau)}{m(\tau)} = \frac{1}{LC(\tau)} \quad (8.56)$$

and it is also typically assumed that the bandwidth 2δ of a resonant circuit is not changed substantially and Q -factor is large and constant.

Under such conditions, functions $A_1(\tau, r)$ and $B_1(\tau, r)$ are defined, by (2.131) and (2.132), to be, respectively,

$$A_1(\tau, r) = -\frac{r C'(\tau)}{4 C(\tau)} - \frac{1}{2\pi\sqrt{LC(\tau)}} \int_0^{2\pi} f_0(\tau, r, \psi) \sin \psi \, d\psi, \quad (8.57)$$

$$B_1(\tau, r) = -\frac{1}{2\pi r\sqrt{LC(\tau)}} \int_0^{2\pi} f_0(\tau, r, \psi) \cos \psi \, d\psi, \quad (8.58)$$

where

$$f_0(\tau, r, \psi) = Q[RC(\tau) - MS(r \cos \psi)]r\omega_0(\tau) \sin \psi. \quad (8.59)$$

Typically, to observe principle effects, the transistor nonlinearity is described with the incomplete cubic polynomial $i = av - bv^3$ that yields $S(v) = a - 3bv^2$ and

$$f_0(\tau, r, \psi) = Q[RC(\tau) - M(a - 3br^2 \cos^2 \psi)]r\omega_0(\tau) \sin \psi. \quad (8.60)$$

Substituting (8.60) to (8.57) and (8.58), then neglecting products of small values and providing the integration produce

$$A_1(\tau, r) = -\frac{rC'(\tau)}{4C(\tau)} - \frac{Q\omega_0^2}{2} \left[RC(\tau) - M \left(a - \frac{3}{4}br^2 \right) \right] r,$$

$$B_1(\tau, r) = 0.$$

By these functions, equations (8.54) and (8.55) become, respectively,

$$r' = -\frac{\omega_0^2}{2} \left[RC(\tau) - M \left(a - \frac{3}{4} br^2 \right) \right] r, \tag{8.61}$$

$$\psi' = \omega_0(\tau). \tag{8.62}$$

The oscillations sustain with the amplitude r_0 and average capacity C_0 if the expression in brackets of (8.61) is zero. This allows us to find the average amplitude

$$r_0 = \sqrt{\frac{4(Ma - RC_0)}{3Mb}}.$$

If we suppose further that $C(\tau) = C_0 + \tilde{C}(\tau)$, where $\tilde{C}(\tau)$ is a variable part of $C(\tau)$, equation (8.61) will attain the final form of

$$r' = -\delta \frac{\tilde{C}(\tau)}{C_0} r + \delta\beta \left(1 - \frac{r^2}{r_0^2} \right) r, \tag{8.63}$$

where $\beta = MQa\omega_0 - 1$. A general solution of (8.63) is given by (8.51) if we let $a(t) = \delta \left[\frac{\tilde{C}(t)}{C_0} - \beta \right]$ and $b = -\frac{\delta\beta}{r_0^2}$. This, however, does not lead to substantial simplifications of (8.51), because $\tilde{C}(t)$ is still indistinct.

Example 8.9. A capacitor $C(\tau)$ is varied harmonically with the frequency Ω as

$$C(\tau) = C_0(1 - 2\alpha \cos \gamma\tau) = C_0 + \tilde{C}(\tau),$$

where $\alpha \ll 1$, $\gamma = \Omega/\epsilon$, $2\delta \sim \Omega \ll \omega_0$, and $\tilde{C}(\tau) = -2C_0\alpha \cos \gamma\tau$. The frequency of an oscillator (Fig. 8.8) is thus modulated with

$$\omega_0(\tau) \cong \omega_0(1 + \alpha \cos \gamma\tau),$$

representing a solution of (8.62).

Neglecting products of small values, the amplitude equation (8.63) attains the form of

$$r' = \delta\beta \left(1 - \frac{r^2}{r_0^2} \right) r + 2\delta\alpha r \cos \Omega t$$

that can be reduced further to the Bernoulli equation (8.50) with $n = 3$ and $a(t) = -\delta(\beta + 2\alpha \cos \Omega t)$ and $b = -\frac{\delta\beta}{r_0^2}$. By $t_0 = 0$, a solution (8.51) becomes

$$r(t) = \left[\frac{\frac{2\delta\beta}{r_0^2} \int_0^t e^{2\delta(\beta t_1 + 2\frac{\alpha}{\Omega} \sin \Omega t_1)} dt_1 + r(0)^{-2}}{e^{2\delta(\beta t + 2\frac{\alpha}{\Omega} \sin \Omega t)}} \right]^{-\frac{1}{2}}, \quad (8.64)$$

where the integral cannot be found in closed form, by simple functions. Fig. 8.9 illustrates a solution (8.64) for $\alpha = 0.2$ and $\Omega = 3\delta$ along with that associated with an unmodulated signal, $\alpha = 0$. As it is seen, inherent spurious AM occurs owing to nonlinearity and variations in the closed loop gain with modulation. \square

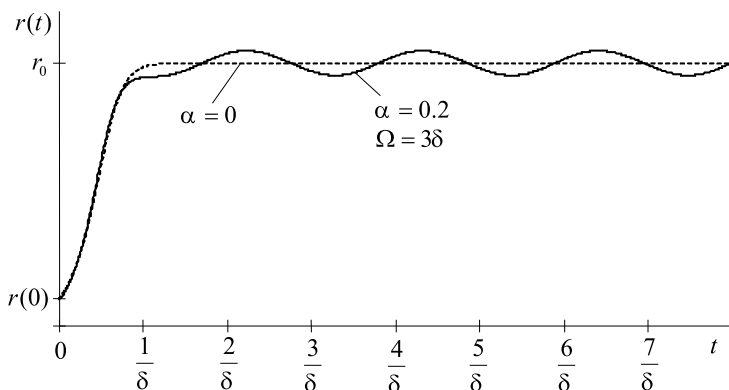


Fig. 8.9. Amplitude transient in the voltage controlled oscillator with a harmonically varied capacitor.

8.5 Nonlinear Periodically Time-varying Systems

In communication systems and specific applications in electronics, oscillators can undergo periodic changes of parameters causing, for example, *frequency modulation* (FM). Nonlinear systems with periodically varying parameters fall to the class of the *nonlinear periodically time-varying* (NPTV) systems. The general theory of NPTV systems was outlined by Krylov, Bogoliubov, and Mitroposkiy both for slow and fast variations. The theory has then been developed by many authors.

Typically, two cases of NPTV systems are recognized. In the first case of slowly varying parameters, the modulation frequency is supposed to be lower than the system bandwidth. That allows considering a system as memoryless for modulation. The second case of rapidly changing parameters presumes that the modulation frequency greatly exceeds the system bandwidth. This

case also has a broad area of applications, because of fast modulation is able to cause many useful as well as nuisance resonance effects associated with overmodulation, frequency jumps, etc.

Commonly, equations of modulated NTV oscillatory systems have not general solutions. On the other hand, rigorous solutions are typically redundant for such systems and near harmonic solutions for the amplitude and phase are searched. Below we observe approximate approaches to investigate NPTV closed loop oscillatory systems.

8.5.1 Bogolubov-Mitropolskiy Model

One of the generalized models of NPTV closed loop systems was proposed and extensively investigated by Bogoliubov and Mitropolskiy. The model is appropriate for both slow and fast modulations. It is represented with the second-order nonlinear ODE (2.123), in which the nonlinear function is supposed to be periodic with period 2π , by the phase function $\phi = \Omega t$,

$$[m(\tau)y']' + k(\tau)y = \epsilon F(\tau, \phi, y, y'), \quad (8.65)$$

where ϵ is still a small parameter, $\tau = \epsilon t$ is a “slow” time, and $m(\tau)$ and $k(\tau)$ are periodically time-variant parameters of a system.

Owing to periodicity, the function $F(\tau, \phi, y, y')$ is expanded to the finite Fourier series

$$F(\tau, \phi, y, y') = \sum_{k=-K}^K F_k(\tau, y, y') e^{jk\Omega t}, \quad (8.66)$$

where the subfunction $F_k(\tau, y, y')$ is supposed to be some polynomial of y and y' with time-variant coefficients dependent on τ . Also, $\Omega = d\phi/dt$ is an instantaneous frequency of the slowly varying external periodic force. As can be seen, (8.66) differs from (2.123) by a periodic function F . In view of that, asymptotic solutions can be built from the common positions.

A solution of the first order approximation is written for such systems as

$$y = r \cos\left(\frac{p}{q}\phi + \vartheta\right), \quad (8.67)$$

where p and q are some mutually simple numbers which choice depends on the effect (resonance) being under investigation. The amplitude r and phase ϑ are defined by the equations, respectively,

$$r' = \epsilon A_1(\tau, r, \vartheta), \quad (8.68)$$

$$\vartheta' = \omega(\tau) - \frac{p}{q}\Omega(\tau) + \epsilon B_1(\tau, r, \vartheta), \quad (8.69)$$

in which the functions A_1 and B_1 periodic for ϕ with period 2π are defined by solving the equations

$$\begin{aligned} & \left[\omega(\tau) - \frac{p}{q} \Omega(\tau) \right] \frac{\partial A_1}{\partial \vartheta} - 2r\omega(\tau)B_1 \\ = & \frac{1}{2\pi^2 m(\tau)} \sum_{\sigma} e^{jq\sigma\vartheta} \int_0^{2\pi} \int_0^{2\pi} F_0(\tau, r, \phi, \psi) e^{-jq\sigma\vartheta'} \cos \psi \, d\phi \, d\psi, \end{aligned} \quad (8.70)$$

$$\begin{aligned} & \left[\omega(\tau) - \frac{p}{q} \Omega(\tau) \right] r \frac{\partial B_1}{\partial \vartheta} + 2\omega(\tau)A_1 = -\frac{1}{m(\tau)} \frac{d[m(\tau)\omega(\tau)]}{d\tau} \\ & - \frac{1}{2\pi^2 m(\tau)} \sum_{\sigma} e^{jq\sigma\vartheta} \int_0^{2\pi} \int_0^{2\pi} F_0(\tau, r, \phi, \psi) e^{-jq\sigma\vartheta'} \sin \psi \, d\phi \, d\psi, \end{aligned} \quad (8.71)$$

and it is implied that

$$\begin{aligned} F_0(\tau, r, \phi, \psi) &= F[\tau, \phi, r \cos \psi, -r\omega(\tau) \sin \psi], \\ \vartheta' &= \psi - \frac{p}{q} \phi. \end{aligned}$$

Special notations need to be made regarding the sums in (8.70) and (8.71). The addition must be carried out over all the values of σ (negative and positive), for which the integrals do not equal to zero. In turn, the integrals are not zero only by σ such that the power of the relevant exponential function (produced by expanding the integrand to the Fourier series) is zero. This means that if $F(\tau, \phi, y, y')$ is a polynomial regarding $y, y', \cos \Omega t$, and $\sin \Omega t$, then σ takes a finite number of integer values.

In spite of the fact that the Bogoliubov-Mitropolskiy method is general for any NPTV closed loop, more engineering features demonstrates the *modulation functions method* exploiting the double harmonic balance approach.

8.5.2 Modulation Functions Method (Slow Modulation)

Let us consider an NPTV closed loop system represented with an oscillator, which frequency is periodically varied with time (modulated). FM oscillators are used in communication systems to convey information.

When an oscillator loop is in steady state, the main question is how the modulating signal results in FM at different modulation frequencies? Because any oscillator having a limit cycle is inherently nonlinear, spurious AM occurs and the other question arises of how high is the spurious AM index? On the other hand, any closed loop nonlinear system is addicted to amplitude-to-frequency conversion and we thus need to know how high is the spurious FM index? The block of questions can be solved by the approach proposed by Shmaliy and called the *modulation functions method* or *dynamic modulation characteristics method*. The method is based on double harmonic balance and motivated by investigations earlier carried out by Sokolinskiy.

In accordance with the method, an FM oscillator is modeled to have the modulating input $x(t)$ and modulated output $y(t)$ as shown in Fig. 8.10a. FM can be provided either externally, by a message signal, or internally, by the flicker noise acting on any of the oscillator components.

For the harmonic test, the input can be represented by the complex signal

$$x(t) = x_0 + \Delta x e^{j\Omega t} = x_0 (1 + \alpha e^{j\Omega t}) , \tag{8.72}$$

where $\alpha = \Delta x/x_0$ is the modulation factor, Ω is the modulation frequency, and x_0 and Δx are the constant value and amplitude of the harmonic addition, respectively.

The output $y(t)$ generated by this NPTV system in steady state consists of an infinite set of overtones of the fundamental frequency ω_0 such that

$$\begin{aligned} y(t) &= \sum_{i=0}^{\infty} y_i(t) = y_0 + \sum_{i=1}^{\infty} r_i(t) e^{j[\int \omega_i(t) dt + \varphi_i]} \\ &= y_0 + r_1(t) e^{j[\int \omega_0(t) dt + \varphi_1]} + \text{harmonics} , \end{aligned} \tag{8.73}$$

where the amplitudes $r_i(t)$ and frequencies $\omega_i(t) = i\omega_0(t)$ of the i th component $y_i(t)$ are varied with time periodically by $x(t)$. With small modulation factor α , the modulator can be supposed to be linear and overtones of the modulation frequency neglected. Under such conditions, instead of a general structure (Fig. 8.10a) two conventional linear channels $x(t) \rightarrow r_i(t)$ and $x(t) \rightarrow \omega_i(t)$ can be considered and described in the frequency domain as in the following.

The amplitude of the i th overtone of $y(t)$ can be performed as

$$\begin{aligned} r_i(t) &= r_{i0} [1 + \text{Re } \mu_{r_i}(j\Omega) e^{j\Omega t}] \\ &= r_{i0} [1 + \mu_{r_i}^* \cos(\Omega t + \Psi_{r_i})] , \end{aligned} \tag{8.74}$$

where $\mu_{r_i}(j\Omega) = \mu_{r_i}^*(\Omega) e^{j\Psi_{r_i}(\Omega)}$ is the *amplitude modulation factor* and $\mu_{r_i}^*$ can be either positive or negative.

A channel $x(t) \rightarrow r_i(t)$ is represented in Fig. 8.10b by the upper branch having an input α and output $\mu_{r_i}(j\Omega)$. The *amplitude modulation function* (AMF) of the i th overtone is defined for this branch by

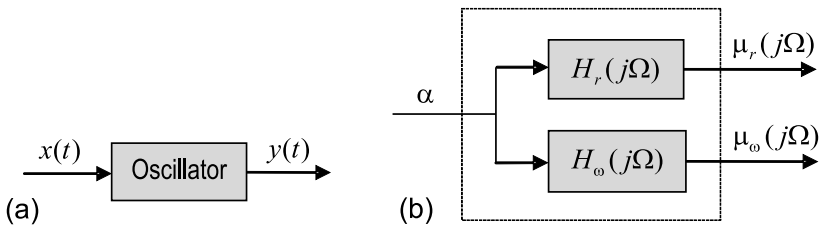


Fig. 8.10. FM oscillator: (a) basic structure and (b) linearized.

$$H_{ri}(j\Omega) = |H_{ri}(j\Omega)|e^{j\Theta_{ri}(\Omega)} = \frac{\mu_{ri}(j\Omega)}{\alpha} = \frac{\mu_{ri}^*(\Omega)}{\alpha}e^{j\Psi_{ri}(\Omega)}, \quad (8.75)$$

where $|H_{ri}(j\Omega)|$ is the *magnitude* AMF and

$$\Theta_{ri}(\Omega) = \begin{cases} \Psi_{ri}(\Omega), & \mu_{ri}^* \geq 0 \\ \Psi_{ri}(\Omega) + \pi, & \mu_{ri}^* < 0 \end{cases}$$

is the *phase* AMF.

Reasoning similarly, we can represent the modulated frequency of the i th overtone with

$$\begin{aligned} \omega_i(t) &= i\omega_0 [1 + \operatorname{Re} \mu_{\omega_i}(j\Omega)e^{j\Omega t}] \\ &= i\omega_0 [1 + \mu_{\omega_i}^* \cos(\Omega t + \Psi_{\omega_i})], \end{aligned} \quad (8.76)$$

where ω_0 is an unmodulated frequency, $\mu_{\omega_i}(j\Omega) = \mu_{\omega_i}^*(\Omega)e^{j\Psi_{\omega_i}(\Omega)}$ is the *frequency modulation factor*, and $\mu_{\omega_i}^*$ can be either positive or negative.

This channel, $x(t) \rightarrow \omega_i(t)$, is represented in Fig. 8.10b by the lower branch having an input α and output $\mu_{\omega_i}(j\Omega)$. For this branch, the *frequency modulation function* (FMF) of the i th overtone is defined by

$$H_{\omega_i}(j\Omega) = |H_{\omega_i}(j\Omega)|e^{j\Theta_{\omega_i}(\Omega)} = \frac{\mu_{\omega_i}(j\Omega)}{\alpha} = \frac{\mu_{\omega_i}^*(\Omega)}{\alpha}e^{j\Psi_{\omega_i}(\Omega)}, \quad (8.77)$$

where $|H_{\omega_i}(j\Omega)|$ is the *magnitude* FMF and

$$\Theta_{\omega_i}(\Omega) = \begin{cases} \Psi_{\omega_i}(\Omega), & \mu_{\omega_i}^* \geq 0 \\ \Psi_{\omega_i}(\Omega) + \pi, & \mu_{\omega_i}^* < 0 \end{cases}$$

is the *phase* FMF. One thus can conclude that both AMF and FMF are akin to the frequency response of an LTI system.

In the above-introduced terms, a real output signal (8.73) can be performed, by $y_0 = 0$, as

$$\begin{aligned} y(t) &= \sum_{i=1}^{\infty} r_{i0} [1 + \operatorname{Re} \mu_{ri}(j\Omega)e^{j\Omega t}] \\ &\times \cos \left\{ \left[i\omega_0 \int [1 + \operatorname{Re} \mu_{\omega_i}(j\Omega)e^{j\Omega t}] dt + \varphi_i \right] \right\}. \end{aligned} \quad (8.78)$$

For the fundamental frequency, $i = 1$, (8.78) is represented with the only term such that

$$y(t) = r_0 [1 + \mu_r^* \cos(\Omega t + \Psi_r)]$$

$$\begin{aligned} & \times \cos \left\{ \left[\omega_0 \int [1 + \mu_\omega^* \cos(\Omega t + \Psi_\omega)] dt + \varphi_1 \right] \right\} \\ & = r_0 [1 + \mu_r^* \cos(\Omega t + \Psi_r)] \\ & \times \cos \left\{ [\omega_0 t + \mu_\varphi^* \sin(\Omega t + \Psi_\omega) + \varphi_1] \right\}, \end{aligned} \tag{8.79}$$

where $\mu_\varphi^*(\Omega) = \frac{\omega_0}{\Omega} \mu_\omega^*(\Omega)$ and

$$\mu_\varphi(j\Omega) = \mu_\varphi^*(\Omega) e^{j\Psi_\omega(\Omega)} = \frac{\omega_0}{\Omega} \mu_\omega^*(\Omega) e^{j\Psi_\omega(\Omega)}$$

is the *phase modulation factor*.

Fig. 8.11 illustrates the modulation processes in the NPTV system modeled with (8.79). As can be seen, both the frequency and amplitude of $y(t)$

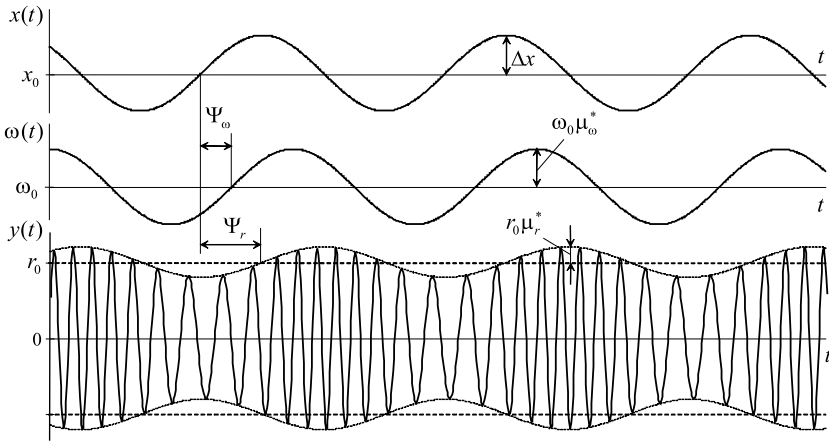


Fig. 8.11. Modulation processes in an FM oscillator.

undergo modulation. The other important point to notice is that the amplitude deviation $r_0 \mu_r^*(\Omega)$ and frequency deviation $\omega_0 \mu_\omega^*(\Omega)$ as well as the relevant phase shifts, $\Psi_r(\Omega)$ and $\Psi_\omega(\Omega)$, are functions of the modulation frequency Ω . Namely this dependence on Ω governs dynamics of modulation processes of FM oscillators via the AMF (8.75) and FMF (8.77).

To describe the AMF $H_{r_i}(j\Omega)$ and FMF $H_{\omega_i}(j\Omega)$ in terms of the oscillator nonlinear ODE, the double harmonic balance method can be used. By this method, a solution of the ODE regarding the i th overtone of the oscillator output is searched in the form of

$$y_i(t) = A_i \cos \phi_i + B_i \sin \phi_i, \tag{8.80}$$

where the amplitudes A_i and B_i are both modulated. By $\alpha \ll 1$, we can further write

$$A_i = A_{i0} + a_{i1} \cos \Omega t + a_{i2} \sin \Omega t, \quad (8.81)$$

$$B_i = B_{i0} + b_{i1} \cos \Omega t + b_{i2} \sin \Omega t, \quad (8.82)$$

where A_{i0} and B_{i0} are values in absence of modulation and the *variable amplitudes* a_{i1} , a_{i2} , b_{i1} , and b_{i2} are assumed to be small values.

In a complex form, (8.80) can be rewritten as

$$y_i(t) = \sqrt{A_i^2 + B_i^2} e^{j(\phi_i - \arctan \frac{B_i}{A_i})} = r_i e^{j\psi_i} \quad (8.83)$$

that allows us to represent the signal amplitude and instantaneous frequency by, respectively,

$$r_i = \sqrt{A_i^2 + B_i^2}, \quad (8.84)$$

$$\omega_i = \frac{d\psi_i}{dt} = \frac{d}{dt} \left(\phi_i - \arctan \frac{B_i}{A_i} \right) \quad (8.85)$$

and we notice that both r_i and ω_i are modulated via (8.81) and (8.82).

The AMF and FMF can now be expressed via A_{i0} , B_{i0} , a_{i1} , a_{i2} , b_{i1} , and b_{i2} if to equate (8.74) to (8.84) and (8.76) to (8.85), respectively, and provide the necessary transformations.

Amplitude Modulation Function

The AMF is represented in terms of (8.80)–(8.82) if we substitute (8.81) and (8.82) to (8.84) and provide the transformations neglecting products of small values as in the following,

$$\begin{aligned} r_i &= \sqrt{(A_{i0} + a_{i1} \cos \Omega t + a_{i2} \sin \Omega t)^2 + (B_{i0} + b_{i1} \cos \Omega t + b_{i2} \sin \Omega t)^2} \\ &= r_{i0} \sqrt{1 + \frac{2}{r_{i0}^2} [(A_{i0} a_{i1} + B_{i0} b_{i1}) \cos \Omega t + (A_{i0} a_{i2} + B_{i0} b_{i2}) \sin \Omega t]} \\ &\cong r_{i0} \left\{ 1 + \frac{1}{r_{i0}^2} [(A_{i0} a_{i1} + B_{i0} b_{i1}) \cos \Omega t + (A_{i0} a_{i2} + B_{i0} b_{i2}) \sin \Omega t] \right\}, \end{aligned}$$

where $r_{i0} = \sqrt{A_{i0}^2 + B_{i0}^2}$. The result can be rewritten as (8.74),

$$r_i = r_{i0} [1 + \mu_{ri}^* \cos(\Omega t + \Psi_{ri})],$$

where

$$\mu_{ri}^* = \frac{1}{r_{i0}^2} \sqrt{(A_{i0} a_{i1} + B_{i0} b_{i1})^2 + (A_{i0} a_{i2} + B_{i0} b_{i2})^2}, \quad (8.86)$$

$$\tan \Psi_{ri} = -\frac{A_{i0} a_{i2} + B_{i0} b_{i2}}{A_{i0} a_{i1} + B_{i0} b_{i1}}. \quad (8.87)$$

Both (8.86) and (8.87) complete representation of the AMF $H_{ri}(j\Omega)$ (8.75) via the solutions (8.80)–(8.82). By high quality factor, $Q \gg 1$, the components B_{i0} , b_{i1} , and b_{i2} become negligible and the AMF for the first overtone can approximately be performed by the functions

$$\mu_r^* \cong \frac{1}{A_0} \sqrt{a_{11}^2 + a_{12}^2}, \quad (8.88)$$

$$\tan \Psi_r \cong -\frac{a_{12}}{a_{11}}, \quad (8.89)$$

suggesting that the sine component in (8.80) can be neglected.

Frequency Modulation Function

In a like manner, the FMF is specified via (8.80)–(8.82) by transforming (8.85). However, as the reader probably remembers, the asymptotic methods give solutions for frequency and phase only in the second order of approximation. Therefore, the derivation of the FMF needs some care.

For the real cosine input (8.72), the modulated frequency $\omega_i(t)$ of the i th overtone, neglecting harmonics of the modulation frequency Ω , can approximately be written as

$$\omega_i^*(t) = i\omega_0 + i\Delta\omega \cos \Omega t,$$

where $\Delta\omega \ll \omega_0$ is a small frequency deviation caused by α .

Inherently, the oscillator nonlinearity causes the amplitude-to-phase conversion via overtones, owing to which additional components $\Delta\omega_{ci} \cos \Omega t$ and $\Delta\omega_{si} \sin \Omega t$ appear in the frequency. If to add these components to $\omega_i^*(t)$, then the modulated frequency can be performed by

$$\begin{aligned} \omega_i(t) &= i\omega_0 + (i\Delta\omega + \Delta\omega_{ci}) \cos \Omega t + \Delta\omega_{si} \sin \Omega t \\ &= i\omega_0 [1 + \mu_{\omega_i}^* \cos(\Omega t + \Psi_{\omega_i})], \end{aligned} \quad (8.90)$$

where

$$\mu_{\omega_i}^* = \frac{1}{i\omega_0} \sqrt{(i\Delta\omega + \Delta\omega_{ci})^2 + \Delta\omega_{si}^2}, \quad (8.91)$$

$$\tan \Psi_{\omega_i} = -\frac{\Delta\omega_{si}}{i\Delta\omega + \Delta\omega_{ci}}, \quad (8.92)$$

and we notice that both $\mu_{\omega_i}^*$ and Ψ_{ω_i} represent the FMF (8.77).

In a manner similar to the AMF, the components $\Delta\omega_{ci}$ and $\Delta\omega_{si}$ can also be expressed via the amplitudes A_i and B_i . To provide, let us transform (8.85) as follows,

$$-\frac{d}{dt} \arctan \frac{B_i}{A_i} = -\frac{B_i' A_i - A_i' B_i}{A_i^2 + B_i^2}$$

$$\begin{aligned}
 &= \Omega \frac{B_{i0}a_{i2} - A_{i0}b_{i2}}{A_{i0}^2 + B_{i0}^2} \cos \Omega t + \Omega \frac{A_{i0}b_{i1} - B_{i0}a_{i1}}{A_{i0}^2 + B_{i0}^2} \sin \Omega t \\
 &= \Delta\omega_{ci} \cos \Omega t + \Delta\omega_{si} \sin \Omega t,
 \end{aligned} \tag{8.93}$$

where

$$\Delta\omega_{ci} = \Omega \frac{B_{i0}a_{i2} - A_{i0}b_{i2}}{A_{i0}^2 + B_{i0}^2}, \tag{8.94}$$

$$\Delta\omega_{si} = \Omega \frac{A_{i0}b_{i1} - B_{i0}a_{i1}}{A_{i0}^2 + B_{i0}^2}. \tag{8.95}$$

By (8.94), (8.95), $\Delta\omega_{ci} \ll \Delta\omega$, and $\Delta\omega_{si} \ll \Delta\omega$, we go from (8.91) to

$$\mu_{\omega i}^* = \frac{\Delta\omega}{\omega_0} \sqrt{\left(1 + \frac{\Omega}{i\Delta\omega} \frac{B_{i0}a_{i2} - A_{i0}b_{i2}}{A_{i0}^2 + B_{i0}^2}\right)^2 + \left(\frac{\Omega}{i\Delta\omega} \frac{A_{i0}b_{i1} - B_{i0}a_{i1}}{A_{i0}^2 + B_{i0}^2}\right)^2} \tag{8.96}$$

$$\cong \frac{\Delta\omega}{\omega_0} \left(1 + \frac{\Omega}{i\Delta\omega} \frac{B_{i0}a_{i2} - A_{i0}b_{i2}}{A_{i0}^2 + B_{i0}^2}\right) \tag{8.97}$$

$$\cong \frac{\Delta\omega}{\omega_0} \left[1 + \frac{\Omega}{i\Delta\omega} \frac{B_{i0}}{A_{i0}} \left(\frac{a_{i2}}{A_{i0}} - \frac{b_{i2}}{B_{i0}}\right)\right]. \tag{8.98}$$

Similarly, (8.92) is transformed to

$$\tan \Psi_{\omega i} = -\frac{\Delta\omega_{si}}{i\Delta\omega + \Delta\omega_{ci}} \tag{8.99}$$

$$\cong -\frac{\Omega(A_{i0}b_{i1} - B_{i0}a_{i1})}{i\Delta\omega(A_{i0}^2 + B_{i0}^2) + \Omega(B_{i0}a_{i2} - A_{i0}b_{i2})} \tag{8.100}$$

$$\cong -\frac{\Omega}{i\Delta\omega} \frac{B_{i0}}{A_{i0}} \left(\frac{b_{i1}}{B_{i0}} - \frac{a_{i1}}{A_{i0}}\right). \tag{8.101}$$

The FMF (8.77) is now approximately described by (8.98) and (8.101) in terms of (8.81) and (8.82). Typically, the modulation processes are of concern to the fundamental frequency ω_0 . If so, functions (8.98) and (8.101) can be rewritten as, respectively,

$$\mu_{\omega}^* \cong \frac{\Delta\omega}{\omega_0} \left[1 + \frac{\Omega}{\Delta\omega} \frac{B_0}{A_0} \left(\frac{a_{12}}{A_0} - \frac{b_{12}}{B_0}\right)\right], \tag{8.102}$$

$$\Psi_{\omega} \cong -\frac{\Omega}{\Delta\omega} \frac{B_0}{A_0} \left(\frac{b_{11}}{B_0} - \frac{a_{11}}{A_0}\right). \tag{8.103}$$

Further, in order to describe dynamics of an FM oscillator in terms of the AMF and FMF, one needs writing the nonlinear oscillator ODE and solve it by the double harmonic balance method for A_0 , B_0 , $a_{11}(\Omega)$, $a_{12}(\Omega)$, $b_{11}(\Omega)$, and $b_{12}(\Omega)$. To illustrate the approach, below we examine electronic and crystal FM oscillators.

8.5.3 Oscillator with a Modulated Inductance

Let us consider a familiar electronic oscillator (Fig. 8.12), which inductance $L(t)$ is supposed to be modulated slowly as

$$L(t) = L_0(1 + \alpha \cos \Omega t), \tag{8.104}$$

where L_0 is constant, $\alpha \ll 1$, and the modulation frequency Ω does not exceed substantially the bandwidth, $0 \leq \Omega \sim 2\delta = \frac{1}{RC}$. This means that Ω

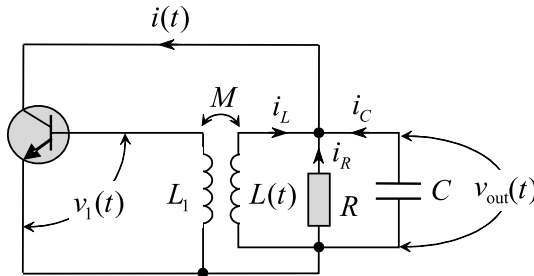


Fig. 8.12. Oscillator with a modulated inductance.

is much smaller than the resonance frequency, $\Omega \ll \omega_0 = \frac{1}{\sqrt{LC}}$. By (8.104), the modulated frequency becomes

$$\begin{aligned} \omega(t) &= \omega_0 + \Delta\omega \cos \Omega t = \omega_0 \left(1 + \frac{\Delta\omega}{\omega_0} \cos \Omega t \right) \\ &\cong \omega_0 \left(1 - \frac{\alpha}{2} \cos \Omega t \right), \end{aligned} \tag{8.105}$$

where $\Delta\omega/\omega_0 = -\alpha/2$. Let us be interested of the oscillator response in the amplitude and frequency to the modulation factor α at different Ω . We thus need to find the relevant AMF (8.75) and FMF (8.77).

The oscillator balance equation can be written as

$$\frac{1}{L} \int v_{out} dt + \frac{v_{out}}{R} + C \frac{dv_{out}}{dt} = i(t).$$

By substituting $v_1 = kv = \frac{M}{L}v$, then describing the nonlinearity with the traditional incomplete cubic polynomial $i = a_1v_1 - a_3v_1^3$, and assigning $y = v_{out}$, we arrive at the ODE

$$y'' + 2\delta(1 - G_1 + 3G_3y^2)y' + \omega_0^2(t)y = 0, \tag{8.106}$$

where the generalized gains $G_1 = a_1kR$ and $G_3 = a_3k^3R$ are associated with the linear and cubic terms. When derived (8.106), we took into account the

fact that $L(t)$ is modulated slowly and hence is almost constant (having a negligible time derivative) during the period of oscillations.

By harmonic balance, a solution of (8.106) is found as (8.80),

$$y = A \cos \phi + B \sin \phi. \quad (8.107)$$

Substituting (8.107) to (8.106), dropping overtones, and equating amplitudes of $\cos \phi$ and $\sin \phi$ to zero produce two equations,

$$A'' + 2B'\omega + B\omega' - 2\delta(G_1 - 1)(A' + B\omega) + \frac{3}{2}\delta G_3(3A^2A' + A^2B\omega + 2ABB' + B^2A' + B^3\omega) = 0, \quad (8.108)$$

$$B'' - 2A'\omega - A\omega' - 2\delta(G_1 - 1)(B' - A\omega) + \frac{3}{2}\delta G_3(3B^2B' - B^2A\omega + 2AA'B + A^2B' - A^3\omega) = 0. \quad (8.109)$$

In frames of double harmonic balance, A and B are represented by (8.81) and (8.82) as

$$A = A_0 + a_{11} \cos \Omega t + a_{12} \sin \Omega t, \quad (8.110)$$

$$B = B_0 + b_{11} \cos \Omega t + b_{12} \sin \Omega t \quad (8.111)$$

and substituted to (8.108) and (8.109). In the following transformations, one needs to use (8.105) and neglect products of small values. Thereafter, if to equate to zero the constant terms, we arrive at two equal equations with two unknown amplitudes, A_0 and B_0 ,

$$A_0^2 + B_0^2 = \frac{4}{3G_3}(G_1 - 1). \quad (8.112)$$

Because (8.112) cannot be solved for two variables, it needs to consider some additional condition to specify B_0 via the overtones.

For the cubic nonlinearity given and initial base-emitter voltage $v_1 = V \cos \omega t$, the collector current can be found as $i(t) = I_{1c} \cos \omega t + I_{3c} \cos 3\omega t$, where the amplitudes are $I_{1c} = \frac{V}{R} (G_L - \frac{3}{4}G_3V^2)$ and $I_{3c} = -\frac{V^3}{4R_1}G_3$. The third overtone induces an extra voltage

$$v_3 = \frac{1}{C} \int I_{3c} \cos 3\omega t dt = -\frac{1}{4} \frac{G_3 V^3}{3\omega CR} \sin 3\omega t \quad (8.113)$$

such that the output voltage becomes

$$v^* = V \cos \omega t - \frac{\delta G_3 V^3}{6\omega} \sin 3\omega t. \quad (8.114)$$

If we now set $v_1^* = kv^*$ and pass over the loop again, we will arrive at the output voltage

$$v \cong V \left(G_L - \frac{3}{4} G_3 V^2 \right) \cos \omega t + \frac{3}{4} G_3^2 \frac{2\delta V^5}{27\omega} \sin \omega t, \quad (8.115)$$

where the amplitudes can be assigned as

$$A_0 = V \left(G_L - \frac{3}{4} G_3 V^2 \right), \quad (8.116)$$

$$B_0 = \frac{3}{4} G_3^2 \frac{2\delta V^5}{27\omega}. \quad (8.117)$$

On the other hand, we have $V^2 = A_0^2 + B_0^2$ and recall that, typically, $B_0^2 \ll A_0^2$. In view of that, (8.116) and (8.117) produce

$$A_0 = \sqrt{\frac{4}{3G_3}(G_1 - 1)}, \quad (8.118)$$

$$B_0 \cong \frac{(G_1 - 1)^2}{9Q} A_0, \quad (8.119)$$

where $Q = \omega_0/2\delta$ is the quality factor. Now note that (8.118) is exactly a solution of (8.112) if we allow $B_0^2 \ll A_0^2$. In turn, the “nonlinear” amplitude B_0 is represented via the main amplitude A_0 , quality factor Q , and linear gain G_1 . That means that if an oscillator is quasi linear, $G_1 \rightarrow 1$, and $Q \rightarrow \infty$, then $B \rightarrow 0$ and no substantial distortions in the phase and frequency can be indicated over all modulation frequencies.

We can now equate to zero the terms with $\cos \Omega t$ and $\sin \Omega t$ in the transformed (8.108) and (8.109), using (8.118) and (8.119). Consequently, we arrive at four algebraic equations for a_{11} , a_{12} , b_{11} , and b_{12} , by $\nu = \Omega/\delta$,

$$\begin{bmatrix} a_{11} \\ a_{12} \\ b_{11} \\ b_{12} \end{bmatrix} \begin{bmatrix} 3G_3 A_0 B_0 & 0 & 3G_3 A_0^2 & 2\nu \\ 0 & 3G_3 A_0 B_0 & -2\nu & 3G_3 A_0^2 \\ 3G_3 A_0^2 & 2\nu & 3G_3 A_0 B_0 & 0 \\ 2\nu & -3G_3 A_0^2 & 0 & -3G_3 A_0 B_0 \end{bmatrix} = \begin{bmatrix} 0 \\ -\frac{\alpha}{2} B_0 \nu \\ 0 \\ \frac{\alpha}{2} A_0 \nu \end{bmatrix}. \quad (8.120)$$

A solution of (8.120), by $G_3 = 4(G_1 - 1)/3A_0^2$, gives the functions

$$a_{11}(\nu) = \frac{1}{4} \alpha A_0 \frac{\nu^2}{\nu^2 + 4(G_L - 1)^2}, \quad (8.121)$$

$$a_{12}(\nu) = -\frac{1}{2} \alpha A_0 \frac{\nu(G_L - 1)}{\nu^2 + 4(G_L - 1)^2}, \quad (8.122)$$

$$b_{11}(\nu) = \frac{1}{4} \alpha B_0 \frac{\nu^2[\nu^2 - 4(G_L - 1)^2]}{[\nu^2 + 4(G_L - 1)^2]^2}, \quad (8.123)$$

$$b_{12}(\nu) = -\alpha B_0 \frac{\nu^3(G_L - 1)}{[\nu^2 + 4(G_L - 1)^2]^2}. \quad (8.124)$$

Alternatively, by substituting B_0 with (8.119), the amplitudes b_{11} and b_{12} can be rewritten as, respectively,

$$b_{11}(\nu) = \frac{1}{4}\alpha A_0 \frac{1}{9Q} \frac{\nu^2(G_L - 1)^2[\nu^2 - 4(G_L - 1)^2]}{[\nu^2 + 4(G_L - 1)^2]^2}, \quad (8.125)$$

$$b_{12}(\nu) = -\alpha A_0 \frac{1}{9Q} \frac{\nu^3(G_L - 1)^3}{[\nu^2 + 4(G_L - 1)^2]^2}. \quad (8.126)$$

Fig. 8.13 illustrates (8.121)–(8.124) for several values of G_1 , among which the value $G_1 = 1.5$ corresponds to the maximum generated power. The first

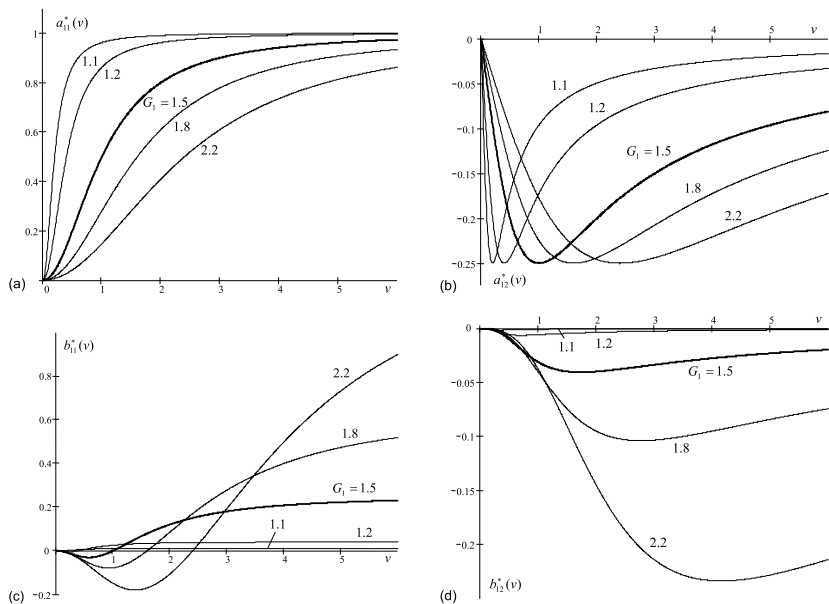


Fig. 8.13. Variable amplitudes: (a) $a_{11}^* = 4a_{11}/\alpha A_0$, (b) $a_{12}^* = 2a_{12}/\alpha A_0$, (c) $b_{11}^* = 36b_{11}Q/\alpha A_0$, and (d) $b_{12}^* = 9b_{12}Q/\alpha A_0$.

point to notice is that, by $0 \leftarrow \nu \ll 1$, the modulation process is memoryless (or static) and all of the variable amplitudes become zero.

As can be seen, increasing ν results in growing $a_{11}^* = 4a_{11}/\alpha A_0$ that asymptotically tends toward unity with a maximum rate at $\nu = 2(G_1 - 1)$. The negative $a_{12}^* = 2a_{12}/\alpha A_0$ changes qualitatively as the derivative of a_{11}^* . However, the peak value -0.25 of a_{12}^* corresponding to the maximum rate of a_{11}^* does not depend on G_L .

One can now realize how strongly G_L affects the modulation dynamics. At the excitation bound, $G_L = 1$, we have $a_{11}^* = 1$ and $a_{12}^* = 0$ for all ν . The explanation lies in the following. With $G_L \rightarrow 1$, the losses of energy are almost

fully recovered by feedback, the loaded quality factor rises dramatically, and the loaded bandwidth therefore becomes extremely narrow. As a consequence, a_{11}^* transfers from zero to unity by utterly low $0 \leftarrow \nu \ll 1$.

In line with a_{11} and a_{12} , the amplitudes b_{11} and b_{12} vary mostly in the range of small ν . The asymptotic level for $b_{11}^* = 36b_{11}Q/\alpha A_0$ is $(G_L - 1)^2$ and it is zero for $b_{12}^* = gb_{12}Q/\alpha A_0$. Because b_{11} and b_{12} are products of overtones, their values are reciprocals of the quality factor. Therefore, when overtones vanish, by $G_L = 1$, both b_{11} and b_{12} become zero. The latter effect is neatly seen in Fig. 8.13c and Fig. 8.13d, by $G_L = 1.1$.

Employing (8.121)–(8.126), the AMF and FMF are now readily defined via (8.86), (8.87), (8.102), and (8.103), respectively,

$$\mu_r^* = \frac{\alpha\nu}{4\sqrt{\nu^2 + 4(G_L - 1)^2}}, \quad (8.127)$$

$$\tan \Psi_r = \frac{2(G_L - 1)}{\nu}, \quad (8.128)$$

$$\mu_\omega^* \cong -\frac{\alpha}{2} \left[1 - \frac{\nu^2(G_1 - 1)^3[\nu^2 - 4(G_L - 1)^2]}{18Q^2[\nu^2 + 4(G_L - 1)^2]^2} \right], \quad (8.129)$$

$$\Psi_\omega \cong -\frac{2\nu^3(G_1 - 1)^4}{9Q^2[\nu^2 + 4(G_L - 1)^2]^2}. \quad (8.130)$$

Accordingly, the AMF is performed with

$$H_r(j\nu) = |H_r(j\nu)|e^{j\Theta_r(\nu)} = \frac{\mu_r^*(\nu)}{\alpha} e^{j\Psi_r(\nu)} \quad (8.131)$$

and thus

$$|H_r(j\nu)| = \frac{\mu_r^*(\nu)}{\alpha} = \frac{\nu}{4\sqrt{\nu^2 + 4(G_L - 1)^2}}, \quad (8.132)$$

$$\tan \Theta_r(\nu) = \tan \Psi_r(\nu) = \frac{2(G_L - 1)}{\nu}. \quad (8.133)$$

In turn, the FMF is specified with

$$H_\omega(j\nu) = |H_\omega(j\nu)|e^{j\Theta_\omega(\nu)} = \frac{\mu_\omega^*(\nu)}{\alpha} e^{j\Psi_\omega(\nu)} \quad (8.134)$$

and, in the view of negative signs in (8.129) and (8.130), we have

$$|H_\omega(j\nu)| = -\frac{\mu_\omega^*(\nu)}{\alpha} = \frac{1}{2} \left[1 - \frac{\nu^2(G_1 - 1)^3[\nu^2 - 4(G_L - 1)^2]}{18Q^2[\nu^2 + 4(G_L - 1)^2]^2} \right], \quad (8.135)$$

$$\Theta_\omega(\nu) = \pi + \Psi_\omega(\nu) = \pi - \frac{2\nu^3(G_1 - 1)^4}{9Q^2[\nu^2 + 4(G_L - 1)^2]^2}. \quad (8.136)$$

Fig. 8.14 sketches the AMF and FMF for several values of G_1 . When FM is “static” or memoryless, by $\nu \ll 1$, spurious AM is very poor and the phase

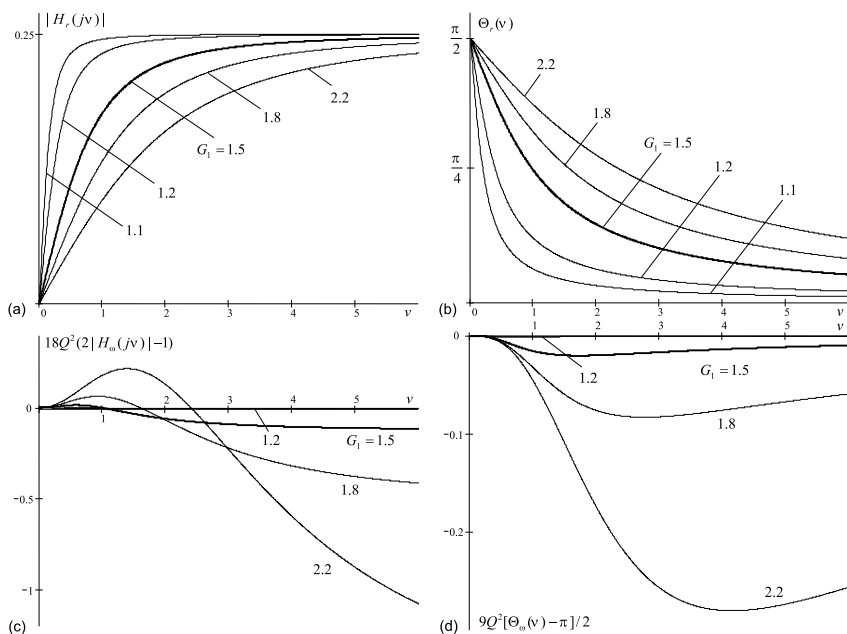


Fig. 8.14. AMF and FMF of an FM oscillator (Fig. 8.12): (a) $|H_r(j\nu)|$, (b) $\Theta_r(\nu)$, (c) $|H_\omega(j\nu)|$, and (d) $\frac{9}{2}Q^2[\Theta_\omega(\nu) - \pi]$.

difference between the modulating signal and envelope of $y(t)$ is almost $\pi/2$. It is seen that frequency distortions are negligible with $\nu \ll 1$.

In this oscillator, spurious AM reaches a maximum, $|H_r(j\nu)| = 0.25$, when $\nu \gg 1$. Moreover, by $\nu \gg 1$, the envelope of $y(t)$ coincides in phase with the modulating function, spurious FM reaches a maximum,

$$|H_\omega(j\nu)|_{\nu \gg 1} \rightarrow \frac{1}{2} \left[1 - \frac{(G_1 - 1)^3}{18Q^2} \right], \quad (8.137)$$

and the phase shift between $\omega(t)$ and $L(t)$ becomes π . Note that this shift is also π at $\nu = 0$ and thus the maximum index of spurious FM corresponds to the bound of the loaded bandwidth.

Relation (8.137) suggests a clear rule to decrease spurious FM, in contrast to spurious AM that commonly cannot be avoided. In fact, if an oscillator is near linear, $G_1 \rightarrow 1$, and its resonator has a high quality factor, $Q \gg 1$, the value (8.137) becomes 0.5 corresponding to (8.105) over all modulation frequencies. We notice that namely two these factors, a near unity G_1 and high Q , are pursued by designers of precision oscillators. Best results are achieved in quantum and crystal oscillators.

8.5.4 Frequency Modulated Crystal Oscillator

As the function (8.137) suggests, to obtain low distortion FM, an oscillator must be quasi linear utilizing a resonator with high quality factor. A commonly accepted solution is to use a piezoelectric resonator instead of an LC circuit and obtain G_1 slightly more than unity. On the other hand, a quasi linear piezoelectric oscillator becomes sensitive to changes in the closed loop occurring with FM. Stability in the steady state must thus be ascertained under the modulation conditions.

An equivalent scheme of the Colpitts² crystal oscillator belonging to the class of *three-point* oscillators is shown in Fig. 8.15. A piezoelectric resonator is represented here with a series branch of motional L_1 , C_1 , and R_1 , in parallel to which a static capacitance C_0 is included. Two auxiliary capacitors, C_2 and C_3 , are included to organize feedback. FM is provided by a voltage applied to a varactor diode, which capacitance C_v is put in series with the resonator.

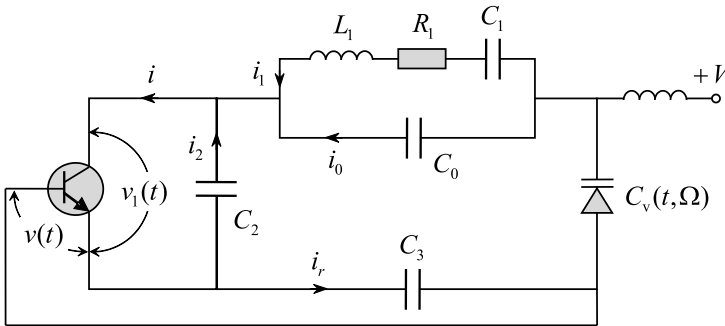


Fig. 8.15. FM Colpitts crystal oscillator.

To derive an equilibrium equation, one can proceed with the Kirchoff's³ laws and write

$$i = i_r + i_2, \quad i_r = i_1 + i_0, \quad \frac{i_0}{C_0} + i_r \frac{C_3 + C_v}{C_v C_3} - \frac{i_2}{C_2} = 0,$$

$$\frac{1}{C_1} \int i_1 dt + R_1 i_1 + L_1 \frac{di_1}{dt} - \frac{1}{C_0} \int i_0 dt = 0.$$

By $i_r = C_3 \frac{dv}{dt}$, the oscillator ODE can then be written as

$$C_3 g_1 v''' + C_3 g_2 v'' + C_3 g_3 v' - \frac{C_0}{C_2} i'' - 2\delta_r \frac{C_0}{C_2} i' - \omega_2^2 \left(\frac{1}{p_r} - 1 \right) i = 0, \quad (8.138)$$

² Edwin H. Colpitts, US engineer and inventor, 1872-1949.

³ Gustav Robert Kirchoff, German mathematician, 12 March 1824–17 October 1887.

where

$$\begin{aligned}\omega_2^2 &= \frac{1}{L_1 C_2}, \quad p_r = \frac{C_1}{C_0}, \quad g_1 = 1 + C_0 \left(\frac{1}{C_2} + \frac{1}{C_3} + \frac{1}{C_v} \right), \\ g_2 &= 2\delta_r g_1 - 2 \frac{C_0 C'_v}{C_v^2}, \quad g_3 = \omega_r^2 [g_1 + p_r (g_1 - 1)] - 2\delta_r \frac{C_0 C'_v}{C_v^2}, \\ 2\delta_r &= \frac{R_1}{L_1} = \frac{1}{Q_r^2 R_1 C_1}, \quad Q_r = \frac{\omega_r}{2\delta_r}, \quad \omega_r^2 = \frac{1}{L_1 C_1}.\end{aligned}$$

By inherently high Q_r , spurious FM is negligible in crystal oscillators. Therefore, to investigate dynamics and ascertain stability of oscillations with FM means studying the spurious AM.

By van der Pol's method, a solution of (8.138) can be written as

$$\begin{aligned}v &= A \cos \phi, \\ v' &= -A\omega \sin \phi, \\ v'' &= -A'\omega \sin \phi - A\omega^2 \cos \phi,\end{aligned}$$

and $v''' = -\omega^2 v'$. For the traditional nonlinearity $i = a_1 v - a_3 v^3$, harmonic balance applied to (8.138) produces two equations,

$$\begin{aligned}A' C_3 (g_3 - 3g_1 \omega^2) - 2\delta_r A' \frac{C_0}{C_2} \left(a_1 + \frac{9}{4} a_3 A^2 \right) - A C_3 g_2 \omega^2 \\ + A \left[\frac{C_0}{C_2} \omega^2 - \omega_r^2 (1 + p_r) \right] \left(a_1 + \frac{3}{4} a_3 A^2 \right) = 0,\end{aligned}\tag{8.139}$$

$$\begin{aligned}A C_3 (g_1 \omega^2 - g_3) + 2\delta_r A \frac{C_0}{C_2} \left(a_1 + \frac{3}{4} a_3 A^2 \right) - 2A' C_3 g_2 \\ + 2A' \frac{C_0}{C_2} \left(a_1 + \frac{9}{4} a_3 A^2 \right) = 0.\end{aligned}\tag{8.140}$$

For the harmonically modulated capacitance C_v of a diode,

$$C_v = C_{v0} (1 + \alpha \cos \Omega t),\tag{8.141}$$

where $\alpha \ll 1$, the oscillator frequency is modulated as

$$\omega = \omega_0 \left(1 - \frac{\alpha_1}{2} \cos \Omega t \right),\tag{8.142}$$

where

$$\begin{aligned}\alpha_1 &= \alpha \frac{C_0 p_r}{C_{v0} r_1 [p_r (r_1 - 1) + r_1]}, \\ r_1 &= 1 + C_0 \left(\frac{1}{C_3} + \frac{1}{C_2} + \frac{1}{C_{v0}} \right),\end{aligned}$$

and auxiliary functions for (8.139) and (8.140) are defined to be

$$\begin{aligned} g_1 &= r_1(1 - \alpha r_2 \cos \Omega t), \\ g_2 &= 2\delta_r g_1 + \alpha r_3 \Omega \sin \Omega t, \\ g_3 &= g_1 \omega_r^2 + \alpha \delta_r r_3 \Omega \sin \Omega t + \omega_r^2 p_r (r_1 - 1) - \alpha \omega_{v_0}^2 \cos \Omega t, \end{aligned}$$

where $r_2 = r_1 C_0 / C_{v_0}$, $r_3 = 2r_1 r_2$, and $\omega_{v_0}^2 = 1 / L_1 C_{v_0}$.

Substituting all the above given functions to (8.139) and (8.140) and thereafter equating to zero the constant terms and the terms with $\cos \Omega t$ and $\sin \Omega t$, we obtain the equations

$$1 - \frac{2C_0 \omega_0 \Delta - C_2 \omega_2^2}{C_3 C_2 \omega_0^2 2\delta_r r_1} \left(a_1 + \frac{3}{4} a_3 A_0^2 \right) = 0, \quad (8.143)$$

$$\begin{bmatrix} a_{11} \\ a_{12} \end{bmatrix} \begin{bmatrix} -(G_1 - 1) & -\nu \\ \nu & -(G_1 - 1) \end{bmatrix} = \begin{bmatrix} -\alpha A_0 r_2 \left(1 + \frac{(G_1 - 1)^2}{18} \right) \\ \alpha A_0 \nu \left(r_2 + \frac{3}{4} \right) \end{bmatrix}, \quad (8.144)$$

where $\nu = \Omega / \delta_r$ and the frequency shift caused by C_{v_0} is

$$\Delta = \omega_0 \frac{p_r}{4r_1} \left(2r_1 - 1 - \sqrt{1 - \frac{4r_1^2}{p_r^2 Q_r^2}} \right).$$

By (8.143), the amplitude A_0 possess the familiar form of

$$A_0 = \sqrt{\frac{4}{3G_3} (G_1 - 1)}, \quad (8.145)$$

where

$$G_1 = a_1 \frac{2C_0 \omega_0 \Delta - C_2 \omega_2^2}{C_3 C_2 \omega_0^2 2\delta_r r_1},$$

$$G_3 = a_3 \frac{2C_0 \omega_0 \Delta - C_2 \omega_2^2}{C_3 C_2 \omega_0^2 2\delta_r r_1}.$$

Thereafter, (8.144) produces two variable amplitudes

$$a_{11} \cong \alpha A_0 \frac{r_2 (G_1 - 1) \left[1 + \frac{(G_1 - 1)^2}{18} \right] + \nu^2 \left(r_2 + \frac{3}{4} \right)}{(G_1 - 1)^2 + \nu^2}, \quad (8.146)$$

$$a_{12} \cong \alpha A_0 \nu \frac{r_2 \left[1 + \frac{(G_1 - 1)^2}{18} \right] - (G_1 - 1) \left(r_2 + \frac{3}{4} \right)}{(G_1 - 1)^2 + \nu^2}. \quad (8.147)$$

An important peculiarity of these functions is that, by the critical values

$$G_{1b} = 1 + \frac{9}{r_2} \left(r_2 + \frac{3}{4} \right) + \frac{3}{r_2} \sqrt{9 \left(r_2 + \frac{3}{4} \right)^2 - 2r_2^2}, \quad (8.148)$$

$$r_{2b} = \frac{27}{2} \frac{G_1 - 1}{(G_1 - 1)^2 - 18(G_1 - 1) + 18}, \tag{8.149}$$

the value of a_{11} becomes constant

$$a_{11b} = \frac{3}{4} \alpha A_0 \frac{18 + (G_1 - 1)^2}{(G_1 - 1)^2 - 18(G_1 - 1) + 18}. \tag{8.150}$$

and a_{12} zero over all modulation frequencies.

Fig. 8.16 answers the question of what happens with $a_{11}(\nu)$ and $a_{12}(\nu)$ if r_2 is fixed and G_1 varies about G_{1b} . It is seen that for any $G_1 \geq G_{1b}$, spurious AM is bounded by (8.150) and the equilibrium point is always stable. Contrary, if G_1 is less than G_{1b} and approaches unity, $1 \leftarrow G_1 < G_{1b}$, the spurious AM index rises dramatically causing instability. A similar picture is watched in changes of a_{12} : by $1 \leftarrow G_1 \leq G_{1b}$, the amplitude a_{12} demonstrates a dramatic overshoot causing instability.

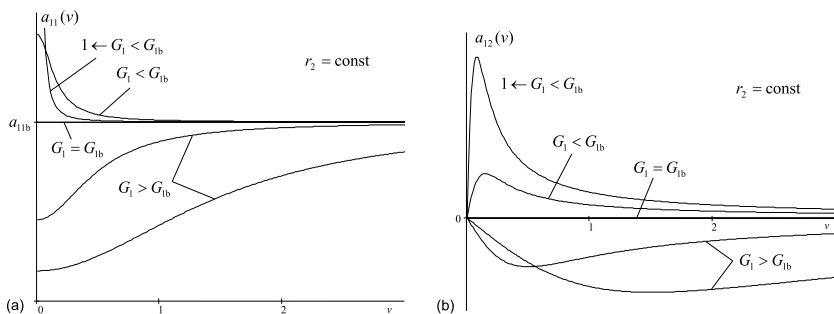


Fig. 8.16. Variable amplitudes, by $r_2 = \text{const}$: (a) $a_{11}(\nu)$ and (b) $a_{12}(\nu)$.

Now needs to be examined the case of a maximum generated power obtained by $G_1 = 1.5$ for r_2 ranging within the allowed bounds, $0 \leq r_2 \leq 1$. Again we infer that there is some critical value r_{2b} for which a_{12} is constant and $a_{12} = 0$ over all ν . However, no critical values of a_{11} and a_{12} exist (Fig. 8.17) to cause instability.

By (8.146) and (8.147), the magnitude and phase AMFs are defined to be, respectively,

$$|H_r(j\nu)| = \sqrt{\frac{\nu^2 \left(r_2 + \frac{3}{4}\right)^2 + r_2^2 \left[1 + \frac{1}{18}(G_1 - 1)^2\right]}{\nu^2 + (G_1 - 1)^2}}, \tag{8.151}$$

$$\tan \Theta_r(\nu) = -\nu \frac{r_2 \left[1 + \frac{(G_1 - 1)^2}{18}\right] - (G_1 - 1) \left(r_2 + \frac{3}{4}\right)}{r_2(G_1 - 1) \left[1 + \frac{(G_1 - 1)^2}{18}\right] + \nu^2 \left(r_2 + \frac{3}{4}\right)}. \tag{8.152}$$

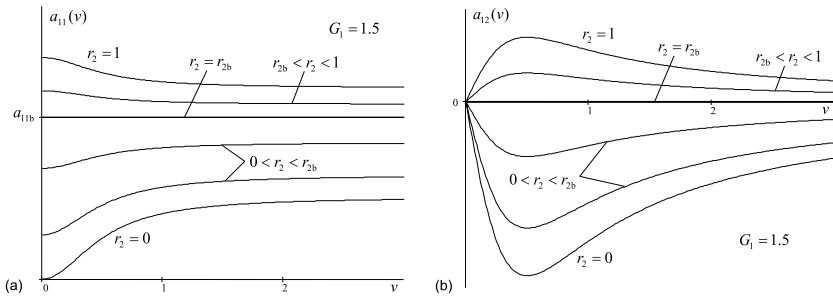


Fig. 8.17. Variable amplitudes for a constant $G_1 = 1.5$: (a) $a_{11}(\nu)$ and (b) $a_{12}(\nu)$.

Inherently, by (8.148) and (8.149), the magnitude AMF becomes constant, $|H_r(j\nu)| = H_{r0} = a_{11b}(\nu)/\alpha A_0$, and phase AMF zero, $\Theta_r(\nu) = 0$, over all frequencies ν . Following a_{11} and a_{12} , the magnitude AMF increases dramatically (Fig. 8.18a) when $1 \leftarrow G_1 < G_{1b}$. The oscillator thus loses stability and it is stable otherwise, if $G_1 \geq G_{1b}$.

A picture similar to Fig. 8.17 can be sketched for the AMF assuming $G_1 = 1.5$. A key point is that there is no value of r_2 between zero and unity to make the oscillator potentially unstable (Fig. 8.19). Moreover, the spurious AM index lowers if $r_2 < r_{2b}$, making this value preferable for FM.

Overall, to avoid potential instability of this NPTV system, it is recommended to choose the value of G_1 such that the spurious AM has almost a constant index over all modulation frequencies.

Example 8.10. An NPTV system shown in Fig. 8.15 utilizes a piezoelectric resonator excited at the first overtone frequency $f_r = 100\text{MHz}$ having the quality factor $Q_r = 10^5$, static capacitance $C_0 = 3 \times 10^{-12}\text{F}$, and losses $R_1 = 100\text{Ohm}$. Additional capacitances are $C_2 = 100 \times 10^{-12}\text{F}$ and $C_3 = 50 \times 10^{-12}\text{F}$. A bias voltage $+V$ of a varactor diode is chosen such that $C_{v0} = 10 \times 10^{-12}\text{F}$. FM is carried out by voice in the frequency range of $(300 - 3000)\text{Hz}$.

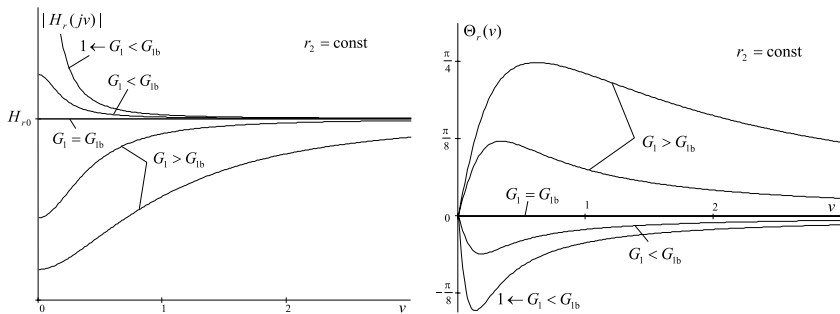


Fig. 8.18. AMFs for a constant r_2 : (a) magnitude $|H_r(j\nu)|$ and (b) phase $\Theta_r(\nu)$.

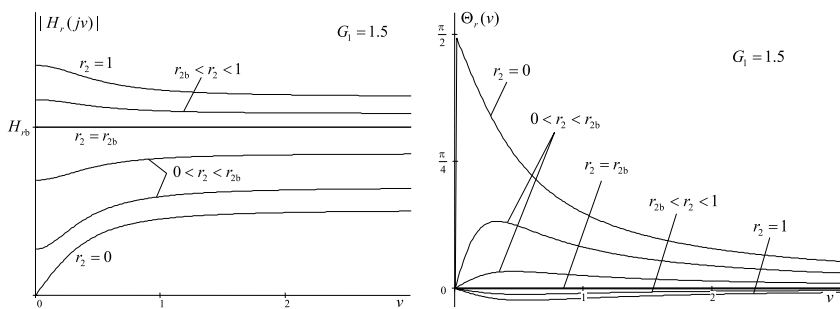


Fig. 8.19. AMF for $G_1 = 1.5$: (a) magnitude $|H_r(j\nu)|$ and (b) phase $\Theta_r(\nu)$.

The resonator bandwidth, $W_r = f_r/Q_r = 1000\text{Hz}$, coincides with the spectral content of the modulating signal. Coefficients r_1 and r_2 are evaluated by $r_1 = 1 + C_0 \left(\frac{1}{C_2} + \frac{1}{C_3} + \frac{1}{C_{v0}} \right) = 1.39$ and $r_2 = \frac{C_0}{r_1 C_{v0}} = 0.216$, respectively. For $r_2 = 0.216$, we have $G_{1b} = 1.224$ and thus, to avoid potential instability, the gain G_1 must be chosen such that $G_1 \geq 1.224$. \square

8.5.5 Modulation Functions Method (Fast Modulation)

As it follows, the modulation functions method (slow modulation) is applicable to an NPTV closed loop system (oscillator) that is periodically varied with the frequency comparable with the resonator bandwidth, $2\delta \sim \Omega \ll \omega_0$. With higher modulation frequencies, $2\delta \ll \Omega \rightarrow \infty$, both AMF and FMF reach their asymptotic levels and, if such a system is characterized with a single resonance (pole), an analysis is complete.

If a system is multiresonant (multipole), the main question arises how the nonuniformity of the open loop frequency response affects modulation. An example is an oscillator with any physical (bulk) resonator (dielectric, crystal, microwave, etc), which resonant system is inherently multimodal. To describe such a system, the modulation functions method needs to be modified for fast modulation.

Let us consider an oscillator represented with the closed loop Hammerstein system, whose linear periodically time-varying (modulated) feedback has two branches as shown in Fig. 8.20. The memoryless nonlinearity $f(\cdot)$ and the principle feedback with the frequency response $H(j\omega, t)$ generate steady-state oscillations at the frequency ω_0 . An additional unexcited feedback is supposed to be multiresonant. For the sake of simplicity, we save in this branch only the i th resonance at $\omega_i > \omega_0$, $i = 1, 2, \dots$, and represent it with the frequency response $H_i(j\omega)$.

Beyond the bandwidth of an additional feedback, the output $y_0(t)$ can be described using (8.79) as follows

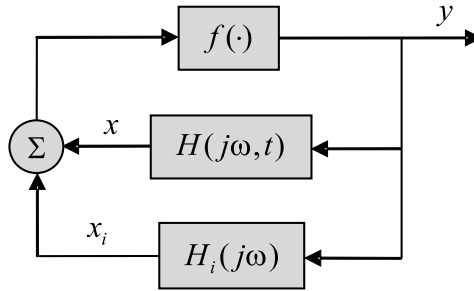


Fig. 8.20. Oscillator with two resonant feedbacks.

$$y_0(t) = r_0 [1 + \mu_r^* \cos(\Omega t + \Psi_r)] \cos [\omega_0 t + \mu_\varphi^* \sin(\Omega t + \Psi_\omega) + \varphi_1] , \quad (8.153)$$

where $\mu_r^*(\Omega)$, $\Psi_r(\Omega)$, $\mu_\varphi^*(\Omega) = \frac{\omega_0}{\Omega} \mu_\omega^*(\Omega)$, and $\Psi_\omega(\Omega)$ are specified with slow modulation by (8.86), (8.87), (8.102), and (8.103), respectively. Here, without loss in generality with FM, φ_1 can be omitted.

Typically, the modulation factors in FM oscillators are such that $|\mu_\omega^*| \ll |\mu_r^*| < 1$ and $|\mu_\varphi^*| \ll 1$. That allows us to let

$$\cos(\beta \sin z) \cong \cos(\beta \cos z) \cong 1 ,$$

$$\sin(\beta \sin z) \cong \beta \sin z ,$$

$$\sin(\beta \cos z) \cong \beta \cos z$$

and represent the spectral content of (8.153) with

$$\begin{aligned} y_0(t) = & V_1 \cos(\omega_0 t + \varphi_0) \\ & + V_{-\Omega} \cos[(\omega_0 - \Omega)t + \varphi_{-\Omega}] + V_{+\Omega} \cos[(\omega_0 + \Omega)t - \varphi_{+\Omega}] \\ & - V_{-2\Omega} \cos[(\omega_0 - 2\Omega)t + \varphi_{-2\Omega}] - V_{+2\Omega} \cos[(\omega_0 + 2\Omega)t - \varphi_{+2\Omega}] , \end{aligned} \quad (8.154)$$

where the amplitudes and phases are defined by

$$V_1 = r_0 \sqrt{1 + \frac{1}{4} \mu_r^{*2} \mu_\varphi^{*2} \sin^2(\Psi_r - \Psi_\omega)} , \quad (8.155)$$

$$\tan \varphi_0 = -\frac{1}{2} \mu_r^* \mu_\varphi^* \sin(\Psi_r - \Psi_\omega) , \quad (8.156)$$

$$V_{\pm\Omega} = r_0 \sqrt{\frac{1}{4} (\mu_r^{*2} + \mu_\varphi^{*2}) \mp \frac{1}{2} \mu_r^* \mu_\varphi^* \cos(\Psi_r - \Psi_\omega)} , \quad (8.157)$$

$$\tan \varphi_{\pm\Omega} = -\frac{\mu_\varphi^* \sin \Psi_\omega \mp \mu_r^* \sin \Psi_r}{\mu_{\varphi,r}^* \cos \Psi_r \mp \mu_{r,\varphi}^* \cos \Psi_\omega} , \quad (8.158)$$

$$V_{\pm 2\Omega} = \frac{r_0}{4} \mu_r^* \mu_\varphi^* , \quad (8.159)$$

$$\varphi_{\pm 2\Omega} = -(\Psi_r + \Psi_\omega). \quad (8.160)$$

Let us now analyze an influence of the additional resonant feedback. Of prime interest is to evaluate spurious AM and FM when the most power side spectral component of (8.154) with the frequency $\omega_0 + \Omega \cong \omega_i$ passes through the additional branch. It can be supposed that, when passed, an auxiliary voltage is generated at the output,

$$y_i(t) = V_{ic} \cos(\omega_0 + \Omega)t + V_{is} \sin(\omega_0 + \Omega)t, \quad (8.161)$$

with amplitudes $V_{1c}(\Omega)$ and $V_{1s}(\Omega)$ caused by $H_i(j\omega)$.

Adding (8.161) to (8.154) forms the output

$$y(t) = y_0(t) + y_i(t) = V_g(t) \cos[\omega_0 t + \varphi_g(t)], \quad (8.162)$$

where

$$V_g(t) = \sqrt{V_{g1}^2 + V_{g2}^2}, \quad (8.163)$$

$$\tan \varphi_g(t) = -\frac{V_{g2}}{V_{g1}}, \quad (8.164)$$

$$\begin{aligned} V_{g1} = & V_1 [1 + \mu_r^* \cos(\Omega t + \Psi_r)] \cos[\mu_\varphi^* \sin(\Omega t + \Psi_\omega)] \\ & + V_{ic} \cos \Omega t + V_{is} \sin \Omega t, \end{aligned} \quad (8.165)$$

$$\begin{aligned} V_{g2} = & V_1 [1 + \mu_r^* \cos(\Omega t + \Psi_r)] \sin[\mu_\varphi^* \sin(\Omega t + \Psi_\omega)] \\ & + V_{is} \cos \Omega t - V_{ic} \sin \Omega t. \end{aligned} \quad (8.166)$$

Similarly to slow modulation, we can now transform (8.163) and (8.164) in order to evaluate the factors of spurious AM and FM.

Spurious Amplitude Modulation

Neglecting harmonics of the modulation frequency, the amplitude (8.163) can be transformed to the AM form of

$$V_g(t) = V_{g0} [1 + \mu_{V_i}^* \cos(\Omega t + \Psi_{V_i})], \quad (8.167)$$

where

$$\mu_{V_i}^* = \frac{1}{2V_{g0}^2} \sqrt{V_{Ci}^4 + V_{Si}^4},$$

$$\tan \Psi_{V_i} = -\frac{V_{Si}^2}{V_{Ci}^2},$$

$$V_{g0}^2 = r_0^2 \left[1 + \frac{\mu_r^2}{2} + k_i^2 + k_i \mu_r^* \cos(\Psi_r - \varphi_i) + k_i \mu_\varphi^* \cos(\Psi_\omega - \varphi_i) \right],$$

$$\begin{aligned}
 V_{Ci}^2 &= r_0^2 \left\{ 2 \left(\frac{V_{ic}}{r_0} + \mu_r^* \cos \Psi_r \right) \right. \\
 &+ \mu_r^* \mu_\varphi^* \left[\frac{V_{is}}{r_0} \sin (\Psi_r - \Psi_\omega) + \frac{k_i}{2} \cos (\Psi_r + \Psi_\omega - \varphi_i) \right] \left. \right\}, \\
 V_{Si}^2 &= r_0^2 \left\{ 2 \left(\frac{V_{is}}{r_0} - \mu_r^* \sin \Psi_r \right) \right. \\
 &- \mu_r^* \mu_\varphi^* \left[\frac{V_{ic}}{r_0} \sin (\Psi_r - \Psi_\omega) - \frac{k_i}{2} \sin (\Psi_r + \Psi_\omega - \varphi_i) \right] \left. \right\}.
 \end{aligned}$$

Also, $V_i = \sqrt{V_{ic}^2 + V_{is}^2}$ and $\tan \varphi_i = -\frac{V_{is}}{V_{ic}}$ are the amplitude and phase of (8.161) and $k_i = V_i/r_0$ is the *modulation coefficient*.

Spurious Frequency Modulation

The instantaneous frequency shift, caused by the phase φ_g (8.164), can be defined by

$$\Delta\omega_g(t) = \frac{d}{dt} \varphi_g(t) = \frac{1}{V_{g1}^2 + V_{g2}^2} \left(V_{g1} \frac{dV_{g2}}{dt} - V_{g2} \frac{dV_{g1}}{dt} \right). \quad (8.168)$$

Substituting (8.165) and (8.166) to (8.168) and neglecting products of small values yield

$$\begin{aligned}
 \Delta\omega_g(t) &\cong \\
 &- \Omega \left[(\mu_\varphi^* \cos \Psi_\omega - k_i \cos \varphi_i) \cos \Omega t - (\mu_\varphi^* \sin \Psi_\omega - k_i \sin \varphi_i) \sin \Omega t \right]. \quad (8.169)
 \end{aligned}$$

The signal modulated frequency can now be performed in the standard FM form as

$$\omega(t) = \omega_0 [1 + \mu_{Wi}^* \cos (\Omega t + \Psi_{Wi})], \quad (8.170)$$

where $\mu_{Wi}(\Omega) = \Delta\omega_g/\omega_0$ and $\Psi_{Wi}(\Omega)$ are provided by

$$\mu_{Wi}^* = \frac{\Omega}{\omega_0} \sqrt{\mu_\varphi^{*2} - 2\mu_\varphi^* k_i \cos (\Psi_\omega - \varphi_i) + k_i^2}, \quad (8.171)$$

$$\tan \Psi_{Wi} = \frac{\mu_\varphi^* \sin \Psi_\omega - k_i \sin \varphi_i}{\mu_\varphi^* \cos \Psi_\omega - k_i \cos \varphi_i}, \quad (8.172)$$

to describe the FMF of an oscillator.

Modulation Factors and Functions

After the transformations, we finally arrive at the output signal

$$y(t) = V_{g0} [1 + \mu_{V_i}^* \cos(\Omega t + \Psi_{V_i})] \times \cos \left\{ \omega_0 \int [1 + \mu_{W_i}^* \cos(\Omega t + \Psi_{W_i})] dt + \varphi_1 \right\}, \quad (8.173)$$

where

$$\mu_{V_i}^* = \mu_{r0}^* \sqrt{1 + 2 \frac{k_i}{\mu_{r0}^*} \cos(\Psi_{r0} - \varphi_i) + \frac{k_i^2}{\mu_{r0}^{*2}}}, \quad (8.174)$$

$$\tan \Psi_{V_i} = \frac{\mu_{r0}^* \sin \Psi_{r0} + k_i \sin \varphi_i}{\mu_{r0}^* \cos \Psi_{r0} + k_i \cos \varphi_i}, \quad (8.175)$$

$$\mu_{W_i}^* = \mu_{\omega 0}^* \sqrt{1 - 2 \frac{k_i}{\mu_{\varphi 0}^*} \cos(\Psi_{\omega 0} - \varphi_i) + \frac{k_i^2}{\mu_{\varphi 0}^{*2}}}, \quad (8.176)$$

$$\tan \Psi_{W_i} = \frac{\mu_{\varphi 0}^* \sin \Psi_{\omega 0} - k_i \sin \varphi_i}{\mu_{\varphi 0}^* \cos \Psi_{\omega 0} - k_i \cos \varphi_i}. \quad (8.177)$$

In these functions, μ_{r0}^* , Ψ_{r0} , $\mu_{\omega 0}^*$, $\mu_{\varphi 0}^*$, and $\Psi_{\omega 0}$ are parameters of modulation beyond the bandwidth of $H_i(j\Omega)$ and the frequency-varying coefficient $k_i = \frac{V_i}{r_0}$ is specified by $H_i(j\Omega)$.

A simple analysis of (8.174)–(8.177) shows that with an extremely small gain of an additional resonance circuit, $k_i \rightarrow 0$, modulation is characterized with the AMF and FMF featured to slow modulation: $\mu_{V_i}^* = \mu_{r0}^*$, $\Psi_{V_i} = \Psi_{r0}$, $\mu_{W_i}^* = \mu_{\omega 0}^*$, and $\Psi_{W_i} = \Psi_{\omega 0}$.

It also follows that when Ω is exactly equal to $\omega_i - \omega_0$, causing $\varphi_i \cong \Psi_{r_i} \cong \Psi_{\omega_i} \cong 0$, then (8.174) and (8.176) reach their extrema, respectively,

$$\begin{aligned} \mu_{V_i}^*|_{\text{ext}} &= \mu_{r0}^* + k_i \max, \\ \mu_{W_i}^*|_{\text{ext}} &= \mu_{\omega 0}^* - \frac{\omega_i - \omega_0}{\omega_0} k_i \max. \end{aligned}$$

Because $0 < |\mu_{\omega 0}^*| \ll |\mu_{r0}^*| < 1$ and k_i can be large, the increase in the modulation factors caused by an additional resonance can be very appreciable. In this sense, the effect is reminiscent of the familiar parametric amplification in LPTV systems demonstrated in Fig. 6.27.

For this model, the AMF and FMF can be defined by

$$|H_{r_i}(j\Omega)| = \left| \frac{\mu_{V_i}^*}{\mu_{r0}^*} \right|, \quad \Theta_{r_i} = \begin{cases} \Psi_{V_i}, & \mu_{V_i}^*/\mu_{r0}^* \geq 0 \\ \Psi_{V_i} + \pi, & \mu_{V_i}^*/\mu_{r0}^* < 0 \end{cases}, \quad (8.178)$$

$$|H_{\omega_i}(j\Omega)| = \left| \frac{\mu_{W_i}^*}{\mu_{\omega_0}^*} \right|, \quad \Theta_{\omega_i} = \begin{cases} \Psi_{W_i}, & \mu_{W_i}^*/\mu_{\omega_0}^* \geq 0 \\ \Psi_{W_i} + \pi, & \mu_{W_i}^*/\mu_{\omega_0}^* < 0 \end{cases}. \quad (8.179)$$

To calculate (8.178) and (8.179), the complex modulation coefficient

$$k_i e^{j\varphi_i} = \frac{\sqrt{V_{ic}^2 + V_{is}^2}}{r_0} e^{-j \arctan \frac{V_{is}}{V_{ic}}} \quad (8.180)$$

must be specified for the particular oscillator scheme.

Example 8.11 (Modulation coefficient). To define k_i and φ_i , by (8.180), the loop (Fig. 8.20) may be reconfigured regarding the frequency ω_i as shown in Fig. 8.21. At ω_i , the nonlinear function $f(\cdot)$ is linearized with a gain factor a and the main feedback omitted.

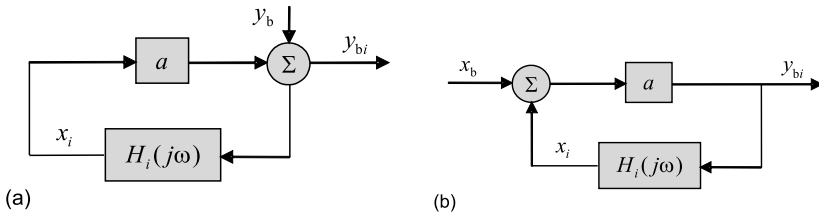


Fig. 8.21. An oscillator loop linearized at ω_i : (a) output-to-output and (b) input-to-output.

The spectral component $y_b = \text{Re}V_{+\Omega}e^{j(\omega_b t - \varphi + \Omega)}$ of $y(t)$ acts at the frequency $\omega_b = \omega_0 + \Omega$ in the output (Fig. 8.21a). Equivalently, it can be transferred to the input as $x_b = \frac{y_b}{a}$ (Fig. 8.21b). The output component y_{bi} caused by x_b is defined by

$$y_{bi} = x_b \frac{a}{1 - aH_i} = y_b \frac{1}{1 - aH_i} = y_b H_b. \quad (8.181)$$

By $H_b(j\omega) = H_{br}(\omega) + jH_{bi}(\omega)$, we rewrite the real part of (8.181) as

$$\begin{aligned} y_{bi} &= V_{+\Omega} |H_b(j\omega)| \cos(\omega_b t + \varphi_b - \varphi + \Omega) \\ &= V_{+\Omega} |H_b(j\omega)| \cos(\varphi_b - \varphi + \Omega) \cos \omega_b t - V_{+\Omega} |H_b(j\omega)| \sin(\varphi_b - \varphi + \Omega) \sin \omega_b t, \end{aligned} \quad (8.182)$$

where

$$|H_b(j\omega)| = \sqrt{H_{br}^2(\omega) + H_{bi}^2(\omega)}, \quad (8.183)$$

$$\tan \varphi_b(\omega) = \frac{H_{bi}(\omega)}{H_{br}(\omega)}. \quad (8.184)$$

Equivalently, y_{bi} can be defined by the sum of two components, $y_b = V_{+\Omega} \cos(\omega_b t - \varphi + \Omega)$ and y_i (8.161); that is,

$$y_{bi} = (V_{+\Omega} \cos \varphi_{+\Omega} + V_{1c}) \cos \omega_b t + (V_{+\Omega} \sin \varphi_{+\Omega} + V_{1s}) \sin \omega_b t. \quad (8.185)$$

By equating (8.182) and (8.185) and making the necessary transformations, we find the amplitudes

$$V_{ic} = V_{+\Omega}[(H_{br} - 1) \cos \varphi_{+\Omega} + H_{bi} \sin \varphi_{+\Omega}], \quad (8.186)$$

$$V_{is} = V_{+\Omega}[(H_{br} - 1) \sin \varphi_{+\Omega} - H_{bi} \cos \varphi_{+\Omega}], \quad (8.187)$$

where $H_{br}(\omega)$ and $H_{bi}(\omega)$ are specified by a particular oscillator scheme. By $H_i(j\omega) = H_1(\omega) + jH_2(\omega)$ and an identity $(1 - aH_i)^{-1} = H_b$ stated by (8.181), the components $H_{br}(\omega)$ and $H_{bi}(\omega)$ become

$$H_{br} = \frac{1 - aH_1}{(1 - aH_1)^2 + a^2H_2^2}, \quad (8.188)$$

$$H_{bi} = -\frac{aH_2}{(1 - aH_1)^2 + a^2H_2^2}. \quad (8.189)$$

Finally, because of $V_i = \sqrt{V_{ic}^2 + V_{is}^2}$, (8.186) and (8.187) yield

$$V_i = V_{+\Omega} \sqrt{(H_{br} - 1)^2 + H_{bi}^2}, \quad (8.190)$$

and the coefficient k_i is defined by

$$k_i = \frac{V_i}{r_0} = \frac{V_{+\Omega}}{r_0} \sqrt{(H_{br} - 1)^2 + H_{bi}^2}. \quad (8.191)$$

The most common property of k_i can now be pointed out by analyzing (8.188) and (8.189). As it is seen, exactly at $\Omega = \omega_i - \omega_0$, we have $H_2 = 0$, thus $H_{br} = (1 - aH_1)^{-1}$ and $H_{bi} = 0$, and k_i reaches a maximum value

$$k_{i \max} = \frac{V_{+\Omega}}{r_0} \left| \frac{aH_1}{1 - aH_1} \right|$$

that in the linearized model tends toward infinity when $aH_1 = 1$. A typical surface plot of $k_i(\Omega, a|H_i(j\omega)|)$ is shown in Fig. 8.22.

The phase, $\tan \varphi_i = -V_{is}/V_{ic}$, ranges from $\pi/2$ to $-\pi/2$. By increasing Ω , it changes from positive to negative values if $a|H_i(j\omega)| < 1$, becomes zero when $a|H_i(j\omega)| = 1$ and $\Omega = \omega_i - \omega_0$, and changes from negative to positive values if $a|H_i(j\omega)| > 1$. A typical surface plot of $\varphi_i(\Omega, a|H_i(j\omega)|)$ is shown in Fig. 8.23.

Such changes in the modulation coefficient $k_i e^{j\varphi_i}$ mean that, similarly to parametric excitation of LPTV systems, modulation of an NPTV closed loop system (oscillator) can cause excitation of its additional resonant branch. \square

So, if the frequency response $H_i(j\omega)$ of an additional resonant feedback is distinct and $k_i e^{j\varphi_i}$ is specified as in Example 8.11, the AMF and FMF of an FM oscillator can be calculated using (8.178) and (8.179) via (8.174)–(8.177). Below, we apply this approach to the Butler type crystal oscillator.

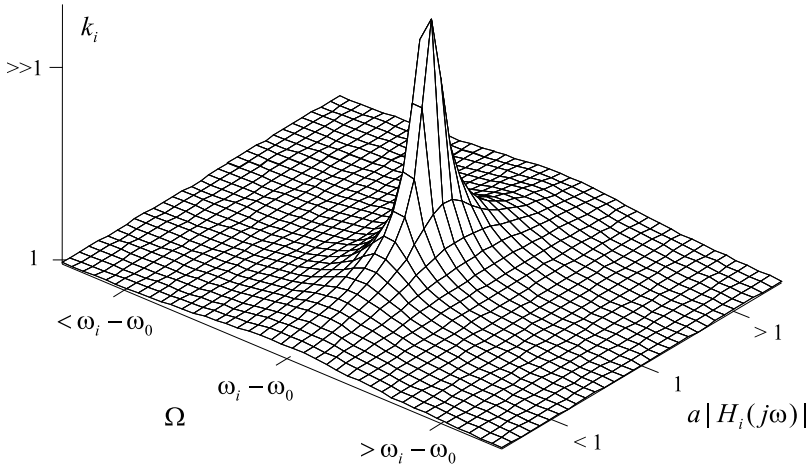


Fig. 8.22. A typical function of $k_i(\Omega, a|H_i(j\omega)|)$.

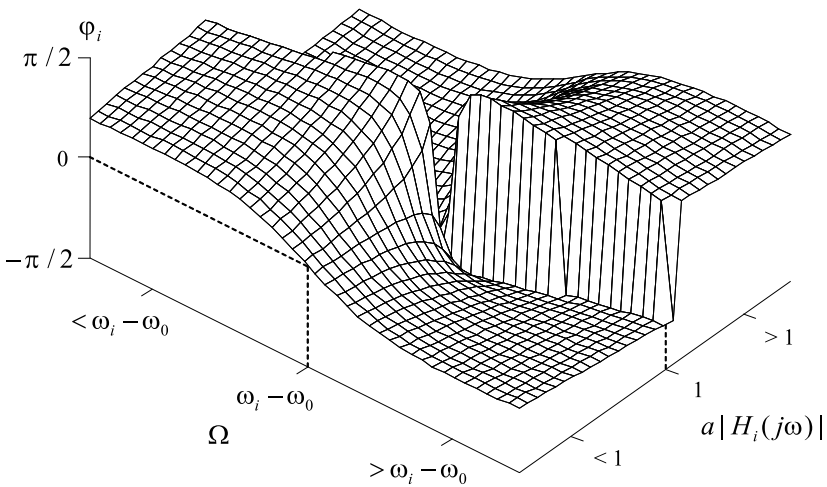


Fig. 8.23. A typical function of $\varphi_i(\Omega, a|H_i(j\omega)|)$.

8.5.6 Butler Type FM Crystal Oscillator

To illustrate application of the approach to fast modulation, we are going to examine in this section the Butler type FM crystal oscillator, whose equivalent scheme is given in Fig. 8.24a. Here, a transistor and the net of L, C_1 and C_2 compose a non-inverting NTI amplifier. A cascade of a crystal resonator and varactor diode represent an LTV resonant feedback. By two series branches of a piezoelectric resonator, the scheme becomes as sketched in Fig. 8.24b,

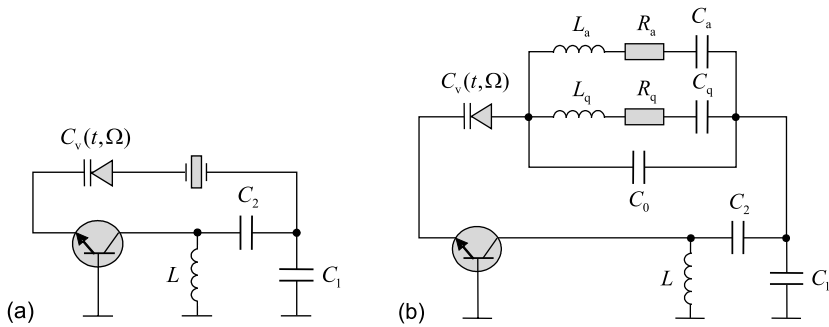


Fig. 8.24. Equivalent scheme of a Butler type FM crystal oscillator: (a) basic and (b) simplified.

where L_q, C_q and R_q represent the fundamental vibration, L_a, C_a and R_a the anharmonic vibration, and C_0 is the resonator static capacitance. The branches are characterized with the resonance frequencies, $\omega_q = 1/\sqrt{L_q C_q}$ and $\omega_a = 1/\sqrt{L_a C_a}$, and nonoverlapped bandwidths, $2\delta_q = R_q/L_q$ and $2\delta_a = R_a/L_a$.

To find the AMF and FMF associated with the feedback frequency response $H_i(j\omega)$, we substitute the loop at the frequency ω_a with the equivalent scheme shown in Fig. 8.25a. The scheme can further be generalized as in Fig. 8.25b for the impedance of an additional branch $Z_{ea} = R_{ea} + jX_{ea}$ and as in Fig. 8.25c for the impedance of an additional feedback $Z_e = R_e + jX_e$. Here, the voltage $v_b(t, \Omega)$ is the output component with the frequency $\omega_q + \Omega \sim \omega_a$.

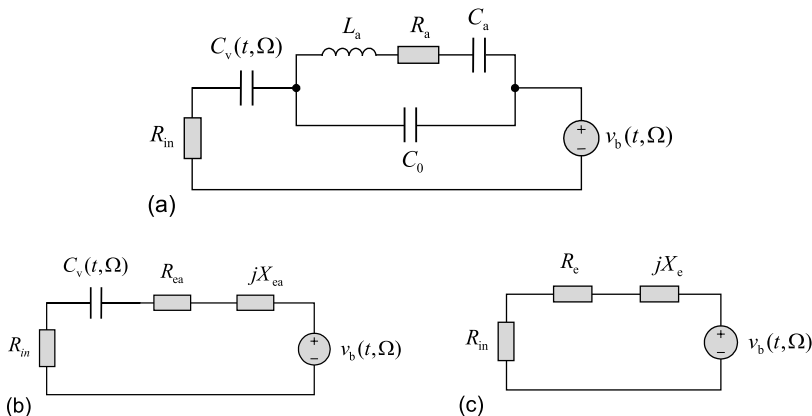


Fig. 8.25. The Butler type FM crystal oscillator linearized at ω_a : (a) basic scheme, (b) with a generalized resonator, and (c) generalized.

Real and imaginary components of the impedance of a crystal resonator additional branch are given by (5.84) and (5.85), respectively,

$$R_{\text{ea}} = R_{\text{a}} \frac{1}{(1 - \nu\kappa_{\text{a}})^2 + \kappa_{\text{a}}^2}, \quad (8.192)$$

$$X_{\text{ea}} = R_{\text{a}} \frac{\nu(1 - \nu\kappa_{\text{a}}) - \kappa_{\text{a}}}{(1 - \nu\kappa_{\text{a}})^2 + \kappa_{\text{a}}^2}, \quad (8.193)$$

where $\nu(\omega) = (\omega - \omega_{\text{a}})/\delta_{\text{a}}$ and $\kappa_{\text{a}} = R_{\text{a}}\omega_{\text{a}}C_0$ is the κ -factor of an additional branch of a crystal resonator. By (8.192) and (8.193), the frequency response of an additional feedback is defined to be

$$H_i = \frac{R_{\text{in}}}{R_{\text{in}} + R_{\text{ea}} + j(X_{\text{ea}} - \bar{X}_{\text{v}})} = H_1 + jH_2, \quad (8.194)$$

where $\bar{X}_{\text{v}}(\omega) = 1/\omega\bar{C}_{\text{v}}$ and \bar{C}_{v} is a mean capacitance of a varactor diode.

By (8.194), the real part $H_1(\omega)$ and imaginary part $H_2(\omega)$ of $H_i(j\omega)$ are defined as

$$H_1 = \frac{R_{\text{in}}(R_{\text{in}} + R_{\text{ea}})}{(R_{\text{in}} + R_{\text{ea}})^2 + (X_{\text{ea}} - \bar{X}_{\text{v}})^2}, \quad (8.195)$$

$$H_2 = \frac{R_{\text{in}}(X_{\text{ea}} - \bar{X}_{\text{v}})}{(R_{\text{in}} + R_{\text{ea}})^2 + (X_{\text{ea}} - \bar{X}_{\text{v}})^2}. \quad (8.196)$$

Exploiting (8.195) and (8.196), the modulation functions of the FM crystal oscillator can easily be calculated numerically. In the following examples, we observe several particular situations.

Example 8.12 (Basic scheme). Consider a scheme (Fig. 8.25a) characterized with $f_{\text{a}} = 5.108$ MHz, $L_{\text{a}} = 10$ H, and $R_{\text{a}} = R_{\text{in}} = 150$ Ohm. For clarity, we let $\mu_{\omega_0}^* = 10^{-6}$, $\Psi_{\omega_0} = 0$, $\mu_{\nu_0}^* = 10^{-2}$, and $\Psi_{\nu_0} = \pi$. The capacitance \bar{C}_{v} is assumed to be extremely large and C_0 negligibly small.

Under such conditions, (8.195) and (8.196) can be simplified to

$$H_1 = \frac{R_{\text{in}}(R_{\text{in}} + R_{\text{ea}})}{(R_{\text{in}} + R_{\text{ea}})^2 + X_{\text{ea}}^2},$$

$$H_2 = \frac{R_{\text{in}}X_{\text{ea}}}{(R_{\text{in}} + R_{\text{ea}})^2 + X_{\text{ea}}^2},$$

where $R_{\text{ea}} = R_{\text{a}}$ and $X_{\text{ea}} = R_{\text{a}}(\omega - \omega_{\text{a}})/\delta_{\text{a}}$. Numerical plots of the magnitude AMF $|H_{ri}(j\Omega)|$ and phase AMF $\Theta_{ri}(\Omega)$ are shown in Fig. 8.26a and Fig. 8.26b, respectively. As can be seen, the functions qualitatively fit Fig. 8.22 and Fig. 8.23. Indeed, increasing $a|H_i|$ makes the magnitude AMF brightly pronounced and such that, by $a|H_i| = 1$, it becomes infinity. Further increasing with $a|H_i| > 1$ reduces the peak value. Contrary to φ_i (Fig. 8.23), the phase AMF (Fig. 8.26b) ranges from π to $-\pi$, but the trend remains qualitatively the same. By increasing Ω , the phase changes from π to $-\pi$, if $a|H_i| < 1$. At $a|H_i| = 1$, it jumps from π to $-\pi$ exactly at $\Omega = \omega_{\text{a}} - \omega_{\text{q}}$ and, by $a|H_i| > 1$, changes the sign. \square

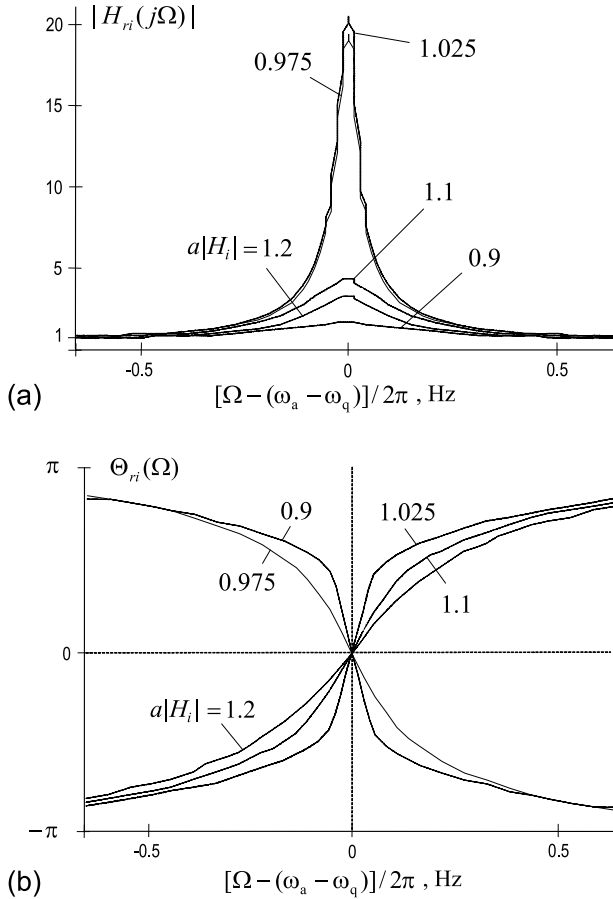


Fig. 8.26. AMF of an oscillator (Example 8.12): (a) magnitude and (b) phase.

Example 8.13 (Effect of C_0). Consider Example 8.12, supposing that \bar{C}_v is still very large, but $C_0 > 0$ is real. For this case, the components H_1 and H_2 are defined, respectively, by (8.195) and (8.196) with $\bar{X}_v = 0$.

The magnitude FMF $|H_{\omega_i}(\Omega)|$ and phase FMF $|\Theta_{\omega_i}(\Omega)|$ are shown in Fig. 8.27a and Fig. 8.27b, respectively, for $a|H_i| = 0.8$ and several feasible values of C_0 . As can be seen, the parallel resonance at the frequency $1/\sqrt{L_a C_0}$ forces the phase to change the sign. It is also seen that the peak value of the magnitude FMF has appeared to be larger than μ_{ω_0} by the factor of about 2000 that coincides with Fig. 8.22. \square

Example 8.14 (Effect of \bar{C}_v). Let us now examine the most general case of Fig. 8.25a when both C_0 and \bar{C}_v are real and another parameters are those given in Example 8.12. Setting for clarity $C_0 = 4 \times 10^{-12}$ F and $aH_{br} = 0.9$,

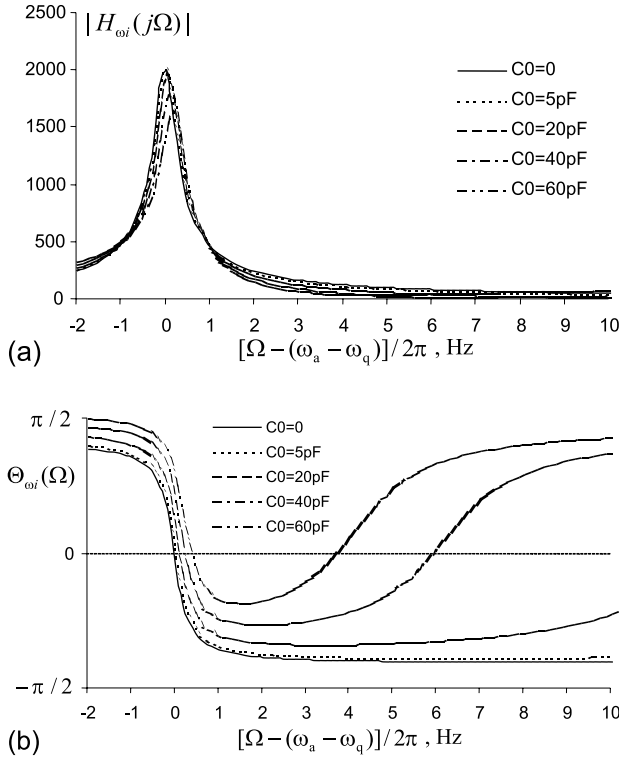


Fig. 8.27. FMF of an oscillator (Example 8.13): (a) magnitude and (b) phase.

we change \bar{C}_v , calculate (8.195) and (8.196), and watch for the AMF and FMF.

The magnitude and phase AMFs are shown in Fig. 8.28a and Fig. 8.28b, respectively, and we indicate some new trends. Reducing \bar{C}_v first results in decreasing the peak value of $|H_{ri}(\Omega)|$. With some boundary value of \bar{C}_v , the magnitude AMF becomes flat and, by further increasing \bar{C}_v , demonstrates a dip, which minimum can locate closely to zero. By very small values of \bar{C}_v , there are almost no changes in the AMF. The latter is because the feedback becomes extremely poor when $\bar{C}_v < 1$. The relevant phase AMFs also differ from those (Fig. 8.26b) observed in the basic structure.

Similarly to the magnitude AMF, the peak value of the magnitude FMF is removed by increased \bar{C}_v toward higher frequencies (Fig. 8.29a) with, however, no dips. Here, the phase FMFs (Fig. 8.29b) behave qualitatively as in Fig. 8.27b, except for shifts at zero. \square

The above-given examples neatly demonstrate several important features of NPTV closed loop systems. First of all, if an LTI resonant part is multi-

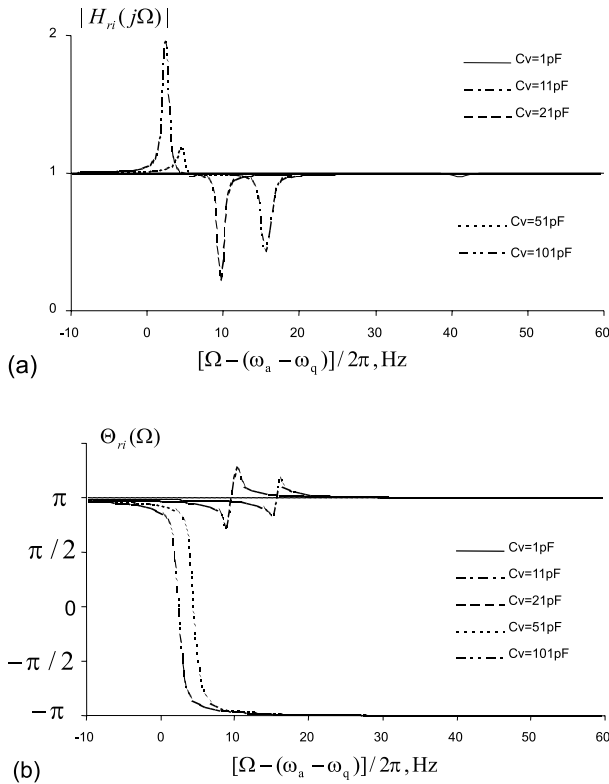


Fig. 8.28. AMF caused by an additional feedback: (a) magnitude and (b) phase.

frequency (multipole), the modulation indexes of both spurious AM and FM can reach extremely large values at some resonance frequencies. Second of all, energy induced with modulation by spectral components of the output to an additional resonant feedback can cause excitation of this feedback. If it occurs, an oscillator becomes either multifrequency, although unstable, or, typically, can no longer fulfill the requirements.

8.6 State Space Representation

As well as other systems, NTV systems can also be represented in state space that often has certain advantages against the ODE form. In fact, the state space model allows finding generalizations and solutions at least for several important particular cases.

Most generally, an NTV system is represented in state space with the equations

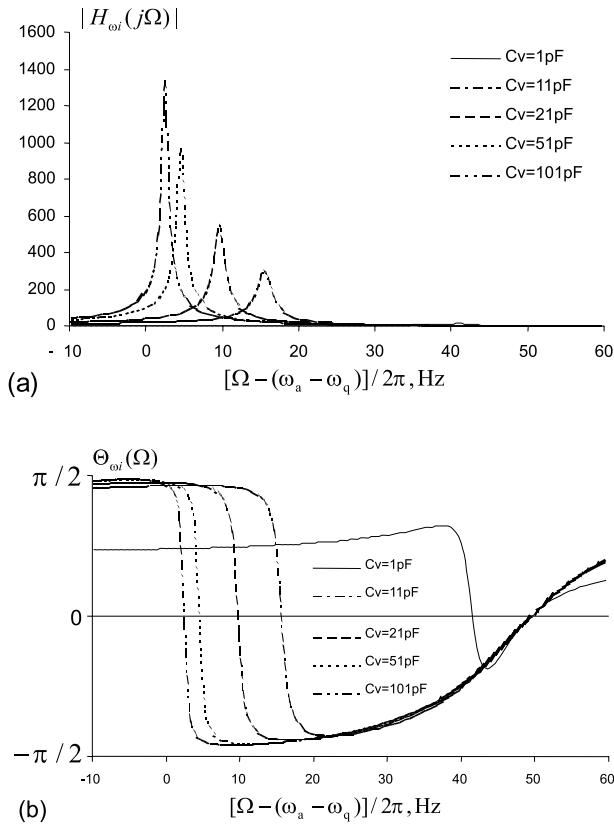


Fig. 8.29. FMF caused by an additional feedback: (a) magnitude and (b) phase.

$$\mathbf{q}'(t) = \Psi[\mathbf{q}(t), \mathbf{x}(t), t], \quad (8.197)$$

$$\mathbf{y}(t) = \Upsilon[\mathbf{q}(t), \mathbf{x}(t), t], \quad (8.198)$$

where $\mathbf{q}(t)$ is the state vector, $\mathbf{x}(t)$ is the input vector, and $\mathbf{y}(t)$ is output vector. Here Ψ and Υ are some nonlinear time-varying vector functions. Like the NTI system case, these generalized equations are unsolvable, until the functions Ψ and Υ are specified. Moreover, a general solution is not of importance, because of real electronic systems are typically described in particular forms. In the below examples, we examine several such forms associated with already familiar electronic systems.

Example 8.15 (Voltage controlled oscillator). Consider a voltage controlled oscillator (Fig. 8.12) with a time-varying capacitance $C(t)$ and all other parameters constant. The oscillator can be described with the ODE

$$y'' + \left[\frac{C'}{C} + \frac{R}{L} + \frac{M}{LC} (a - 3by^2) \right] y' + \frac{1}{LC} y = 0,$$

By assigning the state variables $q_1 = y$, $q_2 = y' = q_1'$, and

$$q_2' = - \left[\frac{C'}{C} + \frac{R}{L} + \frac{M}{LC} (a - 3bq_1^2) \right] q_2 - \frac{1}{LC} q_1,$$

we arrive at the state and output equations, respectively,

$$\mathbf{q}'(t) = \mathbf{A}[\mathbf{q}(t), t]\mathbf{q}(t) + \mathbf{B}x(t), \quad (8.199)$$

$$y(t) = \mathbf{C}\mathbf{q}(t) + \mathbf{D}x(t), \quad (8.200)$$

in which the input and output matrices are both zero, $\mathbf{B} = \mathbf{0}$ and $\mathbf{D} = \mathbf{0}$, respectively, the measurement matrix is $\mathbf{C} = [1 \ 0]$, and the system matrix is nonlinear and time-variant,

$$\mathbf{A}[\mathbf{q}(t), t] = \begin{bmatrix} 0 & 1 \\ -\frac{1}{LC} & -\frac{C'}{C} - \frac{R}{L} - \frac{M}{LC}(a - 3bq_1^2) \end{bmatrix}.$$

In this typical case of an electronic oscillator, the general equations (8.197) and (8.198) become (8.199) and (8.200), respectively. It follows that the state equation is NTV, whereas the measurement equation is LTI. A general solution of (8.199) and (8.200) can be found by regular methods and stability can be ascertained by investigating the system matrix $\mathbf{A}[\mathbf{q}(t), t]$. \square

Example 8.16 (Time-variant Hammerstein-based control system).

Consider a memoryless NTV system, which nonlinearity $f(\cdot, t)$ is adapted to external situation and is thus time-varying. To operate only in the certain frequency region, an LTI filter is placed over to organize a feedback. The system thus becomes the time-varying Hammerstein-based closed loop control system (Fig. 7.45a) with the nonlinearity $f(\cdot, t)$. In state space, such a SISO control loop is represented with the familiar equations (7.253) modified to

$$\begin{aligned} \mathbf{q}'(t) &= \mathbf{A}\mathbf{q} + \mathbf{B}y(t), \\ v(t) &= \mathbf{C}\mathbf{q}, \\ y(t) &= f[x(t) + v(t), t] \end{aligned} \quad (8.201)$$

that has a compact form of

$$\mathbf{q}'(t) = \mathbf{A}\mathbf{q} + \mathbf{B}f[\mathbf{C}\mathbf{q} + x(t), t].$$

To ascertain stability, the Popov's criterion can be applied if to take into consideration time variations if the nonlinearity. \square

Example 8.17 (Time-variant Lur'e control system). A linear BP tracking (thus time-varying) filter is designed with saturation in the feedback representing the time-varying Lur'e control system. The state space presentation of this system (Fig. 7.45b) is given by the modified equations (7.254),

$$\begin{aligned}\mathbf{q}'(t) &= \mathbf{A}(t)\mathbf{q}(t) + \mathbf{B}v(t), \\ y(t) &= \mathbf{C}\mathbf{q}(t), \\ v(t) &= x(t) + f(y),\end{aligned}\tag{8.202}$$

having a compact form of

$$\mathbf{q}'(t) = \mathbf{A}(t)\mathbf{q}(t) + \mathbf{B}\{x(t) + f[\mathbf{C}\mathbf{q}(t)]\}.$$

If the system matrix $\mathbf{A}(t)$ is Hurwitz, then stability of this system is ascertained by the Popov criterion. \square

These examples neatly show that, at least in several important practical cases, the general equations, (8.197) and (8.198), can be substituted with much more simple forms having solutions and analizable for stability. In some other cases, linearization of the state space NTV model often gives nice solutions for particular problems.

8.6.1 Linearization

Linearization of NTV systems in state space is provided similarly to NTI systems. First of all, one needs to examine the model in the vicinity of the point $(\mathbf{y}_0, \mathbf{x}_0)$, state \mathbf{q}_0 , and its time derivative \mathbf{q}'_0 , provided

$$\mathbf{q}(t) = \mathbf{q}_0(t) + \tilde{\mathbf{q}}(t),\tag{8.203}$$

$$\mathbf{x}(t) = \mathbf{x}_0(t) + \tilde{\mathbf{x}}(t),\tag{8.204}$$

$$\mathbf{y}(t) = \mathbf{y}_0(t) + \tilde{\mathbf{y}}(t),\tag{8.205}$$

where $\tilde{\mathbf{q}}(t)$, $\tilde{\mathbf{x}}(t)$, and $\tilde{\mathbf{y}}(t)$ are small time-varying increments. By (8.203)–(8.205), the state space model (8.197) and (8.198) can then be rewritten as

$$\mathbf{q}'_0(t) + \tilde{\mathbf{q}}'(t) = \Psi[\mathbf{q}_0(t) + \tilde{\mathbf{q}}(t), \mathbf{x}_0(t) + \tilde{\mathbf{x}}(t), t],\tag{8.206}$$

$$\mathbf{y}_0(t) + \tilde{\mathbf{y}}(t) = \Upsilon[\mathbf{q}_0(t) + \tilde{\mathbf{q}}(t), \mathbf{x}_0(t) + \tilde{\mathbf{x}}(t), t].\tag{8.207}$$

If to expand the right-hand sides of (8.206) and (8.207) to the Taylor series and save only the constant and linear terms, we can arrive at the linearized equations

$$\tilde{\mathbf{q}}'(t) = \mathbf{A}(t)\tilde{\mathbf{q}}(t) + \mathbf{B}(t)\tilde{\mathbf{x}}(t),\tag{8.208}$$

$$\tilde{\mathbf{y}}(t) = \mathbf{C}(t)\tilde{\mathbf{q}}(t) + \mathbf{D}(t)\tilde{\mathbf{x}}(t),\tag{8.209}$$

in which the time-varying Jacobian matrices are determined by

$$\mathbf{A}(t) = \left. \frac{\partial \Psi}{\partial \mathbf{q}} \right|_0, \quad \mathbf{B}(t) = \left. \frac{\partial \Psi}{\partial \mathbf{x}} \right|_0, \quad \mathbf{C}(t) = \left. \frac{\partial \Upsilon}{\partial \mathbf{q}} \right|_0, \quad \mathbf{D}(t) = \left. \frac{\partial \Upsilon}{\partial \mathbf{x}} \right|_0, \quad (8.210)$$

where “0” still means the point $(\mathbf{x}_0, \mathbf{y}_0)$ and \mathbf{q}_0 .

The linearized NTV system is thus the LTV system with all of the properties featured to the latter.

Example 8.18. An NTV system is described in state space by the equations

$$\begin{bmatrix} q_1' \\ q_2' \end{bmatrix} = \begin{bmatrix} -3q_1 - 2tq_2 + x_1 \\ -q_1q_2 - 4tq_2 + 2x_2 \end{bmatrix}, \quad (8.211)$$

$$y(t) = 2tq_1 + q_1q_2 + x_1 + 2x_2. \quad (8.212)$$

By (8.210), the system is linearized at t_0 to possess the forms (8.208) and (8.209) with the matrices

$$\mathbf{A}(t) = \begin{bmatrix} -3 & -4t \\ -q_2(t_0) & -q_1(t_0) - 4t \end{bmatrix}, \quad \mathbf{B} = \begin{bmatrix} 1 & 0 \\ 0 & 2 \end{bmatrix},$$

$$\mathbf{C}(t) = [2t + q_2(t_0) \quad q_1(t_0)], \quad \mathbf{D} = [1 \ 2].$$

Here only the system and observation matrices are time-varying. \square

The other particular models of NTV systems are associated with the time-varying Hammerstein and Wiener systems.

8.6.2 Time-varying Hammerstein System

Let us recall that the basic Hammerstein system (Fig. 7.37a) is represented with the memoryless (static) NTI subsystem following by the memory (dynamic) LTI subsystem. Implying time variations in the structure, we have three basic realizations of the time-varying Hammerstein system shown in Fig. 8.30. In the first case (Fig. 8.30a), the nonlinear memoryless part is

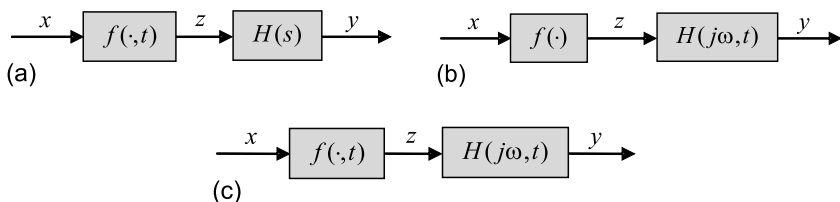


Fig. 8.30. Hammerstein system with time-varying (a) nonlinearity, (b) linear block, and (c) nonlinear and linear parts.

time-varying. The second case (Fig. 8.30b) presumes the linear block to be time-varying. When both blocks are time-variant, we have the time-varying Hammerstein system shown in Fig. 8.30c.

Time-varying Nonlinearity

Similarly to (7.247), the Hammerstein system shown in Fig. 8.30a is described with the equations

$$\begin{aligned} \mathbf{q}'(t) &= \mathbf{A}\mathbf{q}(t) + \mathbf{B}z(t), \\ y(t) &= \mathbf{C}\mathbf{q}(t), \\ z(t) &= f[x(t), t], \end{aligned} \quad (8.213)$$

where, it is supposed, the nonlinear function $f[(x), t]$ has no memory. Otherwise, the system is not Hammerstein.

For the system (8.213) to be stable, the function $z(t)$ must be bounded, $|z(t)| \leq M < \infty$, the input matrix \mathbf{B} and observation matrix \mathbf{C} must have finite components, and the system matrix \mathbf{A} must be Hurwitz.

The general solution $y(t)$ associated with (8.213) is written as

$$y(t) = \mathbf{C}\Phi(t, t_0)\mathbf{q}(t_0) + \mathbf{C} \int_{t_0}^t \Phi(t, \theta)\mathbf{B}f[x(\theta), t]d\theta, \quad (8.214)$$

where $\Phi(t, \tau) = e^{\mathbf{A}(t-\tau)}$ is the state transition matrix. As can be seen, the current time t in the integrand of (8.214) plays a role of a coefficient and is typically assumed to be “slow”.

Example 8.19. Consider an asynchronous demodulator (Fig. 7.38) in which an auxiliary bias voltage $V_b(t)$ applied to the rectifier diode is such that the electric current is time-varying,

$$i(t) = I_0 \left[e^{\frac{x(t)+V_b(t)}{V_T}} - 1 \right]$$

In terms of the variables $x(t) = v(t)$, $q(t) = y(t) = v_C(t)$, and $z(t) = i(t)$, the scheme is represented in state space with

$$\begin{aligned} q'(t) &= Aq(t) + Bz(t), \\ y(t) &= Cq(t), \\ z(t) &= I_0 \left[e^{\frac{x(t)+V_b(t)}{V_T}} - 1 \right], \end{aligned}$$

where $A = -\frac{1}{RC}$, $B = \frac{1}{C}$, and $C = 1$. By (8.214), the output thus becomes

$$y(t) = y_0 e^{-\frac{t}{RC}} + \frac{I_0}{C} e^{-\frac{t}{RC}} \int_0^t e^{\frac{\theta}{RC}} \left[e^{\frac{x(\theta) + V_b(t)}{V_T}} - 1 \right] d\theta, \quad (8.215)$$

where $y_0 = y(0)$. It can be shown that, if to vary $V_b(t)$ properly, the demodulated envelope can be obtained to trace as close to the modulating function as it is allowed by this simplest scheme. The latter can be achieved using an adaptive regulator. \square

Time-varying Linear Part

In the other version of the Hammerstein system (Fig. 8.30b), the linear part is supposed to be time-varying that leads to the equations

$$\begin{aligned} \mathbf{q}'(t) &= \mathbf{A}(t)\mathbf{q}(t) + \mathbf{B}(t)z(t), \\ y(t) &= \mathbf{C}(t)\mathbf{q}(t), \\ z(t) &= f[x(t)]. \end{aligned} \quad (8.216)$$

Employing the general solution (6.115) valid for LTV systems, we can write

$$y(t) = \mathbf{C}(t)\Phi(t, t_0)\mathbf{q}(t_0) + \mathbf{C}(t) \int_{t_0}^t \Phi(t, \theta)\mathbf{B}(\theta)f[x(\theta)]d\theta, \quad (8.217)$$

where $\Phi(t, \tau)$ is still the state transition matrix. This system is stable if $z(t)$ is bounded, $|z(t)| \leq M < \infty$, the matrices $\mathbf{B}(t)$ and $\mathbf{C}(t)$ have finite components, and $\mathbf{A}(t)$ is Hurwitz.

Example 8.20. Let us come back to the scheme (Fig. 7.38) and suppose that the output filter is adapted to the waveform of the modulating signal. The system matrix $\mathbf{A}(t)$ is thus time-varying and the equations (see Example 8.15) become

$$\begin{aligned} q'(t) &= A(t)q(t) + Bz(t), \\ y(t) &= |C|q(t), \\ z(t) &= I_0 \left[e^{\frac{x(t)}{V_T}} - 1 \right], \end{aligned}$$

where $A(t) = -\frac{1}{RC(t)}$, $B = \frac{1}{C}$, and $C = [1]$. Applying the solution (6.63) to the above-defined state equation, one can represent the output $y(t)$ in the form of (8.217). \square

8.6.3 Time-varying Wiener System

In line with the Hammerstein system, the Wiener system is also often described to have time-varying blocks. Because the blocks in the Wiener system are merely interchanged for the Hammerstein one, there are also three possible realizations as shown in Fig. 8.31. As well as in the Hammerstein system case, here either nonlinear or linear or even both linear and nonlinear blocks can be time-varying.

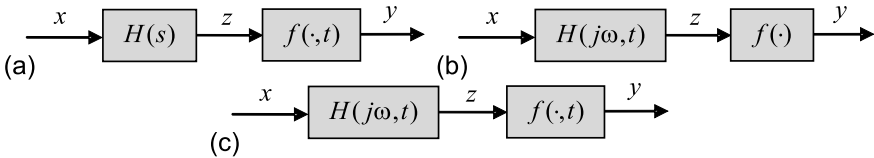


Fig. 8.31. Wiener system system with time-varying (a) nonlinearity, (b) linear block, and (c) nonlinear and linear parts.

Time-varying Nonlinearity

Having a slowly time-varying nonlinear block (Fig. 8.31a), the SISO Wiener system is described, similarly to (7.251), by the equations

$$\begin{aligned} \mathbf{q}'(t) &= \mathbf{A}\mathbf{q}(t) + \mathbf{B}x(t), \\ z(t) &= \mathbf{C}\mathbf{q}(t), \\ y(t) &= f[z(t), t], \end{aligned} \tag{8.218}$$

where the nonlinear function $f(\cdot, t)$ is memoryless. Otherwise, the system is not Wiener. Employing (7.251), the output of the time-varying Wiener system can be written as

$$y(t) = f \left[\mathbf{C}\Phi(t, t_0)\mathbf{q}(t_0) + \mathbf{C} \int_{t_0}^t \Phi(t, \theta)\mathbf{B}x(\theta)d\theta, t \right]. \tag{8.219}$$

The system (8.219) is stable, if the function $f(\cdot, t)$ is bounded for all $t \geq t_0$,

$$|y(t)| = |f(\cdot, t)| \leq M < \infty,$$

\mathbf{A} is Hurwitz, and \mathbf{B} and \mathbf{C} have finite components. As well as in the time-invariant Wiener system case, here the main problem is associated with the identification of nonlinearity and coefficients of the linear block.

Time-varying Linear Part

If a linear part is time-varying (Fig. 8.31b), the equations of a SISO Wiener system become

$$\begin{aligned}\mathbf{q}'(t) &= \mathbf{A}(t)\mathbf{q}(t) + \mathbf{B}(t)x(t), \\ z(t) &= \mathbf{C}(t)\mathbf{q}(t), \\ y(t) &= f[z(t)],\end{aligned}\tag{8.220}$$

where the matrices $\mathbf{A}(t)$, $\mathbf{B}(t)$, and $\mathbf{C}(t)$ are time-varying. By (6.111), the system output can then be specified with

$$y(t) = f \left[\mathbf{C}(t)\Phi(t, t_0)\mathbf{q}(t_0) + \mathbf{C}(t) \int_{t_0}^t \Phi(t, \theta)\mathbf{B}(\theta)x(\theta)d\theta \right]\tag{8.221}$$

It can be shown that this system is stable when the function $f(\cdot)$ is bounded for all $t \geq t_0$,

$$|y(t)| = |f(\cdot)| \leq M < \infty,$$

the matrix \mathbf{A} is Hurwitz, and \mathbf{B} and \mathbf{C} have finite components.

Example 8.21. Consider Example 7.31, in which the selective circuit is designed to be adapted to the input signal. The frequency response of this circuit is thus time varying and the system can be represented with the equations

$$\begin{aligned}\mathbf{q}'(t) &= \mathbf{A}(t)\mathbf{q}(t) + \begin{bmatrix} 1 & 0 \end{bmatrix} \begin{bmatrix} x_1 \\ x_2 \end{bmatrix}, \\ \mathbf{z}(t) &= \begin{bmatrix} z_1 \\ z_2 \end{bmatrix} = \mathbf{C}(t)\mathbf{q}(t), \\ y(t) &= \frac{1}{2}\mathbf{z}^T(t)\mathbf{S}\mathbf{z}(t),\end{aligned}$$

where the matrices $\mathbf{A}(t)$ and $\mathbf{C}(t)$ are time-varying and $\mathbf{S} = \begin{bmatrix} 0 & 1 \\ 1 & 0 \end{bmatrix}$. By (8.221), the system output becomes

$$y(t) = \left[\mathbf{C}(t) \int_{t_0}^t \Phi(t, \theta)\mathbf{B}(\theta)x(\theta)d\theta \right]^T \mathbf{S} \left[\mathbf{C}(t) \int_{t_0}^t \Phi(t, \theta)\mathbf{B}(\theta)x(\theta)d\theta \right],$$

representing an NTV system. □

We notice that an extension of the Hammerstein and Wiener systems to the time-varying case can also be provided with their cascades, parallel connections, and feedbacks as discussed in Chapter 7. Such complicated NTV structures often serve to fit a great deal of practical needs related to both the deterministic and stochastic NTV problems. In line with the Hammerstein and Wiener systems, albeit not commonly, some other particular models of NTV systems are used depending on practical needs. Descriptions of these models can be found in special books.

In this Chapter, we examined NTV systems and most general methods of their analysis. The reader must remember that, unlike linear systems, the nonlinear structures can generally be supposed to have arbitrary nonlinearities. Therefore, the general theory of NTV systems in state space has substantial limitations. In view of that, they usually exploit several well studied models, such as Hammerstein and Wiener, to fit real nonlinear physical systems and describe them with a reasonable accuracy and without redundancy. In many cases, NTV systems with weak nonlinearity are well modeled with the Volterra method. In a few cases, the nonlinear ODE with time-varying coefficients can be solved exactly. For NPTV closed loop oscillatory systems, the Bogoliubov-Mitropolskiy and modulation functions methods can be used. Finally, the Hammerstein and Wiener models and their interconnections allow representing NTV structures in state space with high efficiency.

8.7 Summary

The time-varying models of nonlinear systems are applied, whenever nonlinear modulators, demodulators, voltage controlled oscillators, tracking filters, etc. are analyzed. The most general foundations of the NTV systems theory are the following:

- A system that provides nonlinear transformations with a time-varying operator is the NTV system also called nonlinear nonautonomous system.
- Memoryless NTV systems are typically interpolated with the time-varying Lagrange, Newton, or spline techniques.
- An NTV system can be expanded to the time-varying Taylor series at an arbitrary point.
- The Volterra series with time-varying kernels is fully applicable for NTV systems.
- Solutions of nonlinear ODEs representing NTV systems can be found only in a few particular cases.
- Most generally, a closed loop NPTV system can be analyzed with the Bogoliubov-Mitropolskiy and modulation functions method.

- Linearization of NTV systems is provided in a manner similar to NTI systems.
- In state space, NTV systems are typically described with the time-varying Hammerstein and Wiener models as well as with their series, parallel, and feedback interconnections.

8.8 Problems

8.1. Explain the differences between NTI and NTV systems. How can an NTV system appear from the NTI system? What are the necessary and sufficient conditions to transform an NTV system to an NTI system?

8.2. Observe the electronic systems given in Chapter 1 and find examples of NTV systems and subsystems.

8.3. Given the following electronic nonlinear systems:

- A crystal oscillator, in which the flicker noise in units
 - plays a critical role to shape the phase power spectral density,
 - can be ignored.
- A BP active filter
 - with saturation,
 - included in a square amplifier and having a modulated capacitance,
 - included in a phase tracking system.
- A wireless nonlinear communications channel operating
 - in a homogenous media,
 - under the environment conditions.
- The phase radar intended to measure
 - a constant distance,
 - a variable distance,
 - a distance with tracking the carrier.

Ascertain, which system is NTV and which is NTI? What are the conditions for these systems to be time-variant and time-invariant?

8.4 (Taylor series expansion). A memoryless SISO NTV system is given with the following equation:

1. $y(x, t) = t(3x^2 + \frac{t}{2}x)$
2. $y(x, t) = \arctan(t + x)$
3. $y(x, t) = a(e^{x+bt} - 1)$
4. $y(x, t) = a(e^{x+at} - 1)$
5. $y(x, t) = -a \ln \frac{x+a \cos t}{b}$
6. $y(x, t) = -b \exp \frac{x+a \sin t}{a}$

Using (8.3)–(8.5), linearize the system at some point x_0 , at some time instant t_0 , and at (x_0, t_0) .

8.5 (Volterra series expansion). Find simple words to explain the links between LTI, LTV, NTI, and NTV systems in terms of the Volterra theory. Give simple examples (block-diagrams) demonstrating how an NTI system becomes NTV.

8.6. An NTV system is represented with the block-diagram shown in Fig. 8.32, write the system equation in the Volterra series form.

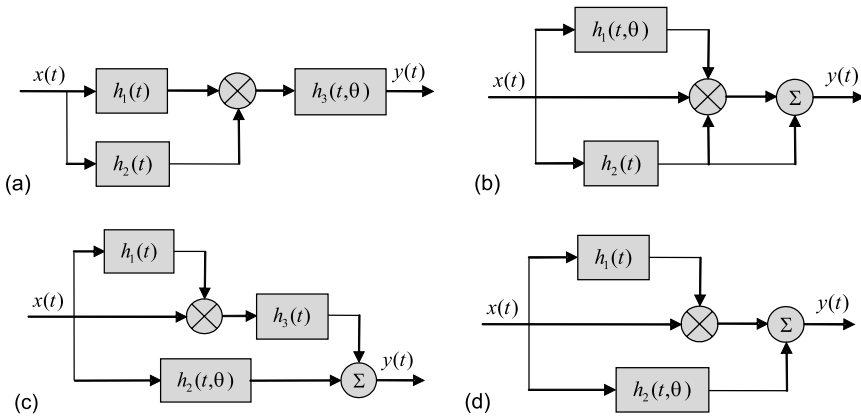


Fig. 8.32. Nonlinear time-varying systems.

8.7. Find the output of an NTV system shown in Fig. 8.32 for the following impulse responses, respectively,

1. $h_1(t) = e^{-|t|}$, $h_2(t) = e^{-2t}u(t)$, $h_3(t, \theta) = e^{-(t^2 - \theta^2)}u(t - \theta)$
2. $h_1(t, \theta) = \frac{\theta+1}{t+1}e^{-(t-\theta)}u(t - \theta)$, $h_2(t) = e^{-t}u(t)$
3. $h_1(t) = e^{-2t}u(t)$, $h_2(t, \theta) = \delta(t - \theta)e^{j\omega_0 t}$, $h_3(t) = e^{-2t} \cos \omega_0 t u(t)$
4. $h_1(t) = e^{-2t} \cos \omega_0 t u(t)$, $h_2(t, \theta) = \delta(t - \theta - \theta_0)$

8.8. Exploiting the output signal found in Problem 8.7 and using (8.25), ascertain stability of an NTV system shown in Fig. 8.32.

8.9. Using the general transformation rule (8.27) and the Volterra kernel derived in Problem 8.6, define the multifrequency time-varying system function for the structure given in Fig. 8.32.

8.10. Define the multiple spectral function (8.37) and total multifrequency system function (8.39) associated with the multifrequency time-varying system function derived in Problem 8.9.

8.11 (Differential equation presentation). A SISO NTV system is represented with the following ODE,

1. $q' + q = x \cos t, \quad y = q + q^2$
2. $2q' - q = xe^{-t}, \quad y = 1 + q^2$
3. $q' + 3q = tx, \quad y = q^2$
4. $4q' - 3q = e^{-t}x \cos t, \quad y = q + q^2 + q^3$

Analyze the system equations and show the block diagram. Write the general solution of the system ODE.

8.12. Define the multifrequency system function described by the ODE (Problem 8.11). First, by applying the transform (8.27) to the Volterra kernels. Second, by letting $x(t) = e^{j\omega t}$ in the ODE. Verify correctness of the general relation (8.36).

8.13. Given an oscillator with a time-varying unit (inductor or capacitor) shown in Fig. 8.33, write the ODE of an oscillator for any energy bearer (voltage or current) supposing arbitrary function of $\Delta L(t)$ and $\Delta C(t)$.

8.14. By the Krylov-Bogoliubov asymptotic method, transform the ODE of an oscillator derived in Problem 8.13 to the ODE for the slowly changing amplitudes and phase, similarly to (8.61) and (8.62).

8.15. Employing the solution of the Bernoulli equation, find the function of the oscillator signal amplitude (problem 8.14) for the modulated $\Delta L(t) =$

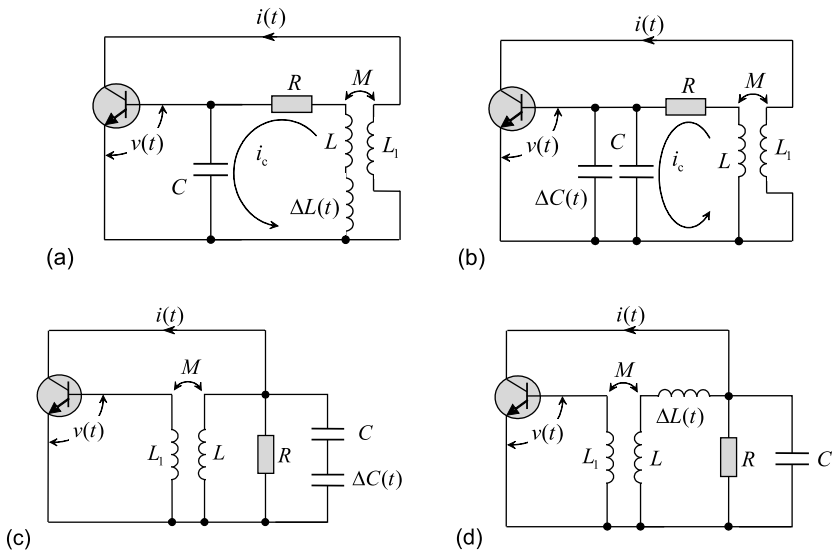


Fig. 8.33. Oscillator with a time-varying component.

$a \cos \Omega t$ and $\Delta C(t) = b \cos \Omega t$. Illustrate this function by some particular values of a , b , and Ω within the resonant circuit bandwidth.

8.16 (Periodically time-varying nonlinear systems). Consider an oscillator given in Fig. 8.33, whose frequency is modulated by the time-varying $\Delta C(t)$ or $\Delta L(t)$. Explain, why spurious AM accompanies FM in nonlinear oscillators. Is it possible to design an FM oscillator with a zero spurious AM index?

8.17. Give simple explanations for the frequency modulation and amplitude modulation functions (FMF and AMF, respectively) of an FM oscillator. What are the conditions for applications of the modulation functions method to NPTV oscillators?

8.18. Consider the ODE of an FM oscillator (Problem 8.13) and suppose that $\Delta L(t) = a \cos \Omega t \ll L$ and $\Delta C(t) = b \cos \Omega t \ll C$. Using the modulation functions method, derive the FMF and AMF of an oscillator.

8.19 (State space presentation). Analyze the state space forms (8.197) and (8.198) of a MIMO NTV system. Why the state equation cannot be solved in closed form? Why a general solution of these equations is commonly redundant for applications?

8.20. Using the ODE of a system (Problem 8.13), represent the system in state space. Ascertain stability of an oscillator via the system matrix.

8.21. Linearize the state space equations of an oscillator (Problem 8.20) at zero and ascertain stability at this point.

8.22. An NTV system is represented in state space with the following equations:

1.
$$\begin{bmatrix} q_1' \\ q_2' \end{bmatrix} = \begin{bmatrix} q_1 - 2q_2^2 + 2x_1 \\ -(q_1 + 4tq_2) + x_2 \end{bmatrix}, \quad y(t) = q_1 + q_1q_2 + x_1 + x_2$$
2.
$$\begin{bmatrix} q_1' \\ q_2' \\ q_3' \end{bmatrix} = \begin{bmatrix} tq_1 - 2q_2q_3 + x_1 \\ -q_1 + x_2 \\ q_3^2 \end{bmatrix}, \quad y(t) = q_1 + x_2$$
3.
$$\begin{bmatrix} q_1' \\ q_2' \end{bmatrix} = \begin{bmatrix} t - 2q_2 \\ -1 - 4tq_1 \end{bmatrix} \begin{bmatrix} q_1 \\ q_2 \end{bmatrix} + \begin{bmatrix} x_1 \\ x_2 \end{bmatrix}, \quad y(t) = q_1 + x_1 + x_2$$
4.
$$\begin{bmatrix} q_1' \\ q_2' \end{bmatrix} = \begin{bmatrix} (q_1 + q_2)(2q_1 - q_2) + x_1 \\ -q_1^2 - 4tq_2^2 + x_2 \end{bmatrix}, \quad y(t) = q_1 - q_2 + x_1 + x_2$$

Linearize the system and ascertain stability at zero.

8.23 (Hammerstein and Wiener systems). A nonlinear time-varying amplifier follows by the LTI resonant circuit of the second order. Represent this system by the Hammerstein model and write equations in state space.

8.24. Solve Problem 8.23 for the LTI resonant circuit of the third order having a time-varying resonance frequency that follows by the nonlinear memoryless amplifier. Use the Wiener model.

8.25. An NTV memoryless system is described in Problem 8.4. The other system of the second order is linear and can be either LTV or LTI. Represent the following cascade of the given systems with the Hammerstein or Wiener models and write the equations in state space.

1. NTV-to-LTI
2. LTI-to-NTV
3. LTV-to-NTV
4. NTV-to-LTV

8.26. Represent the Butler type oscillator shown in Fig. 8.24b with the closed loop Hammerstein system shown in Fig. 8.30b and write the relevant equations in state space.

8.27. Consider the Wiener system given by (8.219). Define the response of this system to the unite impulse for the quadratic nonlinearity.

A

Dirac Delta Function

The *Dirac delta function* $\delta(x)$ (Fig. A.1) is also often referred to as the *unit impulse*, *impulse symbol*, *Dirac impulse*, or *delta function*. It is the function

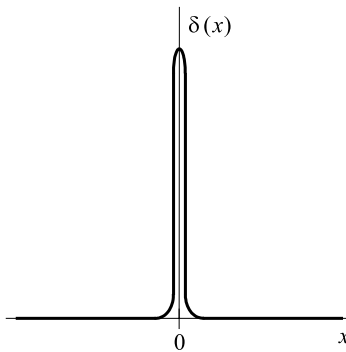


Fig. A.1. Dirac delta function.

that tends toward infinity at zero, is zero otherwise, and has a unit area. These fundamental properties are supported by the following relations

$$\delta(x) = \begin{cases} \infty, & x = 0 \\ 0, & x \neq 0 \end{cases}, \quad (\text{A.1})$$

$$\int_{-\infty}^{\infty} \delta(x) dx = 1. \quad (\text{A.2})$$

In the system theory, the delta-function is used both in the time domain ($x = t$ [sec]) and frequency domain ($x = f$ [Hz] or $x = \omega = 2\pi f$ [rad/sec]).

In the frequency domain, the delta-shaped spectral density appears as a product of the integration

Table A.1. Alternative definitions of the Dirac delta function

Delta function	Definition
$\delta(x - x_0)$	$= \frac{1}{\pi} \lim_{\alpha \rightarrow \infty} \frac{\sin \alpha(x-x_0)}{x-x_0}$ $= \lim_{\alpha \rightarrow 0} \frac{1}{\alpha \sqrt{2\pi}} e^{-\frac{(x-x_0)^2}{2\alpha^2}}$ $= \frac{1}{\pi} \lim_{\alpha \rightarrow \infty} \frac{1-\cos \alpha(x-x_0)}{\alpha(x-x_0)^2}$ $= \frac{1}{\pi} \lim_{\alpha \rightarrow \infty} \frac{\sin^2 \alpha(x-x_0)}{\alpha(x-x_0)^2}$ $= \frac{1}{\pi} \lim_{\alpha \rightarrow \infty} \frac{\alpha}{\alpha^2(x-x_0)^2+1}$ $= \frac{1}{\pi^2(x-x_0)} \lim_{\alpha \rightarrow 0} \int_{(x-x_0)-\alpha}^{(x-x_0)+\alpha} \frac{dy}{y}$ $= \frac{1}{2} \frac{\partial^2}{\partial t^2} x - x_0 $
	Via the inverse Fourier transform:
$\delta(x - x_0)$	$= \frac{1}{2\pi} \int_{-\infty}^{\infty} e^{j\omega(x-x_0)} d\omega$ $= \frac{1}{\pi} \int_0^{\infty} \cos \omega(x - x_0) d\omega$
$\frac{1}{2}[\delta(x + x_0) + \delta(x - x_0)]$	$= \frac{1}{2\pi} \int_{-\infty}^{\infty} \cos \omega x_0 e^{j\omega x} d\omega$ $= \frac{1}{\pi} \int_0^{\infty} \cos \omega x_0 \cos \omega x d\omega$

$$\begin{aligned}
 \delta(f - f_0) &= \int_{-\infty}^{\infty} e^{\pm 2\pi j(f-f_0)t} dt = \int_{-\infty}^{\infty} e^{\pm j(\omega-\omega_0)t} dt \\
 &= 2\pi \int_{-\infty}^{\infty} e^{\pm 2\pi j(\omega-\omega_0)z} dz = 2\pi\delta(\omega - \omega_0), \tag{A.3}
 \end{aligned}$$

where an auxiliary variable is $z = t/2\pi$, f_0 is a regular shift-frequency in Hz, and ω_0 is an angular shift-frequency in rad/sec, $\omega_0 = 2\pi f_0$. Two delta functions expressed in terms of regular and angular frequencies are coupled by the relation

$$\delta(f - f_0) = 2\pi\delta(\omega - \omega_0). \tag{A.4}$$

In line with alternative definitions given in Table A.1 and major properties listed in Table A.2, several other general and particular ones are useful.

If the functions $\phi(x)$ and $\psi(x)$ are continuous at x_0 and $a < x_0 < b$, then

Table A.2. Major properties of the Dirac delta function

Property	LTI system
Variable shifting	$\delta(x - x_0) = \begin{cases} \infty, & x = x_0 \\ 0, & x \neq x_0 \end{cases}$
Integration	$\int_{x_0-\varepsilon}^{x_0+\varepsilon} \delta(x - x_0) dx = 1$
Symmetry (often required, but not obligatory)	$\delta(x - x_0) = \delta(x_0 - x)$ $\int_{x_0}^{x_0+\varepsilon} \delta(x - x_0) dx = \int_{x_0-\varepsilon}^{x_0} \delta(x - x_0) dx = 0.5$
Relationships with the unit-step functions	$\delta(x) = \frac{du(x)}{dx}$ $u(x) = \int_{-\infty}^x \delta(z) dz$ $\delta(x) = \lim_{\xi \rightarrow 0} \frac{dv(x, \xi)}{dx} = \frac{dH(x)}{dx}$
Sifting property (filtering property or sampling property)	$\phi(x_0) = \int_{-\infty}^{\infty} \phi(x)\delta(x - x_0)dx$ $\phi(0) = \int_{-\infty}^{\infty} \phi(x)\delta(x)dx$ $\phi(x)\delta(x) = \phi(0)\delta(x)$ $\phi(x)\delta(x - x_0) = \phi(x_0)\delta(x - x_0)$ $\int_a^b \phi(x)\delta(x)dx = \begin{cases} \phi(0), & a < 0 < b \\ 0, & a < b < 0 \text{ or } 0 < a < b \\ \phi(0)\delta(0), & a = 0 \text{ or } b = 0 \end{cases}$
Scaling	$\delta(ax) = \frac{1}{ a }\delta(x)$ $\delta(\frac{x-x_0}{a}) = a \delta(x - x_0)$
Derivative	$\int_{-\infty}^{\infty} \phi(x) \frac{d\delta(x)}{dx} dx = -\frac{d\phi(x)}{dx} \Big _{x=0}$ $\int_{x_0-\varepsilon}^{x_0+\varepsilon} \phi(x) \frac{d^n \delta(x-x_0)}{dx^n} dx = (-1)^n \frac{d^n \phi(x)}{dx^n} \Big _{x=x_0}$
Fourier transform	$\int_{-\infty}^{\infty} \delta(x - x_0)e^{-j\omega x} dx = e^{-j\omega x_0}$ $\int_{-\infty}^{\infty} \delta(x)e^{-j\omega x} dx = 1$ $\frac{1}{2} \int_{-\infty}^{\infty} [\delta(x + x_0) + \delta(x - x_0)]e^{-j\omega x} dx$ $= \frac{1}{2}[e^{j\omega x_0} + e^{-j\omega x_0}] = \cos \omega x_0$

Here, x_0 is any real value, $\varepsilon > 0$ is real, $u(x) = \begin{cases} 1, & x > 0 \\ 0, & x < 0 \end{cases}$ is the unit step function,

$v(x, \xi) = \begin{cases} 1, & x > \xi \\ 0.5(x/\xi + 1), & -\xi \leq x \leq \xi \\ 0, & x < -\xi \end{cases}$, and $H(x) = \begin{cases} 1, & x > 0 \\ 0.5, & x = 0 \\ 0, & x < 0 \end{cases}$ is the Heaviside unit-step function,

$$\int_a^b \phi(x)\psi(x)\delta(x-x_0) dx = \int_a^b \phi(x)\psi(x_0)\delta(x-x_0) dx = \phi(x_0)\psi(x_0) \quad (\text{A.5})$$

and, in particular, by $a < u$ and $v < b$, we have

$$\int_a^b \delta(x-u)\delta(x-v) dx = \delta(u-v) = \delta(v-u). \quad (\text{A.6})$$

If $\alpha(x)$ is continuous and monotonous with a positive derivative at $a \leq x \leq b$ and crosses the axis x at x_0 , namely $\alpha(a) < \alpha(x_0) = 0 < \alpha(b)$, then

$$\int_a^b \phi(x)\delta[\alpha(x)] dx = \int_{\alpha(a)}^{\alpha(b)} \frac{\phi[x(t)]}{\alpha'[x(t)]} \delta(t) dt = \frac{\phi[x(0)]}{\alpha'[x(0)]} = \frac{\phi(x_0)}{\alpha'(x_0)}. \quad (\text{A.7})$$

If $\alpha(x)$ has a negative derivative at $a \leq x \leq b$, the (A.7) holds true with its sign changed. If $\alpha(x)$ does not cross the axis x at $a \leq x \leq b$, then (A.7) produces zero. Therefore, the following relation is valid

$$\delta[\alpha(x)] = \frac{\delta(x-x_0)}{|\alpha'(x_0)|}. \quad (\text{A.8})$$

The following fundamental relations are valid for the two-dimensional delta function $\delta(x, y)$ and two dimensional continuous function $\phi(x, y)$:

$$\int_{-\infty}^{\infty} \int_{-\infty}^{\infty} \delta(x-x_0, y-y_0) dx dy = 1, \quad (\text{A.9})$$

$$\int_{-\infty}^{\infty} \phi(x, y)\delta(x-x_0, y-y_0) dy = \phi(x, y_0)\delta(x-x_0), \quad (\text{A.10})$$

$$\int_{-\infty}^{\infty} \int_{-\infty}^{\infty} \phi(x, y)\delta(x-x_0, y-y_0) dx dy = \phi(x_0, y_0). \quad (\text{A.11})$$

B

Matrices

A rectangular table (array) of $m \times n$ elements having m rows and n columns is called the rectangular matrix of dimensions $m \times n$. It is denoted as

$$\mathbf{A} = \begin{bmatrix} a_{11} & a_{12} & \dots & a_{1n} \\ a_{21} & a_{22} & \dots & a_{2n} \\ \vdots & \vdots & \ddots & \vdots \\ a_{m1} & a_{m2} & \dots & a_{mn} \end{bmatrix} = [a_{ij}], \quad (\text{B.1})$$

where the numbers a_{ij} are called the *matrix elements*, in which the first index i indicates the number of rows and the second one j the number of columns. The matrix \mathbf{A} is said to be a *square matrix of order n* , if $m = n$.

Basic definitions and operations. Two matrices $\mathbf{A} = [a_{ij}]$ and $\mathbf{B} = [b_{ij}]$ are equal if and only if they have the same order and all relevant elements are equal, namely $a_{ij} = b_{ij}$, $i = 1, 2, \dots, m$, and $j = 1, 2, \dots, n$.

A matrix of dimensions $1 \times n$ is called an n -dimensional *row vector*

$$\mathbf{x} = [x_{11} \ x_{12} \ \dots \ x_{1n}] \equiv [x_1 \ x_2 \ \dots \ x_n] \quad (\text{B.2})$$

and an $n \times 1$ matrix is called an m -dimensional *column vector*

$$\mathbf{y} = \begin{bmatrix} y_{11} \\ y_{21} \\ \vdots \\ y_{m1} \end{bmatrix} \equiv \begin{bmatrix} y_1 \\ y_2 \\ \vdots \\ y_m \end{bmatrix}. \quad (\text{B.3})$$

The vectors are often denoted with small letters, e.g. \mathbf{x} , and matrices with capital letters, e.g. \mathbf{A} .

If a matrix or vector has only one element, then it is *scalar*.

A zero matrix $\mathbf{0}$ is a matrix having all its elements zero.

A square matrix \mathbf{D} having all its elements zero apart the main diagonal is said to be the *diagonal matrix*:

$$\mathbf{D} = \begin{bmatrix} d_{11} & 0 & \dots & 0 \\ 0 & d_{22} & \dots & 0 \\ \vdots & \vdots & \ddots & \vdots \\ 0 & 0 & \dots & d_{nn} \end{bmatrix} \equiv \begin{bmatrix} d_1 & 0 & \dots & 0 \\ 0 & d_2 & \dots & 0 \\ \vdots & \vdots & \ddots & \vdots \\ 0 & 0 & \dots & d_n \end{bmatrix}. \quad (\text{B.4})$$

The other often used expression for the $n \times n$ diagonal matrix is

$$\mathbf{D} = \text{diag} (d_1 \ d_2 \ \dots \ d_n). \quad (\text{B.5})$$

The $n \times n$ diagonal matrix \mathbf{D} is said to be the *identity matrix* (or *unit matrix*) \mathbf{I} if all its components equal to 1,

$$\mathbf{I} = \begin{bmatrix} 1 & 0 & \dots & 0 \\ 0 & 1 & \dots & 0 \\ \vdots & \vdots & \ddots & \vdots \\ 0 & 0 & \dots & 1 \end{bmatrix}. \quad (\text{B.6})$$

Basic operations with matrices are given in Table B.1.

Table B.1. Basic operations with matrices

Given $m \times n$ matrices $\mathbf{A} = [a_{ij}]$, $\mathbf{B} = [b_{ij}]$, and $\mathbf{C} = [c_{ij}]$

Property	Operation
Addition (subtraction)	$\mathbf{A} \pm \mathbf{B} = \mathbf{C} = [c_{ij}] = [a_{ij} \pm b_{ij}]$ $\mathbf{A} - \mathbf{A} = \mathbf{A} + (-\mathbf{A}) = \mathbf{0}$
Commutativity	$\mathbf{A} + \mathbf{B} = \mathbf{B} + \mathbf{A}$ $\mathbf{A} + \mathbf{0} = \mathbf{0} + \mathbf{A} = \mathbf{A}$
Associativity	$(\mathbf{A} + \mathbf{B}) + \mathbf{C} = \mathbf{A} + (\mathbf{B} + \mathbf{C})$
Equating	$\mathbf{A} = \mathbf{B} = [a_{ij}] = [b_{ij}]$
Multiplication by scalars	$\mathbf{B} = \alpha \mathbf{A} = [b_{ij}] = [\alpha a_{ij}]$ $\alpha(\mathbf{A} + \mathbf{B}) = \alpha \mathbf{A} + \alpha \mathbf{B}$ $(\alpha + \beta)\mathbf{A} = \alpha \mathbf{A} + \beta \mathbf{A}$ $\alpha(\beta \mathbf{A}) = (\alpha\beta)\mathbf{A} = \beta(\alpha \mathbf{A})$
Sign changing with $\alpha = -1$	$\mathbf{B} = \alpha \mathbf{A} = [b_{ij}] = -[a_{ij}] = -\mathbf{A}$

The matrix product \mathbf{AB} is defined only when the number of columns of \mathbf{A} is equal to the number of rows of \mathbf{B} . In this case, the matrices \mathbf{A} and \mathbf{B} are said to be *conformable*. Accordingly, the product of an $m \times n$ matrix \mathbf{A} and an $n \times 1$ vector \mathbf{x} produces an $m \times 1$ vector \mathbf{y} , namely $\mathbf{Ax} = \mathbf{y}$.

The product \mathbf{AB} is always definable if \mathbf{A} and \mathbf{B} are square of the same order. Even so, the product commonly does not commute, i.e. $\mathbf{AB} \neq \mathbf{BA}$.

If $\mathbf{AB} = \mathbf{BA}$, then \mathbf{A} and \mathbf{B} are said to be commuting each other. Basic operations of multiplication are postponed to Table B.2.

Table B.2. Basic operations of multiplication

Property	Operation
Product	$\mathbf{C} = \mathbf{AB} = [c_{ij}], c_{ij} = \sum_{k=1}^n a_{ik}b_{kj}$
Commutativity	$\mathbf{AB} \neq \mathbf{BA}$ (non-commuting matrices) $\mathbf{AB} = \mathbf{BA}$ (commuting matrices) $\alpha\mathbf{A} = \mathbf{A}\alpha$ $\mathbf{A}\mathbf{0} = \mathbf{0A} = \mathbf{0}$ $\mathbf{AI} = \mathbf{IA} = \mathbf{A}$
Distributivity	$(\mathbf{A} + \mathbf{B})\mathbf{C} = \mathbf{AC} + \mathbf{BC}$
Associativity	$(\mathbf{AB})\mathbf{C} = \mathbf{A}(\mathbf{BC}) = \mathbf{ABC}$ $\alpha(\mathbf{AB}) = (\alpha\mathbf{A})\mathbf{B} = \mathbf{A}(\alpha\mathbf{B})$
Idempotent matrix	$\mathbf{AA} = \mathbf{A}^2 = \mathbf{A}$

Transpose and inverse. Suppose \mathbf{A} is an $m \times n$ matrix. The *transpose* of \mathbf{A} is denoted by \mathbf{A}^T and is an $n \times m$ matrix formed by interchanging the rows and columns of \mathbf{A} , i.e. $\mathbf{B} = \mathbf{A}^T = [b_{ij}] = [a_{ji}]$. Therefore

$$\mathbf{A}^T = \begin{bmatrix} a_{11} & a_{21} & \dots & a_{m1} \\ a_{12} & a_{22} & \dots & a_{m2} \\ \vdots & \vdots & \ddots & \vdots \\ a_{1n} & a_{2n} & \dots & a_{mn} \end{bmatrix} = [a_{ji}]. \tag{B.7}$$

The $m \times 1$ vector \mathbf{x} and its $1 \times m$ transpose \mathbf{x}^T may thus be performed as, respectively,

$$\mathbf{x} = \begin{bmatrix} x_1 \\ x_2 \\ \vdots \\ x_m \end{bmatrix} = [x_1 \ x_2 \ \dots \ x_m]^T, \tag{B.8}$$

$$\mathbf{x}^T = [x_1 \ x_2 \ \dots \ x_m]. \tag{B.9}$$

It follows that the product of an $n \times 1$ vector \mathbf{x} and a transpose of an $m \times 1$ vector \mathbf{y} produces an $n \times m$ matrix,

$$\mathbf{xy}^T = \begin{bmatrix} x_1 \\ x_2 \\ \vdots \\ x_n \end{bmatrix} [y_1 \ y_2 \ \cdots \ y_m] = \begin{bmatrix} x_1y_1 & x_1y_2 & \cdots & x_1y_m \\ x_2y_1 & x_2y_2 & \cdots & x_2y_m \\ \vdots & \vdots & \ddots & \vdots \\ x_ny_1 & x_ny_2 & \cdots & x_ny_m \end{bmatrix}.$$

If $\mathbf{A}^T = \mathbf{A}$, then \mathbf{A} is said to be *symmetric*. If $\mathbf{A}^T = -\mathbf{A}$, then \mathbf{A} is said to be *skew-symmetric*. If a matrix is skew-symmetric, then its diagonal elements are all zero.

If $\mathbf{A} = [a_{ij}]$ is a square matrix of order $n > 1$, then there exists an associated number called the *determinant* and denoted by $\det \mathbf{A}$ or $|\mathbf{A}|$,

$$\det \mathbf{A} = |\mathbf{A}| = \sum_{k=1}^n (-1)^{k+1} a_{1k} |\mathbf{M}_{1k}|, \quad (\text{B.10})$$

where $|\mathbf{M}_{1k}|$ is the determinant of a square matrix of order $n - 1$ obtained from \mathbf{A} by deleting the 1th row and k th column.

Most generally, the determinant is defined using the Laplace expansion. Let \mathbf{M}_{ij} be the square matrix of order $n - 1$ obtained from \mathbf{A} by deleting the i th row and j th column. The relevant number A_{ij} called the *cofactor* of a_{ij} is defined by

$$A_{ij} = (-1)^{i+j} |\mathbf{M}_{ij}|, \quad (\text{B.11})$$

where $i, j = 1, 2, \dots, n$. The $\det \mathbf{A}$ is then defined by one of the following expressions,

$$|\mathbf{A}| = \sum_{k=1}^n (-1)^{i+k} a_{ik} |\mathbf{M}_{ik}| = \sum_{k=1}^n a_{ik} A_{ik}, \quad (\text{B.12})$$

$$|\mathbf{A}| = \sum_{k=1}^n (-1)^{k+j} a_{kj} |\mathbf{M}_{kj}| = \sum_{k=1}^n a_{kj} A_{kj}. \quad (\text{B.13})$$

Relations (B.12) and (B.13) are known as the *Laplace expansions* of \mathbf{A} along the i th row and along the j th column, respectively. It follows from (B.12) and (B.13) that

$$|\mathbf{A}| = |\mathbf{A}^T|.$$

A square matrix \mathbf{A} is *singular* if $|\mathbf{A}| = 0$. Otherwise, it is *nonsingular*.

For any two square matrices \mathbf{A} and \mathbf{B} of order n the following identity holds true

$$|\mathbf{AB}| = |\mathbf{A}||\mathbf{B}|. \quad (\text{B.14})$$

A matrix \mathbf{A} is said to be *invertible* if there exists a matrix \mathbf{B} such that the product \mathbf{AB} commutes and $\mathbf{BA} = \mathbf{AB} = \mathbf{I}$. The matrix \mathbf{B} is called the *inverse matrix* of \mathbf{A} and is denoted by \mathbf{A}^{-1} . Thus

$$\mathbf{A}^{-1}\mathbf{A} = \mathbf{AA}^{-1} = \mathbf{I}. \quad (\text{B.15})$$

For every nonsingular matrix \mathbf{A} there exists an inverse matrix $\mathbf{A}^{-1} = |a_{ij}^{-1}|$ such that its elements are determined by

$$a_{ij}^{-1} = \frac{A_{ji}}{|\mathbf{A}|}, \tag{B.16}$$

where the cofactor A_{ij} is given by (B.11).

The inverse matrix of an $n \times n$ matrix \mathbf{A} can be computed as

$$\mathbf{A}^{-1} = \frac{1}{|\mathbf{A}|} \text{adj } \mathbf{A}, \tag{B.17}$$

where the *adjugate* or *adjoint* of \mathbf{A} is

$$\text{adj } \mathbf{A} = [A_{ij}]^T = \begin{bmatrix} A_{11} & A_{21} & \dots & A_{n1} \\ A_{12} & A_{22} & \dots & A_{n2} \\ \vdots & \vdots & \ddots & \vdots \\ A_{1n} & A_{2n} & \dots & A_{nn} \end{bmatrix}. \tag{B.18}$$

In particular, if $A = \begin{vmatrix} a & b \\ c & d \end{vmatrix}$ and $|A| = 1$, then $A^{-1} = \begin{vmatrix} d & -b \\ -c & a \end{vmatrix}$.

If \mathbf{A} is invertible, then $\mathbf{A}\mathbf{B} = \mathbf{0}$ means that $\mathbf{B} = \mathbf{0}$.

Basic operations with transposable and inversible matrices are given in Table B.3.

Table B.3. Basic operations with transposable and inversible matrices

Property	Operation
Transpose	$(\mathbf{A} + \mathbf{B})^T = \mathbf{A}^T + \mathbf{B}^T$
	$(\alpha\mathbf{A})^T = \alpha\mathbf{A}^T$
	$(\mathbf{A}\mathbf{B})^T = \mathbf{B}^T\mathbf{A}^T$
Double transpose	$(\mathbf{A}^T)^T = \mathbf{A}$
Inverse	$(\alpha\mathbf{A})^{-1} = \frac{1}{\alpha}\mathbf{A}^{-1}$
	$(\mathbf{A}\mathbf{B})^{-1} = \mathbf{B}^{-1}\mathbf{A}^{-1}$
	$\mathbf{A}^{-1}\mathbf{A}\mathbf{B} = \mathbf{I}\mathbf{B} = \mathbf{B}$
Double inverse	$(\mathbf{A}^{-1})^{-1} = \mathbf{A}$
Duality	$(\mathbf{A}^T)^{-1} = (\mathbf{A}^{-1})^T$

Linear transformations. A linear transformation of an $n \times 1$ vector \mathbf{x} to the other $n \times 1$ vector \mathbf{y} is provided with a square matrix \mathbf{A} of order n as follows:

$$\mathbf{y} = \mathbf{A}\mathbf{x}. \tag{B.19}$$

If for some scalar λ and nonzero column vector $\mathbf{x} \neq \mathbf{0}$ we have

$$\mathbf{Ax} = \lambda \mathbf{x}, \quad (\text{B.20})$$

then λ is called an *eigenvalue* or *characteristic value* of \mathbf{A} and \mathbf{x} is said to be an *eigenvector* associated with λ .

Alternatively, (B.20) can be rewritten as

$$(\lambda \mathbf{I} - \mathbf{A})\mathbf{x} = \mathbf{0}, \quad (\text{B.21})$$

having a nonzero eigenvector \mathbf{x} only if $\lambda \mathbf{I} - \mathbf{A}$ is singular. To find the eigenvalues λ , the following equation must be solved,

$$|\lambda \mathbf{I} - \mathbf{A}| = 0, \quad (\text{B.22})$$

known as the *characteristic equation* of \mathbf{A} . The determinant in (B.22) is commonly defined by the polynomial

$$|\lambda \mathbf{I} - \mathbf{A}| = \eta(\lambda) = \lambda^n + a_{n-1}\lambda^{n-1} + \dots + a_1\lambda + a_0 \quad (\text{B.23})$$

called the *characteristic polynomial* of \mathbf{A} . If all eigenvalues λ_i , $i = 1, 2, \dots, n$, of \mathbf{A} are distinct, then (B.23) may be rewritten as

$$\eta(\lambda) = (\lambda - \lambda_1)(\lambda - \lambda_2) \dots (\lambda - \lambda_n). \quad (\text{B.24})$$

Supposing that all distinct eigenvalues $\lambda_1, \lambda_2, \dots, \lambda_n$ of the characteristic equation (B.22) are known, the relevant eigenvectors $\mathbf{x}_1, \mathbf{x}_2, \dots, \mathbf{x}_n$ may be found from (B.20) to satisfy for $i = 1, 2, \dots, n$ the following equation

$$\lambda_i \mathbf{x}_i = \mathbf{Ax}_i. \quad (\text{B.25})$$

If all distinct eigenvalues $\lambda_1, \lambda_2, \dots, \lambda_n$ of \mathbf{A} are different, then the relevant eigenvectors $\mathbf{x}_1, \mathbf{x}_2, \dots, \mathbf{x}_n$ are linearly independent and orthogonal. Note that, in some cases, n linearly independent eigenvectors x_i may be found for multiple eigenvalues λ_i .

Linear independence. Given an $n \times n$ matrix $\mathbf{A} = [\mathbf{a}_1 \ \mathbf{a}_2 \ \dots \ \mathbf{a}_n]$, where \mathbf{a}_i , $i = 1, 2, \dots, n$, denotes the i th column vector. The vectors \mathbf{a}_i , $i = 1, 2, \dots, n$, are said to be *linearly dependent* if there exist numbers γ_i , $i = 1, 2, \dots, n$, not all zeros such that

$$\gamma_1 \mathbf{a}_1 + \gamma_2 \mathbf{a}_2 + \dots + \gamma_n \mathbf{a}_n = \mathbf{0}. \quad (\text{B.26})$$

If (B.26) holds only for all $\gamma_i = 0$, then the column vectors \mathbf{a}_i , $i = 1, 2, \dots, n$, are said to be *linearly independent*.

Rank of a matrix. The number of linearly independent column vectors in a matrix \mathbf{A} is called the *column rank* of \mathbf{A} . The number of linearly independent row vectors in a matrix \mathbf{A} is said to be the *row rank* of \mathbf{A} . It can be shown

that the rank of \mathbf{A} is equal to the biggest number of linearly independent rows or columns.

The *determinant rank* of a matrix \mathbf{A} is defined by the order of the largest square submatrix \mathbf{N} such that $|\mathbf{N}| \neq 0$. It can be shown that the rank of \mathbf{A} is equal to the determinant rank of \mathbf{A} .

Trace of a matrix. The *trace* of a square matrix \mathbf{A} of order n is the sum

$$\text{Tr}(\mathbf{A}) = \sum_{i=1}^n a_{ii} \tag{B.27}$$

of its diagonal components demonstrating the following properties:

- $\text{Tr}(\mathbf{A} + \mathbf{B}) = \text{Tr}(\mathbf{A}) + \text{Tr}(\mathbf{B})$, □
- $\text{Tr}(\alpha\mathbf{A}) = \alpha\text{Tr}(\mathbf{A})$, □
- $\text{Tr}(\mathbf{BA}) = \text{Tr}(\mathbf{AB})$, □
- $\text{Tr}(\mathbf{AB} - \mathbf{BA}) = \mathbf{0}$. □

Diagonalization. For the matrix $\mathbf{T} = [\mathbf{x}_1 \ \mathbf{x}_2 \ \dots \ \mathbf{x}_n]$, which columns are formed by the linearly independent eigenvectors of a matrix \mathbf{A} , the following identity may be written

$$\mathbf{AT} = \mathbf{T}\mathbf{\Lambda} , \tag{B.28}$$

where the diagonal matrix $\mathbf{\Lambda}$ is defined by

$$\mathbf{\Lambda} = \begin{bmatrix} \lambda_1 & 0 & \dots & 0 \\ 0 & \lambda_2 & \dots & 0 \\ \vdots & \vdots & \ddots & \vdots \\ 0 & 0 & \dots & \lambda_n \end{bmatrix} . \tag{B.29}$$

Because \mathbf{T} is composed with n linearly independent vectors, it is nonsingular and its inverse exists. The matrix $\mathbf{\Lambda}$ may hence be defined by

$$\mathbf{\Lambda} = \mathbf{T}^{-1}\mathbf{AT} \tag{B.30}$$

or, if $\mathbf{\Lambda}$ is known, we have

$$\mathbf{A} = \mathbf{T}\mathbf{\Lambda}\mathbf{T}^{-1} . \tag{B.31}$$

The transformation process (B.31) is known as *diagonalization* of \mathbf{A} . The matrix \mathbf{T} is called the *diagonalization matrix* or *eigenvector matrix* and $\mathbf{\Lambda}$ the *eigenvalue matrix*. Note that the diagonalization matrix is not unique. A new matrix \mathbf{T} may be produced by reordering the columns or multiplying them by nonzero scalars.

Application of the diagonalization matrix gives the other useful relation. By changing the variables, $\mathbf{x} = \mathbf{T}\mathbf{u}$ and $\mathbf{y} = \mathbf{T}\mathbf{v}$, an equation (B.19) may equivalently be rewritten as

$$\mathbf{v} = \mathbf{\Lambda}\mathbf{u} .$$

Similarity transformation. Given two square matrices, \mathbf{A} and \mathbf{B} , of the same order. They say that the matrix \mathbf{B} is *similar* to \mathbf{A} if there exists a nonsingular matrix \mathbf{Q} such that

$$\mathbf{B} = \mathbf{Q}^{-1}\mathbf{A}\mathbf{Q}. \quad (\text{B.32})$$

Equation (B.32) is called the *similarity transformation* having the following properties:

- If \mathbf{B} is similar to \mathbf{A} , then \mathbf{A} is similar to \mathbf{B} . □
- If \mathbf{A} and \mathbf{B} are similar, then they have the same eigenvalues. □
- If \mathbf{A} is similar to \mathbf{B} and \mathbf{B} is similar to \mathbf{C} , then \mathbf{A} is similar to \mathbf{C} . □
- A square matrix \mathbf{A} of order n is similar to a diagonal matrix \mathbf{D} if and only if there exist n linearly independent eigenvectors of \mathbf{A} . □

Functions of a matrix. If a matrix \mathbf{A} is diagonalizable, then, similarly to (B.31), for any analytical function $\phi(\lambda)$ there can be defined a function $\phi(\mathbf{A})$ of a matrix \mathbf{A} such that

$$\phi(\mathbf{A}) = \mathbf{T}\phi(\mathbf{\Lambda})\mathbf{T}^{-1},$$

$$\phi(\mathbf{A}) = \mathbf{T} \begin{bmatrix} \phi(\lambda_1) & 0 & \dots & 0 \\ 0 & \phi(\lambda_2) & \dots & 0 \\ \vdots & \vdots & \ddots & \vdots \\ 0 & 0 & \dots & \phi(\lambda_n) \end{bmatrix} \mathbf{T}^{-1}, \quad (\text{B.33})$$

where λ_i , $i = 1, 2, \dots, n$, are the eigenvalues of \mathbf{A} , if only $\phi(\lambda)$ exists at λ_i .

It can be shown that if $\phi(\lambda)$ is expendable to the power series within a circle $|\lambda| < r$ of a radius r ,

$$\phi(\lambda) = \alpha_0 + \alpha_1\lambda + \alpha_2\lambda^2 + \dots = \sum_{k=0}^{\infty} \alpha_k\lambda^k, \quad (\text{B.34})$$

then this expansion also holds true if to substitute a scalar λ with any matrix \mathbf{A} , all eigenvalues of which, λ_i , $i = 1, 2, \dots, n$, lie entirely within the same circle,

$$\phi(\mathbf{A}) = \alpha_0\mathbf{I} + \alpha_1\mathbf{A} + \alpha_2\mathbf{A}^2 + \dots = \sum_{k=0}^{\infty} \alpha_k\mathbf{A}^k. \quad (\text{B.35})$$

Several particular expansions of $\phi(\mathbf{A})$ are given in Table B.4.

It is of importance that the function of a matrix $\phi(\mathbf{A})$ saves some properties associated with a scalar function $\phi(\lambda)$, for example,

$$\cos^2 \mathbf{A} + \sin^2 \mathbf{A} = \mathbf{I},$$

$$e^{\mathbf{A}}e^{-\mathbf{A}} = \mathbf{I},$$

Table B.4. Series expansions of $\phi(\mathbf{A})$

Function $\phi(\mathbf{A})$	Expansion
$e^{\mathbf{A}}$	$\sum_{k=0}^{\infty} \frac{\mathbf{A}^k}{k!}$
$\cos \mathbf{A}$	$\sum_{k=0}^{\infty} \frac{(-1)^k}{(2k)!} \mathbf{A}^{2k}$
$\sin \mathbf{A}$	$\sum_{k=0}^{\infty} \frac{(-1)^k}{(2k+1)!} \mathbf{A}^{(2k+1)}$
$\cosh \mathbf{A}$	$\sum_{k=0}^{\infty} \frac{1}{(2k)!} \mathbf{A}^{2k}$
$\sinh \mathbf{A}$	$\sum_{k=0}^{\infty} \frac{1}{(2k+1)!} \mathbf{A}^{(2k+1)}$
$\ln \mathbf{A}$	$\sum_{k=1}^{\infty} \frac{(-1)^{k-1}}{k!} (\mathbf{A} - \mathbf{I})^k$, for $ \lambda_i - 1 < 1, i = 1, 2, \dots, n$
$(\mathbf{I} - \mathbf{A})^{-1}$	$\sum_{k=0}^{\infty} \mathbf{A}^k$, for $ \lambda_i < 1, i = 1, 2, \dots, n$

$$e^{j\mathbf{A}} = \cos \mathbf{A} + j \sin \mathbf{A}.$$

On the other hand, an identity $e^{\mathbf{A}+\mathbf{B}} = e^{\mathbf{A}}e^{\mathbf{B}}$ holds true only if $\mathbf{AB} = \mathbf{BA}$, i.e. when \mathbf{A} and \mathbf{B} commute.

The Cayley-Hamilton theorem. Let a square matrix \mathbf{A} of order n is represented with the characteristic polynomial (B.23),

$$\eta(\lambda) = |\lambda\mathbf{I} - \mathbf{A}| = \lambda^n + a_{n-1}\lambda^{n-1} + \dots + a_1\lambda + a_0. \tag{B.36}$$

The *Cayley-Hamilton theorem* states that, if so, the matrix \mathbf{A} satisfies its own characteristic equation (B.22):

$$\eta(\mathbf{A}) = \mathbf{A}^n + a_{n-1}\mathbf{A}^{n-1} + \dots + a_1\mathbf{A} + a_0\mathbf{I} = \mathbf{0}. \tag{B.37}$$

By the Cayley-Hamilton theorem, a function $\phi(\mathbf{A})$ defined by (B.35) with an infinite series, can be represented with the finite series (B.37) as

$$\phi(\mathbf{A}) = \beta_0\mathbf{I} + \beta_1\mathbf{A} + \dots + \beta_{n-1}\mathbf{A}^{n-1} = \sum_{k=0}^{n-1} \beta_k \mathbf{A}^k. \tag{B.38}$$

It then follows that $\phi(\lambda)$ defined by (B.34) can be represented with the finite series (B.36) as

$$\phi(\lambda) = \beta_0 + \beta_1\lambda + \dots + \beta_{n-1}\lambda^{n-1} = \sum_{k=0}^{n-1} \beta_k \lambda^k. \tag{B.39}$$

If all eigenvalues $\lambda_i, i = 1, 2, \dots, n$, of \mathbf{A} are distinct, then the coefficients $\beta_k, k = 0, 1, \dots, n - 1$, are determined by solving the following equations:

$$\begin{aligned}
\phi(\lambda_1) &= \beta_0 + \beta_1\lambda_1 + \dots + \beta_{n-1}\lambda_1^{n-1}, \\
\phi(\lambda_2) &= \beta_0 + \beta_1\lambda_2 + \dots + \beta_{n-1}\lambda_2^{n-1}, \\
&\vdots \\
\phi(\lambda_n) &= \beta_0 + \beta_1\lambda_n + \dots + \beta_{n-1}\lambda_n^{n-1}.
\end{aligned} \tag{B.40}$$

If all eigenvalues $\lambda_i, i = 1, 2, \dots, n$, of \mathbf{A} are not distinct, then (B.40) does not consist of n equations. It is typical that an eigenvalue λ_j has multiplicity p and all other eigenvalues are distinct. In this case, differentiating both sides of (B.39) $p - 1$ times with respect to λ and setting $\lambda = \lambda_j$ gives additionally $p - 1$ equations

$$\begin{aligned}
\left. \frac{d}{d\lambda} \phi(\lambda) \right|_{\lambda=\lambda_j} &= \left. \frac{d}{d\lambda} \sum_{k=0}^{n-1} \beta_k \lambda^k \right|_{\lambda=\lambda_j}, \\
\left. \frac{d^2}{d\lambda^2} \phi(\lambda) \right|_{\lambda=\lambda_j} &= \left. \frac{d^2}{d\lambda^2} \sum_{k=0}^{n-1} \beta_k \lambda^k \right|_{\lambda=\lambda_j}, \\
&\vdots \\
\left. \frac{d^{p-1}}{d\lambda^{p-1}} \phi(\lambda) \right|_{\lambda=\lambda_j} &= \left. \frac{d^{p-1}}{d\lambda^{p-1}} \sum_{k=0}^{n-1} \beta_k \lambda^k \right|_{\lambda=\lambda_j}.
\end{aligned} \tag{B.41}$$

The coefficients β_k are then determined by combining (B.40) and (B.41).

Minimum polynomial of \mathbf{A} . Given a square matrix \mathbf{A} of order n , then its *minimum polynomial* $\mu(\lambda)$ is the polynomial of lowest degree having 1 as its leading coefficient such that $\mu(\mathbf{A}) = \mathbf{0}$. The degree of $\mu(\mathbf{A})$ cannot be greater than n .

It can be shown that $\mu(\lambda)$ can be determined by

$$\mu(\lambda) = \frac{\eta(\lambda)}{v(\lambda)}, \tag{B.42}$$

where $v(\lambda)$ is a greatest common divisor (gcd) of all elements of $\text{adj}(\lambda\mathbf{I} - \mathbf{A})$, thus $\eta(\lambda)$ is divisible by $\mu(\lambda)$ and if all the eigenvalues of \mathbf{A} are distinct, then $\mu(\lambda) = \eta(\lambda)$. Yet, every eigenvalue of \mathbf{A} is a zero of $\mu(\lambda)$.

In the same way $\mu(\lambda)$ may be used as $\eta(\lambda)$ for the expression of higher powers of \mathbf{A} in terms of a limited number of powers of \mathbf{A} .

Spectral decomposition. If a matrix \mathbf{A} of order n is represented with the minimum polynomial of the form

$$\mu(\lambda) = (\lambda - \lambda_1)(\lambda - \lambda_2) \dots (\lambda - \lambda_m), \tag{B.43}$$

then, it can be shown, \mathbf{A} can be represented with

$$\mathbf{A} = \lambda_1 \mathbf{E}_1 + \lambda_2 \mathbf{E}_2 + \dots + \lambda_m \mathbf{E}_m, \tag{B.44}$$

where \mathbf{E}_l , $l = 1, 2, \dots, m$, is termed the *constituent matrix*. The form (B.44) is called the *spectral decomposition* of \mathbf{A} and the set of eigenvalues of \mathbf{A} is called the *spectrum* of \mathbf{A} .

The following properties of \mathbf{E}_l are of importance:

1. $\mathbf{E}_1 + \mathbf{E}_2 + \dots + \mathbf{E}_m = \mathbf{I}$ □
2. $\mathbf{E}_i \mathbf{E}_j = \mathbf{0}$, $i \neq j$ □
3. $\mathbf{E}_l^2 = \mathbf{E}_l$ (idempotent) □
4. $\mathbf{A} \mathbf{E}_l = \mathbf{E}_l \mathbf{A} = \lambda_l \mathbf{E}_l$ □

It can be shown, by the properties of \mathbf{E}_l , that $\phi(\mathbf{A})$ can also be decomposed similarly to (B.44):

$$\phi(\mathbf{A}) = \phi(\lambda_1) \mathbf{E}_1 + \phi(\lambda_2) \mathbf{E}_2 + \dots + \phi(\lambda_m) \mathbf{E}_m. \tag{B.45}$$

To evaluate \mathbf{E}_l , the following relation can be used:

$$\mathbf{E}_l = \frac{\prod_{k=1, k \neq l}^m (\mathbf{A} - \lambda_k \mathbf{I})}{\prod_{k=1, k \neq l}^m (\lambda_l - \lambda_k)}. \tag{B.46}$$

Differentiation and integration of matrices. The operation of differentiation of an $m \times n$ matrix \mathbf{A} over a scalar variable t is provided with the expression

$$\begin{aligned} \frac{d}{dt} \mathbf{A}(t) &= \left[\frac{d}{dt} a_{ij}(t) \right] \\ &= \begin{bmatrix} \frac{d}{dt} a_{11}(t) & \frac{d}{dt} a_{12}(t) & \dots & \frac{d}{dt} a_{1n}(t) \\ \frac{d}{dt} a_{21}(t) & \frac{d}{dt} a_{22}(t) & \dots & \frac{d}{dt} a_{2n}(t) \\ \vdots & \vdots & \ddots & \vdots \\ \frac{d}{dt} a_{m1}(t) & \frac{d}{dt} a_{m2}(t) & \dots & \frac{d}{dt} a_{mn}(t) \end{bmatrix}, \end{aligned} \tag{B.47}$$

meaning that the derivative of \mathbf{A} is a matrix of the same dimensions, each element of which is the derivative of the corresponding element of \mathbf{A} .

In a like manner, the integral of an $m \times n$ matrix \mathbf{A} over a scalar variable t is provided with

$$\int \mathbf{A}(t) dt = \left[\int a_{ij}(t) dt \right]$$

$$= \begin{bmatrix} \int a_{11} dt & \int a_{12} dt & \dots & \int a_{1n} dt \\ \int a_{21} dt & \int a_{22} dt & \dots & \int a_{2n} dt \\ \vdots & \vdots & \ddots & \vdots \\ \int a_{m1} dt & \int a_{m2} dt & \dots & \int a_{mn} dt \end{bmatrix}. \quad (\text{B.48})$$

The following relations hold true for the derivatives of matrix functions:

$$\frac{d}{dt}(\mathbf{AB}) = \left(\frac{d}{dt}\mathbf{A}\right)\mathbf{B} + \mathbf{A}\left(\frac{d}{dt}\mathbf{B}\right), \quad (\text{B.49})$$

$$\frac{d}{dt}\mathbf{A}^{-1} = -\mathbf{A}^{-1}\left(\frac{d}{dt}\mathbf{A}\right)\mathbf{A}^{-1}, \quad (\text{B.50})$$

$$\frac{d}{dt}\mathbf{A}^n = \left(\frac{d}{dt}\mathbf{A}\right)\mathbf{A}^{n-1} + \mathbf{A}\left(\frac{d}{dt}\mathbf{A}\right)\mathbf{A}^{n-2} + \dots + \mathbf{A}^{n-1}\left(\frac{d}{dt}\mathbf{A}\right). \quad (\text{B.51})$$

The derivative of a scalar function $\phi(\mathbf{x})$ over an $n \times 1$ column vector $\mathbf{x} = [x_1, x_2, \dots, x_n]^T$ is a row vector

$$\frac{d}{d\mathbf{x}}\phi(\mathbf{x}) = \left[\frac{d\phi(\mathbf{x})}{dx_1} \quad \frac{d\phi(\mathbf{x})}{dx_2} \quad \dots \quad \frac{d\phi(\mathbf{x})}{dx_n} \right]. \quad (\text{B.52})$$

The derivative of an $m \times 1$ vector function

$$\mathbf{y}(\mathbf{x}) = [y_1(\mathbf{x}), y_2(\mathbf{x}), \dots, y_m(\mathbf{x})]^T$$

over an $n \times 1$ column vector $\mathbf{x} = [x_1, x_2, \dots, x_n]^T$ is called the *Jacobian matrix*

$$\frac{d\mathbf{y}}{d\mathbf{x}} = \left[\frac{dy_i}{dx_j} \right] = \begin{bmatrix} \frac{dy_1}{dx} \\ \frac{dy_2}{dx} \\ \vdots \\ \frac{dy_m}{dx} \end{bmatrix} = \begin{bmatrix} \frac{dy_1}{dx_1} & \frac{dy_1}{dx_2} & \dots & \frac{dy_1}{dx_n} \\ \frac{dy_2}{dx_1} & \frac{dy_2}{dx_2} & \dots & \frac{dy_2}{dx_n} \\ \vdots & \vdots & \ddots & \vdots \\ \frac{dy_m}{dx_1} & \frac{dy_m}{dx_2} & \dots & \frac{dy_m}{dx_n} \end{bmatrix}. \quad (\text{B.53})$$

The derivative of a scalar function $\phi(\mathbf{A})$ over a matrix \mathbf{A} is defined by

$$\frac{d}{d\mathbf{A}}\phi(\mathbf{A}) = \left[\frac{d\phi(\mathbf{A})}{da_{ij}} \right]. \quad (\text{B.54})$$

In a similar manner, partial derivatives are defined of scalar and vector functions over vector functions. For example, derivatives of a scalar function $\phi(\mathbf{y}, \mathbf{x}, t)$ of vectors $\mathbf{y}(\mathbf{x}, t)$ and $\mathbf{x} = \mathbf{x}(t)$ are defined by

$$\frac{d\phi}{d\mathbf{x}} = \left(\frac{\partial\phi}{\partial\mathbf{y}}\right)\frac{\partial\mathbf{y}}{\partial\mathbf{x}} + \frac{\partial\phi}{\partial\mathbf{x}}, \quad (\text{B.55})$$

$$\frac{d\phi}{dt} = \left[\frac{\partial\phi}{\partial\mathbf{x}} + \left(\frac{\partial\phi}{\partial\mathbf{y}}\right)\left(\frac{\partial\mathbf{y}}{\partial\mathbf{x}}\right) \right] \frac{d\mathbf{x}}{dt} + \left[\frac{\partial\phi}{\partial\mathbf{y}} \right] \frac{\partial\mathbf{y}}{\partial t} + \frac{\partial\phi}{\partial t}. \quad (\text{B.56})$$

It can be shown that for a vector function $\mathbf{z}(\mathbf{y}, \mathbf{x}, t)$ and the same \mathbf{x} and \mathbf{y} , we have

$$\frac{d\mathbf{z}}{d\mathbf{x}} = \left[\frac{\partial \mathbf{z}}{\partial \mathbf{y}} \right] \left[\frac{\partial \mathbf{y}}{\partial \mathbf{x}} \right] + \frac{\partial \mathbf{z}}{\partial \mathbf{x}}, \tag{B.57}$$

$$\frac{d\mathbf{z}}{dt} = \left[\frac{\partial \mathbf{z}}{\partial \mathbf{y}} \right] \left[\left(\frac{\partial \mathbf{y}}{\partial \mathbf{x}} \right) \frac{d\mathbf{x}}{dt} + \frac{\partial \mathbf{y}}{\partial t} \right] + \left[\frac{\partial \mathbf{z}}{\partial \mathbf{x}} \right] \frac{d\mathbf{x}}{dt} + \frac{\partial \mathbf{z}}{\partial t}. \tag{B.58}$$

Taylor expansion. Referring to the above-defined derivatives, the Taylor expansion about a point \mathbf{x}_0 for a scalar function $\phi(\mathbf{x})$ and vector function $\mathbf{z}(\mathbf{x})$ can be written as, respectively,

$$\begin{aligned} \phi(\mathbf{x}) &= \phi(\mathbf{x}_0) + \left[\frac{\partial \phi}{\partial \mathbf{x}} \right] \Big|_{\mathbf{x}=\mathbf{x}_0} (\mathbf{x} - \mathbf{x}_0) \\ &+ \frac{1}{2}(\mathbf{x} - \mathbf{x}_0)^T \left[\frac{\partial}{\partial \mathbf{x}} \left(\frac{\partial \phi}{\partial \mathbf{x}} \right)^T \right] \Big|_{\mathbf{x}=\mathbf{x}_0} (\mathbf{x} - \mathbf{x}_0) + \dots, \end{aligned} \tag{B.59}$$

$$\begin{aligned} \mathbf{z}(\mathbf{x}) &= \mathbf{z}(\mathbf{x}_0) + \left[\frac{\partial \mathbf{z}(\mathbf{x})}{\partial \mathbf{x}} \right] \Big|_{\mathbf{x}=\mathbf{x}_0} (\mathbf{x} - \mathbf{x}_0) \\ &+ \frac{1}{2}(\mathbf{x} - \mathbf{x}_0)^T \left[\frac{\partial}{\partial \mathbf{x}} \left(\frac{\partial \mathbf{z}(\mathbf{x}_0)}{\partial \mathbf{x}} \right)^T \right] \Big|_{\mathbf{x}=\mathbf{x}_0} (\mathbf{x} - \mathbf{x}_0) + \dots. \end{aligned} \tag{B.60}$$

The following identities hold true for derivatives of the determinant of independent matrices:

$$\frac{d}{d\mathbf{A}} |\mathbf{A}| = |\mathbf{A}| [\mathbf{A}^{-1}], \tag{B.61}$$

$$\frac{d}{d\mathbf{A}} \ln |\mathbf{A}| = [\mathbf{A}^{-1}]^T, \tag{B.62}$$

$$\frac{d}{d\mathbf{B}} |\mathbf{ABC}| = |\mathbf{ABC}| [\mathbf{B}^{-1}]^T, \tag{B.63}$$

$$\frac{d}{d\mathbf{A}} |\mathbf{A}^n| = n |\mathbf{A}^{n-1}| [\mathbf{A}^{-1}]^T. \tag{B.64}$$

Matrix forms of linear ODEs with constant coefficients. A system of linear ODEs of the first order with constant coefficients can be represented by the matrix differential equation of the first order:

$$\frac{d}{dt} \mathbf{x}(t) = \mathbf{A} \mathbf{x}(t) + \mathbf{y}(t), \tag{B.65}$$

where $\mathbf{x}(t)$ is unknown $n \times 1$ vector of a scalar variable t , $\mathbf{y}(t)$ is a known $n \times 1$ vector of t , and \mathbf{A} is an $n \times n$ matrix with constant components.

A solution of (B.65) is given by

$$\mathbf{x}(t) = e^{\mathbf{A}t} \mathbf{x}_0 + \int_{t_0}^t e^{\mathbf{A}(t-\theta)} \mathbf{y}(\theta) d\theta, \quad (\text{B.66})$$

where $\mathbf{x}_0 = \mathbf{x}(t_0)$. The function $e^{\mathbf{A}t}$ is known as the *matrix exponential* and can be expanded to the series (see Table B.4).

If $\mathbf{y}(t) = \mathbf{x}(t)\mathbf{B}$ and (B.65) hence attains the form

$$\frac{d}{dt} \mathbf{x}(t) = \mathbf{A}\mathbf{x}(t) + \mathbf{x}(t)\mathbf{B}, \quad (\text{B.67})$$

then a solution of (B.67) is defined by

$$\mathbf{x}(t) = e^{\mathbf{A}t} \mathbf{x}_0 e^{\mathbf{B}t}. \quad (\text{B.68})$$

If \mathbf{A} and \mathbf{B} are diagonalizable, then solutions (B.66) and (B.68) are performed in standard matrix forms.

Matrix forms of linear ODEs with variable coefficients. Most generally, the matrix ODE is represented with two variable matrices $\mathbf{A}(t)$ and $\mathbf{B}(t)$ as follows

$$\frac{d}{dt} \mathbf{x}(t) = \mathbf{A}(t)\mathbf{x}(t) + \mathbf{B}(t)\mathbf{y}(t). \quad (\text{B.69})$$

A general solution of (B.69) is given with

$$\mathbf{x}(t) = \Phi(t, t_0) \mathbf{x}_0 + \int_{t_0}^t \Phi(t, \theta) \mathbf{B}(\theta) \mathbf{y}(\theta) d\theta, \quad (\text{B.70})$$

where $\Phi(t, t_0)$ is called the *state transition matrix* satisfying the homogenous equation

$$\frac{d}{dt} \Phi(t, t_0) = \mathbf{A}(t) \Phi(t, t_0) \quad (\text{B.71})$$

and having the following basic properties:

$$\Phi(t_0, t_0) = \mathbf{I}, \quad (\text{B.72})$$

$$\Phi^{-1}(t, t_0) = \Phi(t_0, t), \quad (\text{B.73})$$

$$\Phi(t_2, t_0) = \Phi(t_2, t_1) \Phi(t_1, t_0). \quad (\text{B.74})$$

The state transition matrix $\Phi^{-1}(t, t_0)$ is defined via the *fundamental matrix* $\mathbf{Q}(t)$ as

$$\Phi(t, t_0) = \mathbf{Q}(t) \mathbf{Q}^{-1}(t_0), \quad (\text{B.75})$$

where $\mathbf{Q}(t)$ also satisfies the homogenous equation

$$\frac{d}{dt}\mathbf{Q}(t) = \mathbf{A}(t)\mathbf{Q}(t). \tag{B.76}$$

Because any initial condition may be chosen to solve (B.76), the fundamental matrix $\mathbf{Q}(t)$ for $\mathbf{A}(t)$ is not unique having the following properties:

- It is nonsingular for all t . Otherwise, it does not satisfy (B.76) and cannot be unit matrix \mathbf{I} at t_0 . □
- It is the $n \times n$ square matrix. □

Norms of matrices. Consider two n -dimensional normed vector spaces \mathcal{N} and \mathcal{M} . Let the linear map (matrix) \mathbf{A} belongs to the set T of all linear maps from \mathcal{N} to \mathcal{M} . If a vector \mathbf{x} belongs to \mathcal{N} and \mathbf{y} to \mathcal{M} , we have the transformation $\mathbf{y} = \mathbf{A}\mathbf{x}$. The norm for a vector \mathbf{y} is defined by

$$\|\mathbf{y}\| = \|\mathbf{A}\mathbf{x}\|. \tag{B.77}$$

The norm for a matrix \mathbf{A} is a function $\|\mathbf{A}\|$, satisfying

$$\|\mathbf{A}\| \geq \sup_{\|\mathbf{x}\|=1} \|\mathbf{A}\mathbf{x}\|, \tag{B.78}$$

$$\|\gamma\mathbf{A}\| = |\gamma|\|\mathbf{A}\|, \tag{B.79}$$

where “sup” denotes the upper bound. An inequality (B.78) also means that

$$\|\mathbf{A}\mathbf{x}\| \leq \|\mathbf{A}\|\|\mathbf{x}\| \tag{B.80}$$

and it can be shown that norms of matrices satisfy two fundamental properties called the *submultiplicative property* and *triangle property*, respectively,

$$\|\mathbf{A}\mathbf{B}\| \leq \|\mathbf{A}\|\|\mathbf{B}\|, \tag{B.81}$$

$$\|\mathbf{A} + \mathbf{B}\| \leq \|\mathbf{A}\| + \|\mathbf{B}\|. \tag{B.82}$$

If \mathcal{N} is n -dimensional and \mathcal{M} is m -dimensional, then the matrix \mathbf{A} is of $m \times n$ dimensions. For such a general case, the most frequently used matrix norms are the following:

$$\|\mathbf{A}\|_1 = \sup_{1 \leq j \leq n} \sum_{i=1}^m |a_{ij}|, \tag{B.83}$$

$$\|\mathbf{A}\|_2 = \sqrt{\lambda_M}, \tag{B.84}$$

$$\|\mathbf{A}\|_\infty = \sup_{1 \leq i \leq m} \sum_{j=1}^n |a_{ij}|. \tag{B.85}$$

In (B.84), λ_M denotes the greatest eigenvalue of $\mathbf{A}^T\mathbf{A}$ if \mathbf{A} is real or $\bar{\mathbf{A}}\mathbf{A}$ if \mathbf{A} is complex, where $\bar{\mathbf{A}}$ is a conjugate matrix.

C

**Tables of Fourier Series, Transform, and
Properties**

Table C.1 Properties of the continuous-time Fourier series

$$x(t) = \sum_{k=-\infty}^{\infty} C_k e^{jk\Omega t} \qquad C_k = \frac{1}{T} \int_{-T/2}^{T/2} x(t) e^{-jk\Omega t} dt$$

Property	Periodic function $x(t)$ with period $T = 2\pi/\Omega$	Fourier series C_k
Time-shifting	$x(t \pm t_0)$	$C_k e^{\pm jk\Omega t_0}$
Time-scaling	$x(\alpha t), \alpha > 0$	C_k with period $\frac{T}{\alpha}$
Differentiation	$\frac{d}{dt} x(t)$	$jk\Omega C_k$
Integration	$\int_{-\infty}^t x(\tau) d\tau < \infty$	$\frac{1}{jk\Omega} C_k$
Linearity	$\sum_i \alpha_i x_i(t)$	$\sum_i \alpha_i C_{ik}$
Conjugation	$x^*(t)$	C_{-k}^*
Time-reversal	$x(-t)$	C_{-k}
Modulation	$x(t) e^{jK\Omega t}$	C_{k-K}
Product	$x(t)y(t)$	$\sum_{i=-\infty}^{\infty} C_{xi} C_{y(k-i)}$
Periodic convolution	$\int_T x(\tau) y(t - \tau) d\tau$	$T C_{xk} C_{yk}$
Symmetry	$x(t) = x^*(t)$ real	$\begin{cases} C_k = C_{-k}^*, C_k = C_{-k} , \\ \operatorname{Re} C_k = \operatorname{Re} C_{-k}, \\ \operatorname{Im} C_k = -\operatorname{Im} C_{-k}, \\ \arg C_k = -\arg C_{-k} \end{cases}$
	$x(t) = x^*(t) = x(-t)$ real and even	$\begin{cases} C_k = C_{-k}, C_k = C_k^*, \\ \text{real and even} \end{cases}$
	$x(t) = x^*(t) = -x(-t)$ real and odd	$\begin{cases} C_k = -C_{-k}, C_k = -C_k^*, \\ \text{imaginary and odd} \end{cases}$
Parseval's theorem		$\frac{1}{T} \int_{-T/2}^{T/2} x(t) ^2 dt = \sum_{k=-\infty}^{\infty} C_k ^2$

Table C.2 Properties of the continuous-time Fourier transform

$$x(t) = \frac{1}{2\pi} \int_{-\infty}^{\infty} X(j\omega)e^{j\omega t} d\omega \qquad X(j\omega) = \int_{-\infty}^{\infty} x(t)e^{-j\omega t} dt$$

Property	Non periodic function $x(t)$	Fourier transform $X(j\omega)$
Time shifting	$x(t \pm t_0)$	$e^{\pm j\omega t_0} X(j\omega)$
Time scaling	$x(\alpha t)$	$\frac{1}{ \alpha } X\left(\frac{j\omega}{\alpha}\right)$
Differentiation	$\frac{d}{dt}x(t)$	$j\omega X(j\omega)$
Integration	$\int_{-\infty}^t x(\tau)d\tau$	$\frac{1}{j\omega} X(j\omega) + \pi X(j0)\delta(\omega)$
	$\int_{-\infty}^{\infty} x(t)dt$	$X(j0)$
Frequency integration	$2\pi x(0)$	$\int_{-\infty}^{\infty} X(j\omega)d\omega$
Linearity	$\sum_i \alpha_i x_i(t)$	$\sum_i \alpha_i X_i(j\omega)$
Conjugation	$x^*(t)$	$X^*(-j\omega)$
Time reversal	$x(-t)$	$X(-j\omega)$
Modulation	$x(t)e^{j\omega_0 t}$	$X(j\omega - j\omega_0)$
Product	$x(t)y(t)$	$\frac{1}{2\pi} X(j\omega) * Y(j\omega)$
Convolution	$x(t) * y(t)$	$X(j\omega)Y(j\omega)$
Symmetry	$x(t) = x^*(t)$ real	$\begin{cases} X(j\omega) = X^*(-j\omega), \\ X(j\omega) = X(-j\omega) , \\ \text{Re } X(j\omega) = \text{Re } X(-j\omega), \\ \text{Im } X(j\omega) = -\text{Im } X(-j\omega), \\ \text{arg } X(j\omega) = -\text{arg } X(-j\omega) \end{cases}$
	$x(t) = x^*(t) = x(-t)$ real and even	$\begin{cases} X(j\omega) = X(-j\omega), \\ X(j\omega) = X^*(j\omega), \\ \text{real and even} \end{cases}$
	$x(t) = x^*(t) = -x(-t)$ real and odd	$\begin{cases} X(j\omega) = -X(-j\omega), \\ X(j\omega) = -X^*(j\omega), \\ \text{imaginary and odd} \end{cases}$
Rayleigh's theorem	$E_x = \int_{-\infty}^{\infty} x(t) ^2 dt = \frac{1}{2\pi} \int_{-\infty}^{\infty} X(j\omega) ^2 d\omega$	

Table C.3 The Fourier transform and series of basic signals

Signal $x(t)$	Transform $X(j\omega)$	Series C_k
1	$2\pi\delta(\omega)$	$C_0 = 1, C_{k \neq 0} = 0$
$\delta(t)$	1	$C_k = \frac{1}{T}$
$u(t)$	$\frac{1}{j\omega} + \pi\delta(\omega)$	—
$u(-t)$	$-\frac{1}{j\omega} + \pi\delta(\omega)$	—
$e^{j\Omega t}$	$2\pi\delta(\omega - \Omega)$	$C_1 = 1, C_{k \neq 1} = 0$
$\sum_{k=-\infty}^{\infty} C_k e^{jk\Omega t}$	$2\pi \sum_{k=-\infty}^{\infty} C_k \delta(\omega - k\Omega)$	C_k
$\cos \Omega t$	$\pi[\delta(\omega - \Omega) + \delta(\omega + \Omega)]$	$C_1 = C_{-1} = \frac{1}{2}, C_{k \neq \pm 1} = 0$
$\sin \Omega t$	$\frac{\pi}{j}[\delta(\omega - \Omega) - \delta(\omega + \Omega)]$	$C_1 = -C_{-1} = \frac{1}{2j}, C_{k \neq \pm 1} = 0$
$\frac{1}{\alpha^2 + t^2}$	$e^{-\alpha \omega }$	$\frac{1}{T} e^{-\frac{2\pi\alpha k }{T}}$
Rectangular $x_1(t)$	$\tau \frac{\sin(\omega\tau/2)}{\omega\tau/2}$	$\frac{1}{q} \frac{\sin(k\pi/q)}{k\pi/q}$
Triangular $x_2(t)$	$\frac{\tau}{2} \frac{\sin^2(\omega\tau/4)}{(\omega\tau/4)^2}$	$\frac{1}{2q} \frac{\sin^2(k\pi/2q)}{(k\pi/2q)^2}$
$\frac{\sin \alpha t}{\alpha t}$	$\begin{cases} \frac{\pi}{\alpha}, & \omega < \alpha \\ 0, & \omega > \alpha \end{cases}$	$\begin{cases} \frac{\pi}{\alpha T}, & k < \frac{\alpha T}{2\pi} \\ 0, & k > \frac{\alpha T}{2\pi} \end{cases}$
$e^{-\alpha t} u(t),$ $\text{Re } \alpha > 0$	$\frac{1}{\alpha + j\omega}$	$\frac{1}{\alpha T + j2\pi k}$
$te^{-\alpha t} u(t),$ $\text{Re } \alpha > 0$	$\frac{1}{(\alpha + j\omega)^2}$	$\frac{T}{(\alpha T + j2\pi k)^2}$
$\frac{t^{n-1}}{(n-1)!} e^{-\alpha t} u(t),$ $\text{Re } \alpha > 0$	$\frac{1}{(\alpha + j\omega)^n}$	$\frac{T^{n-1}}{(\alpha T + j2\pi k)^n}$
$e^{-\alpha t }, \alpha > 0$	$\frac{2\alpha}{\alpha^2 + \omega^2}$	$\frac{2\alpha T}{\alpha^2 T^2 + 4\pi^2 k^2}$
$e^{-\alpha^2 t^2}$	$\frac{\sqrt{\pi}}{\alpha} e^{-\frac{\omega^2}{4\alpha^2}}$	$\frac{\sqrt{\pi}}{\alpha T} e^{-\frac{\pi^2 k^2}{\alpha^2 T^2}}$

$x_1(t) = u(t + \frac{\tau}{2}) - u(t - \frac{\tau}{2}), x_2(t) = \frac{2}{\tau} (\frac{\tau}{2} - |t|) [u(t + \frac{\tau}{2}) - u(t - \frac{\tau}{2})], q = \frac{T}{\tau}, C_k$ corresponds to $x(t)$ repeated with period T , and τ is duration.

D

**Tables of Laplace Transform and Transform
Properties**

Table D.1. Properties of the bilateral Laplace transform

$$X(s) = \int_{-\infty}^{\infty} x(t)e^{-st} dt \qquad x(t) = \frac{1}{2\pi j} \int_{\sigma-j\infty}^{\sigma+j\infty} X(s)e^{st} ds$$

Property	Function $z(t)$	Transform $Z(s)$	ROC
Time shifting	$x(t - \tau)$	$e^{-s\tau} X(s)$	$R_z = R_x$
Shifting in s	$e^{\nu t} x(t)$	$X(s - \nu)$	$R_z = R_x + \text{Re}(\nu)$
Time scaling	$x(at)$	$\frac{1}{ a } X(s)$	$R_z = aR_x$
Time reversal	$x(-t)$	$X(-s)$	$R_z = -R_x$
Linearity	$ax(t) + by(t)$	$aX(s) + bY(s)$	$R_z \supset R_x \cap R_y$
Conjugation	$x^*(t)$	$X^*(s^*)$	$R_z = R_x$
Product	$x(t)y(t)$	$Z_1(s)$	$R_z \supset R_x \cap R_y$
Convolution	$x(t) * y(t)$	$X(s)Y(s)$	$R_z \supset R_x \cap R_y$
Differentiation in t	$\frac{d}{dt}x(t)$	$sX(s)$	$R_z \supset R_x$
Differentiation in s	$-tx(t)$	$\frac{d}{ds}X(s)$	$R_z = R_x$
Integration	$\int_{-\infty}^t x(\tau) d\tau$	$\frac{1}{s}X(s)$	$R_z \supset R_x \cap [\text{Re}(s) > 0]$

$$Z_1(s) = \frac{1}{2\pi j} \int_{\sigma-j\infty}^{\sigma+j\infty} X(\nu)Y(s - \nu) d\nu$$

The unilateral (one-sided) Laplace transform is provided by

$$X(s) = \int_{0^-}^{\infty} x(t)e^{-st} dt, \tag{D.1}$$

where $0^- = \lim_{\epsilon \rightarrow 0} (0 - \epsilon)$, having the following properties:

Initial value theorem: If $x(t) = 0$ for $t < 0$ and $x(t)$ contains no impulses or higher-order singularities at $t = 0$, then

$$x(0^+) = \lim_{s \rightarrow \infty} sX(s). \tag{D.2}$$

Final value theorem: If $x(t) = 0$ for $t < 0$ and $x(t)$ has a finite limit as $t \rightarrow 0$, then

$$\lim_{t \rightarrow \infty} x(t) = \lim_{s \rightarrow 0} sX(s). \tag{D.3}$$

Differentiation in time:

Table D.2. Laplace transform pairs of some functions

Function	Transform	ROC
$\delta(t)$	1	All s
$\delta(t - \tau)$	$e^{-s\tau}$	All s
$\frac{d^n}{dt^n}\delta(t)$	s^n	All s
$u(t)$	$\frac{1}{s}$	$\text{Re}(s) > 0$
$-u(-t)$	$\frac{1}{s}$	$\text{Re}(s) < 0$
$\underbrace{u(t) * u(t) * \dots * u(t)}_{n \text{ times}}$	$\frac{1}{s^n}$	$\text{Re}(s) > 0$
$tu(t)$	$\frac{1}{s^2}$	$\text{Re}(s) > 0$
$\frac{1}{\sqrt{\pi t}}u(t)$	$\frac{1}{\sqrt{s}}$	$\text{Re}(s) > 0$
$2\sqrt{\frac{t}{\pi}}u(t)$	$\frac{1}{\sqrt{s^3}}$	$\text{Re}(s) > 0$
$t^n u(t)$	$\frac{n!}{s^{n+1}}$	$\text{Re}(s) > 0$
$\frac{t^{n-1}}{(n-1)!}u(t)$	$\frac{1}{s^n}$	$\text{Re}(s) > 0$
$-\frac{t^{n-1}}{(n-1)!}u(-t)$	$\frac{1}{s^n}$	$\text{Re}(s) < 0$
$e^{-at}u(t)$	$\frac{1}{s+a}$	$\text{Re}(s) > -\text{Re}(a)$
$-e^{-at}u(-t)$	$\frac{1}{s+a}$	$\text{Re}(s) < -\text{Re}(a)$
$te^{-at}u(t)$	$\frac{1}{(s+a)^2}$	$\text{Re}(s) > -\text{Re}(a)$
$-te^{-at}u(-t)$	$\frac{1}{(s+a)^2}$	$\text{Re}(s) < -\text{Re}(a)$
$\frac{t^{n-1}}{(n-1)!}e^{-at}u(t)$	$\frac{1}{(s+a)^n}$	$\text{Re}(s) > -\text{Re}(a)$
$-\frac{t^{n-1}}{(n-1)!}e^{-at}u(-t)$	$\frac{1}{(s+a)^n}$	$\text{Re}(s) < -\text{Re}(a)$
$u(t) \cos \omega_0 t$	$\frac{s}{s^2 + \omega_0^2}$	$\text{Re}(s) > 0$
$u(t) \sin \omega_0 t$	$\frac{\omega_0}{s^2 + \omega_0^2}$	$\text{Re}(s) > 0$
$u(t)e^{-at} \cos \omega_0 t$	$\frac{s+a}{(s+a)^2 + \omega_0^2}$	$\text{Re}(s) > -\text{Re}(a)$
$u(t)e^{-at} \sin \omega_0 t$	$\frac{\omega_0}{(s+a)^2 + \omega_0^2}$	$\text{Re}(s) > -\text{Re}(a)$
$\frac{1}{a-b}(e^{at} - e^{bt})u(t)$	$\frac{1}{(s-a)(s-b)}$	
$\frac{1}{a-b}(ae^{at} - be^{bt})u(t)$	$\frac{s}{(s-a)(s-b)}$	
$u(t) \cosh at$	$\frac{s}{s^2 - a^2}$	
$u(t) \frac{1}{a} \sinh at$	$\frac{1}{s^2 - a^2}$	
$u(t) \frac{1}{a^2} (1 - \cos at)$	$\frac{1}{s(s^2 + a^2)}$	
$u(t) \frac{1}{a^3} (at - \sin at)$	$\frac{1}{s^2(s^2 + a^2)}$	

$$\frac{dx(t)}{dt} \stackrel{\mathcal{L}}{\Leftrightarrow} sX(s) - x(0^-), \quad (\text{D.4})$$

$$\frac{d^2x(t)}{dt^2} \stackrel{\mathcal{L}}{\Leftrightarrow} s^2X(s) - sx(0^-) - x'(0^-), \quad (\text{D.5})$$

$$\frac{d^n x(t)}{dt^n} \stackrel{\mathcal{L}}{\Leftrightarrow} s^n X(s) - s^{n-1}x(0^-) - s^{n-2}x'(0^-) - \dots - x^{(n-1)}(0^-). \quad (\text{D.6})$$

Integration in time:

$$\int_{0^-}^t x(\tau) d\tau \stackrel{\mathcal{L}}{\Leftrightarrow} \frac{1}{s}X(s), \quad (\text{D.7})$$

$$\int_{-\infty}^t x(\tau) d\tau \stackrel{\mathcal{L}}{\Leftrightarrow} \frac{1}{s}X(s) + \frac{1}{s} \int_{-\infty}^{0^-} x(t) dt. \quad (\text{D.8})$$

E

Mathematical Formulas

Basic functions :

$$\triangleright \delta(t) = \begin{cases} \infty, & t = 0 \\ 0, & t \neq 0 \end{cases} \quad (\text{Dirac delta-function, unit impulse})$$
$$\int_{-\infty}^{\infty} \delta(t) dt = 1 \quad , \quad \int_{-\infty}^t \delta(t) dt = u(t)$$

$$\triangleright u(t) = \begin{cases} 1, & t \geq 0 \\ 0, & t < 0 \end{cases} \quad (\text{unit step})$$
$$\frac{d}{dt}u(t) = \delta(t)$$

Limits :

$$\triangleright \lim_{x \rightarrow a} \frac{f(x)}{g(x)} = \lim_{x \rightarrow a} \frac{\partial f(x)/\partial x}{\partial g(x)/\partial x} \quad (\text{L'Hospital's rule})$$

$$\triangleright \lim_{x \rightarrow 0} \frac{\sin x}{x} = 1$$

$$\triangleright \lim_{x \rightarrow 0} \frac{\sin Nx}{\sin x} = N$$

$$\triangleright \int_0^{\infty} \sin bx dx = \lim_{\alpha \rightarrow 1} \int_0^{\infty} x^{\alpha-1} \sin bx dx = \frac{\Gamma(\alpha)}{b^\alpha} \sin \frac{\alpha\pi}{2} \Big|_{\alpha=1} = \frac{1}{b}$$

Trigonometric identities :

$$\triangleright e^{jx} = \cos x + j \sin x \quad (\text{Euler's formula})$$

$$\triangleright e^{(\alpha+jx)} = e^\alpha (\cos x + j \sin x)$$

$$\triangleright \cos x = \frac{e^{jx} + e^{-jx}}{2}$$

$$\triangleright \sin x = \frac{e^{jx} - e^{-jx}}{2j}$$

$$\triangleright \cos^2 x + \sin^2 x = 1$$

- ▷ $\cos^2 x - \sin^2 x = \cos 2x$
- ▷ $2 \cos x \sin x = \sin 2x$
- ▷ $\cos^2 x = \frac{1}{2}(1 + \cos 2x)$
- ▷ $\sin^2 x = \frac{1}{2}(1 - \cos 2x)$
- ▷ $\cos^3 x = \frac{1}{4} \cos 3x + \frac{3}{4} \cos x$
- ▷ $\sin^3 x = -\frac{1}{4} \sin 3x + \frac{3}{4} \sin x$
- ▷ $\cos x \cos y = \frac{1}{2}[\cos(x + y) + \cos(x - y)]$
- ▷ $\sin x \sin y = \frac{1}{2}[\cos(x - y) - \cos(x + y)]$
- ▷ $\sin x \cos y = \frac{1}{2}[\sin(x + y) + \sin(x - y)]$
- ▷ $\cos(x \pm y) = \cos x \cos y \mp \sin x \sin y$
- ▷ $\sin(x \pm y) = \sin x \cos y \pm \cos x \sin y$
- ▷ $\cos x + \cos y = 2 \cos \frac{x+y}{2} \cos \frac{x-y}{2}$
- ▷ $\cos x - \cos y = -2 \sin \frac{x+y}{2} \sin \frac{x-y}{2}$
- ▷ $\sin x \pm \sin y = 2 \sin \frac{x \pm y}{2} \cos \frac{x \mp y}{2}$
- ▷ $a \cos x + b \sin x = r \sin(x + \varphi) = r \cos(x - \psi),$
 $r = \sqrt{a^2 + b^2}, \sin \varphi = \frac{a}{r}, \cos \varphi = \frac{b}{r}, \sin \psi = \frac{b}{r}, \cos \psi = \frac{a}{r}$
- ▷ $\frac{d}{dx} \arcsin x = \frac{1}{\sqrt{1-x^2}}$
- ▷ $\frac{d}{dx} \arccos x = -\frac{1}{\sqrt{1-x^2}}$
- ▷ $\frac{d}{dx} \arctan x = \frac{1}{1+x^2}$
- ▷ $\frac{d}{dx} \operatorname{arccot} x = -\frac{1}{1+x^2}$

Hyperbolic identities :

- ▷ $\sinh x = -\sinh(-x) = \pm \sqrt{\cosh^2 x - 1} = \pm \sqrt{\frac{1}{2}(\cosh 2x - 1)} = \frac{e^x - e^{-x}}{2}$
- ▷ $\cosh x = \cosh(-x) = \sqrt{\sinh^2 x + 1} = \sqrt{\frac{1}{2}(\cosh 2x + 1)} = 2 \cosh^2 \frac{x}{2} - 1 = \frac{e^x + e^{-x}}{2}$
- ▷ $\tanh x = \frac{\sinh x}{\cosh x} = \frac{e^x - e^{-x}}{e^x + e^{-x}}$
- ▷ $\operatorname{coth} x = \frac{\cosh x}{\sinh x} = \frac{e^x + e^{-x}}{e^x - e^{-x}}$

- ▷ $\cosh^2 x - \sinh^2 x = 1$
- ▷ $\cosh x + \sinh x = e^x$
- ▷ $\cosh x - \sinh x = e^{-x}$

Exponents :

- ▷ $e^{\ln x} = x$
- ▷ $\frac{e^x}{e^y} = e^{x-y}$
- ▷ $e^x e^y = e^{x+y}$
- ▷ $(e^x)^\alpha = e^{\alpha x}$

Logarithms :

- ▷ $\ln e^x = x$
- ▷ $\ln \frac{x}{y} = \ln x - \ln y$
- ▷ $\ln \alpha x = \ln \alpha + \ln x$
- ▷ $\ln x^\alpha = \alpha \ln x$

Extension to series :

- ▷ $\sin x = x - \frac{x^3}{3!} + \frac{x^5}{5!} - \dots + (-1)^n \frac{x^{2n+1}}{(2n+1)!} + \dots$
- ▷ $\cos x = 1 - \frac{x^2}{2!} + \frac{x^4}{4!} - \frac{x^6}{6!} + \dots + (-1)^n \frac{x^{2n}}{(2n)!} + \dots$
- ▷ $e^x = 1 + x + \frac{x^2}{2!} + \frac{x^3}{3!} + \dots + \frac{x^n}{n!} + \dots$
- ▷ $e^{j\beta \cos z} = \sum_{k=-\infty}^{\infty} j^k J_k(\beta) e^{jkz}$
- ▷ $\cos(\beta \sin z) = J_0(\beta) + 2 \sum_{k=1}^{\infty} J_{2k}(\beta) \cos 2kz$
- ▷ $\cos(\beta \cos z) = J_0(\beta) + 2 \sum_{k=1}^{\infty} (-1)^k J_{2k}(\beta) \cos 2kz$
- ▷ $\sin(\beta \sin z) = 2 \sum_{k=0}^{\infty} J_{2k+1}(\beta) \sin(2k+1)z$
- ▷ $\sin(\beta \cos z) = 2 \sum_{k=0}^{\infty} (-1)^k J_{2k+1}(\beta) \cos(2k+1)z$
- ▷ $\ln(1+x) = \sum_{n=1}^{\infty} \frac{(-1)^{n+1}}{n} x^n = x - \frac{x^2}{2} + \frac{x^3}{3} - \dots \quad , \quad |x| < 1$

Series :

$$\triangleright \sum_{n=0}^{N-1} x^n = \frac{1-x^N}{1-x}, \quad x \neq 1 \quad (\text{by geometric progression})$$

$$\triangleright \sum_{n=0}^{N-1} e^{\alpha n} = \frac{1-e^{\alpha N}}{1-e^{\alpha}}$$

$$\triangleright \sum_{n=0}^{\infty} x^n = \frac{1}{1-x}, \quad |x| < 1$$

$$\triangleright \sum_{k=1}^{\infty} \frac{\sin^2(k\pi/q)}{k^2} = \frac{\pi^2(q-1)}{2q^2}$$

Indefinite integrals :

$$\triangleright \int f'(x)g(x)dx = f(x)g(x) - \int f(x)g'(x)dx \quad (\text{integration by parts})$$

$$\triangleright \int f(x)dx = \int f[g(y)]g'(y)dy \quad [x = g(y)] \quad (\text{change of variable})$$

$$\triangleright \int \frac{dx}{x} = \ln|x|$$

$$\triangleright \int \frac{x+a}{x+b}dx = x + (a-b)\ln|x+b|$$

$$\triangleright \int e^x dx = e^x$$

$$\triangleright \int \frac{e^{ax}}{x} dx = \text{Ei}(ax), \quad a \neq 0,$$

$$\triangleright \int a^x dx = \frac{a^x}{\ln a}$$

$$\triangleright \int \frac{dx}{x(ax^r+b)} = \frac{1}{rb} \ln \left| \frac{x^r}{ax^r+b} \right|$$

$$\triangleright \int x e^{\alpha x} dx = e^{\alpha x} \left(\frac{x}{\alpha} - \frac{1}{\alpha^2} \right)$$

$$\triangleright \int x^2 e^{\alpha x} dx = e^{\alpha x} \left(\frac{x^2}{\alpha} - \frac{2x}{\alpha^2} + \frac{2}{\alpha^3} \right)$$

$$\triangleright \int x^\lambda e^{\alpha x} dx = \frac{1}{\alpha} x^\lambda e^{\alpha x} - \frac{\lambda}{\alpha} \int x^{\lambda-1} e^{\alpha x} dx$$

$$\triangleright \int \frac{1}{x} e^{\alpha x} dx = \text{Ei}(\alpha x) \quad [\alpha \neq 0]$$

$$\triangleright \int \frac{1}{\sqrt{x}} e^{-\alpha x} dx = \sqrt{\frac{\pi}{\alpha}} \text{erf}(\sqrt{\alpha x}) \quad [\alpha > 0]$$

$$\triangleright \int \frac{e^x}{x^2 + \alpha^2} dx = \frac{1}{\alpha} \text{Im}[e^{j\alpha} \text{Ei}(x - j\alpha)]$$

$$\triangleright \int x e^{-ax^2} dx = -\frac{1}{2a} e^{-ax^2}$$

$$\triangleright \int x^2 e^{-ax^2} dx = -\frac{1}{2a} x e^{-ax^2} + \frac{\sqrt{\pi}}{4a^{3/2}} \text{erf}(ax)$$

$$\triangleright \int x^3 e^{-ax^2} dx = -\frac{ax^2+1}{2a^2} e^{-ax^2}$$

$$\triangleright \int x e^{-a^2 x^2 + bx} dx = \frac{1}{a^2} e^{\frac{b^2}{4a^2}} \left(\frac{b}{2a} \int e^{-t^2} dt + \int t e^{-t^2} dt \right), \quad t = ax - \frac{b}{2a}$$

$$\triangleright \int e^{-(ax^2 + bx + c)} dx = \frac{1}{2} \sqrt{\frac{\pi}{a}} e^{\frac{b^2 - 4ac}{4a}} \operatorname{erf} \left(x\sqrt{a} + \frac{b}{2\sqrt{a}} \right)$$

$$\triangleright \int \sin x dx = -\cos x$$

$$\triangleright \int \cos x dx = \sin x$$

$$\triangleright \int x \begin{Bmatrix} \sin x \\ \cos x \end{Bmatrix} dx = \begin{Bmatrix} \sin x \\ \cos x \end{Bmatrix} \mp x \begin{Bmatrix} \cos x \\ \sin x \end{Bmatrix}$$

$$\triangleright \int \sin^2 x dx = -\frac{1}{4} \sin 2x + \frac{x}{2}$$

$$\triangleright \int \cos^2 x dx = \frac{1}{4} \sin 2x + \frac{x}{2}$$

$$\triangleright \int \sin^3 x dx = \frac{1}{12} \cos 3x - \frac{3}{4} \cos x$$

$$\triangleright \int \cos^3 x dx = \frac{1}{12} \sin 3x + \frac{3}{4} \sin x$$

$$\triangleright \int \sin^4 x dx = \frac{3x}{8} - \frac{1}{4} \sin 2x + \frac{1}{32} \sin 4x$$

$$\triangleright \int \cos^4 x dx = \frac{3x}{8} + \frac{1}{4} \sin 2x + \frac{1}{32} \sin 4x$$

$$\triangleright \int \frac{dx}{a+b \cos x} = \frac{2}{\sqrt{a^2-b^2}} \arctan \frac{\sqrt{a^2-b^2} \tan \frac{x}{2}}{a+b} \quad , \quad [a^2 > b^2]$$

$$= \frac{1}{\sqrt{b^2-a^2}} \ln \frac{\sqrt{b^2-a^2} \tan \frac{x}{2} + a + b}{\sqrt{b^2-a^2} \tan \frac{x}{2} - a - b} \quad , \quad [a^2 < b^2]$$

$$\triangleright \int \frac{dx}{a+b \sin x} = \frac{2}{\sqrt{a^2-b^2}} \arctan \frac{a \tan \frac{x}{2} + b}{\sqrt{a^2-b^2}} \quad , \quad [a^2 > b^2]$$

$$= \frac{1}{\sqrt{b^2-a^2}} \ln \frac{a \tan \frac{x}{2} + b - \sqrt{b^2-a^2}}{a \tan \frac{x}{2} + b + \sqrt{b^2-a^2}} \quad , \quad [a^2 < b^2]$$

$$\triangleright \int \operatorname{erf}(ax) dx = x \operatorname{erf}(ax) + \frac{1}{a\sqrt{\pi}} e^{-a^2 x^2}$$

$$\triangleright \int e^{ax} \cos bx dx = \frac{e^{ax}}{a^2 + b^2} (a \cos bx + b \sin bx)$$

$$\triangleright \int e^{ax} \sin bx dx = \frac{e^{ax}}{a^2 + b^2} (a \sin bx - b \cos bx)$$

Definite integrals :

$$\triangleright \int_{-\infty}^{\infty} \frac{\sin \alpha x}{x} dx = \pi$$

$$\triangleright \int_{-\infty}^{\infty} e^{-\alpha x^2} dx = \sqrt{\frac{\pi}{\alpha}}$$

$$\triangleright \int_0^x e^{a^2 t^2} dt = \frac{\sqrt{\pi}}{2a} \operatorname{erfi}(ax)$$

$$\triangleright \int_{-\infty}^{\infty} x^2 e^{-\alpha x^2} dx = \sqrt{\pi} \alpha^{-3/2}$$

$$\triangleright \int_0^{\infty} \frac{\sin \alpha x}{x} dx = \frac{\pi}{2} \operatorname{sgn} \alpha$$

$$\triangleright \int_0^{\infty} \frac{\sin^2 \alpha x}{x^2} dx = \frac{\pi \alpha}{2}$$

$$\triangleright \int_{-\infty}^{\infty} \frac{\sin^4 \alpha x}{x^2} dx = \frac{\pi \alpha}{2}$$

$$\triangleright \int_0^{\infty} \frac{dx}{\alpha^2 + x^2} = \frac{\pi}{2\alpha}$$

$$\triangleright \int_0^{\infty} x^{\alpha-1} \sin bx dx = \frac{\Gamma(\alpha)}{b^\alpha} \sin \frac{\alpha\pi}{2}$$

$$\triangleright \int_0^{\infty} \sin bx dx = \frac{1}{b}$$

$$\triangleright \int_{-\infty}^{\infty} \frac{\sin x}{x(x-\alpha)} dx = \frac{\pi}{\alpha} (\cos \alpha - 1), \quad \alpha \text{ is real}$$

$$\triangleright \int_{-\infty}^{\infty} \frac{\cos(ax)}{b^2 - x^2} dx = \frac{\pi}{2b} \sin(ab), \quad a, b > 0$$

Inequalities :

$$\triangleright x(t) \leq C + \int_{t_0}^t \gamma(\tau) x(\tau) d\tau \leq C e^{\int_{t_0}^t \gamma(\tau) d\tau} \quad (\text{Gronwall-Bellman})$$

Special functions :

$$\triangleright \operatorname{erf}(x) = \frac{2}{\sqrt{\pi}} \int_0^x e^{-t^2} dt \quad (\text{Error function})$$

$$\triangleright \operatorname{erfi}(x) = -j \operatorname{erf}(jx) = \frac{2}{\sqrt{\pi}} \int_0^x e^{t^2} dt \quad (\text{Imaginary error function})$$

$$\triangleright \operatorname{Ei}(x) = - \int_{-x}^{\infty} \frac{e^{-t}}{t} dt = \int_{-\infty}^x \frac{e^t}{t} dt \quad [x < 0] \quad (\text{Exponential-integral})$$

$$\triangleright \operatorname{Ei}(x) = e^x \left[\frac{1}{x} + \int_0^{\infty} \frac{e^{-t}}{(x-t)^2} dt \right] \quad [x > 0] \quad (\text{Exponential-integral})$$

$$\triangleright J_n(z) = \frac{1}{2\pi} \int_{-\pi}^{\pi} e^{-j(n\vartheta - z \sin \vartheta)} d\vartheta \quad (\text{Bessel function of the first kind})$$

$$\triangleright T_n(\omega) = \begin{cases} \cos(n \arccos \omega), & |\omega| \leq 1 \\ \cosh(n \operatorname{arccosh} \omega), & |\omega| > 1 \end{cases} \quad (\text{Chebyshev polynomials})$$

References

1. Baskakov S. I., *Radio Circuits and Signals*, 2nd ed., Moscow, Vysshaya Shkola, 1988 (in Russian).
2. Bellman, R., *Introduction to Matrix Analysis*, McGraw-Hill, New York, 1960.
3. Bello, Ph., Time-Frequency Duality, *IEEE Trans. Inform. Theory*, IT-10, 18-33, Jan. 1964.
4. Bensoussan, A., Da Prato, G., Delfour, M.C., and Mitter, S.K., *Representation and Control of Infinite Dimensional Systems*, Birkhduser, Boston, 1993.
5. Black H.S., Stabilized feedback amplifiers, *Bell System Techn. J.*, 13, 1-18, 1934.
6. Bogoliubov N.N., and Mitropolskiy Yu.A., *Asymptotic Methods in the Theory of Non-Linear Oscillations*, New York, Gordon and Breach, 1961.
7. Boyd, S., Chua, L.O., and Desoer, C.A., Analytical foundations of Volterra series, *IMA J. of Mathematical Control & Information*, 1, 243-282, 1984.
8. Carmen, C., *Ordinary Differential Equations with Applications*, Springer-Verlag, New York, 1999.
9. Chen, Chi-T., *Linear System Theory and Design*, Oxford Univ. Press, New-York, 1999.
10. Chen, Wai-K., *Passive and Active Filters, Theory and Implementations*, John Wiley & Sons, New York, 1986.
11. Chua L.O., Komuro M., and Matsumoto T., The Double Scroll Family, *IEEE Trans. Circuits and Systems-I*, 33, 11, 1072-1118, 1986.
12. Como M., Grimaldi A., *Theory of Stability of Continuous Elastic Structure*, CRC Press, Boca Raton, Florida, 1995.
13. D'Angelo, A., *Linear Time-Varying Systems: Analysis and Synthesis*, Allyn and Bacon, Boston, 1970.
14. Dewilde, P., van der Veen, A.-J., Wilde P., *Time-Varying Systems and Computations*, Kluwer, Boston, 1998.
15. Director, S.W., and Rohrer, R.A., *Introduction to Systems Theory*, McGraw-Hill, New York, 1972.
16. Doyle J.C., Francis B.A., Tannenbaum A.R., *Feedback Control Theory*, Macmillan Publishing Company, New York, 1992.
17. Dulac, H., Sur les cycles limites, *Bulletin de la S. M. F.*, 51, 45-188, 1923.
18. Dulac, H., *Signals, Systems, and Transforms*, 3rd ed., Prentice Hall, New-York, 2002.

19. Gelb, A., and Velde, W.E., *Multiple-Input Describing Functions and Nonlinear System Design*, McGraw-Hill, New York, 1968.
20. Gil M.I., *Explicit Stability Conditions for Continuous Systems: A Functional Analytic Approach*, Springer, Berlin, 2005.
21. Gonorovsky I. S., *Radio Circuits and Signals*, 2nd ed., Moscow, Radio i sviaz, 1986 (in Russian).
22. Guckenheimer, J., Holmes, P., *Nonlinear Oscillations, Dynamical Systems, and Bifurcations of Vector Fields*, 7th printing, Springer-Verlag, New-York, 2002.
23. Erikson K.R., Fry F.J., and Jones J.P., Ultrasound in Medicine – A Review, *IEEE Trans. Sonics and Ultrasonics*, SU-21, 3, 1974.
24. Floquet, G., Sur les quations differentielles lineaires coefficients priodiques, *Ann. cole Norm. Sup.* 12, 47–88, 1883.
25. Gantmacher, F.R., *Applications of the Theory of Matrices*, translated by J.I. Brenner, Wiley (Interscience), New York, 1959.
26. Hayfeh A.H., and Mook D.T., *Nonlinear Oscillations*, New York, John Wiley & Sons, 1999.
27. Haykin, S., and Van Veen, B., *Signals and Systems*, 2nd ed., New-York, Wiley & Sons, 2002.
28. Hilborn, R., *Chaos and Nonlinear Dynamics: An Introduction for Scientists and Engineers*, 2nd ed., Oxford University Press, New-York, 2004.
29. Hitz, K.L., Fortmann, T.E., *An Introduction to Linear Control Systems*, Marcel Dekker, New York, 1997.
30. Hsu, H. P., *Signals and Systems*, New-York, McGraw-Hill, 1995.
31. Ichikawa, A., Katayama, H., *Linear Time Varying Systems and Sampled-Data Systems*, Springer-Verlag, London, 2001.
32. Jordan D.W., and Smith P., *Nonlinear Ordinary Differential Equations: An Introduction to Dynamical Systems*, 3rd ed., New York, Oxford Univ. Press, 1999.
33. Kahn P.B., *Mathematical Methods for Scientists and Engineers: Linear and Nonlinear Systems*, New York, John Wiley & Sons, 1990.
34. Kailath, T., *Sampling Models for Linear Time-Variant Filters*, Techn. Report 352, MIT, Cambridge, MA, May 25, 1959.
35. Kalman, R.E., A new approach to linear filtering and prediction problems, *Trans. ASME – J. of Basic Engineering*, D, 35–45, 1960.
36. Khalil H.K., *Nonlinear systems*, Prentice-Hall, 3rd. Edition, Upper Saddle River, 2002.
37. Korn, G. A., and Korn, T. M., *Mathematical Handbook for Scientists and Engineers*, McGraw-Hill, New-York, 1961.
38. Lepage, W. R., *Complex Variables and the Laplace Transform for Engineers*, Dover Publ., New-York, 1961.
39. Lillesand T.M., and Kiefer R., *Remote Sensing and Image Interpretation*, 3rd ed., New York, John Wiley, 1993.
40. Lur'e, A.I., and Postnikov, V.N., On the theory of stability of control systems, *Applied Mathematics and Mechanics*, 8, 3, 246–248, 1944.
41. *Low-Power Design Techniques and CAD for Analog and RF Integrated Circuits*, Edited by P. Wambacq, G. Gielen, and J. Gerrits, Kluwer, Boston, 2001.
42. Magnus, K., *Schwingungen: Eine Einführung in die Theoretische Behandlung von Schwingungsproblemen*, B.G. Teubner, Stuttgart, 1976.
43. Manevitch L.I., Andrianov I.V., *Asymptotology: Ideas, Methods, and Applications*, Kluwer, Dordrecht, 2002.

44. Marmarelis, V. Z., *Nonlinear Dynamic Modeling of Physiological Systems*, New-Jersey, John Wiley & Sons, Inc., 2004.
45. Melnikov, V. K., On the stability of the center for time periodic perturbations, *Trans. Moscow Math.*, 12, 1–57, 1963.
46. Morgan, D. P., *Surface-Wave Devices for Signal Processing*, Elsevier, Amsterdam, 1991.
47. Oppenheim, A. V., Willsky, A. S., and Hamid Nawab S., *Signals and Systems*, 2nd ed., New-York, Prentice-Hall, 1994.
48. Peters, M.A., Iglesias P., *Minimum Entropy Control for Time-Varying Systems*, Birkhäuser, Boston, 1997.
49. Polderman, J.W., Mareels, I., *Adaptive Systems: an Introduction*, Birkhäuser, Boston, 1996.
50. Popov, V.M., Absolute stability of nonlinear systems of automatic control, *Automation and Remote Control*, 22, 857–875, 1962.
51. Popov, V.M., *Hyperstability of Control Systems*, Springer-Verlag, New York, 1973.
52. Rabiner, L.R., and Gold, B., *Theory and Applications fo Digital Signal Processing*, Prentice-Hall, Englewood Cliffs, New Jersey, 1975.
53. Richards, J.A., *Analysis of Periodically Time-Varying Systems*, Springer-Verlag, New York, 1983.
54. Rickard, S.T., Balan, R.V., Poor, H.V., and Verdú, S., Canonical time-frequency, time-scale, and frequency-scale representations of time-varying channels, *Commun. in Inform., and Systems*, 5, 2. 197–226, 2005.
55. Rugh W. J., *Nonlinear System Theory: The Volterra/Wiener Approach*, Baltimore, John Hopkins Univ. Press, 1981.
56. Samarskiy, A.A., and Gulin, A.V., *Numerical Methods*, Nauka, Moscow, 1989.
57. Salt, D., *Hy-Q Handbook of Quartz Crystal Devices*, Van Nostrand Reinhold, Wokingham, 1987.
58. Sandberg, I.W., On the response of nonlinear control systems to periodic input signals, *Bell Syst. Tech. J.*, 43, 1964.
59. Sandberg, I.W., A perspective on system theory, *IEEE Trans. Circuits and Systems*, CaS-31, 1, 88–103, 1984.
60. Sastry, S., *Nonlinear Systems: Analysis, Stability and Control*, Springer-Berlag, New York, 1999.
61. Schetzen, M., *The Volterra and Wiener Theories of Nonlinear Systems*, Wiley & Sons, New York, 1980 (in Russian).
62. Shakhtarin, B., *Analysis of Synchronization Systems by Averaging Method*, Radio i zviyaz, Moscow, 1999 (in Russian).
63. Shmaliy, Yu. S., *Continuous-Time Signals*, Springer, Dordrecht, 2006.
64. Shmaliy, Yu.S., Dynamic distortions in frequency-modulated self-oscillatory systems, *Radioelectronics and Communications Systems*, 29, 12, 40–44, 1986.
65. Shmaliy, Yu.S., Spikes in the dynamic modulation characteristics of a precision frequency-modulated quartz sustained oscillator, *Telecommunications and Radio Engineering*, Part 2 (*Radio Engineering*), 46, 8, 86–90, 1991.
66. Sirobaba, Ya.Ya., Teplitskiy, M.E., and Shakhov, V.O., *Fundamentals of Radio Engineering Measurements of Parameters of Movement*, MO USSR, Moscow, 1971 (in Russian).
67. Sokolinskiy, V.G., and Sheinkman, V.G., *Frequency and Phase Modulators and Manipulators*, Radio i Zviyaz, Moscow, 1983 (in Russian).

68. Soliman, S. S., and Srinath, M. D., *Continuous and Discrete Signals and Systems*, New-York, Prentice-Hall, 1990.
69. Sontag, E.D., Smooth stabilization implies coprime factorization, *IEEE Trans. Automatic Control*, AC-34, 435-443, 1989.
70. Sontag, E.D., and Wang, Y., Notions of input to output stability, *Systems and Control Letters*, 38, 4, 235–248. 1999.
71. Stavroulakis, P., *Third Generation Mobil Telecommunication Systems: UMTS and IMT-2000*, Springer-Berlag, New-York, 2001.
72. Stensby, J., *Phase-locked loops: Theory and applications*, CRC Press, Boston, 1997.
73. Tarantovich, T.M., and Khon'kin, V.M., Dynamics of a two-frequency self-excited oscillator with "stiff" excitation, *Radiophysics and Quantum Electronics*, 16, 2, 165–168, 1973.
74. Taylor, F. J., *Principles of Signals and Systems*, New-York, McGraw-Hill, 1994.
75. Verhulst, F., *Nonlinear Differential Equations and Dynamic Systems*, Springer-Verlag, Berlin, 1990.
76. Volterra, V., *Theory of Functionals and of Integral and Integro-Differential Equations*, Dover Publications, Inc., New York, 1959.
77. Vukić Z., Kuljača L., Donlagić D., and Tešnjak S., *Nonlinear Control Systems*, New York, Marcel Dekker, 2003.
78. Umez-Eronini, E.I., *System Dynamics and Control*, Tomson-Engineering, 1998.
79. Wiener, N. *Response of a Non-Linear Device to Noise*, Report No. 129, Radiation Laboratory, M.I.T., Cambridge, MA, Apr. 1942.
80. Zadeh, L.A., Circuits analysis of linear varying-parameter networks, *J. Applied Physics*, 21, 1171-1177, 1950.
81. Zames, G., Realizability conditions for nonlinear feedback systems, *IEEE Trans. Circuit Theory*, Ct-11, 186–194, 1964.

Index

- κ -factor, 571
- s domain, 315, 319, 334
- Acoustic wave, 8
 - bulk (BAW), 267
 - surface (SAW), 267
- Adder, 188, 407
- Addition, 30, 32
- Additivity, 16
- AM radio, 251
- Amplifier, 37, 263, 266, 321
 - exponential, 34
 - feedback, 320
 - gain, 267
 - inverting, 325
 - power, 498
 - regenerative, 330
 - resonant, 264, 266
 - square, 33, 58, 527
 - transistor, 264, 266, 323
- Amplitude, 195, 265, 407
 - modulated, 83
 - peak, 7
 - slowly changing, 72
 - unmodulated, 83
- Amplitude modulation function (AMF),
 - 545, 548, 555, 566
 - magnitude, 546, 560, 571
 - phase, 546, 560, 571
- Amplitude scaling, 28, 32, 162
- Anharmonic, 269
- Antenna, 251
- Approximation, 61
 - exponential, 433
 - polynomial, 61
 - the first order, 71, 74, 77, 78, 83, 487
 - the second order, 71, 76
- Associativity, 159, 367
- Asymptotic method, 70, 74, 78, 80, 83
- Attenuation, 257, 266, 271, 272, 274
 - coefficient, 260
 - parameter, 334, 338
- Attractor, 130, 135, 506
 - n -scroll, 506
 - butterfly, 135
 - map sink, 130
 - regular, 130
 - strange, 130
- Autoregressive (AR) model, 52, 169
- Averaging, 66
 - generalized method, 67
- Backlash, 461
- Bandwidth, 77, 183, 226, 257, 259–261,
 - 263, 266, 328, 352, 364, 378, 409,
 - 474, 551
 - sides, 260
- Bendixson’s criterion, 126, 127, 409, 411
- Bias voltage control, 520, 521
- Bifurcation, 131
 - diagram, 132
 - parameter, 132
 - theory, 131, 134
 - typical types, 134
- Block diagram, 175, 188, 196, 201, 206,
 - 209, 313, 378, 380, 384, 386
 - the first direct (canonic) form, 189,
 - 314, 379

- the second direct (canonic) form, 192, 315, 381
- Bode plot, 244, 257, 260, 325, 328
- Bogoliubov-Mitropolskiy model, 543
- Brownian motion, 447
- Cassinian oval, 140
- Causality, 163, 172, 292, 445, 530
- Channel, 97, 263, 320, 531
 - amplification, 321
 - LTI, 327
 - LTV, 359
 - quadrature, 407
 - RF, 321
 - wireless, 414
- Chaos theory, 130
- Chaotic cell, 505
- Chaotic orbit, 134
- Chaotic system
 - cellular neural network, 505
 - Chua's circuit, 505
 - Lorenz's, 135
 - Lur's, 505
 - n-scroll circuit, 505
- Characteristic exponent, 400, 402, 411
- Characteristic multiplier, 400, 402
- Circuit
 - electrical, 175, 255, 307, 375
 - LTV electrical, 378
 - RC, 251, 256, 309, 376
 - resonant, 266, 407, 414
 - RL, 256, 309, 311
 - RLC, 252, 253, 260, 312, 385
 - selective, 252
- Clock and data recovery, 506
- Closed loop, 562
 - control, 209
 - LTI, 206
 - stability, 207
- Coefficients
 - time-varying, 74, 77
- Commutativity, 158, 442
- Comparator, 36
- Comparison, 36
- Continuous-time
 - autoregressive moving average (CARMA) model, 52, 169
 - system, 2, 134
- Controllability, 394
- Controllability matrix, 217
- Controllable canonic form, 215
- Conversion
 - amplitude-to-frequency, 10
 - amplitude-to-phase, 73, 77, 549
 - phase-to-amplitude, 73
- Convolution, 49, 58, 153, 163, 167, 168, 178, 240, 288, 289, 357, 441, 453, 455
 - Duhamel's principle, 154
 - general, 51, 57, 349
 - generalized, 58, 437, 442
- Critical damping, 182, 183
- Cross-correlation, 161
- Crystal, 267
 - media, 267
 - surface, 267
- Crystal resonator, 571
- Damping factor, 179, 183, 185
- Degree of freedom, 142
- Demodulation, 506
- Demodulator, 3, 37
 - asynchronous, 579
 - synchronous, 497
- Density
 - conservative, 141
 - integral invariant, 141
- Describing function
 - cosine input, 459
 - sinusoidal input, 464
- Describing function (DF), 85, 458, 465
 - cosine input, 86
 - method, 85
 - sinusoidal input, 86
- Detector, 10, 406
 - synchronous, 405, 406, 520, 523
- Differential equation
 - method, 60
- Differentiator, 15
- Direct problem, 165
- Dirichlet conditions, 88, 276, 279
- Discontinuity, 451
- Dissipation rate, 112
- Distortionless transmission, 249
- Distributivity, 158, 366, 443, 529
- Divided differences, 429
- Doppler shift, 359
- Doppler-delay spread function, 361

- Double harmonic balance, 81, 552
- Drive level dependence (DLD), 474
- Duality, 216
- Duhamel's integral, 154
- Dynamic systems theory, 119

- Eigenfrequency, 180
- Eigenfunction, 171
- Eigenvalue, 122, 125, 171, 400–402
 - periodic, 411
 - semiperiodic, 411
- Eigenvector, 122, 125, 126
- Electric charge, 376, 407
- Electric potential, 376
- Energy, 109, 408, 414
- Envelope, 248
- Equalizer, 496
- Equation
 - Bernoulli's, 470, 472, 538
 - characteristic, 108, 121, 124, 171, 179, 226, 322, 490, 495
 - Mathieu's, 409, 411, 413
 - voltage balance, 311, 377
- Equivalent linearization, 66, 77
- Equivalent scheme, 266
- Euler formula, 48, 303, 415
- Evenness, 243
- Excitation, 413
 - biharmonic, 480, 486
 - soft, 484

- Feedback, 207, 321, 328, 504, 562
 - negative, 26, 319, 320
 - positive, 26, 319, 320
- Feedback matrix, 206, 208, 210
- Feedback system
 - LTI, 206
- Figure of merit, 270
- Filter, 37, 96, 251, 254, 260, 261, 264
 - all-pass, 251, 252
 - anti-hum, 254
 - anti-presence, 254
 - band-elimination, 253
 - band-pass (BP), 252, 264, 499, 501, 527, 577
 - band-rejection (BR), 253
 - band-stop, 253, 254
 - band-suppression, 253
 - bass-cut, 251
 - Bessel, 340
 - BP ideal (perfect), 252
 - BR ideal (perfect), 253
 - Butterworth, 333–335, 339
 - Chebyshev, 333, 336
 - elliptic, 340
 - high-cut, 251
 - high-pass (HP), 175, 251, 252, 254, 258
 - hiss, 251
 - HP ideal (perfect), 252
 - ladder, 273
 - lattice, 272
 - low-cut, 251
 - low-pass (LP), 175, 249, 251–253, 255, 258, 273, 406, 508, 527, 536
 - LP ideal (perfect), 251, 254
 - narrow band-pass, 254
 - notch, 253, 254, 261
 - optimal, 254
 - order, 334, 338
 - RC, 256, 497
 - RL, 256
 - rumble, 251
 - selective, 254
 - T-notch, 254
 - tracking, 349, 362
 - treble cut, 251
 - voltage controlled, 536
- Filter approximation, 333
- Filtering, 250
- Fixed point
 - center, 132
 - center (neutral), 122
 - focus, 122
 - node, 122, 124
 - saddle, 122, 124, 132, 142, 146
 - spiral, 122, 124, 126
- Floquet exponent, 400
- Floquet's theory, 398, 400, 402, 411
- Fourier series, 79, 84, 403, 609
- Fractal, 137
- Frequency, 408
 - carrier, 10, 402, 405, 406
 - central, 253, 275, 527
 - cut-off, 251–253, 256, 257, 328, 334, 337, 339
 - gain crossover, 325
 - instantaneous, 565

- intermediate, 404
- linear drift rate, 195
- mean cut-off, 253
- modulated, 546, 565
- modulating, 408
- modulation, 84, 403, 527
- natural (angular), 74, 179, 183, 248, 409
- parallel resonance, 270
- phase crossover, 325
- pumping, 412
- resonance, 260, 261, 263, 267, 407, 474
- resonant, 413
- series resonance, 270
- carrier, 7
- Frequency divider, 414, 506
- Frequency domain, 239, 246, 357, 359, 398, 531
- kernel, 454
- Frequency drift, 11
- Frequency instability, 11
- Frequency modulation factor, 546
- Frequency modulation function (FMF), 546, 549, 555, 566
- magnitude, 546, 573
- phase, 546, 573
- Frequency offset, 11, 269, 412
- Frequency response, 46, 54, 93, 239, 240, 245, 249, 253, 255, 256, 259, 261, 264, 266, 272, 323, 328, 331, 334, 356, 510
- time-varying, 356, 375, 533, 537
- two-dimensional (bi-frequency), 357, 361
- Frequency tracking, 506
- Frequency transformation, 402
- Frequency transformer, 403, 405
- Full-wave rectifier, 36
- Function
 - complex exponent, 276
 - cosine truncated, 303
 - Dirac delta, 43, 228, 302, 359, 532
 - exponential truncated, 303
 - general complex exponent, 277
 - generalized energy, 109
 - Mathieu's, 411
 - positive definite, 109, 112
 - sinc, 254
 - sinusoidal truncated, 303
 - unit step, 302
- Fundamental matrix, 387, 390, 392, 399, 401, 402
- Fundamental solution, 400
- Gain constant, 249
- Gain factor, 321
- Gain stability margin, 325
- Gaussian waveform, 7
- General superposition inntegral, 350
- Generalized detuning, 261–263
- Geometric mean, 253
- Gibbs phenomenon, 449
- Grönwall-Bellman inequality, 107
- Group delay, 247, 248, 250, 255, 256, 259, 334, 339
- Half bandwidth, 84
- Half-wave rectifier, 36
- Hamilton's equations, 142
- Hamiltonian, 142
- Hammerstein system, 439, 496, 497, 499–502, 504, 562, 578
- closed loop control, 576
- generalized, 496
- Harmonic balance, 66, 78, 83, 411, 475, 552, 558
- Harmonic pumping, 409
- Harmonics, 80
- Heterodyne, 405
- High-quality audio coding, 328
- Homogeneity, 159, 366, 444, 451, 529
- Hurwitz, 577
- Hurwitz determinant, 322
- Hurwitz matrix, 219, 500, 506
- Hysteresis, 426
- Ideal differentiation, 30, 32
- Ideal integration, 29, 32
- Identity matrix, 56
- Impedance, 256, 260, 264, 266, 269
- characteristic, 263
- collector-emitter, 264
- phase, 261, 263, 270
- total, 261, 263, 270
- Impulse response, 44, 96, 153, 161, 164, 173, 176, 182, 183, 228, 240, 250–254, 292, 364

- generalized, 58
- matrix, 97, 167
- time-varying, 51, 57, 97, 349, 351, 359, 362, 367, 372, 373, 391, 393, 527, 533
- time-varying modified, 352, 361, 362
- Inconvertibility, 369
- Initial condition, 171, 187, 196, 228, 318
- Input matrix, 54, 198, 204, 318, 384, 386, 495
- Integration factor, 175, 222, 386, 391
- Integrator, 15, 61
 - ideal, 189, 327
- Interdigital transducer (ITD), 274, 275
- Intermediate (IF), 402
- Interpolation, 523
 - Lagrange, 427, 523
 - Newton, 429, 523
 - Nyquist-Kotelnikov-Shannon, 254
- Interpolation polynomial, 428
- Inverse problem, 165
- Isocline, 121

- Jacobian, 65, 121, 123, 126, 144, 495
- Josephson junction, 510

- Kalman decomposition, 217
- Krylov-Bogoliubov method, 66, 482, 487
- Krylov-Bogoliubov-Mitropolskiy method, 70

- Laplace domain kernel, 454
- Laplace transform
 - capacitance, 309
 - electric current, 307
 - electric voltage, 307
 - inductance, 309
 - resistor, 307
- Least upper bound, 93
- Lemniscate, 140
- Limit cycle, 126, 127, 145, 544
 - rough, 144
 - stable, 126, 127
 - unstable, 126
- Limitation, 37
- Linear asynchronously time-varying system, 364
- Linear parametric excitation, 407
- Linear parametric oscillator, 409
- Linear periodically time-varying (LPTV) system, 365, 396, 398, 399, 402, 407
 - stability, 401
- Linear synchronously time-varying system, 364
- Linearity, 159, 162, 172, 244, 286, 366
- Linearization, 61, 471, 577
 - analytical, 62
- Linearization technique, 65, 435
 - feedback, 65, 435
 - feedforward, 65, 435
 - nonlinear predistortion, 65, 436
- Lower sideband (LSB), 273
- LTI system, 499, 504
 - cascade, 266
 - narrowband, 264
 - of high order, 266
 - of the first order, 175, 254, 305
 - of the second order, 179, 260, 263, 306
- LTV system, 364, 371, 394
 - BIBO stability, 371, 393
 - generalized ODE, 378
 - in state space, 386
 - of the first order, 372
- Lur'e system, 502, 505, 506
 - control, 577
- Lyapunov, 218
 - exponent, 135, 137, 138, 400, 401
 - function, 108, 110, 111, 220, 221
 - the first (indirect) method, 105
 - the second (direct) method, 108, 110, 221, 503
 - theorem, 110
 - transformation of variables, 398, 399
- Magnetic flux, 377
- Magnitude response, 47, 239, 242, 245, 249, 255–257, 259, 262, 264, 267, 331, 333, 334, 337, 338, 476, 489
 - logarithmic, 244
 - rectangular, 251, 252
- Manifold, 146
- Matrix exponential, 223, 224, 226, 227
- Matrix theory overview, 593
- Measurement
 - distance, 4

- velocity, 5
- Melnikov integral, 147
- Memory, 162, 425
- Method
 - cover-up, 294, 295
 - electric circuits, 245
 - functional, 437
 - Lagrange of variation, 389
 - Melnikov's, 146
 - qualitative, 112, 119
 - quantitative, 43, 112
 - Volterra series, 437
- Method of expansion (perturbation method), 67
- Mixer, 407, 525
- Modes competition, 484
- Modulation, 290, 402, 408, 506
 - amplitude (AM), 3, 405
 - broadband, 85
 - frequency (FM), 3, 75, 405, 545
 - phase (PM), 3, 405
- Modulation factor, 403, 409, 414, 416, 566
- Modulation function
 - amplitude (AMF), 85
 - frequency (FMF), 84
- Modulation functions method, 84
 - fast modulation, 562
 - slow modulation, 544
- Modulator, 3, 37
- Monodromy matrix, 399
- Motion equation, 170, 474
- Motional
 - capacitance, 269, 474
 - inductance, 269, 474
 - resistance, 269, 474
- Moving average (MA) model, 52, 169
- Multifrequency network function, 532
- Multifrequency system function, 532
- Multivariate system function, 532
- Mutual inductance, 204

- Noble identity, 361
- Non-commutativity, 367, 529
- Nonlinear amplifier
 - classes, 34
- Nonlinear ODE, 470
 - linearized, 471
- Nonlinear periodically time-varying (NPTV) system, 542, 562
- Norm, 87
 - H_2 , 91, 92, 95
 - H_∞ , 93, 95
 - L_1 , 88
 - L_2 , 88
 - L_∞ , 89
 - L_p , 89
 - definition, 87
 - Euclidian, 92, 97
 - Frobenius, 92, 97
 - homogeneity, 87
 - positive definiteness, 87
 - positivity, 87
 - root-mean-square, 90
- Normed space, 87
- NTI system, 425
 - BIBO stable, 446
 - causal, 445
 - in state space, 495
 - memory, 504
 - memoryless, 468, 496, 499
 - noncausal, 445
 - stability, 472
- NTV system, 520
 - BIBO stable, 531
 - causal, 530
 - in state space, 574
 - memoryless, 520, 523
 - noncausal, 530
 - of the first order, 536
- Nuisance parameters, 536
- Nullcline, 121, 126
- Nyquist plot, 324, 326, 504

- Observability, 396
- Observability matrix, 216
- Observable canonic form, 216
- Observation equation, 54, 195, 197, 200, 202, 206, 208, 383, 390
- Observation matrix, 54, 198, 204, 216, 318, 384, 386
- Observation model, 198
- Oddness, 243
- Ordinarily differential equation (ODE),
 - 51, 168, 244, 371, 387, 470, 535
 - forced solution, 170, 172, 181, 374, 375

- general solution, 138
 - homogenous solution, 170, 180, 374, 375
 - linear, 51, 124
 - nonlinear, 63
 - nonlinear linearized, 65
 - operator, 170
 - solution, 304
 - weakly nonlinear, 79
- Oscillations, 407, 409, 414
 - forced, 490
 - harmonic, 74
- Oscillator, 10, 37, 111, 402, 520, 525, 562
 - Butler crystal, 569
 - Colpitts, 557
 - critically damped, 181
 - FM crystal, 557, 561, 571
 - frequency modulated (FM), 545, 563
 - harmonic, 477
 - harmonic synchronized, 486
 - linear, 409
 - Lorenz, 135
 - Mathieu, 411
 - modulated, 551
 - multifrequency, 486
 - oven controlled crystal (OCXO), 10
 - overdamped, 24, 181
 - quartz crystal, 267
 - Rayleigh, 107
 - reference, 10, 183
 - synchronized, 490
 - three-point, 557
 - underdamped, 24, 181
 - voltage controlled, 539, 575
 - voltage controlled crystal (VCXO), 504
- Output matrix, 54, 198, 204, 318, 384, 386
- Overdamping, 182, 183
- Overtone, 83

- Parallel resonance, 474
- Parallel resonant circuit, 260, 263, 264, 274
- Parametric amplification, 414
- Parametric demodulation, 405
- Parametric excitation, 407, 413, 414
- Parametric modulation, 404
- Parametric modulator, 404
- Parametric oscillations, 407
- Parametric resonance, 408
- Partial differential equation (PDE), 139, 140
- Passband, 271, 333, 335, 337
- Periodic orbit, 126, 411
- Phase, 77, 195, 408, 502
 - carrier, 407
 - difference, 99
 - linear drift rate, 195
 - modulo 2π , 242
 - nonstationary, 11
 - principle, 242
 - reference, 99
 - slowly changing, 72
 - trajectory, 132
- Phase delay, 247, 248, 250, 255, 256, 259
- Phase distortions, 246
- Phase locked loop (PLL), 37, 99, 406, 506, 510, 511
- Phase modulation factor, 547
- Phase plane, 112, 119, 120, 124, 126
- Phase portrait, 124, 142, 484
- Phase response, 47, 239, 242, 245, 248, 249, 255, 256, 259, 262, 264, 334, 339, 476
 - linear, 254
- Phase space, 119, 126
- Phase stability margin, 325
- Phase synchronization, 492
- Phase system, 100
- Phase tracking, 506
- Phase trajectory, 120, 124, 126, 140
 - closed, 126
 - heteroclinic, 128
 - homoclinic, 128, 129
- Phase wrapped, 242
- Physical realizability, 51
- Piezoelectric
 - crystal ladder filter, 272
 - effect, 267
 - filter, 267, 271
 - nonlinear filter, 473, 476
 - resonator, 267, 269, 557
 - structure, 267
 - substrate, 274
- Point

- equilibrium, 99, 100, 104, 108
 - fixed, 121, 139, 142
- Positive definite matrix, 220
 - symmetric, 221
- Power amplification, 34
- Product, 35, 83, 289, 452
- Proper ratio, 278

- Qualitative analysis, 119, 120
- Qualitative theory, 119
- Quality factor, 179, 261, 265, 269, 271, 330, 413
- Quartz oscillator clock, 267

- Radio frequency (RF), 274
 - transformer, 500
- Radio station, 252
- Range of existence, 271, 355, 362
- Rate of convergence, 102
- Receiver, 2, 9, 251, 502
 - coherent, 501
 - CW, 272
 - GPS timing, 12
 - radio, 252
 - superheterodyne, 402
- Rectangular pulse, 302
- Rectification, 36
- Region of convergence (ROC), 279, 280, 282, 286, 450
- Relay system, 465
- Resonator
 - crystal, 10
- Ripple, 333, 336, 337, 339
 - factor, 338
- Roll-off, 254, 266, 333, 336, 340
- Roughness, 131

- Saturation, 35, 463, 577
- SAW device, 273, 274
 - filter, 273, 275
 - oscillator, 273
 - resonator, 275
 - sensor, 273
 - transformer, 273
 - typical design, 274
- SAW energy, 275
- SAW propagation velocity, 274
- Scalar multiplier, 188
- Scaling property, 16

- Sensitivity
 - amplitude, 3
 - phase, 3
 - temperature, 10
 - frequency, 3
- Sensor, 10
- Separatrix, 124, 126, 146
- Series resonant circuit, 260, 263
- Shifting property, 177
- Signal
 - absolutely integrable, 88
 - carrier, 248, 527
 - causal, 163
 - energy, 89, 142
 - GPS timing, 12
 - message, 406
 - modulating, 407
 - noncausal, 163
 - pumping, 414
 - spurious, 321
 - total resources, 88
- Signal processing, 271
- Similarity transformation, 211, 213
- Slow time, 74, 77
- Solution
 - exponential, 141
 - harmonic, 412
 - periodic, 411, 475
 - semiperiodic, 411
- Spectral density, 242
 - magnitude, 242
 - phase, 242
- Spectral function, 359
- Splines, 429, 523
 - cubic, 431
- Spread function, 361
- Spurious
 - AM, 558, 564, 574
 - AM index, 544, 556, 560
 - FM, 564, 565, 574
 - FM index, 544
- Stability, 24, 95, 164, 218, 291, 319, 401, 409, 446, 483, 490, 494, 500, 531
 - asymptotic, 100, 104, 106, 108, 110, 221, 394, 401, 495
 - bounded-input/bounded-output (BIBO), 24, 95, 164
 - exponential, 102, 105, 106, 112, 401, 402

- external, 95, 102
- global, 99
- global asymptotic (G.A.S), 110
- global exponential (G.E.S), 102, 112
- in the sense of Lagrange, 102, 104
- in the sense of Lyapunov, 99, 104, 321, 401, 402, 495
- input to output (IOS), 103
- input to state (ISS), 103
- input/output to state (IOSS), 103
- internal, 98
- local, 99
- local exponential, 102
- marginal, 99, 320, 394
- output to state (OSS), 103
- resources, 327
- robustly output (ROS), 103
- structural, 131
- uniform, 100
- Stability criterion
 - circle, 503, 504, 506
 - Lyapunov function, 220
 - Lyapunov's, 219
 - Nyquist, 322, 323
 - Popov's, 503–506, 576
 - Routh-Hurwitz, 220, 322
- State, 212
 - controllability, 213, 216
 - equation, 54, 195, 197, 202, 208, 383, 495
 - observability, 213, 215, 216
 - transition matrix, 103, 104, 223, 389, 390, 393, 394, 399, 401, 402
 - variable, 54, 55, 195, 197
 - variables convertibility, 211
 - vector, 54–56, 61, 211, 389
- State space, 54, 60, 61, 138, 153, 195, 217, 317, 383, 384, 411, 493, 574
- State space equations, 226, 383, 384
 - forced solution, 227
 - general solution, 222
 - homogenous solution, 223, 227
 - solution, 222, 386
- State space model, 55, 64, 195, 198, 203, 206, 212, 226, 383–385
 - linearized, 64, 99, 494
 - the first direct form, 196
 - the second direct form, 200
- Stationarity, 162, 445, 530
- Steady state, 489
- Step response, 46, 157, 173, 178, 183, 185, 228
 - time-varying, 369, 374
- Stopband, 271, 272, 333, 339
- Superposition principle, 16, 158, 366
- Suppression, 272
- Supremum, 89
- Symbol (bit) synchronization, 506
- Synchronization, 489
 - region, 492
- Synchronous detection, 407
- Synthesis, 506
- System, 349
 - biharmonic oscillatory, 480
 - chaotic, 146
 - communication, 2, 273, 506
 - conservative, 138, 141, 142, 183
 - control, 6, 37, 206
 - controlable, 213
 - delay feedback, 331
 - dissipative, 139, 143, 146
 - Doppler radar, 5
 - dynamical, 1
 - Hamiltonian, 141, 143–145
 - input-to-output, 209
 - matrix, 54, 386, 495
 - medical ultrasonography, 7
 - memory, 426, 436
 - memoryless, 427
 - mobile phone, 273
 - near conservative, 143, 145
 - observable, 215
 - open loop, 209
 - precision nonlinear oscillatory, 183
 - radar, 4, 273
 - remote sensing, 10
 - resonant, 260
 - robot positioning, 8
 - rough, 131
 - subtle, 131
 - TV, 273
 - Volterra, 454
 - wireless, 8
- System block diagram, 58
- System characteristic
 - accuracy, 20
 - causality, 15
 - continuity, 13

- controlability, 19
- detectability, 20, 103
- dimensionality, 13
- homogeneity, 16
- linearity, 16
- memory, 14
- observability, 19
- precision, 20
- regularity, 12
- robustness, 21
- Stability, 24
- stabilizability, 20, 103
- uncertainty, 21
- System definition, 1
- System function, 46
- System identification, 166
- System matrix, 108, 204, 224, 226, 318, 383
- System operator, 12, 239, 349, 425
- System state, 195
- System structure
 - cascade, 27, 501
 - closed loop, 25, 143, 206, 319, 502
 - closed loop control, 26, 206
 - feedback, 25, 206, 319
 - open, 25
 - parallel, 27
- System type
 - autonomous, 322
 - causal, 15, 163, 292
 - continuous-time, 13
 - deterministic, 12
 - discrete-time, 13
 - linear, 16
 - linear time-invariant (LTI), 17, 54, 153
 - linear time-varying (LTV), 18, 32, 51, 54, 349
 - memory (or dynamic), 14
 - memoryless (or static), 14, 87
 - multiple-input multiple-output (MIMO), 13, 167
 - multiple-input single-output (MISO), 14, 167
 - noncausal, 15, 163, 292
 - nonlinear, 16
 - nonlinear memoryless, 33
 - nonlinear time-invariant (NTI), 18, 33, 60, 425
 - nonlinear time-varying (NTV), 18, 37, 60, 519
 - random, 13
 - single-input multiple-output (SIMO), 14, 167
 - single-input single-output (SISO), 14, 167
 - stochastic, 13, 519
 - time-invariant, 17
 - time-varying (time-variant), 17
- Taylor series, 57, 63, 64, 137, 195, 223–225, 434, 437, 495, 523
- Test signal, 43
 - complex exponential, 44
 - unit impulse, 44
 - unit step, 44
- Theorem, 129
 - Andronov's, 130
 - Andronov-Pontryagin's, 131
 - Cayley-Hamilton, 225, 227
 - Dulac's, 128
 - final value, 301
 - Floquet's, 398, 412
 - initial value, 300
 - Melnikov's, 147
 - Poincaré-Bendixson, 127
 - Pontryagin's, 143, 144
 - similarity, 284
- Time constant, 177
- Time domain, 153, 240, 315, 378
- Time reversal, 284
- Time scaling, 283
- Time shifting, 31, 162, 225, 283, 451
- Time-invariance, 173
- Topography, 131
- Tract, 263, 320
- Trajectory, 110
 - homoclinic, 146
- Transconductance, 265, 403, 405
- Transducer
 - ultrasonic acoustic, 7
- Transfer function, 52, 56, 97, 239, 291, 292, 294, 314, 315, 319, 323, 334, 337
 - multivariate, 454
 - poles, 279
 - time-varying, 362
 - zeros, 278

- Transform
 - Fourier, 15, 30, 47, 54, 165, 239–241, 244, 249, 255, 276, 278, 356, 357, 361, 397, 450, 609
 - Fourier inverse, 251
 - Laplace, 52, 239, 276, 279, 280, 287, 295, 304, 305, 307, 313, 317, 364, 450, 453, 613
 - Laplace bilateral, 54, 276, 278, 282
 - Laplace inverse, 293
 - Laplace unilateral, 276, 297
 - multivariate, 454
- Transform domain, 239, 455, 535
- Transform domain kernel, 456
- Transient time, 185
- Transmitter, 2, 8
 - SSB, 272
- Triangular inequality, 88

- Uncertainty principle, 22
- Underdamping, 181, 183
- Unit impulse, 43, 163, 305, 356, 373
- Unit step, 157, 306, 374, 454
- Upper sideband (USB), 272

- van der Pol's
 - equation, 68, 70, 72, 119
 - method, 66, 68, 78, 558
 - oscillator, 68, 70, 72, 75, 78, 80, 82, 84, 86, 120, 127, 139, 144, 473
 - solution, 68
- Vandermonde matrix, 427
- Variable amplitudes, 548, 559
- Vibration
 - fundamental, 269
 - spurious, 269
- Volterra kernel, 57, 437, 440, 446, 449, 452, 526, 529, 534
- Volterra operator, 437, 442, 450, 528
- Volterra series, 57, 436, 449, 453, 497, 525, 526
- Volterra system, 451

- Wiener kernel, 447, 449
- Wiener method, 59, 447
- Wiener operator, 447
- Wiener system, 439, 496, 499–502, 581